frontiers | Research Topics

Solving the plasmalogen puzzle – from basic science to clinical application

Edited by
Masanori Honsho, Fabian Dorninger and Johannes Berger

Published in
Frontiers in Cell and Developmental Biology
Frontiers in Molecular Biosciences

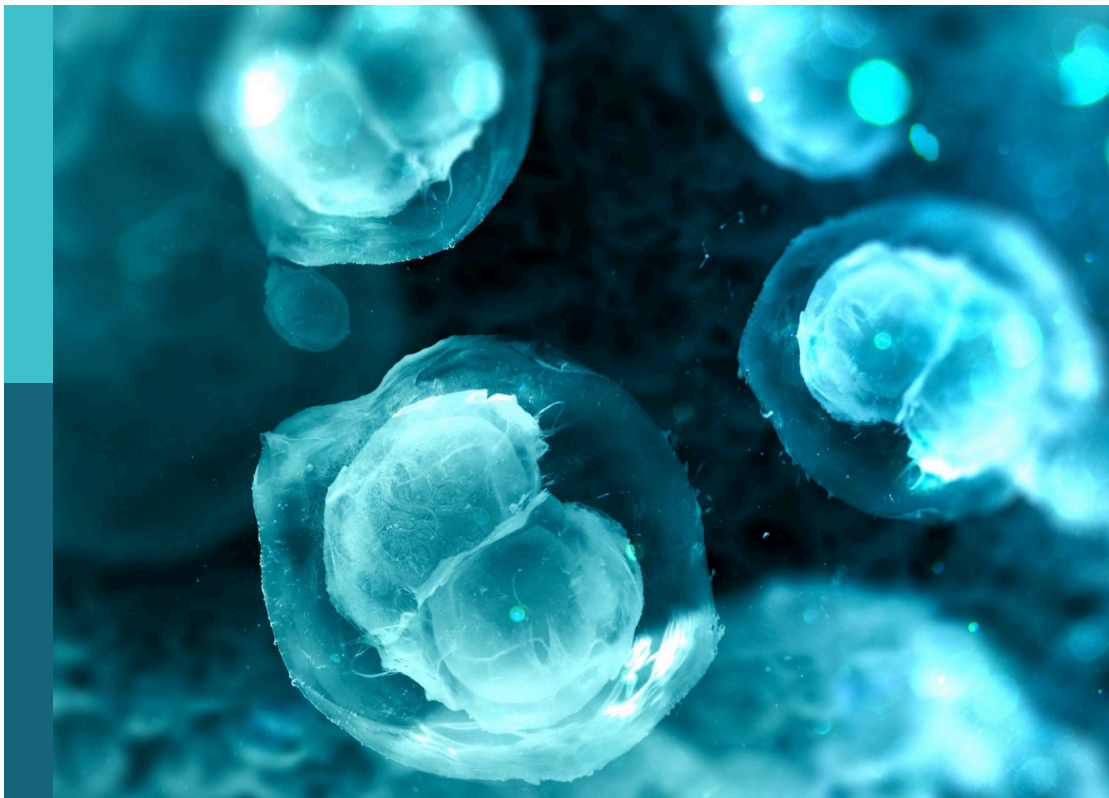

ISSN 1664-8714
ISBN 978-2-83251-494-8
DOI 10.3389/978-2-83251-494-8

About Frontiers

Frontiers is more than just an open access publisher of scholarly articles: it is a pioneering approach to the world of academia, radically improving the way scholarly research is managed. The grand vision of Frontiers is a world where all people have an equal opportunity to seek, share and generate knowledge. Frontiers provides immediate and permanent online open access to all its publications, but this alone is not enough to realize our grand goals.

Frontiers journal series

The Frontiers journal series is a multi-tier and interdisciplinary set of open-access, online journals, promising a paradigm shift from the current review, selection and dissemination processes in academic publishing. All Frontiers journals are driven by researchers for researchers; therefore, they constitute a service to the scholarly community. At the same time, the *Frontiers journal series* operates on a revolutionary invention, the tiered publishing system, initially addressing specific communities of scholars, and gradually climbing up to broader public understanding, thus serving the interests of the lay society, too.

Dedication to quality

Each Frontiers article is a landmark of the highest quality, thanks to genuinely collaborative interactions between authors and review editors, who include some of the world's best academicians. Research must be certified by peers before entering a stream of knowledge that may eventually reach the public - and shape society; therefore, Frontiers only applies the most rigorous and unbiased reviews. Frontiers revolutionizes research publishing by freely delivering the most outstanding research, evaluated with no bias from both the academic and social point of view. By applying the most advanced information technologies, Frontiers is catapulting scholarly publishing into a new generation.

What are Frontiers Research Topics?

Frontiers Research Topics are very popular trademarks of the *Frontiers journals series*: they are collections of at least ten articles, all centered on a particular subject. With their unique mix of varied contributions from Original Research to Review Articles, Frontiers Research Topics unify the most influential researchers, the latest key findings and historical advances in a hot research area.

Find out more on how to host your own Frontiers Research Topic or contribute to one as an author by contacting the Frontiers editorial office: frontiersin.org/about/contact

Solving the plasmalogen puzzle – from basic science to clinical application

Topic editors

Masanori Honsho — Kyushu University, Japan

Fabian Dorninger — Medical University of Vienna, Austria

Johannes Berger — Medical University of Vienna, Austria

Citation

Honsho, M., Dorninger, F., Berger, J., eds. (2023). *Solving the plasmalogen puzzle – from basic science to clinical application*. Lausanne: Frontiers Media SA.

doi: 10.3389/978-2-83251-494-8

Table of contents

frontiers | Frontiers in Cell and Developmental Biology

TYPE Editorial
PUBLISHED 16 January 2023
DOI 10.3389/fcell.2023.1137868

OPEN ACCESS

EDITED AND REVIEWED BY
Graça Soveral,
University of Lisbon, Portugal

*CORRESPONDENCE
Fabian Dorninger,
fabian.dorninger@meduniwien.ac.at

SPECIALTY SECTION
This article was submitted to Cellular Biochemistry, a section of the journal Frontiers in Cell and Developmental Biology

RECEIVED 04 January 2023
ACCEPTED 06 January 2023
PUBLISHED 16 January 2023

CITATION
Dorninger F, Berger J and Honsho M (2023), Editorial: Solving the plasmalogen puzzle—From basic science to clinical application.
Front. Cell Dev. Biol. 11:1137868.
doi: 10.3389/fcell.2023.1137868

Editorial: Solving the plasmalogen puzzle—From basic science to clinical application

Fabian Dorninger[1]*, Johannes Berger[1] and Masanori Honsho[2,3]

[1]Department of Pathobiology of the Nervous System, Center for Brain Research, Medical University of Vienna, Vienna, Austria, [2]Department of Neuroinflammation and Brain Fatigue Science, Graduate School of Medical Sciences, Kyushu University, Fukuoka, Japan, [3]Institute of Rheological Functions of Food-Kyushu University Collaboration Program, Kyushu University, Fukuoka, Japan

KEYWORDS

plasmalogen, ether lipid, membrane, Alzheimer's disease, phospholipid

Editorial on the Research Topic
Solving the plasmalogen puzzle—From basic science to clinical application

In the almost 100 years since their discovery, numerous scientific breakthroughs around plasmalogens have been made, but at the same time the enigmatic phospholipid group is still keeping scientists of various disciplines on their toes. For example, biophysicists have revealed many biophysical properties of plasmalogens, but several aspects of their role in connection with other phospholipids in membrane bilayers remain cloudy. Geneticists have mostly elucidated the genetic basis of ether lipid biosynthesis but some genes involved in plasmalogen metabolism are still unknown; molecular biologists have identified new roles of plasmalogens in cellular processes but many puzzle pieces of the overall picture, particularly in complex organisms, have yet to be added; and clinicians have made major progress in diagnosing diseases involving plasmalogen deficiency but still lack suitable treatment strategies. Certainly, none of these scientific fields works independently, but an interdisciplinary approach is required to explore complex subjects like the biological role of plasmalogens. Many of the disciplines mentioned above have cooperated for the generation of the present Research Topic, which contains a balanced collection of reviews and original articles comprising a broad range of topics associated with plasmalogens, from basic science to clinical application.

Due to their unique biochemical structure and the particular challenge to discriminate the vinyl ether bond at the *sn*-1 position from double bonds of the alkyl chains of other ether lipid species, the reliable analytical determination of plasmalogens has bothered researchers for a long time (Koch et al., 2020). In their review article, Koch et al. give a comprehensive overview over the historic milestones in the analytical detection and quantification of plasmalogens. Subsequently, they highlight the progress made in recent years and demonstrate, how state-of-the-art methodology can be utilized to gather novel information on ether lipid species, their tissue distribution and physiological functions. In addition to technical advances in plasmalogen analysis, recent research has also brought key developments in elucidating the genes and enzymes involved in the generation of these lipids. One of the last orphan enzymes to be assigned to the corresponding gene was plasmanylethanolamine desaturase, the crucial enzyme for the introduction of the vinyl ether bond, which was recently shown by three independent approaches to be encoded by the *TMEM189* gene in humans (Gallego-Garcia et al., 2019; Werner et al., 2020; Wainberg et al., 2021). In the present Research Topic, Padmanabhan et al. outline the hunt for that gene and narrate, how the use of a comparatively unconventional model organism, *Myxococcus xanthus*, enabled the identification of this so crucial gene for

plasmalogen biosynthesis. A more general overview of the steps involved in plasmalogen generation and their regulation is provided in the article authored by Dorninger et al. Moreover, the authors elaborate on the most recent knowledge on plasmalogen metabolism in different tissues as well as under physiological or pathological conditions and discuss the therapeutic potential of exogenous plasmalogen supplementation. While that article focuses mainly on plasmalogen metabolism in mammals, the work of Goldfine reminds us of the unusual distribution of plasmalogens in bacteria. As a long-standing expert in the topic (Goldfine, 2010), the author summarizes current knowledge on plasmalogen biosynthesis under anaerobic conditions and the functions of these lipids in bacterial species.

As a result of continuous research in the last years, important roles of plasmalogens in a variety of cell types and organs have emerged. Compared with other tissues, relatively little is known about their function in the eye. However, here, following up on the previous work of their group (Saab et al., 2014), Karadayi et al. reveal that plasmalogens are essential for the stability and functioning of gap junctions between Müller cells, a glia cell type specific for the retina, thus expanding our understanding of the role of plasmalogens in intercellular communication. On the cellular level, their involvement in signaling processes has become a major focus in the discussion around the physiological role of plasmalogens (Dorninger et al., 2020) and, accordingly, is also well represented in the current Research Topic. Honsho et al. have previously shown that plasmalogen levels in the inner leaflet of the plasma membrane bilayer govern a feedback loop that regulates the stability of FAR1, the rate-limiting enzyme in the plasmalogen biosynthesis pathway (Honsho et al., 2017). In their Original Research article in this Research Topic, they extend their findings and identify ATP8B2 as the flippase enzyme responsible for the asymmetric distribution of plasmalogens in the plasma membrane, thus controlling the feedback loop and, consequently, downstream processes like intracellular signaling. Previous work has shown that in the mammalian nervous system, plasmalogens are crucial for the adequate functioning of the Akt-ERK axis (da Silva et al., 2014), one of the main signaling cascades in many cell types, and that G-protein coupled receptors are important mediators of this effect (Hossain et al., 2016). Following up on these findings, Hossain et al. provide experimental evidence that signaling *via* brain-derived neurotrophic factor is impacted by plasmalogens as a downstream effect of the Akt-ERK modulation. Furthermore, they indicate that this mechanism is responsible for learning and memory deficits observed in mice upon plasmalogen deficiency, which can be alleviated by dietary plasmalogen supplementation.

Based on their association with such important processes like learning and memory, plasmalogens (or their deficiency) have been ascribed major contributions to various human diseases. The most obvious example is the inborn defect in plasmalogen biosynthesis, which causes the rare disorder rhizomelic chondrodysplasia punctata (RCDP). In this Frontiers Research Topic, Fallatah et al. use a series of mouse models with graded plasmalogen deficiency to show that genotype severity determines the levels of several biochemical markers. This renders these mouse models particularly valuable for the clinical evaluation of RCDP, where similar observations have been made (Fallatah et al., 2021). Excitingly, also neurochemical markers and the characteristic neurobehavioral alterations correlate with the degree of plasmalogen deficiency, thus paving the way for establishing novel readouts in clinical trials for this so far uncurable disease. Next to inborn errors in their biosynthesis, a role of plasmalogens has been implicated in a variety of other human diseases. One so far unknown example is studied by Karadayi et al. in the present Research Topic. The research group has previously shown that in children developing retinopathy of prematurity—an eye disease that can lead to early blindness and is associated with abnormal retinal vessel development—arachidonic acid in erythrocyte membranes accumulates with time *in utero* at the expense of docosahexaenoic acid (Pallot et al., 2019). Here, the authors utilize data from a prospective cohort study to support the hypothesis that plasmalogens play a major role in modulating the arachidonic acid/docosahexaenoic acid ratio in children with retinopathy of prematurity.

A disease that has kept the world in suspense in the last 3 years is COVID-19 caused by infection with the SARS-CoV-2 virus. Their previous work on lipids in sepsis (Amunugama et al., 2021) and the comparable disease courses in sepsis and severe COVID-19 prompted the authors around Pike et al. to study plasmalogen levels in a mouse model of SARS-CoV-2 infection. Remarkably, their experiments reveal a reduction of lung plasmalogen levels in the infected mice, thus showing similarities to the situation upon sepsis, for which the authors demonstrate a depletion of plasmalogens in plasma of both rats and humans. More than in any other disease, an involvement of plasmalogens is debated in the pathogenesis of Alzheimer's disease (Senanayake and Goodenowe, 2019), the most common cause of dementia worldwide. Goodenowe and Senanayake add to the intrigue with a post-mortem analysis of temporal brain cortex samples from patients with mild cognitive impairment and Alzheimer's disease compared with controls. The resulting data show an association with cognition and, under certain circumstances, even predictive value of specific ethanolamine phospholipid species, among them plasmalogens.

Their widespread involvement in disease mechanisms and maybe also etiology has raised speculation and curiosity about the potential of plasmalogens (or their precursors) as dietary supplements and therapeutic substances (Paul et al., 2019; Bozelli and Epand, 2021). A prerequisite for the evaluation of dietary supplementation strategies is an understanding of the metabolization of plasmalogens after their ingestion. Interestingly, previous work from Nishimukai and coworkers has shown that the extent of lymphatic absorption is heavily dependent on the type of headgroup (Nishimukai et al., 2011). In their article in the current Research Topic, Sato et al. investigate the metabolic fate of bacterial plasmalogens, which carry different *sn*-1 alkyl chains than those synthesized by mammals. Adding an important piece of knowledge on plasmalogen metabolism, they show that also these atypical plasmalogens are readily absorbed into the lymph after duodenal infusion and remodeled at the *sn*-2 position, similar to what is known for endogenous plasmalogen species. Several promising therapeutic approaches involving plasmalogens or enhancements thereof are featured in our Research Topic: Based on their previous expertise in evaluating potential drugs against Alzheimer's disease (Chowdhury et al., 2021), Gu et al. utilize sea squirts to extract plasmalogens for the treatment of aged mice. Remarkably, intragastric application of the plasmalogen extract improved cognitive performance and aging-related molecular changes, thus raising hope for a future use as anti-neurodegenerative therapy. An alternative strategy is the use of precursor substances, which can be converted to plasmalogens *in situ* after oral application. One example is PPI-1011, a compound with a

preformed vinyl ether bond at the *sn*-1 position, docosahexaenoic acid at *sn*-2 and lipoic acid as a stabilizer at *sn*-3 (Wood et al., 2011). Now, Smith et al. investigate in detail the metabolization and excretion of PPI-1011 in mice by using a radioactively labeled variant. The authors show the distribution of the label across various tissues, including the brain, which is an essential target for all therapeutic strategies in plasmalogen deficiency. In view of these data, we are eagerly awaiting future studies involving functional readouts after the supplementation with PPI-1011. An additional step is taken by Goodenowe et al., who have previously stressed the positive association between blood plasmalogens and cognition in humans (Goodenowe and Senanayake, 2019). Here, they orally provided a plasmalogen precursor and show increased serum plasmalogen levels, reduced signs of oxidative stress and even clinical relevance for cognitive function in a small sample of cognitively impaired trial participants, which warrants further investigation of this compound. Also Fujino et al. have previously emphasized the value of plasmalogens for cognition in certain subgroups of cognitively impaired patients (Fujino et al., 2017). In this Research Topic, they indicate surprisingly positive effects of plasmalogens in a very different population: Results after dietary supplementation of plasmalogens extracted from scallops suggested improved mental health and reduced fatigue in male students. Even though the molecular mechanisms underlying the beneficial effect of plasmalogens or their precursors on cognitive parameters remain largely unclear, these data further position these compounds as complementary therapeutic substances in various neurological diseases. From a different perspective, this is also underlined in the review article of Rong et al.: After previously pointing out potential anti-viral properties of plasmalogens (Deng and Angelova, 2021), the authors here analyze structural similarities between plasmalogens and platelet-activating factor (PAF), an ether lipid without vinyl ether bond. Based on these, they hypothesize that plasmalogens could fine-tune PAF-associated signaling, thus exerting anti-inflammatory function, which may be favorable in pathological conditions involving a pro-inflammatory milieu.

Overall, the variety of articles and wide range of subjects in the present Research Topic well reflect the variegated research landscape in the plasmalogen field and underline the versatility of this lipid subgroup. They also demonstrate that major progress is made continuously to understand the role of plasmalogens in biological systems, and exploit their therapeutic potential. However, as researchers we are well familiar with the fact that every solved scientific question raises several new ones and that is no different for the field of plasmalogens. Accordingly, the research around plasmalogens will remain vivid also in the future and we are looking forward to the next revelations around this fascinating group of phospholipids.

Author contributions

FD wrote the original draft of the manuscript. JB and MH reviewed and edited the manuscript draft. All authors approved the submitted version.

Funding

This work was supported by grants from the Austrian Science Fund (FWF; P34723) and the Japan Society for the Promotion of Science (JSPS; Grant-in-Aid for Scientific Research No. JP21K06839 to MH).

Conflict of interest

The authors declare that the research was conducted in the absence of any commercial or financial relationships that could be construed as a potential conflict of interest.

Publisher's note

References

Amunugama, K., Pike, D. P., and Ford, D. A. (2021). The lipid biology of sepsis. *J. Lipid Res.* 62, 100090. doi:10.1016/j.jlr.2021.100090

Bozelli, J. C., Jr., and Epand, R. M. (2021). Plasmalogen replacement therapy. *Membr. (Basel)* 11, 838. doi:10.3390/membranes11110838

Chowdhury, S. R., Gu, J., Hu, Y., Wang, J., Lei, S., Tavallaie, M. S., et al. (2021). Synthesis, biological evaluation and molecular modeling of benzofuran piperidine derivatives as Aβ antiaggregant. *Eur. J. Med. Chem.* 222, 113541. doi:10.1016/j.ejmech.2021.113541

da Silva, T. F., Eira, J., Lopes, A. T., Malheiro, A. R., Sousa, V., Luoma, A., et al. (2014). Peripheral nervous system plasmalogens regulate Schwann cell differentiation and myelination. *J. Clin. Invest.* 124, 2560–2570. doi:10.1172/JCI72063

Deng, Y., and Angelova, A. (2021). Coronavirus-induced host cubic membranes and lipid-related antiviral therapies: A focus on bioactive plasmalogens. *Front. Cell Dev. Biol.* 9, 630242. doi:10.3389/fcell.2021.630242

Dorninger, F., Forss-Petter, S., Wimmer, I., and Berger, J. (2020). Plasmalogens, platelet-activating factor and beyond - ether lipids in signaling and neurodegeneration. *Neurobiol. Dis.* 145, 105061. doi:10.1016/j.nbd.2020.105061

Fallatah, W., Schouten, M., Yergeau, C., Di Pietro, E., Engelen, M., Waterham, H. R., et al. (2021). Clinical, biochemical, and molecular characterization of mild (nonclassic) rhizomelic chondrodysplasia punctata. *J. Inherit. Metab. Dis.* 44, 1021–1038. doi:10.1002/jimd.12349

Fujino, T., Yamada, T., Asada, T., Tsuboi, Y., Wakana, C., Mawatari, S., et al. (2017). Efficacy and blood plasmalogen changes by oral administration of plasmalogen in patients with mild alzheimer's disease and mild cognitive impairment: A multicenter, randomized, double-blind, placebo-controlled trial. *EBioMedicine* 17, 199–205. doi:10.1016/j.ebiom.2017.02.012

Gallego-Garcia, A., Monera-Girona, A. J., Pajares-Martinez, E., Bastida-Martinez, E., Perez-Castano, R., Iniesta, A. A., et al. (2019). A bacterial light response reveals an orphan desaturase for human plasmalogen synthesis. *Science* 366, 128–132. doi:10.1126/science.aay1436

Goldfine, H. (2010). The appearance, disappearance and reappearance of plasmalogens in evolution. *Prog. Lipid Res.* 49, 493–498. doi:10.1016/j.plipres.2010.07.003

Goodenowe, D. B., and Senanayake, V. (2019). Relation of serum plasmalogens and APOE genotype to cognition and dementia in older persons in a cross-sectional study. *Brain Sci.* 9, 92. doi:10.3390/brainsci9040092

Honsho, M., Abe, Y., and Fujiki, Y. (2017). Plasmalogen biosynthesis is spatiotemporally regulated by sensing plasmalogens in the inner leaflet of plasma membranes. *Sci. Rep.* 7, 43936. doi:10.1038/srep43936

Hossain, M. S., Mineno, K., and Katafuchi, T. (2016). Neuronal orphan G-protein coupled receptor proteins mediate plasmalogens-induced activation of ERK and Akt signaling. *PLoS One* 11, e0150846. doi:10.1371/journal.pone.0150846

Koch, J., Lackner, K., Wohlfarter, Y., Sailer, S., Zschocke, J., Werner, E. R., et al. (2020). Unequivocal mapping of molecular ether lipid species by LC-MS/MS in plasmalogen-deficient mice. *Anal. Chem.* 92, 11268–11276. doi:10.1021/acs.analchem.0c01933

Nishimukai, M., Yamashita, M., Watanabe, Y., Yamazaki, Y., Nezu, T., Maeba, R., et al. (2011). Lymphatic absorption of choline plasmalogen is much higher than that of ethanolamine plasmalogen in rats. *Eur. J. Nutr.* 50, 427–436. doi:10.1007/s00394-010-0149-0

Pallot, C., Mazzocco, J., Meillon, C., Semama, D. S., Chantegret, C., Ternoy, N., et al. (2019). Alteration of erythrocyte membrane polyunsaturated fatty acids in preterm newborns with retinopathy of prematurity. *Sci. Rep.* 9, 7930. doi:10.1038/s41598-019-44476-w

Paul, S., Lancaster, G. I., and Meikle, P. J. (2019). Plasmalogens: A potential therapeutic target for neurodegenerative and cardiometabolic disease. *Prog. Lipid Res.* 74, 186–195. doi:10.1016/j.plipres.2019.04.003

Saab, S., Buteau, B., Leclere, L., Bron, A. M., Creuzot-Garcher, C. P., Bretillon, L., et al. (2014). Involvement of plasmalogens in post-natal retinal vascular development. *PLoS One* 9, e101076. doi:10.1371/journal.pone.0101076

Senanayake, V., and Goodenowe, D. B. (2019). Plasmalogen deficiency and neuropathology in Alzheimer's disease: Causation or coincidence? *Alzheimers Dement. (N Y)* 5, 524–532. doi:10.1016/j.trci.2019.08.003

Wainberg, M., Kamber, R. A., Balsubramani, A., Meyers, R. M., Sinnott-Armstrong, N., Hornburg, D., et al. (2021). A genome-wide atlas of co-essential modules assigns function to uncharacterized genes. *Nat. Genet.* 53, 638–649. doi:10.1038/s41588-021-00840-z

Werner, E. R., Keller, M. A., Sailer, S., Lackner, K., Koch, J., Hermann, M., et al. (2020). The TMEM189 gene encodes plasmanylethanolamine desaturase which introduces the characteristic vinyl ether double bond into plasmalogens. *Proc. Natl. Acad. Sci. U. S. A.* 117, 7792–7798. doi:10.1073/pnas.1917461117

Wood, P. L., Smith, T., Lane, N., Khan, M. A., Ehrmantraut, G., and Goodenowe, D. B. (2011). Oral bioavailability of the ether lipid plasmalogen precursor, PPI-1011, in the rabbit: A new therapeutic strategy for alzheimer's disease. *Lipids Health Dis.* 10, 227. doi:10.1186/1476-511X-10-227

frontiers in Cell and Developmental Biology

ORIGINAL RESEARCH
published: 09 February 2022
doi: 10.3389/fcell.2022.828282

Plasmalogens, the Vinyl Ether-Linked Glycerophospholipids, Enhance Learning and Memory by Regulating Brain-Derived Neurotrophic Factor

Md. Shamim Hossain, Shiro Mawatari and Takehiko Fujino*

Institute of Rheological Functions of Food, Fukuoka, Japan

Plasmalogens (Pls), a kind of glycerophospholipids, have shown potent biological effects but their role in hippocampus-dependent memory remained mostly elusive. Here, we first report Pls can enhance endogenous expression of brain-derived neurotrophic factor (*Bdnf*) in the hippocampus and promotes neurogenesis associated with improvement of learning and memory in mice. Genomic and proteomic studies revealed that Pls enhanced recruitment of CREB transcription factor onto the murine *Bdnf* promoter region via upregulating ERK-Akt signaling pathways in neuronal cells. Reduction of endogenous Pls in murine hippocampus significantly reduced learning and memory associated with the reduction of memory-related protein expression, suggesting that Pls can regulate memory-related gene expression in the hippocampus.

Keywords: plasmalogens, memory, BDNF, synaptic plasticity, lipid raft, long-term potentiation (LTP), dendritic spine density

OPEN ACCESS

Edited by:
Fabian Dorninger,
Medical University of Vienna, Austria

Reviewed by:
Sonja Forss-Petter,
Medical University of Vienna, Austria
Steve Holly,
Campbell University, United States
Raphael Zoeller,
Boston University School of Medicine, United States

****Correspondence:***
Md. Shamim Hossain
shamim@rheology.po-jp.com

Specialty section:
This article was submitted to Cellular Biochemistry, a section of the journal Frontiers in Cell and Developmental Biology

Received: *03 December 2021*
Accepted: *17 January 2022*
Published: *09 February 2022*

Citation:
Hossain MS, Mawatari S and Fujino T (2022) Plasmalogens, the Vinyl Ether-Linked Glycerophospholipids, Enhance Learning and Memory by Regulating Brain-Derived Neurotrophic Factor. Front. Cell Dev. Biol. 10:828282. doi: 10.3389/fcell.2022.828282

INTRODUCTION

Plasmalogens (PLs) are ether-linked glycerophospholipids that contain a vinyl ether bond at the *sn*-1 position of the glycerol moiety and consist of two main types, ethanolamine Pls (Pls-Etn) and choline Pls (Pls-Cho) (Braverman and Moser, 2012). The Pls-Etn are enriched mostly in the brain whereas the Pls-Cho are mostly abundant in other tissues including the heart and kidney (Braverman and Moser, 2012). It has been reported that up to two-thirds of the Etn-phospholipids in the whole brain is Pls-Etn (Nagan and Zoeller, 2001). Reduction of Pls-Etn in the brain and blood samples of Alzheimer's disease (AD) patients and its association with the cognitive decline (Ginsberg et al., 1995; Wood et al., 2010; Braverman and Moser, 2012) has raised the question of whether there is a direct relation between Pls and the hippocampal-dependent memory.

Genetic mutation of two major peroxisomal enzymes related to Pls synthesizing enzymes, glyceronephosphate O-acyltransferase (GNPAT) and alkylglycerone phosphate synthase (AGPS), and their modulator Pex-7 has been found in Rhizomelic Chondrodysplasia Punctata (RCDP), which is a disorder characterized by developmental problems, congenital contractures, and severe intellectual disability (Braverman and Moser, 2012; Itzkovitz et al., 2012). The knockout mice of *AGPS* are lethal and those of *Pex-7* and *GNPAT* showed eye cataracts (Braverman and Moser, 2012; da Silva et al., 2014; Liegel et al., 2014) giving a difficulty to use these Pls-reduced mice models for a memory test. Due to the limitation of using the knockout mice, we employed a lentivirus system (sh-RNA) to knock down *GNPAT* mRNA expression, aiming to reduce local Pls content in the mouse hippocampus.

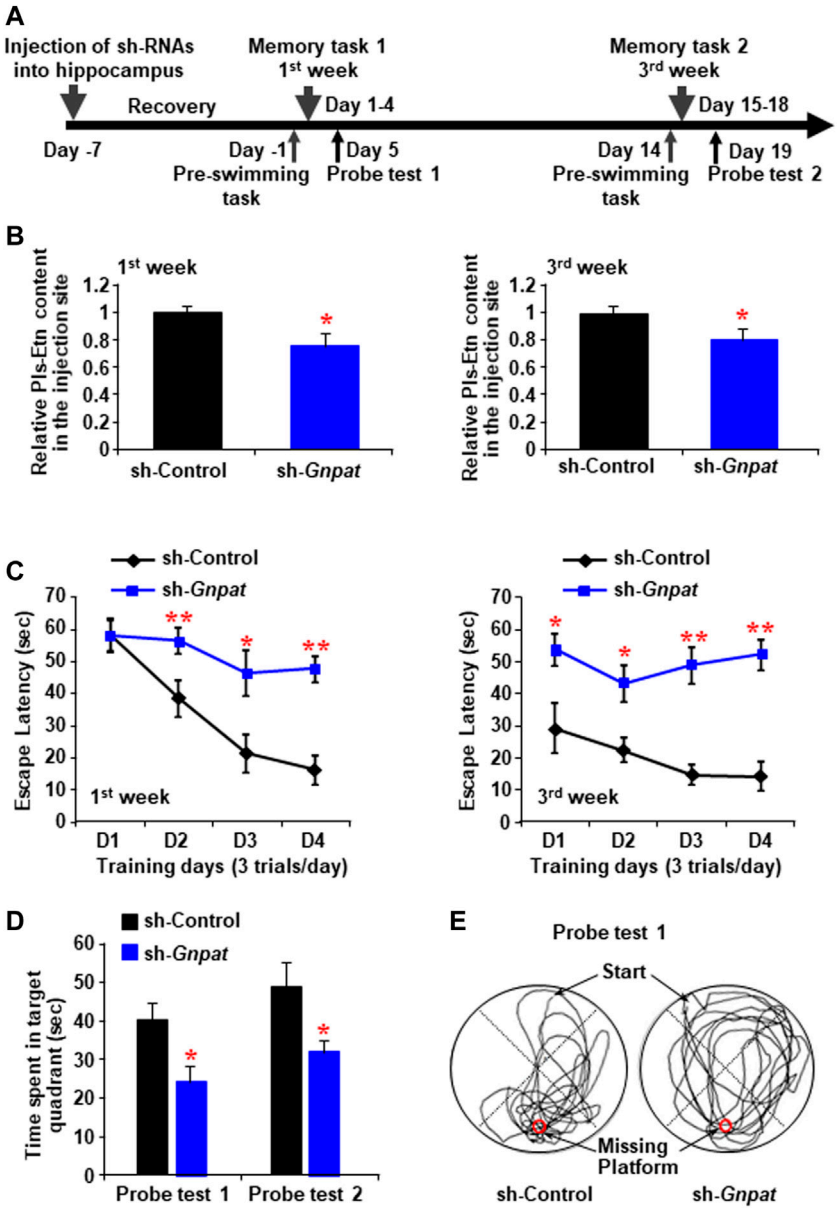

FIGURE 1 | Memory impairment by the reduction of plasmalogen in the hippocampus. **(A)** Schematic diagram shows the memory tasks and probe trials schedule after the intrahippocampal injection of sh-RNA against *Gnpat*. **(B)** Mass spectroscopic data show the relative amount of ethanolamine Pls (Pls-Etn) in the hippocampus infected with lentiviruses (5×10^5 TDU). **(C)** Morris water maze task shows in the change in escape latency at the first week (left panel) and third week (right panel). Data are the mean ± S.E.M. of three independent experiments. Each experiment included more than five mice whose hippocampus was successfully infected by sh-*GNPAT*. **(D)** Probe tests showed the time spent in the target quadrant. **(E)** Examples of traces for control (left) and sh-*GNPAT* (right) mice in probe test one performed after memory task 1. The red circle shows the place of the missing platform. *, $p < 0.05$ and **, $p < 0.01$, in each experimental group compared with the respective control group were analyzed by ANOVA test followed by post hoc Bonferroni's tests.

Our previous study showed that direct application of Pls activated cellular survival signaling of Akt and ERK1/2, resulting in the inhibition of neuronal cells death (Hossain et al., 2013). Consistent with our report, *Pex-7* and *GNPAT* knockout mice showed a deficit in Akt signaling in the peripheral Schwann cells, resulting in the development and differentiation problem of the myelination (da Silva et al., 2014). Our recent study showed that the Pls-induced activation of Akt and ERK signaling might be mediated by specific orphan G-protein coupled receptors (GPCR) expressed in neurons (Hossain et al., 2016). These studies indicate that Pls may act as mediators of cellular signaling in the nervous system.

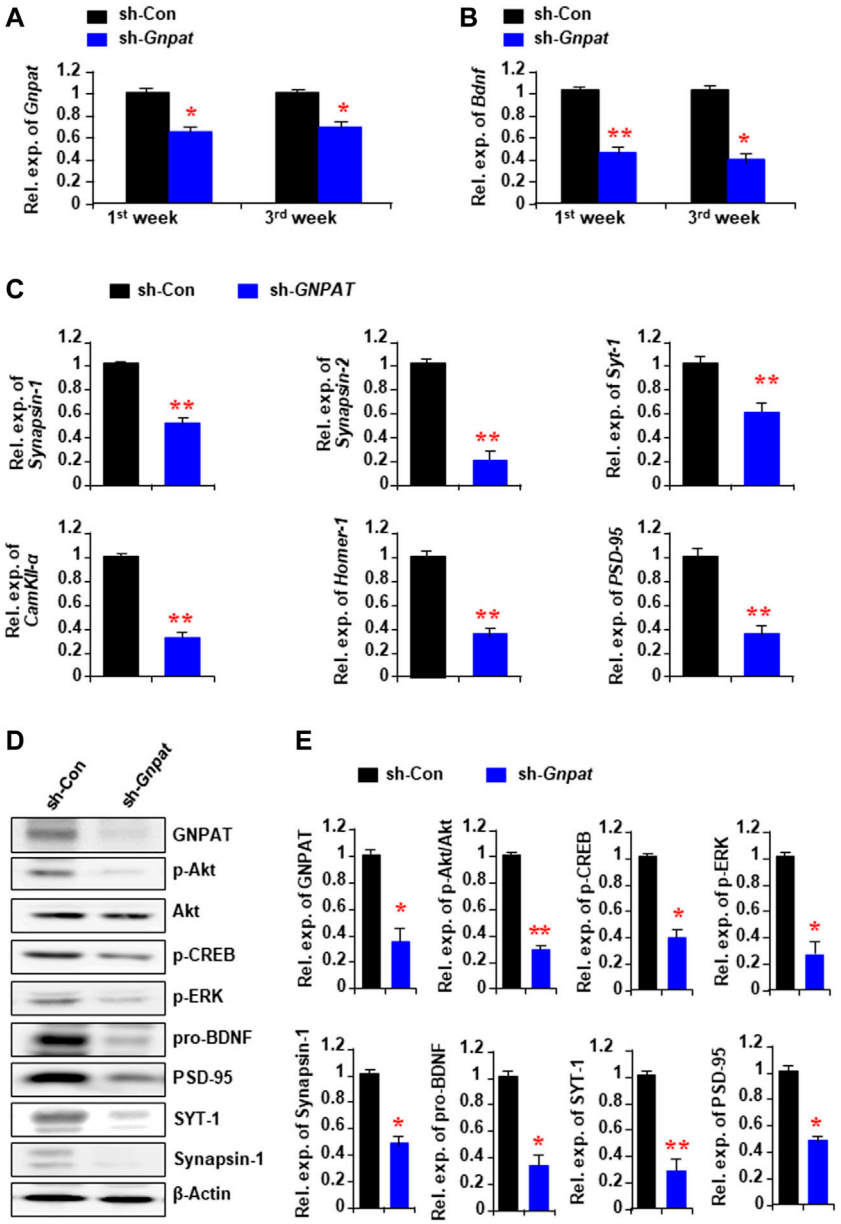

FIGURE 2 | Alteration of memory-related gene expression and cellular signaling in the hippocampus following the Gnpat knockdown. **(A,B)** Real-time PCR data show the changes of *Gnpat* **(A)** and *Bdnf* **(B)** mRNA expressions in the hippocampus following 1 and 3 weeks after microinjection of sh-*Gnpat* lentiviruses. **(C)** Real-time PCR data show the changes in memory-related gene expressions in the hippocampus 3 weeks after the injections of lentiviruses. **(D)** Western blotting assays show the representative protein expressions in the hippocampus 3 weeks after the sh-control and sh-*Gnpat* injection. **(E)** Quantification data of panel **(D)** show the relative change of GNPAT, p-Akt, p-CREB, p-ERK, pro-BDNF, Synapsin-1, SYT-1, and PSD-95 in the hippocampus. The protein expression was normalized with the endogenous expression of β-Actin. The data represent the mean ± S.E.M. Each experiment included more than five mice. *, $p < 0.05$ and **, $p < 0.01$. The p values were obtained by Student's t-tests.

BDNF is well known to regulate memory-related changes in the brain such as adult neurogenesis, synaptic protein expression, dendritic spine maturation, and synaptic plasticity including long-term potentiation (LTP) (Yamada and Nabeshima, 2003; Binder and Scharfman, 2004). It has been reported that BDNF can recruit TrkB, a target receptor of BDNF, into the membrane microdomains called lipid rafts to induce cellular signaling (Suzuki et al., 2004). Here, we studied the effects of Pls in the memory process and examined its regulating effects on BDNF-TrkB signaling. We also investigated whether oral ingestion of Pls could improve learning and memory in mice.

RESULTS

Reduction of Hippocampal Plasmalogens Promoted Learning and Memory Loss in Adult Male Mice

To reduce the endogenous Pls synthesis, we injected lentiviral shRNA to knockdown *GNPAT* expression bilaterally into the mouse hippocampus (**Figure 1A**). Morris water maze tasks were performed following 1 (Memory task 1) and 3 weeks (Memory task 2) of the injection, each of which was followed by a probe test (**Figure 1A**). Reduction of brain Pls in the sh-*GNPAT* injected hippocampus was confirmed by liquid chromatography-mass spectrometry (LC-MS) analysis (**Figure 1B**). At both time points, significant increases in escape latency were observed in the sh-*GNPAT* group of mice compared with the control lentiviral (sh-Luciferase) group (**Figure 1C**). These data suggest that reduction of the hippocampal Pls reduced the learning performance in the mice. To assess the memory performance, we performed the probe tests after finishing the training phases. Probe tests showed that there was a significant reduction of the memory in mice groups lacking hippocampal Pls (**Figures 1D,E**). These findings suggest that the reduction of hippocampal Pls causes impairment of spatial learning and memory in mice. Control lentiviral injection showed no significant changes in the memory performance compared with the uninfected mice (**Supplementary Figure S1A**), indicating that the hippocampal injection itself did not disturb the spatial memory. In addition, the swimming speed of the mice was not affected by the lentivirus injection (**Supplementary Figure S1B**), suggesting that the decrease in learning and memory process in the sh-*GNPAT* mice was not associated with the motor activities.

Knockdown of Hippocampal Plasmalogens Reduced the Memory-Related Gene Expression

To find out the cause of memory loss by the reduction of Pls in the hippocampus, we performed real-time PCR analysis with the infected hippocampal tissue samples, which showed a reduction of *GNPAT* mRNA expression both 1 and 3 weeks after the sh-*GNPAT* injection (**Figure 2A**). BDNF, one of the major memory-related neurotrophic factors, showed a significant reduction of its mRNA expression in the sh-*GNPAT* infected hippocampus (**Figure 2B**). Quantitative PCR data also showed a significant reduction of other memory-related gene expressions; e.g., *synapsin-1*, *synapsin-2*, *synaptotagmin-1* (*SYT-1*), Ca^{2+}*/calmodulin-dependent protein kinase II-α* (*CamKII-α*), *Homer-1*, and *PSD-95* in the Pls reduced hippocampus (**Figure 2C**).

We have previously found that the extracellular addition of Pls can activate ERK and Akt signaling in neuronal cells (Hossain et al., 2013). To examine the relationship between the reduction of Pls and the signaling of these kinases in the hippocampus, we performed Western blotting assays and found a significant reduction of phosphorylated proteins of ERK and Akt in the sh-*GNPAT* infected brain compared with the control group (**Figure 2D**). Protein expression of BDNF, synapsin-1, SYT-,1, and PSD95 was also found to be reduced in the knockdown tissues (**Figures 2D,E**) consistent with the mRNA expression data (**Figures 2B,C**). To confirm the regulatory effects of ERK and Akt phosphorylation on the expression of BDNF, synapsin-1, and SYT-1, we injected either ERK (U0126, 20 μM) or PI3K/Akt inhibitor (LY294002, 0.19 nmol) into the hippocampus (0.5 μL of 50 μM solution/site) stereotaxically in normal mice. It has been reported that these doses of U0126 and LY294002 were effective in blocking the signaling pathways in the brain tissues (Arroyo et al., 2018; Wang et al., 2018). Twenty-four hours after the injection we found a significant decrease in the mRNA expression of *Bdnf*, *synapsin-1*, and *SYT-1* in the hippocampus (**Supplementary Figure S2**). We, therefore, suggest that the reduction of the memory-related gene expression could be due to the down-regulation of ERK and Akt signaling pathways by the reduction of Pls in the hippocampus tissues.

Plasmalogens Diet Enhances Memory and Memory-Related Gene Expression in the Hippocampus

After confirming that the reduction of Pls in the hippocampus resulted in memory loss, we investigated whether the oral intake of Pls had any effect on learning and memory. Mice were given 0.01% Pls-containing or control diet for 6 weeks. There were no differences in food intake and body weight increase between Pls-feeding and control mice. After 6 weeks of Pls feeding, we found that Pls content in the hippocampus increased significantly (**Figure 3A**). The Pls diet improved the learning process in the water maze tasks compared with the control group (**Figure 3B**). The probe test also showed a significant increase in the exploration time in the target compartment (**Figure 3C**), suggesting that Pls diet enhanced memory acquisition and maintenance. The enhancement of the memory was not associated with the physical activity of the mice since the swimming speed was not affected by the Pls diet (**Figures 3D,E**). Consistent with the knockdown data, we observed that Pls diet enhanced phosphorylation of ERK and Akt in the mouse hippocampus, especially in the CA3 region (**Figure 3F**). Western blotting data showed that the Pls diet increased p-ERK, p-Akt, phosphorylated cAMP-regulated element-binding proteins (p-CREB), synapsin-1, PSD-95, and SYT-1 proteins in the hippocampus (**Figures 3G,H**). Real-time PCR data also showed the upregulation of mRNA expression of *Bdnf*, *synapsin-1*, *SYT-1*, and *PSD-95* in the hippocampus (**Figure 3I**). The increases in hippocampal p-Akt and p-CREB expression induced by Pls diet were completely abolished by bilateral microinjection of a phosphoinositide 3-kinase (PI3K)/Akt inhibitor (LY294002) into the hippocampus (0.5 μL of 50 μM solution/site) when measured 24 h after the injection (**Supplementary Figure S3A**). Quantitative analysis showed that not only p-Akt and p-CREB, but also the Pls-induced increase in *Bdnf* mRNA was suppressed by PI3K/Akt inhibitor (**Supplementary Figure S3B**). These findings suggest that the Pls diet-induced enhancement of *Bdnf* expression in the

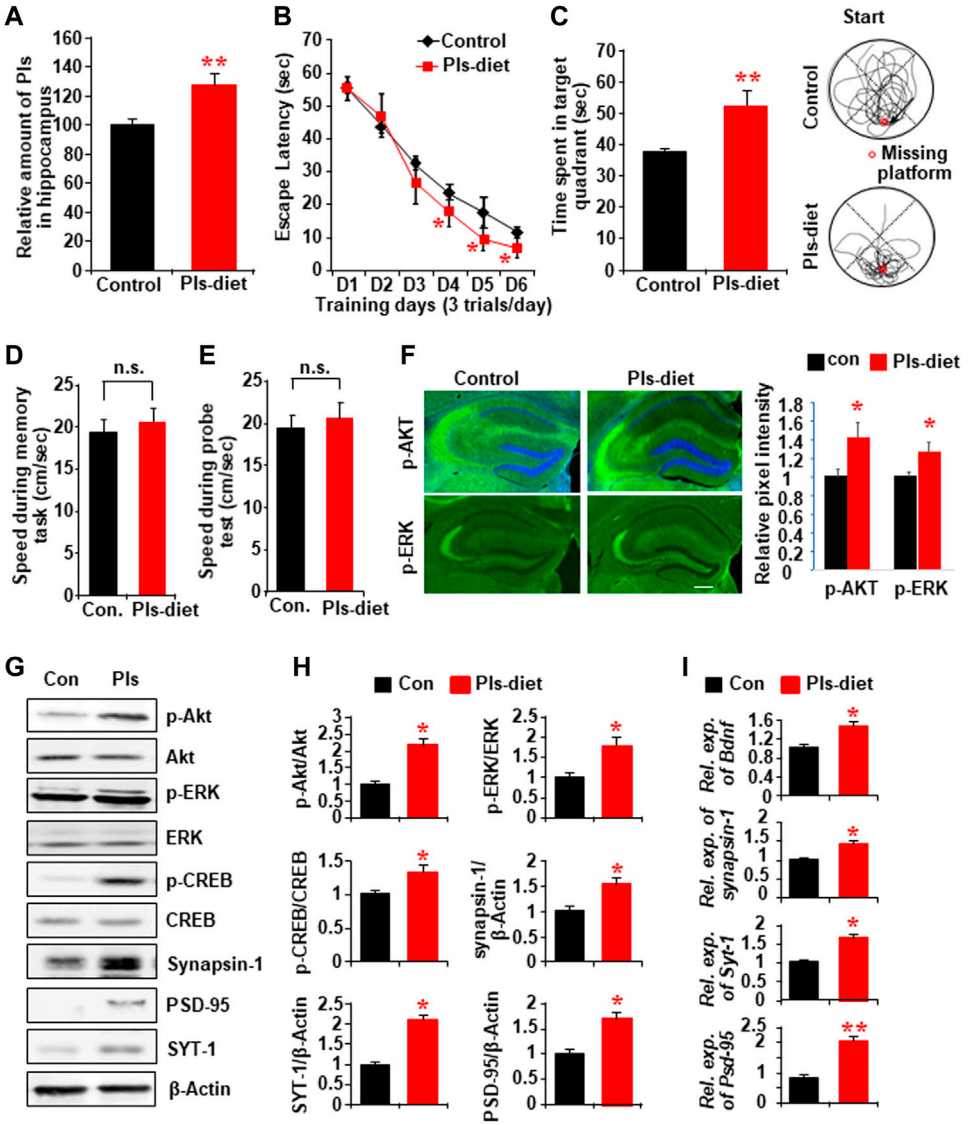

FIGURE 3 | Impact of Pls diet in spatial memory and memory-related protein expression in the hippocampus. **(A)** Mass spectroscopic data show the expression of hippocampal Pls in the mice fed with the diet containing 0.01% Pls for 6 weeks (0.2–0.25 mg Pls/day/mouse, $n = 5$). **(B)** Memory tasks show the change in escape latency by Pls diet. **(C)** The probe test following the memory task shows the changes of time spent in the target quadrant. The right panel shows examples of traces for control (upper) and Pls diet (lower) mice. The red circle indicates the place of the missing platform. **(D,E)** The swimming speed of the mice in both groups during the memory tasks **(D)** and the probe tests **(E)**. **(F)** Immunohistochemistry data show the expression of p-Akt and p-ERK in the control and Pls diet mice hippocampus. Scale bar, 300 μm. The right panel shows the image intensities in relative pixel values. **(G)** Representative Western blotting assays show the protein expression in the control and Pls diet mice hippocampus tissue. **(H)** Quantification data of the panel **(G)** show the relative change in the expression of p-Akt, p-ERK, p-CREB, synapsin-1, PSD-95, and SYT-1 by the Pls diet in the mice hippocampus ($n = 5$). **(I)** Real-time PCR data show the mRNA expression of *Bdnf*, *Synapsin-1*, *Syt-1*, and *Psd-95* in the mice hippocampus ($n = 5$). The data represent mean ± S.E.M. *, $p < 0.05$ and **, $p < 0.01$. The p values of panel B were obtained from ANOVA analysis followed by post hoc Bonferroni's tests. Student's t-tests were performed in panels **(D,E,F,H,I)**.

hippocampus could be affected by the activation of Akt-induced phosphorylation of CREB proteins.

Plasmalogens-Feeding Enhances Synaptic Plasticity of Hippocampal Synapses

We investigated hippocampal plasticity by recording long-term potentiation (LTP) of the synaptic transmission. We have recorded the field excitatory postsynaptic potentials (EPSPs) from the stratum radiatum in the area CA1 of hippocampal slices in control and Pls diet mice (**Figure 4A**, left) and added tetanic stimulation to the Shaffer collaterals to evoke LTP. The basal averages of the first EPSP amplitude and slope of control-diet mice were 0.31 ± 0.02 mV and 0.11 ± 0.01 mV/ms ($n = 12$) and those of Pls diet mice were 0.33 ± 0.02 mV and 0.10 ± 0.01 mV/ms ($n = 15$), respectively. Two superimposed traces showed EPSPs

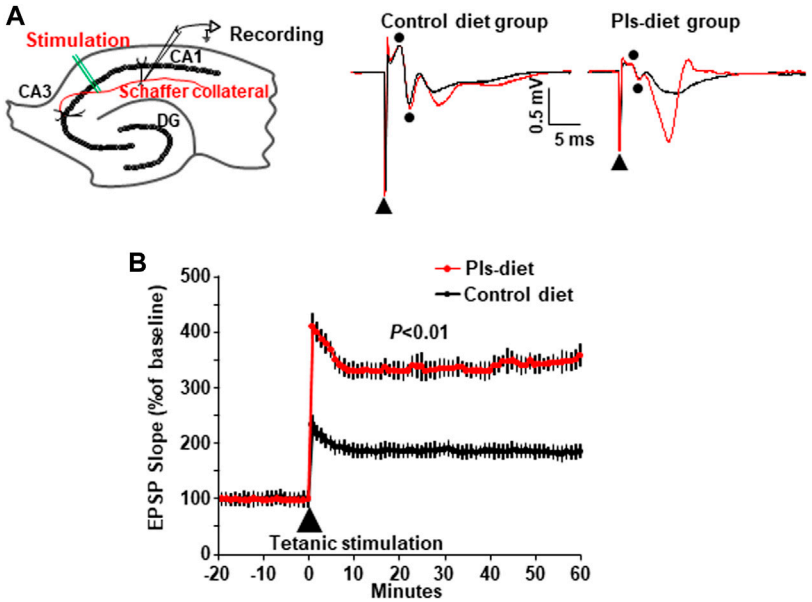

FIGURE 4 | Enhancement of synaptic plasticity by Pls diet. **(A)** The field EPSPs were evoked by stimulation of Schaffer collaterals and recorded in stratum radiatum in the mouse hippocampal slices (left panel). DG, dentate gyrus. The superimposed traces show the EPSP field potentials at time −10 min (black) and 60 min (red) in control and Pls diet mice (middle and right panels). In the traces of control diet [**(A)**, middle], the biphasic wave (dots) just after the stimulus artifact (triangle) was considered to be a fiber volley recorded from nerve fibers since the amplitude was not affected by stimulation (black and red). Then the next downward wave was the first EPSP. The small fiber volley was also observed in the Pls diet. **(B)** Percent changes in the field EPSPs of Pls diet mice (n = 15) show a significant enhancement of LTP after the tetanus stimuli compared with the control slices (n = 12). The data represent five mice in each group and three to four slices from each mouse were examined). The data represent mean ± S.E.M., n = 5 in each group. **, p < 0.01 (Student's t-test).

following stimulus artifact (triangle) and fiber volleys (two dots) at time −10 min (black) and 60 min (red) recorded from control and Pls diet mice (**Figure 4A**, middle and right panels), Percentage changes in field EPSPs showed a significant enhancement of LTP in Pls-feeding mice compared with control-diet mice (**Figure 4B**). This data suggest that Pls diet could enhance synaptic transmission of the hippocampal neurons.

Plasmalogens Treatments Enhance the Maturation of Dendritic Spines of Hippocampal Neurons and Enhance Neurogenesis in the Dentate Gyrus

To examine whether the Pls diet mediated enhancement of synaptic plasticity is correlated with the changes in the synaptic morphology, we performed Golgi-Cox staining and observed a significant increase in the number of dendritic spines (shown as dots) in CA1 and CA3 regions of the hippocampus in the Pls group mice (**Figures 5A, B**). To see the direct effects, we treated primary hippocampal neurons with Pls. After application of Pls (5 μg/ml) on the DIV (Disc *in vitro*) 3, the number of branching from the neuronal cell body was increased at DIV 6, 14, and 22 (**Figures 5C,D**), suggesting that Pls enhanced neuronal cell body differentiation to form mature neurons. We further checked the number of dendritic spines in the matured neurons of DIV 14 and DIV 22 since the dendritic spines appeared at these time points. The presence of Pls in the neuronal culture medium increased dendritic spines (dots) significantly at both time points (**Figures 5E,F**). In addition, the quantity of matured spines called mushroom spines (shown as yellow dots), as well as stubby spines (white dots) at DIV 22, was also found to be increased by the Pls treatments (**Figures 5G,H**).

Neurogenesis in the hippocampus is known to play a role in memory. To address whether Pls diet enhances neurogenesis, we stained newborn neurons in the hippocampus with the antibody against doublecortin (DCX). There was a significant increase in the DCX-positive neurons in the dentate gyrus region of the hippocampus in the Pls diet mice compared to the control group mice (**Figures 5I,J**).

To confirm the signaling mechanism of Pls-treatments induced enhancement of dendritic spines, we examined ERK and Akt proteins. Western blotting assays showed significant increases in p-ERK and p-Akt in the neurons of DIV 14 and DIV 22 (**Supplementary Figure S4A**). The treatments of ERK and Akt inhibitors reduced the Pls-induced increase in dendritic spines at DIV 14 and DIV 22 (**Supplementary Figure S4B**), suggesting that the Pls could enhance the spine formation by a mechanism dependent on ERK and Akt signaling.

Plasmalogens Treatments Enhance *Bdnf* Gene Expression by Activating the Transcriptional Factor CREB

We investigated whether Pls-treatments could induce *Bdnf* gene expression by promoting the recruitment of CREB proteins onto the *Bdnf* promoter regions. Genomic sequence analysis revealed that there are eleven possible CREB recruitment sites onto the mouse

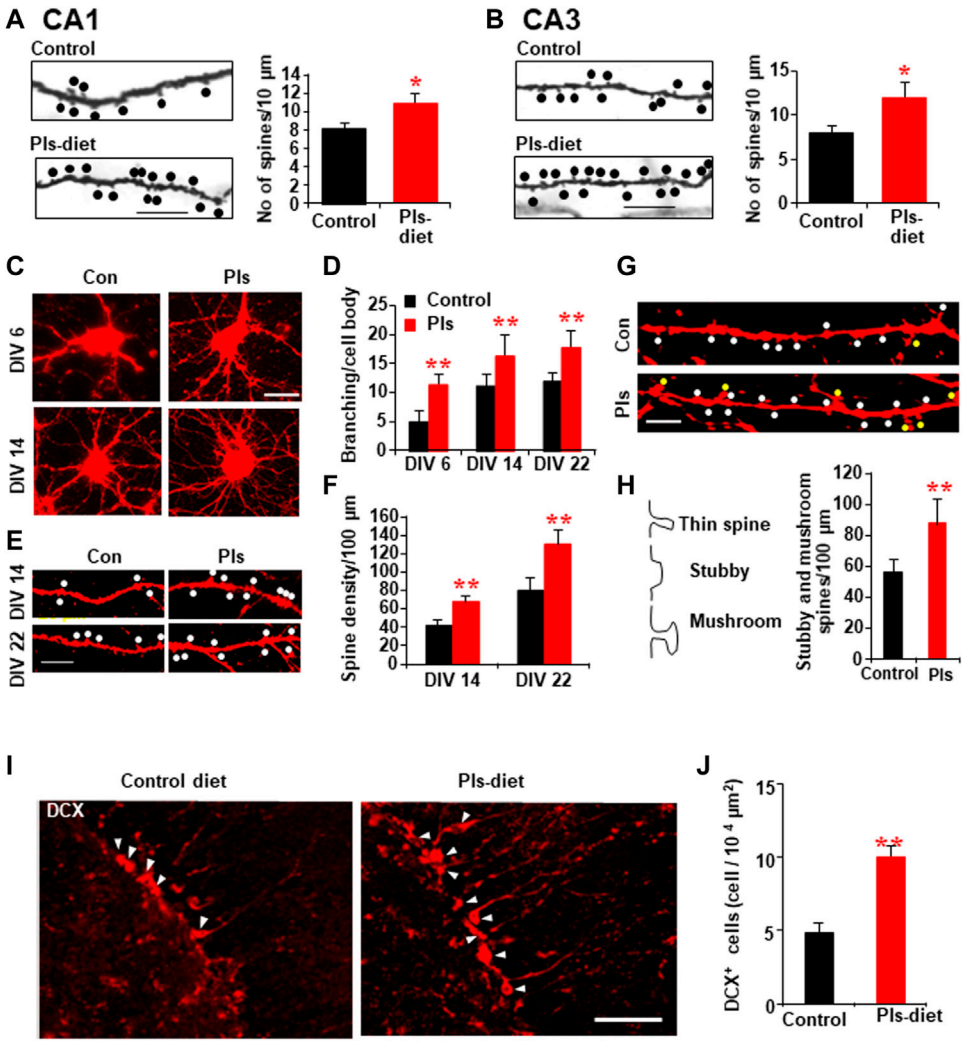

FIGURE 5 | PLs-induced increase in dendritic spines in vivo and in vitro. **(A,B)** Golgi-cox staining shows the representative dendritic-like spines (dots) of CA1 **(A)** and CA3 neurons **(B)** in control and Pls diet mice. Quantification data show the changes in the number of spines in Pls diet mice. Scale bar, 10 µm. **(C–H)** Effects of Pls (5 µg/ml) application on the cultured neuronal cells. Neuronal cells derived from E18 mice embryo were cultured with Pls-containing medium for the indicated days (DIV = disc *in vitro* culture) and stained by DiI to visualize (red color) the morphology of the cells. Pls were added on the DIV3. Branching per cell body **(C,D)** and the number of spines (dots) were enhanced by Pls **(E,F)**. The stubby spines (white dots) and mushroom-shaped spines (yellow dots) were also enhanced by Pls **(G,H)**. Scale bar, 20 µm. **(I)** Immunohistochemistry data show the increased amount of doublecortin (DCX) positive neurons (arrowheads) in the dentate gyrus of Pls diet mice hippocampus. Scale bar, 50 µm. **(J)** Quantification data of panel **(I)** show the significant increase in the DCX-positive neurons in Pls diet mice. The data represent mean ± S.E.M. These values were drawn from the three independent experiments with triplicates. For each sample, more than 20 different locations were photographed by the microscope (40 and 60 X) and scored the spines number per unit length and branching per cell body. *****, $p < 0.05$ and ******, $p < 0.01$. The p values in panels of D and F were calculated by ANOVA followed by Bonferroni's post hoc tests whereas Student's t-tests were performed in panels **(A,B,H,J)**.

Bdnf genomic regions (**Figure 6A**). We found that Pls diet enhanced expression of all the *Bdnf* isoforms in the mouse hippocampus (**Figure 6B**) and in the primary cultured neurons at DIV 22 treated with Pls (Figure 10C), suggesting a possibility that Pls could enhance CREB recruitments onto those promoter sites. Extensive ChIP assays data showed that Pls diet significantly enhanced CREB recruitments onto the putative binding sites of RE (Responsive elements) 1, 2, 3, 5, 6, 7, 8, and 11 (**Figures 6D–F**). Negative control was performed to amplify the genomic region between the exon10 and 11, which did not show any recruitment of CREB (data not shown). IgG control of the ChIP assays did not show any nonspecific recruitments (**Figure 6E**) onto these recruitment sites. To our knowledge, it is the first report of comprehensive ChIP data that suggests a CREB-mediated regulation of the *Bdnf* isoforms in neuronal cells.

Plasmalogens Are Enriched in the Lipid Rafts and Enhance TrkB Expression in the Rafts to Accelerate BDNF Signaling

It has been known that the receptor for BDNF, TrkB, can be recruited in lipid raft microdomains of the cell membrane to induce BDNF signaling (Suzuki et al., 2004; Assaife-Lopes et al.,

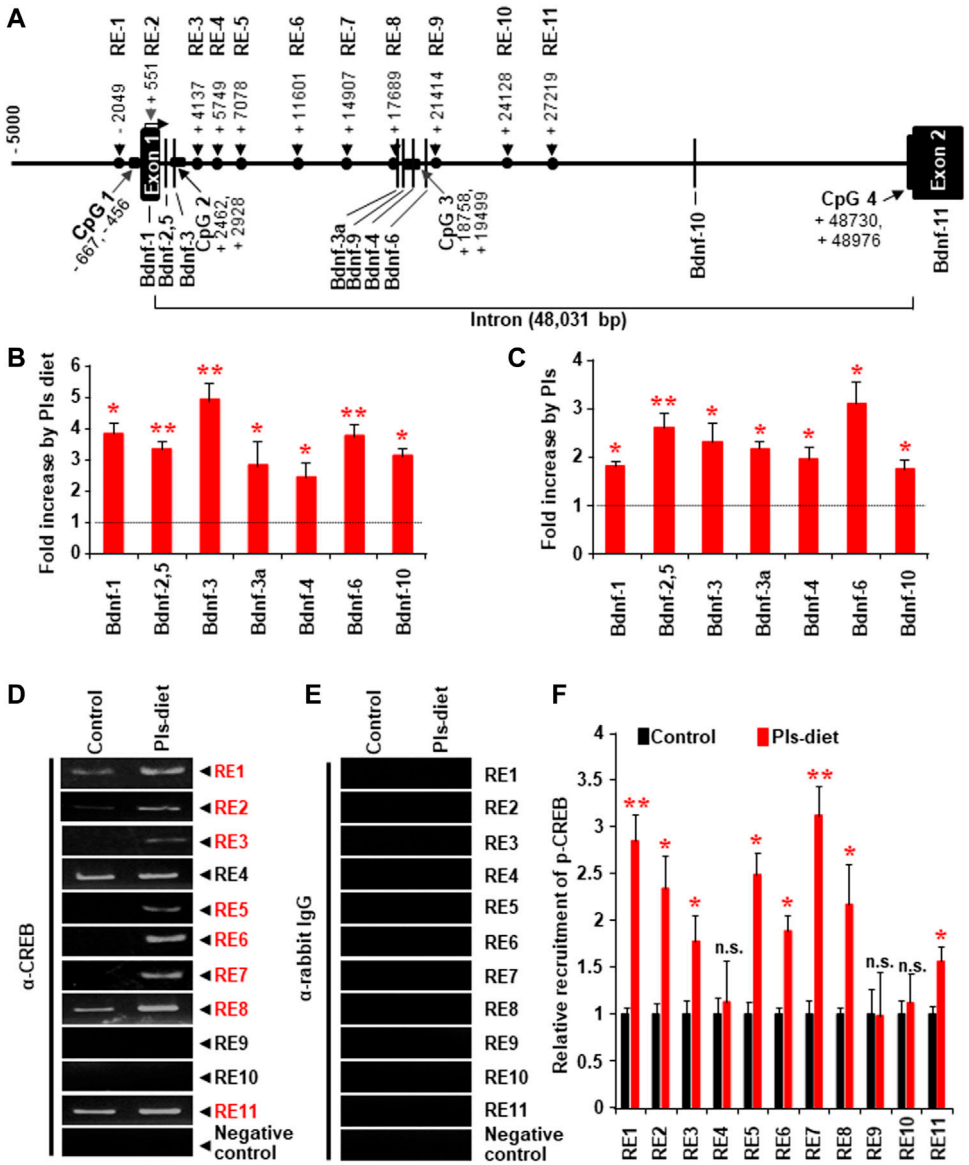

FIGURE 6 | Changes of CREB recruitment onto the Bdnf promoters in the hippocampus tissue by Pls diet. **(A)** The possible CREB recruitment sites (RE indicates responsive element) and the reported promoters onto the mouse *Bdnf* genomic DNA. **(B)** Real-time PCR data show the relative increase in the *Bdnf* transcripts from the different promoters by Pls diet in the mice hippocampus. The values show relative increases compared with the control diet ($n = 5$, in each group). **(C)** Real-time PCR data show the relative increase in *Bdnf* transcripts in primary neuronal cells (at DIV 22) cultured with Pls (5 μg/ml). Pls were added on the DIV3. **(D,E)** ChIP assays show the relative pulldown of the genomic DNA fragments by the phosphorylated CREB antibody **(D)** and the control rabbit IgG **(E)** in the hippocampus of a control diet and Pls diet mice. **(F)** Real-time PCR data following the ChIP assays show the relative recruitment of the p-CREB onto the different responsive elements. In panels, **(B,C,F)** the data represent mean ± S.E.M. ($n = 5$, *****, $p < 0.05$ and ******, $p < 0.01$). The p values were calculated by ANOVA followed by Bonferroni's post hoc tests to compare the multiple groups.

2010). The membrane fraction assays of the mouse hippocampal tissues showed a significant amount of TrkB in the lighter upper fractions (Fraction No. 4, 5, and 6), which were enriched in lipid raft marker protein Flotillin (**Figure 7A**) as well as cholesterol (**Figure 7B**). The LC-MS assays revealed that the lipid raft fractions have more Pls than the non-raft fractions (fraction no. 8, 9, and 10) (**Figure 7C**). We, therefore, suggest that a high content of Pls-Etn in the hippocampal lipid rafts might promote BDNF-TrKB signaling from the lipid rafts. The LC-MS assay also showed that Pls containing monounsaturated fatty acids such as oleic acid and eicosanoic acid, and ω-6 polyunsaturated fatty acids (PUFA) such as arachidonic acid and docosatetraenoic acid were enriched in lipid rafts compared with non-rafts whereas the amount of ω-3 PUFA, docosahexaenoic acid-containing Pls was similar in both the rafts and non-rafts (**Figure 7D**).

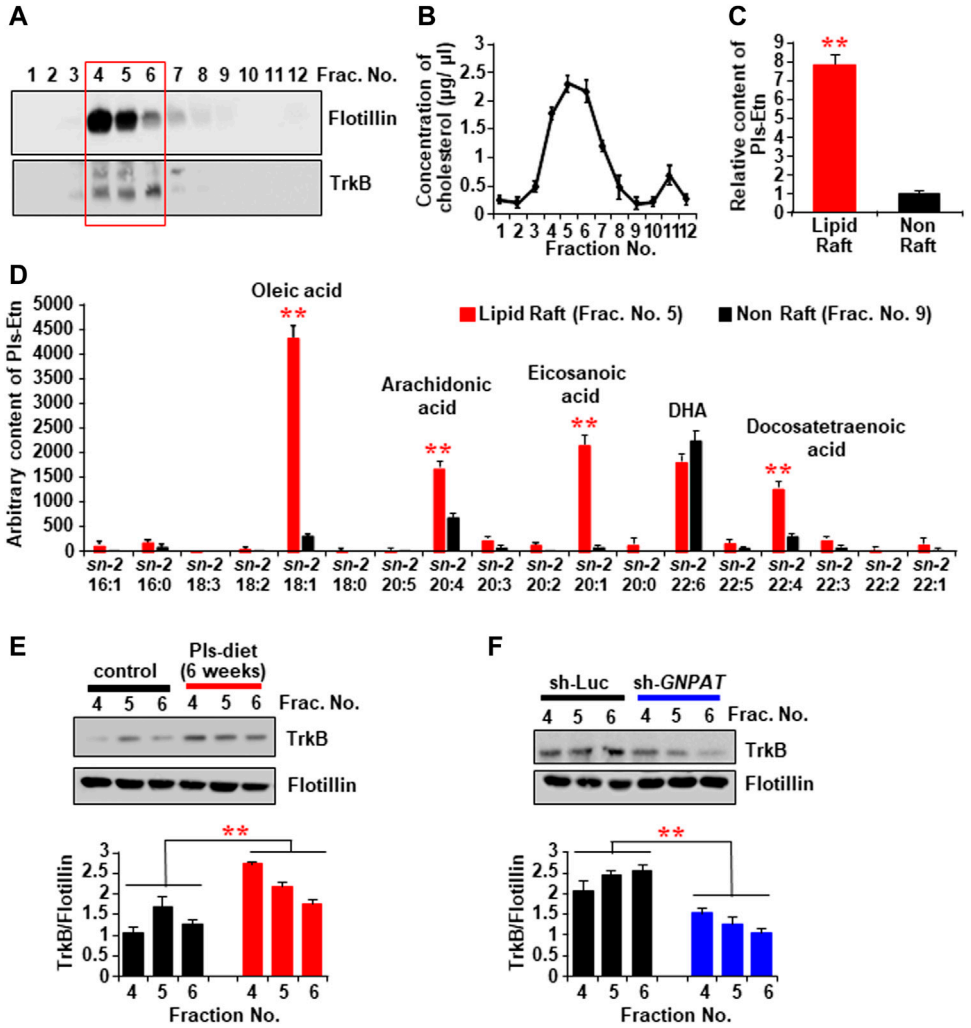

FIGURE 7 | The changes of TrkB recruitment into the lipid rafts of hippocampal tissues by the Pls diet. **(A)** Western blotting data show the expression of TrkB protein in the lipid raft fractions (sucrose gradient fraction no. 4, 5, and 6) of the hippocampus tissue. The Flotillin was used as a lipid raft marker. **(B)** Concentration of cholesterol in the sucrose gradient fractions of the hippocampus tissue. **(C)** LC-MS analysis shows the total Pls content in the rafts and non-raft factions of the hippocampus tissue. **(D)** LC-MS analysis shows the distribution of *sn-2* fatty acid components of Pls in the raft and non-raft fractions. **(E)** Western blotting data show the expression of TrkB in the lipid raft fractions in the control and Pls diet mice hippocampus. **(F)** TrkB contents in the hippocampal lipid raft fractions of control and sh-*GNPAT* group. The data represent mean ± S.E.M. The values were drawn from the three independent experiments with triplicates ($n = 3$). *****, $p < 0.05$ and ******, $p < 0.01$. The *p* values in the panels **(C,D)** were calculated by Student's t-test whereas ANOVA test (followed by Bonferroni's post hoc tests) was performed to get the significance values in the panels **(E,F)**.

We examined the TrkB expression in the lipid rafts of hippocampal tissues in Pls diet mice and found an increase in TrkB proteins in the raft fractions compared with the control-diet mice (**Figure 7E**). We also detected a reduction of TrkB protein in the hippocampus raft fraction in *GNPAT* knockdown mice (**Figure 7F**), suggesting that hippocampal Pls could control TrkB expression level in the lipid raft fractions. These cumulative data, together with the evidence that expression of BDNF itself is dependent on Akt/ERK activation (**Supplementary Figure S2**), suggest that Pls may not only induce BDNF expression through the Akt/ERK activation but also enhance the BDNF actions through the TrkB expression in the lipid rafts.

Plasmalogens-Induced Enhancements of Learning and Memory Are Dependent on the BDNF-TrkB Signaling Pathway

To address whether the Pls-induced enhancements of learning and memory are dependent on BDNF-TrkB signaling in the hippocampus, we injected the lentiviral sh-RNA vectors against either *TrkB* or *Bdnf* bilaterally into the hippocampus 4 weeks after the start of Pls-feeding in mice. The Pls diet was continued for additional 2 weeks following the injection. The water maze test was performed after a total of 6 weeks of Pls diet (**Figure 8A**). Pls diet-mediated improved learning was attenuated in the mice injected with sh-Bdnf and sh-TrkB (**Figure 8B**). In addition,

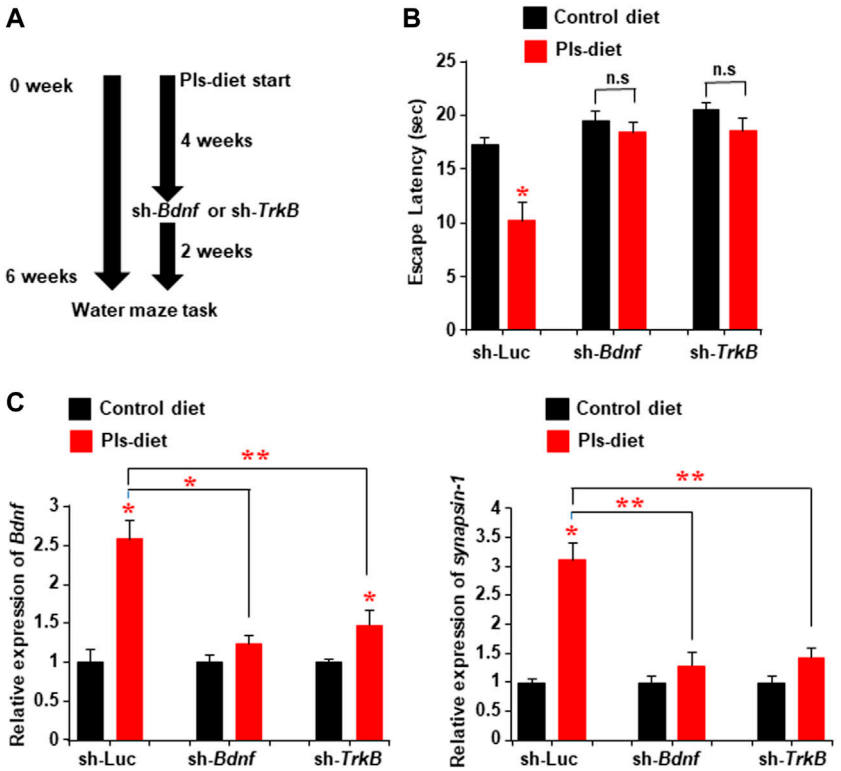

FIGURE 8 | Attenuation of Pls-mediated memory enhancement by knockdown of hippocampal *TrkB* or *Bdnf* expression. **(A)** Mice were subjected to the Pls feeding for 4 weeks followed by the sh-*Bdnf* or sh-*TrkB* injection bilaterally into the hippocampus. The water maze task was performed 6 weeks after Pls feeding. **(B)** Water maze data show the difference in escape latency between the experimental group mice. The data represent the mean values of the swimming time to reach the goal on the fourth-day trails (3 trails per day). **(C)** Real-time PCR data show the expression of *Bdnf* and *synapsin-1* in the hippocampus tissues of the mice. The data represent the mean ± S.E.M. Each experiment included more than five mice. *, $p < 0.05$ and **, $p < 0.01$ (ANOVA followed by Bonferroni's post hoc tests).

the Pls-induced enhancement of *Bdnf* and *synapsin-1* expression was canceled in the *Bdnf* and *TrkB* knockdown mice (**Figure 8C**). These findings suggest that the Pls-induced enhancements of learning and memory are dependent on BDNF-TrkB signaling in the hippocampus.

Effects of the Plasmalogens Derived From Scallop in Learning and Memory

Recent clinical studies showed that scallop-derived Pls (sPls) improved cognition among AD patients (Fujino et al., 2017; Fujino et al., 2018). To screen the effects of sPls, we have performed the learning and memory tests and compared with the effects of the Pls derived from chicken (cPls). We employed a novel object recognition test to check short and long memory (**Figure 9A**). Both the Pls treatments (sPls and cPls) improved the novel object exploration time in the short-term memory training (**Figure 9B**). sPls-treated mice showed an increase of novel object exploration time during the long-term memory training, whereas cPls-treated mice failed to do so (**Figure 9C**). When we examined the discrimination index (DI), we observed the same effect in short-term memory training (**Figure 9D**). In the long-term memory training, the sPls-treated mice showed a significant increase in DI values compared to the control group (**Figure 9E**). These data suggest that scallop-derived Pls which are rich at DHA Pls showed relatively better effects than chicken-derived Pls in the long-term memory performance.

DISCUSSION

The mechanism of progressive memory loss in patients with AD remained largely unknown. It has been shown that patients with AD have reduced Pls-Etn levels in the cortex and hippocampus (Ginsberg et al., 1995; Guan et al., 1999; Han et al., 2001), suggesting a possibility that Pls content in the hippocampus might regulate the memory process in humans. Interestingly, oral intake of Pls has improved cognition among AD patients (Fujino et al., 2017; Fujino et al., 2020). This evidence indicated a possibility that Pls could play a significant role in the memory process of the human brain, especially in the hippocampus. Our recent findings of the mice study clearly showed that the reduction of hippocampal Pls reduced learning and memory associated with the reduction of BDNF-TrkB signaling. To our knowledge, it is the first report indicating the possibility that a reduction of brain Pls could be a risk factor for memory loss in humans. The patients with AD also showed a reduction of BDNF expression in the brain (Peng et al., 2009). Since BDNF plays a

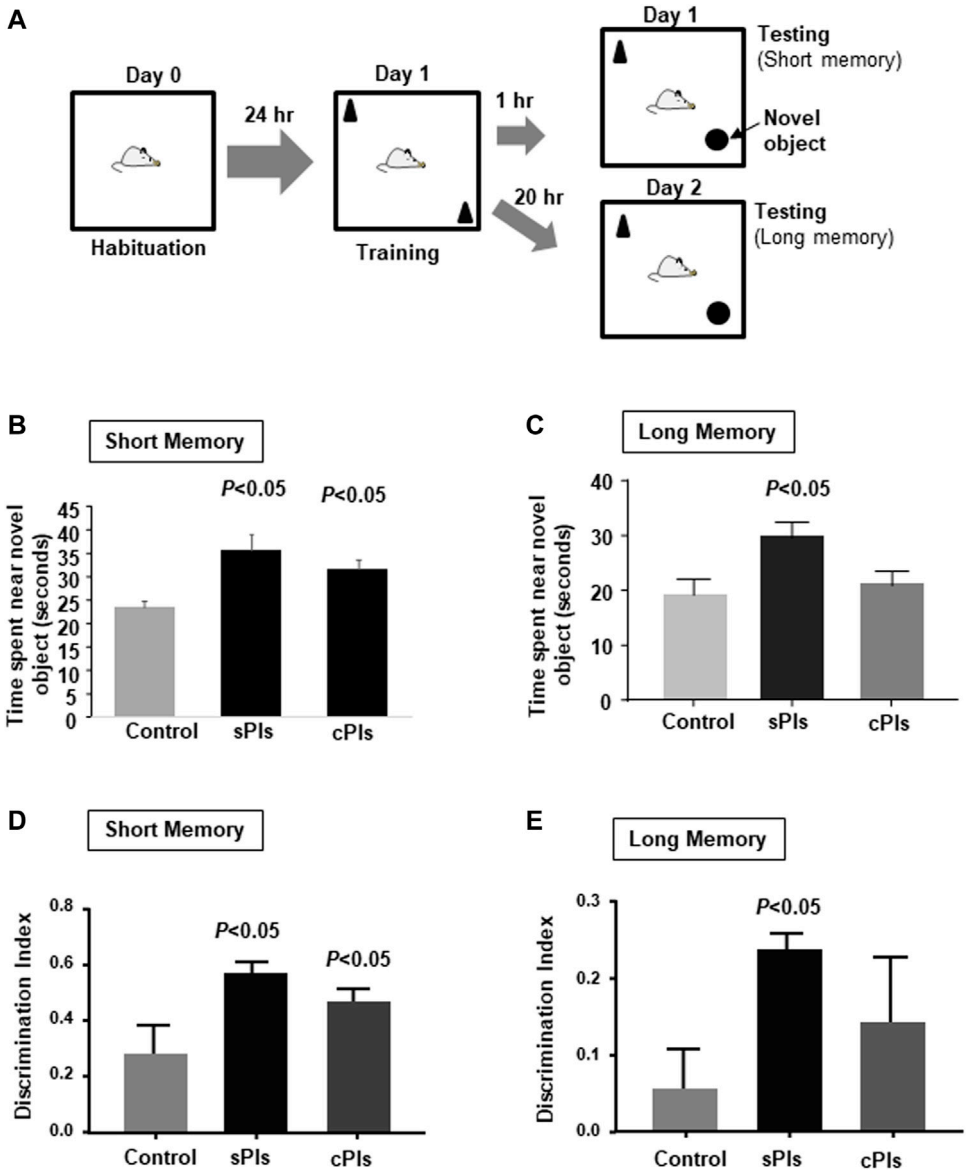

FIGURE 9 | Memory enhancing effects of plasmalogens derived from scallop and chicken. **(A)** Diagram of the novel object recognition test. The mice were subjected to the cPls (Pls from chicken) and sPls (Pls from scallop) drinking (0.01% w/v) for 6 weeks before the tests. **(B)** The data show the time spent near the novel platform when the mice were placed in the chamber after 1 h of the testing phase. **(C)** The data show the average time spent near the novel platform when mice were subjected to the testing phase of 18 h following the training phase. **(D)** The data show the discrimination index in the short-term memory. **(E)** Discrimination index of the long-term memory. Each experimental group contained five mice ($n = 5$). The p values were calculated by ANOVA followed by Bonferroni's post hoc tests to compare the multiple groups.

crucial role in synaptic plasticity and neuronal survival (Peng et al., 2009; Cunha et al., 2010; Lu et al., 2014), we propose that brain Pls can improve hippocampus-dependent learning and memory by regulating the BDNF expression. As with the neuroprotective effects of BDNF, we previously found that Pls inhibited apoptosis of neuronal cells (Hossain et al., 2013). It has been known that BDNF treatments could induce synaptic plasticity as measured by the increase of LTP (Miao et al., 2021). Therefore, we suggest that Pls treatments-mediated increase in BDNF expression in the hippocampus could enhance the synaptic transmission of hippocampal neurons as measured by LTP assays. It was known that BDNF treatments could enhance spine maturation of hippocampal neurons, which is similar to the effects of the Pls treatments, suggesting further that the Pls treatments showed BDNF-like effects. We also noticed that Pls diet-induced learning and memory was inhibited when hippocampal *Bdnf and TrkB* were knockdown, suggesting that Pls could enhance memory by increasing the BDNF signaling n the hippocampus.

The precise mechanism of Pls diet-induced *Bdnf* expression in the hippocampus remained unknown. We observed a slight increase of hippocampal Pls by the Pls diet, suggesting that this increase of Pls content could enhance the *Bdnf* expression in the hippocampus. Activation of Akt is known to be an upstream event of CREB phosphorylation and the transcriptional regulation of *Bdnf* gene (Du and Montminy, 1998). We previously reported that Pls enhanced phosphorylation of Akt and ERK protein in neuronal cells (Hossain et al., 2013). Inconsistent with the previous findings, the Pls treatments have been shown to enhance the expression of p-ERK and p-Akt protein in the hippocampus tissues. In addition, the Inhibition of Akt and ERK attenuated the Pls-induced *Bdnf* expression and reduced the dendritic spine formation, suggesting that Pls-mediated activation of ERK and Akt proteins could play a significant role in the memory process possibly by inducing *Bdnf* expression. In the present study, we cannot claim that the Pls treatment-induced alteration of cellular signaling is a direct effect of Pls because Pls can be degraded in the cells to produce PUFA and lyso-Pls. Further studies will be necessary to address whether the PUFA and lyso-Pls can regulate the cellular signaling in our experimental condition. However, we could suggest that Pls might function as ligands to activate the cellular signaling. It can be supported by the previous findings that membrane-bound GPCRs were critical to induce Pls-mediated cellular signaling in the neuronal cells (Hossain et al., 2016). The previous report showed that CREB was localized at upstream of exon-1 of *Bdnf* gene (Zheng et al., 2012). However, we detected the CREB recruitment in other regions within the *Bdnf* genomic region and found the transcriptional upregulation of various *Bdnf* isoforms. These findings suggested that Pls treatments could induce the expression of the *Bdnf* isoforms by promoting the CREB recruitments onto those promoter regions of *Bdnf*. It has been known that the Bdnf transcription in neuronal cells can be regulated by other transcriptional factors including AP-1 (Tuvikene et al., 2016), In addition to the CREB recruitment, the promoter activity can also be regulated by the epigenetic factor such as histone acetyl transferase (HAT) and it has been known that the *Bdnf* expression was critically controlled by the treatments of HAT inhibitor (SAHA) (Mattson and Meffert, 2006; Guan et al., 2009; Sartor et al., 2019). We have not studied whether Pls treatments could regulate AP-1 and HAT activity and future experiments will be necessary to address this issue. The involvement of *Bdnf* isoform in the learning and memory process is complex and further experiments will be necessary to identify which *Bdnf* isoform is involved in the regulation of memory by the Pls treatments.

It has been shown that Pls are important for the organization of cholesterol-rich lipid raft microdomains in the membrane (Thai et al., 2001; Pike et al., 2002), which is known to participate in cellular signaling (Allen et al., 2007). Pls-deficient mice lacking *GNPAT* showed disruption of these membrane microdomains (Rodemer et al., 2003). Our data showed the localization of Pls in the lipid rafts of mice hippocampus tissue where TrkB was found to be accumulated. Our results, increased TrkB localization by the Pls-diet, could suggest that an association of Pls to the raft could enhance the localization of TrkB because we detected a reduction of TrkB in the Gnpat knockdown hippocampus. The localization of membrane proteins including TrkB in the lipid-raft microdomains is known to enhance Akt and ERK signaling (Suzuki et al., 2004; Cao et al., 2013; Assaife-Lopes et al., 2014). Therefore, it is likely that the Pls could facilitate TrkB-signaling in the lipid rafts to induce *Bdnf* expression. However, the mechanism of how the Pls enhanced TrkB localization in the lipid-raft remained unknown. We have observed that the knockdown of TrkB and Bdnf in the hippocampus resulted in an increase in escape latency, suggesting that the TrkB signaling can regulate the memory which can be supported by the published literature (Yamada and Nabeshima, 2003; Wang et al., 2019).

In the present study, we observed that scallop-derived Pls treatments significantly enhanced the short-term and long-term memory whereas chicken-derived Pls only enhanced the short-term memory. We still do not know why the cPls treatments in contrast to the sPls treatments failed to show a significant effect at long-term memory. It is known that sPls are enriched in DHA-containing Pls which are absent in cPls (Youssef et al., 2019). We previously found that DHA-containing Pls were more effective in inhibiting the microglial activation (Ali et al., 2019; Youssef et al., 2019). The neuroinflammation, characterized by microglial activation in the brain, is a well-known pathological event associated with memory impairment in patients with AD (Heneka et al., 2015). Therefore, we suggest that the presence of DHA-containing Pls in the sPls could have a better effect in reducing neuroinflammation in the brain and improving the long-term memory than the cPls. We still do not know whether the DHA-Pls content in the lipid-raft could be involved in the long-term memory as we also observed enrichment in the non-raft fraction. Further experiments will be necessary to address whether the DHA-Pls content in the sPls is important for long-term memory. Our previous study showed that the reduction of the Pls induced neuroinflammation in the hippocampus (Hossain et al., 2017), suggesting that the deficiency of memory by the Pls knockdown in hippocampus might be due to the neuroinflammation. Although further studies will be necessary to address the mechanism of memory-enhancing effects by sPls and cPls, our findings indicate that there might be a difference in pharmacological function of Pls depending on the source. Though the Pls treatments enhanced cellular signaling to induce *Bdnf* expression and neuronal differentiation (*in vitro* studies) which might explain that a reduction of brain Pls could lead to the loss of memory, our present findings have the limitation in understanding how the oral intake of Pls improved memory (*in vivo* effects) because it remains unknown whether Pls can cross the blood-brain barrier (BBB). It has been known that PUFA can improve cognitive function (Yurko-Mauro et al., 2015; Pifferi et al., 2021), The sn-2 position of Pls can be cleaved by enzymatic reaction in the blood giving rise to PUFA, suggesting a possibility that PUFA derived from the dietary Pls could also improve learning and memory. Although PUFA can cross the BBB, it has been known that PUFA can also alter the intestinal microbial flora and gut hormone secretion

TABLE 1 | The fatty acid composition of the Pls-Etn in the purified Pls from chicken (cPls) and scallop (sPls).

Fatty acid	sPls (% w/w)	cPls (% w/w)
Linoleic acid	0.1	5.1
Oleic acid	2.5	33.1
Eicosapentaenoic acid, EPA	27.8	0.9
Arachidonic acid	24.9	21.9
Docosahexaenoic acid, DHA	37.1	23.8
Other acids	7.6	15.2
Total	100.0	100.0

TABLE 2 | Composition of control and chicken derived Pls (0.01% w/w) containing pellet food.

Component	Control food (%) (AIN-93M, Clea, Japan)	Pls—Containing food (%)
cornstrach	61.1	60.6
Milk casein	14.0	14.0
Sugar	10.0	10.0
cellulose	5.0	5.0
Soybean oil	4.0	4.5 (0.01% Pls)
Mineral mixture	3.5	3.5
Vitamin mixture	1.0	1.0
α-cornstarch	1.0	1.0
Choline bitartrate	0.22	0.22
L-cystine	0.18	0.18
Total	100.0	100.0

including glucagon-like peptide-1 (GLP-1) (Shida et al., 2013; Menni et al., 2017; Parolini, 2019), which could stimulate the vagus nerve to modulate learning and memory (Clark et al., 1999; Hossain et al., 2020). Therefore, PUFA and the dietary Pls might have a significant effect to alter the gut microbial flora and secretion of gut hormones to regulate learning and memory. Further studies will be necessary to address whether the dietary Pls could affect the gut-brain axis to improve learning and memory in mice. However, our present results could suggest that a reduction of brain Pls, which is common in patients with AD, might lead to a reduction in learning and memory.

Our cumulative pieces of evidence suggest that a reduction of hippocampal Pls could be a risk factor for AD. These lines of evidence of Pls-mediated memory improvement in experimental mice and patients with AD (Fujino et al., 2017) suggest that the oral intake of Pls could be a potent therapeutic strategy to improve memory by enhancing the synaptic plasticity in the hippocampus.

MATERIALS AND METHODS

Animal, and Cell Treating Reagents

All the animal experiments were followed by the guidelines provided by the Committee on the Ethics of Animal Experiments, Kyushu University, and carried out by the Guidelines provided by the National Institute of Health in the United States regarding the care and use of animals for experimental procedures. All efforts were made to minimize animals' suffering and the number of animals used for the study.

Male C57BL/6 mice (8 weeks old) were used for *in vivo* study. Primary hippocampal neurons were prepared from the E-18 embryo of mice. After dissection of anesthetized pregnant mice, the meninges of the embryo were removed carefully. The hippocampus was cleared with the surrounding cortex and dissolved in trypsin solution containing phosphate-buffered saline (PBS), bovine serum albumin (BSA), and glucose at 37°C for 15 min. FBS was used to neutralize the trypsin activity. The hippocampus was then dissociated in neurobasal medium (GIBCO) supplemented with B27 (GIBCO) by appropriate pipetting using different pour-sized Pasteur pipettes. The dissociated neurons were then cultured on poly-D-lysine coated glass coverslips (30,000 cells/15 mm coverslip) with the neurobasal medium in a 5% CO_2 humidified incubator. On DIV (Disk *In Vitro*) 3, 90% of the cultured medium was replaced with a B27 free neurobasal medium. Cytosine arabinoside (Ara-C) purchased from Sigma was added to DIV three primary neurons at a concentration of 1 μM to inhibit microglial proliferation. More than 95% pure primary hippocampal pyramidal neuronal cells (on DIV 21) were used as primary neurons (Hossain et al., 2013). To visualize the neuronal cells, we performed Dil (tetramethylindocarbocyanine perchlorate) staining by following the recommended protocol (Invitrogen). PI3K/AKT and MAPK ERK Kinase (MEK) inhibitors named LY294002 (Catalog number #9901) and U0126 (#9903), respectively, were purchased from Cell Signaling Technology (Boston, MA, United States) and human recombinant BDNF from WAKO (Osaka, Japan).

Preparation of Plasmalogens Containing Food and Water

The Pls used in the present study were extracted from chicken and scallop by using a previously reported method (Mawatari et al., 2009) and kindly donated by Central Research Institute, Marudai Food Co. Ltd. (Osaka, Japan) and B&S Corporation Co., Ltd. (Tokyo, Japan). The purified Pls consisted of 96.5% Pls-Etn, 2.5% Pls-Cho, 0.5% sphingomyelin (SM) and 0.5% other phospholipids (Mawatari et al., 2007). The composition of fatty acids of Pls-Etn was analyzed using the high-performance liquid chromatography method (Mawatari et al., 2009) and shown in **Tables 1**, **2**. Pls (0.01%)-containing pellet food was prepared by Clea Japan Inc. (Tokyo, Japan). The composition of control and chicken Pls containing food was shown in **Table 2**. We have used Pls (chicken and scallop derived Pls) dissolved (0.01% w/v) in drinking water for the novel object recognition test.

Preparation of sh-RNA Lentiviruses and *in vivo* Injection Into Mouse Brain

The sh-RNA sequences were cloned into the pLL3.7 lentiviral vector following the protocol provided in the Addgene website (Plasmid No 11795 (Rubinson et al., 2003)). The target sequences were as follows: sh-*GNPAT* (5′-GTCCCAATTAGCATCAGT-3′), sh-*Bdnf* (5′-AGTCCCGGTATCCAAAGG-3′), sh-*TrkB* (5′-

CCTGTACATGATGCTCTC-3′) and sh-Luc (5′-CTTACGCTG AGTACTTCGAG-3′). For the viral constructs, we transfected the Hek-293T cells with the cloned pLL3.7 vectors along with the vectors pMD2. G (Addgene plasmid 12,259), pRSV-Rev (Addgene plasmid 12,253), and pMDLg/pRRE (Addgene plasmid 12,251). The cells supernatant was centrifuged at 24,000 rpm for 3 h at 4°C and the viral pellet was dissolved in PBS (1% BSA). After checking the viral titer in N2A cells, 5×10^5 TDU (transduction units) were injected stereotaxically into the bilateral hippocampus through the 30-gauge stainless steel tube at an injection rate of 0.05 μL/min after making holes on the temporal bone. The stereotaxic coordinates of the hippocampus were A, 1.67 mm posterior to bregma; L, 1.25; and H, 2.0 from the surface of the brain. The wound was sutured and treated with an antibiotic. After the experiments, the injection site was confirmed by immunohistochemistry.

Morris Water Maze Task

Morris water maze task was performed in a black plastic circular pool (diameter, 100 cm; wall height, 45 cm) containing water at 22–23°C. The pool was surrounded by a gray curtain wall, on which 3 rectangular, triangle, and circular drawings brightly illuminated were placed and served as the spatial cues. A circular, transparent plastic platform (diameter, 12 cm) was placed in one quadrant of the pool 2 cm below the surface of the water. After the pre-swimming task performed 1 day before the maze task, mice were released from one of four randomly chosen starting points in the circular pool to search for the hidden escape platform for 60 s. They were allowed to rest for 30 s on the platform after they found it. If mice could not find the platform within 60 s, the experimenter placed the animal on the platform for 10 s. Mice were then placed for 30 min in a waiting cage for the next trial and were dried under a heating lamp. The mice received 4 trials in a day for 4 consecutive days. There were no mice that did not show motivation for swimming (floating behavior). The mice were tracked by an infrared-sensitive camera connected to a maze analysis unit (SMART, Panlab S. L., Barcelona, Spain). A probe test was performed after the end of the maze task, in which the mice were allowed to search for 60 s in the absence of the platform. The duration of cumulative time they spent in the target quadrants was measured in the probe test. In the experiments of Pls diet mice, they received three trials in a day until day 6 (D6).

Novel Object Recognition Test

The novel object recognition test was performed according to the published paper (Lueptow, 2017). Mice were subjected to Pls drinking (cPls and sPls) at the dose of 0.01% w/v for 6 weeks. Before starting the habituation phase, mice were kept in the experimental room for 1 hour to adjust the room condition. For the habituation phase, mice were placed in a chamber (65 cm × 65 cm x 30 cm) and allowed to explore for 10 min. For the training phase, mice were placed in the same chamber containing two similar objects for 5 min while being recorded by camera overhead. To remove the odor left by the previous mice, we cleaned the chambers with 70% alcohol. For the testing of short-term memory, mice were placed in the same box with the novel object for 5 min after 1 hour of the training phase. To check the long-term memory, mice were placed in the chambers after about 18 h of the training phase. The discrimination index was calculated by the formula: (time exploring near the novel object—time exploring the familiar object)/(time exploring the novel object + time exploring the familiar object).

Real-Time PCR Analyses

Mice were deeply anesthetized with pentobarbital (50 mg/kg) and transcardially perfused with sterile PBS. For each animal, the brain was removed and the hippocampus was dissected in a dish filled with ice-cold PBS. The tissue samples were stored at −80°C until PCR analyses. Total RNAs were extracted from tissues using TRIZOL reagents (Life Technologies) following standard protocols. cDNAs were then prepared from the purified total RNAs using ReverTra Ace qPCR RT Kit (Toyobo). All the Real-time qPCR reactions were carried out by SYBR Premix ExTaq (RR420Q, Takara) followed by the real-time quantification using 7,500 Real-Time PCR System (Applied Biosystems). The specific primer sets used for amplifying each mouse gene were as follows: *GNPAT*, forward 5′-GCGCTGTCTCAGACTTCCAT-3′ and reverse 5′-GGAGGACATCCACACCTGTC-3′; *Bdnf*, forward 5′-TGCAGGGGCATAGACAAAAGG-3′ and reverse 5′-CTT ATGAATCGCCAGCCAATTCTC-3′; *synapsin-1*, forward 5′-GGCCTACATGAGGACATCAG-3′ and reverse 5′-ACCACA AGTTCCACGATGAG-3′; *synapsin-2* forward 5′-CAGGTA CTTCGGAATGGCAC-3′ and reverse 5′-CAAATGCATGCT GTCGGAT-3′; *synaptotagmin-1 (SYT-1)*, forward 5′-CACCGT GGGCCTTAATTGC-3′ and reverse 5′-TGTTAATGGCGTTCT TCCCTC-3′; *Ca^{2+}/calmodulin-dependent protein kinase II-α* (*CamKII-α*), forward 5′- ATGCTCCGTCCAAATACCCTCC-3′ and reverse 5′-GCAGTGGTCATTCAAGTTCACAGC-3′; *Homer-1*, forward 5′-CTATATTCTCCGCGCAACCT-3′ and reverse 5′-GCAACTCAACAAGGCAGACA-3′; *PSD-95*, forward 5′-CACCGACTACCCCACAGC-3′ and reverse 5′-ACTGGCATTGCGGAGGTC-3′; and *β-Actin*, forward 5′-CAC TGTGCCCATCTACGA-3′ and reverse 5′-CAGGATTCCATA CCCAAG-3′. To amplify the different isoforms of mouse *Bdnf* genes, we have used the following primers *Bdnf1*, forward 5′-CTG TAGTCGCCAAGGTGGAT-3′ and reverse 5′-AGAAGTTCG GCTTTGCTCAG-3′; *Bdnf2/5*, forward 5′-TGGAAGAAACCG TCTAGAGCA-3′ and reverse 5′-TCTGTCCAAGGTGCTGAA TG-3′; *Bdnf3*, forward 5′-CGATCCTCGATGGATAGTTCTT-3′ and reverse 5′-CTTCCCTTGAGAAGCAGGAG-3′; *Bdnf4*, forward 5′-CTGGGAGGCTTTGATGAGAC-3′ and reverse 5′-CATTGTTGTCACGCTTCTGG-3′; *Bdnf6*, forward 5′-CTC CAGGACAGCCTGTATCC-3′ and reverse 5′-TCCCGGATG AAAGTCAAAAC-3′; and *Bdnf10*, forward 5′-GGAACCACC AGTTTTCTCCA-3′ and reverse 5′-TGTGTGGGTAGATGC CAAAA-3′. The mRNA expression was calculated using delta-delta Ct method and the expressional level of mRNA was normalized with the endogenous expression of mouse *Gapdh* (forward: 5′-CAATGTGTCCGTCGTGGATCT-3′ and reverse: 5′-GTCCTCAGTGTAGCCCAAGATG-3′).

Western Blotting Assays

Western blotting assays were carried out by standard protocols (Hossain et al., 2013) using antibodies against GNPAT (ab75060,

Abcam, Cambridge, MA), CREB (9,197, Cell signaling), p-CREB (9,191, cell signaling), Akt (610,860, BD Biosciences), p-Akt (s-473, 4,060, Cell signaling), ERK (4,695, Cell signaling), p-ERK (4,370, Cell signaling), pro-BDNF (ANT-006, alomone labs), Synapsin-1 (AB1543, Millipore), SYT-1 (AB5600, Millipore), PSD-95 (MAB1598, Millipore), Flotillin (610,820, BD Biosciences), TrkB (610,102, BD Biosciences) and β-Actin (sc-47778, Cell Signaling).

Hippocampal tissues were dissected in the same way as PCR analyses and lysed using the RIPA buffer (1% NP40, 0.5% sodium deoxycholate, and 0.1% SDS dissolved in 1X TBS) mixed with the complete protease inhibitor cocktail tablets (Roche). After 30 min on ice with the lysis buffer, cells were subjected to brief sonication at 4°C followed by centrifugation at 15,000 rpm for 10 min to remove insoluble cell debris. For subcellular fractionation assays, cells were suspended in mild buffer (0.5% NP40, 1 mM EDTA, and 10 mM Tris-HCl) followed by centrifugation at 15,000 rpm and the supernatant (cytoplasmic fraction) was collected. The precipitate was then washed three times by the same mild buffer and dissolved with RIPA buffer to collect the nuclear fraction. Protein concentration was measured by the BCA protein assay kit (Thermo Scientific) and a total of 20 μg protein was loaded for analysis by SDS-PAGE. After the protein transfer, nitrocellulose membranes (BIO-RAD) were blocked with Tris-buffered saline containing 5% Difco Skim Milk (BD) and 0.1% Tween 20 for 1 h at room temperature. Membranes were then incubated at 4°C overnight with the primary antibodies. After treatments with primary antibodies, membranes were washed, and then incubated with horseradish peroxidase-coupled goat anti-mouse or anti-rabbit IgG secondary antibody (Cell Signaling Technology, Boston, MA, United states) at room temperature for 2 h. Specific signals from the transferred protein were then visualized by SuperSignal West Pico Chemiluminescent Substrate (Thermo Scientific) using a LAS4000 biomolecular imager. ImageJ software was used to quantify the signals.

Chromatin Immunoprecipitation (ChIP) Assays

ChIP assays were conducted as the published protocol (Carey et al., 2009). DNA/protein complexes in culturing cells were cross-linked with 4% paraformaldehyde (PFA) for 20 min at 4°C, and those in brain tissues were cross-linked by the transcardial perfusion of 4% PFA (30 ml/mice). Cells and tissues were then lysed in the lysis buffer (5 mM PIPES of pH8.0, 85 mM KCl, and 0.5% Nonidet P-40 dissolved in dH_2O). DNA in the DNA/protein complexes was fragmented to 200–400 bp, which correspond to the size of mono-to di-nucleosomes, by sonication in ice-cold water. We then used 1 mg DNA-protein complexes in dilution buffer (16.7 mM Tris, 167 mM NaCl, 1.2 mM EDTA, 0.01% SDS, and 1.1% Triton X-100) for each experimental group, and treated with the protein A-agarose/salmon sperm DNA (Millipore) for 2 h at 4°C with rotation. After centrifuging at 3,000 rpm for 2 min, supernatants were collected into a new tube and rotated with 500 ng of the primary antibodies (p-CREB, 9,197, Cell Signaling) overnight at 4°C. We then added protein A-agarose/salmon sperm DNA to the supernatant and rotated for 2 h followed by centrifugation at 3,000 rpm for 2 min. The precipitated beads were then washed with high-salt wash buffer (50 mM HEPES, 500 mM NaCl, 1 mM EDTA, 0.1% SDS, 1% Triton X-100, and 0.1% deoxycholate) with rotation for 10 min at room temperature followed by centrifugation at 3,000 rpm for 2 min. This high-salt wash was repeated 8 times followed by 2 times wash with the TE buffer (1mM EDTA and 10 mM Tris). The precipitated chromatins were then re-suspended in elution buffer (50 mM Tris pH8.0, 10 mM EDTA and 1% SDS) followed by treatment with Proteinase-K (20 μg/ml) at 55°C for 2 h. To reverse cross-links, samples were then treated at 65°C overnight followed by centrifugation at 12,000 rpm for 5 min. The supernatant was then collected and subjected to DNA purification by standard phenol: chloroform extraction method. Amplification of CREB binding sites mentioned here as responsive elements (RE) onto the mouse *Bdnf* genomic region was carried out using conventional PCR with rTaq DNA polymerase (R001A, Takara) as well as by the real-time PCR assays using the following primer sets: for RE-1, forward 5′-CCTCCCACGTCATTTTACGA-3′ and reverse 5′-AGCCAGTTTCCTGAGAATGC-3′; for RE-2, forward 5′-CTG AGCAAAGCCGAACTTCT-3′ and reverse 5′-GCTTTGCTG TCCTGGAGACT-3′; for RE-3, forward 5′-TCTGGGCGACAA GGAGAAAA-3′ and reverse 5′-TGGGTGTAAGAGGATGAC GT-3′, for RE-4, forward 5′-GGGGTTGCCTTAAGTGGAGA-3′ and reverse 5′-GAACAGCTCTACATTCCCAACT-3′; for RE-5, forward 5′-CACAGTGACTTGGGTTCAAAGA-3′ and reverse 5′-TGTGCATGGAAACAGAAACTG-3′, for RE-6, forward 5′-GCTGAATTTATTGTACATGCGGT-3′ and reverse 5′-CCC ACACTAACCAGCCTGAT-3′; for RE-7, forward 5′-TTTTCC CCAAAGAAGAGTGAAG-3′ and reverse 5′-TTGGATGAG GTCAATCCTACTATG-3′, for RE-8, forward 5′-TGTCTA TTTCGAGGCAGAGGA-3′ and reverse 5′-CTCCTCGGTGAA TGGGAAAG-3′; for RE-9, forward 5′-CAACGACACAGAACA CACGTT-3′ and reverse 5′-GCACAACAGTCTTGTTTATCT GG-3′, for RE-10, forward 5′-TGTAATAGAAAGTCAGAT AAATGTTTCAA-3′ and reverse 5′-TACTGGGAAGTCTGG GGAAA-3′; and RE-11, forward 5′-CCTCTTGGAAAGCAA CGTGT-3′ and reverse 5′-TGGTGGGAGACTGACATCAA-3′. For the negative control of ChIP assays, we amplified the intron-region right after the exon-10 (Bdnf-10) by the primers forward 5′-TCACCGTATCCGCTGCCT-3′ and reverse 5′-CCAGGT GGTGTCTCAGATAC-3′. The size of the amplified genome by these primer sets was within 100–150 bp.

Immunohistochemical Staining

To prepare the cryosections, mice were perfused transcardially with phosphate-buffered saline (PBS) followed by 4% PFA solution. The brains were then collected in 4% PFA solution, fixed overnight at 4°C followed by treatment with 30% sucrose solution, embedded in optimum cutting temperature (O. C. T.) compound, and frozen in −70°C before making thin sections (30 μm thick). Sections were collected in ice-cold PBS and treated to 3N HCl for 30 min followed by extensive washing with PBS on a shaker. After 1 h treatment with a blocking solution (0.2% TritonX-100 and 5% BSA dissolved in PBS), tissue slices were incubated with the antibodies, dissolved in the same blocking solution, overnight at 4°C on a shaker. Antibodies were diluted as

follows: p-Akt (Cell signaling, 1:500), p-ERK (Cell signaling, 1: 500), and DCX (Abcam, 1:500). After brief washing in PBS, the brain slices were then incubated with fluorochrome-conjugated secondary antibodies (1:1,000 in blocking solution; Alexa Fluor 488/568, Life technologies) for 3 h at room temperature. 4′,6-diamidino-2-phenylindole (DAPI) was used for nuclear staining. The images were analyzed by BZ-9000 Fluorescence Microscope (KEYENCE, Osaka, Japan).

Electrophysiology

The electrophysiology assay of the mice hippocampal slices was performed according to the protocol described in the published paper (Hossain et al., 2018). Under deep anesthesia with isoflurane, mice were sacrificed and the brain was quickly excised. The hippocampal slices (350 μm thick) were made perpendicular to the septotemporal axis and incubated in Krebs-Ringer solution (124 mM NaCl, 4 mM KCl, 1.3 mM MgSO4, 1.23 mM NaH2PO4, 26 mM NaHCO3, 2.4 mM CaCl2, and 10 mM glucose) bubbled with 95% O_2 and 5% CO_2 at 32–34°C with pH 7.4. After 2 h incubation, slices were transferred to a recording chamber, which was perfused with Krebs-Ringer solution at a constant rate of about 2.5 ml/min. Extracellular recording of field excitatory postsynaptic potential (EPSP) was made from the stratum radiatum in the area CA1 by a glass microelectrode filled with Krebs-Ringer solution (tip diameter, 15–25 μm; DC resistance, 3–5 MΩ). Orthodromic stimuli were delivered through a coaxial bipolar electrode (diameter, 0.3 mm) that was placed in the stratum radiatum in the CA3 region to stimulate the Schaffer collateral-CA1 pathway. The test-stimulus intensity of 50 μs square pulses ranged from 0.15 to 0.4 mA to give a field EPSP amplitude of 0.2–0.4 mV at 0.03 Hz. After confirmation of stable amplitude of EPSP at least for 10 min, tetanic stimulation was delivered, and data were collected further for 60 min. To induce LTP, a train of 100 Hz for 1 s was delivered at the same stimulus intensity used for the test stimulus. Responses were acquired, digitized, and stored by a Macintosh computer interfaced with PowerLab (AD instruments, New South Wales, Australia) at 20 kHz for 64 ms, beginning 4 ms before the stimulation. For LTP analysis, the initial slope of the EPSP at each time point was expressed as a percentage of control values (averages before tetanic stimulation).

Golgi Cox Staining

To prepare the Golgi-Cox solution, we first prepared three solutions: solution A (5% potassium dichromate, $K_2Cr_2O_7$, in distilled water), solution B (5% mercuric chloride, Hg_2Cl_2, in dH_2O), and solution C (5% potassium chromate, K_2CrO_4, in dH_2O). 200 ml of each solution A and B were mixed in a glass bottle followed by adding 160 ml of solution C slowly under continuous agitation by glass rods (special precaution was taken to avoid the skin and inhalation contact and all these mixings were done under fume hood chamber). The mixed solution (Golgi-Cox solution) was kept in the dark for 5 days followed by adding the intracardiac saline perfused mice brains. After 14 days in the solution, the brains were kept in 30% sucrose solution overnight followed by freezing at −70°C with the O.C.T. compound (Tissue-Tek). The frozen brain tissues were then cut into 30 μm slices and collected on FRONTIER coated glass slides (FRC-03, Matsunami Glass Ind. Ltd., Osaka, Japan) followed by stock in −70 °C. Before use, the slides were kept in 70% EtOH for 3 min followed by drying at room temperature aimed to improve the tissue adhesion. The slides were then subjected to dH_2O for 1 min followed by 30 min treatments with 10% ammonium hydroxide solution in a dark room. Slides were then washed in dH_2O for 1 min followed by 30min treatments with Kodak Fix Solution (251 ml of Kodak Fix Solution A and 28 ml of Kodak Fix Solution B in 2000ml dH_2O). Slides were washed in dH2O for 1 min followed by the alcohol dehydration process: 30 s in 70% ethanol, 30 s in 80% EtOH, 30 s in 90% ethanol, 30 s in 95% ethanol, and 2 min in 100% ethanol (2 times). Before mounting with the Permafluor (Thermo scientific) the slides were treated with CXA (Chloroform, Xylene, and Alcohol in a ratio of 1:1:1) for 15 min. Photographs were taken by the BZ-9000 Fluorescence Microscope by using the bright field filter.

Lipid Raft Isolation and Cholesterol Assays

Brain tissues were dissolved in the raft buffer composed of 100 mM HEPES, 5 M NaCl, and 50 mM EGTA by passing through 25 G needles 15 times. We then added 1% Brij-58 (P5884, Sigma) and passed through 25 G needles for 15 times followed by keeping the solution in Ice for 30 min. A total of 1 mg protein was then dissolved in sucrose-PBS solution to make 4 ml volume of 40% sucrose mixture followed by adding it in the centrifuge tube (13PET TUBE ASSY, S303276A, Hitachi, Japan) keeping on ice. We then slowly added 4 ml of 25% sucrose-PBS solution followed by adding 4 ml of 5% sucrose-PBS solution to make a total of 12 ml solution in the tube. The centrifuge tubes were then placed in the ultracentrifuge machine (himac CP 65β, Hitachi Centrifuges, Japan) at a speed of 36,000 rpm for 26 h at 4°C. After the centrifuge, 12 fractions of 1ml volume were collected gently from top to the bottom and labeled fractions No. 1–12. A total of 250 μL 59% (w/v) trichloroacetic acid (TCA) solution was added to each 1 ml fraction and mixed vigorously followed by centrifugation at 14,000 rpm for 10 min. The protein precipitates were then washed with acetone 3 times followed by being subjected to the heat block at 95°C until dried up. SDS sample buffer (50 μL) was used to dissolve the protein before performing Western blotting. The cholesterol contents of the lipid raft fractions were analyzed by the total cholesterol assay kit (Cell Biolabs, Inc. Catalog number STA-384) by following the recommended protocol.

Liquid Chromatography-Electronspray Ionization-Tandem Mass Spectrometry (LC-MS) Assays

Extraction of the total lipids was performed by Bligh and Dyer method (Bligh and Dyer, 1959; Abe et al., 2014). Briefly, the cells

and tissues were dissolved in PBS followed by sonication in the ice-cold water. After checking the protein concentration, equal amount (50 μg) of protein was dissolved in methanol/chloroform/water (v/v/v: 2:1:0.8) and 50 pmol internal standard (1-heptadecanoylsn-glycero-3-phosphocholine, 1, 2-didodecanoyl-sn-glycero-3-phosphocholine and 1, 2-didodecanoyl-sn-glycero-3-phosphoethanolamine). After 5 min, 1 ml each of water and chloroform was added and the whole centrifuged to collect the lower organic phase. 1 ml chloroform was added again to re-extract the lipids. Collected organic phase was then evaporated under the nitrogen stream and suspended in pure methanol. LC-MS assay was performed using a 4000 Q-TRAP quadrupole linear ion trap hybrid mass Q8 spectrometer (AB Sciex) with ACQUITY UPLC System (Waters). Samples were injected into an ACQUIRY UPLC BEH C18 column and then directly subjected to ESI-MS/MS analysis. A 10 μL aliquot of each sample was directly introduced by autosampler injector and the samples were separated by step gradient elution with mobile phase A (acetonitrile:methanol:water at 2:2:1 (v/v/v), 0.1% formic acid and 0.028% ammonium) and mobile phase B (isopropanol, 0.1% formic acid and 0.028% ammonium) at the ratios: 100:0 (for 0–5 min), 95:5 (5–20 min), 70:30 (20–21 min), 50:50 (21–45 min), 50:50 (45–100 min) and 100:0 (100–120 min). The flow rate (70 μL/min at 30°C), source temperature (200°C), declustering potential (60), and collision cell exit potential (15) was kept constant. Ethanolamine Pls (PlsEtns) with alkenyl p16:0, p18:0, and p18:1 at the sn-1 position was detected by precursor ion scan of m/z 364, m/z 392, and m/z 390, respectively, at positive ion mode. The data were analyzed and quantified using the Analyst software (AB Sciex).

Statistical Analyses

All data were expressed as mean ± S.E.M (standard error of mean). To analyze the statistical significance among experimental groups, we performed one-way ANOVA followed by a post hoc test (Bonferroni's test). Student's t-tests were performed to find the significance values in the case of two experimental groups. p values less than 0.05 were considered significant.

DATA AVAILABILITY STATEMENT

The original contributions presented in the study are included in the article/**Supplementary Material**, further inquiries can be directed to the corresponding author.

ETHICS STATEMENT

The animal study was reviewed and approved by the Graduate School of Medical Sciences, Kyushu University.

AUTHOR CONTRIBUTIONS

MH and SM performed experiments. MH and TF supervised experiments. MH and TF wrote the paper. MH, TF and SM edited the paper.

FUNDING

This work was supported by JSPS KAKENHI Grant Number 26460320 to T. Katafuchi and JSPS Grant-in-Aid for Young Scientists (Wakate B) (16K19007) to MH.

ACKNOWLEDGMENTS

We thank Yukio Fujiki's research team (Kyushu University, Japan) for LC-MS analysis and the technical assistance of the Research Support Center, Graduate School of Medical Sciences, Kyushu University. We are grateful to Chizuko Kanemaru for her support in preparing the manuscript.

SUPPLEMENTARY MATERIAL

The Supplementary Material for this article can be found online at: https://www.frontiersin.org/articles/10.3389/fcell.2022.828282/full#supplementary-material

REFERENCES

Abe, Y., Honsho, M., Nakanishi, H., Taguchi, R., and Fujiki, Y. (2014). Very-long-chain Polyunsaturated Fatty Acids Accumulate in Phosphatidylcholine of Fibroblasts from Patients with Zellweger Syndrome and Acyl-CoA Oxidase1 Deficiency. *Biochim. Biophys. Acta (Bba) - Mol. Cel Biol. Lipids* 1841 (4), 610–619. doi:10.1016/j.bbalip.2014.01.001

Ali, F., Hossain, M. S., Sejimo, S., and Akashi, K. (2019). Plasmalogens Inhibit Endocytosis of Toll-like Receptor 4 to Attenuate the Inflammatory Signal in Microglial Cells. *Mol. Neurobiol.* 56 (5), 3404–3419. doi:10.1007/s12035-018-1307-2

Allen, J. A., Halverson-Tamboli, R. A., and Rasenick, M. M. (2007). Lipid Raft Microdomains and Neurotransmitter Signalling. *Nat. Rev. Neurosci.* 8 (2), 128–140. doi:10.1038/nrn2059

Arroyo, D. S., Gaviglio, E. A., Peralta Ramos, J. M., Bussi, C., Avalos, M. P., Cancela, L. M., et al. (2018). Phosphatidyl-Inositol-3 Kinase Inhibitors Regulate Peptidoglycan-Induced Myeloid Leukocyte Recruitment, Inflammation, and Neurotoxicity in Mouse Brain. *Front. Immunol.* 9, 770. doi:10.3389/fimmu.2018.00770

Assaife-Lopes, N., Sousa, V. C., Pereira, D. B., Ribeiro, J. A., Chao, M. V., and Sebastiao, A. M. (2010). Activation of Adenosine A2A Receptors Induces TrkB Translocation and Increases BDNF-Mediated Phospho-TrkB Localization in Lipid Rafts: Implications for Neuromodulation. *J. Neurosci.* 30 (25), 8468–8480. doi:10.1523/JNEUROSCI.5695-09.2010

Assaife-Lopes, N., Sousa, V. C., Pereira, D. B., Ribeiro, J. A., and Sebastião, A. M. (2014). Regulation of TrkB Receptor Translocation to Lipid Rafts by Adenosine A2A Receptors and its Functional Implications for BDNF-Induced Regulation of Synaptic Plasticity. *Purinergic Signal.* 10 (2), 251–267. doi:10.1007/s11302-013-9389-910.1007/s11302-013-9383-2

Binder, D. K., and Scharfman, H. E. (2004). Brain-Derived Neurotrophic Factor. *Growth Factors* 22 (3), 123–131. doi:10.1080/08977190410001723308

Bligh, E. G., and Dyer, W. J. (1959). A Rapid Method of Total Lipid Extraction and Purification. *Can. J. Biochem. Physiol.* 37 (8), 911–917. doi:10.1139/o59-099

Braverman, N. E., and Moser, A. B. (2012). Functions of Plasmalogen Lipids in Health and Disease. *Biochim. Biophys. Acta (Bba) - Mol. Basis Dis.* 1822 (9), 1442–1452. doi:10.1016/j.bbadis.2012.05.008

Cao, C., Rioult-Pedotti, M. S., Migani, P., Yu, C. J., Tiwari, R., Parang, K., et al. (2013). Impairment of TrkB-PSD-95 Signaling in Angelman Syndrome. *Plos Biol.* 11 (2), e1001478. doi:10.1371/journal.pbio.1001478

Carey, M. F., Peterson, C. L., and Smale, S. T. (2009). Chromatin Immunoprecipitation (ChIP). *Cold Spring Harb Protoc.* 2009 (9), pdb.prot5279. doi:10.1101/pdb.prot5279

Clark, K. B., Naritoku, D. K., Smith, D. C., Browning, R. A., and Jensen, R. A. (1999). Enhanced Recognition Memory Following Vagus Nerve Stimulation in Human Subjects. *Nat. Neurosci.* 2 (1), 94–98. doi:10.1038/4600

Cunha, C., Brambilla, R., and Thomas, K. L. (2010). A Simple Role for BDNF in Learning and Memory? *Front. Mol. Neurosci.* 3, 1. doi:10.3389/neuro.02.001.2010

da Silva, T. F., Eira, J., Lopes, A. T., Malheiro, A. R., Sousa, V., Luoma, A., et al. (2014). Peripheral Nervous System Plasmalogens Regulate Schwann Cell Differentiation and Myelination. *J. Clin. Invest.* 124 (6), 2560–2570. doi:10.1172/JCI72063

Du, K., and Montminy, M. (1998). CREB Is a Regulatory Target for the Protein Kinase Akt/PKB. *J. Biol. Chem.* 273 (49), 32377–32379. doi:10.1074/jbc.273.49.32377

Fujino, T., Yamada, T., Asada, T., Ichimaru, M., Tsuboi, Y., Wakana, C., et al. (2018). Effects of Plasmalogen on Patients with Mild Cognitive Impairment: A Randomized, Placebo-Controlled Trial in Japan. *J. Alzheimer's Dis. Parkinsonism* 8 (419), 1–5. doi:10.4172/2161-0460.1000419

Fujino, T., Hossain, M. S., and Mawatari, S. (2020). Therapeutic Efficacy of Plasmalogens for Alzheimer's Disease, Mild Cognitive Impairment, and Parkinson's Disease in Conjunction with a New Hypothesis for the Etiology of Alzheimer's Disease. *Adv. Exp. Med. Biol.* 1299, 195–212. doi:10.1007/978-3-030-60204-8_14

Fujino, T., Yamada, T., Asada, T., Tsuboi, Y., Wakana, C., Mawatari, S., et al. (2017). Efficacy and Blood Plasmalogen Changes by Oral Administration of Plasmalogen in Patients with Mild Alzheimer's Disease and Mild Cognitive Impairment: A Multicenter, Randomized, Double-Blind, Placebo-Controlled Trial. *EBioMedicine* 17, 199–205. doi:10.1016/j.ebiom.2017.02.012

Ginsberg, L., Rafique, S., Xuereb, J. H., Rapoport, S. I., and Gershfeld, N. L. (1995). Disease and Anatomic Specificity of Ethanolamine Plasmalogen Deficiency in Alzheimer's Disease Brain. *Brain Res.* 698 (1-2), 223–226. doi:10.1016/0006-8993(95)00931-f

Guan, J.-S., Haggarty, S. J., Giacometti, E., Dannenberg, J.-H., Joseph, N., Gao, J., et al. (2009). HDAC2 Negatively Regulates Memory Formation and Synaptic Plasticity. *Nature* 459 (7243), 55–60. doi:10.1038/nature07925

Guan, Z., Wang, Y., Cairns, N. J., Lantos, P. L., Dallner, G., and Sindelar, P. J. (1999). Decrease and Structural Modifications of Phosphatidylethanolamine Plasmalogen in the Brain with Alzheimer Disease. *J. Neuropathol. Exp. Neurol.* 58 (7), 740–747. doi:10.1097/00005072-199907000-00008

Han, X., Holtzman, D. M., and McKeel, D. W., Jr (2001). Plasmalogen Deficiency in Early Alzheimer's Disease Subjects and in Animal Models: Molecular Characterization Using Electrospray Ionization Mass Spectrometry. *J. Neurochem.* 77 (4), 1168–1180. doi:10.1046/j.1471-4159.2001.00332.x

Heneka, M. T., Carson, M. J., Khoury, J. E., Landreth, G. E., Brosseron, F., Feinstein, D. L., et al. (2015). Neuroinflammation in Alzheimer's Disease. *Lancet Neurol.* 14 (4), 388–405. doi:10.1016/S1474-4422(15)70016-5

Hossain, M. S., Abe, Y., Ali, F., Youssef, M., Honsho, M., Fujiki, Y., et al. (2017). Reduction of Ether-type Glycerophospholipids, Plasmalogens, by NF-Kb Signal Leading to Microglial Activation. *J. Neurosci.* 37 (15), 4074–4092. doi:10.1523/jneurosci.3941-15.2017

Hossain, M. S., Ifuku, M., Take, S., Kawamura, J., Miake, K., and Katafuchi, T. (2013). Plasmalogens rescue Neuronal Cell Death through an Activation of AKT and ERK Survival Signaling. *PloS one* 8 (12), e83508. doi:10.1371/journal.pone.0083508

Hossain, M. S., Mineno, K., and Katafuchi, T. (2016). Neuronal Orphan G-Protein Coupled Receptor Proteins Mediate Plasmalogens-Induced Activation of ERK and Akt Signaling. *PloS one* 11 (3), e0150846. doi:10.1371/journal.pone.0150846

Hossain, M. S., Oomura, Y., Fujino, T., and Akashi, K. (2020). Glucose Signaling in the Brain and Periphery to Memory. *Neurosci. Biobehavioral Rev.* 110, 100–113. doi:10.1016/j.neubiorev.2019.03.018

Hossain, M. S., Oomura, Y., and Katafuchi, T. (2018). Glucose Can Epigenetically Alter the Gene Expression of Neurotrophic Factors in the Murine Brain Cells. *Mol. Neurobiol.* 55 (4), 3408–3425. doi:10.1007/s12035-017-0578-3

Itzkovitz, B., Jiralerspong, S., Nimmo, G., Loscalzo, M., Horovitz, D. D. G., Snowden, A., et al. (2012). Functional Characterization of Novel Mutations in GNPAT and AGPS, Causing Rhizomelic Chondrodysplasia Punctata (RCDP) Types 2 and 3. *Hum. Mutat.* 33 (1), 189–197. doi:10.1002/humu.21623

Liegel, R. P., Ronchetti, A., and Sidjanin, D. J. (2014). Alkylglycerone Phosphate Synthase (AGPS) Deficient Mice: Models for Rhizomelic Chondrodysplasia Punctata Type 3 (RCDP3) Malformation Syndrome. *Mol. Genet. Metab. Rep.* 1, 299–311. doi:10.1016/j.ymgmr.2014.06.003

Lu, B., Nagappan, G., and Lu, Y. (2014). BDNF and Synaptic Plasticity, Cognitive Function, and Dysfunction. *Handbook Exp. Pharmacol.* 220, 223–250. doi:10.1007/978-3-642-45106-5_9

Lueptow, L. M. (2017). Novel Object Recognition Test for the Investigation of Learning and Memory in Mice. *JoVE*. doi:10.3791/55718

Mattson, M. P., and Meffert, M. K. (2006). Roles for NF-Kb in Nerve Cell Survival, Plasticity, and Disease. *Cell Death Differ* 13 (5), 852–860. doi:10.1038/sj.cdd.4401837

Mawatari, S., Okuma, Y., and Fujino, T. (2007). Separation of Intact Plasmalogens and All Other Phospholipids by a Single Run of High-Performance Liquid Chromatography. *Anal. Biochem.* 370 (1), 54–59. doi:10.1016/j.ab.2007.05.020

Mawatari, S., Yunoki, K., Sugiyama, M., and Fujino, T. (2009). Simultaneous Preparation of Purified Plasmalogens and Sphingomyelin in Human Erythrocytes with Phospholipase A1fromAspergillus Orizae. *Biosci. Biotechnol. Biochem.* 73 (12), 2621–2625. doi:10.1271/bbb.90455

Menni, C., Zierer, J., Pallister, T., Jackson, M. A., Long, T., Mohney, R. P., et al. (2017). Omega-3 Fatty Acids Correlate with Gut Microbiome Diversity and Production of N-Carbamylglutamate in Middle Aged and Elderly Women. *Sci. Rep.* 7 (1), 11079. doi:10.1038/s41598-017-10382-2

Miao, H.-H., Miao, Z., Pan, J.-G., Li, X.-H., and Zhuo, M. (2021). Brain-derived Neurotrophic Factor Produced Long-Term Synaptic Enhancement in the Anterior Cingulate Cortex of Adult Mice. *Mol. Brain* 14 (1), 140. doi:10.1186/s13041-021-00853-z

Nagan, N., and Zoeller, R. A. (2001). Plasmalogens: Biosynthesis and Functions. *Prog. Lipid Res.* 40 (3), 199–229. doi:10.1016/s0163-7827(01)00003-0

Parolini, C. (2019). Effects of Fish N-3 PUFAs on Intestinal Microbiota and Immune System. *Mar. Drugs* 17 (6), 374. doi:10.3390/md17060374

Peng, S., Garzon, D. J., Marchese, M., Klein, W., Ginsberg, S. D., Francis, B. M., et al. (2009). Decreased Brain-Derived Neurotrophic Factor Depends on Amyloid Aggregation State in Transgenic Mouse Models of Alzheimer's Disease. *J. Neurosci.* 29 (29), 9321–9329. doi:10.1523/JNEUROSCI.4736-08

Pifferi, F., Laurent, B., and Plourde, M. (2021). Lipid Transport and Metabolism at the Blood-Brain Interface: Implications in Health and Disease. *Front. Physiol.* 12, 645646. doi:10.3389/fphys.2021.645646

Pike, L. J., Han, X., Chung, K.-N., and Gross, R. W. (2002). Lipid Rafts Are Enriched in Arachidonic Acid and Plasmenylethanolamine and Their Composition Is Independent of Caveolin-1 Expression: a Quantitative Electrospray Ionization/mass Spectrometric Analysis. *Biochemistry* 41 (6), 2075–2088. doi:10.1021/bi0156557

Rodemer, C., Thai, T.-P., Brugger, B., Kaercher, T., Werner, H., Nave, K.-A., et al. (2003). Inactivation of Ether Lipid Biosynthesis Causes Male Infertility, Defects in Eye Development and Optic Nerve Hypoplasia in Mice. *Hum. Mol. Genet.* 12 (15), 1881–1895. doi:10.1093/hmg/ddg191

Rubinson, D. A., Dillon, C. P., Kwiatkowski, A. V., Sievers, C., Yang, L., Kopinja, J., et al. (2003). A Lentivirus-Based System to Functionally Silence Genes in Primary Mammalian Cells, Stem Cells and Transgenic Mice by RNA Interference. *Nat. Genet.* 33 (3), 401–406. doi:10.1038/ng1117

Sartor, G. C., Malvezzi, A. M., Kumar, A., Andrade, N. S., Wiedner, H. J., Vilca, S. J., et al. (2019). Enhancement of BDNF Expression and Memory by HDAC Inhibition Requires BET Bromodomain Reader Proteins. *J. Neurosci.* 39 (4), 612–626. doi:10.1523/JNEUROSCI.1604-18.2018

Shida, T., Kamei, N., Takeda-Morishita, M., Isowa, K., and Takayama, K. (2013). Colonic Delivery of Docosahexaenoic Acid Improves Impaired Glucose Tolerance via GLP-1 Secretion and Suppresses Pancreatic Islet Hyperplasia in Diabetic KK-Ay Mice. *Int. J. pharmaceutics* 450 (1-2), 63–69. doi:10.1016/j.ijpharm.2013.04.029

Suzuki, S., Numakawa, T., Shimazu, K., Koshimizu, H., Hara, T., Hatanaka, H., et al. (2004). BDNF-induced Recruitment of TrkB Receptor into Neuronal Lipid Rafts: Roles In Synaptic Modulation. *J. Cel Biol* 167 (6), 1205–1215. doi:10.1083/jcb.200404106

Thai, T.-P., Rodemer, C., Jauch, A., Hunziker, A., Moser, A., Gorgas, K., et al. (2001). Impaired Membrane Traffic in Defective Ether Lipid Biosynthesis. *Hum. Mol. Genet.* 10 (2), 127–136. doi:10.1093/hmg/10.2.127

Tuvikene, J., Pruunsild, P., Orav, E., Esvald, E.-E., and Timmusk, T. (2016). AP-1 Transcription Factors Mediate BDNF-Positive Feedback Loop in Cortical Neurons. *J. Neurosci.* 36 (4), 1290–1305. doi:10.1523/jneurosci.3360-15.2016

Wang, J.-Z., Long, C., Li, K.-Y., Xu, H.-T., Yuan, L.-L., and Wu, G.-Y. (2018). Potent Block of Potassium Channels by MEK Inhibitor U0126 in Primary Cultures and Brain Slices. *Sci. Rep.* 8 (1), 8808. doi:10.1038/s41598-018-27235-1

Wang, Z.-H., Xiang, J., Liu, X., Yu, S. P., Manfredsson, F. P., Sandoval, I. M., et al. (2019). Deficiency in BDNF/TrkB Neurotrophic Activity Stimulates δ-Secretase by Upregulating C/EBPβ in Alzheimer's Disease. *Cel Rep.* 28 (3), 655–669. doi:10.1016/j.celrep.2019.06.054

Wood, P. L., Mankidy, R., Ritchie, S., Heath, D., Wood, J. A., Flax, J., et al. (2010). Circulating Plasmalogen Levels and Alzheimer Disease Assessment Scale-Cognitive Scores in Alzheimer Patients. *jpn* 35 (1), 59–62. doi:10.1503/jpn.090059

Yamada, K., and Nabeshima, T. (2003). Brain-derived Neurotrophic factor/TrkB Signaling in Memory Processes. *J. Pharmacol. Sci.* 91 (4), 267–270. doi:10.1254/jphs.91.267

Youssef, M., Ibrahim, A., Akashi, K., and Hossain, M. S. (2019). PUFA-plasmalogens Attenuate the LPS-Induced Nitric Oxide Production by Inhibiting the NF-kB, P38 MAPK and JNK Pathways in Microglial Cells. *Neuroscience* 397, 18–30. doi:10.1016/j.neuroscience.2018.11.030

Yurko-Mauro, K., Alexander, D. D., and Van Elswyk, M. E. (2015). Docosahexaenoic Acid and Adult Memory: a Systematic Review and Meta-Analysis. *PloS one* 10 (3), e0120391. doi:10.1371/journal.pone.0120391

Zheng, F., Zhou, X., Moon, C., and Wang, H. (2012). Regulation of Brain-Derived Neurotrophic Factor Expression in Neurons. *Int. J. Physiol. Pathophysiol Pharmacol.* 4 (4), 188–200. doi:10.1038/tp.2015.114

Conflict of Interest: The authors declare that the research was conducted in the absence of any commercial or financial relationships that could be construed as a potential conflict of interest.

Publisher's Note: All claims expressed in this article are solely those of the authors and do not necessarily represent those of their affiliated organizations, or those of the publisher, the editors and the reviewers. Any product that may be evaluated in this article, or claim that may be made by its manufacturer, is not guaranteed or endorsed by the publisher.

frontiers in Molecular Biosciences

ORIGINAL RESEARCH
published: 23 February 2022
doi: 10.3389/fmolb.2022.815320

Plasmalogens Eliminate Aging-Associated Synaptic Defects and Microglia-Mediated Neuroinflammation in Mice

*Jinxin Gu[1], Lixue Chen[1], Ran Sun[1], Jie-Li Wang[2], Juntao Wang[1], Yingjun Lin[1], Shuwen Lei[1], Yang Zhang[1], Dan Lv[1], Faqin Jiang[1], Yuru Deng[2], James P. Collman[3] and Lei Fu[1,4]**

[1]School of Pharmacy, Shanghai Jiao Tong University, Shanghai, China, [2]Wenzhou Institute, University of Chinese Academy of Sciences, Wenzhou, China, [3]Department of Chemistry, Stanford University, Stanford, CA, United States, [4]Academy of Pharmacy, Xi'an Jiaotong-Liverpool University, Suzhou, China

Neurodegeneration is a pathological condition in which nervous system or neuron losses its structure, function, or both leading to progressive neural degeneration. Growing evidence strongly suggests that reduction of plasmalogens (Pls), one of the key brain lipids, might be associated with multiple neurodegenerative diseases, including Alzheimer's disease (AD). Plasmalogens are abundant members of ether-phospholipids. Approximately 1 in 5 phospholipids are plasmalogens in human tissue where they are particularly enriched in brain, heart and immune cells. In this study, we employed a scheme of 2-months Pls intragastric administration to aged female C57BL/6J mice, starting at the age of 16 months old. Noticeably, the aged Pls-fed mice exhibited a better cognitive performance, thicker and glossier body hair in appearance than that of aged control mice. The transmission electron microscopic (TEM) data showed that 2-months Pls supplementations surprisingly alleviate age-associated hippocampal synaptic loss and also promote synaptogenesis and synaptic vesicles formation in aged murine brain. Further RNA-sequencing, immunoblotting and immunofluorescence analyses confirmed that plasmalogens remarkably enhanced both the synaptic plasticity and neurogenesis in aged murine hippocampus. In addition, we have demonstrated that Pls treatment inhibited the age-related microglia activation and attenuated the neuroinflammation in the murine brain. These findings suggest for the first time that Pls administration might be a potential intervention strategy for halting neurodegeneration and promoting neuroregeneration.

Keywords: aging, plasmalogen, synaptogenesis, neurogenesis, microglia, neuroinflammation

OPEN ACCESS

Edited by:
Masanori Honsho,
Kyushu University, Japan

Reviewed by:
Pedro Brites,
Universidade do Porto, Portugal
Richard M. Epand,
McMaster University, Canada

****Correspondence:***
Lei Fu
leifu@sjtu.edu.cn

Specialty section:
This article was submitted to Cellular Biochemistry, a section of the journal Frontiers in Molecular Biosciences

Received: *15 November 2021*
Accepted: *02 February 2022*
Published: *23 February 2022*

Citation:
Gu J, Chen L, Sun R, Wang J-L, Wang J, Lin Y, Lei S, Zhang Y, Lv D, Jiang F, Deng Y, Collman JP and Fu L (2022) Plasmalogens Eliminate Aging-Associated Synaptic Defects and Microglia-Mediated Neuroinflammation in Mice. Front. Mol. Biosci. 9:815320. doi: 10.3389/fmolb.2022.815320

1 INTRODUCTION

Plasmalogens (Pls) are a special type of vinyl ether-bonded phospholipids actively participating in structure and function of biological membranes. Approximately 20% of phospholipids are plasmalogens in human tissue, where they are particularly rich in the brain, heart, and immune cells (Lessig and Fuchs 2009; Braverman and Moser 2012). In brain, ethanolamine plasmalogens (PlsEtns) constitute approximately 60 and 80% of the total ethanolamine phospholipids in gray and white matter, respectively (Macala et al., 1983). Pls are also concentrated in specialized membranes,

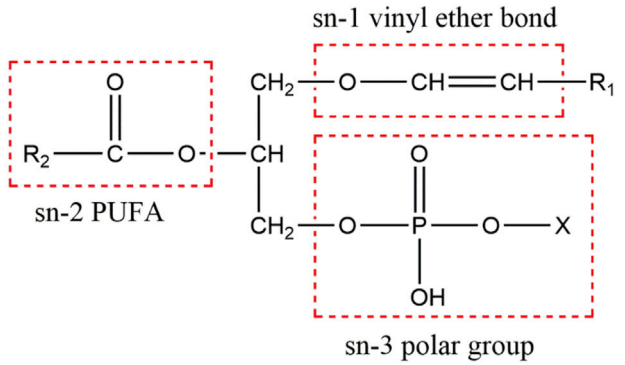

FIGURE 1 | The chemical structure of plasmalogens. Plasmalogen is characterized by a vinyl ether linkage with 16:0, 18:0, and 18:1 hydrocarbon chains at sn-1 position, an ester bond linking PUFAs at sn-2 position, and a phosphate group at sn-3 position (X denotes ethanolamine or choline) of the glycerol backbone.

such as sarcolemma, myelin, and synaptic vesicles (Post et al., 1988; Takamori et al., 2006; Poitelon et al., 2020). Reduced levels of PlsEtns have been found to be associated with aging (Pradas et al., 2019) and several neurodegenerative diseases, including Alzheimer's disease (AD) (Guan et al., 1999; Han et al., 2001; Goodenowe et al., 2007; Wood 2010; Wood et al., 2015; Yamashita et al., 2016b), Parkinson's disease (PD) (Dragonas et al., 2009; Fabelo et al., 2011; Xicoy et al., 2019), Niemann-Pick type C disease (Schedin and Pavel 1997), multiple sclerosis (MS) (Ferreira et al., 2021) and Zellweger syndrome (Heymans et al., 1983).

Plasmalogens are one of the key determinants in membrane dynamics and trafficking (Glaser and Gross 1994; Rog and Koivuniemi 2016; Skotland et al., 2019; Jimenez-Rojo and Riezman 2019; Dorninger et al., 2019). A recent structural study revealed that Pls could strongly influence the membrane thickness and curvature (Angelova et al., 2021). Due to their abundance in brain and their "fusogenic" property, plasmalogens have been proposed to play an important role in neurotransmission (Dorninger et al., 2017). The Pls-containing biomembranes have an increased propensity to undergo the transition from lamellar to non-lamellar structures, which may result in an increased leakage of membranes to ions and induction of membrane fusion (Glaser and Gross 1994; Lohner, 1996; Siegel and Epand 1997; Nagan and Zoeller 2001; Koivuniemi 2017). Plasmalogens as a major lipid component in the membranes of synapses and synaptic vesicles (Hofteig et al., 1985; Takamori et al., 2006), together with their proposed role in membrane fusion and fission processes have led to the speculations about their roles in synaptic vesicle cycle and neurotransmission (Brites et al., 2004; Han 2005; Gorgas et al., 2006; Dorninger et al., 2017). The reduction of PlsEtns may change the biophysical properties of phospholipid-bilayered cell membranes and correlate with the impairments of synaptic transmission and neurotransmitter release (Brodde et al., 2012; Dorninger et al., 2019). A neurolipidomics study showed that the aberrant PlsEtns might be involved in synaptic dysfunction in AD (Bennett et al., 2013). Moreover, plasmalogens tend to carry polyunsaturated fatty acids (PUFAs), specifically docosahexaenoic acid (DHA) or arachidonic acid (AA) at sn-2 position of glycerol backbone (**Figure 1**). These PUFAs may regulate the SNARE proteins, which mediate synaptic vesicle exocytosis and membrane fusion (Darios and Davletov 2006; Davletov et al., 2007; Davletov and Montecucco 2010; Bazinet and Laye 2014; Lauwers et al., 2016).

Normal function of a brain requires the formation of complex neuronal networks built based on numerous synaptic connections appropriately formed and maintained. Synaptic loss correlates strongly with cognitive decline mainly because the integrity of structure and function of synapses underlie the cognitive performance. It is widely recognized that alterations of synaptic function are not only a core feature, but also a leading cause of several neurodegenerative diseases, including AD (Selkoe 2002). The synaptic loss, triggered by amyloidosis, tauopathy and inflammation, has been considered as a potential disease biomarker in AD (Colom-Cadena et al., 2020). A recent report showed a widespread synaptic loss across the brains of early AD patients and the synapse loss was even more extensive than the decrease of volume of gray matter, suggesting the synaptic degeneration may precede the occurrence of neurodegeneration and brain atrophy (Mecca et al., 2020). Aging is thought to drive a progressive decline in synaptic connectivity of the brain, resulting in cognitive impairments and predisposition to neurodegenerative disorders (Burke and Barnes 2006; Bishop et al., 2010; Fan et al., 2017). The genetic profiling studies of aging mouse, monkey and human brains have revealed significant alterations in the expression of synapse-associated genes (Jiang et al., 2001; Lu et al., 2004; Fraser et al., 2005).

Accumulated evidence and data support that plasmalogens are able to halt neuroinflammation mediated by microglial activation both *in vitro* and *in vivo* (Ifuku et al., 2012; Hossain et al., 2018; Sejimo et al., 2018; Ali et al., 2019; Youssef et al., 2019; Nguma et al., 2021). Various inflammatory stimuli may reduce Pls levels in murine microglia, and the reduction of Pls in the murine cortex further increases the activated phenotype of microglia and also the expression of pro-inflammatory cytokines (Hossain et al., 2017). PlsEtns are also important in the phagocytosis of macrophages (Rubio et al., 2018). Microglia of aged rodent brain are less active in phagocytosis compared to those of young rodent brain (Njie et al., 2012), suggesting the reduction of brain plasmalogen level may contribute to the decline in microglial phagocytosis. The impacts of aging on both microglial and synaptic dysfunctions might be related to the reduction of plasmalogen level in the brain. Aging brains are often accompanying with the increased neuroinflammation and synaptic loss, which may attribute to aging-dependent microglial dysfunction (Niraula et al., 2017; Angelova and Brown 2019). Based on these, we thus boldly speculate that plasmalogens may act to modulate synaptic and microglial function separately in addition to microglia-synapse interaction pathways.

Thus, we investigated the effects of an ascidian-derived plasmalogens supplementation on the prevention of age-related cognitive decline in mice. In the present study, we for

the first time showed that the administration of Pls could promote synaptic plasticity and neurogenesis, and inhibit the age-related microglia-mediated neuroinflammation in a natural aging mouse model. Our TEM data, immunoblotting and immunofluorescence analyses demonstrate that plasmalogens, the key brain phospholipids, improved cognition and memory by reducing neuroinflammation and supporting synaptogenesis and neurogenesis in aged mice. Our studies strongly suggest that Pls administration may serve as a potential intervention strategy for halting neurodegeneration and promoting neuroregeneration.

2 MATERIALS AND METHODS

2.1 Preparation of Plasmalogens

Plasmalogens (Pls) were extracted from ascidian (*Halocynthia roretzi*) following the protocol described before (Mawatari et al., 2009). The extracted plasmalogens were analyzed and confirmed by HPLC and LC-MS methods (Mawatari et al., 2007; Otoki et al., 2017). These purified Pls are enriched with eicosapentaenoic acid (EPA), docosahexaenoic acid (DHA), and other omega-3 fatty acids. Pls were dissolved in the sterilized water to the final concentration of 50 mg/ml by sonication.

2.2 Animals and Study Design

7-month old ($n = 40$) female C57BL/6J mice were purchased from GemPharmatech Co. Ltd., and raised to 16-month old in Laboratory Animal Center of Shanghai Jiao Tong University. 16-month old mice were then randomly divided into two groups: aged control group and aged Pls-fed group. To discern cognitive function status in aged mice, 4-week old (n = 15) female C57BL/6J mice (GemPharmatech) were used as young control group, and raised in the same condition as aged mice. Mice in aged Pls-fed group were supplemented with Pls in water by intragastric administration for 2 months and mice in aged control group were given the same amount of water. Pls were administrated at a dosage of 300 mg/kg, once a day, and 5 days per week. Behavioral tests were performed after 2 months of the Pls treatment. At the time of behavioral tests, mice in aged Pls-fed group and aged control group were 18 months old, and mice in young controls group were 3 months old. The animal protocol was reviewed and approved by the Shanghai Jiao Tong University Institutional Animal Care and Use Committee (SJTU-IACUC). All mice were housed in a pathogen-free facility with 12-h light/12-h dark cycles, received food and water ad libitum.

2.3 Morris Water Maze Test

The Morris water maze test was performed as described previously (Vorhees and Williams 2006). The apparatus was a circular pool (120 cm diameter) filled with water. Tests were performed at 22°C. A 10 cm diameter transparent platform was placed 1 cm below the water surface at a fixed position. Mice were taken to the behavior room, acclimatized, and trained on five consecutive days, four trials per day. The starting point changed after each trial of a daily training session. Each trial lasted 60 s or until the mouse found the platform. If the platform was not located during the time period, then the mouse was guided to the platform, and allowed to stay there for 15 s. On day six, the platform was removed for the probe trial. The duration of probe trial was 60 s. All parameters were recorded by a video tracking system.

2.4 Transmission Electron Microscope Study

Mice were anesthetized with 1% pentobarbital sodium. Mice were perfused transcardially with phosphate buffered saline (PBS) followed by 4% paraformaldehyde (PFA) solution. The brains were rapidly removed and placed on ice. CA1 parts of hippocampus were dissected out immediately. Tissue blocks were first fixed in 2.5% glutaraldehyde overnight, followed by 2nd fixation of 1% osmium tetroxide for 20 min. Samples were dehydrated through an ethanol gradient and finally infiltrated and embedded in low viscosity epoxy resin kit (Spurr) containing initiator and polymerized at 70°C for 12 h. Ultrathin (50–75 nm) sections were cut with a diamond knife (DiATOME, ultra 45°) on ultramicrotome (Leica, EM UC7) and collected on 200-mesh copper grids. Sections were then stained with lead citrate for 10 min. Sections were then viewed on a transmission electron microscope (FEI, Talos F200S) at 200 kV.

2.5 Western Blot Analysis

Mice hippocampus were dissected after sacrificed, snap frozen and lysed in RIPA buffer (YoBiBio, China) with 1% phenylmethanesulfonyl fluoride (PMSF) (YoBiBio, China). The lysates were firstly separated on 8–12% SDS-PAGE and transferred to Polyvinylidene difluoride (PVDF) membrane. The separated proteins were immunoblotted with the following antibodies: β-Tubulin (ab6046, Abcam), Synaptophysin (ab52636, Abcam). Western blotting images were obtained by ECL exposure and quantified by Image J software. The amount of protein was expressed as a relative value to the levels of β-Tubulin.

2.6 RNA Sequencing Analysis

RNA purification, reverse transcription, library construction, and sequencing were performed at Shanghai Biochip Co., Ltd. (Shanghai, China) according to the manufacturer's instructions. The expression level of each transcript was calculated according to the fragments per kilobase of exon per million mapped reads method. RNA-Seq by expectation–maximization was used to quantify gene abundances. Gene ontology (GO) annotation enrichment analysis of differentially expressed genes was analyzed at database for annotation, visualization and integrated discovery (DAVID) version 6.8 (https://david.ncifcrf.gov/home.jsp).

2.7 Real-Time PCR Analysis

Total RNA was extracted from the mouse brain tissue using Trizol reagent (Invitrogen), according to the manufacturer's instructions. Reverse transcription of RNA was performed with the ReverTra Ace qPCR RT Master Mix with gDNA Remover Kit (Toyobo). The cDNA was subsequently subjected to Real-Time PCR by using SYBR Green Real-time PCR Master

Mix (Toyobo). The qPCR primers used for amplifying each mouse gene were as follows: Sox2, 5′-forward CCCACCTAC AGCATGTCCTAC-3′ and reverse 5′-GCCTCGGACTTGACC ACAG-3'; IL-1β, forward 5′-GAAATGCCACCTTTTGACAGT G-3′ and reverse 5′-TGGATGCTCTCATCAGGACAG-3'; TNF-α, forward 5′-AAGCCTGTAGCCCACGTCGT-3′ and reverse 5′-AGGTACAACCCATCGGCTGG-3'; IL-6, forward 5′-TAG TCCTTCCTACCCCAATTTCC-3′ and reverse 5′-TTGGTC CTTAGCCACTCCTTC-3'; GAPDH, forward 5′-CAATGT GTCCGTCGTGGATCT-3′ and reverse 5′-GTCCTCAGTGTA GCCCAAGATG-3'. The quantitative fold changes in mRNA in each sample were normalized to GAPDH expression and calculated using the $2^{(-\triangle\triangle Ct)}$ method.

2.8 Immunofluorescence Study

Anesthetized mice were perfused with PBS buffer and then with 4% paraformaldehyde (PFA) in PBS buffer. The brains were then collected in 4% PFA solution, fixed overnight at 4°C followed by the treatment with the sucrose solutions 30% until they sink. The brains were then embedded in optimum cutting temperature (O.C.T.) compound, and sectioned into 10 μm slices on a freezing microtome. Sections were incubated overnight at 4 C with primary antibodies in 3% bovine serum albumin (BSA) in PBS containing 0.1% Tween 20. Primary antibodies used in this study were rabbit anti-Synaptophysin (ab52636, Abcam), rabbit anti-Sox2 (ab93689, Abcam), rabbit anti-Iba1 (17198S, Cell Signaling Technology). Following the overnight primary antibody incubation, sections were washed five times with PBS or TBS buffer solution, incubated with the appropriate secondary antibodies (1:100, Jackson ImmunoResearch Laboratories). For quantification of the expression of Sox2, Sox2-positive cells were counted in the DG of hippocampus. For quantification of the expression of Synaptophysin, the immunofluorescence intensity was quantified using the Image J.

2.9 Morphometric Analysis of Iba1+ Microglia

Microglia were classified as activated when cells presented shortening of processes and increase in cell body size (dystrophic morphology) (Streit et al., 2004). The overall morphologies of Iba1+ microglia from young control, aged control and aged Pls-fed groups were analyzed with ImageJ (NIH) by using skeleton analysis and sholl analysis as described previously (Young and Morrison 2018). Iba1+ microglia were chosen randomly in the CA1 region of hippocampus, and investigators who performed tracings were blinded to the experimental groups. Simple neurite tracer plugin was used for tracing processes of microglia cells. Cells were skeletonized using 3D skeletonize plugin and labeled for slab, junctions, or end of branches. Conformational Sholl analysis was performed through concentric envelopes computed with a 1 μm radius step starting from the cell body. In each group, 30 microglia (7-8 cells/animal, 4 animals/group) were analyzed by Sholl analysis.

2.10 Statistical Analysis

GraphPad Prism 7.0 was used for statistical analysis. The data are shown as the mean ± SEM. Group differences were analyzed with one-way ANOVA followed by the Tukey multiple comparisons test for comparison among multiple groups. The two-tailed unpaired *t* test was applied for comparisons between two groups. Differences were considered statistically significant with $^{*}p < 0.05$, $^{**}p < 0.01$ and $^{***}p < 0.001$.

3 RESULTS

3.1 Plasmalogens-Fed Intervention Improves Memory and Cognition of Aged Mice

In this report, we used a natural aged mice model to investigate the effect of plasmalogens (Pls) supplementation on the cognition performance. Supplementation with water or Pls by oral gavage in the aged mice started at age of 16 months and continued until age of 18 months. The body weight (**Supplementary Figure S1**) was not statistically different between the aged control and aged Pls-fed mice during the gavage administration period. The effect of Pls supplementation on murine cognition behavior was assessed by Morris Water Maze test. The aged mice swam a longer distance (**Figure 2B**) and took a longer time (**Figure 2C**) to find the escape platform compared to the young mice, suggesting the cognitive impairments might occur in aged mice. In comparison with aged controls, the data of aged Pls-fed mice showed a significant shorter swimming distance and escape latency to reach the escape platform on the 4th day and 5th day (**Figures 2B,C**). In the probe trial, with the platform removed, trials were performed to evaluate the spatial reference memory of the mice. The aged Pls-fed mice spent more time in the target quadrant and the crossing numbers were significantly increased over that of aged control mice (**Figures 2D,E**). These outcomes reveal that aged mice with 2-months Pls supplementation have better spatial learning and memory capacity compared to aged control mice. Of note, by the age of 18 months, the appearance of aged control mice showed striking signs of senescence, characterized by gray body hair and obvious hair loss, while aged Pls-fed mice look healthy in appearance with glossier and thicker hair compared to aged controls (**Figure 2A**). These data suggest that Pls supplementation may alleviate age-related cognitive decline and reverse the aged symptoms in mice.

3.2 Plasmalogen Treatment Alleviates Age-dependent Synaptic Loss in Murine Hippocampus

Synapses are specialized intercellular junctions with two apposed compartments, pre-synaptic terminal and post-synaptic domain, and synaptic cleft, a gap about 20 nm between pre- and post-synaptic components (Hernandez-Nicaise 1973). As shown in

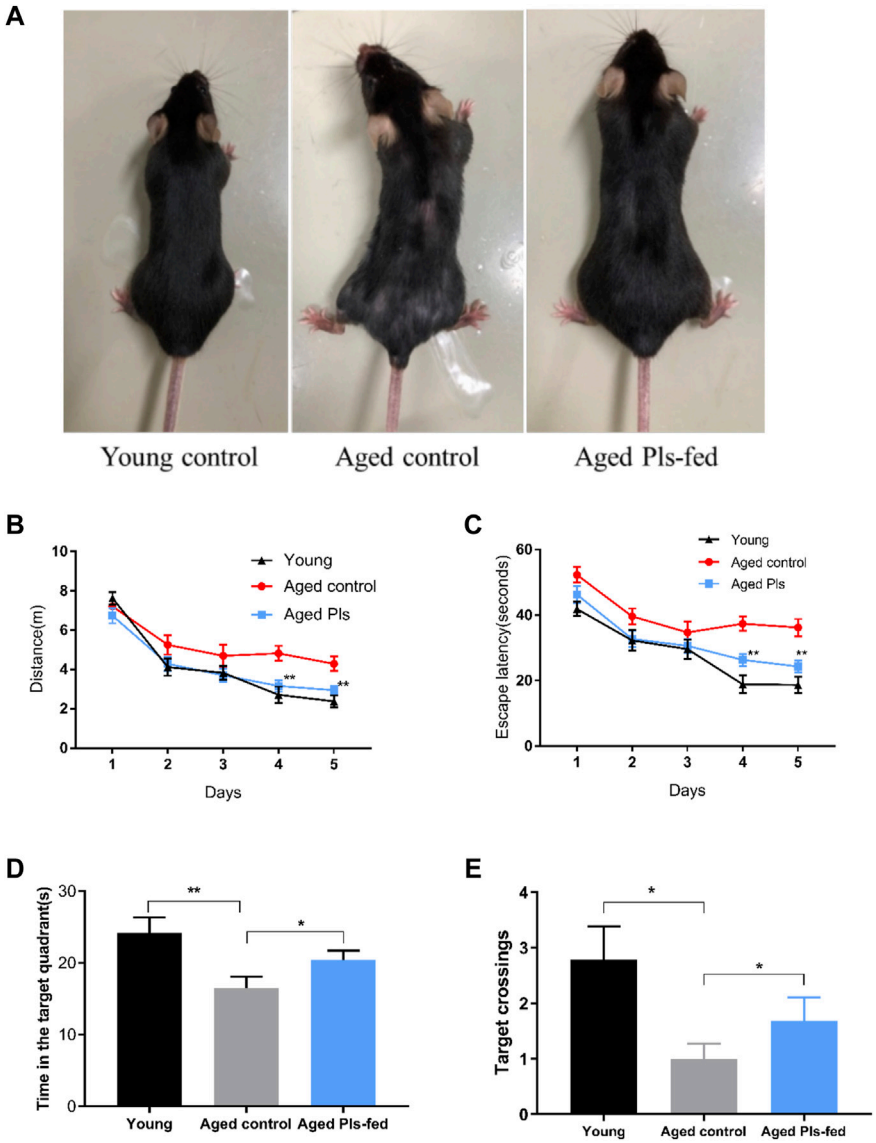

FIGURE 2 | Effects of 2-months Pls supplementation on the appearance and cognitive behaviors of aged mice. **(A)** Representative photos of young mice (3 months), aged Pls-fed mice (18 months), aged control mice (18 months). **(B–E)** Spatial reference learning and memory were determined and characterized in a Morris water maze study. Mice were trained in Morris water maze for consecutive 5 days, four trials per day. The probe trials were tested on the 6th day. The distance traveled **(B)** and time spent **(C)** to reach the escape platform are demonstrated respectively. A bar graph summarizes the time spent within the target quadrant **(D)** and platform crossing numbers **(E)**. Data are presented as mean ± SEM, with 13–16 mice in each group (Young, $n = 14$; Aged control, $n = 13$; Aged Pls-fed, $n = 16$). Asterisks indicate statistical significances compared to Aged control using one-way ANOVA; Statistical significance (*$p < 0.05$; **$p < 0.01$).

Figure 3, pre-synaptic domains are marked with blue color, and post-synaptic domains with pink color. The typical ultrastructures of synapse of young control (**Figure 3B**) and aged Pls-fed mice (**Figures 3C,D**) were examined by TEM. Remarkably, abundant synaptic structures are present in both young controls (**Figure 3B**) and aged Pls-fed mice (**Figures 3C,D**), and the numbers of synapse are far more than we have observed in those of aged controls (**Figure 3A**). There are plenty of synaptic vesicles in the presynaptic domains in both young controls and aged Pls-fed mice. Although young controls (**Figure 3B**) and aged Pls-fed mice (**Figures 3C,D**) have similar and comparable numbers of synapses, the number of synaptic vesicles in young mice is greater compared to aged Pls-fed group in the total viewed TEM images (each group 30–40 images from 3-4 biologically independent samples), nevertheless both young controls (**Figure 3B**) and aged Pls-fed mice (**Figures 3C,D**) have much greater numbers of synaptic vesicles compared to aged controls (**Figure 3A**). In aged control samples, synaptic loss is visually obvious and synaptic ultrastructures showed severe deterioration with few synaptic vesicles (**Figure 3A**). In aged Pls-fed mice (**Figures 3C,D**), the synaptic structures are intact and look similar to those of young controls (**Figure 3B**), with synaptic

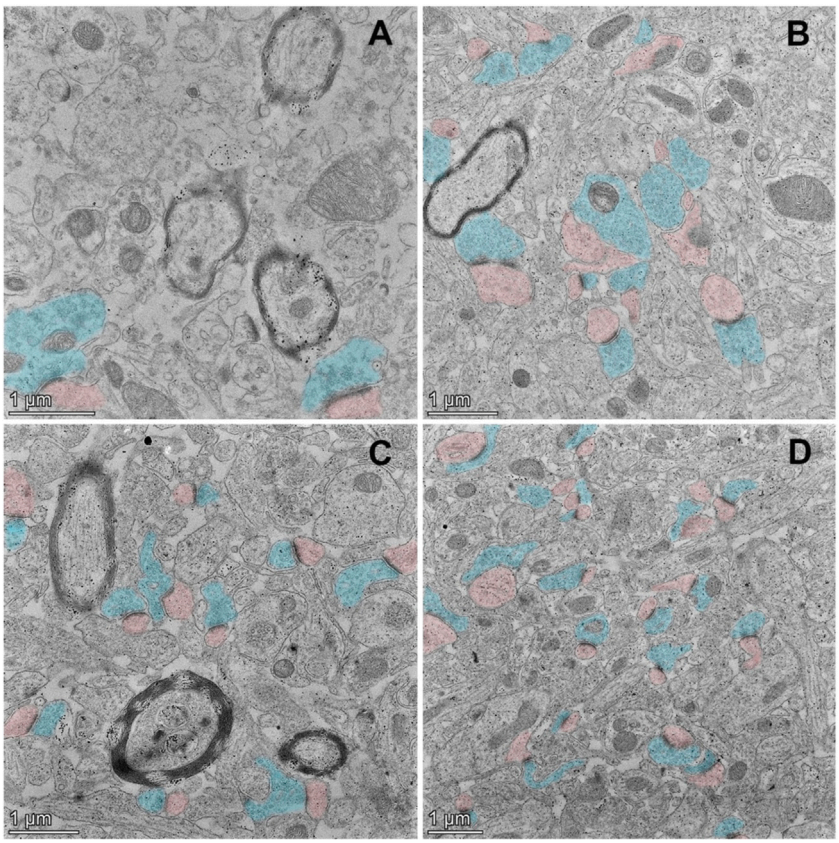

FIGURE 3 | TEM ultrastructural study on murine hippocampal CA1 region. The TEM micrographs of aged control mice **(A)**, young control mice **(B)**, and aged Pls-fed mice **(C,D)**. Pre-synaptic terminals are marked with blue color, and post-synaptic domains with pink color. The synaptic loss, synaptic degradation and deterioration were observed in aged controls **(A)**. On the contrary, abundant synaptic vesicles are present in the pre-synaptic terminals (marked in blue) of young controls **(B)**. There is a pronounced increase in the numbers and density of synapses in aged Pls-fed murine hippocampus with moderate numbers of synaptic vesicles **(C,D)**. Bars = 1 μm.

vesicles evenly distributed in the presynaptic domains. The TEM data strongly indicate that Pls supplementation may protect against the hippocampal synaptic loss in aged mice.

3.3 Plasmalogens Treatment Changed the Transcriptomics Profile of Hippocampus in Aging Mice

To investigate the molecular mechanism of plasmalogens improving learning and memory of aged mice, transcriptome analysis was performed by RNA-sequencing (RNA-seq) on the experimental murine hippocampus tissues. There are 802 differentially expressed genes (Ratio >1.2 or Ratio <0.8, and $p < 0.05$) in the aged Pls-fed mice compared with aged control (**Supplementary Table S1**), and heatmap analysis of all the differentially expressed genes was shown in **Figure 4A**. GeneAnalytics pathway analysis showed that these differentially expressed genes were involved in several pathways, including ERK, PI3K-AKT signaling (**Figure 4B**). The DAVID version 6.8 was used for function annotation analysis and enrichment analysis, which shown that these genes were engaged in synapse (Synpo, Synpr, Erbb3, and Slc6a9, etc.), neurogenesis (Fabp7, Nrp2, Ephb1, and Insc, etc.), neural stem cell (Nestin, Sox2, and Msi1), nervous system development (Ephb3, Dpysl3, Smarca2, and Efnb3, etc.), neuotrophin signaling pathway (Vgf, Ntf3, Gab1, and Irs1, etc.), lipid metabolic process (Agpat4, Elovl1, Elovl7, and Fa2h, etc.) (**Figure 4C**). Neurotrophins including VGF and neurotrophin-3 (Ntf-3), are considered powerful molecular mediators in synaptic plasticity (Poo 2001; Park and Poo 2013). The elevated level of neurotrophins in aged Pls-fed mice may contribute to potential neurogenesis and observed synaptogenesis in aged Pls-fed murine hippocampus. These RNA-sequencing data point out that Pls administration may upregulate the expression of synapse-associated genes and promote synaptogenesis and neurogenesis in aged murine hippocampus.

3.4 Plasmalogens Enhance the Hippocampal Synaptic Plasticity in the Aged Mice

Learning and memory are associated with the remodeling and growth of synapses (Bailey et al., 2015). Above-mentioned

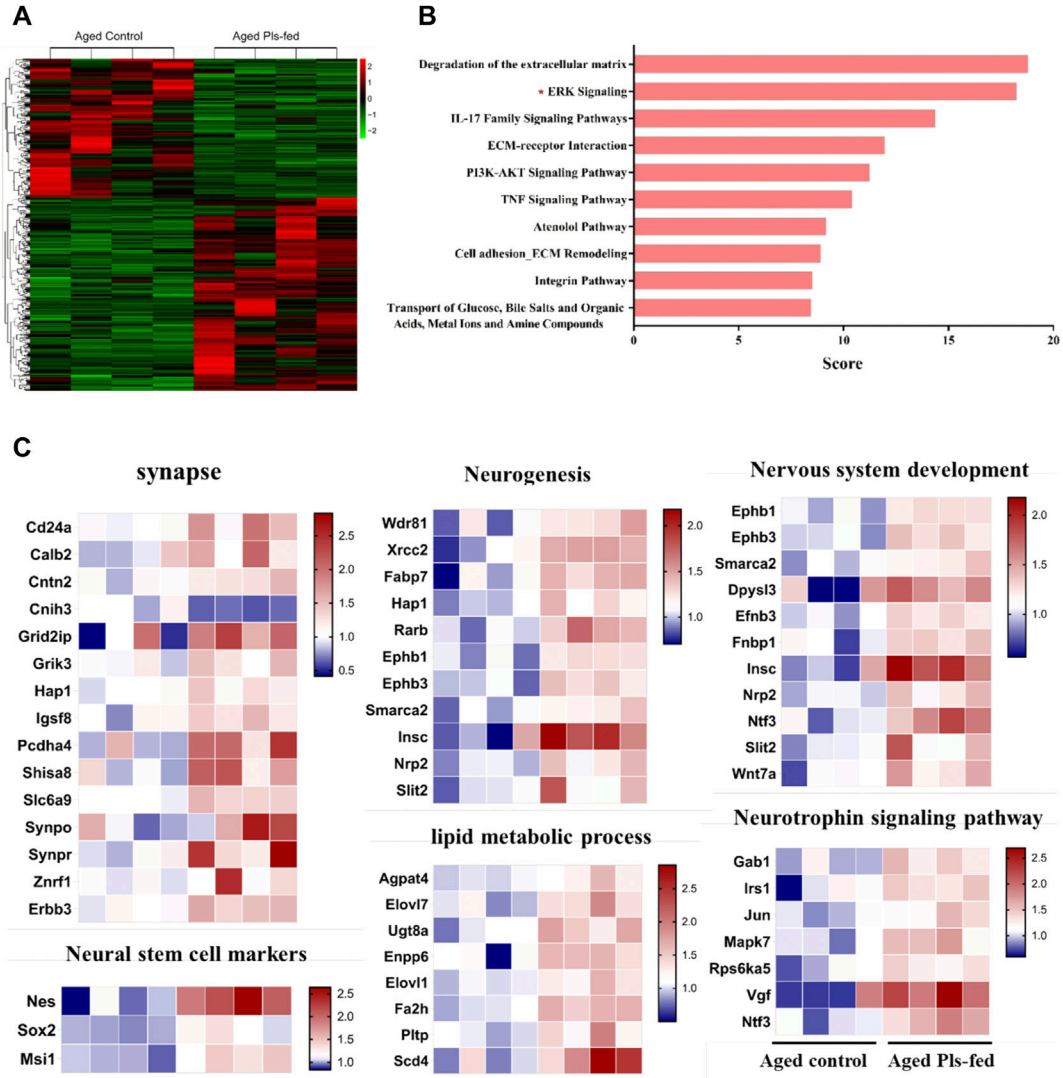

FIGURE 4 | Transcriptomics profile of hippocampus in aged Pls-fed mice. **(A)** A heat map shows all differentially expressed genes in aged control versus aged Pls-fed murine hippocampus based on RNA-seq (*n* = 4 mice per group). **(B)** GeneAnalytics pathway analysis of differentially expressed genes in hippocampus of aged control vs. aged Pls-fed mice, the top ten pathways are highlighted here. **(C)** Plasmalogen treatment changed the transcriptomics profile of hippocampus in the aged mice. (*n* = 4 mice per group).

TEM and RNA-seq results have suggested that Pls may enhance the hippocampal synaptic plasticity. To further verify the alterations of synaptic plasticity, we investigated the expression of synaptic plasticity-related protein, synaptophysin, by immunoblotting and immunofluorescence techniques. Immunofluorescence studies showed that, the expression of synaptophysin was significantly reduced in the CA1 and DG regions of hippocampus of aged controls mice compared with that of young mice, and significantly increased in aged Pls-fed mice compared with that of the aged controls (**Figures 5A–C**). Furthermore, immunoblotting analysis also showed that synaptophysin was markedly upregulated in the hippocampus of aged Pls-fed mice (**Figures 5D,E**). These results indicate that synaptic plasticity decreases in an age-related manner and can be enhanced by Pls supplementation.

3.5 Plasmalogens Promote Neurogenesis in the Aged Murine Hippocampus

In the aged brain, neurogenesis decline leading to reduced neuroplasticity and cognitive function (Villeda et al., 2011). Adult neurogenesis usually occurs in neurogenic niches in the dentate gyrus (DG) of hippocampus (Villeda et al., 2011). To further investigate whether plasmalogens can affect the neurogenesis, we examined the proliferative Sox2+ stem

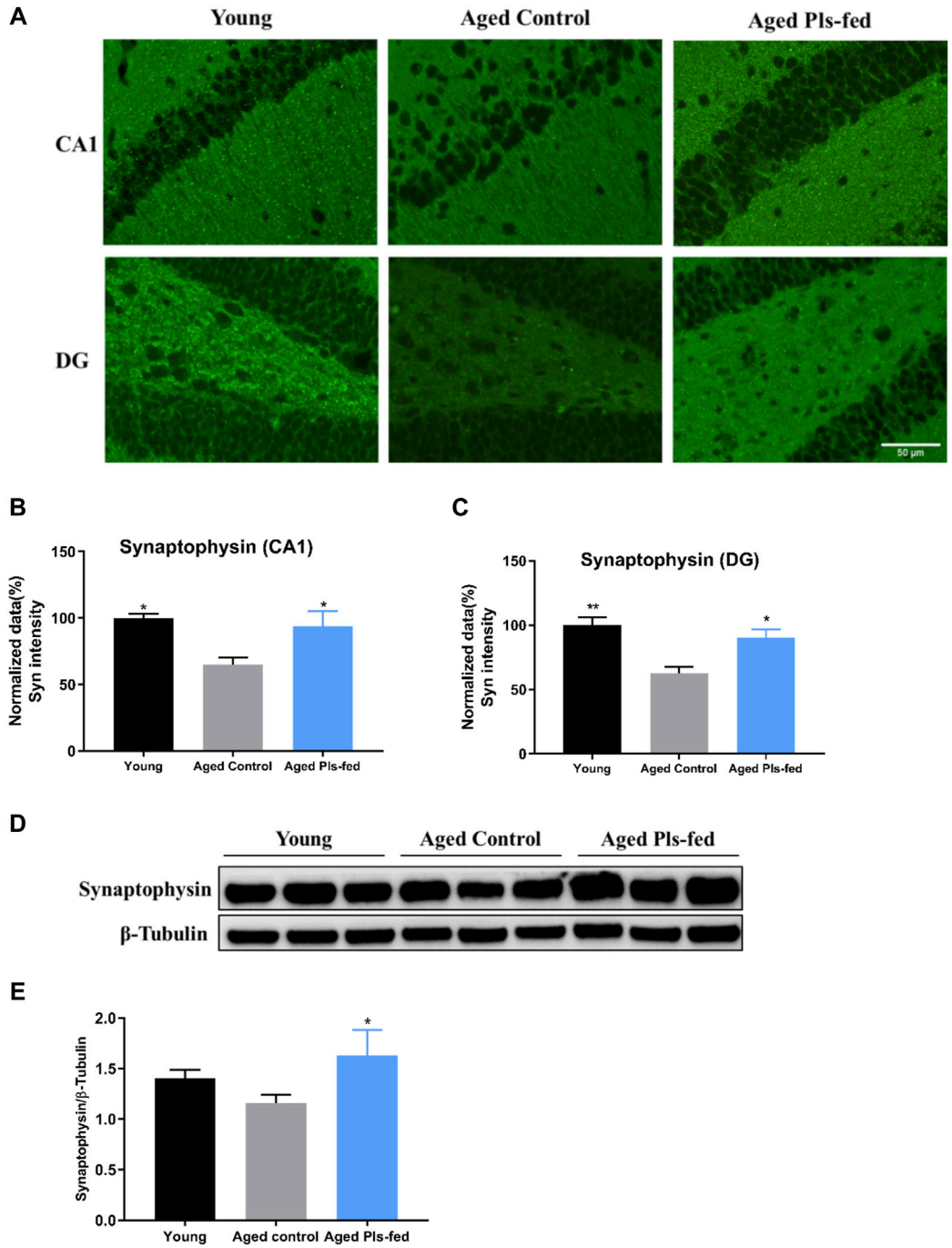

FIGURE 5 | Plasmalogens enhance synaptic plasticity in the hippocampus of aged mice. **(A)** Representative images showing the expression of synaptophysin (green) in the CA1 and DG region of mice hippocampus. **(B–C)** Graph showing quantification of the immunostaining of synaptophysin in the CA1 and DG region of murine hippocampus ($n = 4$ mice for each group), and values are presented as mean ± SEM. **(D)** Representative immunoblotting of synaptophysin levels and **(E)** graph showing quantification of synaptophysin levels. The quantification is a ratio of synaptophysin/β-tubulin levels ($n = 3$ mice per group), and values are presented as mean ± SD. Asterisks indicate statistical significances compared to Aged control by one-way ANOVA; significance (*$p < 0.05$; **$p < 0.01$), scale bars, 50 μm.

cells in the murine hippocampal sections. Immunofluorescence data showed that, the number of Sox2+ stem cells was significantly reduced in the DG regions of hippocampus of aged controls compared with that of young controls, and significantly increased in the aged Pls-fed mice compared with that of the aged controls (**Figures 6A,B**). Furthermore, the increased Sox2 mRNA level (**Figure 6C**) in the aged Pls-fed mice compared with that of

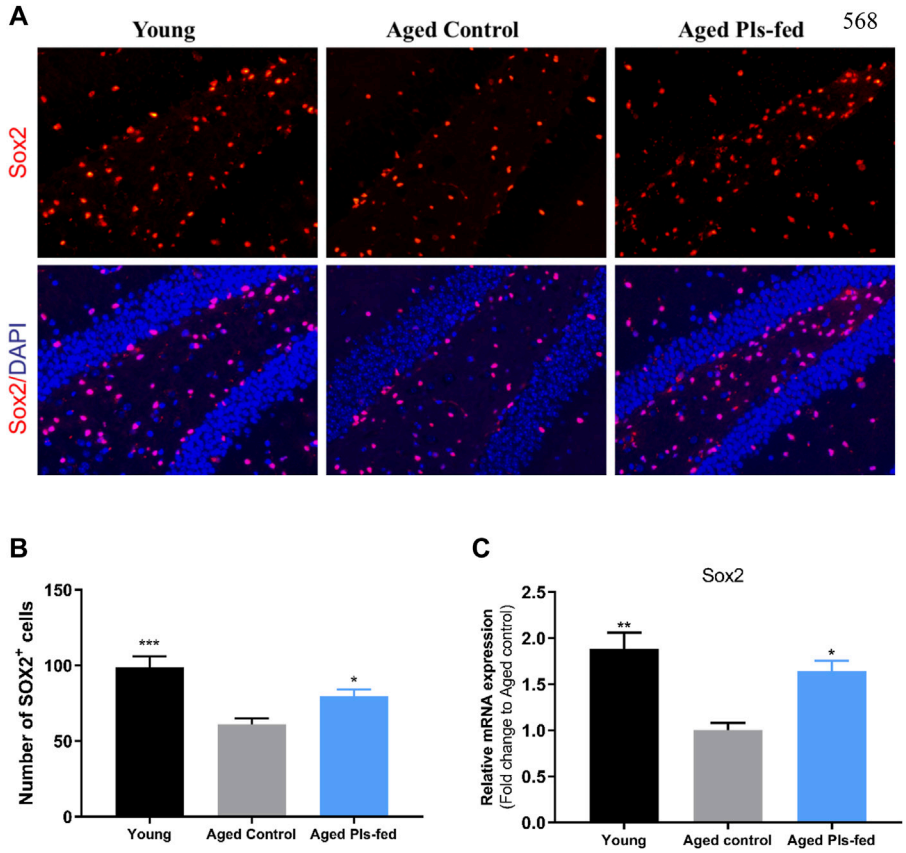

FIGURE 6 | Plasmalogens promote neurogenesis in the aged murine hippocampus. **(A)** Representative fluorescence images showing neural stem cells in young control, aged control and aged Pls-fed mice of hippocampal dentate gyrus (DG). Cells are identified based on anti-Sox2 (red). DAPI indicates nuclear staining (blue). **(B)** graph showed quantification of Sox2+ cells among groups. **(C)** The real-time PCR data showed mRNA expression of Sox2 in hippocampus of young control, aged control and aged Pls-fed mice. All values are presented as mean ± SEM. Asterisks indicate statistical significances compared to Aged control by one-way ANOVA; significance (*$p < 0.05$; **$p < 0.01$; ***$p < 0.001$), scale bars, 50 μm n = 4 mice for each group.

the aged controls is consistent with previous RNA-seq data (**Figure 4C**). These results demonstrate that plasmalogens may activate the NSCs proliferation, which is beneficial to stabilize the neural network in hippocampus.

3.6 Plasmalogens Suppress the Microglia Activation and Attenuate Neuroinflammation in the Aged Murine Brain

Microglia partake in many important events in adult brain including neurogenesis, synaptic plasticity, synaptic pruning and maintenance of neuronal health (Kierdorf and Prinz 2017). In healthy brain, microglia exhibit a ramified morphology, termed as "resting" or "surveying" microglia. Whereas microglia in the aged brain display a dystrophic morphology, classified as a "primed" or "sensitized" phenotype (Niraula et al., 2017; Hanisch and Kettenmann 2007). Immunofluorescence analysis of Iba1+ cells allowed us to view microglial shapes in the murine hippocampus (**Figure 7A**). The morphological features of surveying microglia with branched long processes were observed in young control and aged Pls-fed samples, whereas the dystrophic microglia were observed in aged control mice (**Figure 7A**). Quantitative analysis of morphological changes of microglia demonstrated the noticeable differences among three groups. The skeleton analysis data showed that endpoints were lower in the aged control compared to young control and aged Pls-fed mice (**Figure 7B**). The Sholl analysis data showed an increase in the number of branches in microglia of aged Pls-fed mice compared to those of aged controls (**Figure 7C**). The experimental results indicate that plasmalogens may alleviate age-related microglia activation. The primed phenotype of microglia in the aged brain may produce more pro-inflammatory cytokines such as TNF-α, IL-1β and IL-6 (Sierra et al., 2007). The measurements of pro-inflammatory cytokines, revealed that the levels of IL-1β, IL-6 and TNF-α (**Figures 7D–F**) were significantly reduced in the hippocampal tissues of aged Pls-fed mice compared to aged controls. These experimental outcomes demonstrate that plasmalogens may inhibit microglial

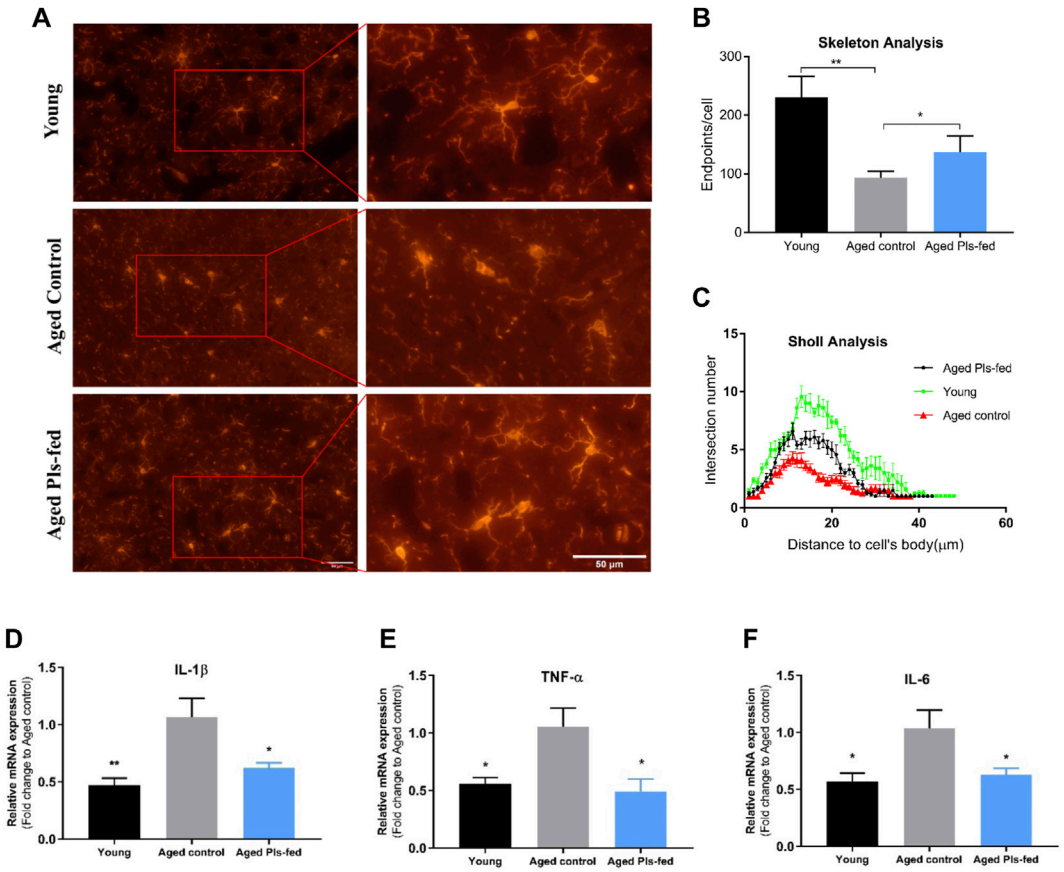

FIGURE 7 | Effects of plasmalogens intervention on microglia activation and inflammatory cytokines expression. **(A)** Immunofluorescence staining of Iba1+ microglia cells (red) in the hippocampus of young control, aged control and aged Pls-fed mice, scale bars, 50 μm. Note that microglia of aged control mice display shorter processes and diminished ramification of processes, whereas microglia of aged Pls-fed and young control show longer and ramified processes. **(B)** The graph bar of skeleton analysis on microglia showed that the endpoints are increased in microglia of aged Pls-fed mice. **(C)** Sholl analysis of the number of branches plotted as a distance from cell body (n = 30, microglial cells per experimental group). **(D–F)** The real-time PCR data showed mRNA expression of pro-inflammatory cytokines IL-1β, TNF-α, IL-6 in hippocampus of young control, aged control and aged Pls-fed mice. All values are presented as mean ± SEM. Asterisks indicate statistical significances compared to Aged control by one-way ANOVA (*p < 0.05; **p < 0.01).

activation and reduce pro-inflammatory cytokines in the aged mice.

4 DISCUSSION

There has been an increasing interest in plasmalogens research due to the emerging roles they play in health and diseases (Su et al., 2019; Dorninger et al., 2020; Bozelli et al., 2021). The reduced level of plasmalogens has been commonly observed in the patients suffering from neurodegenerative disorders and appears to meet Bradford Hill criteria for causal association with neurodegeneration to a considerable extent (Senanayake and Goodenowe 2019). Moreover, plasmalogen replacement therapy (PRT) has been shown to be a successful way to restore plasmalogen levels as well as to ameliorate pathological phenotypes (Bozelli and Epand 2021), and an increasing number of studies suggests that plasmalogens may serve as potential therapeutic intervention for multiple neurodegenerative diseases, including AD and PD (Fujino et al., 2017; Yamashita et al., 2017; Bourque et al., 2018; Fujino et al., 2018; Nadeau et al., 2019; Mawatari et al., 2020). These reports all point to a fact that the significance of plasmalogens in neuro-degeneration and neuro-regeneration. However, these studies also raised some puzzling questions about the actual mechanisms of plasmalogens that remain to be revealed. Based on others' and our own experimental data, we thus boldly propose that plasmalogens may improve age-related cognitive decline through the promotion of neurogenesis, especially synaptogenesis and synaptic vesicles formation to counteract the loss of synaptic connectivity and networking in aging and neurodegenerative process.

In the present study, we attempt to answer these important questions by examining the synaptic and microglial response to plasmalogens treatment in the aged female mice. The decline of cognitive function in humans is progressive, usually starting at middle age (Schönknecht et al., 2005). Compared to males, age-related cognitive decline and brain atrophy occur earlier in

females (Yuan et al., 2012; Podgórski et al., 2021). Women have a higher life expectancy than men, but reported a higher prevalence of dementia (Corrada et al., 2008). For these reasons, naturally aged female mice were used as experimental subjects in this study. The 18-month old C57BL/6J mice showed significant cognitive impairments compared to young controls, while the aged Pls-fed mice have significantly better spatial learning and memory performance than that of aged controls. Moreover, aged Pls-fed mice look healthy in appearance with glossier and thicker body hair comparable to young control mice. From our close observations, the aged mice began to grow new black hair clearly visible to the naked eyes since the 3rd week of Pls supplementation. As Pls administration was continuously introduced to the aged mice, the black hair became thicker with glossy look. The intragastric administration of plasmalogens effectively improved the physiological structure and function of synapses in the aged murine hippocampus and might further reverse the age-related cognitive functions of the brains.

Aging is thought to drive a progressive decline in synaptic connectivity and neurogenesis in brain, resulting in cognitive impairments and predisposition to neurodegenerative disorders (Burke and Barnes 2006; Dickstein et al., 2007; Rossi et al., 2008; Villeda et al., 2011; Fan et al., 2017). Synaptic loss is correlated most strongly with cognitive decline and synaptic function; the latter is underlying the cognitive performance. In this report, the hippocampal synaptic ultrastructures of CA1 area in aged Pls-fed mice appear comparable to those of young controls. Whereas the number and density of synapses and synaptic vesicles of aged controls are visibly much less compared to those of young controls and aged Pls-fed mice. Our observations of synaptic damage and loss in the aged controls are consistent with that of previous reports (Bondareff and Geinisman 1976; Geinisman et al., 1986; Geinisman et al., 1992). TEM data in this report provide the first direct visual evidence that plasmalogens supplementations may alleviate age-dependent synaptic loss and also promote synaptogenesis and synaptic vesicles (SVs) formation. Therefore, we further examined neurogenesis and synaptic plasticity associated proteins. Synaptophysin is a synaptic vesicle glycoprotein, involved in the fusion of neurotransmitter vesicles and regulation of synaptic vesicle exocytosis (Südhof 1995; Janz et al., 1999). The markedly increased expression of synaptophysin in aged Pls-fed mice, suggests that plasmalogens as a major lipid component of synapses may play role in promoting the formation of SVs and synaptic membrane. Moreover, plasmalogens can activate the neural stem cells and promote neurogenesis in aged murine brain, and both may have significant effects on maintaining the cognitive function of animals. Furthermore, RNA-seq analysis on the murine hippocampus revealed the obvious changes in synapse, neurotrophins, neurogenesis, neural stem cell and lipid metabolism at the genetic and molecular level in response to plasmalogen administration. All these findings support that Pls may reverse cognitive aging by enhancing the synaptic plasticity and neurogenesis in aging mice.

During aging process, activated microglia release a plethora of cytokines, chemokines, and reactive oxygen species, which in turn affect various aspects of adult neurogenesis (Sierra et al., 2010; Harry 2013). The continuous over-activated microglia may lead to the development of neurodegeneration. Microglia in the aged brain have been characterized by the dystrophic morphologies (Niraula et al., 2017), which are arguably less capable in securing CNS homeostasis and may trigger the neuroinflammation to further develop neurodegenerative disorders. The dystrophic microglia as an indicator of pathological precursor may contribute to overall weakening of synaptic connectivity and plasticity, often underlying age-dependent cognitive decline. Downregulation of plasmalogens synthesis by injection of lentiviral shRNAs targeting the Gnpat mRNA causes activated NF-κB in the cerebral cortex of mice, an observation accompanied by a pro-inflammatory state of microglia in the manipulated brain region (Hossain et al., 2017). Vice versa, complementary experiments *in vitro* and *in vivo* indicate that plasmalogens supplementation can halt inflammatory response, through shifting microglia cell to a less pro-inflammatory state (Hossain et al., 2018; Sejimo et al., 2018; Ali et al., 2019; Youssef et al., 2019). In our study, microglia in aged Pls-fed mice brain are less activated (**Figures 7A,B**), suggesting that plasmalogens may alleviate age-related microglial activation and retain them in a surveillance state.

Neuroinflammation is a common feature of multiple neurodegenerative disorders, including AD. Neuroinflammation is known as a negative regulator of adult hippocampal neurogenesis (Ekdahl et al., 2003; Monje et al., 2003) and its progressive enhancement in hippocampus has been considered as one of the hallmarks of aging. The aged microglia produce more pro-inflammatory cytokines including TNF-α, IL1-β, and IL-6 (Sierra et al., 2007). Our examinations on microglia-mediated pro-inflammatory cytokines (IL-1β, IL-6 and TNF-α), demonstrated a significant decline of these inflammatory factors in the hippocampus of aged Pls-fed mice compared to that of aged controls. The reduced neuroinflammation mediated by plasmalogens supplementation in aged brain may help maintain a healthy nervous system and against cognitive decline.

The bioavailability of oral supplements of plasmalogens to the neuronal cells is still not clear. Although some studies suggest that plasmalogen precursors can pass through the blood-brain barrier (BBB) (Wood et al., 2011; Malheiro et al., 2019) the penetration of plasmalogens across BBB may be low in efficacy (Fallatah et al., 2020). Plasmalogen can be hydrolysed into PUFA and lyso-plasmalogen by gut phospholipase A2 (Jurkowitz et al., 1999; Wu et al., 2011). Lyso-plasmalogen could be transported to various tissues and organs and be reused to synthesize new plasmalogen species (Yamashita et al., 2021). Plasmalogens from ascidians (*Halocynthia roretzi*) contain unsaturated fatty acids such as DHA and EPA (Yamashita et al., 2014; Yamashita et al., 2016a). One study has suggested that the phospholipid form of DHA could cross the blood-brain barrier at a rate of approximately 10 times faster than that of the free fatty acid form of DHA (Lagarde et al., 2015). Therefore, the ingestion of plasmalogens with DHA might exert enhanced neuroprotective and neural function maintenance effects in the brain. Further studies are necessary to examine whether 2 months of oral Pls supplements may improve the plasmalogen levels and/or change the plasmalogen profiles or fatty acids profiles in the aged brain.

In conclusion, our results in the aging mouse model provide novel evidence that ascidian-derived plasmalogens treatment for

2 months is effective in improving cognitive function of the elderly. Further analyses of suggested that improved cognitive function following Pls treatment is linked to the enhanced synaptic plasticity, anti-inflammatory effects, and enhanced neurogenesis in the aged hippocampus. These results suggest that administration of plasmalogens may offer a promising strategy to improve cognitive function as we age.

DATA AVAILABILITY STATEMENT

The datasets presented in this study can be found in online repositories. The names of the repository/repositories and accession number(s) can be found below: https://www.ncbi.nlm.nih.gov/bioproject/PRJNA781063.

ETHICS STATEMENT

The animal study was reviewed and approved by Shanghai Jiao Tong University Institutional Animal Care and Use Committee.

AUTHOR CONTRIBUTIONS

LF and JC conceived the project, designed research, provided study resources, analyzed data, and revised the manuscript. JG performed the study, carried out data analyses, and drafted the paper. RS helped with animal studies. JW performed TEM study. YD provided a few study resources and revised the manuscript.

FUNDING

YD was supported by the National Natural Science Foundation of China (Grant No. 31670841) and Wenzhou Institute, University of Chinese Academy of Sciences (Grant No. WIUCASQD2019005).

ACKNOWLEDGMENTS

We would like to extend our gratitude to the Electron Microscopy Unit (Wenzhou Institute, University of Chinese Academy of Sciences) for providing the facility for this work. Special thanks go to Bin Xu for his technical assistance in TEM analysis.

SUPPLEMENTARY MATERIAL

The Supplementary Material for this article can be found online at: https://www.frontiersin.org/articles/10.3389/fmolb.2022.815320/full#supplementary-material

REFERENCES

Ali, F., Hossain, M. S., Sejimo, S., and Akashi, K. (2019). Plasmalogens Inhibit Endocytosis of Toll-like Receptor 4 to Attenuate the Inflammatory Signal in Microglial Cells. *Mol. Neurobiol.* 56 (5), 3404–3419. doi:10.1007/s12035-018-1307-2

Angelova, D. M., and Brown, D. R. (2019). Microglia and the Aging Brain: Are Senescent Microglia the Key to Neurodegeneration. *J. Neurochem.* 151 (6), 676–688. doi:10.1111/jnc.14860

Angelova, A., Angelov, B., Drechsler, M., Bizien, T., Gorshkova, Y. E., and Deng, Y. (2021). Plasmalogen-Based Liquid Crystalline Multiphase Structures Involving Docosapentaenoyl Derivatives Inspired by Biological Cubic Membranes. *Front. Cel. Dev. Biol.* 9, 617984. doi:10.3389/fcell.2021.617984

Bailey, C. H., Kandel, E. R., and Harris, K. M. (2015). Structural Components of Synaptic Plasticity and Memory Consolidation. *Cold Spring Harb Perspect. Biol.* 7 (7), a021758. doi:10.1101/cshperspect.a021758

Bazinet, R. P., and Layé, S. (2014). Polyunsaturated Fatty Acids and Their Metabolites in Brain Function and Disease. *Nat. Rev. Neurosci.* 15 (12), 771–785. doi:10.1038/nrn3820

Bennett, S. A. L., Valenzuela, N., Xu, H., Franko, B., Fai, S., and Figeys, D. (2013). Using Neurolipidomics to Identify Phospholipid Mediators of Synaptic (Dys)function in Alzheimer's Disease. *Front. Physiol.* 4, 168. doi:10.3389/fphys.2013.00168

Bishop, N. A., Lu, T., and Yankner, B. A. (2010). Neural Mechanisms of Ageing and Cognitive Decline. *Nature* 464 (7288), 529–535. doi:10.1038/nature08983

Bondareff, W., and Geinisman, Y. (1976). Loss of Synapses in the Dentate Gyrus of the Senescent Rat. *Am. J. Anat.* 145 (1), 129–136. doi:10.1002/aja.1001450110

Bourque, M., Grégoire, L., and Di Paolo, T. (2018). The Plasmalogen Precursor Analog PPI-1011 Reduces the Development of L-DOPA-Induced Dyskinesias in De Novo MPTP Monkeys. *Behav. Brain Res.* 337, 183–185. doi:10.1016/j.bbr.2017.09.023

Bozelli, J. C., and Epand, R. M. (2021). Plasmalogen Replacement Therapy. *Membranes* 11 (11), 838. doi:10.3390/membranes11110838

Bozelli, J. C., Jr., Azher, S., and Epand, R. M. (2021). Plasmalogens and Chronic Inflammatory Diseases. *Front. Physiol.* 12, 730829. doi:10.3389/fphys.2021.730829

Braverman, N. E., and Moser, A. B. (2012). Functions of Plasmalogen Lipids in Health and Disease. *Biochim. Biophys. Acta (Bba) - Mol. Basis Dis.* 1822 (9), 1442–1452. doi:10.1016/j.bbadis.2012.05.008

Brites, P., Waterham, H. R., and Wanders, R. J. A. (2004). Functions and Biosynthesis of Plasmalogens in Health and Disease. *Biochim. Biophys. Acta (Bba) - Mol. Cel Biol. Lipids* 1636 (2-3), 219–231. doi:10.1016/j.bbalip.2003.12.010

Brodde, A., Teigler, A., Brugger, B., Lehmann, W. D., Wieland, F., Berger, J., et al. (2012). Impaired Neurotransmission in Ether Lipid-Deficient Nerve Terminals. *Hum. Mol. Genet.* 21 (12), 2713–2724. doi:10.1093/hmg/dds097

Burke, S. N., and Barnes, C. A. (2006). Neural Plasticity in the Ageing Brain. *Nat. Rev. Neurosci.* 7 (1), 30–40. doi:10.1038/nrn1809

Colom-Cadena, M., Spires-Jones, T., Spires-Jones, T., Zetterberg, H., Blennow, K., Caggiano, A., et al.Group Synaptic Health Endpoints Working (2020). The Clinical Promise of Biomarkers of Synapse Damage or Loss in Alzheimer's Disease. *Alz Res. Ther.* 12 (1), 21. doi:10.1186/s13195-020-00588-4

Corrada, M. M., Brookmeyer, R., Berlau, D., Paganini-Hill, A., and Kawas, C. H. (2008). Prevalence of Dementia after Age 90: Results from the 90+ Study. *Neurology* 71 (5), 337–343. doi:10.1212/01.wnl.0000310773.65918.cd

Darios, F., and Davletov, B. (2006). Omega-3 and omega-6 Fatty Acids Stimulate Cell Membrane Expansion by Acting on Syntaxin 3. *Nature* 440 (7085), 813–817. doi:10.1038/nature04598

Davletov, B., and Montecucco, C. (2010). Lipid Function at Synapses. *Curr. Opin. Neurobiol.* 20 (5), 543–549. doi:10.1016/j.conb.2010.06.008

Davletov, B., Connell, E., and Darios, F. (2007). Regulation of SNARE Fusion Machinery by Fatty Acids. *Cell. Mol. Life Sci.* 64 (13), 1597–1608. doi:10.1007/s00018-007-6557-5

Dickstein, D. L., Kabaso, D., Rocher, A. B., Luebke, J. I., Wearne, S. L., and Hof, P. R. (2007). Changes in the Structural Complexity of the Aged Brain. *Aging Cell* 6 (3), 275–284. doi:10.1111/j.1474-9726.2007.00289.x

Dorninger, F., Forss-Petter, S., and Berger, J. (2017). From Peroxisomal Disorders to Common Neurodegenerative Diseases - the Role of Ether Phospholipids in the Nervous System. *FEBS Lett.* 591 (18), 2761–2788. doi:10.1002/1873-3468.12788

Dorninger, F., König, T., Scholze, P., Berger, M. L., Zeitler, G., Wiesinger, C., et al. (2019). Disturbed Neurotransmitter Homeostasis in Ether Lipid Deficiency. *Hum. Mol. Genet.* 28 (12), 2046–2061. doi:10.1093/hmg/ddz040

Dorninger, F., Forss-Petter, S., Wimmer, I., and Berger, J. (2020). Plasmalogens, Platelet-Activating Factor and beyond - Ether Lipids in Signaling and Neurodegeneration. *Neurobiol. Dis.* 145, 105061. doi:10.1016/j.nbd.2020.105061

Dragonas, C., Bertsch, T., Sieber, C. C., and Brosche, T. (2009). Plasmalogens as a Marker of Elevated Systemic Oxidative Stress in Parkinson's Disease. *Clin. Chem. Lab. Med.* 47 (7), 894–897. doi:10.1515/CCLM.2009.205

Ekdahl, C. T., Claasen, J.-H., Bonde, S., Kokaia, Z., and Lindvall, O. (2003). Inflammation Is Detrimental for Neurogenesis in Adult Brain. *Proc. Natl. Acad. Sci.* 100 (23), 13632–13637. doi:10.1073/pnas.2234031100

Fabelo, N., Martín, V., Santpere, G., Marín, R., Torrent, L., Ferrer, I., et al. (2011). Severe Alterations in Lipid Composition of Frontal Cortex Lipid Rafts from Parkinson's Disease and Incidental Parkinson's Disease. *Mol. Med.* 17 (9-10), 1107–1118. doi:10.2119/molmed.2011.00119

Fallatah, W., Smith, T., Cui, W., Jayasinghe, D., Di Pietro, E., Ritchie, S. A., et al. (2020). Oral Administration of a Synthetic Vinyl-Ether Plasmalogen Normalizes Open Field Activity in a Mouse Model of Rhizomelic Chondrodysplasia Punctata. *Dis. Model. Mech.* 13 (1), dmm042499. doi:10.1242/dmm.042499

Fan, X., Wheatley, E. G., and Villeda, S. A. (2017). Mechanisms of Hippocampal Aging and the Potential for Rejuvenation. *Annu. Rev. Neurosci.* 40 (1), 251–272. doi:10.1146/annurev-neuro-072116-031357

Ferreira, H. B., Melo, T., Monteiro, A., Paiva, A., Domingues, P., and Domingues, M. R. (2021). Serum Phospholipidomics Reveals Altered Lipid Profile and Promising Biomarkers in Multiple Sclerosis. *Arch. Biochem. Biophys.* 697, 108672. doi:10.1016/j.abb.2020.108672

Fraser, H. B., Khaitovich, P., Plotkin, J. B., Pääbo, S., and Eisen, M. B. (2005). Aging and Gene Expression in the Primate Brain. *Plos Biol.* 3 (9), e274. doi:10.1371/journal.pbio.0030274

Fujino, T., Yamada, T., Asada, T., Tsuboi, Y., Wakana, C., Mawatari, S., et al. (2017). Efficacy and Blood Plasmalogen Changes by Oral Administration of Plasmalogen in Patients with Mild Alzheimer's Disease and Mild Cognitive Impairment: A Multicenter, Randomized, Double-Blind, Placebo-Controlled Trial. *EBioMedicine* 17, 199–205. doi:10.1016/j.ebiom.2017.02.012

Fujino, T., Yamada, T., Asada, T., Ichimaru, M., Tsuboi, Y., Wakana, C., et al. (2018). Effects of Plasmalogen on Patients with Mild Cognitive Impairment: A Randomized, Placebo-Controlled Trial in Japan. *J. Alzheimers Dis. Parkinsonism* 08 (01), 419. doi:10.4172/2161-0460.1000419

Geinisman, Y., de Toledo-Morrell, L., and Morrell, F. (1986). Loss of Perforated Synapses in the Dentate Gyrus: Morphological Substrate of Memory Deficit in Aged Rats. *Proc. Natl. Acad. Sci.* 83 (9), 3027–3031. doi:10.1073/pnas.83.9.3027

Geinisman, Y., de Toledo-Morrell, L., Morrell, F., Persina, I. S., and Rossi, M. (1992). Age-related Loss of Axospinous Synapses Formed by Two Afferent Systems in the Rat Dentate Gyrus as Revealed by the Unbiased Stereological Dissector Technique. *Hippocampus* 2 (4), 437–444. doi:10.1002/hipo.450020411

Glaser, P. E., and Gross, R. W. (1994). Plasmenylethanolamine Facilitates Rapid Membrane Fusion: a Stopped-Flow Kinetic Investigation Correlating the Propensity of a Major Plasma Membrane Constituent to Adopt an HII Phase with its Ability to Promote Membrane Fusion. *Biochemistry* 33 (19), 5805–5812. doi:10.1021/bi00185a019

Goodenowe, D. B., Cook, L. L., Liu, J., Lu, Y., Jayasinghe, D. A., Ahiahonu, P. W. K., et al. (2007). Peripheral Ethanolamine Plasmalogen Deficiency: a Logical Causative Factor in Alzheimer's Disease and Dementia. *J. Lipid Res.* 48 (11), 2485–2498. doi:10.1194/jlr.P700023-JLR200

Gorgas, K., Teigler, A., Komljenovic, D., and Just, W. W. (2006). The Ether Lipid-Deficient Mouse: Tracking Down Plasmalogen Functions. *Biochim. Biophys. Acta (Bba) - Mol. Cel Res.* 1763 (12), 1511–1526. doi:10.1016/j.bbamcr.2006.08.038

Guan, Z., Wang, Y., Cairns, N. J., Lantos, P. L., Dallner, G., and Sindelar, P. J. (1999). Decrease and Structural Modifications of Phosphatidylethanolamine Plasmalogen in the Brain with Alzheimer Disease. *J. Neuropathol. Exp. Neurol.* 58 (7), 740–747. doi:10.1097/00005072-199907000-00008

Han, X., Holtzman, D. M., and McKeel, D. W., Jr. 2001. "Plasmalogen Deficiency in Early Alzheimer's Disease Subjects and in Animal Models: Molecular Characterization Using Electrospray Ionization Mass Spectrometry." *J. Neurochem.* 77 (4):1168–1180. doi: doi:doi:10.1046/j.1471-4159.2001.00332.x

Han, X. (2005). Lipid Alterations in the Earliest Clinically Recognizable Stage of Alzheimers Disease: Implication of the Role of Lipids in the Pathogenesis of Alzheimers Disease. *Curr. Alzheimer Res.* 2 (1), 65–77. doi:10.2174/1567205052772786

Hanisch, U.-K., and Kettenmann, H. (2007). Microglia: Active Sensor and Versatile Effector Cells in the normal and Pathologic Brain. *Nat. Neurosci.* 10 (11), 1387–1394. doi:10.1038/nn1997

Harry, G. J. (2013). Microglia during Development and Aging. *Pharmacol. Ther.* 139 (3), 313–326. doi:10.1016/j.pharmthera.2013.04.013

Hernandez-Nicaise, M.-L. (1973). The Nervous System of Ctenophores III. Ultrastructure of Synapses. *J. Neurocytol* 2 (3), 249–263. doi:10.1007/BF01104029

Heymans, H. S. A., Schutgens, R. B. H., Tan, R., van den Bosch, H., and Borst, P. (1983). Severe Plasmalogen Deficiency in Tissues of Infants without Peroxisomes (Zellweger Syndrome). *Nature* 306 (5938), 69–70. doi:10.1038/306069a0

Hofteig, J. H., Noronha, A. B., Druse, M. J., and Keresztes-Nagy, C. (1985). Synaptic Membrane Phospholipids: Effects of Maternal Ethanol Consumption. *Exp. Neurol.* 87 (1), 165–171. doi:10.1016/0014-4886(85)90142-6

Hossain, M. S., Abe, Y., Ali, F., Youssef, M., Honsho, M., Fujiki, Y., et al. (2017). Reduction of Ether-type Glycerophospholipids, Plasmalogens, by NF-Kb Signal Leading to Microglial Activation. *J. Neurosci.* 37 (15), 4074–4092. doi:10.1523/JNEUROSCI.3941-15.2017

Hossain, M. S., Tajima, A., Kotoura, S., and Katafuchi, T. (2018). Oral Ingestion of Plasmalogens Can Attenuate the LPS-Induced Memory Loss and Microglial Activation. *Biochem. Biophys. Res. Commun.* 496 (4), 1033–1039. doi:10.1016/j.bbrc.2018.01.078

Ifuku, M., Katafuchi, T., Mawatari, S., Noda, M., Miake, K., Sugiyama, M., et al. (2012). Anti-inflammatory/anti-amyloidogenic Effects of Plasmalogens in Lipopolysaccharide-Induced Neuroinflammation in Adult Mice. *J. Neuroinflamm.* 9 (1), 197. doi:10.1186/1742-2094-9-197

Janz, R., Südhof, T. C., Hammer, R. E., Unni, V., Siegelbaum, S. A., and Bolshakov, V. Y. (1999). Essential Roles in Synaptic Plasticity for Synaptogyrin I and Synaptophysin I. *Neuron* 24 (3), 687–700. doi:10.1016/S0896-6273(00)81122-8

Jiang, C. H., Tsien, J. Z., Schultz, P. G., and Hu, Y. (2001). The Effects of Aging on Gene Expression in the Hypothalamus and Cortex of Mice. *Proc. Natl. Acad. Sci.* 98 (4), 1930–1934. doi:10.1073/pnas.98.4.1930

Jiménez-Rojo, N., and Riezman, H. (2019). On the Road to Unraveling the Molecular Functions of Ether Lipids. *FEBS Lett.* 593, 2378–2389. doi:10.1002/1873-3468.13465

Jurkowitz, M. S., Horrocks, L. A., and Litsky, M. L. (1999). Identification and Characterization of Alkenyl Hydrolase (Lysoplasmalogenase) in Microsomes and Identification of a Plasmalogen-Active Phospholipase A2 in Cytosol of Small Intestinal Epithelium. *Biochim. Biophys. Acta (Bba) - Mol. Cel. Biol. Lipids* 1437 (2), 142–156. doi:10.1016/S1388-1981(99)00013-X

Kierdorf, K., and Prinz, M. (2017). Microglia in Steady State. *J. Clin. Invest.* 127 (9), 3201–3209. doi:10.1172/JCI90602

Koivuniemi, A. (2017). The Biophysical Properties of Plasmalogens Originating from Their Unique Molecular Architecture. *FEBS Lett.* 591 (18), 2700–2713. doi:10.1002/1873-3468.12754

Lagarde, M., Hachem, M., Bernoud-Hubac, N., Picq, M., Véricel, E., and Guichardant, M. (2015). Biological Properties of a DHA-Containing Structured Phospholipid (AceDoPC) to Target the Brain. *Prostaglandins, Leukot. Essent. Fatty Acids* 92, 63–65. doi:10.1016/j.plefa.2014.01.005

Lauwers, E., Goodchild, R., and Verstreken, P. (2016). Membrane Lipids in Presynaptic Function and Disease. *Neuron* 90 (1), 11–25. doi:10.1016/j.neuron.2016.02.033

Lessig, J., and Fuchs, B. (2009). Plasmalogens in Biological Systems: Their Role in Oxidative Processes in Biological Membranes, Their Contribution to Pathological Processes and Aging and Plasmalogen Analysis. *Curr. Med. Chem.* 16 (16), 2021–2041. doi:10.2174/092986709788682164

Lohner, K. (1996). Is the High Propensity of Ethanolamine Plasmalogens to Form Non-lamellar Lipid Structures Manifested in the Properties of Biomembranes. *Chem. Phys. Lipids* 81 (2), 167–184. doi:10.1016/0009-3084(96)02580-7

Lu, T., Pan, Y., Kao, S.-Y., Li, C., Kohane, I., Chan, J., et al. (2004). Gene Regulation and DNA Damage in the Ageing Human Brain. *Nature* 429 (6994), 883–891. doi:10.1038/nature02661

Macala, L. J., Yu, R. K., and Ando, S. (1983). Analysis of Brain Lipids by High Performance Thin-Layer Chromatography and Densitometry. *J. Lipid Res.* 24 (9), 1243–1250. doi:10.1016/S0022-2275(20)37906-2

Malheiro, A. R., Correia, B., Ferreira da Silva, T., Bessa-Neto, D., Van Veldhoven, P. P., and Brites, P. (2019). Leukodystrophy Caused by Plasmalogen Deficiency Rescued by Glyceryl 1-myristyl Ether Treatment. *Brain Pathol.* 29, 622–639. doi:10.1111/bpa.12710

Mawatari, S., Okuma, Y., and Fujino, T. (2007). Separation of Intact Plasmalogens and All Other Phospholipids by a Single Run of High-Performance Liquid Chromatography. *Anal. Biochem.* 370 (1), 54–59. doi:10.1016/j.ab.2007.05.020

Mawatari, S., Yunoki, K., Sugiyama, M., and Fujino, T. (2009). Simultaneous Preparation of Purified Plasmalogens and Sphingomyelin in Human Erythrocytes with Phospholipase A1fromAspergillus Orizae. *Biosci. Biotechnol. Biochem.* 73 (12), 2621–2625. doi:10.1271/bbb.90455

Mawatari, S., Ohara, S., Taniwaki, Y., Tsuboi, Y., Maruyama, T., and Fujino, T. (2020). Improvement of Blood Plasmalogens and Clinical Symptoms in Parkinson's Disease by Oral Administration of Ether Phospholipids: A Preliminary Report. *Parkinson's Dis.* 2020, 2671070. doi:10.1155/2020/2671070

Mecca, A. P., Chen, M. K., O'Dell, R. S., Naganawa, M., Toyonaga, T., Godek, T. A., et al. (2020). *In Vivo* measurement of Widespread Synaptic Loss in Alzheimer's Disease with SV2A PET. *Alzheimer's Demen.* 16 (7), 974–982. doi:10.1002/alz.12097

Monje, M. L., Toda, H., and Palmer, T. D. (2003). Inflammatory Blockade Restores Adult Hippocampal Neurogenesis. *Science* 302 (5651), 1760–1765. doi:10.1126/science.1088417

Nadeau, J., Smith, T., Lamontagne-Proulx, J., Bourque, M., Al Sweidi, S., Jayasinghe, D., et al. (2019). Neuroprotection and Immunomodulation in the Gut of Parkinsonian Mice with a Plasmalogen Precursor. *Brain Res.* 1725, 146460. doi:10.1016/j.brainres.2019.146460

Nagan, N., and Zoeller, R. A. (2001). Plasmalogens: Biosynthesis and Functions. *Prog. Lipid Res.* 40 (3), 199–229. doi:10.1016/S0163-7827(01)00003-0

Nguma, E., Yamashita, S., Kumagai, K., Otoki, Y., Yamamoto, A., Eitsuka, T., et al. (2021). Ethanolamine Plasmalogen Suppresses Apoptosis in Human Intestinal Tract Cells *In Vitro* by Attenuating Induced Inflammatory Stress. *ACS Omega* 6 (4), 3140–3148. doi:10.1021/acsomega.0c05545

Niraula, A., Sheridan, J. F., and Godbout, J. P. (2017). Microglia Priming with Aging and Stress. *Neuropsychopharmacol* 42 (1), 318–333. doi:10.1038/npp.2016.185

Njie, E. G., Boelen, E., Stassen, F. R., Steinbusch, H. W. M., Borchelt, D. R., and Streit, W. J. (2012). *Ex Vivo* cultures of Microglia from Young and Aged Rodent Brain Reveal Age-Related Changes in Microglial Function. *Neurobiol. Aging* 33 (1), e1–195. doi:10.1016/j.neurobiolaging.2010.05.008

Otoki, Y., Kato, S., Kimura, F., Furukawa, K., Yamashita, S., Arai, H., et al. (2017). Accurate Quantitation of Choline and Ethanolamine Plasmalogen Molecular Species in Human Plasma by Liquid Chromatography-Tandem Mass Spectrometry. *J. Pharm. Biomed. Anal.* 134, 77–85. doi:10.1016/j.jpba.2016.11.019

Park, H., and Poo, M.-m. (2013). Neurotrophin Regulation of Neural Circuit Development and Function. *Nat. Rev. Neurosci.* 14 (1), 7–23. doi:10.1038/nrn3379

Podgórski, P., Bladowska, J., Sasiadek, M., and Zimny, A. (2021). Novel Volumetric and Surface-Based Magnetic Resonance Indices of the Aging Brain - Does Male and Female Brain Age in the Same Way. *Front. Neurol.* 12 (774), 645729. doi:10.3389/fneur.2021.645729

Poitelon, Y., Kopec, A. M., and Belin, S. (2020). Myelin Fat Facts: An Overview of Lipids and Fatty Acid Metabolism. *Cells* 9 (4), 812. doi:10.3390/cells9040812

Poo, M.-m. (2001). Neurotrophins as Synaptic Modulators. *Nat. Rev. Neurosci.* 2 (1), 24–32. doi:10.1038/35049004

Post, J. A., Verkleij, A. J., Roelofsen, B., and Op de Kamp, J. A. (1988). Plasmalogen Content and Distribution in the Sarcolemma of Cultured Neonatal Rat Myocytes. *FEBS Lett.* 240 (1), 78–82. doi:10.1016/0014-5793(88)80343-0

Pradas, I., Jové, M., Huynh, K., Puig, J., Ingles, M., Borras, C., et al. (2019). Exceptional Human Longevity Is Associated with a Specific Plasma Phenotype of Ether Lipids. *Redox Biol.* 21, 101127. doi:10.1016/j.redox.2019.101127

Rog, T., and Koivuniemi, A. (2016). The Biophysical Properties of Ethanolamine Plasmalogens Revealed by Atomistic Molecular Dynamics Simulations. *Biochim. Biophys. Acta (Bba) - Biomembr.* 1858 (1), 97–103. doi:10.1016/j.bbamem.2015.10.023

Rossi, D. J., Jamieson, C. H. M., and Weissman, I. L. (2008). Stems Cells and the Pathways to Aging and Cancer. *Cell* 132 (4), 681–696. doi:10.1016/j.cell.2008.01.036

Rubio, J. M., Astudillo, A. M., Casas, J., Balboa, M. A., and Balsinde, J. (2018). Regulation of Phagocytosis in Macrophages by Membrane Ethanolamine Plasmalogens. *Front. Immunol.* 9, 1723. doi:10.3389/fimmu.2018.01723

Schedin, S., Sindelar, P. J., Pentchev, P., Brunk, U., and Dallner, G. (1997). Peroxisomal Impairment in Niemann-Pick Type C Disease. *J. Biol. Chem.* 272 (10), 6245–6251. doi:10.1074/jbc.272.10.6245

Schönknecht, P., Pantel, J., Kruse, A., and Schröder, J. (2005). Prevalence and Natural Course of Aging-Associated Cognitive Decline in a Population-Based Sample of Young-Old Subjects. *Am. J. Psychiatry* 162 (11), 2071–2077. doi:10.1176/appi.ajp.162.11.2071

Sejimo, S., Hossain, M. S., and Akashi, K. (2018). Scallop-derived Plasmalogens Attenuate the Activation of PKCδ Associated with the Brain Inflammation. *Biochem. Biophys. Res. Commun.* 503 (2), 837–842. doi:10.1016/j.bbrc.2018.06.084

Selkoe, D. J. (2002). Alzheimer's Disease Is a Synaptic Failure. *Science* 298 (5594), 789–791. doi:10.1126/science.1074069

Senanayake, V., and Goodenowe, D. B. (2019). Plasmalogen Deficiency and Neuropathology in Alzheimer's Disease: Causation or Coincidence. *Alzheimers Dement (N Y)* 5, 524–532. doi:10.1016/j.trci.2019.08.003

Siegel, D. P., and Epand, R. M. (1997). The Mechanism of Lamellar-To-Inverted Hexagonal Phase Transitions in Phosphatidylethanolamine: Implications for Membrane Fusion Mechanisms. *Biophys. J.* 73 (6), 3089–3111. doi:10.1016/S0006-3495(97)78336-X

Sierra, A., Gottfried-Blackmore, A. C., McEwen, B. S., and Bulloch, K. (2007). Microglia Derived from Aging Mice Exhibit an Altered Inflammatory Profile. *Glia* 55 (4), 412–424. doi:10.1002/glia.20468

Sierra, A., Encinas, J. M., Deudero, J. J. P., Chancey, J. H., Enikolopov, G., Overstreet-Wadiche, L. S., et al. (2010). Microglia Shape Adult Hippocampal Neurogenesis through Apoptosis-Coupled Phagocytosis. *Cell Stem Cell* 7 (4), 483–495. doi:10.1016/j.stem.2010.08.014

Skotland, T., Hessvik, N. P., Sandvig, K., and Llorente, A. (2019). Exosomal Lipid Composition and the Role of Ether Lipids and Phosphoinositides in Exosome Biology. *J. Lipid Res.* 60 (1), 9–18. doi:10.1194/jlr.R084343

Streit, W. J., Sammons, N. W., Kuhns, A. J., and Sparks, D. L. (2004). Dystrophic Microglia in the Aging Human Brain. *Glia* 45 (2), 208–212. doi:10.1002/glia.10319

Südhof, T. C. (1995). The Synaptic Vesicle Cycle: a cascade of Protein-Protein Interactions. *Nature* 375 (6533), 645–653. doi:10.1038/375645a0

Su, X. Q., Wang, J., and Sinclair, A. J. (2019). Plasmalogens and Alzheimer's Disease: a Review. *Lipids Health Dis.* 18 (1), 100. doi:10.1186/s12944-019-1044-1

Takamori, S., Holt, M., Stenius, K., Lemke, E. A., Grønborg, M., Riedel, D., et al. (2006). Molecular Anatomy of a Trafficking Organelle. *Cell* 127 (4), 831–846. doi:10.1016/j.cell.2006.10.030

Villeda, S. A., Luo, J., Mosher, K. I., Zou, B., Britschgi, M., Bieri, G., et al. (2011). The Ageing Systemic Milieu Negatively Regulates Neurogenesis and Cognitive Function. *Nature* 477 (7362), 90–94. doi:10.1038/nature10357

Vorhees, C. V., and Williams, M. T. (2006). Morris Water Maze: Procedures for Assessing Spatial and Related Forms of Learning and Memory. *Nat. Protoc.* 1 (2), 848–858. doi:10.1038/nprot.2006.116

Wood, P. L., Smith, T., Lane, N., Khan, M. A., Ehrmantraut, G., and Goodenowe, D. B. (2011). Oral Bioavailability of the Ether Lipid Plasmalogen Precursor, PPI-1011, in the Rabbit: a New Therapeutic Strategy for Alzheimer's Disease. *Lipids Health Dis.* 10, 227. doi:10.1186/1476-511X-10-227

Wood, P. L., Barnette, B. L., Kaye, J. A., Quinn, J. F., and Woltjer, R. L. (2015). Non-targeted Lipidomics of CSF and Frontal Cortex Grey and white Matter in Control, Mild Cognitive Impairment, and Alzheimer's Disease Subjects. *Acta Neuropsychiatr.* 27 (5), 270–278. doi:10.1017/neu.2015.18

Wood, P. L., Mankidy, R., Ritchie, S., Heath, D., Wood, J. A., Flax, J., et al. (2010). Circulating Plasmalogen Levels and Alzheimer Disease Assessment Scale-Cognitive Scores in Alzheimer Patients. *J. Psychiatry Neurosci.* 35 (1), 59–62. doi:10.1503/jpn.090059

Wu, L.-C., Pfeiffer, D. R., Calhoon, E. A., Madiai, F., Marcucci, G., Liu, S., et al. (2011). Purification, Identification, and Cloning of Lysoplasmalogenase, the Enzyme that Catalyzes Hydrolysis of the Vinyl Ether Bond of Lysoplasmalogen. *J. Biol. Chem.* 286 (28), 24916–24930. doi:10.1074/jbc.M111.247163

Xicoy, H., Wieringa, B., and Martens, G. J. M. (2019). The Role of Lipids in Parkinson's Disease. *Cells* 8 (1), 27. doi:10.3390/cells8010027

Yamashita, S., Honjo, A., Aruga, M., Nakagawa, K., and Miyazawa, T. (2014). Preparation of Marine Plasmalogen and Selective Identification of Molecular Species by LC-MS/MS. *J. Oleo Sci.* 63 (5), 423–430. doi:10.5650/jos.ess13188

Yamashita, S., Kanno, S., Honjo, A., Otoki, Y., Nakagawa, K., Kinoshita, M., et al. (2016a). Analysis of Plasmalogen Species in Foodstuffs. *Lipids* 51 (2), 199–210. doi:10.1007/s11745-015-4112-y

Yamashita, S., Kiko, T., Fujiwara, H., Hashimoto, M., Nakagawa, K., Kinoshita, M., et al. (2016b). Alterations in the Levels of Amyloid-β, Phospholipid Hydroperoxide, and Plasmalogen in the Blood of Patients with Alzheimer's Disease: Possible Interactions between Amyloid-β and These Lipids. *J. Alzheimers Dis.* 50 (2), 527–537. doi:10.3233/JAD-150640

Yamashita, S., Hashimoto, M., Haque, A. M., Nakagawa, K., Kinoshita, M., Shido, O., et al. (2017). Oral Administration of Ethanolamine Glycerophospholipid Containing a High Level of Plasmalogen Improves Memory Impairment in Amyloid β-Infused Rats. *Lipids* 52 (7), 575–585. doi:10.1007/s11745-017-4260-3

Yamashita, S., Fujiwara, K., Tominaga, Y., Nguma, E., Takahashi, T., Otoki, Y., et al. (2021). Absorption Kinetics of Ethanolamine Plasmalogen and its Hydrolysate in Mice. *J. Oleo Sci.* 70 (2), 263–273. doi:10.5650/jos.ess20223

Young, K., and Morrison, H. (2018). Quantifying Microglia Morphology from Photomicrographs of Immunohistochemistry Prepared Tissue Using ImageJ. *J. Vis. Exp.* 136, e57648. doi:10.3791/57648

Youssef, M., Ibrahim, A., Akashi, K., and Hossain, M. S. (2019). PUFA-plasmalogens Attenuate the LPS-Induced Nitric Oxide Production by Inhibiting the NF-kB, P38 MAPK and JNK Pathways in Microglial Cells. *Neuroscience* 397, 18–30. doi:10.1016/j.neuroscience.2018.11.030

Yuan, Y., Chen, Y. P. P., Boyd-Kirkup, J., Khaitovich, P., and Somel, M. (2012). Accelerated Aging-related Transcriptome Changes in the Female Prefrontal Cortex. *Aging Cell* 11 (5), 894–901. doi:10.1111/j.1474-9726.2012.00859.x

Conflict of Interest: The authors declare that the research was conducted in the absence of any commercial or financial relationships that could be construed as a potential conflict of interest.

Publisher's Note: All claims expressed in this article are solely those of the authors and do not necessarily represent those of their affiliated organizations, or those of the publisher, the editors, and the reviewers. Any product that may be evaluated in this article, or claim that may be made by its manufacturer, is not guaranteed or endorsed by the publisher.

frontiers in Cell and Developmental Biology

ORIGINAL RESEARCH
published: 22 March 2022
doi: 10.3389/fcell.2022.836186

Lymphatic Absorption of Microbial Plasmalogens in Rats

Nana Sato[1†], *Aki Kanehama*[1†], *Akiko Kashiwagi*[2], *Miwa Yamada*[1,3*] and *Megumi Nishimukai*[3,4*]

[1]Faculty of Agriculture, Department of Biological Chemistry and Food Science, Iwate University, Morioka, Japan, [2]Faculty of Agriculture and Life Science, Hirosaki University, Hirosaki, Japan, [3]Agri-Innovation Center, Iwate University, Morioka, Japan, [4]Department of Animal Science, Faculty of Agriculture, Iwate University, Morioka, Japan

OPEN ACCESS

Edited by:
Masanori Honsho,
Kyushu University, Japan

Reviewed by:
Mikhail Y. Golovko,
University of North Dakota, United States
Oskar Engberg,
University Hospital Leipzig, Germany
Yuichi Abe,
Kyushu University, Japan

***Correspondence:**
Miwa Yamada
myamada@iwate-u.ac.jp
Megumi Nishimukai
nmegumi@iwate-u.ac.jp

[†]These authors have contributed equally to this work

Specialty section:
This article was submitted to Cellular Biochemistry, a section of the journal Frontiers in Cell and Developmental Biology

Received: 15 December 2021
Accepted: 21 February 2022
Published: 22 March 2022

Citation:
Sato N, Kanehama A, Kashiwagi A, Yamada M and Nishimukai M (2022) Lymphatic Absorption of Microbial Plasmalogens in Rats. Front. Cell Dev. Biol. 10:836186. doi: 10.3389/fcell.2022.836186

Plasmalogens, functional glycerophospholipids with biological roles in the human body, are associated with various diseases. Although a variety of saturated and/or unsaturated fatty acids in plasmalogens are presumed to have different functions in the human body, there are limited reports validating such functions of plasmalogens. In this study, we focused on the bacterial plasmalogen derived from *Selenomonas ruminantium* subsp. *lactilytica* (NBRC No. 103574) with different main species of hydrocarbon chains at the *sn*-1 position and shorter fatty acids at the *sn*-2 position than animal plasmalogens. Optimum culture conditions of *S. ruminantium* for high-yield production of plasmalogens, such as pH and the concentration of caproic acid, were investigated under anaerobic conditions using a 2-L scale jar fermenter. The obtained plasmalogen mainly consisted of the ethanolamine plasmalogen (PlsEtn). The molar ratios of PlsEtn species obtained from *S. ruminantium*, at *sn*-1/*sn*-2 positions, were p16:1/14:0 (68.4%), p16:1/16:1 (29.2%), p16:1/16:0 (0.7%), p16:1/15:0 (0.3%), and p17:1/14:0 (0.3%). Subsequently, duodenal infusion of the emulsion carrying the lipid extracted from *S. ruminantium* was carried out in lymph duct-cannulated rats. In the lymphatic plasmalogen of rats, the level of PlsEtns with molar ratios p16:1/14:0 and p16:1/16:1, the main species of plasmalogens from *S. ruminantium*, increased gradually until 3–4 h after lipid injection and then gradually decreased. In addition, the level of PlsEtns with p16:1/20:4 and p16:1/22:6 rapidly increased, peaking at 1–1.5 h and 1.5–2 h after lipid injection, respectively. The increase in the number of PlsEtns with p16:1/20:4 and p16:1/22:6 suggested that 20:4 and 22:6, the main fatty acids at the *sn*-2 position in the rat lymphatic plasmalogen, were preferentially re-esterified at the *sn*-2 position, regardless of the types of hydrocarbon chains at the *sn*-1 position. Thus, we showed that bacterial PlsEtns with "unnatural" structures against rats could be absorbed into the lymph. Our findings provide insights into the association between the chemical structure of plasmalogens and their biological functions in humans.

Keywords: ethanolamine plasmalogen, *Selenomonas ruminantium*, lymphatic absorption, molecular species, microbial plasmalogen

INTRODUCTION

Glycerophospholipids, the main components of biological membranes, play important roles in maintaining the structure and function of biological membranes, as well as in the overall physiology of the organism. They are classified into three subclasses: diacyl, alkyl, and alkenyl, based on the aliphatic hydrocarbon chain at the *sn*-1 position of the glycerol backbone, *via* ester, ether, and vinyl-ether binding, respectively.

Plasmalogens that we focused on the present study are a subclass of glycerophospholipids containing a vinyl-ether bond at the *sn*-1 position and an ester bond at the *sn*-2 position of the glycerol backbone (**Figure 1**). The *sn*-1 and -2 positions consist of saturated and/or unsaturated fatty acids (FAs) with various carbon chains. It is well known that plasmalogens are present in human and animal tissues (Bradley et al., 2015). In the brain and lungs, the content of ethanolamine plasmalogen (PlsEtn), which has ethanolamine bound to the phosphate group at the *sn*-3 position, is relatively higher than that in other organs (Panganamala et al., 1971; Heymans et al., 1983). In addition, the heart contains choline plasmalogen (PlsCho), which has choline bound to the phosphate group at the *sn*-3 position (Panganamala et al., 1971; Heymans et al., 1983).

Multiple physiological functions of plasmalogens have been presumed: 1) structural components of the cell membrane (Lee, 1998; Nagan and Zoeller, 2001), 2) maintaining cell membrane dynamics (Koivuniemi, 2017), 3) storage compounds of arachidonic acid, a precursor of functional lipid mediators (Garg and Haerdi, 1993), and 4) antioxidants. The antioxidant effect was confirmed by both *in vivo* and *in vitro* radical scavenger examination of reactive oxygen species, and was found to be a result of the vinyl-ether double bond of plasmalogens (Hahnel et al., 1999a; Maeba and Ueta, 2003; Wu et al., 2019). It is not certain whether this antioxidative ability of plasmalogens is the main cause or not, but many previous studies have reported that the composition of plasmalogens is strongly related to the etiopathogenesis of many kinds of diseases (Ginsberg et al., 1995; Hahnel et al., 1999b; Maeba et al., 2007; Khan et al., 2008; Nishimukai et al., 2014a; Nishimukai et al., 2014b). For instance, the presence of plasmalogens in the serum reportedly prevented arteriosclerosis, and a deficiency of plasmalogens was involved in nerve degeneration in Alzheimer's disease (Goodenowe et al., 2007; Su et al., 2019). Thus, understanding of the physiological function of plasmalogens can provide clarity on disease pathogenesis and/or its prevention.

Plasmalogens are contained in the cell membrane of not only animals but also some strictly anaerobic bacteria such as *Selenomonas ruminantium*, *Ruminococcus albus*, *Ruminococcus flavefaciens*, *Bacteroides succinogenes*, *Borrelia* sp., and *Clostridium butyricum*, which are classified as rumen bacteria (Kamio et al., 1969). In particular, *S. ruminantium* has been well studied as a typical bacterium which contains plasmalogens in the cell membrane (Kamio et al., 1970). Kanegasaki and Takahashi demonstrated that plasmalogens are derived from FA present in the medium containing glucose and ^{14}C-labeled FAs used for cultivating *S. ruminantium* and the phospholipid (PL) fraction obtained from ethanol–ether extraction of the cultivated cells

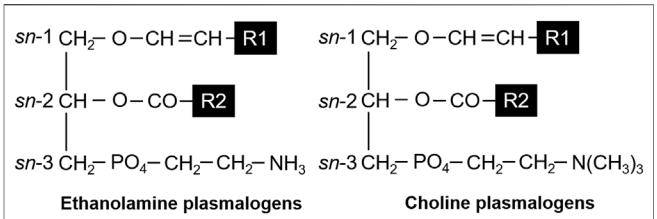

FIGURE 1 | Structures of ethanolamine plasmalogens (PlsEtn) and choline plasmalogens (PlsCho). R1 and R2 denote the carbon chain at the *sn*-1 and *sn*-2 positions, respectively.

(Kanegasaki and Takahashi, 1968). Furthermore, it was reported that the type of energy source in the culture medium affects the plasmalogen content in *S. ruminantium* (Kamio et al., 1969; Kim et al., 1970; Takatsuka and Kamio, 2004). The plasmalogen content of *S. ruminantium* cultivated in a medium containing lactate was approximately three times higher than that of the cells cultivated in a medium containing glucose. Although microbial cells mainly contain PlsEtns, a difference in the chemical structure is found between microbial and animal plasmalogens. Microbial plasmalogens have FAs with a shorter carbon chain length at the *sn*-1 and -2 positions compared to animal plasmalogens (Watanabe et al., 1982). Thus, microorganisms are a good source of plasmalogens which consist of FAs different from that of animal plasmalogens.

In this study, our final goal is to elucidate the physiological structure–function correlation of plasmalogens in humans by comparing the function of plasmalogens having "unnatural" chemical structures against mammals. We investigated optimum large-scale culture conditions, such as the concentration of FAs and pH, to obtain high productivity of microbial plasmalogens derived from *S. ruminantium*. However, plasmalogens are unstable compounds and easily broken under acidic conditions, such as in the stomach, because of its vinyl-ether bond at the *sn*-1 position (**Figure 1**). We assumed to utilize capsules containing plasmalogens to absorb intact plasmalogens into the small intestine in our future experiments. It is important to perform not only general gavage experiments but also lymphatic absorption experiments. Thus, the lymphatic absorption of microbial plasmalogens from the small intestine was studied using lymph duct-cannulated rats as a first step toward our goal.

MATERIALS AND METHODS

Strain and Culture Conditions

S. ruminantium subsp. *lactilytica* (NBRC No. 103574) (Kaneko et al., 2015) was obtained from the National Institute of Technology and Evaluation. The seed culture was carried out in 100-ml sealed vials containing 100 ml of the 988TYG medium (pH 7.0) at 37°C for 24 h under anaerobic conditions. Eighty milliliters of the culture was inoculated into a 2-L jar fermenter (M-1000B, EYELA, Tokyo, Japan) containing 2.1 L of the 988TYG medium and then incubated at 37°C with N_2 gas

flowing. The 988TYG medium contained 0.2% trypticase, 0.2% yeast extract, 0.5% glucose, 0.02% caproic acid sodium salt, 0.3% Na_2CO_3, 0.09% KH_2PO_4, 0.09% NaCl, 0.09% $(NH_4)_2SO_4$, 0.001% $MnCl_2{\cdot}4H_2O$, 0.001% $CoCl_2{\cdot}6H_2O$, 0.001% $CaCl_2{\cdot}2H_2O$, and 0.0001% resazurin. After air in the 988TYG medium was partially replaced with N_2, the medium was autoclaved, and then, 0.2 ml (for 100 ml medium) or 4.2 ml (for 2.1 L medium) of filter-sterilized L-cysteine hydrochloride solution (250 mg/ml) was aseptically added to the medium using syringes.

Extraction of Lipids From *S. ruminantium* and Porcine Brain

After cultivation, the cells were harvested by centrifugation (6,400 g × 15 min, 4°C) and washed thrice with distilled water. The microbial cells or porcine brain were lyophilized using an FD-1000 vacuum freeze dryer (EYELA, Japan) at −80°C for 2 days. Lipids were extracted with chloroform/methanol/1% KCl solution (1.1: 1.1: 1, by volume), followed by extraction with chloroform twice. All extract solutions were collected, evaporated to dryness, and dissolved in methanol. This fraction was analyzed by ultra-performance liquid chromatography–electrospray ionization tandem mass spectrometry (UPLC/ESI-MS/MS) and subjected to further experiments.

Preparation of Emulsion

The extracted lipids (25 g/L) from *S. ruminantium* and porcine brain in a 1 ml emulsified solution contained 1.83 and 2.77 μmol PlsEtn (estimated average molecular weight, 638 and 768), respectively. The FA composition and molecular species composition of plasmalogens in the PlsEtn are shown in **Table 2**. These test lipid preparations were emulsified with sodium taurocholate (10 g/L) and triolein (75 g/L) using a sonicator just prior to use.

Animals

Male Wistar/ST rats (Japan SLC Inc., Hamamatsu, Japan), aged 9 weeks, were fed a standard diet (AIN 93G formula) for a 3-day acclimation period.

After overnight fasting, a vinyl catheter and a silicone catheter were implanted in the thoracic lymph duct and the duodenum, respectively, as described previously (Nishimukai et al., 2011). After the collection of lymph for 30 min (initial lymph) on the day after implanting the indwelling catheter, the rats were administered 1 ml of an emulsified test solution containing 25 mg test lipids for 1 min. The glucose-NaCl isotonic solution without test lipids was infused continuously at 1.8 ml/h through the duodenal tube after the implants of the catheter until the end of the experiment except during an administration of the emulsified test solution.

The lymph was collected from the thoracic duct lymph over time, that is, at 0.5 h intervals during the first 2 h and at 1-h intervals during the next 7 h, following the administration of the test solution. The collected lymph was frozen immediately and kept at −80°C until subsequent analyses.

This study was approved by the Iwate University Animal Committee (approval number; A201450), and animals were maintained in accordance with the Iwate University guideline for the care and use of laboratory animals.

Analyses

Total lipids in the lymphatic fluid were extracted by the Bligh & Dyer method (Bligh and Dyer, 1959). All plasmalogens in the lipid extracts were analyzed by UPLC/ESI-MS/MS, as previously described (Nishimukai et al., 2011; Nishimukai et al., 2014b). Briefly, liquid chromatography (LC) separation was performed using a Dionex UltiMate 3000 system (Thermo Fisher Scientific, Waltham, MA, United States) with a BEH C8 column (1.7 μm, 100 mm × 2.1 mm I.D.; Waters Corp., Milford, MA, United States) at 60°C and a flow rate of 0.45 ml/min. The mobile phase A consisted of water containing 5 mM ammonium formate, and the mobile phase B consisted of acetonitrile. Mass spectrometry (MS) analysis was performed using a TSQ Quantum Access MAX instrument (Thermo Fisher Scientific) equipped with an ESI probe in the positive ion mode. We checked many molecular species in a preliminary experiment and selected those in order of the quantity contained in the sample. PlsEtn was quantified according to the principles described (Zemski Berry and Murphy, 2004). In brief, PlsEtn was identified by fragments derived from the *sn*-1 position (p16:0, p16:1, p17:0, p17:1, and p18:1). "p" indicates the carbon chain of *sn*-1 in plasmalogens with a vinyl-ether linkage. PlsCho was identified by three fragments and was quantified by phosphocholine as a fragment ion at m/z 184 after the separation of each PlsCho molecule by UPLC. In addition, the presence of plasmalogens was confirmed by the disappearance of the peak after treatment with acid. The parent and fragment ions of the plasmalogen molecular species measured in this study are shown in **Table 1**. The collision energy for PlsCho and PlsEtn was 32 and 18 eV, respectively.

Synthetic p18:0–18:1 and p18:0–20:4 of PlsCho and PlsEtn, (Avanti Polar Lipids, Alabaster, AL, United States) were used to generate a standard curve to quantify individual species of ether glycerophospholipids. Total PlsEtn and PlsCho were taken as the sum of all molecular species in each class measured by UPLC-MS/MS. The lipid composition in the lipid extracts from bacteria and porcine brain was measured by thin layer chromatography on chromarods with flame ionization detection (FID) using an Iatroscan MK-6 instrument (Mitsubishi Chemical Yatron, Tokyo, Japan) (Watanabe et al., 2019).

Calculation and Statistical Analysis

Data are expressed as mean ± SEM (standard error of the mean). The results were analyzed by one-way analysis of variance followed by Dunnett multiple comparisons. Data analysis was performed by the add-in software Statcel 3 (OMS, Tokyo, Japan). Differences with $p < 0.05$ were taken to be statistically significant.

TABLE 1 | The parent and CID (collision induced dissociation) fragment ions of the measured plasmalogen molecular species.

PlsEtn				PlsCho			
***sn*-1**	***sn*-2**	**[M + H]$^+$**	**CID fragment ion**	***sn*-1**	***sn*-2**	**[M + H]$^+$**	**CID fragment ion**
p16:0	14:0	648.49	364	p16:0	14:0	690.54	184
	15:0	662.50	364		15:0	704.55	184
	15:1	660.49	364		15:1	702.54	184
	16:0	676.52	364		16:0	718.57	184
	16:1	674.50	364		16:1	716.55	184
	17:0	690.54	364		17:0	732.58	184
	17:1	688.52	364		17:1	730.57	184
	18:0	704.55	364		18:0	746.60	184
	18:1	702.54	364		18:1	744.58	184
	18:2	700.52	364		18:2	742.57	184
	20:4	724.52	364		20:4	766.57	184
	20:5	722.51	364		20:5	764.55	184
	22:4	752.55	364		22:4	794.60	184
	22:5	750.54	364		22:5	792.58	184
	22:6	748.52	364		22:6	790.57	184
p16:1	14:0	646.47	362	p16:1	14:0	688.52	184
	15:0	660.48	362		15:0	702.53	184
	15:1	658.47	362		15:1	700.52	184
	16:0	674.50	362		16:0	716.55	184
	16:1	672.48	362		16:1	714.53	184
	17:0	688.52	362		17:0	730.56	184
	17:1	686.50	362		17:1	728.55	184
	18:0	702.53	362		18:0	744.58	184
	18:1	700.52	362		18:1	742.56	184
	18:2	698.51	362		18:2	740.55	184
	20:4	722.51	362		20:4	764.55	184
	20:5	720.49	362		20:5	762.54	184
	22:4	750.54	362		22:4	792.58	184
	22:5	748.52	362		22:5	790.57	184
	22:6	746.51	362		22:6	788.55	184
p17:0	14:0	662.51	378	p17:0	14:0	704.56	184
	15:0	676.52	378		15:0	718.57	184
	15:1	674.51	378		15:1	716.56	184
	16:0	690.54	378		16:0	732.59	184
	16:1	688.52	378		16:1	730.57	184
	17:0	704.56	378		17:0	746.60	184
	17:1	702.54	378		17:1	744.59	184
	18:0	718.57	378		18:0	760.62	184
	18:1	716.56	378		18:1	758.60	184
	18:2	714.54	378		18:2	756.58	184
	20:4	738.54	378		20:4	780.58	184
	20:5	736.52	378		20:5	778.57	184
	22:4	766.57	378		22:4	808.61	184
	22:5	764.55	378		22:5	806.60	184
	22:6	762.54	378		22:6	804.58	184
p17:1	14:0	660.49	376	p17:1	14:0	702.54	184
	15:0	674.50	376		15:0	716.55	184
	15:1	672.49	376		15:1	714.54	184
	16:0	688.52	376		16:0	730.57	184
	16:1	686.50	376		16:1	728.55	184
	17:0	702.54	376		17:0	744.58	184
	17:1	700.52	376		17:1	742.57	184
	18:0	716.55	376		18:0	758.60	184
	18:1	714.54	376		18:1	756.58	184
	18:2	712.52	376		18:2	754.57	184
	20:4	736.52	376		20:4	778.57	184
	20:5	734.51	376		20:5	776.55	184
	22:4	764.55	376		22:4	806.60	184
	22:5	762.54	376		22:5	804.58	184
	22:6	760.52	376		22:6	802.57	184

(Continued on following page)

TABLE 1 | (*Continued*) The parent and CID (collision induced dissociation) fragment ions of the measured plasmalogen molecular species.

PlsEtn				PlsCho			
***sn*-1**	***sn*-2**	**[M + H]$^+$**	**CID fragment ion**	***sn*-1**	***sn*-2**	**[M + H]$^+$**	**CID fragment ion**
p18:0	14:0	676.52	392	p18:0	14:0	718.57	184
	15:0	690.53	392		15:0	732.58	184
	15:1	688.52	392		15:1	730.57	184
	16:0	704.55	392		16:0	746.60	184
	16:1	702.53	392		16:1	744.58	184
	17:0	718.57	392		17:0	760.61	184
	17:1	716.55	392		17:1	758.60	184
	18:0	732.58	392		18:0	774.63	184
	18:1	730.57	392		18:1	772.61	184
	18:2	728.55	392		18:2	770.60	184
	20:4	752.55	392		20:4	794.60	184
	20:5	750.54	392		20:5	792.58	184
	22:4	780.58	392		22:4	822.63	184
	22:5	778.57	392		22:5	820.62	184
	22:6	776.55	392		22:6	818.60	184
p18:1	14:0	674.51	390	p18:1	14:0	716.56	184
	15:0	688.52	390		15:0	730.57	184
	15:1	686.51	390		15:1	728.56	184
	16:0	702.54	390		16:0	744.59	184
	16:1	700.52	390		16:1	742.57	184
	17:0	716.56	390		17:0	758.60	184
	17:1	714.54	390		17:1	756.59	184
	18:0	730.57	390		18:0	772.62	184
	18:1	728.56	390		18:1	770.60	184
	18:2	726.54	390		18:2	768.58	184
	20:4	750.54	390		20:4	792.58	184
	20:5	748.52	390		20:5	790.57	184
	22:4	778.57	390		22:4	820.61	184
	22:5	776.55	390		22:5	818.60	184
	22:6	774.54	390		22:6	816.58	184

RESULTS

Effects of Caproic Acid Concentration and pH on Biosynthesis of PlsEtn in *S. ruminantium*

First, we optimized culture conditions such as the concentration of caproic acid and pH in a glucose medium for 2.1-L scale anaerobic cultivation of *S. ruminantium*. The effects from 0.001 to 0.04% caproic acid in the glucose medium (component is similar to the 988TYG medium except to concentration of caproic acid sodium salt) were examined at 37 °C and pH 7.0 for 24 h. Although there was no effect on the cell growth at different caproic acid concentrations (0.001–0.04%) (**Figure 2A**), PlsEtn production per 1 L culture broth was the maximum in the glucose medium containing 0.02% caproic acid (**Figure 2B**). Subsequently, we investigated the effect of pH on growth and PlsEtn production when *S. ruminantium* was cultured in the glucose medium containing 0.02% caproic acid at 37°C for 24 h. Growth increased along with pH from 6 to 8 (**Figure 2C**), but PlsEtn production was the highest at pH 7 (**Figure 2D**). The maximum PlsEtn production was 10.5 ± 3.5 μmol/L of culture broth, and the molar ratios of PlsEtn species were p16:1/14:0 (68.4%), p16:1/16:1 (29.2%), p16:1/15:0 (0.3%), p16:1/15:1 (0.1%), p16:1/16:0 (0.7%), and p17:1/14:0 (0.3%) (**Table 2**). Furthermore, phosphatidyl ethanolamine including PlsEtn accounted for 73% of the lipid extract from *S. ruminantium* (**Table 3**).

Lymphatic Absorption of PlsEtn Derived From *S. ruminantium* and Porcine Brain in Rats

To examine the characteristic of absorption of plasmalogens derived from *S. ruminantium*, the lymphatic output of plasmalogens in rats administered with bacterial plasmalogens from *S. ruminantium* or porcine brain was analyzed using the UPLC-MS/MS method and compared. In the lipid extract from porcine brain, the molar ratios of PlsEtn species were p18:1/18:1 (21.4%), p18:1/20:4 (13.7%), and p18:0/22:6 (12%) (**Table 2**). Phosphatidyl ethanolamine including PlsEtn accounted for 40.4% of the lipid extract (**Table 3**). In addition, phosphatidyl choline and sphingomyelin including PlsCho accounted for 23.3% of the lipid extract.

After the injection of the lipid derived from *S. ruminantium* containing the PlsEtn, the total PlsEtn output in the lymph was not significantly increased compared to that prior to the administration of the lipid emulsion containing plasmalogens

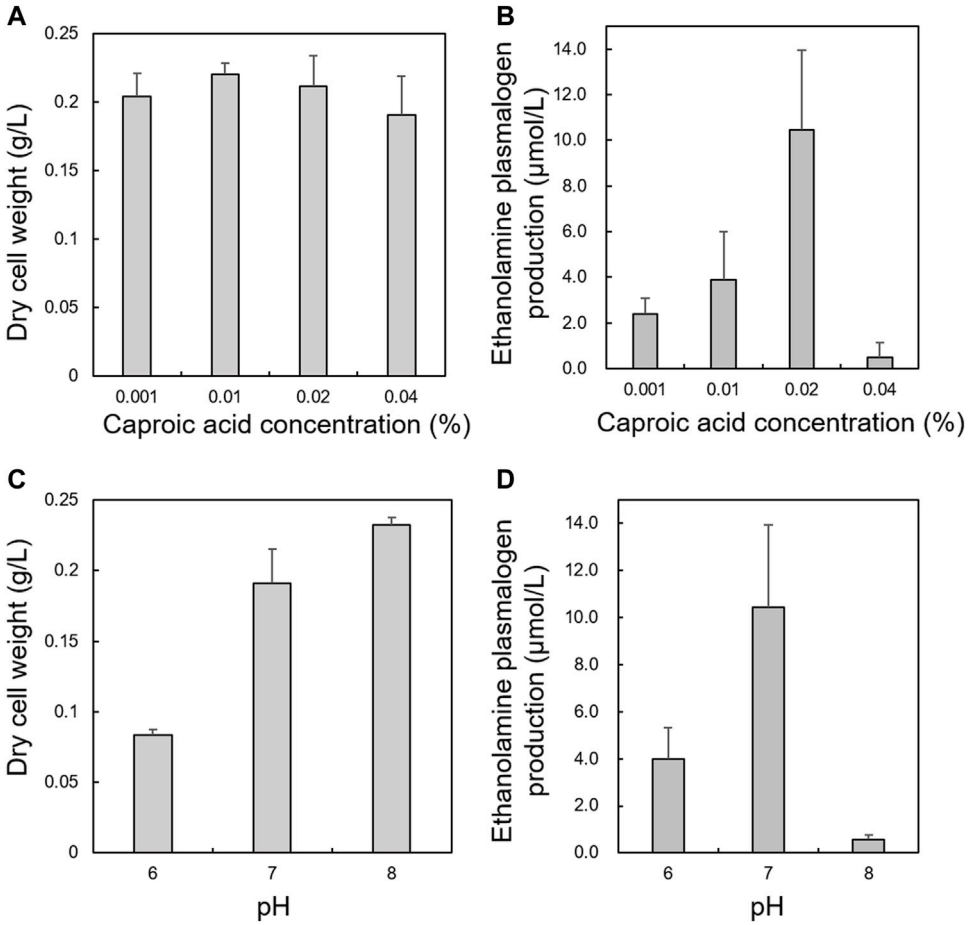

FIGURE 2 | Effects of caproic acid concentration and pH on growth and PlsEtn production in *S. ruminantium*. Effect of caproic acid at different concentrations on **(A)** growth of *S. ruminantium* and **(B)** PlsEtn production of *S. ruminantium* in the glucose medium at 37°C and pH 7.0 for 24 h. Effect of pH on **(C)** the growth of *S. ruminantium* and **(D)** PlsEtn production of *S. ruminantium* in the glucose medium containing 0.02% caproic acid at 37°C for 24 h. Dry cell weight was measured after freeze drying. PlsEtn production was measured by LC-MS/MS analysis of lipids extracted from dry cells. The data represent mean ± SD (n = 3).

(initial) (**Figure 3**). However, the level of PlsEtn containing p16:1 at the *sn*-1 position was increased, reaching a peak value at 1–4 h (**Figure 4A**). The molecular species of PlsEtn with p16:1 at *sn*-1 detected using the UPLC-MS/MS method were p16:1/14:0, p16:1/16:1, p16:1/18:1, p16:1/18:2, p16:1/20:4, p16:1/20:5, and p16:1/22:6 (**Figure 4C**). The amounts of PlsEtns with p16:1/14:0 and p16:1/16:1 peaked at 3–4 h and nearly returned to the initial level at 4–5 h. Furthermore, the levels of PlsEtn with p16:1/20:4, p16:1/22:6, p16:1/18:1, and p16:1/20:5 peaked at 1–3 h after administration and remained higher than the initial level thereon; the levels of PlsEtns, especially with p16:1/20:4 and p16:1/22:6, rapidly increased. However, the amounts of PlsEtn containing p16:0, p18:0, and p18:1 at the *sn*-1 position decreased over time and remained at levels lower than that of the initial level up to 7 h (**Figure 4A**). The molar ratios of the hydrocarbon chain at the *sn*-1 position of PlsEtn in the lymph are as follows: 21.4%, p16:0; 0.2%, p16:1; 64.3%, p18:0; and 14.1%, p18:1 for the initial lymph, and 9.9%, p16:0; 43.3%, p16:1; 35.9%, p18:0; and 10.9%, p18:1 at 1–1.5 h after the administration of plasmalogens from *S. ruminantium*, which were mostly maintained up to 7 h. With regards to FAs at the *sn*-2 position, the amounts of PlsEtn with 18:2, 22:4, and 22:5 decreased after administration, whereas those with 14:0, 16:1, 18:1, and 20:5 increased (**Figure 4B**).

We used the lipid extract from porcine brain, which is known to be rich in PlsEtn, as a comparison control. After the injection of the lipid derived from porcine brain, the molecular species of PlsEtn containing p16:1 at the *sn*-1 position was barely detected in the lymph, and the level of PlsEtn containing p16:0, p18:0, and p18:1 at the *sn*-1 position increased, particularly that of 18:0 (**Figure 5A**). As for the molar ratios of the hydrocarbon chain at the *sn*-1 position of the PlsEtn, the levels of the PlsEtn with p18:0 and p18:1 at the *sn*-1 position increased after administration and that of p16:0 decreased as follows: 25.2%, p16:0; 0.5%, p16:1; 58.3%, p18:0; and 15.8%, p18:1 for the initial lymph, and 13.1%, p16:0; 0.5%, p16:1; 66.6%, p18:0; and 19.8%, p18:1 at 1–1.5 h. However, the ratios were returning to a level closer to that as the initial lymph as follows: 24.2%, p16:0; 0.2%, p16:1; 55.5%, p18:0; and 20.1%, p18:1 at 6–7 h. Furthermore, with regard to FAs at the *sn*-2 position, the amounts of almost all

TABLE 2 | The composition of fatty acids in the lipid extracts and molecular species composition in ethanolamine plasmalogen of lipid extracts from *Selenomonas ruminantium* and porcine brain.

Origin			
			Fatty acids (%)
S. ruminantium	14:0		26.71
	15:0		0.51
	16:0		11.38
	16:1		42.56
	17:1		2.53
	18:0		1.27
	18:1		7.18
	18:2		1.78
	Others		6.09
			100
	sn-1 Alkenyl	*sn*-2 Acyl	Ethanolamine plasmalogen (%)
	p16:1	14:0	68.4
	p16:1	15:0	0.3
	p16:1	15:1	0.1
	p16:1	16:0	0.7
	p16:1	16:1	29.2
	p17:1	14:0	0.3
	Others		1.0
			100.0
			Fatty acids (%)
Porcine brain	16:0		31.22
	16:1		2.55
	17:1		3.38
	18:0		21.77
	18:1		22.88
	18:1		5.07
	20:4		5.44
	22:5		1.30
	22:6		2.73
	Others		3.66
			100
	sn-1 Alkenyl	*sn*-2 Acyl	Ethanolamine plasmalogen (%)
	p18:1	18:1	21.4
	p18:1	20:4	13.7
	p18:0	22:6	12
	Others		52.9
			100

TABLE 3 | The composition (%) of lipids in the lipid extracts from *S. ruminantium* and porcine brain.

	Amount of lipid (%) in lipid extracts	
	S. ruminantium	**Porcine brain**
PE	73	40.4
PC + SM	—	23.3
ChoE + TG	3.59	4.87
Chol	3.66	22.3
Others	19.75	9.13
	100	100

PE, phosphatidyl ethanolamine including PlsEtn; PC + SM, phosphatidyl choline + sphingomyelin; ChoE + TG, cholesterolester + triglyceride; Chol, cholesterol.

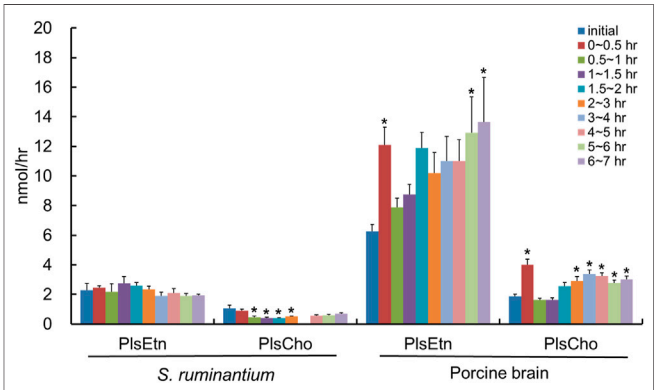

FIGURE 3 | Total amounts of PlsEtn and PlsCho in the lymph of thoracic lymph-cannulated rats for 7 h after duodenal administration of the emulsion containing lipids extracted from *S. ruminantium* or porcine brain. Lipids extracted from *S. ruminantium* and porcine brain were adjusted to the same amount in total lipids when the duodenal administration was conducted. Data are represented as mean ± SEM (n = 5–6). Asterisk indicates significant difference with respect to the values at time 0 ($p < 0.05$).

PlsEtns were time-dependently increased compared to that in the initial lymph; in particular, the level of the molecular species with 20:4 at the *sn*-2 position increased (**Figure 5B**). As a result, the total PlsEtn output in the lymph was increased time-dependently by the injection of the porcine brain lipid (p = 0.050) (**Figure 3**).

The total lymphatic outputs of PlsEtn for 7 h after the administration of plasmalogens derived from *S. ruminantium* and porcine brain were 6.2 ± 0.5 nmol and 33.0 ± 6.5 nmol, respectively. The absorption percentage of total PlsEtn from *S. ruminantium* into the lymph was approximately one-fourth compared to that derived from the porcine brain (0.33 ± 0.03% for *S. ruminantium* and 1.19 ± 0.23% for porcine brain).

Lymphatic Absorption of PlsCho Derived From *S. ruminantium* and Porcine Brain in Rats

After the injection of the lipid derived from *S. ruminantium* containing PlsEtn, the lymphatic output of total PlsCho was decreased and then gradually recovered by half of the initial value at 6–7 h (**Figure 3**). The level of PlsCho containing p16:0, p18:0, and p18:1 at the *sn*-1 position reached its lowest at 1–2 h after administration and then gradually increased (**Figure 6A**). On the other hand, the level of PlsCho containing p16:1 at the *sn*-1 position, particularly that of p16:1/18:1, reached the peak value at 2–3 h after administration and remained high until 7 h (**Figure 6A**); however, p16:1/14:0 and p16:1/16:1 were not

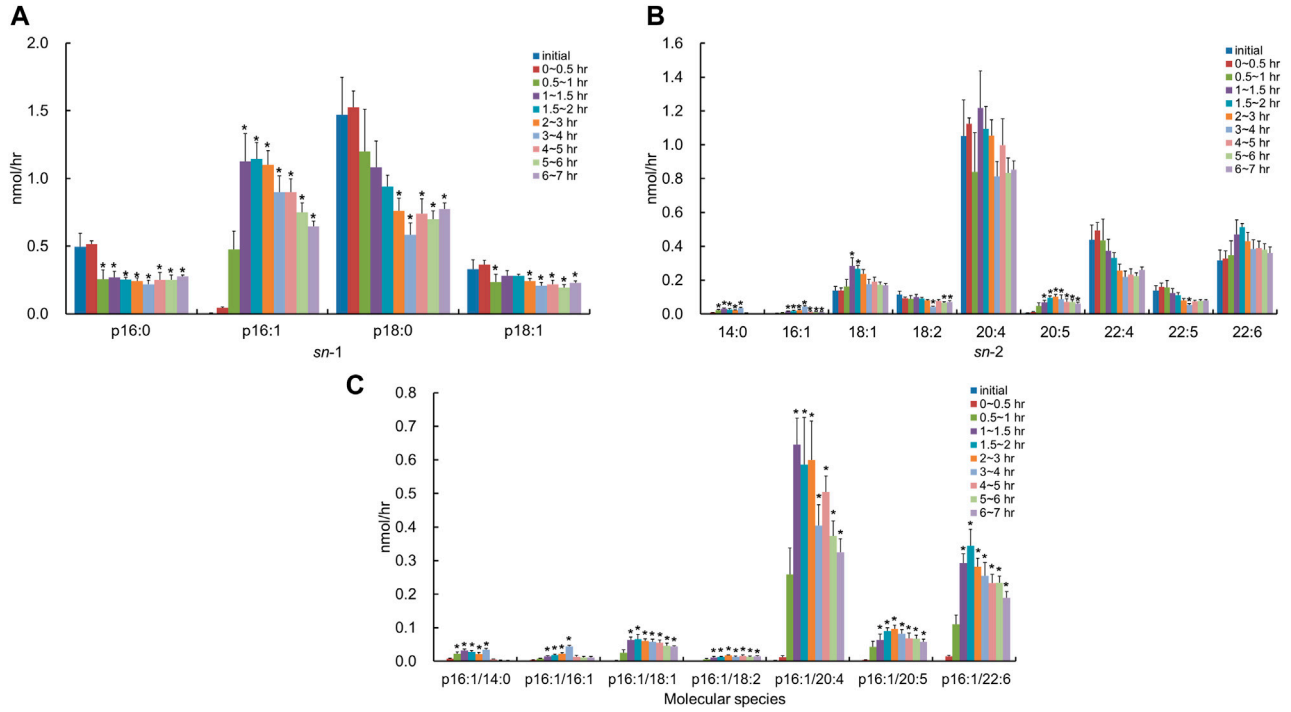

FIGURE 4 | Change in molecular species due to the classification in **(A)** the hydrocarbon chain at the *sn*-1 position and **(B)** FA at the *sn*-2 position and **(C)** change in molecular species with p16:1 at the *sn*-1 position, in lymphatic PlsEtn of thoracic lymph-cannulated rats for 7 h after duodenal administration of the emulsion containing the lipid extracted from *S. ruminantium*. Data are represented as mean ± SEM (n = 5–6). Asterisk indicates significant difference with respect to the values at time 0 ($p < 0.05$).

detected (**Figure 6C**). The molar ratios of the hydrocarbon chain at the *sn*-1 position of PlsCho in the initial lymph are as follows: 54.7%, p16:0; 1.1%, p16:1; 29.8%, p18:0; and 14.4%, p18:1, whereas those in the lymph 1–1.5 h after plasmalogen (from *S. ruminantium*) administration are as follows: 41.0%, p16:0; 13.5%, p16:1; 32.6%, p18:0; and 12.9%, p18:1. Moreover, only the p16:1 ratio was maintained until after 6–7 h. With regard to FAs at the *sn*-2 position, PlsCho with 16:0, 18:2, 20:4, 22:4, 22:5, and 22:6 was decreased after administration of porcine plasmalogens, whereas those with 18:1 and 20:5 was increased (**Figure 6B**).

In contrast, after the injection of the lipid derived from porcine brain containing PlsEtn, the molecular species of PlsCho containing p16:1 at the *sn*-1 position was barely detected in the lymph, and the level of PlsCho with p16:0, p18:0, and p18:1 increased to the same extent time-dependently (**Figure 7A**). With regard to FAs at the *sn*-2 position, the lymphatic output of almost all PlsCho, and especially that of the molecular species with 20:4 at the *sn*-2 position, was time-dependently increased compared to the initial lymph, regardless of the type of FA binding at the *sn*-2 position in PlsCho (**Figure 7B**). There was almost no change in the composition of both *sn*-1 and *sn*-2 in PlsCho after the injection of the lipid extract from porcine brain.

There were no significant differences in the amount of lymph flow among rats administered with each plasmalogen emulsion (data not shown).

DISCUSSION

The results of plasmalogen production by *S. ruminantium* in the present study show differences when compared to results of other previous experiments. A previous study showed that glucose media containing volatile FAs or lactate media containing biotin were appropriate for the growth of *S. ruminantium* (Kanegasaki and Takahashi, 1967). However, in the present study, *S. ruminantium* grew well in the glucose medium and not so much in the lactate medium (data not shown). In addition, the production of serine plasmalogens (PlsSer) was not detected in our study, although it is reported that PlsEtn and PlsSer are the main plasmalogens produced in *S. ruminantium* (Watanabe et al., 1982). These differences could be due to differences in culture conditions such as the culture volume and anaerobic level.

In general, in the small intestine, most of the dietary PLs are hydrolyzed at the *sn*-2 position by pancreatic phospholipase A2 (pPLA2) and then absorbed by the intestinal mucosal cells as free FAs and lyso-phospholipids (Lyso-PLs) in the small intestinal lumen (**Figure 8**). Lyso-PLs and some free-FAs are re-esterified to

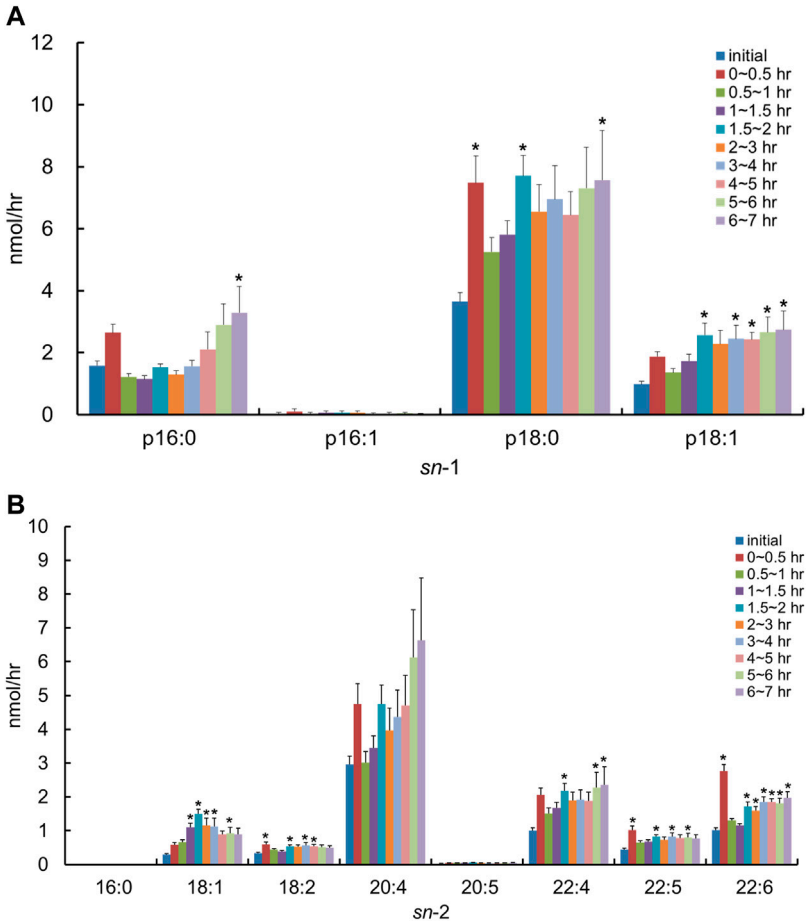

FIGURE 5 | Change in molecular species due to the classification in **(A)** the hydrocarbon chain at the *sn*-1 position and **(B)** FA at the *sn*-2 position in lymphatic PlsEtn of thoracic lymph-cannulated rats for 7 h after duodenal administration of the emulsion containing the lipid extracted from porcine brain. Data are represented as mean ± SEM (n = 5–6). Asterisk indicates significant difference with respect to the values at time 0 ($p < 0.05$).

PLs by acyltransferase in the small intestinal epithelial cells and released into the lymph flow incorporated in chylomicrons. However, it has been assumed that some intestinal PLs are absorbed passively and without hydrolyzation (Scow et al., 1967; Zierenberg and Grundy, 1982). The most common PL present in food is phosphatidylcholine, whereas other PLs, such as phosphatidylethanolamine, phosphatidylserine, and phosphatidylinositol, are present in much smaller amounts (Murru et al., 2013). Therefore, although there are more reports about phosphatidylcholine compared to other PLs, it is reported that phosphatidylethanolamine goes through similar stages of digestion and absorption as phosphatidylcholine, despite their differences in the efficiency of digestion and uptake (Ikeda et al., 1987; Nishimukai et al., 2011). Based on this knowledge, it is considered that plasmalogens are absorbed in the small intestine through a process similar to that of the absorption of other PLs.

After administration of the lipid from *S. ruminantium* to rats, the level of PlsEtn containing the p16:1 hydrocarbon chain at the *sn*-1 position increased in the lymph (**Figure 4A**). The PlsEtn with p16:1 at *sn*-1 is characteristic of PlsEtn from *S. ruminantium* and is barely detected from the initial lymph fluid of rats under normal diet. In contrast, after the injection of the lipid from porcine brain, the level of PlsEtn with p18:0 and p18:1 at the *sn*-1 position, which is the main hydrocarbon chain at the *sn*-1 position of plasmalogens in mammalian tissues such as brain (Nishimukai et al., 2011), increased without an increase in the level of PlsEtn with the p16:1 hydrocarbon chain. Thus, the compositions of the *sn*-1 position of plasmalogens in the lymph roughly reflected the composition of the administered plasmalogens, which suggests that at least part of microbial plasmalogens administered to rats was absorbed from the small intestine and released into the lymph while maintaining the molecular structure of *sn*-1 (**Figure 8**).

The level of PlsEtn with p16:1/20:4 and p16:1/22:6 (**Figures 4**, **8**) increased significantly in the lymph compared to that in the initial lymph after administration of plasmalogens from *S. ruminantium*. Lipids from *S. ruminantium* were rich in 14:0 and 16:1 but not in 20:4 and 22:6 (**Table 2**). On the other hand, FAs of the *sn*-2 position in PlsEtn in the lymph were very rich in 20:4 and 22:6 but only slightly in 14:0 and 16:1. Similarly, after the administration of plasmalogens from porcine brain, nearly half of

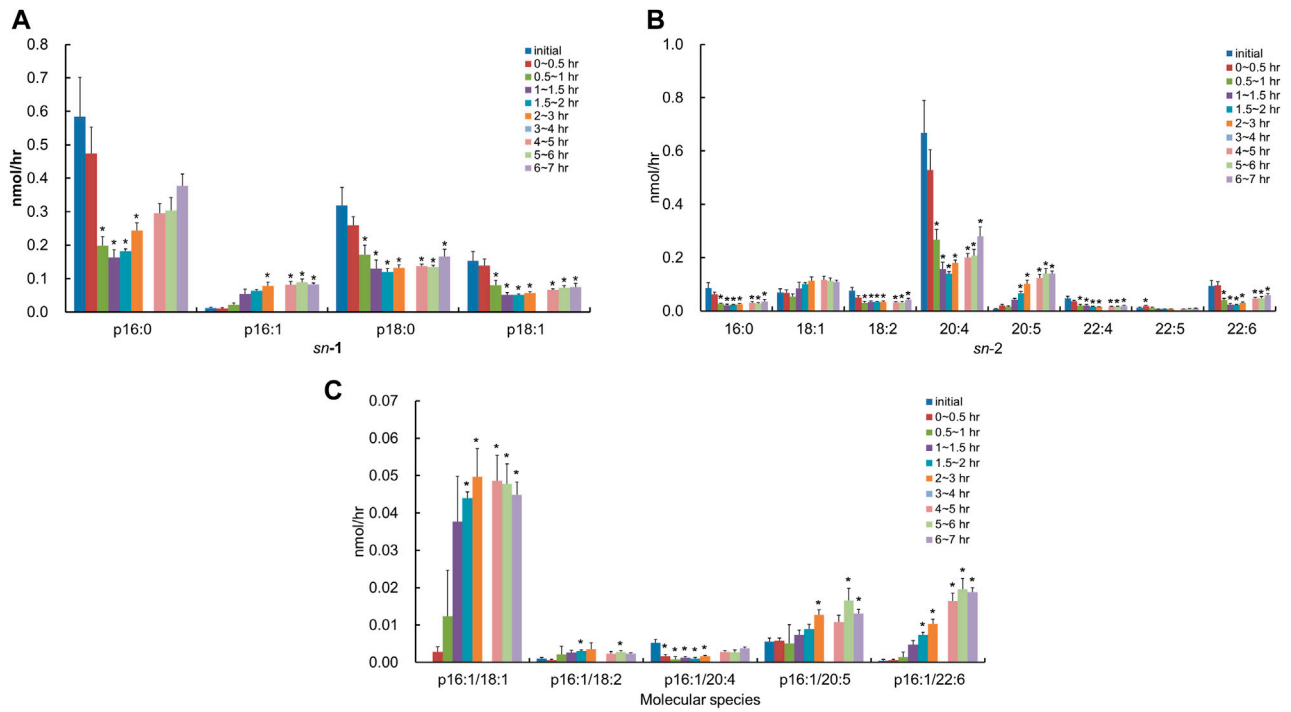

FIGURE 6 | Change in molecular species due to the classification in **(A)** the hydrocarbon chain at the *sn*-1 position and **(B)** FA at the *sn*-2 position and **(C)** change in molecular species with p16:1 at the *sn*-1 position in the lymphatic PlsCho of thoracic lymph-cannulated rats for 7 h after duodenal administration of the emulsion containing the lipid extracted from *S. ruminantium*. Data are represented as mean ± SEM (n = 5–6). Asterisk indicates significant difference with respect to the values at time 0 ($p < 0.05$). The data of 3–4 h were missing in order to mistake analyzing.

the FAs at the *sn*-2 position in the lymphatic plasmalogens were 20:4 and 22:6 and did not reflect the FA composition of the injected lipid. From these results, we confirmed that 20:4 and 22:6 were preferentially re-esterified at the *sn*-2 position during absorption of PlsEtn in the small intestine, regardless of the types of carbon chain at the *sn*-1 position. Previously, studies conducted by us and others have shown that PlsEtn preferentially selected 20:4 for re-esterification in the intestine using plasmalogens with p16:0, p18:0, and p18:1 at the *sn*-1 position (Nishimukai et al., 2011; Takahashi et al., 2020). However, the present study is the first to show that plasmalogens containing p16:1, which is rarely found at the *sn*-1 position in animal plasmalogens, have similar characteristics to those containing p16:0, p18:0, and p18:1. The level of PlsEtn with 20:5 at the *sn*-2 position (**Figure 4B**) also increased significantly in the lymph compared to that in the initial lymph after administration of plasmalogens from *S. ruminantium*. This phenomenon is interesting because the abundance of 20:5 in phospholipids is generally at the low level in the phospholipids. However, we have no reasonable reasons until now.

The structural change, which is the replacement of FAs with 20:4 and 22:6, is possibly involved in FA turnover during PL remodeling by reacylation of lyso-PL by lysophospholipid acyltransferases (LPLATs) (Cao et al., 2008; Harayama et al., 2014; Bradley et al., 2015; Hashidate-Yoshida et al., 2015; Eto et al., 2020). Lyso-phosphatidylcholine acyltransferase 3 (LPCAT3) is highly expressed in the small intestine and involved in incorporating 20:4 into PLs (Hashidate-Yoshida et al., 2015). Further, lyso-phosphatidylethanolamine acyltransferase 2 (LPEAT2) preferentially incorporates 22:6 into PLs in mouse brain cells, unfortunately but not the report about LPEAT2 in the small intestine (Cao et al., 2008; Eto et al., 2020). Though not certain, it is possible that these lysophospholipid acyltransferases equally act for the re-esterification of PlsEtn. As mentioned earlier, most of the PlsEtn absorbed in the small intestine was released into the lymph as PlsEtn with polyunsaturated FAs (20:4 and 22:6) at the *sn*-2 position. However, the levels of PlsEtn having p16:1/14:0 and p16:1/16:1 were also increased in the lymph significantly (**Figure 4B**). The ratio of these species was 4.3% of the total PlsEtn released into the lymph after administration of plasmalogens from *S. ruminantium*. This result may be consistent with the activity of lysophospholipid acyltransferase mentioned previously. It is possible that lysophospholipid acyltransferases in the rat intestine act weakly in incorporating 14:0 and 16:1 into the *sn*-2 position in PlsEtn. Further studies are required to evaluate the structural change that where and how the ingested lipids are re-esterified.

The absorption rate of PlsEtn derived from *S. ruminantium* (0.33 ± 0.03%) into the lymph for 7 h after administration was lower than that of PlsEtn derived from porcine brain (1.19 ±

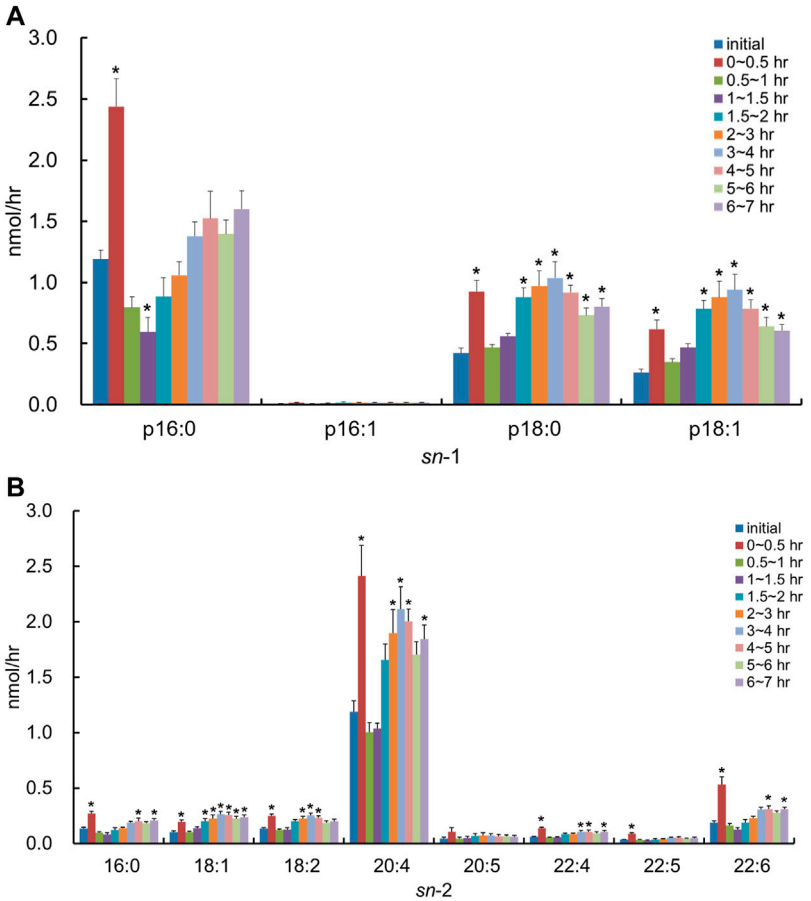

FIGURE 7 | Change in molecular species due to the classification in **(A)** the hydrocarbon chain at the *sn*-1 position and **(B)** FA at the *sn*-2 position in the lymphatic PlsCho of thoracic lymph-cannulated rats for 7 h after duodenal administration of the emulsion containing the lipid extracted from porcine brain. Data are represented as mean ± SEM (n = 5–6). Asterisk indicates significant difference with respect to the values at time 0 ($p < 0.05$).

0.23%). This might be a result of the LPLAT activity for PlsEtn with p16:1 being weaker than that for PlsEtn with p18:0 and p16:0 during re-esterification. Moreover, bacterial lipids consist of relatively short-chain FAs with less than 16 carbons such as 14:0 and 16:1, while pig brain lipids consist of long-chain FAs with more than 18 carbons including 20:4 and 22:6 (**Table 2**). There are many kinds of PLAs, which hydrolyze FAs at the *sn*-2 position of PLs, with various substrate specificities. Therefore, it is possible that the difference in composition, that is, the number of carbon and double bonds in PlsEtn, has an effect on the activity of phospholipase A2 for PlsEtn. However, the detailed mechanisms are still unclear. Therefore, further study is needed to clarify the relation between these enzymes and the structure of plasmalogens.

The lipid from *S. ruminantium* used in this study was rich in 16:1 (palmitoleic acid), according to the composition analysis using the GC and LC-MS/MS method (**Table 2**). However, the level of PlsEtn with 16:1 at the *sn*-2 position was not high in the lymph after the injection of the lipid derived from *S. ruminantium* (**Figure 4C**). In this case, 16:1, which is produced by hydrolysis, is re-esterified to other PLs and triglycerides, and released into the lymph after incorporation into chylomicrons. Consumption of palmitoleic acid prevents hypercholesterolemia, atherosclerosis, fatty liver, and metabolic disorders caused by a high-fat, high-carbohydrate diet (Nunes and Rafacho, 2017; Huang et al., 2020; Souza et al., 2020). Although 16:1 incorporated in the *sn*-2 position of PlsEtn was detected in traces, 16:1 incorporated in other lipids is possibly beneficial to the human body, suggesting new usage of bacterial lipids.

After administration of PlsEtn from *S. ruminantium*, PlsCho with the p16:1 at the *sn*-1 position increased significantly in the lymph, even though PlsCho was absent in the lipid from *S. ruminantium* (**Figure 6**). This result shows that ingested microbial PlsEtn was converted to PlsCho in the small intestinal absorptive cells. PlsCho is known to be formed from PlsEtn by enzymes such as phospholipase C and choline phosphotransferase (Strum et al., 1992; Strum and Daniel, 1993). Previous reports have also indicated the conversion of PlsEtn to PlsCho in small intestinal cells in rats (Nishimukai et al., 2011; Takahashi et al., 2020). Furthermore, we have confirmed such conversion in Caco-2 cells (data not shown). Furthermore,

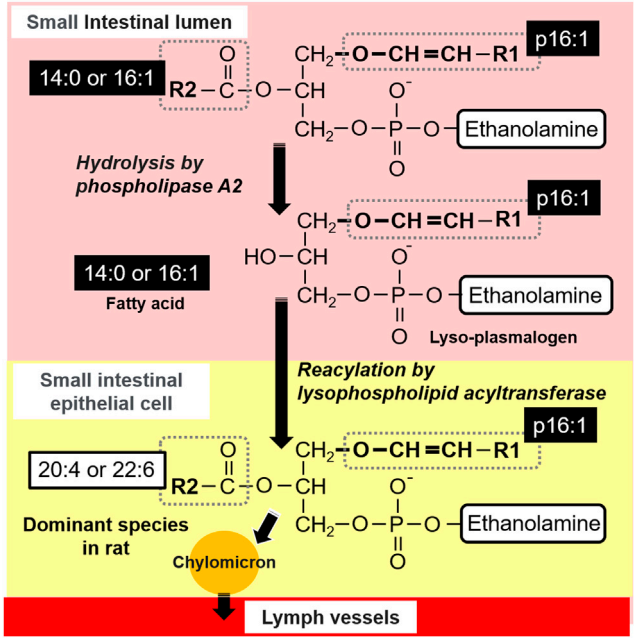

FIGURE 8 | Predicted lymphatic adsorption of plasmalogens from *S. ruminantium* in rats.

the administration of lipids from *S. ruminantium*, containing PlsEtn, time-dependently increased the level of PlsCho containing p16:1 at the *sn*-1 position, temporarily decreasing the levels of PlsEtn containing p16:0, p18:0, and p18:1 at the *sn*-1 position. Furthermore, the peak lymphatic release of PlsCho with p16:1 at the *sn*-1 position was delayed by about 1 h compared with that of PlsEtn with p16:1 at the *sn*-1 position. This is because, immediately after administration, the re-synthesis of PlsEtn is promoted preferentially according to the amounts of lyso-PlsEtn and FA, following which, the conversion of PlsEtn to PlsCho proceeds. Moreover, unexpectedly, we found that the level of PlsCho with p16:1/18:1 was significantly increased in the lymph after the administration of the lipid from *S. ruminantium* (**Figure 6**). Previous reports have suggested a strong correlation between blood concentrations of PlsCho having an 18:1 FA bound at the *sn*-2 position and atherosclerosis-related factors, as well as a protective function against atherosclerosis (Nishimukai et al., 2014a; Nishimukai et al., 2014b); the increase in the level of p16:1/18:1 PlsCho in the body after administration of microbial plasmalogens may have some positive effect on atherosclerosis.

In this study, we focused on bacteria as the resource of plasmalogens. However, bacteria such as *S. ruminantium* are not appropriate to food resource, because *S. ruminantium* is classified into gram-negative bacteria containing endotoxin in the outer membrane of their cell walls. We assumed to utilize plasmalogens extracted from bacteria for dietary supplement in future work. Also, both general gavage experiments as well as lymphatic absorption experiments are required to understand the structure–function correlation of plasmalogens. Therefore, in this study, the lymphatic absorption of microbial plasmalogens in the small intestine was investigated using lymph duct-cannulated rats as a first step toward this goal. In the future, owing to the instability of plasmalogens under acidic conditions, such as in the stomach, we will develop how to facilitate delivery of intact plasmalogens into the small intestine as utilization of capsules containing plasmalogens.

CONCLUSION

In this study, we focused on *S. ruminantium* as a new source of PlsEtn and investigated the absorption mechanism of bacterial PlsEtns with an "unnatural" structure in lymph-cannulated rats. As a result, despite having different chemical structures, it was suggested that a part of bacteria PlsEtn shows the structural change as similar to animal PlsEtn during intestinal absorption, that is, it undergoes 20:4 and 22:6 re-esterification and base conversion (PlsEtn into PlsCho). This finding is expected to not only lead the effective utilization of bacterial resources as food but also clarify the relationship between the chemical structure of plasmalogens and their biological functions in humans.

DATA AVAILABILITY STATEMENT

The raw data supporting the conclusion of this article will be made available by the authors, without undue reservation.

ETHICS STATEMENT

The animal study was reviewed and approved by the Iwate University Animal Committee.

AUTHOR CONTRIBUTIONS

All authors viewed and approved the manuscript and contributed significantly to the work. MN and MY designed the study and revised the manuscript. NS, AK [Aki Kanehama], MY, and MN wrote the manuscript with the help of AK [Akiko Kashiwagi]. NS and AK [Aki Kanehama] performed the experiments with the help of MY and MN. MY and MN analyzed the results.

FUNDING

The study was supported by the research support program of the Initiative for the Implementation of the Diversity Research Environment (Traction Type) (to MN) from the MEXT, Japan, the NAGASE Science Technology foundation (to MY), and the KOBAYASHI foundation (to AK (Akiko Kashiwagi)).

REFERENCES

Bligh, E. G., and Dyer, W. J. (1959). A Rapid Method of Total Lipid Extraction and Purification. *Can. J. Biochem. Physiol.* 37, 911–917. doi:10.1139/o59-099

Bradley, R. M., Marvyn, P. M., Aristizabal Henao, J. J., Mardian, E. B., George, S., Aucoin, M. G., et al. (2015). Acylglycerophosphate Acyltransferase 4 (AGPAT4) Is a Mitochondrial Lysophosphatidic Acid Acyltransferase that Regulates Brain Phosphatidylcholine, Phosphatidylethanolamine, and Phosphatidylinositol Levels. *Biochim. Biophys. Acta (BBA) - Mol. Cell Biol. Lipids* 1851, 1566–1576. doi:10.1016/j.bbalip.2015.09.005

Cao, J., Shan, D., Revett, T., Li, D., Wu, L., Liu, W., et al. (2008). Molecular Identification of a Novel Mammalian Brain Isoform of Acyl-CoA: lysophospholipid Acyltransferase with Prominent Ethanolamine Lysophospholipid Acylating Activity, LPEAT2. *J. Biol. Chem.* 283, 19049–19057. doi:10.1074/jbc.m800364200

Eto, M., Shindou, H., Yamamoto, S., Tamura-Nakano, M., and Shimizu, T. (2020). Lysophosphatidylethanolamine Acyltransferase 2 (LPEAT2) Incorporates DHA into Phospholipids and Has Possible Functions for Fatty Acid-Induced Cell Death. *Biochem. Biophysical Res. Commun.* 526, 246–252. doi:10.1016/j.bbrc.2020.03.074

Garg, M. L., and Haerdi, J. C. (1993). The Biosynthesis and Functions of Plasmalogens. *J. Clin. Biochem. Nutr.* 14, 71–82. doi:10.3164/jcbn.14.71

Ginsberg, L., Rafique, S., Xuereb, J. H., Rapoport, S. I., and Gershfeld, N. L. (1995). Disease and Anatomic Specificity of Ethanolamine Plasmalogen Deficiency in Alzheimer's Disease Brain. *Brain Res.* 698, 223–226. doi:10.1016/0006-8993(95)00931-f

Goodenowe, D. B., Cook, L. L., Liu, J., Lu, Y., Jayasinghe, D. A., Ahiahonu, P. W. K., et al. (2007). Peripheral Ethanolamine Plasmalogen Deficiency: a Logical Causative Factor in Alzheimer's Disease and Dementia. *J. Lipid Res.* 48, 2485–2498. doi:10.1194/jlr.p700023-jlr200

Hahnel, D., Huber, T., Kurze, V., Beyer, K., and Engelmann, B. (1999a). Contribution of Copper Binding to the Inhibition of Lipid Oxidation by Plasmalogen Phospholipids. *Biochem. J.* 340 (Pt 2) (Pt 2), 377–383. doi:10.1042/bj3400377

Hahnel, D., Thiery, J., Brosche, T., and Engelmann, B. (1999b). Role of Plasmalogens in the Enhanced Resistance of LDL to Copper-Induced Oxidation after LDL Apheresis. *Atvb* 19, 2431–2438. doi:10.1161/01.atv.19.10.2431

Harayama, T., Eto, M., Shindou, H., Kita, Y., Otsubo, E., Hishikawa, D., et al. (2014). Lysophospholipid Acyltransferases Mediate Phosphatidylcholine Diversification to Achieve the Physical Properties Required *In Vivo*. *Cell Metab.* 20, 295–305. doi:10.1016/j.cmet.2014.05.019

Hashidate-Yoshida, T., Harayama, T., Hishikawa, D., Morimoto, R., Hamano, F., Tokuoka, S. M., et al. (2015). Fatty Acid Remodeling by LPCAT3 Enriches Arachidonate in Phospholipid Membranes and Regulates Triglyceride Transport. *Elife* 4. doi:10.7554/eLife.06328

Heymans, H. S. A., Schutgens, R. B. H., Tan, R., Van Den Bosch, H., and Borst, P. (1983). Severe Plasmalogen Deficiency in Tissues of Infants without Peroxisomes (Zellweger Syndrome). *Nature* 306, 69–70. doi:10.1038/306069a0

Huang, W.-w., Hong, B.-h., Bai, K.-k., Tan, R., Yang, T., Sun, J.-p., et al. (2020). Cis- and Trans-palmitoleic Acid Isomers Regulate Cholesterol Metabolism in Different Ways. *Front. Pharmacol.* 11, 602115. doi:10.3389/fphar.2020.602115

Ikeda, I., Imaizumi, K., and Sugano, M. (1987). Absorption and Transport of Base Moieties of Phosphatidylcholine and Phosphatidylethanolamine in Rats. *Biochim. Biophys. Acta* 921, 245–253.

Kamio, Y., Kanegasaki, S., and Takahashi, H. (1970). Fatty Acid and Aldehyde Compositions in Phospholipids of Selenomonas Ruminantium with Reference to Growth Conditions. *J. Gen. Appl. Microbiol.* 16, 29–37. doi:10.2323/jgam.16.1_29

Kamio, Y., Kanegasaki, S., and Takahashi, H. (1969). Occurrence of Plasmalogens in Anaerobic Bacteria. *J. Gen. Appl. Microbiol.* 15, 439–451. doi:10.2323/jgam.15.439

Kanegasaki, S., and Takahashi, H. (1968). Function of Growth Factors for Rumen Microorganisms. II. Metabolic Fate of Incorporated Fatty Acids in Selenomonas Ruminantium. *Biochim. Biophys. Acta* 152, 40–49.

Kanegasaki, S., and Takahashi, H. (1967). Function of Growth Factors for Rumen Microorganisms I. Nutritional Characteristics of Selenomonas Ruminantium. *J. Bacteriol.* 93, 456–463. doi:10.1128/jb.93.1.456-463.1967

Kaneko, J., Yamada-Narita, S., Abe, N., Onodera, T., Kan, E., Kojima, S., et al. (2015). Complete Genome Sequence of Selenomonas Ruminantium Subsp. Lactilytica Will Accelerate Further Understanding of the Nature of the Class Negativicutes. *FEMS Microbiol. Lett.* 362. doi:10.1093/femsle/fnv050

Khan, M., Singh, J., and Singh, I. (2008). Plasmalogen Deficiency in Cerebral Adrenoleukodystrophy and its Modulation by Lovastatin. *J. Neurochem.* 106, 1766–1779. doi:10.1111/j.1471-4159.2008.05513.x

Kim, K. C., Kamio, Y., and Takahashi, H. (1970). Glyceryl Ether Phospholipid in Anaerobic Bacteria. *J. Gen. Appl. Microbiol.* 16, 321–325. doi:10.2323/jgam.16.4_321

Koivuniemi, A. (2017). The Biophysical Properties of Plasmalogens Originating from Their Unique Molecular Architecture. *FEBS Lett.* 591, 2700–2713. doi:10.1002/1873-3468.12754

Lee, T.-c. (1998). Biosynthesis and Possible Biological Functions of Plasmalogens. *Biochim. Biophys. Acta (BBA) - Lipids Lipid Metab.* 1394, 129–145. doi:10.1016/s0005-2760(98)00107-6

Maeba, R., Maeda, T., Kinoshita, M., Takao, K., Takenaka, H., Kusano, J., et al. (2007). Plasmalogens in Human Serum Positively Correlate with High- Density Lipoprotein and Decrease with Aging. *Jat* 14, 12–18. doi:10.5551/jat.14.12

Maeba, R., and Ueta, N. (2003). Ethanolamine Plasmalogens Prevent the Oxidation of Cholesterol by Reducing the Oxidizability of Cholesterol in Phospholipid Bilayers. *J. Lipid Res.* 44, 164–171. doi:10.1194/jlr.m200340-jlr200

Murru, E., Banni, S., and Carta, G. (2013). Nutritional Properties of Dietary omega-3-enriched Phospholipids. *Biomed. Res. Int.* 2013, 965417. doi:10.1155/2013/965417

Nagan, N., and Zoeller, R. A. (2001). Plasmalogens: Biosynthesis and Functions. *Prog. Lipid Res.* 40, 199–229. doi:10.1016/s0163-7827(01)00003-0

Nishimukai, M., Maeba, R., Ikuta, A., Asakawa, N., Kamiya, K., Yamada, S., et al. (2014a). Serum Choline Plasmalogens-Those with Oleic Acid in Sn− 2-are Biomarkers for Coronary Artery Disease. *Clinica Chim. Acta* 437, 147–154. doi:10.1016/j.cca.2014.07.024

Nishimukai, M., Maeba, R., Yamazaki, Y., Nezu, T., Sakurai, T., Takahashi, Y., et al. (2014b). Serum Choline Plasmalogens, Particularly Those with Oleic Acid in Sn-2, Are Associated with Proatherogenic State. *J. Lipid Res.* 55, 956–965. doi:10.1194/jlr.p045591

Nishimukai, M., Yamashita, M., Watanabe, Y., Yamazaki, Y., Nezu, T., Maeba, R., et al. (2011). Lymphatic Absorption of Choline Plasmalogen Is Much Higher Than that of Ethanolamine Plasmalogen in Rats. *Eur. J. Nutr.* 50, 427–436. doi:10.1007/s00394-010-0149-0

Nunes, E., and Rafacho, A. (2017). Implications of Palmitoleic Acid (Palmitoleate) on Glucose Homeostasis, Insulin Resistance and Diabetes. *Cdt* 18, 619–628. doi:10.2174/1389450117666151209120345

Panganamala, R. V., Horrocks, L. A., Geer, J. C., and Cornwell, D. G. (1971). Positions of Double Bonds in the Monounsaturated Alk-1-Enyl Groups from the Plasmalogens of Human Heart and Brain. *Chem. Phys. Lipids* 6, 97–102. doi:10.1016/0009-3084(71)90031-4

Scow, R. O., Stein, Y., and Stein, O. (1967). Incorporation of Dietary Lecithin and Lysolecithin into Lymph Chylomicrons in the Rat. *J. Biol. Chem.* 242, 4919–4924. doi:10.1016/s0021-9258(18)99456-1

Souza, C. O., Teixeira, A. A. S., Biondo, L. A., Silveira, L. S., De Souza Breda, C. N., Braga, T. T., et al. (2020). Palmitoleic Acid Reduces High Fat Diet-Induced Liver Inflammation by Promoting PPAR-γ-independent M2a Polarization of Myeloid Cells. *Biochim. Biophys. Acta (BBA) - Mol. Cell Biol. Lipids* 1865, 158776. doi:10.1016/j.bbalip.2020.158776

Strum, J. C., and Daniel, L. W. (1993). Identification of a Lysophospholipase C that May Be Responsible for the Biosynthesis of Choline Plasmalogens by Madin-Darby Canine Kidney Cells. *J. Biol. Chem.* 268, 25500–25508. doi:10.1016/s0021-9258(19)74420-2

Strum, J. C., Emilsson, A., Wykle, R. L., and Daniel, L. W. (1992). Conversion of 1-O-Alkyl-2-Acyl-Sn-Glycero-3-Phosphocholine to 1-O-Alk-1'-Enyl-2-Acyl-Sn-Glycero-3-Phosphoethanolamine. A Novel Pathway for the Metabolism of Ether-Linked Phosphoglycerides. *J. Biol. Chem.* 267, 1576–1583. doi:10.1016/s0021-9258(18)45984-4

Su, X. Q., Wang, J., and Sinclair, A. J. (2019). Plasmalogens and Alzheimer's Disease: a Review. *Lipids Health Dis.* 18, 100. doi:10.1186/s12944-019-1044-1

Takahashi, T., Kamiyoshihara, R., Otoki, Y., Ito, J., Kato, S., Suzuki, T., et al. (2020). Structural Changes of Ethanolamine Plasmalogen during Intestinal Absorption. *Food Funct.* 11, 8068–8076. doi:10.1039/d0fo01666g

Takatsuka, Y., and Kamio, Y. (2004). Molecular Dissection of theSelenomonas ruminantiumCell Envelope and Lysine Decarboxylase Involved in the Biosynthesis of a Polyamine Covalently Linked to the Cell Wall Peptidoglycan Layer. *Biosci. Biotechnol. Biochem.* 68, 1–19. doi:10.1271/bbb.68.1

Watanabe, N., Suzuki, T., Yamazaki, Y., Sugiyama, K., Koike, S., and Nishimukai, M. (2019). Supplemental Feeding of Phospholipid-Enriched Alkyl Phospholipid from Krill Relieves Spontaneous Atopic Dermatitis and Strengthens Skin Intercellular Lipid Barriers in NC/Nga Mice. *Biosci. Biotechnol. Biochem.* 83, 717–727. doi:10.1080/09168451.2018.1559024

Watanabe, T., Okuda, S.-I., and Takahashi, H. (1982). Physiological Importance of Even-Numbered Fatty Acids and Aldehydes in Plasmalogen Phospholipids of Selenomonas Ruminantium. *J. Gen. Appl. Microbiol.* 28, 23–33. doi:10.2323/jgam.28.23

Wu, Y., Chen, Z., Darwish, W. S., Terada, K., Chiba, H., and Hui, S.-P. (2019). Choline and Ethanolamine Plasmalogens Prevent lead-induced Cytotoxicity and Lipid Oxidation in HepG2 Cells. *J. Agric. Food Chem.* 67, 7716–7725. doi:10.1021/acs.jafc.9b02485

Zemski Berry, K. A., and Murphy, R. C. (2004). Electrospray Ionization Tandem Mass Spectrometry of Glycerophosphoethanolamine Plasmalogen Phospholipids. *J. Am. Soc. Mass. Spectrom.* 15, 1499–1508. doi:10.1016/j.jasms.2004.07.009

Zierenberg, O., and Grundy, S. M. (1982). Intestinal Absorption of Polyenephosphatidylcholine in Man. *J. Lipid Res.* 23, 1136–1142. doi:10.1016/s0022-2275(20)38050-0

Conflict of Interest: The authors declare that the research was conducted in the absence of any commercial or financial relationships that could be construed as a potential conflict of interest.

Publisher's Note: All claims expressed in this article are solely those of the authors and do not necessarily represent those of their affiliated organizations, or those of the publisher, the editors, and the reviewers. Any product that may be evaluated in this article, or claim that may be made by its manufacturer, is not guaranteed or endorsed by the publisher.

frontiers in Cell and Developmental Biology

ORIGINAL RESEARCH
published: 31 March 2022
doi: 10.3389/fcell.2022.864599

Plasmalogens Regulate Retinal Connexin 43 Expression and Müller Glial Cells Gap Junction Intercellular Communication and Migration

*Rémi Karadayi[1], Julie Mazzocco[1], Laurent Leclere[1], Bénédicte Buteau[1], Stéphane Gregoire[1], Christine Belloir[2], Mounzer Koudsi[1], Pauline Bessard[1], Jean-Baptiste Bizeau[1], Elisabeth Dubus[1], Claire Fenech[3], Loïc Briand[2], Lionel Bretillon[1], Alain M. Bron[1,4], Xavier Fioramonti[5] and Niyazi Acar[1]**

[1]Eye and Nutrition Research Group, CSGA, Université de Bourgogne Franche-Comté, Dijon, France, [2]Taste and Olfaction Research Group, CSGA, Université de Bourgogne Franche-Comté, Dijon, France, [3]Brain Nutrient Sensing and Energy Homeostasis, CSGA, Université de Bourgogne Franche-Comté, Dijon, France, [4]Department of Ophthalmology, University Hospital, Dijon, France, [5]INRAE, UMR NutriNeuro, Bordeaux, France

OPEN ACCESS

Edited by:
Fabian Dorninger, Medical University of Vienna, Austria

Reviewed by:
Sanjoy K. Bhattacharya, University of Miami, United States
Johannes Berger, Medical University of Vienna, Austria

***Correspondence:**
Niyazi Acar
Niyazi.acar@inrae.fr

Specialty section:
This article was submitted to Cellular Biochemistry, a section of the journal Frontiers in Cell and Developmental Biology

Received: *28 January 2022*
Accepted: *16 March 2022*
Published: *31 March 2022*

Citation:
Karadayi R, Mazzocco J, Leclere L, Buteau B, Gregoire S, Belloir C, Koudsi M, Bessard P, Bizeau J-B, Dubus E, Fenech C, Briand L, Bretillon L, Bron AM, Fioramonti X and Acar N (2022) Plasmalogens Regulate Retinal Connexin 43 Expression and Müller Glial Cells Gap Junction Intercellular Communication and Migration. Front. Cell Dev. Biol. 10:864599. doi: 10.3389/fcell.2022.864599

Plasmalogens are a specific glycerophospholipid subtype characterized by a vinyl-ether bound at their *sn*-1 moiety. Their biosynthesis is initiated in the peroxisome by dihydroxyacetone phosphate-acyltransferase (DHAPAT), which is encoded by the *DAPAT* gene. Previous studies have shown that plasmalogen-deficient mice exhibit major physiological dysfunctions including several eye defects, among which abnormal vascular development of the retina and a reactive activation of macroglial Müller cells. Interestingly, plasmalogen deficiency in mice is also associated with a reduced expression of brain connexin 43 (Cx43). Cx43 is the main connexin subtype of retinal glial cells and is involved in several cellular mechanisms such as calcium-based gap junction intercellular communication (GJIC) or cell migration. Thus, the aim of our work was 1) to confirm the alteration of Cx43 expression in the retina of plasmalogen-deficient DAPAT$^{-/-}$ mice and 2) to investigate whether plasmalogens are involved in crucial functions of Müller cells such as GJIC and cell migration. First, we found that plasmalogen deficiency was associated with a significant reduction of Cx43 expression in the retina of DAPAT$^{-/-}$ mice *in vivo*. Secondly, using a siRNA targeting DHAPAT *in vitro*, we found that a 50%-reduction of Müller cells content in plasmalogens was sufficient to significantly downregulate Cx43 expression, while increasing its phosphorylation. Furthermore, plasmalogen-depleted Müller cells exhibited several alterations in ATP-induced GJIC, such as calcium waves of higher amplitude that propagated slower to neighboring cells, including astrocytes. Finally, *in vitro* plasmalogen depletion was also associated with a significant downregulation of Müller cells migration. Taken together, these data confirm that plasmalogens are critical for the regulation of Cx43 expression and for characteristics of retinal Müller glial cells such as GJIC and cell migration.

Keywords: plasmalogens, retina, müller cells, connexin 43, gap junctional intercellular communication, cell migration

1 INTRODUCTION

The ether-lipid plasmalogens represent a specific glycerophospholipid subgroup that is characterized by the presence of a vinyl-ether bond at the *sn*-1 position of the glycerol backbone. They are synthesized by a multi-step process that starts in the peroxisome with the first and key enzyme of plasmalogen biosynthesis DHAPAT (dihydroxyacetone phosphate-acyltransferase) (Liu et al., 2005). Plasmalogens are present in various concentrations in all cell types and tissues. The heart and nervous tissues are particularly enriched in plasmalogens, where they can make up to 20–30% of total phospholipids (Nagan and Zoeller, 2001). As an extension of the central nervous system, the retina also contains high amounts of plasmalogens, which are mostly represented in the ethanolamine phospholipids subclass (PE) and can make up to 30% of total PE species (Dorman et al., 1976; Acar et al., 2007; Nagy et al., 2012). Interestingly, plasmalogen-deficient mice exhibit several eye defects, including retinal vascular development abnormalities (Saab et al., 2014), as well as a downregulation of brain connexin 43 (Cx43) (Rodemer et al., 2003).

Cx43 is considered as being ubiquitously distributed and is the major connexin in mammal cells (Laird, 2006). Cx43 is implicated in several key cellular functions of glial cells such as gap junction-intercellular communication (GJIC) (Goodenough et al., 1996) or cell migration (Homkajorn et al., 2010). In the retina, Müller cells represent the main glial cell type as they can make up to 90% of macroglial cells (Bringmann et al., 2006). Müller cells are involved in crucial features of the retina, including water and ions homeostasis, angiogenesis, and inflammation (Bringmann et al., 2006; Reichenbach and Bringmann, 2013; Vecino et al., 2016; Toft-Kehler et al., 2018). Such abilities require multiple means of communication between Müller cells, but also with other cell types. For instance, it has been shown that Müller cells can communicate directly through gap junctions-dependent pathways, namely GJIC (Newman and Zahs, 1997; Newman, 2001). Gap junctions are intercellular channels that allow for calcium waves to propagate between adjacent cells among cell networks (Herve and Derangeon, 2013). In the retina, gap junctions between glial cells mostly rely on Cx43 (Zahs and Ceelen, 2006; Kerr et al., 2010), including with astrocytes, which are critical for proper vascular development of the retina (O'Sullivan et al., 2017).

Interestingly, previous data from our laboratory revealed high plasmalogen levels in the retina and suggested that Müller cells play a leading role in plasmalogens biosynthesis (Acar et al., 2007). Thus, using complementary *in vivo* and *in vitro* approaches targeting DHAPAT, our study aimed at determining the impact of plasmalogen depletion on Cx43 expression in the retina as well as on key functional tasks of Müller cells.

2 MATERIALS AND METHODS

2.1 Animals and Cells

2.1.1 Animals

Experiments on animals were performed in accordance with the ARRIVE guidelines, the Association for Research in Vision Ophthalmology (ARVO) statement for the use of animals in ophthalmic and vision research, and with French legislation (personal authorization number 21CAA086 for N.A and animal quarters agreement number A21231010 EA), after approval by ethics committees (#105 Comité d'Ethique de l'Expérimentation Animale Grand Campus Dijon) and by the French Ministry of Higher Education and Research (reference number 02271.1).

2.1.2 Müller Cells

Primary Müller cells were prepared from rat retinas according to a procedure previously described by Hicks and Courtois with slight modifications (Hicks and Courtois, 1990). Nine to 12 days-old animals were obtained from a Wistar rat colony established in our animal quarters. Animals were killed by decapitation. Eyes were isolated and placed in Dulbecco's Modified Eagles Medium (DMEM; Pan Biotech, Germany) with 10% Fetal Bovine Serum (FBS) overnight at room temperature in the dark. Eyeballs were then pre-digested in DMEM containing 0.1% Trypsin-EDTA 10X (Sigma-Aldrich, United States) and 70 U/ml collagenase (Sigma-Aldrich, United States) at 37°C for 45 min. Eyeballs were then placed in DMEM—10% FBS, corneas were incised, lenses and vitreous bodies taken out, and retinas were gently isolated. Retinas were dissociated into small pieces and placed into a Petri dish containing DMEM with 4.5 g/L of glucose, 10% FBS and 10 µL/ml of streptomycin (10 mg/ml)—penicillin (10,000 U/mL) (Pan Biotech, Germany). The medium was not changed during the first 2 days and then progressively substituted by DMEM with 1 g/L of glucose. Cells at 80% confluence were reseeded on different materials depending on their final use (P1) (**Figure 1**). They were used at second generation (P2).

2.1.3 Astrocytes

Primary astrocytes were extracted from rat cerebral cortex. Twenty-one days-old pups were obtained from the same Wistar rat colony established in our animal quarters. Anesthesia was performed *via* an intraperitoneal injection of pentobarbital (Ceva, France) at 0.1 mg/100 g. Animals were perfused through heart's left ventricle with a cold PBS solution. The brain was removed and astroglial cells isolation was performed according to a previously described protocol (Schildge et al., 2013) with slight modifications. Briefly, cortices were separated from the brain and the meninges removed. Cortices were cut into small pieces using sharp blades, and cells were then dissociated by three successive trituration and sedimentation steps in DMEM F12 + 10 µL/ml of streptomycin-penicillin medium. Dissociated cells were then plated onto a 75 cm^2 culture flask, previously pre-coated with poly-L-lysine (1X) and maintained in culture medium (DMEM F12 + 10% FBS +10 µL/ml of streptomycin-penicillin) in an incubator at 37°C with 5% CO2 and 95% humidity. The media was changed every 3–4 days. At 80% confluence, the flask was shaken overnight at 200 rpm to remove non-astroglial cells.

2.1.4 Co-Culture Model

At second generation, Müller cells and astrocytes were seeded on poly-L-lysine coated glass coverslips (18 mm diameter) in 6-wells

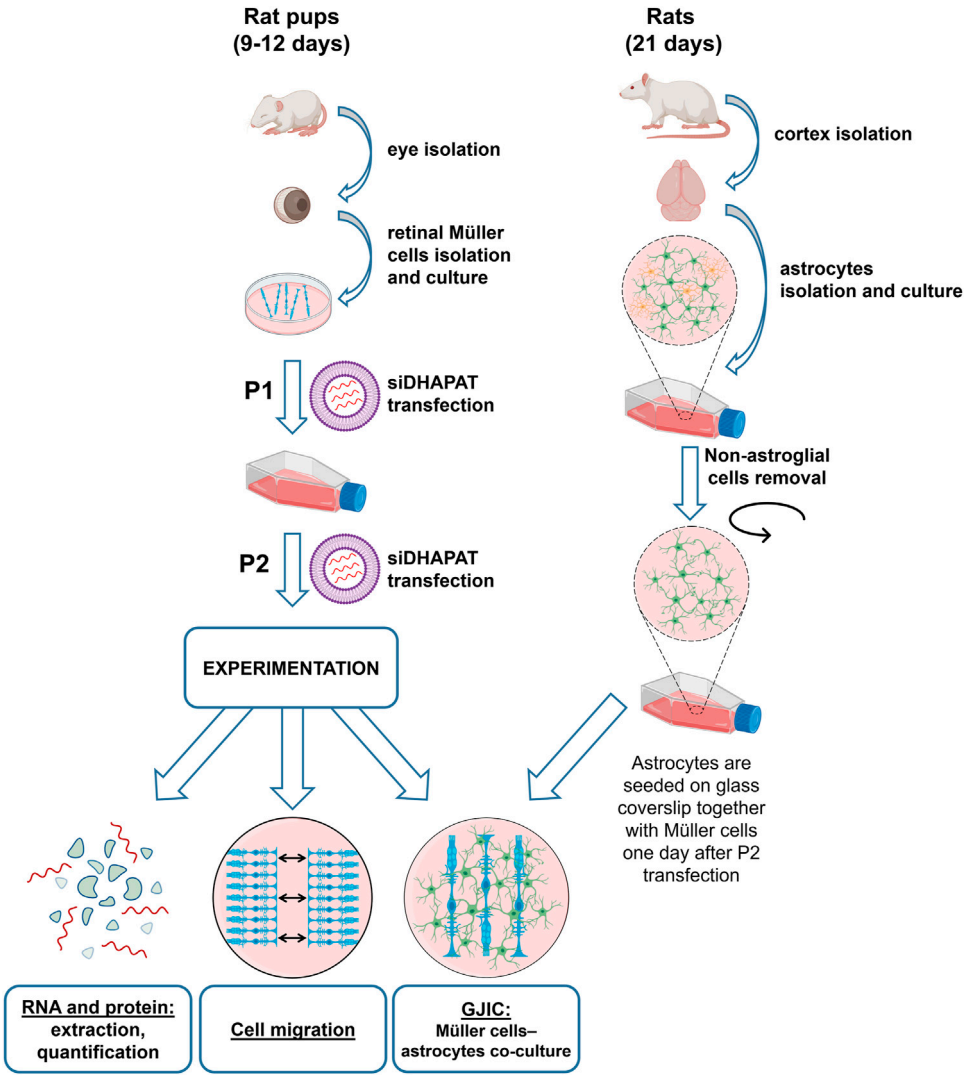

FIGURE 1 | Experimental procedure of plasmalogen depletion using a siRNA-based approach targeting DHAPAT in primary rat retinal Müller cells. Primary Müller cells were prepared from rat retinas according to a previously described procedure (Hicks and Courtois, 1990) with slight modifications. Briefly, eyes were isolated from 9 to 12 days-old rats. Isolated retinas were then dissociated into small pieces and placed into a petri dish. Cells at 80% confluence were reseeded (P1) in a 75 cm^2 culture flask and transfected with a control or DHAPAT-targeting siRNA depending on their final use. The procedure was repeated until the cells have received a second transfection and were then used at second generation (P2). See Materials and methods 2.1 for the complete primary Müller cells and astrocytes isolation, transfection and co-culture procedure.

plates (25 mm diameter) at 5.10^5 cells/ml and 8.10^5 cells/ml, respectively. Müller cells were seeded 1 day before astrocytes to allow the transfection with siRNA. Cells were co-cultured together during 4 days before the experiment in DMEM F12 + 10% FBS +10 µL/ml of streptomycin-penicillin medium (**Figure 1**).

2.2 Immunohistochemistry

Adult C57BL/6 mice (3 months of age, Centre d'Elevage Janvier, France) were euthanized by CO2 exposure. The eyeballs were isolated and fixed overnight in formaldehyde solution (PFA) 4% (Sigma-Aldrich, United States). Lens and cornea were then taken out and eyecups were dehydrated in sucrose baths with gradually increasing sucrose concentrations before being embedded in Tissue-Tek O.C.T. (Sakura Finetek, Netherlands) and frozen into liquid nitrogen. 10 µm-thick cryo-sections were performed on a Leica microtome (CM 3050 S, Leica Microsystemes, France) and were mounted on SuperFrost PlusTM slides (Thermo Scientific, United States). Primary Müller cells were isolated as previously described and seeded on microscope slides fixed for 2 h in PFA 4% and kept in 1X PBS +0.01% thimerosal (Sigma-Aldrich, United States) until further experiments. Prior to antibody labeling, both eye cryo-sections and Müller cells-slides were blocked for 1 h in 1% BSA (Sigma-Aldrich, United States) + 0,1% Triton X-100 (Sigma-Aldrich, United States) + 0,05% Tween (Sigma-Aldrich, United States).

They were then incubated overnight at +4°C in the same BSA/Triton/Tween solution with the following primary antibodies: GNPAT at a dilution of 1:250 (PA5-36447, rabbit polyclonal, Invitrogen, United States), and Glutamin synthetase at a dilution of 1:10,000 (MA5-27749, mouse monoclonal, Invitrogen, United States). After 5 consecutive washes in 1X-PBS, samples were then incubated for 1 h at room temperature in BSA/Triton/Tween solution with DAPI (1:200, Sigma-Aldrich, United States), Alexa Fluor 488 (A11001, goat anti-mouse, Invitrogen, United States) and Alexa Fluor 594 conjugated secondary antibodies (A-11032, goat anti-rabbit, Invitrogen, United States). Samples were then washed again with 5 consecutive 5 min PBS before being sealed in mounting media (Dako, Denmark) for imaging on an inverted confocal microscope (TCS SP8, Leica Microsystemes, France).

2.3 Inhibition of DHAPAT-Mediated Plasmalogen Biosynthesis by siRNA Transfection

Silencer® Select siRNAs were used to knockdown expression of DHAPAT. DHAPAPT-targeting siRNA (siDHAPAT) (siRNA ID s136618 sense 5′-CAUCGUUCUCAAUUCUGAAtt-3′, anti-sense 5′-UUCAGAAUUGAGAACGAUGga-3′ and siRNA ID s136619 sense 5′-GGAUGUCCUUCAGUUGCUUUtt-3′, anti-sense 5′-AAGCAACUGAAGACAUCCtc-3′) and the non-targeting controls (siCTL) were purchased from Ambion (references 4390771 and 4404020, ThermoFisher Scientific, United States). The siRNA transfection of Müller cells was performed using Lipofectamine RNAiMAX transfection reagent (ThermoFisher Scientific, United States) in OPTIMEM medium (ThermoFisher Scientific, United States) overnight at 37°C in 5% CO2 humidified atmosphere according to manufacturer's instructions. Medium was then replaced by DMEM supplemented with 10% FBS on the next morning. Finally, cells were used for experiments 5 days after the second transfection.

2.4 Evaluation of Müller Cells Plasmalogen Content

Total lipid from Müller cells were extracted according to the method described by Folch and collaborators (Folch et al., 1957) by using a mixture of chloroform/methanol (2:1, v:v). Lipid extracts were stored at −20°C under inert gas until further analyses. Total lipids previously extracted were transmethylated using boron trifluoride (BF3) in methanol according to Morrison and Smith (Morrison and Smith, 1964). Fatty acid methyl esters (FAMEs; formed by the transmethylation of fatty acids at *sn*-1 and *sn*-2 positions of diacylglycerophospholipids and the *sn*-2 of plasmalogens) and dimethylacetals (DMAs; formed by the transmethylation of the aldehyde aliphatic groups on *sn*-1 position of plasmalogens) were subsequently extracted with hexane and analyzed by gas chromatography on a Trace 1310 gas chromatograph (ThermoScientific, Waltham, MA, United States) using a CPSIL-88 column (100 m × 0.25 mm i. d, film thickness 0.20 µm; Varian, France) equipped with a flame ionization detector. Hydrogen was used as the carrier gas (inlet pressure 210 kPa). The oven temperature was held at 60°C for 5 min, increased at 165°C with a 15°C/min rate, held for 1 min and then to 225°C at 2°C/min and finally held at 225°C for 17 min. FAMEs and DMAs were identified by comparison with their commercial and synthetic standards. The data were processed using the EZChrom Elite software (Agilent Technologies, France) and reported as a percentage of total FAMEs and DMAs. Plasmalogen levels were calculated as 2 x (% of total DMAs) as previously described by Acar and collaborators (Acar et al., 2007).

2.5 Protein Expression

Proteins were first extracted from Müller cells in RIPA lysis buffer (ThermoFisher Scientific, United States) with extemporaneous addition of a phosphatase inhibitor (Roche, Sigma-Aldrich, United States) and protease inhibitor (Roche, Sigma-Aldrich, United States) cocktails. After a 30-min centrifugation at 10,000 x g, the supernatant containing proteins was isolated. Protein content was measured by using Pierce BCA Protein Assay Kit (ThermoFisher Scientific, United States) at 562 nm by a multilabel plate reader (Victor 3V, PerkinElmer, United States). Dilutions of known concentrations of BSA were prepared and used to determine standard curve.

Twenty five micrograms of protein extracts were boiled for 5 min in a 4X Laemmli buffer (40% glycerol, 240 mM Tris/HCl pH 6.8, 8% SDS, 0.04% bromophenol blue, 5% beta-mercaptoethanol) and then separated by electrophoresis at 125V for 1 h (Mini-PROTEAN® Tetra System, BioRad, United States) using 4–15% SDS-PAGE Stain-Free precast gels (Mini-PROTEAN®, TGX Stain-Free, BioRad, United States). After UV activation of the protein gels on a Chemidoc (BioRad, United States), proteins were subsequently transferred on a nitrocellulose membrane (BioRad, United States) using a Transblot Turbo (BioRad, United States). Membranes were blocked for 1 h at room temperature in a PBS solution with 3% BSA (Sigma-Aldrich, United States) and then incubated for 1 h at room temperature with primary antibodies. Primary antibodies used were 1:1,000 rabbit anti DHAPAT (ref 14931-1-AP, ProteinTech, United Kingdom), mouse anti-Cx43 at 1:1,000 dilution (ref 610062, BD Biosciences, United States), 1:1,000 mouse anti-pCx43 (S368) (ref 52559, Cell Signaling Technology, Netherlands), 1:1,000 rabbit anti-pCx43 (Y265) (ref ab193373, Abcam, United Kingdom), rabbit anti GFAP (1:1,000 dilution, ref sc-6171-R, Santa Cruz Biotechnology, United States), mouse anti β -tubulin (1:2000 dilution, ref 32–26,000, ThermoFisher) and rabbit anti β-actin (1:2000 dilution, ref A2066, Sigma-Aldrich). Membranes were then rinsed for 30 min at room temperature using a mixture of PBS-T (10 mM Na2HPO4, 1,76 mM KH2PO4, 137 mM NaCl, 2,7 mM KCl, and 0.1% Tween 20 w/v) and incubated with HRP-conjugated secondary goat anti-mouse antibodies (reference P0161, Dako, Denmark) for 1 h at room temperature. After another 30min-rinsing, blots were incubated for 2min with ECL reagents (Perkin Elmer, United States) and visualized by chemiluminescence using a charge-coupled device

(CCD) camera (Chemidoc, BioRad, United States). Protein expression was then quantified using total protein loads.

2.6 Gene Expression

After being grown and transfected as described in 2.1, primary Müller cells were collected from culture flask in PBS solution, snap-frozen in liquid nitrogen and stored at −80°C. Total RNA was isolated from primary Müller cells using the NucleoSpin RNA Plus XS Kit (Macherey-Nagel, France) and quantified using a NanoDrop 2000 (Thermo Scientific, United States). RNA samples were then divided in 10 µL aliquots each containing 100 ng of RNA and stored at −20°C. cDNA was synthesized from RNA samples using the high capacity cDNA reverse transcription Kit (Applied Biosystems, United States) and stored in 20 µL aliquots at −20°C. 2µL of cDNA sample were added to 10 µL of iTaq Universal SYBR® Green Supermix (BioRad, United States) plus the corresponding primers. Finally, qPCR was performed on a StepOnePlusTM (ThermoFisher, United States). The qPCR run consisted of a first step at 95°C for 10 min, followed by 40 cycles of 15 s at 95°C, 1 min at 60°C and 30 s at 72°C. In addition to the Cx43-encoding gene (*Gja1*), *Gusb,* and *B2m* were used as housekeeping genes. Primers sequences were as follows: *Gja1*: Forward 5′-CAGCTGTTG AGTCAGCTTGG - 3′, Reverse 5′-ACATGGGCCAAGTAC AGGAG-3'; *Gusb*: Forward 5′-CTCGAACAATCGGTTGCA-3′, Reverse 5′- TCATTGAAGCTGCAAGGGACC-3'; *B2m*: Forward 5′-CCGTGATCTTTCTGGTGCTTG -3′, Reverse 5′-CGGTGGATGGCGAGAGTACA-3'.

2.7 ATP-Stimulated Müller Cells Calcium Response

Primary Müller cells were isolated, cultured and transfected according to the previously described conditions in 2.1 (Hicks and Courtois, 1990). Cells were seeded in Poly-D-lysine coated 96-wells plastic plates (Corning BiocoatTM, Falcon, United States). Müller cells were loaded for 45 min at 37°C with the calcium probe Fluo-4 AM (Molecular Probes, United States) and the organic anion transporters inhibitor probenecid (Invitrogen, United States) in the same modified HBSS. After incubation, plates were placed in a multi-mode microplate reader FlexStation® 3 (Molecular Devices, United States) together with a 500 µM ATP-containing stimulation plate. Müller cells were then stimulated with ATP using the following injection parameters: volume = 50 µL, speed rate 6 (~94 µL/s), height = 60 µL. Calcium response was recorded during 90 s with the following recording parameters: sensitivity = 50 readings, PMT high; reading interval = 5.04 sec. Data were recorded and analyzed using the SoftMax Pro 5.4.6 software (Molecular Devices, United States). Three 96-wells plates were used as replicates for each experiment. The mean of the three plates was used for analysis.

2.8 Calcium Imaging

Co-cultured astrocytes and Müller cells were loaded for 45 min at 37°C under gentle agitation with 2, 5 µM of Fura-2 acetoxymethylester (Fura-2AM, Molecular Probes, United States) in a modified Hanks buffered saline solution (HBSS: 135 mM NaCl, 5 mM KCl, 1.3 mM CaCl2, 1 mM MgCl2, 10 mM HEPES, 2.5 D-glucose, and pH 7.4) supplemented with 0.002% pluronic acid (P3000MP, Molecular Probes, United States). After incubation, glass plates covered with cells were mounted in a thermostatically regulated microscope chamber on an inverted Olympus microscope (IX 70, Olympus Corporation, Japan) and visualized with a 20X objective. Intercellular calcium waves were induced by the application of 100 µM ATP onto a single Müller cell with an 8.4-µm glass micropipette. Two 100 msec-pulses at 10 psi were delivered with a pneumatic PicoPump (PV830, World Precision Instruments, United States). A real-time movie of intercellular calcium waves of stimulated Müller cell and neighboring astrocytes following stimulation was recorded at 2 Hz for 4 min by alternating excitations at 340 and 380 nm (emission spectrum: 420–600 nm). Images were recorded using a CCD camera with the live acquisition software (TiLL photonics, United States). The 340/380 nm fluorescence ratio was calculated after correction for background fluorescence values. A baseline recording was performed for 2 min before stimulation.

2.9 Quantitative Analysis of Intercellular Ca2+ Waves

Each cell was considered as an individual region of interest (ROI). For each ROI, we obtained a curve representing the 340/380 nm fluorescence ratio. Since the fluorescence intensity of Fura-2AM is proportional to calcium concentrations, changes in cytosolic calcium concentrations were inferred from the fluorescence profile of individual cells. The mask of each ROI was imported on ImageJ software (National Institute of Health, United States, https://imagej.nih.gov/ij) to measure the distance between the stimulated Müller cell and the subsequently activated astrocytes. Astrocytes were considered as activated once they reached a 10% increase of the baseline (0.1 x Imax + baseline), and the corresponding latency time was evaluated (activation time). The velocity of calcium wave propagation was calculated and expressed in µm/s. Finally, astrocytes calcium response intensity following their activation was evaluated and expressed as a percentage of increase of the baseline (activation amplitude = ((Imax x 100)/baseline)—100). The change in fluorescence intensity was normalized to the level of baseline fluorescence.

2.10 Cell Migration

Müller cells migration was evaluated by a wound healing assay. Müller cells were isolated and generated as previously described (see 2.1 and **Figure 1**). At P2, cells were seeded in a culture-Insert (Ibidi, Germany) at a density of 1×10^4 cells/well. Inserts were removed 5 days after the second siRNA transfection (P2), thus creating a cell-free gap of 500 µm. Cell migration was monitored under microscope by recording a picture each hour during 72 h. Three fields per insert were observed and the results were averaged. The cell-free area and the percentage of recovery were measured and calculated using the ImageJ software (National Institutes of Health, United States).

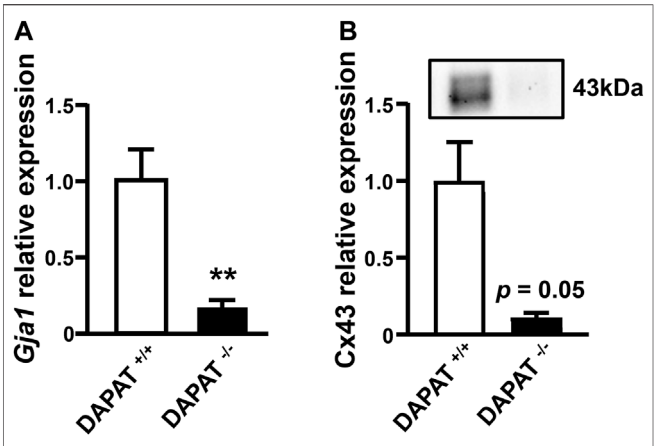

FIGURE 2 | Downregulation of Cx43 gene and protein expression in the retina of plasmalogen-deficient DAPAT adult mice. **(A)** RT-qPCR analysis of *Gja1* expression shows a significant downregulation in 13 weeks-old plasmalogen-deficient DAPAT$^{-/-}$ mice retina compared to DAPAT$^{+/+}$ mice retina (**$p < 0.01$; n = 6–8). **(B)** Western-blot analysis of Cx43 expression reveals a downregulation in 13 weeks-old plasmalogen-deficient DAPAT$^{-/-}$ mice retina compared to DAPAT$^{+/+}$ retina ($p = 0.05$; $n = 3$). Mann & Whitney test. Data shown as mean ± SEM.

2.11 Cell Proliferation

Cell proliferation was evaluated by Ki-67 labeling of Müller cells. Briefly, Müller cells were washed with PBS and fixed for 10 min with 4% formaldehyde in PBS. After washes and permeabilization steps with TritonX100 (Sigma-Aldrich), cells were incubated with primary antibodies (mouse anti-ki67, dilution 1:1,000, reference M7248, Dako, Denmark) overnight at 4°C. Then, secondary antibody (reference A11001, Thermo Fischer Scientific, dilution 1:1,000) and DAPI were added and cells were cover slipped using a fluorescence-mounting medium. Fluorescence microphotographs were taken using a Nikon microscope (Eclipse E600, Nikon, France) and a Nikon digital camera (DS-Ri2, Nikon) equipped with the Nikon Nis BR software. Images were analyzed with ImageJ software. Proliferation was evaluated as a ratio between the numbers of cells stained by Ki-67 to total cells stained by DAPI.

2.12 Statistical Analysis

Statistical analysis was performed using GraphPad Prism v6.05 (GraphPad software, United States). For gene and protein expression, comparisons between two groups were performed using a non-parametric Mann-Whitney test. For the calcium wave quantitative analysis, Pearson correlation coefficients were determined to assess linear associations between astrocytes activation time and their distance from the ATP-stimulated Müller cell. Radius-dependent comparisons between groups were performed by Mann & Whitney test. A p value lower than 0.05 was considered as statistically significant and noted by one star (*). Two (**) and three stars (***) were used for p values lower than 0.01 and 0.001, respectively.

3 RESULTS

3.1 Plasmalogen Deficiency is Associated With Retinal Cx43 Downregulation

Cx43 gene and protein expression were quantified in 13 weeks-old DAPAT$^{+/+}$ and DAPAT$^{-/-}$ mice retinas. Both Cx43 gene (*Gja1*) and protein were significantly downregulated in a similar fashion, as RT-qPCR revealed a reduction of *Gja1* expression by 83% ($p < 0.01$, $n = 6–8$) (**Figure 2A**), while western-blots revealed a reduction of Cx43 protein expression by 89% ($p = 0.05$; $n = 3$) (**Figure 2B**).

3.2 Plasmalogens Are Synthesized and Concentrated in Retinal Müller Glial Cells

Immunohistochemical staining of retinal cryosections revealed DHAPAT expression in several layers corresponding to the ganglion cell layer (GCL), the inner nuclear layer (INL) and the photoreceptors inner segments (IS) (**Figures 3A,B**). Such a pattern is consistent with the localization of Müller cells endfeet, Soma and distal processes, respectively. DHAPAT expression in Müller glia was then further confirmed by immunocytochemistry. A glutamine synthetase (GS)-DHAPAT double immunolabeling first confirmed the purity of our Müller cells culture and that Müller cells strongly express DHAPAT (**Figures 3C–F**). Finally, in order to assess the extent of plasmalogen biosynthesis activity in Müller glia, plasmalogen concentrations were compared in total lipid extracts from primary rat Müller cells and whole mouse retinas. A significantly higher concentration of plasmalogen in Müller cells compared to whole retina extracts (17.67 ± 0.30% vs. 7.53 ± 0.30% of total phospholipids, $p < 0.001$) (**Figure 3G**), confirming Müller glia as a major reservoir of plasmalogens in the retina. These data also reinforce the idea that plasmalogens might play specific roles in Müller cells physiology.

3.3 DHAPAT-Targeting siRNA Treatment is Associated to a Depletion of Plasmalogen Cell Content

In a second series of experiments, we decided to assess the efficiency of our siRNA-based plasmalogen depletion protocol. Plasmalogen content in Müller cells was assessed by a double transfection of primary Müller cells with a DHAPAT-targeted siRNA (siDHAPAT). siDHAPAT treatment induced a significant decrease in DHAPAT protein expression (−56%, $p < 0.01$) (**Figure 4A**) as well as a significant 56%-decrease in the cellular plasmalogen content (7.74 ± 0.59% *vs.* 17.61 ± 0.35% of total phospholipids, $p < 0.001$) (**Figure 4B**).

3.4 Plasmalogen Depletion of Müller Cells is Associated With Cx43 Protein Downregulation

Reduced levels of plasmalogens were significantly associated with a 47%-decrease in Cx43 protein expression ($p < 0.01$)

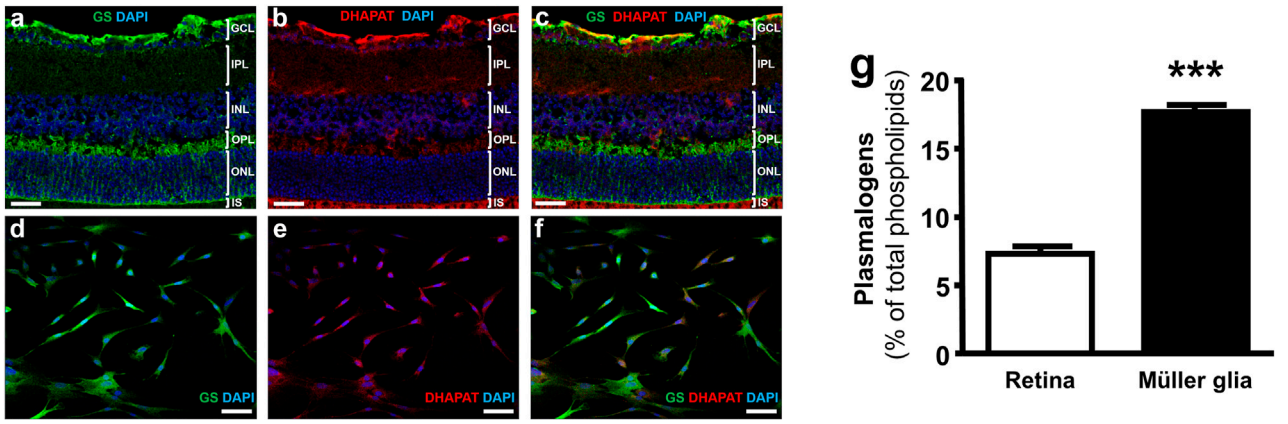

FIGURE 3 | Müller glia express DHAPAT and concentrate plasmalogens in the retina. **(A–C)** Immunohistochemical staining of glutamine synthetase (GS) and DHAPAT in retinal slices. GS expression pattern confirmed the radial Müller cells localization **(A,B)**. DHAPAT-positive cells showed a strong expression pattern in the ganglion cells layer (GCL), the inner nuclear layer (INL) and photoreceptors inner segments (IS) **(B,C)**, corresponding to the localization of Müller cells endfeet, Soma and distal processes, respectively. **(D–F)** Micrographs of primary rat Müller cells labeled with GS and DHAPAT primary antibody showing that GS-positive Müller cells also displayed a strong expression of DHAPAT. **(G)** Plasmalogen quantification by GC-FID reveals a strong concentration in Müller glia compared to whole retina extracts, suggesting a particular function of these ether-lipids in their physiology. $n = 10$. Mann & Whitney test. $^{***}p < 0.001$. Data shown as mean ± SEM. GCL = ganglion cell layer; IPL = inner plexiform layer; INL = inner nuclear layer; ONL = outer nuclear layer; OS = outer segments of the photoreceptors. Scale bars = 50 μM.

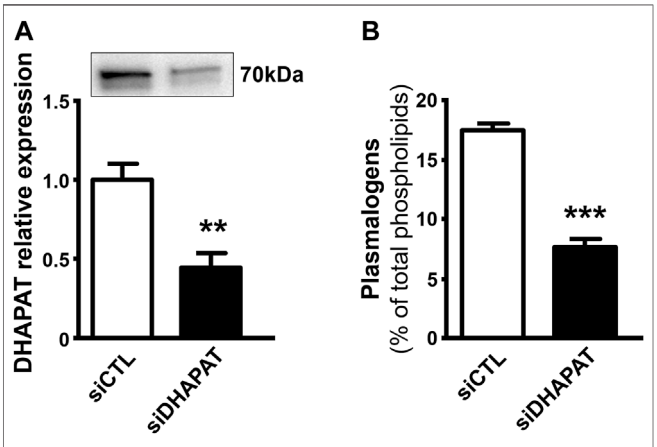

FIGURE 4 | Loss of DHAPAT expression in siDHAPAT-transfected Müller glial cells. **(A)** Western-blot analysis shows a significantly reduced expression of DHAPAT in primary Müller cells transfected with a DHAPAT-targeting siRNA (siDHAPAT) compared to control siRNA-transfected Müller cells (siCTL). **(B)** Plasmalogen concentrations determined by GC-FID are significantly reduced in siDHAPAT-transfected cells. Mann & Whitney test. $^{**}p < 0.01$; $^{***}p < 0.001$. $n = 10$. Data shown as mean ± SEM.

(**Figure 5A**). RT-qPCR analyses further showed that *Gja1* expression was also significantly downregulated in siDHAPAT-transfected Müller cells (−47%, $p < 0.01$) (**Figure 5B**). In order to determine whether other Cx43-dependent mechanisms are involved in Cx43 downregulation, we assessed Cx43 phosphorylation status, as it was shown that phosphorylation of Cx43 on S368 and Y265 residues triggers its degradation through the ubiquitin-proteasome pathway (Leithe

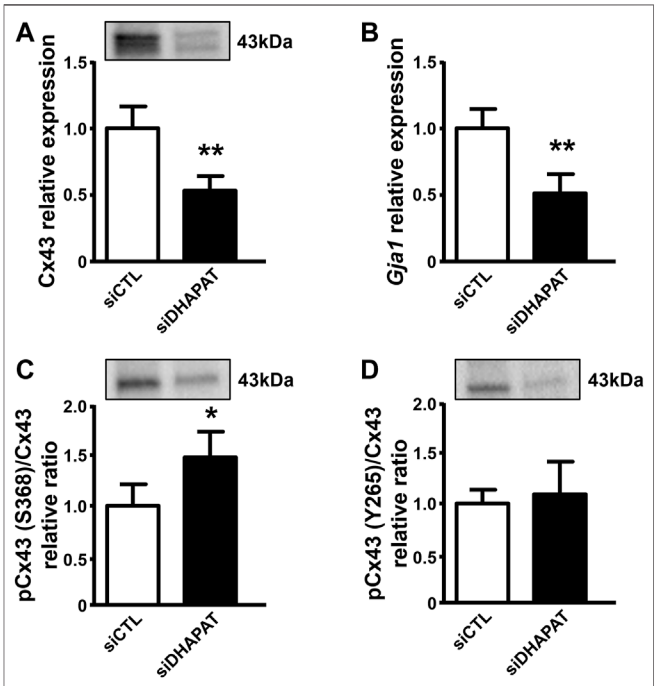

FIGURE 5 | Plasmalogen depletion impacts Cx43 expression in primary Müller cells culture. **(A)** Cx43 protein expression is significantly decreased in siDHAPAT-transfected primary Müller cells. **(B)** Reverse transcription quantitative PCR (RT-qPCR) indicates that siDHAPAT transfection significantly downregulated *Gja1* expression. **(C,D)** Western-blot analyses show a significant increase in the phosphorylation status of Cx43 on its S368 residue **(C)** but not on its Y265 residue **(D)**. $n = 6–8$ cell cultures. Mann & Whitney test. $^{*}p < 0.05$; $^{**}p < 0.01$. Data shown as mean ± SEM.

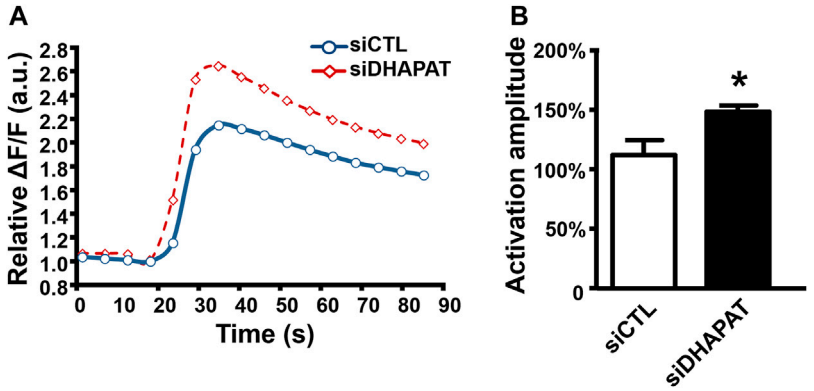

FIGURE 6 | Plasmalogen depletion enhances the calcium response of ATP-stimulated Müller cells. **(A)** Mean kinetic curves responses of control (siCTL) and plasmalogen-depleted (siDHAPAT) primary Müller cells stimulated with ATP. **(B)** Activation amplitude of ATP-stimulated Müller cells show that plasmalogen-depleted Müller cells display a significantly increased calcium response. $n = 4$. Mann & Whitney test. *$p < 0.05$. Data shown as mean ± SEM.

et al., 2018). We found that plasmalogen depletion was associated with a significant increase by 52% on the S368 ($p < 0.05$) (**Figure 5C**) but not on the Y265 residue (**Figure 5D**).

3.5 Plasmalogen Depletion Affects Müller Glia Response to ATP

To evaluate whether Cx43 downregulation could be associated with functional defects of Müller cells, we investigated Müller cells direct response to ATP stimulation (**Figure 6**). Müller cells treated with siDHAPAT exhibited a significant increase of the ATP-mediated calcium response, which was 36%-higher when compared to siCTL-treated cells (149 ± 5% vs. 113 ± 12%, $p < 0.05$) (**Figures 6A,B**).

3.6 Plasmalogen Depletion Alters Retinal Glial Cells Gap Junction-dependent Intercellular Communication

In the retina, Müller cells not only engage in GJIC with other Müller cells, but also with astrocytes, which are critical for numerous physiological features, including vascular development (O'Sullivan et al., 2017). We then used calcium imaging to determine whether plasmalogen depletion affects Müller cells-astrocytes intercellular calcium-based communication. siDHAPAT or siCTL-treated Müller cells were selectively activated in response to topical ATP application using a glass micropipette placed adjacently to the cell (**Figure 7A**). Astrocytes could be morphologically distinguished from Müller cells (**Figures 7A,B**), and the activation of neighboring astrocytes could be effectively monitored as the calcium wave propagated among the astrocytic network (**Figures 7C,D**). Astrocytes activation time data were plotted against the radius from the stimulated Müller cell and Pearson's correlation coefficients were determined to assess the statistical relationship between these two variables. The data showed positive linear associations for each group, confirming that astrocytes activation time is directly correlated to their distance from the ATP-stimulated Müller cell (rPearson: siCTL = 0.517; siDHAPAT = 0.5175) (**Figure 8A**). To further analyze astrocytes responses, we decided to split these data among 3 radius tertiles according to their distance from the ATP-stimulated Müller cell (T1 = 0–50 µm; T2 = 50–100 µm; T3 > 100 µm). Tertiles analyses confirmed that the increase in activation delay of neighboring astrocytes was maintained as the distance increased from the ATP-stimulated stimulated Müller cell (**Figure 8B**). Plasmalogen-depletion of Müller cells was associated to an increase of astrocytes activation time (**Figure 8B**) as well as a decrease of calcium wave velocity (**Figure 8C**), regardless of the distance between the astrocyte and the Müller cell (0–50 µm, $p < 0.05$; 50–100 µm, $p < 0.001$; >100 µm, $p < 0.01$). ATP stimulation of plasmalogen-depleted Müller cells also led to a significant increase in the activation amplitude of astrocytes whatever their distance to the ATP-stimulated Müller cells ($p < 0.05$) (**Figure 8D**), suggesting that the previously shown over-activation of plasmalogen-depleted Müller cells (**Figure 5**) is maintained throughout the calcium propagation to neighboring astrocytes.

Taken together, these results suggest that plasmalogens are involved in the regulation of ATP-stimulated calcium response of retinal Müller cells as well as its propagation through gap junctions to the neighboring astrocyte networks.

3.7 Plasmalogen Depletion Alters Müller Cells Migration

Through wound healing assays, we observed that the wound closure was about 70% after 72 h for siCTL-treated cells (**Figures 9A,B**). Inhibition of plasmalogen biosynthesis strongly affected the migration ability of retinal Müller cells as the rate of wound closure was significantly reduced by 35–40% after 72 h in siDHAPAT-treated Müller cells ($p < 0.05$) (**Figures 9A,B**). Interestingly, plasmalogen depletion was also associated with a 28%-decrease in GFAP protein expression ($p = 0.057$) (**Figure 9E**), but not that of other cytoskeleton proteins such as β-Actin (**Figure 9F**) or β-Tubulin (**Figure 9G**). Finally,

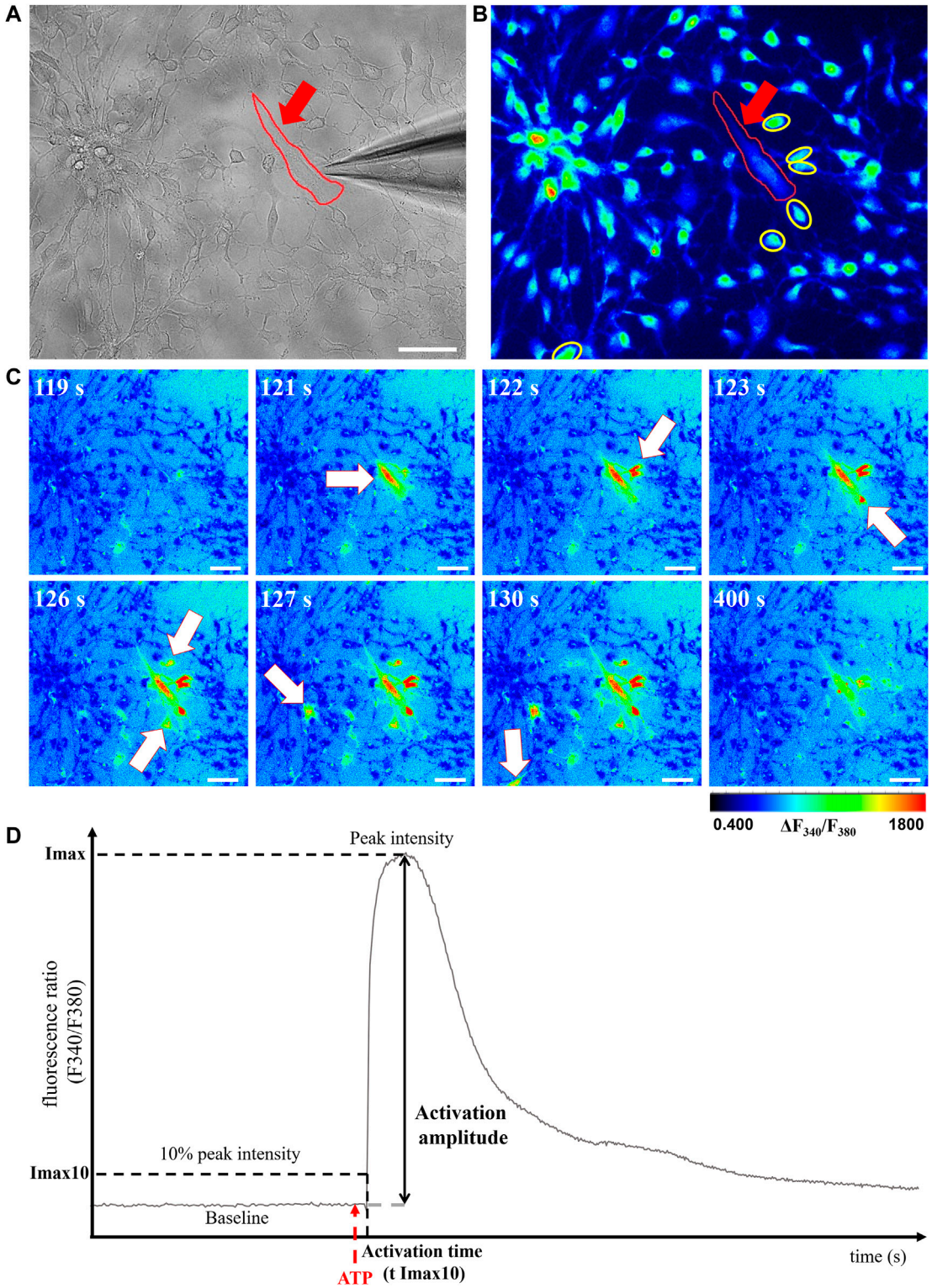

FIGURE 7 | Evaluation of GJIC between retinal Müller cells and astrocytes. **(A,B)** Calcium imaging. Müller cells (red arrow) can be morphologically distinguished from astrocytes (yellow circles) under brightfield **(A)** and fluorescent **(B)** modes. **(C)** ATP-stimulated calcium response of the Müller cell and neighboring astrocytes could be monitored under fluorescent microscopy as a function of time (white arrows). Pseudocolor images were obtained by the 340 nm/380 nm fluorescence ratio and the pseudocolor scale indicates fluorescence ratio values. **(D)** Graphical representation of astrocytes calcium response curves with the parameters selected for further analyses: cell activation threshold (Imax10), activation amplitude (% of baseline increase) and cell activation threshold time (T Imax10) were analyzed. Scale bars = 50 μm.

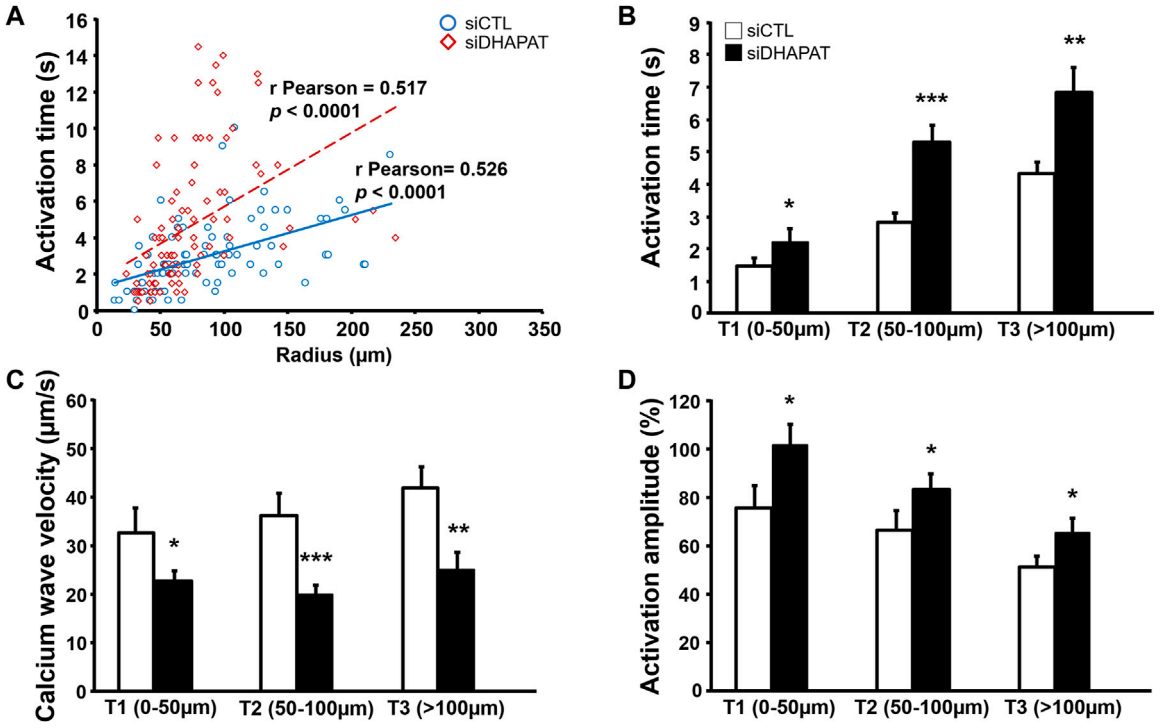

FIGURE 8 | GJIC alterations in astrocytes neighboring plasmalogen-depleted Müller cells. **(A,B)** Astrocytes stimulated by plasmalogen-depleted Müller cells display a significant increase in the activation time **(A,B)** and amplitude **(D)**, as well as in calcium wave velocity in all tertiles of distance **(C)**. n ≥ 75 astrocytes. Student *t* test. **p* < 0.05; ***p* < 0.01; ****p* < 0.001. Data shown as mean ± SEM.

alteration of Müller cells migration was not associated with modifications of cell proliferation as plasmalogen-depleted Müller cells did not exhibited any change in Ki-67 labeling (**Figures 9C,D**).

4 DISCUSSION

In this study, we used a double approach that relied on both *in vivo* and *in vitro* models to investigate the role of plasmalogens in Cx43-related functions of Müller cells. First, we used a plasmalogen-deficient mouse model (DAPAT mice) to assess the existence of an association between plasmalogens and Cx43 in the retina, which was previously identified in plasmalogen-deficient mice brains (Rodemer et al., 2003). Our results show that plasmalogen deficiency is associated with a significant downregulation of both Cx43 protein and gene (*Gja1*) in the retina of 13 weeks-old mice. To our knowledge, this is the first time that Cx43 downregulation is highlighted in the retina of adult DAPAT$^{-/-}$ mice, thereby confirming previously published results in the brain and the heart of plasmalogen-deficient mice (Rodemer et al., 2003; Todt et al., 2020) and suggesting that several tissues may face the same dysregulation mechanisms regarding Cx43 expression. Further studies are required to determine if such a Cx43 downregulations takes place progressively during post-natal growth or if mice pups are born with these alterations already in place, which could be another mechanism underlying the vascular development and glial abnormalities described in the developing DAPAT$^{-/-}$ mouse (Saab et al., 2014).

We then confirmed that not only Müller cells do express the plasmalogen-synthetizing enzyme DHAPAT, but that they also concentrate plasmalogens when compared to whole retinal extracts, suggesting a specific role for these ether-lipids in Müller cells. Yet, we did not know to what extent they are significant for their physiological functions. Furthermore, considering that plasmalogen metabolism seem to be associated with Cx43 regulation, we decided to further investigate this association and the main mechanisms involved *in vitro* using primary Müller cells.

Using molecular and biochemical approaches, we showed that plasmalogen depletion was sufficient to trigger Cx43 downregulation by affecting both transcriptional and post-translational mechanisms in Müller cells *in vitro*. *Gja1* expression is known to be regulated by numerous mechanisms such as transcription factors, epigenetic mechanisms (Oyamada et al., 2013), and even vitamin-associated compounds (Vine et al., 2005). It would be of particular interest to conduct dedicated studies in order to determine the mechanisms leading to *Gja1* downregulation in plasmalogen-depleted Müller cells. Moreover, one of the key features of the Cx43 stands to its C-terminus tail. Cx43 C-terminus consists in an unusually long intracytoplasmic tail with many binding sites for several enzymes, making it a target for various regulation mechanisms such as

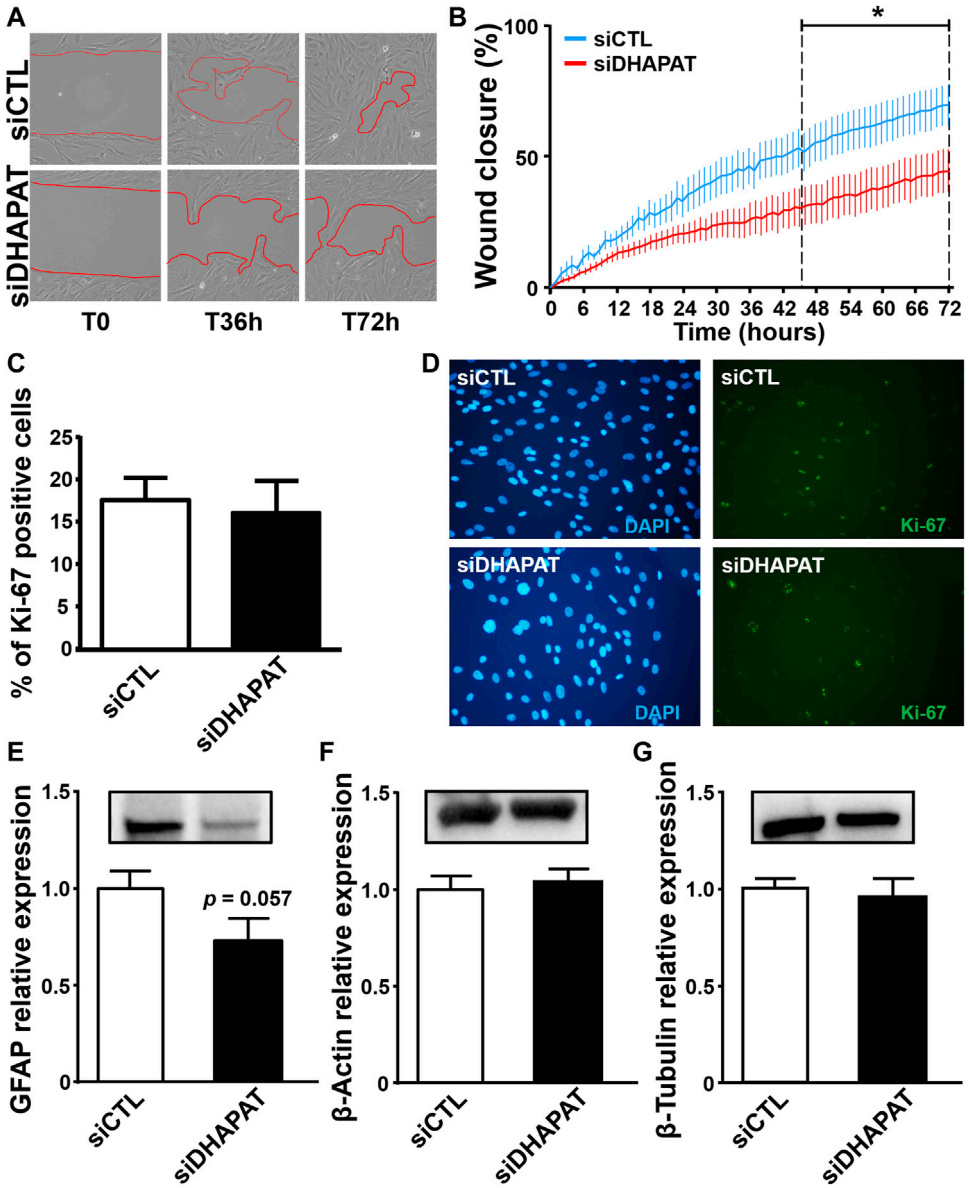

FIGURE 9 | Plasmalogen depletion of primary Müller cells is associated with a decrease of cell migration as well as GFAP expression, but does not modify cell proliferation or other cytoskeleton-related proteins expression. **(A)** Representative micrographs of primary Müller cells treated with a control siRNA (siCTL) or a DHAPAT-targeting siRNA (siDHAPAT) in a wound closure assay before treatment (T0), 36 and 72 h after treatment. **(B)** Quantification of wound closure assays. Summary graph of Müller cells migration speed represented as a percentage of wound closure at indicated time points. Plasmalogen-depleted Müller cells exhibited a significant reduction of migration speed when compared to controls (siDHAPAT vs. siCTL, $p < 0.05$) ($n = 10$ for siCTL, $n = 9$ for siDHAPAT). Two-way ANOVA with Tukey's multiple comparisons test. **(C)** Müller cells proliferation. Ki-67-labeled Müller cells were quantified as a percentage (%) of DAPI-positive cells. Plasmalogen-depleted Müller cells did not show any alteration of proliferation when compared to controls (siDHAPAT vs. siCTL) ($n = 10$ for siCTL, $n = 9$ for siDHAPAT). **(D)** Fluorescence microphotographs of DAPI and Ki-67-labeled Müller cells in siCTL and siDHAPAT-transfected groups. **(E–G)** Western-blot analyses show a reduction of GFAP expression in siDHAPAT-transfected Müller cells ($p = 0.05$) **(E)**, while other cytoskeleton-related proteins expression such as β-Actin **(F)** or β -Tubulin (g) remained unchanged. $n = 4$-5 cell cultures. Mann & Whitney test. $^*p < 0.05$. Data shown as mean ± SEM.

phosphorylation (Leithe et al., 2018), which is known to regulate its degradation by the ubiquitin-proteasome pathway (Leithe and Rivedal, 2004; Kimura and Nishida, 2010). Here we focused on the main phosphorylation sites linked to PKC (S368) and Src (Y265) activities. Our results indicate that plasmalogen depletion resulted in Cx43 overphosphorylation by PKC, but not by Src. Therefore, we suggest that Cx43 degradation is increased by a PKC-mediated overphosphorylation that may be further reducing cell content in Cx43. Cx43 overphosphorylation by PKC in plasmalogen-depleted Müller cells could be a direct consequence of the changes in cell membrane composition. Indeed, previous studies have shown that unlike usual diacyl

glycerol (DAG) generated from phospholipids by phospholipase C (PLC) activity, alkenylacyl-glycerides (plasmalogen-derived DAG) does not induce PKC activation despite being ligands of the enzyme (Cabot and Jaken, 1984; Ganong et al., 1986; Heymans et al., 1987; Daniel et al., 1988). Instead, they would rather act as DAG competitive inhibitors, therefore representing an inhibition mechanism for PKC activity (Clark and Murray, 1995; Warne et al., 1995; Mandal et al., 1997). Besides, PKC activation requires prior docking to the cell membrane. Several phospholipid species of the choline (PC) and serine (PS) subgroups, as well as DAG or even phosphoinositides such as phosphatidylinositol bisphosphate (PIP2) are involved in this mechanism (Gould and Newton, 2008; Guerrero-Valero et al., 2009; Lucic et al., 2016). Accordingly, one could hypothesize that plasmalogen depletion induces spatial and molecular rearrangements of the cell membrane, leading to a facilitated recruitment of PKC. Further studies are needed to elucidate the association between plasmalogens and Cx43 expression and phosphorylation in Müller cells.

Moreover, Cx43 being the major component of retinal gap junctions, we aimed to look for potential alterations of GJIC in a two-steps manner: 1) the initiation steps in Müller cells, and 2) propagation of the calcium wave to neighboring cells. By using the Flexstation 3® plate reader device, we were able to precisely study the isolated calcium response of Müller cells to ATP-stimulation with reproducible and well-calibrated parameters. Our data reveal an increase in the activation amplitude of plasmalogen-depleted Müller cells (siDHAPAT = 85% vs. siCTL = 64%). Interestingly, previous research reported a decrease of the activation amplitude in Cx43 KO astrocytes (Scemes et al., 1998). Even though our model only exhibited partial Cx43 depletion, this suggests the existence of some distinct mechanisms between Müller cells and astrocytes to ATP-induced calcium response. To our knowledge, our data are the first reporting an increase of ATP-induced calcium response following a plasmalogen depletion in Müller cells. Interestingly, previous studies have linked calcium release from the endoplasmic reticulum (ER) to n-3 polyunsaturated fatty acids (PUFAs) such as docosahexaenoic acid (DHA) in astrocytes (Sergeeva et al., 2005; Begum et al., 2012) showing that DHA reduces astrocytic calcium response amplitudes, partly by inhibiting the IP3 receptors activity. As plasmalogens are known to be "reservoirs" of PUFAs (including DHA) in the cell membrane (Nagan and Zoeller, 2001), we could hypothesize that plasmalogen depletion is associated to a lower DHA bioavailability in Müller cells, thereby preventing its inhibitory effects on the calcium release from the ER. This hypothesis is supported by a significant reduction of the n-6/n-3 PUFAs ratio in siDHAPAT-treated Müller cells (data not shown), and by a previous work from our laboratory showing that inhibiting PUFAs release from plasmalogens leads to alterations similar to plasmalogen deficiency in mouse (Saab et al., 2014).

Considering that Müller cells also engage in GJIC with astrocytes, which are crucial for vascular development of the retina (Saab et al., 2014) and other key features of retinal physiology like blood flow regulation (Metea and Newman, 2006; Newman, 2015), we aimed at checking for potential alterations of GJIC between plasmalogen-depleted Müller cells and astrocytes. Our data show that siDHAPAT-treated Müller cells evoked calcium waves that propagated slower than calcium waves originating from control Müller cells (**Figure 8C**), thus resulting in a delayed activation of neighboring astrocytes (**Figure 8B**). The average activation time of astrocytes closer than 50 µm from the Müller cell was 1.8 s for the siCTL group, while it rose to 2.5 s for the siDHAPAT group. Here, we show that calcium waves from control Müller cells propagated at an average speed of 37.3 µm/s, which is consistent with previous studies (Newman and Zahs, 1997; Scemes et al., 1998) measuring calcium wave velocities of 25.3 µm/s and 18.8 µm/s, respectively. Calcium waves originating from plasmalogen-depleted Müller cells propagated at 23.7 µm/s, which represents a 37%-diminution in propagation velocity. Interestingly, Scemes, Dermietzel and Spray also found a 36% reduction of calcium wave velocity in Cx43-KO astrocytes (Scemes et al., 1998). However, they also found that knocking out Cx43 induced a reduction in astrocytes activation amplitude, while we found that astrocytes stimulated by plasmalogen-depleted Müller cells (with downregulated Cx43) exhibited stronger activation amplitudes (**Figure 8D**), which seems consistent with the fact that plasmalogen-depleted Müller cells displayed an increase in their ATP-induced calcium response (**Figure 6**). Accordingly, our results allow us to hypothesize that astrocytes alteration in the plasmalogen-deficient DAPAT$^{-/-}$ mouse could be associated with (at least partly) functional defects of Müller cells. In order to validate our findings, it would be of particular interest to assess Müller cells response to ATP and the subsequent GJIC *in situ* on whole retinas or on isolated Müller cells from *ex vivo* DAPAT$^{-/-}$ mice retinas using previously described procedures (Uckermann et al., 2002; Kurth-Nelson et al., 2009; Tchernookova et al., 2018). Further studies would then be needed to evaluate to what extent the defects in GJIC between Müller cells and astrocytes participate to the abnormal astrocytic template formation in the DAPAT$^{-/-}$ mice as observed previously (Saab et al., 2014).

Besides, the functions of Cx43 in glial cells are not restricted to GJIC since several studies pointed out the implication of Cx43 in other cellular mechanisms such as cell migration (Homkajorn et al., 2010; Lagos-Cabre et al., 2019; Olk et al., 2010). Indeed, Cx43 is a transmembrane protein that acts as a membrane anchor for cytoskeletal proteins (Butkevich et al., 2004; Crespin et al., 2010; Matsuuchi and Naus, 2013), thereby regulating cell cytoskeleton network. Therefore, it seemed likely that alterations of Cx43 may induce modifications of the cytoskeleton network organization and subsequent cell migration (**Figures 9A,B**), potentially even without altering the expression of its protein actors like β-actin or β-tubulin (**Figures 9F,G**). Surprisingly, we found that reducing levels of plasmalogens was associated with a downregulation of GFAP (**Figure 9E**) in Müller cells. As GFAP is overexpressed in activated Müller cells during gliosis and considering its implication in cell migration mechanisms, our data suggest that lowering Müller cells plasmalogen content may influence the reactivity of Müller cells to gliosis but also their ability to migrate. To our knowledge, this is the first time that plasmalogen metabolism is associated with such functional alterations of

Müller cells. Although these data could provide an interesting insight into retinal gliosis mechanisms, further studies are needed to unravel the precise cellular and molecular mechanisms linking plasmalogen levels to GFAP and Cx43 protein metabolism. Several mechanisms can be hypothesized. First, GFAP and Cx43 have several common transcription factors regulating sites in their promoter sequence such as NFkB, AP-1 or AP-2 (Geimonen et al., 1996; Gomes et al., 1999; Wu et al., 2013; Brenner et al., 2019). Quantifying these transcriptional regulators could therefore be of great interest. Secondly, it has been shown that plasmalogens regulate Protein Kinase C (PKC) activity (Daniel et al., 1988; Sejimo et al., 2018), which is responsible for Cx43 phosphorylation and subsequent degradation by the ubiquitin-proteasome pathway (Leithe, 2016). Interestingly, GFAP is also regulated by several mechanisms including phosphorylation (Harrison and Mobley, 1991; Inagaki et al., 1994), and it have been suggested that phosphorylation status of GFAP in glial cells may play an important role in astrocyte remodeling during development and disease (Sullivan et al., 2012). Accordingly, we can hypothesize that plasmalogen depletion could induce a greater activity of PKC and then contribute at least partially to Cx43 and/or GFAP downregulation.

It can be underlined that our model of partial reduction of cellular plasmalogens presented in this study could be of particular interest to investigate the plasmalogen-related cellular mechanisms, as it may mimic biochemical alterations that are closer to pathological conditions when compared to fully-deficient cell lines, which are only relevant for rare diseases such as Rhizomelic chondrodysplasia punctata (RCDP).

To conclude, we show that cell levels of plasmalogens influence the expression and phosphorylation of Cx43, the major protein in gap junctions. In addition to the Cx43 downregulation, plasmalogen-depleted Müller cells displayed defects in both the ATP-stimulated calcium response (initiation) as well as calcium wave's propagation to neighboring astrocytes. Finally, we show that plasmalogen depletion of Müller cells was associated with an alteration of their migration abilities, as well as a downregulation of GFAP expression, a glia-specific cytoskeleton protein involved in glial activation, but not with other cytoskeleton-related proteins. Therefore, our data support the hypothesis that plasmalogen metabolism is involved in the regulation of Cx43 in the retina and Müller cells, and regulates crucial functions of Müller cells such as GJIC and cell migration.

DATA AVAILABILITY STATEMENT

The raw data supporting the conclusion of this article will be made available by the authors, without undue reservation.

ETHICS STATEMENT

The animal study was reviewed and approved by #105 Comite d Ethique de l'Experimentation Animale Grand Campus Dijon.

AUTHOR CONTRIBUTIONS

RK, JM, LBd, LBn, AB, XF, and NA designed the study. RK, JM, LL, BB, SG, CB, MK, PB, J-BB, ED, CF, XF, and NA acquired, analyzed and interpreted the data. RK, JM, LBd, LBn, AB, XF, and NA drafted the manuscript. All authors reviewed the manuscript.

ACKNOWLEDGMENTS

The authors would like to thank Laurence Decocq and Patrick Cailler for animal care. The authors thank VISIO Foundation; National Research Institute for Agriculture, Food and Environment (INRAE); Regional Council of Burgundy (PARI Grant); European Regional Development Fund (FEDER); Agence Nationale de la Recherche (ANR-11-LABX-0021-01); Fondation de France/Fondation de l'Oeil; Groupe Lipides et Nutrition (GLN) for their financial support.

SUPPLEMENTARY MATERIAL

The Supplementary Material for this article can be found online at: https://www.frontiersin.org/articles/10.3389/fcell.2022.864599/full#supplementary-material

REFERENCES

Acar, N., Gregoire, S., Andre, A., Juaneda, P., Joffre, C., Bron, A. M., et al. (2007). Plasmalogens in the Retina: *In Situ* Hybridization of Dihydroxyacetone Phosphate Acyltransferase (DHAP-AT) - the First Enzyme Involved in Their Biosynthesis - and Comparative Study of Retinal and Retinal Pigment Epithelial Lipid Composition. *Exp. Eye Res.* 84 (1), 143–151. doi:10.1016/j.exer.2006.09.009

Begum, G., Kintner, D., Liu, Y., Cramer, S. W., and Sun, D. (2012). DHA Inhibits ER Ca2+ Release and ER Stress in Astrocytes Following *In Vitro* Ischemia. *J. Neurochem.* 120 (4), 622–630. doi:10.1111/j.1471-4159.2011.07606.x

Brenner, M., Messing, A., and Olsen, M. L. (2019). AP-1 and the Injury Response of the GFAP Gene. *J. Neuro Res.* 97 (2), 149–161. doi:10.1002/jnr.24338

Bringmann, A., Pannicke, T., Grosche, J., Francke, M., Wiedemann, P., Skatchkov, S., et al. (2006). Müller Cells in the Healthy and Diseased Retina. *Prog. Retin. Eye Res.* 25 (4), 397–424. doi:10.1016/j.preteyeres.2006.05.003

Butkevich, E., Hülsmann, S., Wenzel, D., Shirao, T., Duden, R., and Majoul, I. (2004). Drebrin Is a Novel Connexin-43 Binding Partner that Links gap Junctions to the Submembrane Cytoskeleton. *Curr. Biol.* 14 (8), 650–658. doi:10.1016/j.cub.2004.03.063

Cabot, M. C., and Jaken, S. (1984). Structural and Chemical Specificity of Diradylglycerols for Protein Kinase C Activation. *Biochem. Biophysical Res. Commun.* 125 (1), 163–169. doi:10.1016/s0006-291x(84)80349-6

Clark, K. J., and Murray, A. W. (1995). Evidence that the Bradykinin-Induced Activation of Phospholipase D and of the Mitogen-Activated Protein Kinase cascade Involve Different Protein Kinase C Isoforms. *J. Biol. Chem.* 270 (13), 7097–7103. doi:10.1074/jbc.270.13.7097

Crespin, S., Bechberger, J., Mesnil, M., Naus, C. C., and Sin, W.-C. (2010). The Carboxy-Terminal Tail of Connexin43 gap junction Protein Is Sufficient to Mediate Cytoskeleton Changes in Human Glioma Cells. *J. Cel. Biochem.* 110 (3), 589–597. doi:10.1002/jcb.22554

Daniel, L. W., Small, G. W., Schmitt, J. D., Marasco, C. J., Ishaq, K., and Piantadosi, C. (1988). Alkyl-linked Diglycerides Inhibit Protein Kinase C Activation by Diacylglycerols. *Biochem. Biophysical Res. Commun.* 151 (1), 291–297. doi:10.1016/0006-291x(88)90592-x

Dorman, R. V., Dreyfus, H., Freysz, L., and Horrocks, L. A. (1976). Ether Lipid Content of Phosphoglycerides from the Retina and Brain of Chicken and Calf. *Biochim. Biophys. Acta* 486 (1), 55–59. doi:10.1016/0005-2760(77)90069-8

Folch, J., Lees, M., and Stanley, G. H. S. (1957). A Simple Method for the Isolation and Purification of Total Lipides from Animal Tissues. *J. Biol. Chem.* 226 (1), 497–509. doi:10.1016/s0021-9258(18)64849-5

Ganong, B. R., Loomis, C. R., Hannun, Y. A., and Bell, R. M. (1986). Specificity and Mechanism of Protein Kinase C Activation by Sn-1,2-Diacylglycerols. *Proc. Natl. Acad. Sci. U.S.A.* 83 (5), 1184–1188. doi:10.1073/pnas.83.5.1184

Geimonen, E., Jiang, W., Ali, M., Fishman, G. I., Garfield, R. E., and Andersen, J. (1996). Activation of Protein Kinase C in Human Uterine Smooth Muscle Induces Connexin-43 Gene Transcription through an AP-1 Site in the Promoter Sequence. *J. Biol. Chem.* 271 (39), 23667–23674. doi:10.1074/jbc.271.39.23667

Gomes, F. C. A., Paulin, D., and Moura Neto, V. (1999). Glial Fibrillary Acidic Protein (GFAP): Modulation by Growth Factors and its Implication in Astrocyte Differentiation. *Braz. J. Med. Biol. Res.* 32 (5), 619–631. doi:10.1590/s0100-879x1999000500016

Goodenough, D. A., Goliger, J. A., and Paul, D. L. (1996). Connexins, Connexons, and Intercellular Communication. *Annu. Rev. Biochem.* 65, 475–502. doi:10.1146/annurev.bi.65.070196.002355

Gould, C., and Newton, A. (2008). The Life and Death of Protein Kinase C. *Cdt* 9 (8), 614–625. doi:10.2174/138945008785132411

Guerrero-Valero, M., Ferrer-Orta, C., Querol-Audí, J., Marin-Vicente, C., Fita, I., Gómez-Fernández, J. C., et al. (2009). Structural and Mechanistic Insights into the Association of PKCα-C2 Domain to PtdIns(4,5)P 2. *Proc. Natl. Acad. Sci. U.S.A.* 106 (16), 6603–6607. doi:10.1073/pnas.0813099106

Harrison, B. C., and Mobley, P. L. (1991). Phorbol Myristate Acetate and 8-Bromo-Cyclic AMP-Induced Phosphorylation of Glial Fibrillary Acidic Protein and Vimentin in Astrocytes: Comparison of Phosphorylation Sites. *J. Neurochem.* 56 (5), 1723–1730. doi:10.1111/j.1471-4159.1991.tb02073.x

Hervé, J.-C., and Derangeon, M. (2013). Gap-junction-mediated Cell-To-Cell Communication. *Cell Tissue Res.* 352 (1), 21–31. doi:10.1007/s00441-012-1485-6

Heymans, F., Da Silva, C., Marrec, N., Godfroid, J.-J., and Castagna, M. (1987). Alkyl Analogs of Diacylglycerol as Activators of Protein Kinase C. *FEBS Lett.* 218 (1), 35–40. doi:10.1016/0014-5793(87)81013-x

Hicks, D., and Courtois, Y. (1990). The Growth and Behaviour of Rat Retinal Müller Cells *In Vitro* 1. An Improved Method for Isolation and Culture. *Exp. Eye Res.* 51 (2), 119–129. doi:10.1016/0014-4835(90)90063-z

Homkajorn, B., Sims, N. R., and Muyderman, H. (2010). Connexin 43 Regulates Astrocytic Migration and Proliferation in Response to Injury. *Neurosci. Lett.* 486 (3), 197–201. doi:10.1016/j.neulet.2010.09.051

Inagaki, M., IMakamura, Y., Takeda, M., Nishimura, T., and Inagaki, N. (1994). Glial Fibrillary Acidic Protein: Dynamic Property and Regulation by Phosphorylation. *Brain Pathol.* 4 (3), 239–243. doi:10.1111/j.1750-3639.1994.tb00839.x

Kerr, N. M., Johnson, C. S., de Souza, C. F., Chee, K.-S., Good, W. R., Green, C. R., et al. (2010). Immunolocalization of gap junction Protein Connexin43 (GJA1) in the Human Retina and Optic Nerve. *Invest. Ophthalmol. Vis. Sci.* 51 (8), 4028–4034. doi:10.1167/iovs.09-4847

Kimura, K., and Nishida, T. (2010). Role of the Ubiquitin-Proteasome Pathway in Downregulation of the Gap-Junction Protein Connexin43 by TNF-α in Human Corneal Fibroblasts. *Invest. Ophthalmol. Vis. Sci.* 51 (4), 1943–1947. doi:10.1167/iovs.09-3573

Kurth-Nelson, Z. L., Mishra, A., and Newman, E. A. (2009). Spontaneous Glial Calcium Waves in the Retina Develop over Early Adulthood. *J. Neurosci.* 29 (36), 11339–11346. doi:10.1523/JNEUROSCI.2493-09.2009

Lagos-Cabré, R., Burgos-Bravo, F., Avalos, A. M., and Leyton, L. (2019). Connexins in Astrocyte Migration. *Front. Pharmacol.* 10, 1546. doi:10.3389/fphar.2019.01546

Laird, D. W. (2006). Life Cycle of Connexins in Health and Disease. *Biochem. J.* 394 (Pt 3), 527–543. doi:10.1042/BJ20051922

Leithe, E., Mesnil, M., and Aasen, T. (2018). The Connexin 43 C-Terminus: A Tail of many Tales. *Biochim. Biophys. Acta (Bba) - Biomembr.* 1860 (1), 48–64. doi:10.1016/j.bbamem.2017.05.008

Leithe, E. (2016). Regulation of Connexins by the Ubiquitin System: Implications for Intercellular Communication and Cancer. *Biochim. Biophys. Acta (Bba) - Rev. Cancer* 1865 (2), 133–146. doi:10.1016/j.bbcan.2016.02.001

Leithe, E., and Rivedal, E. (2004). Ubiquitination and Down-Regulation of gap junction Protein Connexin-43 in Response to 12-O-Tetradecanoylphorbol 13-acetate Treatment. *J. Biol. Chem.* 279 (48), 50089–50096. doi:10.1074/jbc.M402006200

Liu, D., Nagan, N., Just, W. W., Rodemer, C., Thai, T.-P., and Zoeller, R. A. (2005). Role of Dihydroxyacetonephosphate Acyltransferase in the Biosynthesis of Plasmalogens and Nonether Glycerolipids. *J. Lipid Res.* 46 (4), 727–735. doi:10.1194/jlr.m400364-jlr200

Lučić, I., Truebestein, L., and Leonard, T. A. (2016). Novel Features of DAG-Activated PKC Isozymes Reveal a Conserved 3-D Architecture. *J. Mol. Biol.* 428 (1), 121–141. doi:10.1016/j.jmb.2015.11.001

Mandal, A., Wang, Y., Ernsberger, P., and Kester, M. (1997). Interleukin-1-induced Ether-Linked Diglycerides Inhibit Calcium-Insensitive Protein Kinase C Isotypes. *J. Biol. Chem.* 272 (32), 20306–20311. doi:10.1074/jbc.272.32.20306

Matsuuchi, L., and Naus, C. C. (2013). Gap junction Proteins on the Move: Connexins, the Cytoskeleton and Migration. *Biochim. Biophys. Acta (Bba) - Biomembr.* 1828 (1), 94–108. doi:10.1016/j.bbamem.2012.05.014

Metea, M. R., and Newman, E. A. (2006). Glial Cells Dilate and Constrict Blood Vessels: a Mechanism of Neurovascular Coupling. *J. Neurosci.* 26 (11), 2862–2870. doi:10.1523/JNEUROSCI.4048-05.2006

Morrison, W. R., and Smith, L. M. (1964). Preparation of Fatty Acid Methyl Esters and Dimethylacetals from Lipids with boron Fluoride-Methanol. *J. Lipid Res.* 5, 600–608. doi:10.1016/s0022-2275(20)40190-7

Nagan, N., and Zoeller, R. A. (2001). Plasmalogens: Biosynthesis and Functions. *Prog. Lipid Res.* 40 (3), 199–229. doi:10.1016/s0163-7827(01)00003-0

Nagy, K., Brahmbhatt, V. V., Berdeaux, O., Bretillon, L., Destaillats, F., and Acar, N. (2012). Comparative Study of Serine-Plasmalogens in Human Retina and Optic Nerve: Identification of Atypical Species with Odd Carbon Chains. *J. Lipid Res.* 53 (4), 776–783. doi:10.1194/jlr.D022962

Newman, E. A. (2015). Glial Cell Regulation of Neuronal Activity and Blood Flow in the Retina by Release of Gliotransmitters. *Phil. Trans. R. Soc. B* 370 (1672), 20140195. doi:10.1098/rstb.2014.0195

Newman, E. A. (2001). Propagation of Intercellular Calcium Waves in Retinal Astrocytes and Müller Cells. *J. Neurosci.* 21 (7), 2215–2223. doi:10.1523/jneurosci.21-07-02215.2001

Newman, E. A., and Zahs, K. R. (1997). Calcium Waves in Retinal Glial Cells. *Science* 275 (5301), 844–847. doi:10.1126/science.275.5301.844

O′Sullivan, M. L., Puñal, V. M., Kerstein, P. C., Brzezinski, J. A., Glaser, T., Wright, K. M., et al. (2017). Astrocytes Follow Ganglion Cell Axons to Establish an Angiogenic Template during Retinal Development. *Glia* 65 (10), 1697–1716. doi:10.1002/glia.23189

Olk, S., Turchinovich, A., Grzendowski, M., Stühler, K., Meyer, H. E., Zoidl, G., et al. (2009). Proteomic Analysis of Astroglial Connexin43 Silencing Uncovers a Cytoskeletal Platform Involved in Process Formation and Migration. *Glia* 58 (4), NA. doi:10.1002/glia.20942

Oyamada, M., Takebe, K., and Oyamada, Y. (2013). Regulation of Connexin Expression by Transcription Factors and Epigenetic Mechanisms. *Biochim. Biophys. Acta (Bba) - Biomembr.* 1828 (1), 118–133. doi:10.1016/j.bbamem.2011.12.031

Reichenbach, A., and Bringmann, A. (2013). New Functions of Müller Cells. *Glia* 61 (5), 651–678. doi:10.1002/glia.22477

Rodemer, C., Thai, T.-P., Brugger, B., Kaercher, T., Werner, H., Nave, K.-A., et al. (2003). Inactivation of Ether Lipid Biosynthesis Causes Male Infertility, Defects in Eye Development and Optic Nerve Hypoplasia in Mice. *Hum. Mol. Genet.* 12 (15), 1881–1895. doi:10.1093/hmg/ddg191

Saab, S., Buteau, B., Leclère, L., Bron, A. M., Creuzot-Garcher, C. P., Bretillon, L., et al. (2014). Involvement of Plasmalogens in post-natal Retinal Vascular Development. *PLoS One* 9 (6), e101076. doi:10.1371/journal.pone.0101076

Scemes, E., Dermietzel, R., and Spray, D. C. (1998). Calcium Waves between Astrocytes from Cx43 Knockout Mice. *Glia* 24 (1), 65–73. doi:10.1002/(sici)1098-1136(199809)24:1<65::aid-glia7>3.0.co;2-#

Schildge, S., Bohrer, C., Beck, K., and Schachtrup, C. (2013). Isolation and Culture of Mouse Cortical Astrocytes. *JoVE* 71, 50079. doi:10.3791/50079

Sejimo, S., Hossain, M. S., and Akashi, K. (2018). Scallop-derived Plasmalogens Attenuate the Activation of PKCδ Associated with the Brain Inflammation. *Biochem. Biophysical Res. Commun.* 503 (2), 837–842. doi:10.1016/j.bbrc.2018.06.084

Sergeeva, M., Strokin, M., and Reiser, G. (2005). Regulation of Intracellular Calcium Levels by Polyunsaturated Fatty Acids, Arachidonic Acid and Docosahexaenoic Acid, in Astrocytes: Possible Involvement of Phospholipase A2. *Reprod. Nutr. Dev.* 45 (5), 633–646. doi:10.1051/rnd:2005050

Sullivan, S. M., Sullivan, R. K. P., Miller, S. M., Ireland, Z., Björkman, S. T., Pow, D. V., et al. (2012). Phosphorylation of GFAP Is Associated with Injury in the Neonatal Pig Hypoxic-Ischemic Brain. *Neurochem. Res.* 37 (11), 2364–2378. doi:10.1007/s11064-012-0774-5

Tchernookova, B. K., Heer, C., Young, M., Swygart, D., Kaufman, R., Gongwer, M., et al. (2018). Activation of Retinal Glial (Müller) Cells by Extracellular ATP Induces Pronounced Increases in Extracellular H+ Flux. *PLoS One* 13 (2), e0190893. doi:10.1371/journal.pone.0190893

Todt, H., Dorninger, F., Rothauer, P. J., Fischer, C. M., Schranz, M., Bruegger, B., et al. (2020). Oral Batyl Alcohol Supplementation Rescues Decreased Cardiac Conduction in Ether Phospholipid-deficient Mice. *Jrnl Inher Metab. Disea* 43 (5), 1046–1055. doi:10.1002/jimd.12264

Toft-Kehler, A. K., Skytt, D. M., and Kolko, M. (2018). A Perspective on the Müller Cell-Neuron Metabolic Partnership in the Inner Retina. *Mol. Neurobiol.* 55 (6), 5353–5361. doi:10.1007/s12035-017-0760-7

Uckermann, O., Grosche, J., Reichenbach, A., and Bringmann, A. (2002). ATP-evoked Calcium Responses of Radial Glial (Müller) Cells in the Postnatal Rabbit Retina. *J. Neurosci. Res.* 70 (2), 209–218. doi:10.1002/jnr.10406

Vecino, E., Rodriguez, F. D., Ruzafa, N., Pereiro, X., and Sharma, S. C. (2016). Glia-neuron Interactions in the Mammalian Retina. *Prog. Retin. Eye Res.* 51, 1–40. doi:10.1016/j.preteyeres.2015.06.003

Vine, A. L., Leung, Y. M., and Bertram, J. S. (2005). Transcriptional Regulation of Connexin 43 Expression by Retinoids and Carotenoids: Similarities and Differences. *Mol. Carcinog.* 43 (2), 75–85. doi:10.1002/mc.20080

Warne, T. R., Buchanan, F. G., and Robinson, M. (1995). Growth-dependent Accumulation of Monoalkylglycerol in Madin-Darby Canine Kidney Cells. *J. Biol. Chem.* 270 (19), 11147–11154. doi:10.1074/jbc.270.19.11147

Wu, X., Huang, W., Luo, G., and Alain, L. A. (2013). Hypoxia Induces Connexin 43 Dysregulation by Modulating Matrix Metalloproteinases via MAPK Signaling. *Mol. Cel Biochem.* 384 (1-2), 155–162. doi:10.1007/s11010-013-1793-5

Zahs, K. R., and Ceelen, P. W. (2006). Gap Junctional Coupling and Connexin Immunoreactivity in Rabbit Retinal Glia. *Vis. Neurosci.* 23 (1), 1–10. doi:10.1017/S0952523806231018

Conflict of Interest: The authors declare that the research was conducted in the absence of any commercial or financial relationships that could be construed as a potential conflict of interest.

Publisher's Note: All claims expressed in this article are solely those of the authors and do not necessarily represent those of their affiliated organizations, or those of the publisher, the editors and the reviewers. Any product that may be evaluated in this article, or claim that may be made by its manufacturer, is not guaranteed or endorsed by the publisher.

frontiers | Frontiers in Cell and Developmental Biology

REVIEW
published: 12 April 2022
doi: 10.3389/fcell.2022.859421

Plasmalogenic Lipid Analogs as Platelet-Activating Factor Antagonists: A Potential Novel Class of Anti-inflammatory Compounds

Pu Rong[1†], *Jie-Li Wang*[1‡], *Angelina Angelova*[2], *Zakaria A. Almsherqi*[3*] *and Yuru Deng*[1*]

[1]Wenzhou Institute, University of Chinese Academy of Sciences, Wenzhou, China, [2]CNRS, Institut Galien Paris-Saclay, Université Paris-Saclay, Châtenay-Malabry, France, [3]Department of Physiology, Yong Loo Lin School of Medicine, National University of Singapore, Singapore, Singapore

OPEN ACCESS

Edited by:
Masanori Honsho,
Kyushu University, Japan

Reviewed by:
Ernst Robert Werner,
Medical University of Innsbruck, Austria
Hideo Shindou,
National Center For Global Health and Medicine, Japan

***Correspondence:**
Zakaria A. Almsherqi
phszama@nus.edu.sg
Yuru Deng
dengyr@wibe.ac.cn

[†]These authors have contributed equally to this work

[‡]These authors have contributed equally to this work and share first authorship

Specialty section:
This article was submitted to Cellular Biochemistry, a section of the journal Frontiers in Cell and Developmental Biology

Received: 21 January 2022
Accepted: 24 March 2022
Published: 12 April 2022

Citation:
Rong P, Wang J-L, Angelova A, Almsherqi ZA and Deng Y (2022) Plasmalogenic Lipid Analogs as Platelet-Activating Factor Antagonists: A Potential Novel Class of Anti-inflammatory Compounds. Front. Cell Dev. Biol. 10:859421. doi: 10.3389/fcell.2022.859421

Plasmalogens and Platelet-Activating Factor (PAF) are both bioactive ether phospholipids. Whereas plasmalogens are recognized for their important antioxidant function and modulatory role in cell membrane structure and dynamics, PAF is a potent pro-inflammatory lipid mediator known to have messenger functions in cell signaling and inflammatory response. The relationship between these two types of lipids has been rarely studied in terms of their metabolic interconversion and reciprocal modulation of the pro-inflammation/anti-inflammation balance. The vinyl-ether bonded plasmalogen lipid can be the lipid sources for the precursor of the biosynthesis of ether-bonded PAF. In this opinion paper, we suggest a potential role of plasmalogenic analogs of PAF as modulators and PAF antagonists (anti-PAF). We discuss that the metabolic interconversion of these two lipid kinds may be explored towards the development of efficient preventive and relief strategies against PAF-mediated pro-inflammation. We propose that plasmalogen analogs, acting as anti-PAF, may be considered as a new class of bioactive anti-inflammatory drugs. Despite of the scarcity of available experimental data, the competition between PAF and its natural plasmalogenic analogs for binding to the PAF receptor (PAF-R) can be proposed as a mechanistic model and potential therapeutic perspective against multiple inflammatory diseases (*e.g.,* cardiovascular and neurodegenerative disorders, diabetes, cancers, and various manifestations in coronavirus infections such as COVID-19).

Keywords: ether lipids, plasmalogen, platelet-activating factor, anti-PAF, anti-inflammation

INTRODUCTION

The interest in new classes of lipid-based anti-inflammatory drugs constantly increases in view of their critical role in the strategies to inhibit the inflammatory component of the coronavirus SARS-CoV-2 (severe acute respiratory syndrome-coronavirus-2) infection (Casari et al., 2021; Deng and Angelova, 2021; Schwarz et al., 2021), modulation of respiratory distress diseases (Mirastschijski et al., 2020; Zhuo et al., 2021) as well as in cancer and diabetes (Paul et al., 2019), and neuro-inflammation (Ifuku et al., 2012). Plasmalogens exert anti-inflammatory effects and have been first described by Feulgen and Voit in 1924 in relation to their characteristic production of aldehydes in acidic environment (Rapport, 1984). Plasmalogens are an unique type of ether glycerophospholipids

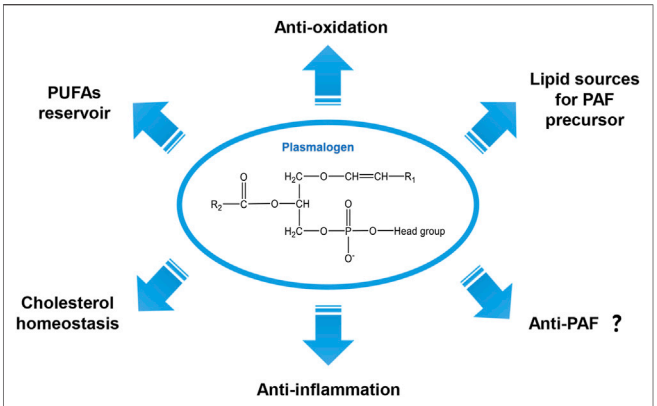

FIGURE 1 | General chemical structure of the vinyl-ether bonded plasmalogen lipid and its proposed biological functions.

carrying a vinyl-ether bond at sn-1 position of the glycerol backbone (Dorninger et al., 2020; Eiriksson et al., 2018) and typically a very long polyunsaturated fatty acid (PUFA) chain at sn-2 position (**Figure 1**). The head group usually comprises ethanolamine or choline at sn-3 position of glycerol backbone, which distinguishes plasmalogen phosphatidylethanolamine (pPE, or PE[P]) and plasmalogen phosphatidylcholine (pPC, or PC[P]) derivatives respectively (Dorninger et al., 2020). The levels of pPE often predominate over those of pPC (Paul et al., 2019). Of note, pPE is abundant in brain, especially in gray matter and white matter (Naughton and Trewhella, 1984; Lessig and Fuchs, 2009), whereas pPC is highly enriched in heart and skeletal muscles (Lessig and Fuchs, 2009; Braverman and Moser, 2012). Various biological functions have been proposed for plasmalogens including their protective role against oxidative damage as well as modulatory role in cell membrane structure and dynamics (Braverman and Moser, 2012; Almsherqi, 2021). In addition, plasmalogen deficiency has been reported to be associated with multiple diseases categorized as chronic inflammation triggered by oxidative stress (Pham et al., 2021).

Platelet activating factor (PAF), also known as acetyl-glyceryl-ether-phosphorylcholine, is an ether phosopholipid which is a potent lipid chemical mediator of inflammation (Demopoulos et al., 1979). PAFs are a family of endogenous pro-inflammatory lipids that may trigger many inflammatory and allergic responses (Palur Ramakrishnan et al., 2017). Noteworthy, plasmalogens can be the lipid sources for the precursor of PAF in lipid biosynthesis (Dorninger et al., 2020). However, the relationship between these two lipid species has been rarely studied in terms of their metabolic interconversion and reciprocal modulation in inflammation/anti-inflammation processes. The plasmalogenic analogs of PAF have been first introduced by Kulikov and Muzia (1992), referring to a family of molecules with similar chemical structures to plasmalogen or PAF. Compounds that inhibit PAF function are referred to as PAF antagonists (anti-PAF) and they may act as potential anti-inflammatory agents (Lordan et al., 2019). In this work, we argue and discuss the potential role of plasmalogenic analogs of PAF as PAF antagonists (anti-PAF). In our opinion, targeting the PAF receptor (PAF-R) by plasmalogenic analogs of PAF (anti-PAF) may provide an alternative strategy in the prevention and therapy for inflammation-mediated diseases.

SIGNIFICANCE OF PLASMALOGENS AS BIOACTIVE VINYL-ETHER LIPIDS

Plasmalogens represent approximately one in five phospholipids in mammalian and human tissues, and they are particularly abundant in brain, heart, skeletal muscles and immune cells (Braverman and Moser, 2012). These vinyl-ether bonded lipids are also richly distributed in food products including fish, mollusk, livestock and poultry (Yamashita et al., 2016; Wu et al., 2019), however they have not been reported in plants or fungi yet (Braverman and Moser, 2012). Of interest, they have a multistage evolutionary history emphasizing their first appearance in anaerobic bacteria and absence in most aerobic bacteria and re-appearance in protozoa and animals (Goldfine, 2010). Plasmalogens also have been found accounting for 21–24 mol % of total phosopholipids in the slime molds (Physarum polycephalum) (Poulos et al., 1971), belonging to the class of Myxomycetes (Fiore-Donno et al., 2008).

Figure 1 summarizes a variety of proposed biological functions for plasmalogens as antioxidants in addition to their modulatory role in membrane structure and dynamics (Bozelli et al., 2021). The high susceptibility of the vinyl-ether bond at sn-1 position to radicals including reactive oxygen species (ROS) and reactive nitrogen species (RNS) as well as to the traces of acids supports their important role as a first-line defense system in biology against oxidative damages (Zhuo et al., 2021; Bozelli et al., 2021). Previously, Deng and colleagues have proposed that plasmalogens carrying PUFA chains may promote intracellular cubic membranes (CM) formation (Deng et al., 2009) with the implication in virus-induced host CM formation (Deng et al., 2010; Deng and Angelova, 2021). In addition, PUFA-plasmalogens may also act as an integrated antioxidant defense system to provide a protective shelter for nucleic acids (RNAs) and other biomolecules (Almsherqi et al., 2008; Deng and Almsherqi, 2015). It has been reported that plasmalogens are highly concentrated in lipid bilayer microdomains in cellular and subcellular organelle membranes (Messias et al., 2018). They naturally participate in multiple cellular processes including membrane fusion (Zhuo et al., 2021), cholesterol homeostasis (Honsho et al., 2015), ion transport (Messias et al., 2018) and immunomodulation (Deng and Angelova, 2021). In lipid biosynthesis, plasmalogens can be the source of supply for the precursor of PAF (Dorninger et al., 2020) (**Figure 1**). The modulatory role of plasmalogens in membrane dynamics mainly relies on their preference for the formation of non-lamellar inverted hexagonal (H_{II}) structures (Lohner, 1996) and cubic phases (Angelova et al., 2021). Their role in membrane fusion and fission processes has been suggested and reviewed (Koivuniemi, 2017; Dean and Lodhi, 2018). Plasmalogens may also serve as a reservoir of omega-6 and/or omega-3 PUFAs whose metabolites are important in various cell signaling pathways (Messias et al., 2018; Dorninger et al., 2020).

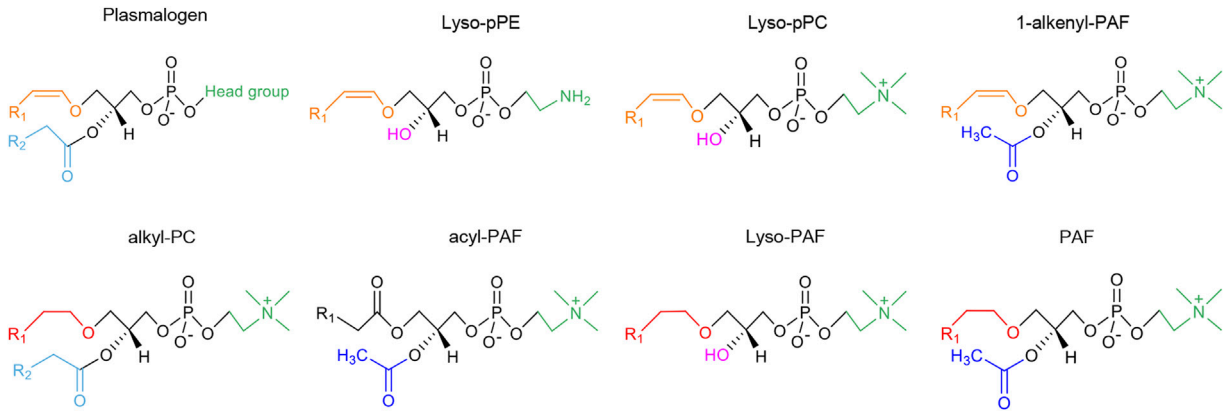

FIGURE 2 | The chemical structures of vinyl ether-bonded plasmalogen lipids as compared to the family of plasmalogen analogs and plasmalogenic analogs of PAF. The head group of plasmalogen at the sn-3 position of glycerol backbone can be either ethanolamine or choline, designated as pPE or pPC, respectively. The lyso forms of plasmalogen are labeled as lyso-pPE and lyso-pPC. The chemical structures of plasmalogens (pPE and pPC) and lyso-plasmalogens (lyso-pPE and lyso-pPC), PAF and its analogs (1-alkenyl-PAF, alkyl-PC, acyl-PAF and lyso-PAF) are all structurally related. The different colors represent the specific chemical structure and functional group: alkyl groups (ether-bond) at sn-1 position are marked in red color; alkenyl groups (vinyl ether-bond) are marked in orange color; acyl groups (ester-bond) at sn-2 position are marked in blue (acyl groups are light blue while acetyl groups are dark blue); the lyso form (hydroxyl-bond) are marked with pink color; and the head groups at sn-3 position are green. R_1 represents the alkyl chains. The saturated or unsaturated fatty acyl chains are labeled as R_2, which is usually PUFA in plasmalogens and alkyl-PC, an acetyl group in PAF, acyl-PAF and 1-alkenyl-PAF, or a hydroxyl group in lyso-plasmalogens and lyso-PAF. The head groups of PAF and plasmalogenic analogs of PAF are often choline type, but can be ethanolamine type for pPE or lyso-pPE. In the upper row of the figure, the molecular structures are considered as plasmalogen analogs. In the lower row, the molecular structures are more similar to PAF, and therefore termed as plasmalogenic analogs of PAF.

Moreover, plasmalogen has shown its anti-inflammatory effect both *in vitro* and *in vivo* (Sejimo et al., 2018).

The biosynthesis of plasmalogens starts in the subcellular organelle peroxisome and completed in the endoplasmic reticulum (ER) (Rangholia et al., 2021). Plasmalogen deficiency has been reported to be associated with several human diseases as well as aging (Bozelli et al., 2021; Pham et al., 2021). Low levels of plasmalogens have been manifested in Zellweger Syndrome (ZS) (Heymans et al., 1983,1984), and Rhizomelic Chondrodysplasia Punctata (RCDP) (Huffnagel et al., 2013; Buchert et al., 2014), both belong to the peroxisome biogenesis disorders (PBDs) (Wanders and Waterham, 2006). Reduced levels of plasmalogens have been found in the brain and serum of patients with neurodegenerative diseases including Alzheimer's disease (AD), Parkinson's disease (PD), Multiple Sclerosis (MS), depression and Niemann-Pick type C disease (Schedin et al., 1997; Dragonas et al., 2009; Wood et al., 2016; Bozelli et al., 2021; Rangholia et al., 2021). Plasmalogens deficit is also implicated in other neurological disorders. For instance, the total level of plasmalogens is reduced by 15–20 % in the plasma of autistic patients (Dorninger et al., 2017). Similarly, pPE levels are decreased by 15% in the brain of autism rat model (Thomas et al., 2010). A significant drop of plasmalogens levels has been reported in the red blood cells and fibroblasts of schizophrenia patients as well (Thomas et al., 2010). Plasmalogens deficiency may be a secondary effect outcome of metabolic and inflammatory disorders including cancer, diabetes mellitus, various cardiac and respiratory diseases (Braverman and Moser, 2012; Pham et al., 2021). Plasmalogen supplementations have been reported to improve cognition (Hossain et al., 2018) and inhibit oxidative damage, neuro-inflammation and apoptosis (Che et al., 2018; Bozelli et al., 2021). Restoring plasmalogens levels has been achieved by the use of plasmalogen replacement therapy (Bozelli and Epand, 2021), which turned out to be a successful way to restore plasmalogen level as well as to improve diseased conditions *via* the potential anti-inflammatory property of plasmalogens (Bozelli et al., 2021).

CHEMICAL ANALOGS OF PLASMALOGEN AND PAF

The ether-bonded phospholipid PAF has attracted much attention (Dorninger et al., 2020), similarly to its precursor vinyl-ether bonded plasmalogen derivatives (Braverman and Moser, 2012; Pham et al., 2021), due to their importance in cell signaling, neurodegeneration, and severe coronavirus COVID-19 disease manifestations (Demopoulos et al., 2020; Deng and Angelova, 2021).

Figure 2 summarizes the chemical structures of plasmalogens (pPE and pPC), lyso-plasmalogens (lyso-pPE and lyso-pPC), PAF and its analogs (1-alkenyl-PAF, alkyl-PC, acyl-PAF and lyso-PAF). The latter are similar to PAF, with differences as the vinyl ether bond or the ether bond at sn-1 position, and specific chemical groups at sn-2 position while PAF includes an alkyl ether bond. In the following, 1-alkenyl-PAF (PAF-like molecule with vinyl ether bond at sn-1 position) is referred to as a plasmalogenic analog of PAF. This designation was first termed by Kulikov and Muzia (1992) in their study in the effect of acyl-PAF and vinyl-PAF (1-alkenyl-PAF) on the PAF-platelet interaction. Thus, the polar lipid molecules

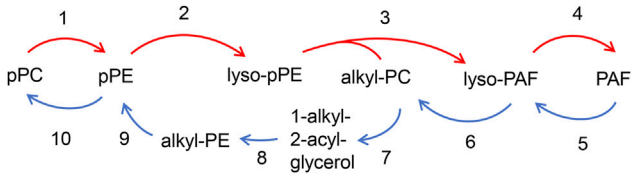

FIGURE 3 | Interconversion pathway between plasmalogen and PAF. pPC can interconvert with pPE *via* head group transfer (reaction 1 and 10), Plasmalogen PE (pPE) is hydrolyzed by PLA_2 to form lyso-pPE (reaction 2). The lyso-PE can be further reacylated by CoA-IT to form lyso-PAF (reaction 3) with the presence of alkyl-PC, and is subsequently converted to PAF by lyso-PAF AcT (reaction 4). PAF can be converted to pPE through the several steps. Losing its acetyl group by PAF-AH (reaction 5) forms lyso-PAF, which can be further converted to alkyl-PC by LPCAT (reaction 6). The alkyl-PC might be hydrolyzed by PLC to form 1-alkyl-2-acyl-glycerol (reaction 7), which then is converted to alkyl-PE by E-PT (reaction 8), and alkyl-PE is further converted to pPE with Δ1 desaturase (reaction 9).

shown in **Figure 2**, which are structurally similar to plasmalogen or PAF, are considered as plasmalogen analogs or plasmalogenic analogs of PAF, respectively.

Figure 3 depicts the interconversion pathway between plasmalogen and PAF. Plasmalogens may supply as lipid source of precursors for the generation of eicosanoids and PAF (Toyoshima et al., 1995). Evidence shows that interconversion beween pPC and pPE can be through the head group transfer (Nagan and Zoeller, 2001) (reaction 1 and 10). Lyso-pPE can be generated through the hydrolytic cleavage of pPE by phospholipase A_2 (PLA_2, EC 3.1.1.4, reaction 2, red arrow). The lyso-pPE can be reacylated by a coenzyme A-independent transacylase (CoA-IT, reaction 3, red arrow) (Uemura et al., 1991), and the donor in reaction 3 is alkyl-PC. The latter reaction may result in the production of lyso-PAF that can be further converted to PAF by acetyl-CoA: lyso-PAF acetyltransferase (lyso-PAF AcT, EC 2.3.1.67, reaction 4, red arrow) (Shindou et al., 2007; Goracci et al., 2009). The remodeling pathway of PAF biosynthesis is considered to be responsible for the pro-inflammatory behavior of PAF in response to acute and/or chronic inflammation (Lordan et al., 2019).

PAF can be converted to pPE *via* a series of enzymatic reactions (Frenkel and Johnston, 1992; Lee et al., 1992) (**Figure 3**). *In vivo* pPE can be converted into pPC through the head group transfer (reaction 10, blue arrow in **Figure 3**) (Nagan and Zoeller, 2001). PAF may lose its acetyl group by PAF acetylhydrolase (PAF-AH, EC 3.1.1.47, reaction 5, blue arrow) to form lyso-PAF, which can be further converted to alkyl-PC by the enzymatic action of lysophosphatidylcholine acyltransferase (LPCAT, EC 2.3.1.23, reaction 6, blue arrow) (Snyder, 1995; Shindou et al., 2007). The 1-alkyl-2-acyl-glycerol is formed by the hydrolytic cleavage of alkyl-PC at the sn-3 position by phospholipase C (PLC, EC 3.1.4.3, reaction 7, blue arrow), resulting in alkyl-PE geneartion by a ethanolamine-phosphotransferase (E-PT, EC 2.7.8.1, reaction 8, blue arrow). The alkyl-PE can be further converted to pPE with Δ1 desaturase (EC 1.14.19.77, reaction 9, blue arrow) (Maeba et al., 2018). Both direction of chemical reaction processes, namely pPC to pPE, lyso-PAF to alkyl-PC and PAF to lyso-PAF, are reversible (**Figure 3**). The relation between PAF and plasmalogen is most likely interconvertible and therefore several potential analogs of PAF and plasmalogen might be generated as shown in **Figure 3**.

SIGNIFICANCE OF PAF AS A BIOACTIVE ALKYL-ETHER LIPID

PAF is a pro-inflammatory lipid mediator with well-known messenger functions (Damiani and Ullrich, 2016). Compounds, which inactivate PAF-R, can act as PAF-R inhibitors. Demopoulos and colleagues have discovered the chemical structure of PAF and have synthesized it for confirmation using plasmalogen with a semi-synthetic method, and the alkenyl ether double bond at the sn-1 position is chemically converted into ether bond through catalytic hydrogenation (Demopoulos et al., 1979). Structurally, PAF is characterized by an alkyl ether linkage at sn-1 position, acetyl groups at sn-2 position, and a phosphocholine group at sn-3 position of the glycerol backbone (Demopoulos et al., 1979) (**Figure 2**). At variance, the potential plasmalogen analogs of PAF have a vinyl-ether bond at sn-1 position and a PUFA chain at sn-2 position (**Figure 2**). PAF analog per se has been commonly referred to as phospholipids similar in chemical or spatial structure as PAF. Notably, these PAF analogs may compete for binding to the PAF-R and are collectively known as PAF-like lipids or PAF-agonists (Lordan et al., 2019; Tsoupras et al., 2018) (see **Figure 2**). PAF is produced by a plethora of blood and immune cells including platelets, neutrophils, monocytes/macrophages, lymphocytes, basophiles, eosinophils and mast cells (Papakonstantinou et al., 2017). They can further act back to stimulate the cells of its origin *via* autocrine action (Demopoulos et al., 2020).

The pathophysiological role of PAF is primarily determined by its produced amount *via* lipid biosynthesis and by the extent of its enzymatic regulation. There are two enzymes that regulate the PAF activity (**Figure 3**), namely acetyl transferase (PAF-AT) and acetyl hydrolase (PAF-AH). The latter is a subtype of the PLA_2 enzyme (Palur Ramakrishnan et al., 2017; Papakonstantinou et al., 2017). The homeostatic level of PAF present in plasma and biological tissues, is regulated by the balance between its anabolic and catabolic pathways (Tsoupras et al., 2018). There are two synthetic pathways of PAF, namely "*de novo*" and "*re-modeling*" pathways (Liu et al., 2017; Tsoupras et al., 2018; Rangholia et al., 2021). The latter is considered as the main pathway of PAF biosynthesis in response to inflammatory stimuli.

PAF may participate in multiple cellular processes, including inflammation, apoptosis, reproduction, angiogenesis, and glycogen degradation in addition to its physiological roles in brain function, lung maturation, regulation of blood circulation, blood pressure and coagulation (Tsoupras et al., 2018; Lordan et al., 2019). Under the diseased conditions, the excess PAF may act as a potent pro-inflammatory mediator, involved in a variety of chronic inflammatory diseases, including cardiovascular

diseases, atherosclerosis, diabetes, neurodegenerative disorders and cancers. Moreover, several recent reports have suggested the implication of PAF in viral infections such as HIV (Papakonstantinou et al., 2017; Lordan et al., 2019) and even COVID-19 pathogenesis (Demopoulos et al., 2020; Klein et al., 2021).

PAF/ANTI-PAF SIGNALING CASCADES IN INFLAMMATORY RESPONSES

Human and guinea pig PAFRs consist of a single polypeptide chain composed of 342 amino acids with seven transmembrane domains, with the characteristics of G-protein coupled receptors (GPCRs) superfamily (Chaudhary and Kim, 2021; Ishii et al., 2002). GPCRs are the largest and most diverse group of membrane receptors in the eukaryotes. These cell surface receptors act like sensors for receiving the information in the form of light energy, peptides, proteins, lipids, and sugars (Ritter and Hall, 2009), and they are the molecular targets for nearly half of the therapeutic drugs prescribed worldwide (Bridges and Lindsley, 2008). Approximately 1,000 members of the GPCRs family exhibit a conserved 7-transmembrane domain topology and can be divided into 3 main subfamilies, termed A, B and C, based on sequence similarity. The canonical view of how GPCRs may modulate cellular physiology is that the binding of ligands (such as hormones, neurotransmitters or sensory stimuli) induces the conformational changes of transmembrane and intracellular domains of the receptor, further allowing interactions with heterotrimeric G proteins (Ritter and Hall, 2009). Up to July 2021, there are total 99 GPCR structures deposited in the Protein Data Bank (PDB: www.pdbus.org), and most of them were determined by the cryo-EM method (García-Nafría and Tate, 2021). After binding to PAF-R, PAF may activate intracellular signaling pathways, including NF-κB and MAPK pathways (Lordan et al., 2019). These important inflammatory signaling pathways are initiated in macrophages (Jeong et al., 2016). They may further trigger the expression and release of a wide range of PAF-mediated inflammatory factors such as tumor necrosis factor (TNF)-α, interleukin (IL)-6, and IL-1β. All together they may orchestrate the inflammatory responses (Jeong et al., 2016). Particularly, NF-κB pathway is one of the key transcriptional pathways in PAF-mediated inflammatory response associated with the regulation of pro-inflammatory factors expression (Jeong et al., 2016). It has been demonstrated that both endogenous and exogenous anti-PAF (PAF antagonists) may inhibit the PAF activities (Lordan et al., 2019). The absence of circulating anti-PAF in the blood may result in an increase of the PAF activity and further worsen the situations of inflammation. The PAF antagonists may halt or diminish the expressions of pro-inflammatory mediators at different levels (Lordan et al., 2019).

There is a vast number of natural and synthetic anti-PAF compounds known to inhibit PAF activity and act as potential anti-inflammatory agents. The anti-PAF compounds of synthetic origin, such as statin drugs (Tsantila et al., 2011), thiazolium derivative (CV-3988), thienodiazepine derivatives such as brotizolam, WEB 2086 (apafant), and WEB 2170 (bepafant) or the natural origin, such as Ginkgolides (Papakonstantinou et al., 2017), may competitively or non-competitively inhibit PAF activity through binding to the active site of PAF-R on the cell membrane, and therefore, directly inhibit PAF signaling cascades (Papakonstantinou et al., 2017). The anti-PAF may exert anti-inflammatory effects by impeding the binding of PAF to PAF-R. This may result in the down-regulation of pro-inflammatory mediators and cytokine production *via* inhibition of NF-κB and/or MAPK pathways (Singh et al., 2013; Jeong et al., 2016; Zhaocheng et al., 2016; Li et al., 2017; Sarkar et al., 2020). It has been reported that other PAF agonists may also indirectly affect the PAF/anti-PAF signaling cascades by affecting the upstream and/or the downstream of nearby microenvironment of the PAF-R in the cell membrane or of other related membrane receptors (Tsoupras et al., 2018).

PLASMALOGENIC ANALOGS OF PAF AS POTENTIAL ANTI-PAF AND ANTI-INFLAMMATION AGENTS

Oxidation of PC phospholipids (including pPC) may generate a series of lyso-phospholipids. Lyso-pPC carrying PUFA, usually arachidonic acid (AA), can be further fragmented to shorter-chain-length fatty acid (McIntyre et al., 1999). Some of these oxidized phospholipids carrying very short sn-2 residues (among other structural features) make them recognizable by PAF-R receptor (Zimmerman et al., 2002). There is a strong preference for PAF-R to bind PAF-like lipid molecules with ether bond at sn-1 position, acetyl residue at sn-2 position, and choline head group at sn-3 position (McIntyre et al., 1999). Plasmalogens, especially pPC (1-alkenyl PC), together with its hydrolysated form of lyso-pPC, are important polar phospholipids with similar spatial structure to PAF. The structural match between pPC/lyso-pPC and PAF may determine the high affinity to the same binding site at PAF-R (Snyder, 1990). Either pPC or lyso-pPC is potentially as a PAF analog that may compete with PAF for binding to PAF-R.

In this way, plasmalogenic analogs may effectively inhibit PAF-induced platelet aggregation through competitive binding to the receptor PAF-R (McManus et al., 1993; Smaragdi Antonopoulou and Demopoulos, 2008). It has been reported that 1-alkenyl-PAF, a plasmalogenic analog of PAF (similar to pPC or lyso-pPC), exhibited high anti-inflammatory activity in two inflammatory models of rat paw edema (Kulikov and Muzya, 2002). The authors have examined the mechanism of interaction of the plasmalogenic analogs of PAF with human platelets (Kulikov and Muzya, 1999). Of interest, 1-alkenyl-PAF has been established to act as an inhibitor of PAF-induced platelet aggregation without the influence on ADP- or thrombin-induced platelet aggregation (Kulikov and Muzya, 1999; Lordan et al., 2017). The acyl-PAF has been reported to act as potential anti-inflammatory molecules to suppress the action of PAF (Chaithra et al., 2018), Therefore, we speculate plasmalogens may be also work as a potential anti-PAF lipid compound.

Here we emphasize that plasmalogens and some plasmalogenic analogs of PAF (**Figure 2**) may act as novel

PAF antagonists, which play an important role in modulating PAF/anti-PAF signaling cascades with implication in inflammation and inflammation-mediated disease processes (Kulikov and Muzya, 1999; Lordan et al., 2017). More about the anti-PAF effect of plasmalogen together with their analogs may inspire more future studies to approve or disapprove the hypothesis.

Plasmalogen has been demonstrated to exert an anti-inflammatory activity (Sejimo et al., 2018; Ali et al., 2019), to ameliorate neurotoxicity and inhibit neuro-inflammation and neuronal apoptosis (Yamashita et al., 2016; Che et al., 2018). A recent report showed that the intake of pPE with vinyl ether linkages at sn-1 and omega-3 PUFA at sn-2 position efficiently inhibited the downstream inflammatory and apoptotic signaling cascades in a human colon (Nguma et al., 2021). The intracellular anti-apoptotic effect of pPE has been achieved through suppressing the generation of pro-inflammatory cytokines and pro-apoptotic factors (Nguma et al., 2021).

PUFAs carried by plasmalogens at sn-2 position, especially omega-3 long-chain PUFAs, are good ligands for peroxisome proliferator-activated receptors (PPARs). These PUFAs may effectively reduce inflammatory responses through activating the PPARs proteins (Deplanque et al., 2003; Farooqui et al., 2007; Korbecki et al., 2019). Moreover, PUFAs can easily be oxidized to further activate PPARs (Echeverría et al., 2016) and form a heterodimer with the 9-cis retinoic acid receptor (RXR) (D'Angelo et al., 2018) and modulate the transcription of the target genes. In brief, plasmalogens carrying omega-3 long-chain PUFAs may provide anti-inflammatory activity through: 1) inhibiting the expression of transcription factors (*e.g.*, NF-κB), intracellular signaling proteins (*e.g.*, MAP kinases) and inflammatory mediators (Carvalho et al., 2021); 2) reducing the level of reactive oxygen species (ROS) by upregulation of antioxidant enzyme expression (Carvalho et al., 2021); and 3) inhibiting microglial activation and generation of pro-inflammatory factors (Yan et al., 2003).

Plasmalogen and cholesterol are both enriched in microdomains of cell membranes. Thus, there may exist a metabolic reciprocity between them (Paul et al., 2019). Plasmalogens are proved to play important roles at multiple steps in cholesterol homeostasis *via* regulation of membrane cholesterol esterification and transportation (Mandel et al., 1998; Munn et al., 2003; Mankidy et al., 2010). The esterification of cholesterol is also dependent on the amount of pPE present in the membranes (Mankidy et al., 2010). A plasmalogen-deficient cell has lower esterified cholesterol and lower rate of HDL-mediated cholesterol efflux compared to normal wild-type cell (Mandel et al., 1998) in addition to the reduced synthesis of cholesterol (Mankidy et al., 2010). Nevertheless, these impairments are repaired by restoring the level of plasmalogens (Honsho and Fujiki, 2017), suggesting that cholesterol homeostasis is tightly regulated by plasmalogen metabolism.

Statin drugs can lower the biosynthesis of both cholesterol and farnesol (Honsho and Fujiki, 2017), the latter being involved in PAF/anti-PAF signaling cascades (Stancu and Sima, 2001). Statins have

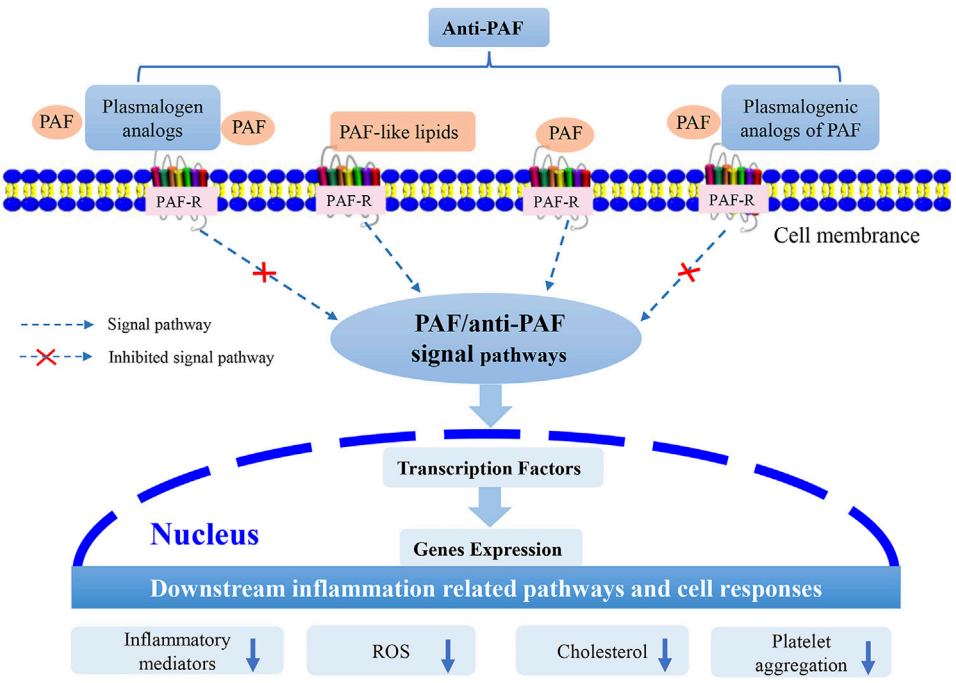

FIGURE 4 | Suggested modes of action of plasmalogen, plasmalogen analogs and plasmalogenic analogs of PAF as PAF antagonists (*i.e.,* anti-PAF). Plasmalogen and its analogs, as well as plasmalogenic analogs of PAF, may compete with the other PAF lipid family (PAF and PAF-like lipids) to bind to the membrane receptor, PAF-R. Consequently, they may modulate the PAF/anti-PAF signaling pathways, such as NF-κB and MAPK, and further inhibit the expression of transcription factors and genes. The potential PAF antagonists (anti-PAF) may modulate the downstream inflammation-mediated pathways and other cellular responses.

pleiotropic functions beyond cholesterol reduction, such as improvement of endothelial function, thrombogenesis reduction, and protection against oxidative stress and inflammation (Harada et al., 2015). In addition, statins may exhibit anti-PAF activity and suppress PAF biosynthesis *via* the "*de novo*" pathway *in vivo* (Tsantila et al., 2011). Hence, plasmalogens have been suggested as an alternative of statin drugs to reduce cholesterol levels (Mankidy et al., 2010; Deng and Angelova, 2021). Of interest, PUFA-pPE precursors are approximately twice as effective as statins at lowering cholesterol levels (Mankidy et al., 2010). Both outcomes of lowering cholesterol and anti-inflammation can be achieved by either plasmalogens or statins. In addition, plasmalogen is a natural product that may avoid the side effects of statin drugs, including hepatotoxicity and increased risk of diabetes mellitus (Sirtori, 2014). Thus, plasmalogens are potentially safe and efficient candidates as PAF antagonists (anti-PAF) compared to statin drugs.

CONCLUSION

Plasmalogens, especially pPC, lyso-pPC and other plasmalogenic analogs of PAF (**Figure 2**), are characterized by the similar chemical structures as PAF, and may be considered as natural PAF analogs acting as anti-PAF compounds (PAF antagonists). This structural analogy is suggested to be beneficial for modulation of inflammatory/anti-inflammatory responses. Plasmalogens and plasmalogenic analogs of PAF may compete with PAF or PAF-like molecules (PAF agonists) for binding to the PAF-R (**Figure 4**). As a consequence, they may modulate PAF/anti-PAF signaling cascades and further re-balance PAF levels in various inflammation-mediated disease processes. Plasmalogens, with a vinyl-ether bond at sn-1 position and PUFA chain at sn-2 position, reveal per se their remarkable roles as antioxidants and anti-inflammatory agents as well as regulators of cholesterol homeostasis. Plasmalogen, plasmalogen analogs and plasmalogenic analogs of PAF may thus offer novel therapeutic developments as potential anti-PAF compounds for the prevention and treatment of a variety of inflammation-mediated diseases including diabetes, cancers, cardiovascular and neurodegenerative disorders in addition to the expansive manifestations of the COVID-19 pathology (Demopoulos et al., 2020). In addition, the prevention and inhibition of neuro-inflammation is of particular interest for slowing down neuro-degeneration.

In conclusion, we propose that plasmalogens supplementation together with anti-PAF enriched food, such as the Mediterranean diet (Tsoupras et al., 2018; Detopoulou et al., 2021), may provide an alternative strategy (Bozelli and Epand, 2021) in inflammatory disease prevention and treatment through rebalancing of the inflammatory mediators and radicals, consequently return or regain system homeostasis.

AUTHOR CONTRIBUTIONS

YD and PR conceived the content and wrote the manuscript. J-LW contributed to the figures and the literature collection and helped in preparing the manuscript. PR drafted the manuscript. AA reviewed and edited the paper. YD and ZA supervised the overall project and edited the manuscript. All authors contributed to the article and approved the submitted version.

FUNDING

This work was supported by grants from the Wenzhou Institute, University of Chinese Academy of Sciences (Grant No. WIUCASQD2019005) to YD.

ACKNOWLEDGMENTS

The authors are grateful to Constantinos Demopoulos for the inspiration.

REFERENCES

Ali, F., Hossain, M. S., Sejimo, S., and Akashi, K. (2019). Plasmalogens Inhibit Endocytosis of Toll-like Receptor 4 to Attenuate the Inflammatory Signal in Microglial Cells. *Mol. Neurobiol.* 56 (5), 3404–3419. doi:10.1007/s12035-018-1307-2

Almsherqi, Z. A. (2021). Potential Role of Plasmalogens in the Modulation of Biomembrane Morphology. *Front. Cel Dev. Biol.* 9, 673917. doi:10.3389/fcell.2021.673917

Almsherqi, Z., Hyde, S., Ramachandran, M., and Deng, Y. (2008). Cubic Membranes: A Structure-Based Design for DNA Uptake. *J. R. Soc. Interf.* 5 (26), 1023–1029. doi:10.1098/rsif.2007.1351

Angelova, A., Angelov, B., Drechsler, M., Bizien, T., Gorshkova, Y. E., and Deng, Y. (2021). Plasmalogen-Based Liquid Crystalline Multiphase Structures Involving Docosapentaenoyl Derivatives Inspired by Biological Cubic Membranes. *Front. Cel Dev. Biol.* 9, 617984. doi:10.3389/fcell.2021.617984

Bozelli, J. C., Azher, S., and Epand, R. M. (2021). Plasmalogens and Chronic Inflammatory Diseases. *Front. Physiol.* 12, 730829. doi:10.3389/fphys.2021.730829

Bozelli, J. C., and Epand, R. M. (2021). Plasmalogen Replacement Therapy. *Membranes* 11 (11), 838. doi:10.3390/membranes11110838

Braverman, N. E., and Moser, A. B. (2012). Functions of Plasmalogen Lipids in Health and Disease. *Biochim. Biophys. Acta (Bba) - Mol. Basis Dis.* 1822 (9), 1442–1452. doi:10.1016/j.bbadis.2012.05.008

Bridges, T. M., and Lindsley, C. W. (2008). G-Protein-Coupled Receptors: From Classical Modes of Modulation to Allosteric Mechanisms. *ACS Chem. Biol.* 3 (9), 530–541. doi:10.1021/cb800116f

Buchert, R., Tawamie, H., Smith, C., Uebe, S., Innes, A. M., Al Hallak, B., et al. (2014). A Peroxisomal Disorder of Severe Intellectual Disability, Epilepsy, and Cataracts Due to Fatty Acyl-CoA Reductase 1 Deficiency. *Am. J. Hum. Genet.* 95 (5), 602–610. doi:10.1016/j.ajhg.2014.10.003

Carvalho, M. V. D., Gonçalves-de-Albuquerque, C. F., and Silva, A. R. (2021). PPAR Gamma: From Definition to Molecular Targets and Therapy of Lung Diseases. *Ijms* 22 (2), 805. doi:10.3390/ijms22020805

Casari, I., Manfredi, M., Metharom, P., and Falasca, M. (2021). Dissecting Lipid Metabolism Alterations in SARS-CoV-2. *Prog. Lipid Res.* 82, 101092. doi:10.1016/j.plipres.2021.101092

Chaithra, V. H., Jacob, S. P., Lakshmikanth, C. L., Sumanth, M. S., Abhilasha, K. V., Chen, C.-H., et al. (2018). Modulation of Inflammatory Platelet-Activating Factor (PAF) Receptor by the Acyl Analogue of PAF. *J. Lipid Res.* 59 (11), 2063–2074. doi:10.1194/jlr.M085704

Chaudhary, P. K., and Kim, S. (2021). An Insight into GPCR and G-Proteins as Cancer Drivers. *Cells* 10 (12), 3288. doi:10.3390/cells10123288

Che, H., Zhou, M., Zhang, T., Zhang, L., Ding, L., Yanagita, T., et al. (2018). EPA Enriched Ethanolamine Plasmalogens Significantly Improve Cognition of Alzheimer's Disease Mouse Model by Suppressing β-amyloid Generation. *J. Funct. Foods* 41, 9–18. doi:10.1016/j.jff.2017.12.016

Damiani, E., and Ullrich, S. E. (2016). Understanding the Connection between Platelet-Activating Factor, a UV-Induced Lipid Mediator of Inflammation, Immune Suppression and Skin Cancer. *Prog. Lipid Res.* 63, 14–27. doi:10.1016/j.plipres.2016.03.004

D'Angelo, M., Antonosante, A., Castelli, V., Catanesi, M., Moorthy, N., Iannotta, D., et al. (2018). PPARs and Energy Metabolism Adaptation during Neurogenesis and Neuronal Maturation. *Ijms* 19 (7), 1869. doi:10.3390/ijms19071869

Dean, J. M., and Lodhi, I. J. (2018). Structural and Functional Roles of Ether Lipids. *Protein Cell* 9 (2), 196–206. doi:10.1007/s13238-017-0423-5

Demopoulos, C., Antonopoulou, S., and Theoharides, T. C. (2020). COVID-19, Microthromboses, Inflammation, and Platelet Activating Factor. *Biofactors* 46 (6), 927–933. doi:10.1002/biof.1696

Demopoulos, C. A., Pinckard, R. N., and Hanahan, D. J. (1979). Platelet-activating Factor. Evidence for 1-O-Alkyl-2-Acetyl-Sn-Glyceryl-3-Phosphorylcholine as the Active Component (A New Class of Lipid Chemical Mediators). *J. Biol. Chem.* 254 (19), 9355–9358. doi:10.1016/S0021-9258(19)83523-8

Deng, Y., and Almsherqi, Z. A. (2015). Evolution of Cubic Membranes as Antioxidant Defence System. *Interf. Focus.* 5 (4), 20150012. doi:10.1098/rsfs.2015.0012

Deng, Y., Almsherqi, Z. A., Ng, M. M. L., and Kohlwein, S. D. (2010). Do viruses Subvert Cholesterol Homeostasis to Induce Host Cubic Membranes? *Trends Cel Biol.* 20 (7), 371–379. doi:10.1016/j.tcb.2010.04.001

Deng, Y., Almsherqi, Z. A., Shui, G., Wenk, M. R., and Kohlwein, S. D. (2009). Docosapentaenoic Acid (DPA) Is a Critical Determinant of Cubic Membrane Formation in Amoeba Chaos Mitochondria. *FASEB j.* 23 (9), 2866–2871. doi:10.1096/fj.09-130435

Deng, Y., and Angelova, A. (2021). Coronavirus-Induced Host Cubic Membranes and Lipid-Related Antiviral Therapies: A Focus on Bioactive Plasmalogens. *Front. Cel Dev. Biol.* 9, 551. doi:10.3389/fcell.2021.630242

Deplanque, D., Gelé, P., Pétrault, O., Six, I., Furman, C., Bouly, M., et al. (2003). Peroxisome Proliferator-Activated Receptor-α Activation as a Mechanism of Preventive Neuroprotection Induced by Chronic Fenofibrate Treatment. *J. Neurosci.* 23 (15), 6264–6271. doi:10.1523/JNEUROSCI.23-15-06264.2003

Detopoulou, P., Demopoulos, C. A., and Antonopoulou, S. (2021). Micronutrients, Phytochemicals and Mediterranean Diet: A Potential Protective Role against COVID-19 through Modulation of PAF Actions and Metabolism. *Nutrients* 13 (2), 462. doi:10.3390/nu13020462

Dorninger, F., Forss-Petter, S., and Berger, J. (2017). From Peroxisomal Disorders to Common Neurodegenerative Diseases - the Role of Ether Phospholipids in the Nervous System. *FEBS Lett.* 591 (18), 2761–2788. doi:10.1002/1873-3468.12788

Dorninger, F., Forss-Petter, S., Wimmer, I., and Berger, J. (2020). Plasmalogens, Platelet-Activating Factor and beyond - Ether Lipids in Signaling and Neurodegeneration. *Neurobiol. Dis.* 145, 105061. doi:10.1016/j.nbd.2020.105061

Dragonas, C., Bertsch, T., Sieber, C. C., and Brosche, T. (2009). Plasmalogens as a Marker of Elevated Systemic Oxidative Stress in Parkinson's Disease. *Clin. Chem. Lab. Med.* 47 (7), 894–897. doi:10.1515/CCLM.2009.205

Echeverría, F., Ortiz, M., Valenzuela, R., and Videla, L. A. (2016). Long-chain Polyunsaturated Fatty Acids Regulation of PPARs, Signaling: Relationship to Tissue Development and Aging. *Prostaglandins, Leukot. Essent. Fatty Acids* 114, 28–34. doi:10.1016/j.plefa.2016.10.001

Eiriksson, F. F., Rolfsson, O., Ogmundsdottir, H. M., Haraldsson, G. G., Thorsteinsdottir, M., and Halldorsson, S. (2018). Altered Plasmalogen Content and Fatty Acid Saturation Following Epithelial to Mesenchymal Transition in Breast Epithelial Cell Lines. *Int. J. Biochem. Cel Biol.* 103, 99–104. doi:10.1016/j.biocel.2018.08.003

Farooqui, A. A., Horrocks, L. A., and Farooqui, T. (2007). Modulation of Inflammation in Brain: A Matter of Fat. *J. Neurochem.* 101 (3), 577–599. doi:10.1111/j.1471-4159.2006.04371.x

Fiore-Donno, A. M., Meyer, M., Baldauf, S. L., and Pawlowski, J. (2008). Evolution of Dark-Spored Myxomycetes (Slime-molds): Molecules versus Morphology. *Mol. Phylogenet. Evol.* 46 (3), 878–889. doi:10.1016/j.ympev.2007.12.011

Frenkel, R. A., and Johnston, J. M. (1992). Metabolic Conversion of Platelet-Activating Factor into Ethanolamine Plasmalogen in an Amnion-Derived Cell Line. *J. Biol. Chem.* 267 (27), 19186–19191. doi:10.1016/S0021-9258(18)41759-0

García-Nafría, J., and Tate, C. G. (2021). Structure Determination of GPCRs: Cryo-EM Compared with X-ray Crystallography. *Biochem. Soc. T.* 49 (5), 2345–2355. doi:10.1042/BST20210431

Goldfine, H. (2010). The Appearance, Disappearance and Reappearance of Plasmalogens in Evolution. *Prog. Lipid Res.* 49 (4), 493–498. doi:10.1016/j.plipres.2010.07.003

Goracci, G., Balestrieri, M. L., and Nardicchi, V. (2009). "Metabolism and Functions of Platelet-Activating Factor (PAF) in the Nervous Tissue," in *Handbook of Neurochemistry and Molecular Neurobiology* (Boston, MA: Springer US), 311–352. doi:10.1007/978-0-387-30378-9_13

Harada, M., Van Wagoner, D. R., and Nattel, S. (2015). Role of Inflammation in Atrial Fibrillation Pathophysiology and Management. *Circ. J.* 79 (3), 495–502. doi:10.1253/circj.CJ-15-0138

Heymans, H. S. A., Bosch, H. V. D., Schutgens, R. B. H., Tegelaers, W. H. H., Walther, J.-U., Muller-Hocker, J., et al. (1984). Deficiency of Plasmalogens in the Cerebro-Hepato-Renal (Zellweger) Syndrome. *Eur. J. Pediatr.* 142 (1), 10–15. doi:10.1007/BF00442582

Heymans, H. S. A., Schutgens, R. B. H., Tan, R., van den Bosch, H., and Borst, P. (1983). Severe Plasmalogen Deficiency in Tissues of Infants without Peroxisomes (Zellweger Syndrome). *Nature* 306 (5938), 69–70. doi:10.1038/306069a0

Honsho, M., Abe, Y., and Fujiki, Y. (2015). Dysregulation of Plasmalogen Homeostasis Impairs Cholesterol Biosynthesis. *J. Biol. Chem.* 290 (48), 28822–28833. doi:10.1074/jbc.M115.656983

Honsho, M., and Fujiki, Y. (2017). Plasmalogen Homeostasis - Regulation of Plasmalogen Biosynthesis and its Physiological Consequence in Mammals. *FEBS Lett.* 591 (18), 2720–2729. doi:10.1002/1873-3468.12743

Hossain, M. S., Tajima, A., Kotoura, S., and Katafuchi, T. (2018). Oral Ingestion of Plasmalogens Can Attenuate the LPS-Induced Memory Loss and Microglial Activation. *Biochem. Biophysical Res. Commun.* 496 (4), 1033–1039. doi:10.1016/j.bbrc.2018.01.078

Huffnagel, I. C., Clur, S.-A. B., Bams-Mengerink, A. M., Blom, N. A., Wanders, R. J. A., Waterham, H. R., et al. (2013). Rhizomelic Chondrodysplasia Punctata and Cardiac Pathology. *J. Med. Genet.* 50 (7), 419–424. doi:10.1136/jmedgenet-2013-101536

Ifuku, M., Katafuchi, T., Mawatari, S., Noda, M., Miake, K., Sugiyama, M., et al. (2012). Anti-inflammatory/anti-amyloidogenic Effects of Plasmalogens in Lipopolysaccharide-Induced Neuroinflammation in Adult Mice. *J. Neuroinflammation* 9 (1), 197. doi:10.1186/1742-2094-9-197

Ishii, S., Nagase, T., and Shimizu, T. (2002). Platelet-activating Factor Receptor. *Prostaglandins & Other Lipid Mediators* 68-69, 599–609. doi:10.1016/S0090-6980(02)00058-8

Jeong, Y. H., Oh, Y.-C., Cho, W.-K., Yim, N.-H., and Ma, J. Y. (2016). Anti-Inflammatory Effect of Rhapontici Radix Ethanol Extract via Inhibition of NF-Kb and MAPK and Induction of HO-1 in Macrophages. *Mediators Inflamm.* 2016, 1–13. doi:10.1155/2016/7216912

Klein, M., Dao, V., and Khan, F. (2021). A Review of Platelet-Activating Factor as a Potential Contributor to Morbidity and Mortality Associated with Severe COVID-19. *Clin. Appl. Thromb. Hemost.* 27, 107602962110517. doi:10.1177/10760296211051764

Koivuniemi, A. (2017). The Biophysical Properties of Plasmalogens Originating from Their Unique Molecular Architecture. *FEBS Lett.* 591 (18), 2700–2713. doi:10.1002/1873-3468.12754

Korbecki, J., Bobiński, R., and Dutka, M. (2019). Self-regulation of the Inflammatory Response by Peroxisome Proliferator-Activated Receptors. *Inflamm. Res.* 68 (6), 443–458. doi:10.1007/s00011-019-01231-1

Kulikov, V. I., and Muzia, G. I. (1992). Acyl and Plasmalogen Analogs of Platelet Activating Factor-Nnew Lipid Cellular Bioregulators. *Biokhimiia* 57 (6), 803–816.

Kulikov, V. I., and Muzya, G. I. (1999). Mechanisms of Interaction of a Plasmalogenic Analog of Platelet-Activating Factor with Human Platelets. *Biochemistry (Mosc)* 64 (6), 631–635.

Kulikov, V. I., and Muzya, G. I. (2002). Influence of Acyl and Plasmalogenic Analogs of Platelet Activating Factor on Chemotaxis of Human Leukocytes *In*

Vitro and Their Inflammatory and Antiinflammatory Activity *In Vivo*. *Biochemistry (Moscow)* 67 (11), 1248–1252. doi:10.1023/A:1021349304885

Lee, T. C., Uemura, Y., and Snyder, F. (1992). A Novel CoA-independent Transacetylase Produces the Ethanolamine Plasmalogen and Acyl Analogs of Platelet-Activating Factor (PAF) with PAF as the Acetate Donor in HL-60 Cells. *J. Biol. Chem.* 267 (28), 19992–20001. doi:10.1016/S0021-9258(19)88655-6

Lessig, J., and Fuchs, B. (2009). Plasmalogens in Biological Systems: Their Role in Oxidative Processes in Biological Membranes, Their Contribution to Pathological Processes and Aging and Plasmalogen Analysis. *Cmc* 16 (16), 2021–2041. doi:10.2174/092986709788682164

Li, Y., Wu, Y., Yao, X., Hao, F., Yu, C., Bao, Y., et al. (2017). Ginkgolide a Ameliorates LPS-Induced Inflammatory Responses *In Vitro* and *In Vivo*. *Ijms* 18 (4), 794. doi:10.3390/ijms18040794

Liu, Y., Shields, L. B. E., Gao, Z., Wang, Y., Zhang, Y. P., Chu, T., et al. (2017). Current Understanding of Platelet-Activating Factor Signaling in central Nervous System Diseases. *Mol. Neurobiol.* 54 (7), 5563–5572. doi:10.1007/s12035-016-0062-5

Lohner, K. (1996). Is the High Propensity of Ethanolamine Plasmalogens to Form Non-lamellar Lipid Structures Manifested in the Properties of Biomembranes? *Chem. Phys. Lipids* 81 (2), 167–184. doi:10.1016/0009-3084(96)02580-7

Lordan, R., Tsoupras, A., Zabetakis, I., and Demopoulos, C. A. (2019). Forty Years since the Structural Elucidation of Platelet-Activating Factor (PAF): Historical, Current, and Future Research Perspectives. *Molecules* 24 (23), 4414. doi:10.3390/molecules24234414

Lordan, R., Tsoupras, A., and Zabetakis, I. (2017). Phospholipids of Animal and marine Origin: Structure, Function, and Anti-inflammatory Properties. *Molecules* 22 (11), 1964. doi:10.3390/molecules22111964

Maeba, R., Araki, A., and Fujiwara, Y. (2018). Serum Ethanolamine Plasmalogen and Urine Myo-Inositol as Cognitive Decline Markers. *Adv. Clin. Chem.* 87, 69–111. doi:10.1016/bs.acc.2018.08.001

Mandel, H., Sharf, R., Berant, M., Wanders, R. J. A., Vreken, P., and Aviram, M. (1998). Plasmalogen Phospholipids Are Involved in HDL-Mediated Cholesterol Efflux: Insights from Investigations with Plasmalogen-Deficient Cells. *Biochem. Biophysical Res. Commun.* 250 (2), 369–373. doi:10.1006/bbrc.1998.9321

Mankidy, R., Ahiahonu, P. W., Ma, H., Jayasinghe, D., Ritchie, S. A., Khan, M. A., et al. (2010). Membrane Plasmalogen Composition and Cellular Cholesterol Regulation: A Structure Activity Study. *Lipids Health Dis.* 9 (1), 1–17. doi:10.1186/1476-511X-9-62

McIntyre, T. M., Zimmerman, G. A., and Prescott, S. M. (1999). Biologically Active Oxidized Phospholipids. *J. Biol. Chem.* 274 (36), 25189–25192. doi:10.1074/jbc.274.36.25189

McManus, L. M., Woodard, D. S., Deavers, S. I., and Pinckard, R. N. (1993). PAF Molecular Heterogeneity: Pathobiological Implications. *Lab. Invest.* 69 (6), 639–650.

Messias, M. C. F., Mecatti, G. C., Priolli, D. G., and de Oliveira Carvalho, P. (2018). Plasmalogen Lipids: Functional Mechanism and Their Involvement in Gastrointestinal Cancer. *Lipids Health Dis.* 17 (1), 1–12. doi:10.1186/s12944-018-0685-9

Mirastschijski, U., Dembinski, R., and Maedler, K. (2020). Lung Surfactant for Pulmonary Barrier Restoration in Patients with COVID-19 Pneumonia. *Front. Med.* 7, 254. doi:10.3389/fmed.2020.00254

Munn, N. J., Arnio, E., Liu, D., Zoeller, R. A., and Liscum, L. (2003). Deficiency in Ethanolamine Plasmalogen Leads to Altered Cholesterol Transport. *J. Lipid Res.* 44 (1), 182–192. doi:10.1194/jlr.M200363-JLR200

Nagan, N., and Zoeller, R. A. (2001). Plasmalogens: Biosynthesis and Functions. *Prog. Lipid Res.* 40, 199–229. doi:10.1016/s0163-7827(01)00003-0

Naughton, J. M., and Trewhella, M. A. (1984). Positional Distribution of Acyl and Alk-1-Enyl Groups in Grey and White Matter Ethanolamine and Choline Phosphoglycerides of a Marsupial, the Koala (*Phascolarctos cinereus*). *J. Neurochem.* 42 (3), 685–691. doi:10.1111/j.1471-4159.1984.tb02737.x

Nguma, E., Yamashita, S., Kumagai, K., Otoki, Y., Yamamoto, A., Eitsuka, T., et al. (2021). Ethanolamine Plasmalogen Suppresses Apoptosis in Human Intestinal Tract Cells *In Vitro* by Attenuating Induced Inflammatory Stress. *ACS Omega* 6 (4), 3140–3148. doi:10.1021/acsomega.0c05545

Palur Ramakrishnan, A. V. K., Varghese, T. P., Vanapalli, S., Nair, N. K., and Mingate, M. D. (2017). Platelet Activating Factor: A Potential Biomarker in Acute Coronary Syndrome? *Cardiovasc. Ther.* 35 (1), 64–70. doi:10.1111/1755-5922.12233

Papakonstantinou, V. D., Lagopati, N., Tsilibary, E. C., Demopoulos, C. A., and Philippopoulos, A. I. (2017). A Review on Platelet Activating Factor Inhibitors: Could a New Class of Potent Metal-Based Anti-inflammatory Drugs Induce Anticancer Properties? *Bioinorganic Chem. Appl.* 2017, 1–19. doi:10.1155/2017/6947034

Paul, S., Lancaster, G. I., and Meikle, P. J. (2019). Plasmalogens: A Potential Therapeutic Target for Neurodegenerative and Cardiometabolic Disease. *Prog. Lipid Res.* 74, 186–195. doi:10.1016/j.plipres.2019.04.003

Pham, T. H., Manful, C. F., Pumphrey, R. P., Hamilton, M. C., Adigun, O. A., Vidal, N. P., et al. (2021). Big Game Cervid Meat as a Potential Good Source of Plasmalogens for Functional Foods. *J. Food Compost. Anal.* 96, 103724. doi:10.1016/j.jfca.2020.103724

Poulos, A., Le Stourgeon, W. M., and Thompson, G. A. (1971). Ether-containing Lipids of the Slime mold,Physarum Polycephalum: I. Characterization and Quantification. *Lipids* 6 (7), 466–469. doi:10.1007/BF02531230

Rangholia, N., Leisner, T. M., and Holly, S. P. (2021). Bioactive Ether Lipids: Primordial Modulators of Cellular Signaling. *Metabolites* 11 (1), 41. doi:10.3390/metabo11010041

Rapport, M. M. (1984). The Discovery of Plasmalogen Structure. *J. Lipid Res.* 25 (13), 1522–1527. doi:10.1016/S0022-2275(20)34427-8

Ritter, S. L., and Hall, R. A. (2009). Fine-tuning of GPCR Activity by Receptor-Interacting Proteins. *Nat. Rev. Mol. Cel Biol* 10 (12), 819–830. doi:10.1038/nrm2803

Sarkar, C., Quispe, C., Jamaddar, S., Hossain, R., Ray, P., Mondal, M., et al. (2020). Therapeutic Promises of Ginkgolide a: A Literature-Based Review. *Biomed. Pharmacother.* 132, 110908. doi:10.1016/j.biopha.2020.110908

Schedin, S., Sindelar, P. J., Pentchev, P., Brunk, U., and Dallner, G. (1997). Peroxisomal Impairment in Niemann-Pick Type C Disease. *J. Biol. Chem.* 272 (10), 6245–6251. doi:10.1074/jbc.272.10.6245

Schwarz, B., Sharma, L., Roberts, L., Peng, X., Bermejo, S., Leighton, I., et al. (2021). Cutting Edge: Severe SARS-CoV-2 Infection in Humans Is Defined by a Shift in the Serum Lipidome, Resulting in Dysregulation of Eicosanoid Immune Mediators. *J.I.* 206 (2), 329–334. doi:10.4049/jimmunol.2001025

Sejimo, S., Hossain, M. S., and Akashi, K. (2018). Scallop-derived Plasmalogens Attenuate the Activation of PKCδ Associated with the Brain Inflammation. *Biochem. Biophysical Res. Commun.* 503 (2), 837–842. doi:10.1016/j.bbrc.2018.06.084

Shindou, H., Hishikawa, D., Nakanishi, H., Harayama, T., Ishii, S., Taguchi, R., et al. (2007). A Single Enzyme Catalyzes Both Platelet-Activating Factor Production and Membrane Biogenesis of Inflammatory Cells. *J. Biol. Chem.* 282 (9), 6532–6539. doi:10.1074/jbc.M609641200

Singh, P., Singh, I. N., Mondal, S. C., Singh, L., and Garg, V. K. (2013). Platelet-activating Factor (PAF)-antagonists of Natural Origin. *Fitoterapia* 84, 180–201. doi:10.1016/j.fitote.2012.11.002

Sirtori, C. R. (2014). The Pharmacology of Statins. *Pharmacol. Res.* 88, 3–11. doi:10.1016/j.phrs.2014.03.002

Smaragdi Antonopoulou, T. N. H. C., and Demopoulos, E. F. A. C. (2008). "PAF, a Potent Lipid Mediator," in *Bioactive Phospholipids. Role In Inflammation And Atherosclerosis*. Editor A. D. Tselepis (Transworld Research Network: Kerala, India), 85–134.

Snyder, F. (1990). Platelet-activating Factor and Related Acetylated Lipids as Potent Biologically Active Cellular Mediators. *Am. J. Physiology-Cell Physiol.* 259 (5), C697–C708. doi:10.1152/ajpcell.1990.259.5.C697

Snyder, F. (1995). Platelet-activating Factor: The Biosynthetic and Catabolic Enzymes. *Biochem. J.* 305 (3), 689–705. doi:10.1042/bj3050689

Stancu, C., and Sima, A. (2001). Statins: Mechanism of Action and Effects. *J. Cell. Mol. Med.* 5 (4), 378–387. doi:10.1111/j.1582-4934.2001.tb00172.x

Thomas, R. H., Foley, K. A., Mepham, J. R., Tichenoff, L. J., Possmayer, F., and MacFabe, D. F. (2010). Altered Brain Phospholipid and Acylcarnitine Profiles in Propionic Acid Infused Rodents: Further Development of a Potential Model of Autism Spectrum Disorders. *J. Neurochem.* 113 (2), 515–529. doi:10.1111/j.1471-4159.2010.06614.x

Toyoshima, K., Narahara, H., Furukawa, M., Frenkel, R. A., and Johnston, J. M. (1995). Platelet-Activating Factor: Role in Fetal Lung Development and Relationship to Normal and Premature Labor. *Clin. Perinatology* 22 (2), 263–280. doi:10.1016/s0095-5108(18)30285-9

Tsantila, N., Tsoupras, A. B., Fragopoulou, E., Antonopoulou, S., Iatrou, C., and Demopoulos, C. A. (2011). *In Vitro* and *In Vivo* Effects of Statins on Platelet-Activating Factor and its Metabolism. *Angiology* 62 (3), 209–218. doi:10.1177/0003319710375089

Tsoupras, A., Lordan, R., and Zabetakis, I. (2018). Inflammation, Not Cholesterol, Is a Cause of Chronic Disease. *Nutrients* 10 (5), 604. doi:10.3390/nu10050604

Uemura, Y., Lee, T. C., and Snyder, F. (1991). A Coenzyme A-independent Transacylase Is Linked to the Formation of Platelet-Activating Factor (PAF) by Generating the Lyso-PAF Intermediate in the Remodeling Pathway. *J. Biol. Chem.* 266 (13), 8268–8272. doi:10.1016/S0021-9258(18)92972-8

Wanders, R. J. A., and Waterham, H. R. (2006). Peroxisomal Disorders: The Single Peroxisomal Enzyme Deficiencies. *Biochim. Biophys. Acta (Bba) - Mol. Cel Res.* 1763 (12), 1707–1720. doi:10.1016/j.bbamcr.2006.08.010

Wood, P. L., Locke, V. A., Herling, P., Passaro, A., Vigna, G. B., Volpato, S., et al. (2016). Targeted Lipidomics Distinguishes Patient Subgroups in Mild Cognitive Impairment (MCI) and Late Onset Alzheimer's Disease (LOAD). *BBA Clin.* 5, 25–28. doi:10.1016/j.bbacli.2015.11.004

Wu, Y., Chen, Z., Darwish, W. S., Terada, K., Chiba, H., and Hui, S.-P. (2019). Choline and Ethanolamine Plasmalogens Prevent Lead-Induced Cytotoxicity and Lipid Oxidation in HepG2 Cells. *J. Agric. Food Chem.* 67 (27), 7716–7725. doi:10.1021/acs.jafc.9b02485

Yamashita, S., Kanno, S., Honjo, A., Otoki, Y., Nakagawa, K., Kinoshita, M., et al. (2016). Analysis of Plasmalogen Species in Foodstuffs. *Lipids* 51 (2), 199–210. doi:10.1007/s11745-015-4112-y

Yan, Q., Zhang, J., Liu, H., Babu-Khan, S., Vassar, R., Biere, A. L., et al. (2003). Anti-Inflammatory Drug Therapy Alters β-Amyloid Processing and Deposition in an Animal Model of Alzheimer's Disease. *J. Neurosci.* 23 (20), 7504–7509. doi:10.1523/JNEUROSCI.23-20-07504.2003

Zhaocheng, J., Jinfeng, L., Luchang, Y., Yequan, S., Feng, L., and Kai, W. (2016). Ginkgolide A Inhibits Lipopolysaccharide-Induced Inflammatory Response in Human Coronary Artery Endothelial Cells via Downregulation of TLR4-NF-Kb Signaling through PI3K/Akt Pathway. *Pharmazie* 71 (10), 588–591. doi:10.1691/ph.2016.6576

Zhuo, R., Rong, P., Wang, J., Parvin, R., and Deng, Y. (2021). The Potential Role of Bioactive Plasmalogens in Lung Surfactant. *Front. Cel Dev. Biol.* 9, 618102. doi:10.3389/fcell.2021.618102

Zimmerman, G. A., McIntyre, T. M., Prescott, S. M., and Stafforini, D. M. (2002). The Platelet-Activating Factor Signaling System and its Regulators in Syndromes of Inflammation and Thrombosis. *Crit. Care Med.* 30 (Suppl. ment), S294–S301. doi:10.1097/00003246-200205001-00020

Conflict of Interest: The authors declare that the research was conducted in the absence of any commercial or financial relationships that could be construed as a potential conflict of interest.

Publisher's Note: All claims expressed in this article are solely those of the authors and do not necessarily represent those of their affiliated organizations, or those of the publisher, the editors and the reviewers. Any product that may be evaluated in this article, or claim that may be made by its manufacturer, is not guaranteed or endorsed by the publisher.

frontiers in Cell and Developmental Biology

ORIGINAL RESEARCH
published: 25 April 2022
doi: 10.3389/fcell.2022.867138

Pharmacokinetics, Mass Balance, Excretion, and Tissue Distribution of Plasmalogen Precursor PPI-1011

Tara Smith, Kaeli J. Knudsen and Shawn A. Ritchie*

Med-Life Discoveries LP, Saskatoon, SK, Canada

PPI-1011 is a synthetic plasmalogen precursor in development as a treatment for multiple plasmalogen-deficiency disorders. Previous work has demonstrated the ability of PPI-1011 to augment plasmalogens and its effects *in vitro* and *in vivo*, however, the precise uptake and distribution across tissues *in vivo* has not been investigated. The purpose of this study was to evaluate the pharmacokinetics, mass balance, and excretion of [^{14}C]PPI-1011 following a single oral administration at 100 mg/kg in Sprague-Dawley rats. Further tissue distribution was examined using quantitative whole-body autoradiography after both single and repeat daily doses at 100 mg/kg/day. Non-compartmental analysis showed that following a single dose, PPI-1011 exhibited peak levels between 6 and 12 h but also a long half-life with mean $t_{1/2}$ of 40 h. Mass balance showed that over 50% of the compound-associated radioactivity was absorbed by the body, while approximately 40% was excreted in the feces, 2.5% in the urine, and 10% in expired air within the first 24 h. Quantitative whole-body autoradiography following a single dose showed uptake to nearly all tissues, with the greatest initial uptake in the intestines, liver, and adipose tissue, which decreased time-dependently throughout 168 h post-dose. Following 15 consecutive daily doses, uptake was significantly higher across the entire body at 24 h compared to single dose and remained high out to 96 h where 75% of the initially-absorbed compound-associated radioactivity was still present. The adipose tissue remained particularly high, suggesting a possible reserve of either plasmalogens or alkyl diacylglycerols that the body can pull from for plasmalogen biosynthesis. Uptake to the brain was also definitively confirmed, proving PPI-1011's ability to cross the blood-brain barrier. In conclusion, our results suggest that oral administration of PPI-1011 results in high uptake across the body, and that repeated dosing over time represents a viable therapeutic strategy for treating plasmalogen deficiencies.

Keywords: PPI-1011, plasmalogen augmentation, absorption, excretion, distribution, metabolism

OPEN ACCESS

Edited by:
Fabian Dorninger,
Medical University of Vienna, Austria

Reviewed by:
Pedro Brites,
Universidade do Porto, Portugal
Long Nam Nguyen,
National University of Singapore, Singapore

****Correspondence:***
Tara Smith
t.smith@med-life.ca

Specialty section:
This article was submitted to Cellular Biochemistry, a section of the journal Frontiers in Cell and Developmental Biology

Received: *31 January 2022*
Accepted: *03 March 2022*
Published: *25 April 2022*

Citation:
Smith T, Knudsen KJ and Ritchie SA (2022) Pharmacokinetics, Mass Balance, Excretion, and Tissue Distribution of Plasmalogen Precursor PPI-1011. Front. Cell Dev. Biol. 10:867138. doi: 10.3389/fcell.2022.867138

INTRODUCTION

Plasmalogens are naturally-occurring ethanolamine phospholipids derived in the peroxisome and endoplasmic reticulum that contain a vinyl-ether bond at the *sn*1 position. Plasmalogens play diverse roles within the body, but they primarily function as lipid membrane components modulating cell membrane architecture (Rog and Koivuniemi, 2016), fluidity (Lohner et al., 1984; Hermetter et al., 1989; Lohner et al., 1991) and vesicular fusion (Glaser and Gross, 1994; Glaser and Gross, 1995; Dorninger et al., 2017b). Plasmalogen deficiency is associated with several neurological disorders,

including the pediatric rare disease Rhizomelic Chondrodysplasia Punctata (RCDP) (Wanders et al., 1992; Wanders et al., 1994; Braverman et al., 1997), Parkinson's disease (Dragonas et al., 2009; Fabelo et al., 2011), and Alzheimer's disease (Han, 2005; Goodenowe et al., 2007). Attention is therefore being given to the potential of plasmalogen replacement as a therapeutic approach for treating these conditions. Although there are some natural dietary sources enriched in plasmalogens including select marine invertebrates such as sea squirts (Yamashita et al., 2017) and scallops (Fujino et al., 2017; Fujino et al., 2020), the concentrations are well below what is anticipated for therapeutic efficacy in humans (Bozelli and Epand, 2021). This leaves the synthetic production of plasmalogens as the only viable and practical approach for clinically-relevant therapeutic intervention.

To address this issue, we have engineered a synthetic plasmalogen precursor, PPI-1011, which has excellent shelf-life stability and is amenable to formulation up to concentrations as high as 500 mg/ml; a concentration high enough to provide the dosing anticipated for clinical efficacy. To our knowledge, PPI-1011 represents the first plasmalogen-augmenting compound undergoing a formal drug development process including preclinical safety-toxicology testing and multi-kilogram GMP manufacturing. PPI-1011 contains an ether-linked, 16:0 fatty alcohol at the *sn*1 position, 22:6 fatty acid (DHA) at the *sn*2 position, and lipoic acid at the *sn*3 position (Wood et al., 2011d). The lipoic acid is a critical component that stabilizes the molecule for long-term storage and prevents migration of the DHA fatty acid from *sn*2 to *sn*3 of the glycerol backbone (Wood et al., 2011a). Endogenously, introduction of the ether bond in the peroxisome is the critical step in plasmalogen biosynthesis, which is catalyzed by alkylglycerone phosphate synthase (AGPS) following the acylation of dihydroxyacetone phosphate by glyceronephosphate O-transferase (GNPAT) (Nagan and Zoeller, 2001). The ether is subsequently reduced to a vinyl-ether by an enzyme of the endoplasmic reticulum following export from the peroxisome (Gallego-García et al., 2019; Werner et al., 2020). Although diseases such as Parkinson's and Alzheimer's have several possible explanations for the associated plasmalogen deficiency, it has been suggested to result from impairment of the peroxisomal steps of the biosynthetic pathway (Kou et al., 2011; Dorninger et al., 2017a; Jo and Cho, 2019). Therefore, therapeutically providing an ether precursor bypasses the enzymes of the peroxisome, leaving the body to catalyze the reduction of the ether to the plasmalogen-defining vinyl-ether bond.

Despite extensive academic *in vitro* and *in vivo* studies examining multiple aspects of various plasmalogen extracts on both biochemical and behavioral endpoints, none have been scaled up and tested in a traditional safety program required for all new drug products. PPI-1011 is one of several fully synthetic plasmalogen precursors under development in our lab, which we have shown over the years to not only augment plasmalogens in multiple cell lines and species (Wood et al., 2011b; Wood et al., 2011c; Wood et al., 2011d; Wood et al., 2011e; Gregoire et al., 2015), but also exhibit a vast array of effects including neuroprotection (Miville-Godbout et al., 2016; Miville-Godbout et al., 2017; Nadeau et al., 2019), protection against inflammation and loss of dopaminergic neurons (Miville-Godbout et al., 2016; Miville-Godbout et al., 2017; Nadeau et al., 2019), shift towards non-amyloidogenic processing (Wood et al., 2011a), reduction of cholesterol (Mankidy et al., 2010), improvement of remyelination in a model of multiple sclerosis (Wood et al., 2011a), regulation of membrane protein function (Wood et al., 2011c), potent anti-dyskinetic effect when administered in combination with levodopa to primates treated with MPTP (Gregoire et al., 2015; Bourque et al., 2018) and normalization of behavior in plasmalogen-deficient mice (Fallatah et al., 2019). Furthermore, PPI-1011 has an acceptable safety profile and shows no toxicity or adverse effects to date, including doses up to 1,000 mg/kg in adult rats and 28-day repeat dosing at 400 mg/kg in primates (manuscript in preparation).

Although we have previously demonstrated brain uptake of PPI-1011 using a [^{13}C]PPI-1011 as well as uptake to peripheral tissues (Wood et al., 2011b), there remains a general uncertainty about the *in vivo* pharmacokinetic behavior, absorption, and distribution of orally administered plasmalogens or ether precursors, as a quantitative assessment of pharmacokinetics has never been performed. Therefore, as part of our ongoing preclinical safety and toxicity program, and to better understand plasmalogen disposition and excretion after treatment, we report herein the pharmacokinetics and tissue distribution of [^{14}C]PPI-1011 following both single and repeat oral dosing in Sprague-Dawley male rats.

MATERIALS AND METHODS

Chemicals

PPI-1011 (1-*O*-hexadecyl-2-*O*-cis-4, 7, 10, 13, 16, 19-docosahexaenoyl-3-*O*-lipoyl glycerol) was synthesized at Laxai Life Sciences Pvt Ltd. using a previously described synthetic route (Wood et al., 2011a). Structure was confirmed by mass spectrometry and NMR analysis. [^{14}C] PPI-1011 was synthesized by RTI International using [^{14}C] sodium cyanide to introduce a single [^{14}C] label onto the first carbon of palmitoyl alcohol, which was linked to the *sn*1 position of the glycerol backbone. [^{14}C]PPI-1011 had a specific activity of 70.2 µCi/mg and a radiochemical purity of 95.9%. Handling of this material was in accordance with US Nuclear Regulatory Commission (NRC), Pennsylvania Bureau of Radiation Protection regulations, Frontage QWBA final study protocol, and all applicable Frontage Standard Operating Procedures (SOP).

Ethanolamine and 2-methoxyethanolamine were purchased from Sigma. Carbo-Sorb® E, PermaFluor® E+, Ultima Gold™, Hionic-Fluor, and Ultima-Flo™ M liquid scintillation cocktails were obtained from Perkin Elmer Life Sciences. Stopflow AQ liquid scintillation cocktails were purchased from AIM Research Company. Solvents used for chromatographic analysis were HPLC or ACS reagent grade and purchased from Fisher. All other reagents were of analytical or ACS reagent grade.

Animals

All animal studies were performed by Frontage Laboratories using male Sprague-Dawley (SD) rats (Charles River Breeding Laboratories) 8–10 weeks old with body weights between 208 and 283 g. Animals were acclimated for a minimum of 3 days and examined to ensure their health status prior to dosing. The animal room was controlled to maintain a temperature of 20 ± 5°C, relative humidity between 30 and 70%, and a 12 h light/12 h dark cycle. Reverse osmosis filtered water and food (certified Purina Rodent Diet) were available to animals *ad libitum*. Final study plans were reviewed and approved by the Institutional Animal Care and Use Committee at Frontage Laboratories and complied with the applicable sections of the Final Rules of the Animal Welfare Act regulations (9 CFR) and were in accordance with the Association for the Assessment and Accreditation of Laboratory Animal Care recommendation.

Dose Formulation

PPI-1011 and [^{14}C]PPI-1011 were formulated together in liquid coconut oil (LCO) containing 0.1% 1-thioglycerol for oral dosing. For single dose studies, PPI-1011 and [^{14}C]PPI-1011 were combined to generate an oral formulation with a concentration of 20 mg/ml and 40 μCi/ml on the day before dosing and stored at 4°C. Formulation for the repeat dosing QWBA experiment was made on the day prior to the first dose with a concentration of 20 mg/ml and 20 μCi/ml. This formulation was then aliquoted and stored frozen at −20°C until the day of use. Concentration and radiochemical purity of all formulations were confirmed by HPLC prior to dosing.

Pharmacokinetic Study

The pharmacokinetics of [^{14}C]PPI-1011 were performed in four rats that were surgically implanted with femoral artery catheters (FAC) for blood collection at least 2 days before dosing began. [^{14}C]PPI-1011 was administered as a single oral dose at 100 mg/kg (200 μCi/kg). Blood samples were collected in EDTA tubes and centrifuged to obtain plasma at 1, 3, 6, 12, 18, 24, 48, and 72 h after drug administration. Duplicate aliquots of plasma (~25 μl or higher) were transferred to liquid scintillation vials and the weights of sample aliquots were recorded. Aliquots were mixed with Ultima Gold (5 ml) as scintillation fluid and total radioactivity was determined by liquid scintillation counting (LSC) and used to calculate the total radioactive concentration.

Mass Balance and Excretion Study

Four male rats were administered a single oral dose of [^{14}C]PPI-1011 at 100 mg/kg (200 μCi/kg). Feces, urine, and the cage rinse samples were collected at pre-determined times up to 168 h post-dose (HPD). The expired air was collected using a carbon dioxide trapping apparatus equipped with airflow apparatus. Expired [^{14}C]CO_2 was collected for two of the four dosed animals for 24 h after the dose in a solution of ethanolamine:2-methoxyethanol (1:3, v/v) in two traps. Rats were sacrificed by overdose of CO_2 and each cage was rinsed with 25% ethanol in water (>50 ml) at the end of the study. The cage rinse sample and the expired [^{14}C]CO_2 was stored at 4°C.

Diluted dose solutions, plasma, urine, and cage rinse were analyzed in duplicate by LSC, as described above. The expired CO_2 was analyzed the same day it was collected by mixing a 1 ml aliquot of the carbon dioxide absorbents with 5 ml of Hionic-Fluor for radioactivity concentrations with LSC. Feces samples were homogenized in 5-fold volume of purified water then duplicate fecal homogenate aliquots were transferred to Combusto Cones and combusted with a Sample Oxidizer (Model A307, Perkin Elmer) equipped with an Oximate 80 Robotic Automatic Samples. The [^{14}C]CO_2 generated by the combustion was also collected in Carbo Sorb E and radioactivity was determined with PermaFluor as the scintillant using a Tri-Carb LSC.

Single Dose Tissue Distribution Study

Six male rats were administered a single oral dose of [^{14}C]PPI-1011 at 100 mg/kg (200 μCi/kg) and one rat was sacrificed at each of the following time points after the administration of the dose: 8, 12, 18, 24, 48, or 168 h. Terminal blood was collected by cardiac puncture directly into tubes with K_2EDTA, an aliquot was stored at 4°C until LSC was performed for radioactivity, while the remaining blood was processed to plasma and stored at −20°C until LSC. Following blood collection, the carcasses were frozen in a cold bath with hexanes and dry ice for at least 8 min and then dried and stored at −70°C for at least 5 h. The carcasses were transferred to a −20°C freezer for at least 12 h before embedding.

Repeat Dose Tissue Distribution Study

Three male rats were administered [^{14}C]PPI-1011 at 100 mg/kg (100 μCi/kg) once daily for 15 days. One rat was sacrificed at each of the following time points after the administration of the day 15 dose: 24, 48, and 96 h. Terminal blood was collected by cardiac puncture directly into tubes with K_2EDTA, an aliquot was stored at 4°C until LSC was performed for radioactivity, while the remaining blood was processed to plasma and stored at −20°C until LSC. Following blood collection, the carcasses were frozen in a cold bath with hexanes and dry ice for at least 8 min and then dried and stored at −70°C for at least 12 h. The carcasses were transferred to a −20°C freezer for at least 12 h before embedding.

QWBA Sectioning and Quantification

QWBA was used to determine radioactivity concentrations in the caecum (contents and mucosa), large intestine (contents and mucosa), small intestine (contents and mucosa), stomach (contents and mucosa), brain, choroid plexus, spinal cord, bone, skin, adrenal gland, pineal body, pituitary gland, thyroid gland, liver, kidney (cortex, medulla and whole kidney), urinary bladder (contents and wall), brown fat, white fat, eye (lens, uveal tract and whole eye), epididymis, prostate gland, testis, ovary, uterus, lung, exorbital lachrymal gland, Harderian gland, pancreas, salivary gland, skeletal muscle, myocardium, cardiac blood, bone marrow, lymph node, spleen, and thymus. As well, LSC was used to determine the total radioactivity in the whole blood and plasma.

The whole-body cryosectioning technique described by (Ullberg, 1977) was the basis for embedding and

cryosectioning the rats assigned to this study. Each frozen carcass was shaved, and then the limbs and tail were removed prior to embedding. Chilled (4°C) 3% CMC (low viscosity) was utilized to provide a firm support of reinforced ice around each rat and for a secure attachment to the microtome stage. Upon thorough freezing of the embedding medium surrounding each rat, the frozen CMC block was removed from the freezing bath and four 3/8 inch holes were drilled into the block. One cryosection quality control standard (CQCS) was prepared with a known amount of radioactivity and at least 1 ml aliquots were added to each of the four drilled holes. CQCS data were utilized to evaluate the overall performance of the QWBA assay.

Each frozen rat was sagittally trimmed (50–100 µm) at −20°C until exposure of a few target tissues employing a Leica Cryomacrocut heavy-duty microtome (Leica Microsystems Inc.,). Disposable stainless steel Feather type H45L knives (Feather Safety Razor Co., Ltd.) were utilized for trimming and sectioning each frozen rat. Several thinner sections (50 µm) were discarded prior to obtaining multiple 50 µm sections at various cryosectioning levels for QWBA analysis. Upon the collection of at least 60 target tissues in multiple cryosectioning levels, the cryosections were kept in the Cryomacrocut cryochamber for a minimum of 18 h for dehydration depending upon the number of cryosections within the cryochamber. After dehydration was complete, the cryosections were transferred to ambient temperature for processing. Mounted whole-body cryosections and a set of 15 standards were sandwiched between a standard phosphor screen and an exposure cassette. All cryosections were exposed to the phosphor screen for 4-days in a cabinet protected with lead prior to scanning using a Typhoon PhosphorImager (Cytiva). MCID™ Analysis software (InterFocus Ltd.) was utilized to generate a calibration curve of the STD nominal concentrations (nCi/g) versus PhosphorImager response (counts/µm^2 minus background) by weighted (1/x) linear regression analysis (Potchoiba et al., 1995; Potchoiba et al., 1998). The linear regression curve was then utilized to determine the concentration (nCi/g) of total radioactivity in whole-body tissues and blood. Radioactivity concentrations were expressed as µg Eq/g based on the specific activity of the compound in the final dose formulations. Radioactivity concentrations represent the mean of all determinations for all whole-body cryosections that contained the target tissue or blood for each individual rat.

Statistical Analysis

The PK calculations of total radioactivity in plasma were analyzed with non-compartmental analyses using Phoenix® WinNonlin® software (version 8.1). Statistical calculations for the other studies were limited to simple parameters such as means or averages, standard deviations (sd), and percentages (%). The amount of compound equivalents (Eq) in samples was calculated as concentrations expressed in µg Eq/g. Dose, MCID™ generated tissue concentrations, pharmacokinetic, and radioanalysis data were compiled using Microsoft Excel for Microsoft 365, Version 2010.

RESULTS

Dose Formulation Analysis

Radiochemical concentrations and purity of the oral dose formulations were all confirmed to be >97% by HPLC with radioactivity detection. The mean radioactivity concentrations of dose formulations were 21.24 µCi/g. Representative radiochromatograms obtained from analysis of dose formulation of [^{14}C]PPI-1011 are shown in **Supplementary Figure S1**. The retention time of [^{14}C]PPI-1011 was approximately 12 min. The stability of the dose formulation at 20 mg/ml concentration was examined at 4°C and at −20°C for up to 24 h. The results are shown in **Supplementary Figure S2**. Under the experimental conditions utilized in this study, the radioactive purity of [^{14}C]PPI-1011 at 20 mg/ml in LCO with 0.1% 1-thioglycerol dose vehicle was stable up to 24 h at 4°C (96.5%) and −20°C (97.2%). The actual dose administered to each rat in µCi as well as the animal weights are shown in **Supplementary Table S1**.

For the repeat dose tissue distribution study, the radiochemical purity of the pre-dose formulation on day one was 97.9%. After being stored at −20°C, the presence of [^{14}C]PPI-1011 + O was detected in the pre-dose formulation on day seven and the post-dose formulations on day eight and on day 15 at levels ranging between 3.6 and 10.1%. The overall total radiochemical purity of these formulations ranged between 95.4 and 97.9%, confirming the stability of [^{14}C] PPI-1011 over the initial 15 consecutive daily dose administration interval.

Pharmacokinetic Profile

Pharmacokinetics of PPI-1011 were evaluated in male rats following a single oral dose of [^{14}C]PPI-1011 at 100 mg/kg (200 µCi/kg). The total radioactivity concentrations in ng Eq/g in rat plasma up to 72 h are plotted in **Figures 1A,B**. The mean total radioactivity in plasma was approximately 500 ng Eq/g at 1 h, increased to ~27,000 ng Eq/g at 6 h, and then decreased with time to ~4,000 ng Eq/g at 72 h. Pharmacokinetics were characterized by a long elimination half-life (40 h), a mean t_{max} of 7.5 h, C_{max} of 27,900 ng/ml, and AUC_{inf} of 867,000 h*ng/ml (**Table 1**).

Recovery of Total Radioactivity

Recovery of total radioactivity was determined by measuring radioactivity excreted in the urine and feces as well as expired air (**Figure 2**). Following a single oral dose at 100 mg/kg (200 µCi/kg) of [^{14}C]PPI-1011 in male SD rats, approximately 50% of dosed radioactivity (45.10 ± 7.34%) was recovered in urine and feces including cage rinses within the 168 h collection period. Approximately 11% of the dosed radioactivity was in expired air (as ^{14}C-CO_2) within 24 HPD, the only timepoint collected for expired air. Feces was the major excretion pathway and recovered 42.51 ± 7.16% of the dose, while a small amount of the dose (2.40 ± 0.59%) was found in urine up to day seven. Between 24 and 48 h, approximately 6% of the total dose was excreted in urine

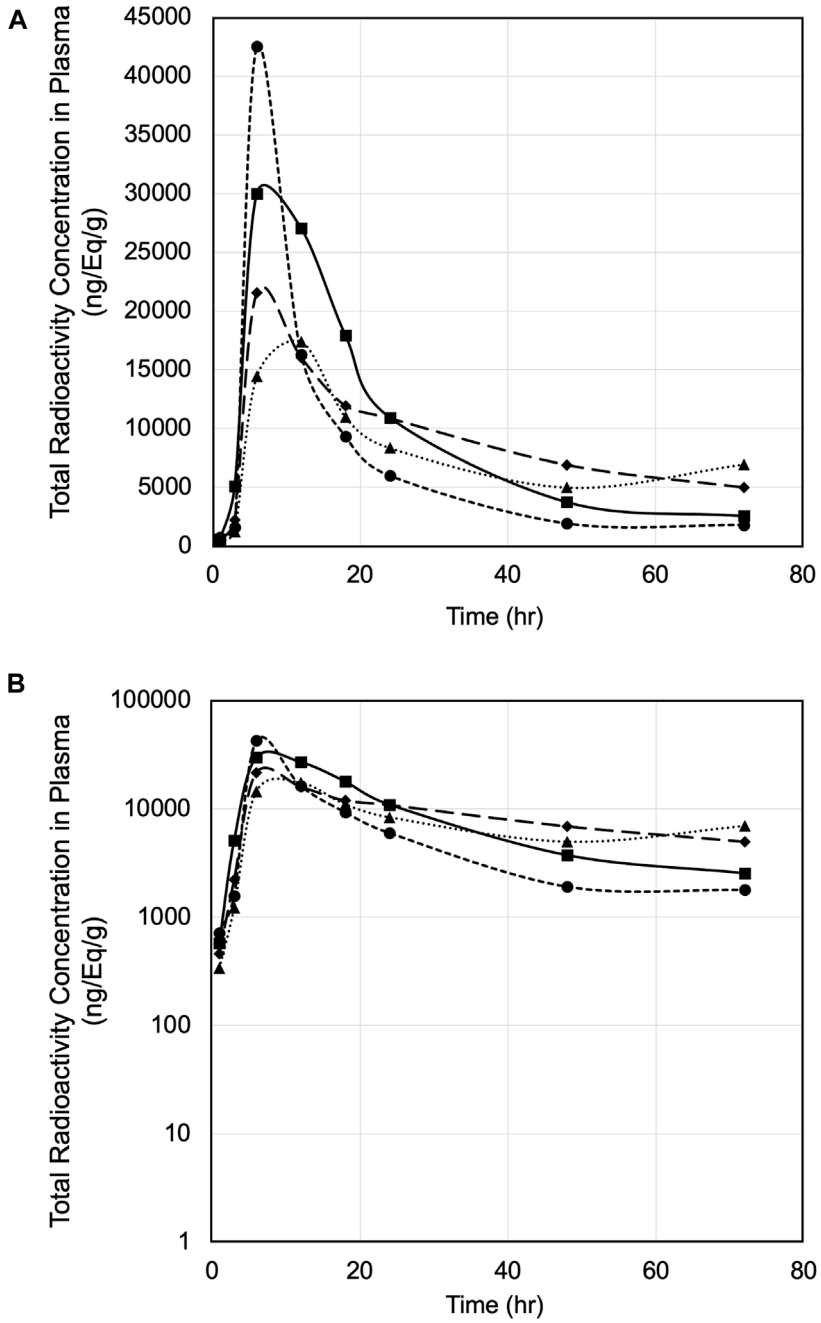

FIGURE 1 | (A) Plasma concentration versus time of [^{14}C]PPI-1011 in four male rats following single-dose oral administration at 100 mg/kg. **(B)** Log10 scale of A.

and feces, with little additional excretion observed between 48 and 168 h (<3%). A complete breakdown of the excretion data is available in **Supplementary Table S2**. The results indicate that significant amounts of dosed radioactivity were not recovered in male SD rats, suggesting high rate of absorption of [^{14}C]PPI-1011 following oral administration, and that a large proportion of the absorbed material is retained within the tissue and serum beyond 7 days.

Tissue Uptake and Distribution Following a Single Dose

[^{14}C]PPI-1011 absorption across tissues was first determined by QWBA for up to 168 h following a single dose at 100 mg/kg. Compound-associated radioactivity was widely distributed into most evaluated tissues (N = 51) at the first sampling time of 8 HPD after oral administration of a single, bolus dose of [^{14}C]PPI-1011 to Sprague-Dawley male rats (**Table 2** and **Figure 3**). The

TABLE 1 | Plasma pharmacokinetic parameters of total radioactivity following a single dose of 100 mg/kg [^{14}C]PPI-1011 (200 μCi/kg) in male Sprague-Dawley rats.

	Rat 1	Rat 2	Rat 3	Rat 4	Mean	SD	%CV
AUC_{last} (h*ng/ml)	702,000	659,000	507,000	565,000	608,000	88,500	14.6
AUC_{Inf} (h*ng/ml)	753,000	953,000	542,000	1,220,000	867,000	289,000	33.3
AUC Extr (%)	6.8	31	6.5	54	20	20	92.5
MRT_{Inf} (h)	27	61	23	110	55	40	73
$t_{1/2}$ (h)	18	42	19	80	40	29	73
t_{max} (h)	6.0	6.0	6.0	12	7.5	3.0	40
C_{max} (ng/ml)	30,000	21,500	42,500	17,400	27,900	88,500	39.8

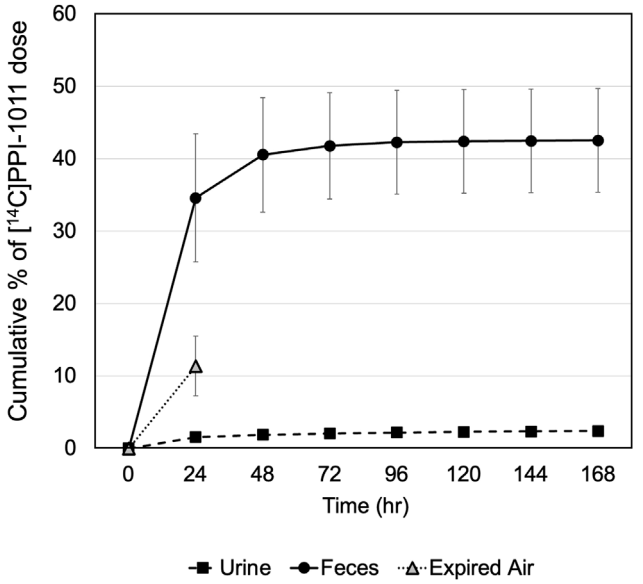

FIGURE 2 | Recovery of radioactivity in excreta of male rats following a single oral dose of [^{14}C]PPI-1011 at 100 mg/kg.

highest concentrations of radioactivity occurred at 8 or 12 HPD in most tissues (N = 17 and 21, respectively) with some exceptions. Tissues with the highest peak concentrations of radioactivity were observed in gastrointestinal tract tissues, adipose (brown, subcutaneous, and visceral), adrenal gland, liver, and preputial gland. Tissues with the lowest peak concentrations of radioactivity were observed in the whole eye, the non-circumventricular CNS tissues, bone surfaces, testis, and uveal tract. Non-circumventricular CNS tissue was grouped separately from other CNS tissues due to differences in the blood-brain barrier. Rather than a true barrier, circumventricular CNS tissues are surrounded instead by fenestrated capillaries that result in their exposure to larger and more polar chemicals than other regions of the CNS (Benarroch, 2011). The ocular lens and vitreous body were the only tissues that were devoid of radioactivity throughout the course of this study. Although tissue radioactivity concentrations slowly declined over time in most tissues after reaching peak levels, compound-associated radioactivity was present in all but five tissues (bladder wall, bone surfaces, ocular lens, vitreous body, and seminal vesicles) at the last sampling time of 168 HPD.

Brown adipose, subcutaneous adipose, and visceral adipose had some of the highest concentrations of compound-associated radioactivity at all timepoints through the last sampling time of 168 HPD. The highest peak concentrations occurred at 12 HPD for all three adipose tissues. By 168 HPD, radioactivity declined approximately 5, 2, and 3 -fold in brown adipose, subcutaneous adipose, and visceral adipose, respectively, when compared with peak concentrations. Except for the adrenal gland, preputial gland, and small intestines, which had similar concentrations, the average last measured radioactivity concentrations in the three adipose tissues were 5 to 56 -fold greater than for all other tissues. This suggests that the retained radioactivity present in adipose tissue, along with its relatively slow release, may serve as a potential reservoir for continual re-distribution to other tissues prior to elimination.

The non-circumventricular CNS tissues (cerebellum, cerebrum, colliculus, medulla oblongata, olfactory bulb, spinal cord, and thalamus) had relatively low radioactivity concentrations throughout the study compared to other tissues. However, presence of radioactivity in CNS tissue at all samples times illustrated that [^{14}C]PPI-1011 does distribute across the blood-brain barrier, and while levels in the non-circumventricular CNS tissue did not substantially change throughout the sampling times, they all demonstrated peak levels at 168 HPD. The choroid plexus, pineal gland, and pituitary gland are CNS tissues that reside behind leaky junctions of the blood-brain barrier. Concentrations of compound-associated radioactivity were higher (approximately 4-fold higher) in these three brain tissues than those measured in the non-circumventricular CNS tissues throughout the time course of this study. The highest peak concentrations occurred at 12, 18, and 48 HPD for the choroid plexus, pituitary gland, and pineal gland, respectively.

The ocular lens and vitreous body were devoid of radioactivity throughout the course of this study. Concentrations of compound-associated radioactivity present in the uveal tract did not substantially change between the first sampling time of 8 HPD through the last sampling time of 168 HPD. The distribution pattern for the whole eye was similar to the uveal tract, but radioactivity concentrations were 3 to 4 -fold lower than the uveal tract due to the lack of radioactivity present in other ocular tissues such as the lens and vitreous body.

Radioactivity concentrations were present in all male-specific tissues from the first sampling time of 8 HPD through the last sampling time of 168 HPD with one exception. By 168 HPD, the radioactivity concentration in the seminal vesicles declined below

TABLE 2 | Radioactivity concentrations (μg equivalents/g) determined by quantitative whole-body autoradiography in tissues and blood through 168 h after a single oral dose of [^{14}C]PPI-1011 to Group 1 Sprague-Dawley male rats (Nominal Dose Levels: 200 μCi/kg and 100 mg/kg).

Rat Identification:	01M	02M	03M	04M	05M	06M
Time (Post-Dose):	**8 h**	**12 h**	**18 h**	**24 h**	**48 h**	**168 h**
Adipose - Brown	171	426	66.0	133	132	89.0
Adipose - Brown (Vessel Wall)	301	383	94.2	110	98.6	76.7
Adipose - Visceral	83.1	170	75.6	71.6	111	90.7
Adipose - Subcutaneous	74.0	242	73.9	70.1	82.1	89.3
Adrenal Gland[a]	195	367	185	155	201	142
Bladder Wall	86.0	19.3	14.5	7.69	10.7	nd
Blood - QWBA	35.4	16.4	9.62	5.62	4.19	2.56
Bone Marrow	23.5	23.0	22.3	18.3	15.7	4.69
Bone Surface	2.30	1.15	1.25	0.513	0.508	nd
Diaphragm	55.6	59.9	40.4	37.4	23.0	11.7
Exorbital Lacrimal Gland	28.7	34.5	8.74	9.66	6.13	7.36
Harderian Gland	14.4	10.8	14.7	10.5	11.1	3.67
Intra-Orbital Lacrimal Gland	10.4	8.89	8.91	7.56	6.64	5.01
Kidney	42.9	45.3	36.1	24.7	24.6	14.5
Renal Cortex	41.4	46.6	38.1	26.8	24.3	15.3
Renal Medulla	51.0	53.2	23.0	25.8	22.7	11.8
Liver	313	269	121	73.4	40.0	7.50
Lung	74.0	51.9	45.4	30.2	22.9	11.2
Lymph Node	22.7	22.6	22.5	17.4	20.0	12.3
Muscle	10.3	12.6	9.63	7.57	8.42	7.01
Myocardium	92.0	72.6	42.4	31.0	26.6	13.4
Nasal Turbinates	16.0	10.6	6.43	4.81	5.03	4.29
Pancreas	66.3	52.7	39.8	24.8	28.0	18.2
Parotid Gland	39.1	30.4	35.2	20.5	20.9	12.3
Salivary Gland	53.3	31.4	28.8	21.3	22.9	15.4
Skin - Non-Pigmented	15.0	18.0	12.0	9.26	13.4	10.2
Spleen	105	111	71.3	46.3	33.1	9.36
Thymus	10.7	12.2	11.8	9.79	9.58	7.84
Thyroid	49.9	43.1	38.5	27.7	27.2	18.9
Ocular - Lens	nd	nd	nd	nd	nd	nd
Ocular - Uveal Tract	6.97	6.57	5.32	4.27	4.78	6.48
Ocular - Vitreous Body	nd	nd	nd	nd	nd	nd
Ocular - Whole Eye	1.83	2.03	1.65	1.14	1.30	1.55
Cerebellum	2.70	2.69	3.03	2.08	2.60	3.59
Cerebrum	2.39	2.22	2.49	1.61	2.23	2.94
Choroid Plexus	14.9	17.1	12.8	9.85	14.4	10.4
Colliculus	3.50	3.03	2.94	2.06	3.30	3.97
Medulla Oblongata	2.40	2.44	2.23	1.98	2.45	3.13
Olfactory Bulb	2.16	2.01	1.75	2.07	2.01	2.25
Pineal Gland	11.9	12.1	16.2	10.8	16.4	12.0
Pituitary Gland	21.2	21.2	22.0	16.7	19.2	12.9
Spinal Cord	2.71	2.76	3.20	1.75	2.56	3.33
Thalamus	2.27	2.31	2.20	1.71	1.91	2.78
Whole Brain	2.60	2.48	2.70	1.95	2.45	3.08
Epididymis	39.8	70.9	67.7	40.4	6.81	7.75
Preputial Gland	33.6	214	78.0	112	76.5	69.0
Prostate	49.6	11.8	28.0	56.7	7.15	4.44
Seminal Vesicles	12.8	2.99	as	5.38	9.12	nd
Testis	2.65	4.12	5.09	4.31	4.02	3.08
Cecum	as	450	177	231	34.3	as
Esophagus	17.4	16.9	15.0	9.46	10.8	5.34
Gastric Mucosa	91.2	67.8	70.1	48.7	37.5	14.5
Large Intestines	12.5	209	154	180	19.1	14.0
Small Intestines	609	347	239	247	43.3	139
Stomach	22.6	22.9	21.6	10.8	8.01	4.97

[a]*as: tissue was soaked with adipose. nd: radioactivity was not detectable*

the lower limit of quantitation (LLOQ) of 0.485 μg Eq/g. The highest peak concentrations in the epididymis, preputial gland, testis, prostate, and seminal vesicles occurred at 12, 12, 18, 24, and 48 HPD, respectively. The testis was the only male-specific tissue where the concentrations of compound-associated radioactivity did not substantially change throughout the course of this study. These concentrations in the testis ranged from a low of 2.65 μg Eq/g at 8 HPD, to a high of 5.09 μg Eq/g at 18 HPD, with a C_{last} of 3.08 μg Eq/g at 168 HPD.

Radioactivity concentrations were present in the esophagus, gastrointestinal tract tissues, and the bladder wall from the first sampling time of 8 HPD through the last sampling time of 168 HPD with one exception. By 168 HPD, the radioactivity concentration in the bladder wall declined below the LLOQ of 0.485 μg Eq/g. The highest peak concentrations occurred in the bladder wall, esophagus, gastric mucosa, and small intestines at 8 HPD and in the cecum, large intestines, and stomach at 12 HPD. There was no detection of radioactivity in urine within the urinary bladder.

Concentrations of compound-associated radioactivity were present in blood from the first sampling time of 8 HPD through the last sampling time of 168 HPD. The highest blood concentration of compound-associated radioactivity occurred at 8 HPD with a concentration of 35.4 μg Eq/g. Blood concentrations of radioactivity declined at each subsequent sampling time with a last measurable concentration of 2.56 μg Eq/g at 168 HPD. Blood:plasma concentration ratios ranged from 0.685 to 1.11 from 8 to 48 HPD suggesting that there was not an apparent preferential uptake of [^{14}C]PPI-1011 associated radioactivity into the cellular components of blood. By 168 HPD the blood:plasma concentration ratio more than doubled to 2.96 from the 48 HPD ratio suggesting an apparent uptake of [^{14}C]PPI-1011 associated radioactivity into the cellular components of blood over time.

Tissue Uptake and Distribution Following Repeat Dosing

QWBA was next used to determine [^{14}C]PPI-1011 uptake following 15-consecutive daily oral bolus doses of [^{14}C]PPI-1011 at 100 mg/kg (100 μCi/kg) to Sprague-Dawley male rats (**Table 3** and **Figure 4**). Compound-associated radioactivity was present in all evaluated tissues (N = 54) at 24, 48, and 96 HPD. The highest concentrations of radioactivity occurred at 24 HPD in most tissues (N = 42) except for five tissues showing highest levels at 48 HPD (adrenal gland, bladder wall, nasal turbinates, subcutaneous adipose, and visceral adipose) and five tissues at 96 HPD (cerebrum, medulla oblongata, spinal cord, ocular lens, and prostate).

Other than the adrenal gland, brown adipose, subcutaneous adipose, and visceral adipose had the highest concentrations of compound-associated radioactivity at 24, 48, and 96 HPD. The highest peak concentrations occurred at 24 HPD for brown adipose and at 48 HPD for subcutaneous and visceral adipose. By 96 HPD, radioactivity concentrations declined approximately 1.4, 1.1, and 1.2 -fold in brown adipose, subcutaneous adipose, and visceral adipose, respectively, when compared with peak concentrations. Except for the adrenal gland, the average last measured radioactivity concentrations in the three adipose tissues were 4 to 629 -fold greater than for all other tissues. Although tissue radioactivity concentrations slowly declined over time in most tissues after reaching peak levels, compound-associated radioactivity exhibited a greater

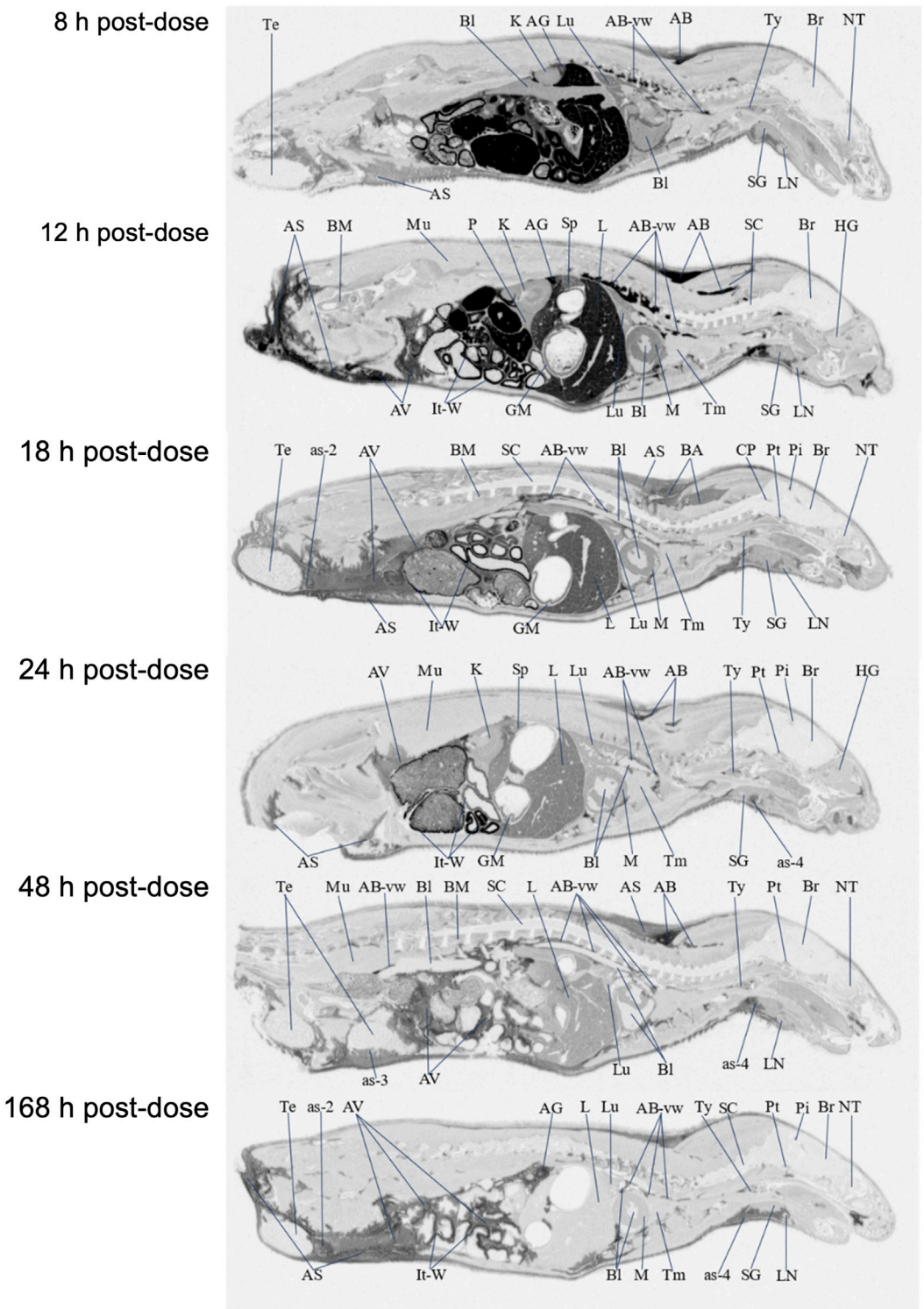

FIGURE 3 | Selected autoradiography images (8, 12, 18, 24, 48, and 168 h post dose) of tissue distribution of in the whole rat body after single-dose oral administration at 100 mg/kg [^{14}C]PPI-1011. The abbreviations are: AB, adipose brown; AS, adipose subcutaneous; AV, adipose visceral; AB-vw, adipose brown:vessel wall; as-2, adipose-soaked:epididymis; as-3, adipose-soaked:testis; as-4, adipose-soaked:salivary gland; AG, adrenal gland; Bl, blood; BM, bone marrow; Br, brain; CP, choroid plexus; GM, gastric mucosa; HG, harderian gland; It-W, intestinal tract wall; K, kidney; L, liver; LN, lymph node; Lu, lung; M, myocardium; Mu, muscle; NT, nasal tubinates; P, pancreas; Pi, pineal gland; Pt, pituitary gland; SC, spinal cord; SG, salivary gland; Sp, spleen; Te, testis; Tm thymus; Ty, thyroid.

TABLE 3 | Radioactivity concentrations (μg equivalents/g) determined by quantitative whole-body autoradiography in tissues and blood through 96 h after daily, multiple oral doses[1,2] of [^{14}C]PPI-1011 to Group 2 Sprague-Dawley male rats (Nominal Dose Levels: 100 μCi/kg and 100 mg/kg).

Rat Identification:	07M	08M	09M
Time (Post-Dose):	24 hr	48 hr	96 hr
Adipose - Brown	2211	1917	1301
Adipose - Brown (Vessel Wall)	1423	1017	1249
Adipose - Visceral	1402	1500	1265
Adipose - Subcutaneous	1316	1498	1373
Adrenal Gland[a]	1830	2346	1636
Bladder Wall	102	108	101
Blood - QWBA	55.0	34.3	29.5
Bone Marrow	160	113	77.3
Bone Surface	11.6	7.66	10.5
Diaphragm	204	172	125
Exorbital Lacrimal Gland	98.0	82.5	71.0
Harderian Gland	113	69.6	47.9
Intra-Orbital Lacrimal Gland	100	84.5	76.5
Kidney	304	221	238
Renal Cortex	323	244	250
Renal Medulla	238	183	186
Liver	412	186	129
Lung	217	181	191
Lymph Node	347	165	127
Muscle	115	95.4	97.9
Myocardium	292	222	172
Nasal Turbinates	180	184	80.2
Pancreas	355	312	333
Parotid Gland	296	257	220
Salivary Gland	308	271	227
Skin - Non-Pigmented	161	101	129
Spleen	319	209	147
Thymus	153	131	107
Thyroid	373	297	259
Ocular - Lens	5.82	5.05	6.92
Ocular - Uveal Tract	105	59.6	68.9
Ocular - Vitreous Body	2.55	2.01	2.06
Ocular - Whole Eye	22.7	15.8	18.2
Cerebellum	57.8	54.9	55.8
Cerebrum	45.7	39.9	47.5
Choroid Plexus	186	131	121
Colliculus	68.3	68.0	67.3
Medulla Oblongata	51.0	48.4	51.8
Olfactory Bulb	47.8	35.0	42.2
Pineal Gland	230	156	179
Pituitary Gland	266	226	191
Spinal Cord	46.8	51.2	53.0
Thalamus	45.4	42.3	45.4
Whole Brain	48.8	43.7	47.3
Epididymis	as	as	as
Preputial Gland	as	as	as
Prostate	74.6	72.1	84.8
Seminal Vesicles	63.2	60.7	54.7
Testis	70.3	47.2	43.3
Cecum	300	95.7	as
Esophagus	161	94.8	87.1
Gastric Mucosa	415	307	210
Large Intestines	255	122	94.3
Small Intestines	420	164	112
Stomach	133	78.9	109

[a]*as: tissue was soaked with adipose.*

than 2-fold decrease in only six tissues (bone marrow, Harderian gland, liver, lymph nodes, nasal turbinates, and spleen) at the last sampling time of 96 HPD. The data illustrated a retention of compound-associated radioactivity in all tissues after multiple doses at concentrations substantially greater than after a single oral dose.

Radioactivity present in the non-circumventricular CNS tissues did not substantially change in concentration across the three sampling times. This CNS concentration data showed that after multiple doses [^{14}C]PPI-1011 radioactivity was present in greater concentrations, approximately 16 to 33 -fold higher at the 24 HPD timepoint, compared to concentrations at the same timepoint after a single oral dose.

After the 15-consecutive daily-dose administrations, radioactivity was now of measurable concentration in the ocular lens and vitreous body at the 24, 48, and 96 HPD. Concentrations of compound-associated radioactivity present in all ocular tissues did not substantially change in concentration across the three sampling times. The highest peak concentrations occurred at 24 HPD for the uveal tract, vitreous body, and whole eye and at 96 HPD for the ocular lens. The distribution pattern for the whole eye was similar to the uveal tract, but radioactivity concentrations were 4 to 5 -fold lower than the uveal tract due to the lower concentrations of radioactivity in other ocular tissues such as the lens and vitreous body.

Radioactivity concentrations were present in all the evaluated male-specific tissues at the three sampling times. However, due to adipose soaking, radioactivity concentrations were not measured in the epididymis and preputial gland at all sampling times. The highest peak concentrations occurred in the seminal vesicles and testis at 24 HPD and in the prostate at 96 HPD, respectively.

Radioactivity concentrations were present in esophagus, gastrointestinal tract tissues and the bladder wall at all three sampling times of 24, 48, and 96 HPD. The highest peak concentrations occurred in the cecum, esophagus, gastric mucosa, large intestines, small intestines, and stomach at 24 HPD and in the bladder wall at 48 HPD. There was no detection of radioactivity in urine within the urinary bladder.

Concentrations of compound-associated radioactivity were present in blood for all three sampling times of 24, 48, and 96 HPD. The highest blood concentration of compound-associated radioactivity occurred at 24 HPD with a concentration of 55.0 μg Eq/g. Blood concentrations of radioactivity declined at each subsequent sampling time with measurable concentrations of 34.3 μg Eq/g at 48 HPD and 29.5 μg Eq/g at 96 HPD. Blood:plasma concentration ratios were 2.31, 2.86, and 4.23 at 24, 48, and 96 HPD, respectively, suggesting that there was an apparent preferential uptake of [^{14}C]PPI-1011 associated radioactivity into the cellular components of blood following multiple dose administration.

In general, compound-associated radioactivity was detectable in all tissues, including CNS, after 15-consecutive daily oral doses, and radioactivity concentrations were substantially greater when compared to those tissues from male rats after a single oral dose. This QWBA study illustrated that all tissues accumulated and retained [^{14}C]PPI-1011 associated radioactivity after multiple doses.

DISCUSSION

We report herein the comprehensive pharmacokinetics and tissue distribution of synthetic plasmalogen precursor PPI-1011

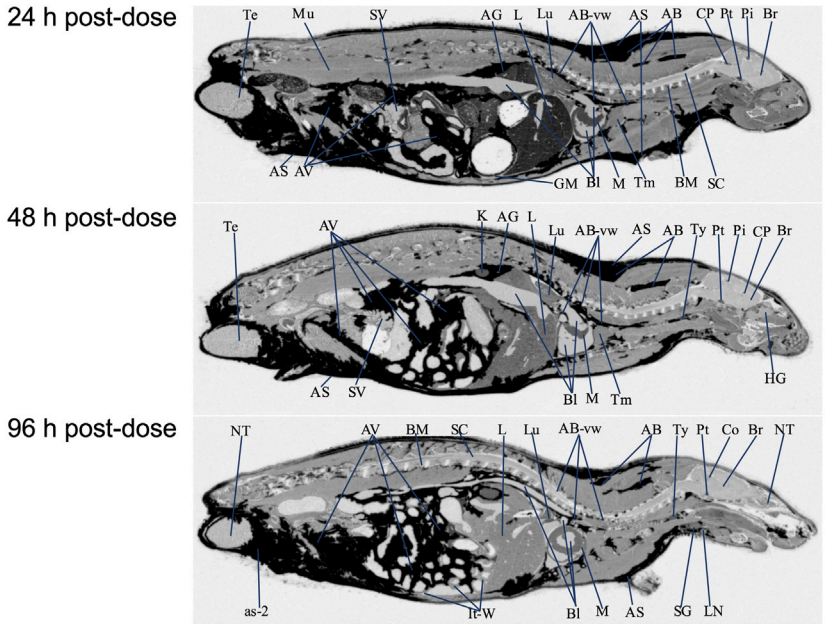

FIGURE 4 | Selected autoradiography images (24, 48, and 96 h post final dose) of tissue distribution of in the whole rat body after 15 daily oral doses at 100 mg/kg [^{14}C]PPI-1011. The abbreviations are: AB, adipose brown; AS, adipose subcutaneous; AV, adipose visceral; AB-vw, adipose brown:vessel wall; as-2, adipose-soaked: epididymis; AG, adrenal gland; Bl, blood; BM, bone marrow; Br, brain; Co, colliculus; CP, choroid plexus; GM, gastric mucosa; HG, harderian gland; It-W, intestinal tract wall; K, kidney; L, liver; LN, lymph node; Lu, lung; M, myocardium; Mu, muscle; NT, nasal tubinates; Pi, pineal gland; Pt, pituitary gland; SC, spinal cord; SG, salivary gland; SV, seminal vesicles; Te, testis; Tm thymus; Ty, thyroid.

following oral administration. Although previous research has addressed various aspects of the oral bioavailability, metabolism, and tissue incorporation of PPI-1011 *in vivo* (Wood et al., 2011b; Wood et al., 2011d; Gregoire et al., 2015; Miville-Godbout et al., 2016), the precise endogenous metabolic fate of PPI-1011 remained unknown. As far as we are aware, this is the first report of mass balance and tissue distribution using a radiolabeled orally-dosed plasmalogen precursor compound.

Pharmacokinetic analysis based on the single oral dose revealed key observations. First, the elimination half-life appears to be long, at approximately 40 h on average, but varied widely between 18 and 80 h. While there was a relatively high level of variation among the peak radioactivity levels between animals observed in the first 12 h, the overall PK profiles were similar. Furthermore, even at 72 h, radioactivity was still well above background. These observations match the previously reported time course of augmentation of the target 16:0/22:6 plasmalogen levels in rabbits following a single dose of PPI-1011, which peaked 12 h after a single dose and remained elevated at 48 h (Wood et al., 2011d).

The second key observation was that over half of the drug is retained and incorporated into the body following a single dose, matching historical estimates of uptake of other ether precursors (Das and Hajra, 1988). The vast majority of excretion of [^{14}C] PPI-1011 was observed within the first 48 h after administration, with the primary route of excretion being in feces and only small amounts (<2.5%) detectable in urine. What did surprise us was the approximately 10% radioactivity present in expired air. Although we only had the 24-h timepoint, expired radioactivity past 24 h would likely have been minimal given the plateau in the total cumulative percent of dose excreted, and the relatively steady tissue levels observed between 24 and 168 h. Given the location of the [^{14}C] label on the alpha carbon of the 16 carbon *sn*1 chain, the results suggest that the ether and/or vinyl-ether bond is cleaved, and the resulting fatty aldehyde/acid amenable to oxidation and release of radioactive CO_2. We expand on this point later in the discussion. Overall, the rapid uptake, long half-life, and high absorption are all highly desirable PK characteristics for a therapy that is intended to systemically replenish deficient levels of an endogenous metabolite. While this [^{14}C] data allowed for the first truly quantitative assessment of the PK characteristics of PPI-1011, it supports all of our previous work which has demonstrated that synthetic plasmalogens have good bioavailability (Wood et al., 2011d), tissue absorption (Wood et al., 2011a; Wood et al., 2011b; Fallatah et al., 2019), and plasmalogen augmentation (Fallatah et al., 2019; Miville-Godbout et al., 2017; Miville-Godbout et al., 2016; Gregoire et al., 2015, Wood et al., 2011e) *in vivo*. Further, we have previously demonstrated the pharmacodynamics of these compounds, which have been shown to result in behavioral (Gregoire et al., 2015; Bourque et al., 2018; Fallatah et al., 2019) and functional improvements within the cells (Wood et al., 2011a; Miville-Godbout et al., 2016; Miville-Godbout et al., 2017; Nadeau et al., 2019) of treated animals.

Although the elevation of plasmalogens in the circulation and tissues has been previously demonstrated following treatment with various supplements and precursors (including PPI-1011),

the assessment of tissue distribution has been at best restricted to crude assays of homogenized whole tissues samples from a few target tissues (Brites et al., 2011; Fujino et al., 2017; Yamashita et al., 2017; Fujino et al., 2020; Todt et al., 2020; Nguma et al., 2021; Paul et al., 2021). This has prevented a true understanding of how orally administered ethers and plasmalogens are distributed *in vivo*. Our QWBA results represent the first visualization of plasmalogen uptake and metabolism *in vivo* over time. Following a single oral administration, uptake of PPI-1011 was observed widely throughout the body, with the ocular lens and vitreous body being the only two tissues without measurable levels at 8 h post-dose. Tissue levels peaked in most tissues between 8 and 12 h following a single administration of [^{14}C]PPI-1011, mirroring the PK profile observed in plasma. Also, as observed in the PK study, significant radioactivity was still seen within tissues 7 days after a single dose, with only three tissues that had originally displayed [^{14}C]PPI-1011 associated radioactivity (bladder wall, bone surfaces, and seminal vesicles) no longer showing detectable radioactivity.

Following 15 consecutive daily doses, the relative tissue distribution pattern mirrored that of the single dose, albeit with much higher uptake across all tissues as well as detectable radioactivity in the ocular lens and vitreous body. As expected by the lipophilic nature of plasmalogens, high levels of radioactivity were observed in adipose tissue, including brown adipose, subcutaneous adipose, and visceral adipose. Except for the adrenal gland, preputial gland, and small intestines, which had similar concentrations, the average last measured radioactivity concentrations in the three adipose tissues were 5 to 56 -fold greater than for all other tissues. This suggests that adipose tissue may act as a reservoir for plasmalogens or alkyl diacylglycerols, which are then slowly released over time and re-distributed to other tissues in the body as required. Interestingly, adipose tissue has been shown to be abnormal in severely plasmalogen deficient mice, with decreased size and shape of the adipocytes. Treatment with alkylglycerol was able to normalize these differences in adipocytes, which corresponded with a normalization of body weight in the animals (Brites et al., 2011), suggesting a physiological function for plasmalogens within adipose tissue. The rapid and robust uptake of PPI-1011 into adipose tissue could be clinically beneficial, particularly as a treatment for RCDP where patients have serious challenges maintaining their body weight (Duker et al., 2017).

Although comparing relative image intensity between the single dose and multiple dose cross sections must be approached with caution, it is worth noting the significant increase in retained radioactivity at 24 h and beyond following multiple doses compared to the single dose (compare **Figure 3** to **Figure 4** at 24 h). Although the 24-h timepoint following 15 doses did show the highest overall level of radioactivity in most tissues, the mean percentage radioactivity (normalized by tissue) at 96 h was still 75% that of the 24-h timepoint. This suggests that under a daily dosing regimen, tissues continue to take up and incorporate the drug throughout the body, and that due to the long half-life, withdrawal of compound up to 96 h appears to have little effect on overall levels in the body. One area worthy of future investigation would be studies aimed at better characterizing the ADME of multiple sequential doses to optimize dosing strategies for ensuring maximum augmentation at the lowest required dose.

Of particular interest in this study was the evaluation of whether the labeled ether backbone or resulting plasmalogens are capable of crossing the blood-brain barrier and incorporating into brain tissue. A historical ^{13}C-labeled study suggested incorporation in a homogenized total brain sample (Wood et al., 2011b), but regional distribution in the brain of treated animals has never been possible due to analytical challenges. QWBA imaging allowed for a detailed evaluation of the distribution within the brain after single and repeated administration of [^{14}C]PPI-1011. In both the single-dose and repeat-dose QWBA studies, there were detectable radioactivity concentrations present in these CNS tissues at all sampling times, confirming that the [^{14}C]PPI-1011 ether backbone, and/or target plasmalogens, were able to cross the blood-brain barrier. Whole brain concentrations of total radioactivity were 4 to 6 -fold greater than the LLOQ of 0.485 µg Eq/g from 8 through 168 HPD, confirming uptake [^{14}C]PPI-1011 to the brain after a single dose. Although this uptake to non-circumventricular CNS tissues (cerebellum, cerebrum, colliculus, medulla oblongata, olfactory bulb, spinal cord, and thalamus) was relatively low compared to other tissues, uptake following 15 doses in the brain was on average 16–18 times higher than after the single dose, further proving that metabolized PPI-1011 can make it to the brain in a dose-dependent manner. Previous work in a plasmalogen-deficient mouse model demonstrated that with chronic administration of an alkylglycerol over months, there was a robust augmentation of plasmalogen levels in peripheral tissue and a small but detectable increase in levels within the brain (Brites et al., 2011). These observations, combined with slow turnover and what appears to be the body's ability to store reserves in adipose tissue, suggests that a daily dosing regimen over an extended period of time will result in plasmalogen augmentation in the CNS. Our work also suggests that minor changes in plasmalogen levels within the brain likely have a meaningful impact, with PPI-1011 demonstrating neuroprotective effects within the brain even when the difference in total plasmalogen levels did not reach statistical significance (Wood et al., 2011a; Miville-Godbout et al., 2016).

With respect to circumventricular tissues, the choroid plexus, pineal gland, and pituitary gland are CNS tissues that reside behind leaky junctions of the blood-brain barrier. Not surprisingly, concentrations of [^{14}C]PPI-1011 associated radioactivity were substantially higher in these three brain regions than those measured in the non-circumventricular CNS tissues. Seven days following a single dose of [^{14}C]PPI-1011, the average radioactivity concentration for choroid plexus, pineal gland, and pituitary gland was approximately 4-fold higher when compared with the average concentration for the non-circumventricular CNS tissues. This further supports that while the blood-brain barrier does partially impede the uptake of plasmalogen lipids, it does not prevent it.

Our study has a couple of limitations to address. First, the determination of various *in vivo* radiolabeled plasmalogen species originating from [^{14}C]PPI-1011 was not possible

within this study due to restrictions on processing radioactive samples. However, we have previously carried out numerous studies with PPI-1011 that have clearly demonstrated its ability to augment the entire *sn*1 16:0 plasmalogen pool (Gregoire et al., 2015; Miville-Godbout et al., 2016; Nadeau et al., 2019). In addition, we have previously evaluated the metabolic fate of the ether backbone *in vivo* and *in vitro* using a [^{13}C] labeled version of PPI-1011 (Wood et al., 2011b). This study clearly demonstrated that the ether bond remains intact following oral administration and that once absorbed, remodeling of the glycerol backbone is limited to the *sn*2 position. Further, a more recent study using a [^{13}C] labeled intact plasmalogen (PPI-1040) demonstrated that following absorption, rearrangement did not occur at the *sn*1 position (Fallatah et al., 2019). Additionally, loss of the *sn*3 phosphoethanolamine group was undetectable, suggesting that remodeling at the *sn*3 position is also minimal. However, we cannot exclude the possibility that the ether backbone is incorporated into non-ethanolamine glycerolipids. While it was outside of the scope of this study, we suggest the need for a future study using a [^{13}C] labeled version of PPI-1011 to evaluate the metabolic fate of the ether backbone in non-phosphoethanolamine lipids.

A second limitation was our assumption that at least the majority of radioactivity uptake, as measured, represented intact plasmalogen. Previous studies with PPI-1011 have demonstrated a rapid reacylation of the *sn*2 fatty acid, but that removal of the *sn*1 was limited (Wood et al., 2011b; Wood et al., 2011d). Other reports using radiolabeled 1-*O*-alkyl-sn-glycerols have also concluded that absorption occurs without cleavage of the ether bond (Bergstrom and Blomstrand, 1956; Das et al., 1992). Nevertheless, our studies clearly demonstrate a large uptake to adipose tissue, of which it is reasonable to assume that the lipid species would predominantly be in an alkyl-acyl-acyl form given that adipose is primary a triglyceride storage depot (Dawkins and Stevens, 1966). This is consistent with studies by Paltauf who used tritium-labeled I-*O*-octadecyl *sn*-glycerol to conclude preferential acylation of the labelled precursor to form alkyl diacyl glycerols, whose stearic configuration is that of naturally occurring alkyl glycerol lipids (Paltauf, 1971). Our interpretation, therefore, based on our results herein and all historical data available to date, is that the absorbed radioactivity is represented by either alkyl diacyl species or by 1-alkenyl (vinyl-ether) containing phosphoglycerolipids. We also know that from previous PK studies in various species, PPI-1011 effectively results in detectable increases in circulating plasmalogen levels within hours of oral administration, confirming a rapid conversion to the *sn*1 vinyl-ether bond (Wood et al., 2011d; Gregoire et al., 2015). Our previous data using a [^{13}C] radiolabeled vinyl-ether containing plasmalogen precursor, shows that the vinyl-ether is very stable endogenously, and that at least under normal physiological conditions, does not undergo rapid cleavage or rearrangement (Fallatah et al., 2019).

However, despite the historical evidence suggesting that the *sn*1 ether is maintained intact during absorption, we cannot disregard the expired radioactivity that we observed in this study. The only route by which this could occur would be through the fatty oxidation of the radiolabeled *sn*1 16:0 fatty acid. This would require cleavage of the ether, yielding an aldehyde that would likely undergo further oxidation to the acid by fatty aldehyde dehydrogenase (FALDH), followed by oxidation and subsequent release of the CO_2 during the Krebb's cycle. Alkylglycerol-mono-oxygenase (AGMO) has recently been reported to cleave alkylglyercols into a glyerol and fatty aldehyde (Tokuoka et al., 2013; Watschinger and Werner, 2013). AGMO is expressed primarily in the liver (Yu et al., 2019) making it likely that a small portion of the alkyl-acyl glycerol absorbed in the gastrointestinal tract following [^{14}C]PPI-1011 administration was broken down in the liver by AGMO following first pass metabolism, leading to the observed radioactive CO_2. Our PK results following a single oral dose showed that after 24 h, there was little further excretion in either the feces or urine. We would expect a similar observation for expired air, although the possibility that a small amount of radioactivity could have been expired post 24 h cannot be excluded. Our overall interpretation, therefore, is that relatively little of the compound-associated radioactivity would likely be due to the free 16:0 aldehyde following a cleavage event of the ether.

In summary, the results suggest that over half of the orally administered dose of PPI-1011 is retained by the body and that the ether backbone is well-absorbed in the gastrointestinal tract and redistributed throughout the body, including into CNS tissue. The long half-life (mean $T_{1/2}$ of 40 h) along with high uptake to the adipose tissue suggests that the adipose tissue might be acting as a reservoir from which the body can continue to pull alkyl-diacyl glycerols for further incorporation into plasmalogens. Overall, this supports the use of PPI-1011 as an oral formulation for the augmentation of plasmalogens in deficient individuals, including those with neurodegenerative diseases that display deficient plasmalogen levels within the brain.

DATA AVAILABILITY STATEMENT

The original contributions presented in the study are included in the article/**Supplementary Material**, further inquiries can be directed to the corresponding author.

ETHICS STATEMENT

The animal study was reviewed and approved by the Institutional Animal Care and Use Committee and Frontage Laboratories.

AUTHOR CONTRIBUTIONS

SR and TS conceived of the study, TS and KK designed and monitored the execution of the study, TS, KK, and SR performed the data analysis and interpretation. All authors contributed to the drafting of the article and approved the submitted version.

FUNDING

All studies were funded by Med-Life Discoveries LP.

ACKNOWLEDGMENTS

The authors would like to acknowledge Li Shen and Michael Potchoiba, and their teams at Frontage Laboratories, for the assistance in the planning and execution of the animal studies.

SUPPLEMENTARY MATERIAL

The Supplementary Material for this article can be found online at: https://www.frontiersin.org/articles/10.3389/fcell.2022.867138/full#supplementary-material

REFERENCES

Benarroch, E. E. (2011). Circumventricular Organs: Receptive and Homeostatic Functions and Clinical Implications. *Neurology* 77, 1198–1204. doi:10.1212/wnl.0b013e31822f04a0

Bergstrom, S., and Blomstrand, R. (1956). The Intestinal Absorption and Metabolism of Chimyl Alcohol in the Rat. *Acta Physiol. Scand.* 38, 166–172. doi:10.1111/j.1748-1716.1957.tb01380.x

Bourque, M., Grégoire, L., and DI Paolo, T. (2018). The Plasmalogen Precursor Analog PPI-1011 Reduces the Development of L-DOPA-Induced Dyskinesias in De Novo MPTP Monkeys. *Behav. Brain Res.* 337, 183–185. doi:10.1016/j.bbr.2017.09.023

Bozelli, J. C., and Epand, R. M. (2021). Plasmalogen Replacement Therapy. *Membranes (Basel)* 11. doi:10.3390/membranes11110838

Braverman, N., Steel, G., Obie, C., Moser, A., Moser, H., Gould, S. J., et al. (1997). Human PEX7 Encodes the Peroxisomal PTS2 Receptor and Is Responsible for Rhizomelic Chondrodysplasia Punctata. *Nat. Genet.* 15, 369–376. doi:10.1038/ng0497-369

Brites, P., Ferreira, A. S., Ferreira da Silva, T., Sousa, V. F., Malheiro, A. R., Duran, M., et al. (2011). Alkyl-glycerol Rescues Plasmalogen Levels and Pathology of Ether-Phospholipid Deficient Mice. *PLoS One* 6, e28539. doi:10.1371/journal.pone.0028539

Das, A. K., and Hajra, A. K. (1988). High Incorporation of Dietary 1-O-Heptadecyl Glycerol into Tissue Plasmalogens of Young Rats. *FEBS Lett.* 227, 187–190. doi:10.1016/0014-5793(88)80895-0

Das, A. K., Holmes, R. D., Wilson, G. N., and Hajra, A. K. (1992). Dietary Ether Lipid Incorporation into Tissue Plasmalogens of Humans and Rodents. *Lipids* 27, 401–405. doi:10.1007/bf02536379

Dawkins, M. J. R., and Stevens, J. F. (1966). Fatty Acid Composition of Triglycerides from Adipose Tissue. *Nature* 209, 1145–1146. doi:10.1038/2091145a0

Dorninger, F., Forss-Petter, S., and Berger, J. (2017a). From Peroxisomal Disorders to Common Neurodegenerative Diseases - the Role of Ether Phospholipids in the Nervous System. *FEBS Lett.* 591, 2761–2788. doi:10.1002/1873-3468.12788

Dorninger, F., Herbst, R., Kravic, B., Camurdanoglu, B. Z., Macinkovic, I., Zeitler, G., et al. (2017b). Reduced Muscle Strength in Ether Lipid-Deficient Mice Is Accompanied by Altered Development and Function of the Neuromuscular junction. *J. Neurochem.* 143, 569–583. doi:10.1111/jnc.14082

Dragonas, C., Bertsch, T., Sieber, C. C., and Brosche, T. (2009). Plasmalogens as a Marker of Elevated Systemic Oxidative Stress in Parkinson's Disease. *Clin. Chem. Lab. Med.* 47, 894–897. doi:10.1515/CCLM.2009.205

Duker, A. L., Niiler, T., Eldridge, G., Brereton, N. H., Braverman, N. E., and Bober, M. B. (2017). Growth Charts for Individuals with Rhizomelic Chondrodysplasia Punctata. *Am. J. Med. Genet.* 173, 108–113. doi:10.1002/ajmg.a.37961

Fabelo, N., Martín, V., Santpere, G., Marín, R., Torrent, L., Ferrer, I., et al. (2011). Severe Alterations in Lipid Composition of Frontal Cortex Lipid Rafts from Parkinson's Disease and Incidental Parkinson's Disease. *Mol. Med.* 17, 1107–1118. doi:10.2119/molmed.2011.00119

Fallatah, W., Smith, T., Cui, W., Jayasinghe, D., DI Pietro, E., Ritchie, S. A., et al. (2019). Oral Administration of a Synthetic Vinyl-Ether Plasmalogen Normalizes Open Field Activity in a Mouse Model of Rhizomelic Chondrodysplasia Punctata. *Dis. Model. Mech.* 13, dmm042499. doi:10.1242/dmm.042499

Fujino, T., Hossain, M. S., and Mawatari, S. (2020). "Therapeutic Efficacy of Plasmalogens for Alzheimer's Disease, Mild Cognitive Impairment, and Parkinson's Disease in Conjunction with a New Hypothesis for the Etiology of Alzheimer's Disease," in *Peroxisome Biology: Experimental Models, Peroxisomal Disorders and Neurological Diseases*. Editor G. LIZARD (Cham: Springer International Publishing).

Fujino, T., Yamada, T., Asada, T., Tsuboi, Y., Wakana, C., Mawatari, S., et al. (2017). Efficacy and Blood Plasmalogen Changes by Oral Administration of Plasmalogen in Patients with Mild Alzheimer's Disease and Mild Cognitive Impairment: A Multicenter, Randomized, Double-Blind, Placebo-Controlled Trial. *EBioMedicine* 17, 199–205. doi:10.1016/j.ebiom.2017.02.012

Gallego-García, A., Monera-Girona, A. J., Pajares-Martínez, E., Bastida-Martínez, E., Pérez-Castaño, R., Iniesta, A. A., et al. (2019). A Bacterial Light Response Reveals an Orphan Desaturase for Human Plasmalogen Synthesis. *Science* 366, 128–132.

Glaser, P. E., and Gross, R. W. (1994). Plasmenylethanolamine Facilitates Rapid Membrane Fusion: a Stopped-Flow Kinetic Investigation Correlating the Propensity of a Major Plasma Membrane Constituent to Adopt an HII Phase with its Ability to Promote Membrane Fusion. *Biochemistry* 33, 5805–5812. doi:10.1021/bi00185a019

Glaser, P. E., and Gross, R. W. (1995). Rapid Plasmenylethanolamine-Selective Fusion of Membrane Bilayers Catalyzed by an Isoform of Glyceraldehyde-3-Phosphate Dehydrogenase: Discrimination between Glycolytic and Fusogenic Roles of Individual Isoforms. *Biochemistry* 34, 12193–12203. doi:10.1021/bi00038a013

Goodenowe, D. B., Cook, L. L., Liu, J., Lu, Y., Jayasinghe, D. A., Ahiahonu, P. W. K., et al. (2007). Peripheral Ethanolamine Plasmalogen Deficiency: a Logical Causative Factor in Alzheimer's Disease and Dementia. *J. Lipid Res.* 48, 2485–2498. doi:10.1194/jlr.p700023-jlr200

Grégoire, L., Smith, T., Senanayake, V., Mochizuki, A., Miville-Godbout, E., Goodenowe, D., et al. (2015). Plasmalogen Precursor Analog Treatment Reduces Levodopa-Induced Dyskinesias in Parkinsonian Monkeys. *Behav. Brain Res.* 286, 328–337. doi:10.1016/j.bbr.2015.03.012

Han, X. (2005). Lipid Alterations in the Earliest Clinically Recognizable Stage of Alzheimers Disease: Implication of the Role of Lipids in the Pathogenesis of Alzheimers Disease. *Car* 2, 65–77. doi:10.2174/1567205052772786

Hermetter, A., Rainer, B., Ivessa, E., Kalb, E., Loidl, J., Roscher, A., et al. (1989). Influence of Plasmalogen Deficiency on Membrane Fluidity of Human Skin Fibroblasts: a Fluorescence Anisotropy Study. *Biochim. Biophys. Acta (Bba) - Biomembranes* 978, 151–157. doi:10.1016/0005-2736(89)90510-5

Jo, D. S., and Cho, D.-H. (2019). Peroxisomal Dysfunction in Neurodegenerative Diseases. *Arch. Pharm. Res.* 42, 393–406. doi:10.1007/s12272-019-01131-2

Kou, J., Kovacs, G. G., Höftberger, R., Kulik, W., Brodde, A., Forss-Petter, S., et al. (2011). Peroxisomal Alterations in Alzheimer's Disease. *Acta Neuropathol.* 122, 271–283. doi:10.1007/s00401-011-0836-9

Lohner, K., Balgavy, P., Hermetter, A., Paltauf, F., and Laggner, P. (1991). Stabilization of Non-bilayer Structures by the Etherlipid Ethanolamine Plasmalogen. *Biochim. Biophys. Acta (Bba) - Biomembranes* 1061, 132–140. doi:10.1016/0005-2736(91)90277-f

Lohner, K., Hermetter, A., and Paltauf, F. (1984). Phase Behavior of Ethanolamine Plasmalogen. *Chem. Phys. Lipids* 34, 163–170. doi:10.1016/0009-3084(84)90041-0

Mankidy, R., Ahiahonu, P. W., Ma, H., Jayasinghe, D., Ritchie, S. A., Khan, M. A., et al. (2010). Membrane Plasmalogen Composition and Cellular Cholesterol Regulation: a Structure Activity Study. *Lipids Health Dis.* 9, 62. doi:10.1186/1476-511x-9-62

Miville-Godbout, E., Bourque, M., Morissette, M., AL-Sweidi, S., Smith, T., Jayasinghe, D., et al. (2017). Plasmalogen Precursor Mitigates Striatal Dopamine Loss in MPTP Mice. *Brain Res.* 1674, 70–76. doi:10.1016/j.brainres.2017.08.020

Miville-Godbout, E., Bourque, M., Morissette, M., AL-Sweidi, S., Smith, T., Mochizuki, A., et al. (2016). Plasmalogen Augmentation Reverses Striatal Dopamine Loss in MPTP Mice. *PLoS One* 11, e0151020. doi:10.1371/journal.pone.0151020

Nadeau, J., Smith, T., Lamontagne-Proulx, J., Bourque, M., AL Sweidi, S., Jayasinghe, D., et al. (2019). Neuroprotection and Immunomodulation in the Gut of Parkinsonian Mice with a Plasmalogen Precursor. *Brain Res.* 1725, 146460. doi:10.1016/j.brainres.2019.146460

Nagan, N., and Zoeller, R. A. (2001). Plasmalogens: Biosynthesis and Functions. *Prog. Lipid Res.* 40, 199–229. doi:10.1016/s0163-7827(01)00003-0

Nguma, E., Yamashita, S., Han, K.-H., Otoki, Y., Yamamoto, A., Nakagawa, K., et al. (2021). Dietary Ethanolamine Plasmalogen Alleviates DSS-Induced Colitis by Enhancing Colon Mucosa Integrity, Antioxidative Stress, and Anti-inflammatory Responses via Increased Ethanolamine Plasmalogen Molecular Species: Protective Role of Vinyl Ether Linkages. *J. Agric. Food Chem.* 69, 13034–13044. doi:10.1021/acs.jafc.1c04420

Paltauf, F. (1971). Metabolism of the Enantiomeric 1-O-Alkyl Glycerol Ethers in the Rat Intestinal Mucosa *In Vivo*; Incorporation into 1-O-Alkyl and 1-O-Alk-1′-Enyl Glycerol Lipids. *Biochim. Biophys. Acta (Bba) - Lipids Lipid Metab.* 239, 38–46. doi:10.1016/0005-2760(71)90190-1

Paul, S., Rasmiena, A. A., Huynh, K., Smith, A. A. T., Mellett, N. A., Jandeleit-Dahm, K., et al. (2021). Oral Supplementation of an Alkylglycerol Mix Comprising Different Alkyl Chains Effectively Modulates Multiple Endogenous Plasmalogen Species in Mice. *Metabolites* 11. doi:10.3390/metabo11050299

Potchoiba, M. J., Tensfeldt, T. G., Nocerini, M. R., and Silber, B. M. (1995). A Novel Quantitative Method for Determining the Biodistribution of Radiolabeled Xenobiotics Using Whole-Body Cryosectioning and Autoradioluminography. *J. Pharmacol. Exp. Ther.* 272, 953–962.

Potchoiba, M. J., West, M., and Nocerini, M. R. (1998). Quantitative Comparison of Autoradioluminographic and Radiometric Tissue Distribution Studies Using Carbon-14 Labeled Xenobiotics. *Drug Metab. Dispos* 26, 272–277.

Rog, T., and Koivuniemi, A. (2016). The Biophysical Properties of Ethanolamine Plasmalogens Revealed by Atomistic Molecular Dynamics Simulations. *Biochim. Biophys. Acta (Bba) - Biomembranes* 1858, 97–103. doi:10.1016/j.bbamem.2015.10.023

Todt, H., Dorninger, F., Rothauer, P. J., Fischer, C. M., Schranz, M., Bruegger, B., et al. (2020). Oral Batyl Alcohol Supplementation Rescues Decreased Cardiac Conduction in Ether Phospholipid-deficient Mice. *Jrnl Inher Metab. Disea* 43, 1046–1055. doi:10.1002/jimd.12264

Tokuoka, S. M., Kita, Y., Shindou, H., and Shimizu, T. (2013). Alkylglycerol Monooxygenase as a Potential Modulator for PAF Synthesis in Macrophages. *Biochem. Biophysical Res. Commun.* 436, 306–312. doi:10.1016/j.bbrc.2013.05.099

Ullberg, S. (1977). The Technique of Whole Body Autoradiography. Cryosectioning Large Specimen. *Sci. Tools, LKB Instrument J.*, 2–28.

Wanders, R. J. A., Dekker, C., Hovarth, V. A. P., Schutgens, R. B. H., Tager, J. M., VAN Laer, P., et al. (1994). Human Alkyldihydroxyacetonephosphate Synthase Deficiency: a New Peroxisomal Disorder. *J. Inherit. Metab. Dis.* 17, 315–318. doi:10.1007/bf00711817

Wanders, R. J. A., Schumacher, H., Heikoop, J., Schutgens, R. B. H., and Tager, J. M. (1992). Human Dihydroxyacetonephosphate Acyltransferase Deficiency: a New Peroxisomal Disorder. *J. Inherit. Metab. Dis.* 15, 389–391. doi:10.1007/bf02435984

Watschinger, K., and Werner, E. R. (2013). Alkylglycerol Monooxygenase. *IUBMB Life* 65, 366–372. doi:10.1002/iub.1143

Werner, E. R., Keller, M. A., Sailer, S., Lackner, K., Koch, J., Hermann, M., et al. (2020). TheTMEM189gene Encodes Plasmanylethanolamine Desaturase Which Introduces the Characteristic Vinyl Ether Double Bond into Plasmalogens. *Proc. Natl. Acad. Sci. USA* 117, 7792–7798. doi:10.1073/pnas.1917461117

Wood, P. L., Khan, A. M., Mankidy, R., Smith, T., and Goodenowe, D. (2011a). "Plasmalogen Deficit: A New and Testable Hypothesis for the Etiology of Alzheimer's Disease," in *Alzheimer's Disease Pathogenesis-Core Concepts, Shifting Paradigms and Therapeutic Targets*. Editor S. DE LA MONTE (InTech).

Wood, P. L., Khan, M. A., Smith, T., Ehrmantraut, G., Jin, W., Cui, W., et al. (2011b). *In Vitro* and *In Vivo* Plasmalogen Replacement Evaluations in Rhizomelic Chrondrodysplasia Punctata and Pelizaeus-Merzbacher Disease Using PPI-1011, an Ether Lipid Plasmalogen Precursor. *Lipids Health Dis.* 10, 182. doi:10.1186/1476-511x-10-182

Wood, P. L., Khan, M., Smith, T., and Goodenowe, D. B. (2011c). Cellular Diamine Levels in Cancer Chemoprevention: Modulation by Ibuprofen and Membrane Plasmalogens. *Lipids Health Dis.* 10, 214. doi:10.1186/1476-511x-10-214

Wood, P. L., Smith, T., Lane, N., Khan, M. A., Ehrmantraut, G., and Goodenowe, D. B. (2011d). Oral Bioavailability of the Ether Lipid Plasmalogen Precursor, PPI-1011, in the Rabbit: a New Therapeutic Strategy for Alzheimer's Disease. *Lipids Health Dis.* 10, 227. doi:10.1186/1476-511x-10-227

Wood, P. L., Smith, T., Pelzer, L., and Goodenowe, D. B. (2011e). Targeted Metabolomic Analyses of Cellular Models of Pelizaeus-Merzbacher Disease Reveal Plasmalogen and Myo-Inositol Solute Carrier Dysfunction. *Lipids Health Dis.* 10, 102. doi:10.1186/1476-511x-10-102

Yamashita, S., Hashimoto, M., Haque, A. M., Nakagawa, K., Kinoshita, M., Shido, O., et al. (2017). Oral Administration of Ethanolamine Glycerophospholipid Containing a High Level of Plasmalogen Improves Memory Impairment in Amyloid β-Infused Rats. *Lipids* 52, 575–585. doi:10.1007/s11745-017-4260-3

Yu, H., Dilbaz, S., Coßmann, J., Hoang, A. C., Diedrich, V., Herwig, A., et al. (2019). Breast Milk Alkylglycerols Sustain Beige Adipocytes through Adipose Tissue Macrophages. *J. Clin. Invest.* 129, 2485–2499. doi:10.1172/jci125646

Conflict of Interest: TS, KK, and SR are paid employees of Med-Life Discoveries LP.

frontiers | Frontiers in Cell and Developmental Biology

REVIEW
published: 27 April 2022
doi: 10.3389/fcell.2022.864716

Tricky Isomers—The Evolution of Analytical Strategies to Characterize Plasmalogens and Plasmanyl Ether Lipids

Jakob Koch[1], *Katrin Watschinger*[2], *Ernst R. Werner*[2] *and Markus A. Keller*[1]*

[1]Institute of Human Genetics, Medical University of Innsbruck, Innsbruck, Austria, [2]Institute of Biological Chemistry, Biocenter, Medical University of Innsbruck, Innsbruck, Austria

Typically, glycerophospholipids are represented with two esterified fatty acids. However, by up to 20%, a significant proportion of this lipid class carries an ether-linked fatty alcohol side chain at the *sn*-1 position, generally referred to as ether lipids, which shape their specific physicochemical properties. Among those, plasmalogens represent a distinct subgroup characterized by an *sn*-1 vinyl-ether double bond. The total loss of ether lipids in severe peroxisomal defects such as rhizomelic chondrodysplasia punctata indicates their crucial contribution to diverse cellular functions. An aberrant ether lipid metabolism has also been reported in multifactorial conditions including Alzheimer's disease. Understanding the underlying pathological implications is hampered by the still unclear exact functional spectrum of ether lipids, especially in regard to the differentiation between the individual contributions of plasmalogens (plasmenyl lipids) and their non-vinyl-ether lipid (plasmanyl) counterparts. A primary reason for this is that exact identification and quantification of plasmalogens and other ether lipids poses a challenging and usually labor-intensive task. Diverse analytical methods for the detection of plasmalogens have been developed. Liquid chromatography–tandem mass spectrometry is increasingly used to resolve complex lipid mixtures, and with optimized parameters and specialized fragmentation strategies, discrimination between ethers and plasmalogens is feasible. In this review, we recapitulate historic and current methodologies for the recognition and quantification of these important lipids and will discuss developments in this field that can contribute to the characterization of plasmalogens in high structural detail.

Keywords: ether lipid biosynthesis, mass spectrometry, phospholipid analytics, PEDS1, plasmalogen physiology, plasmenyl and plasmanyl isomers

OPEN ACCESS

Edited by:
Masanori Honsho,
Kyushu University, Japan

Reviewed by:
Md Shamim Hossain,
Institute of Rheological Functions of Food, Japan
Matthieu Ruiz,
Université de Montréal, Canada

***Correspondence:**
Markus A. Keller
markus.keller@i-med.ac.at

Specialty section:
This article was submitted to Cellular Biochemistry, a section of the journal Frontiers in Cell and Developmental Biology

Received: *28 January 2022*
Accepted: *23 March 2022*
Published: *27 April 2022*

Citation:
Koch J, Watschinger K, Werner ER and Keller MA (2022) Tricky Isomers—The Evolution of Analytical Strategies to Characterize Plasmalogens and Plasmanyl Ether Lipids. Front. Cell Dev. Biol. 10:864716. doi: 10.3389/fcell.2022.864716

1 INTRODUCTION TO PLASMALOGENS AND OTHER ETHER LIPIDS

Many complex lipids are made up of simple lipid building blocks such as fatty acids. In the case of glycerophospholipids, these fatty acids are derivatized to a glycerol backbone as fatty acyl esters (**Figure 1A**). However, besides this esterification, other linkage types also exist that lead to structurally distinct subclasses of glycerophospholipids with divergent physicochemical properties and cellular functions. The so-called ether lipids carry ether-linked fatty alcohols instead of fatty acyls (**Figure 1A**). A well-known subgroup of ether lipids are plasmalogens,

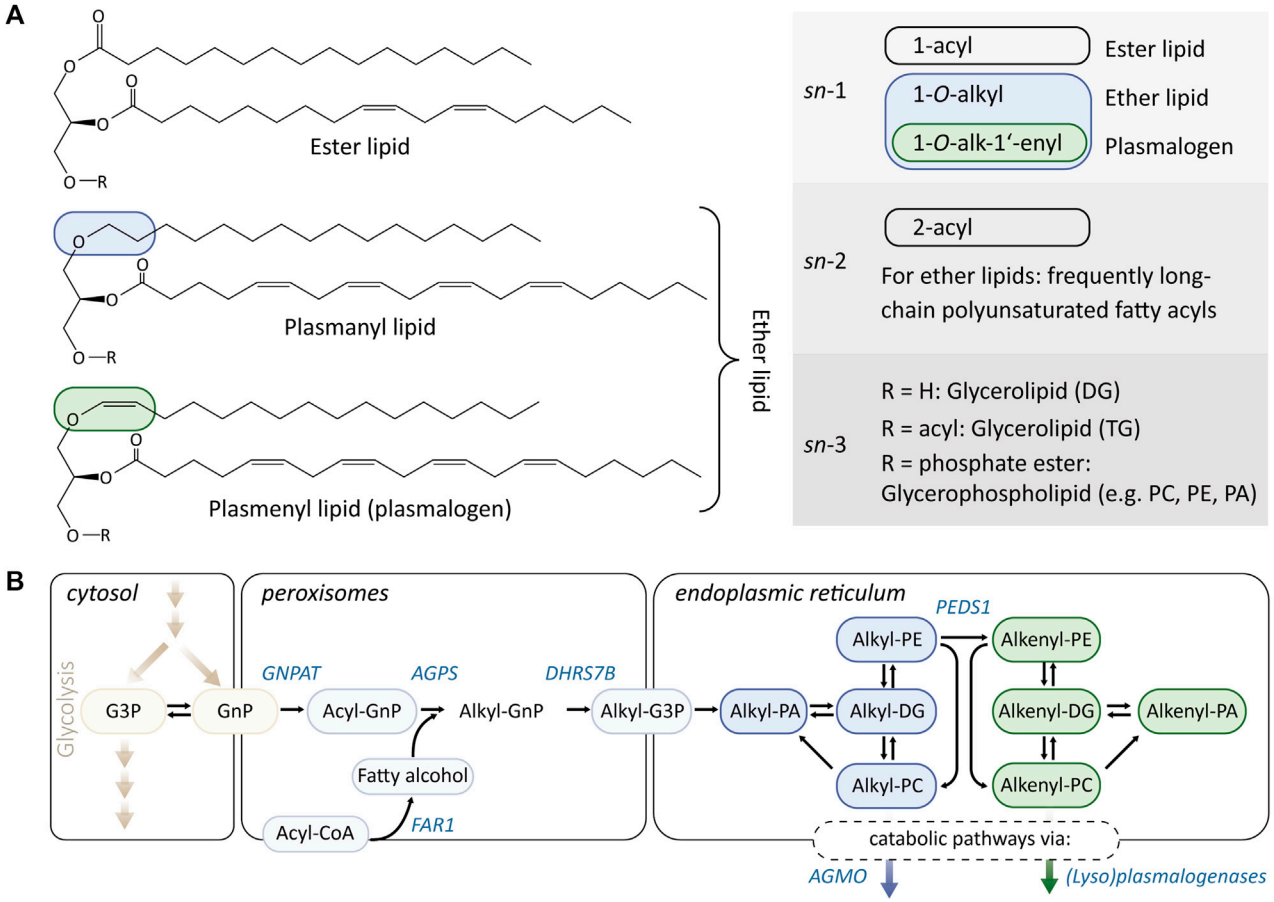

FIGURE 1 | (A) Overview of the chemical structures and unique features of diacyl (ester) lipids, and plasmanyl and plasmenyl lipids. Ether lipids comprise lipids that harbor both alkyl (1-*O*-alkyl, plasmanyl, indicated in blue) and alkenyl (1-*O*-alk-1′-enyl, plasmenyl, indicated in green) residues, while the latter is also referred to as plasmalogens. The alkyl/alkenyl residues of mammalian ether lipids are predominantly localized at the *sn*-1 position, while the *sn*-2 position is frequently substituted with polyunsaturated fatty acyls. Ether lipids belong for the most part to the lipid classes phosphatidylethanolamines (PEs), phosphatidylcholines (PCs), and 1-*O*-alkyl-2-acylglycerols (alkyl-DG). **(B)** Ether lipid metabolism. The initial steps of ether lipid biosynthesis take place in the peroxisomes and are based on substrates derived from glycolysis and fatty acid metabolism. The rate-determining step is the provision of fatty alcohols, which are formed from acyl-CoA by fatty acid reductase 1 (FAR1). Remodeling/interconversion pathways of ether lipids are partially shared with their ester lipid analogs. The enzyme plasmanylethanolamine desaturase (PEDS1) is responsible for converting plasmanyl lipids (blue) into their plasmenyl counterparts (green) and accepts PE as substrates. The catabolism of ether lipids proceeds from their lyso-forms and is catalyzed by alkylglycerol monooxygenase (AGMO; in the case of plasmanyl lipids) and (lyso)plasmalogenases (in the case of plasmenyl lipids).

which are characterized by a vinyl ether double bond (alkenyl) instead of an ether bond (alkyl). Consequently, every plasmalogen can be regarded as an ether lipid, while not every ether lipid is a plasmalogen.

1.1 Occurrence and Molecular Composition of Plasmanyl and Plasmenyl Lipids

In mammals, the ether bond of plasmalogens and other ether lipids is predominantly located at the *sn*-1 position of the glycerol backbone (Marinetti and Erbland, 1957; Rapport et al., 1957; Debuch, 1958), typically substituted with a saturated or mono-unsaturated alkyl/alkenyl residue, such as palmitoyl, stearyl, and oleyl alcohols (Debuch, 1958). In contrast, the fatty acyls of ether lipids, which are generally derivatized to the *sn*-2 position, are frequently long-chained (≥20) and polyunsaturated (Arthur et al., 1985). The exact fatty acyl composition strongly depends not only on the respective organisms (Vítová et al., 2021) but also follows a pronounced tissue-specificity (Koch et al., 2020). The main substituents at the *sn*-3 position of the glycerol backbone are ethanolamine and choline, generating ether-linked phosphatidylethanolamines (PEs) and phosphatidylcholines (PCs), respectively. However, ether lipid analogs to the neutral di- and triacylglycerides (DG and TG, respectively) exist, which have already been known for decades (Schmid et al., 1967; Snyder and Wood, 1968; Lin et al., 1977) and have recently been getting more and more attention (Schievano et al., 2013; Draijer et al., 2020; Meletis, 2020; Wang et al., 2020; Beyene et al., 2021). Additionally, the presence of small proportions of ether lipid species has also been described for other lipid classes (Ivanova et al., 2010).

Plasmalogens and ether lipids are abundant in animals across invertebrate and vertebrate species (Goldfine, 2010), where they can account for up to 20% of the phospholipid mass, depending on the respective tissues (Nagan and Zoeller, 2001; Braverman and Moser, 2012). Furthermore, plasmalogens are also present in many anaerobic bacteria (Řezanka et al., 2012) and archaea (Jain et al., 2014). However, these lipids typically do not occur in aerobic bacteria (Kamio et al., 1969), fungi (Horrocks and Sharma, 1982), and possibly plants (Felde and Spiteller, 1994).

1.2 Biosynthesis and Metabolism of Plasmanyl and Plasmenyl Lipids

As shown in **Figure 1B**, ether lipids are initially synthesized in peroxisomes (Wanders and Brites, 2010), where the glycolysis intermediate glycerone-phosphate [GnP; previously called dihydroxyacetone phosphate (DHAP)] is first acylated by glycerone-phosphate *O*-acyltransferase (GNPAT). This produces acyl-GnP (which is a precursor for both diacylglycerols and ether lipids) and is followed by replacement of the acyl group for a fatty alcohol by alkylglycerone-phosphate synthase (AGPS) (Nagan and Zoeller, 2001). The so-formed alkyl-GnP is then reduced by an alkylglycerone-phosphate reductase activity (encoded by DHRS7B; also acting on acylglycerone-phosphate) to 1-alkyl-glycero-*sn*-3-phosphate (alkyl-G3P) and exported from the peroxisomes. The availability of fatty alcohols is thought to be the rate-limiting factor in ether lipid and plasmalogen biosynthesis and is controlled by fatty acid reductase 1 and 2 (FAR1/2) (Cheng and Russell, 2004; Honsho et al., 2010; Ferdinandusse et al., 2021). A series of lipid metabolic enzymes that catalyze reactions at the *sn*-2 and *sn*-3 positions of glycerophospholipids are thought to also accept their ether lipid analogs as substrates and are responsible for generating the main ether lipid classes 1-*O*-alkyl-2-acyl-glycerol, alkyl-PE, and alkyl-PC. The formation of plasmalogens is catalyzed by the enzyme plasmanylethanolamine desaturase (PEDS1), which is capable of introducing the vinyl ether double bond at the Δ1 position of an alkyl-PE. Despite its central position in plasmalogen biosynthesis, the gene coding for PEDS1 has only recently been identified (Gallego-García et al., 2019; Werner et al., 2020; Wainberg et al., 2021). In contrast to the molecular oxygen requiring PEDS1, the anaerobic biosynthetic pathway of plasmalogens that has been characterized recently operates in an oxygen independent manner (Jackson et al., 2021). This is in line with the hypothesis that the capability of species to synthesize plasmalogens was once lost during evolution and only later reemerged in eukaryotes (Goldfine, 2010). Once formed, plasmalogens follow a different catabolism regime from other ether lipids. While the alkyl bond of ether lipids is cleaved by the tetrahydrobiopterin-dependent enzyme alkylglycerol monooxygenase (AGMO) (Watschinger et al., 2010), the removal of an alkenyl residue requires specialized (lyso)plasmalogenases (Warner and Lands, 1961; Jenkins et al., 2018). However, the plasmanyl and plasmenyl catabolic pathways both form fatty aldehydes that are toxic to cells if not readily oxidized by the enzyme fatty aldehyde dehydrogenase (FALDH) (Keller et al., 2014; Weustenfeld et al., 2019). Genetic impairment of FALDH function leads to the inherited metabolic disease Sjögren–Larsson Syndrome (SLS) (Weustenfeld et al., 2019), in which fatty aldehydes are interconverted into fatty alcohols, instead of fatty acids (Rizzo and Craft, 2000; Keller et al., 2012). This represents a FAR1-independent source of fatty alcohols that can induce the biosynthesis of ether lipids, which accumulate, for example, in the brain of SLS patients (Staps et al., 2020). Further significant crosstalk has been reported between ether lipid metabolism and other lipid classes such as cholesterol and sphingolipids, indicating that the metabolic routes shown in **Figure 1B** are additionally deeply rooted in the regulation of cellular phospholipid homeostasis (Braverman and Moser, 2012; Dean and Lodhi, 2018; Harayama and Riezman, 2018).

1.3 Physiological Roles of Plasmanyl and Plasmenyl Lipids

The full functional spectrum of plasmalogens and other ether lipids is still far from being comprehensively elucidated. However, it is clear that they are structural components of cellular membranes across a broad range of different tissues (Braverman and Moser, 2012) because ether lipids are found in the plasma membrane and in different subcellular compartments (Sun, 1973; Kuerschner et al., 2012). Due to their frequently polyunsaturated fatty acid (PUFA)-rich *sn*-2 side chains, they are considered to be an important reservoir for lipid second messenger precursors (Nagan and Zoeller, 2001). In previous research studies, particular attention has been paid to the specific properties of the vinyl ether bond of plasmalogens, which was demonstrated to be much more susceptible to oxidative cleavage than analog ester lipids (Broniec et al., 2011). Because of that, and due to their high PUFA content, plasmalogens are considered to be efficient membrane-localized antioxidants (Brites et al., 2004; Engelmann, 2004). More recently (however due to the same physicochemical properties), ether lipids have been implicated in the promotion of and robustness against ferroptosis (Zou et al., 2020). Some individual ether lipid species have been found to encompass highly specific functions. An important representative is certainly the platelet-activating factor (PAF), a 1-*O*-alkyl-2-acetyl-*sn*-glycero-3-phosphocholine which acts as a highly potent intracellular signaling molecule, that is involved in the regulation of many cellular processes [discovered in Demopoulos et al. (1979) and reviewed in Snyder (1999) and Lordan et al. (2019)]. Another example is the ether lipid seminolipid - besides sulfatide the only other major sulfoglycolipid - which is mainly synthesized in primary spermatocytes and essential for spermatogenesis (Goto-Inoue et al., 2009). A third important example are glycosylphosphatidylinositol (GPI) anchors that posttranslationally attach more than 250 different eukaryotic proteins to the surface of membranes (Paulick and Bertozzi, 2008). A neglected aspect in many functional studies on ether lipids is the clear differentiation between the potentially different

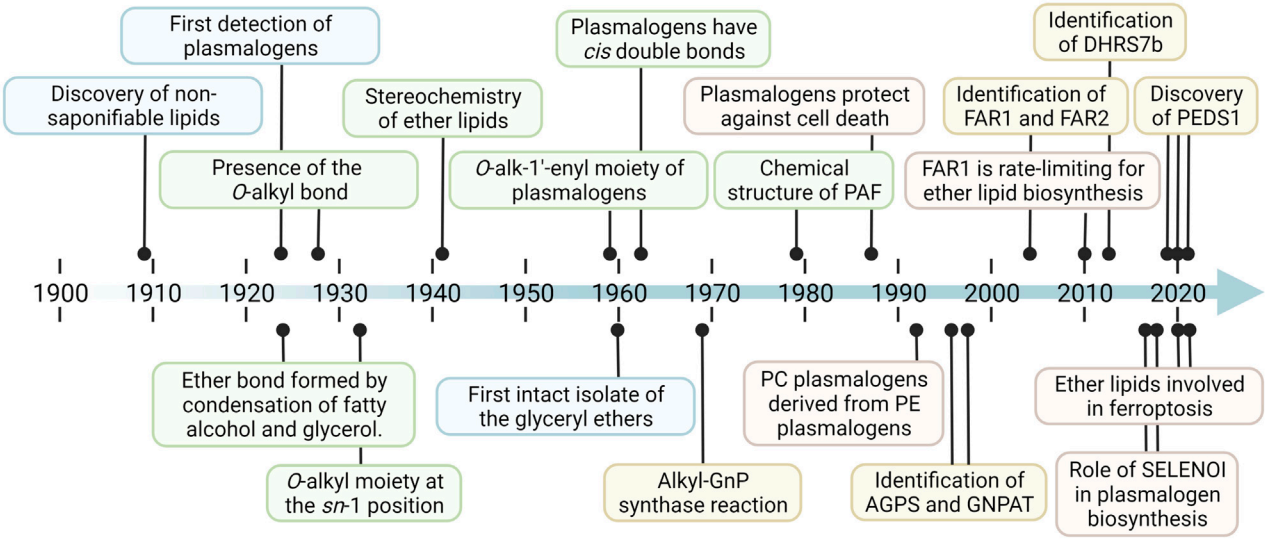

FIGURE 2 | Timeline of selected noteworthy discoveries and milestones in plasmalogen and ether lipid research. In the more than a hundred years since the first evidence for the existence of ether lipids was found, there have been groundbreaking results on a wide variety of conceptual levels. These include their 1) discovery (blue), 2) structural characterization (green), 3) enzymology and metabolism (yellow), and 4) function and physiological roles (red). Corresponding references and additional pioneering findings are listed in **Table 1**.

biological functional spectrum of plasmanyl and plasmenyl lipids (Jiménez-Rojo and Riezman, 2019).

2 THE ANALYTICAL CHALLENGE

Novel breakthroughs and findings in the field of plasmalogen and ether lipid research are strongly linked to the available analytical possibilities. An overview of respective developments throughout the last century is provided in the **Section 3**. In the past until today, reliable differentiation between plasmanyl and plasmenyl lipids represents a major analytical challenge that determines the pace of scientific progress. An important analytical principle that can be exploited for the quantification of ether lipids is that their alkyl and alkenyl residues are nonsaponifiable. Furthermore, the vinyl ether bond of plasmalogens—but not the ether bond of all other ether lipids—can be cleaved under acidic conditions, thereby yielding the respective fatty aldehydes (Werner et al., 2018). Subsequent derivatization of the released aldehydes allows for the quantification of plasmalogen levels; however, the disadvantage is that the presence of free fatty aldehydes, produced from other sources, can significantly distort the validity of the results. With measurement methods based on this principle, the concentrations of plasmanyl ether lipids remain completely obscure.

In recent years, the use of liquid chromatography–tandem mass spectrometry (LC-MS/MS) has become increasingly popular, also for ether lipid analytics. Despite the great possibilities this technology offers for characterizing complex lipid mixtures, ether lipids still remain a challenging class of analytes, as will be discussed in **Section 4**. Specifically, it is not possible to univocally differentiate between monounsaturated plasmanyl and saturated plasmenyl residues based on exact mass-to-charge ratios and fragment spectra alone (Koch et al., 2020). This challenge can be overcome by employing specialized instrumentation and techniques (**Section 3**, **4**). Another possibility is to exploit the differential chromatographic behavior of isobaric plasmanyl and plasmenyl lipids, which can, however, not always readily be integrated due to the lack of sufficiently complete sets of commercially available standards (Koch et al., 2020). One property that eases the analysis of molecular ether lipid species is that their structural variability is less diverse than that of other phospholipid classes (Keller, 2021) because at the *sn*-1 position only a limited set of relevant fatty alcohols is found (Cheng and Russell, 2004), while the *sn*-2 position is often occupied by polyunsaturated fatty acids (Arthur et al., 1985; Koch et al., 2020). A further aspect that represents a major challenge in the research of plasmalogens and other ether lipids is that our knowledge about the respective metabolic pathways for a long time (and partially still) showed substantial gaps because the genes of several important enzymes were not known. This rendered the establishment of suitable model systems very difficult.

3 HISTORY OF ETHER LIPID RESEARCH AND THE PROGRESS IN ETHER LIPID ANALYTICS

3.1 Discovery and Characterization of Ether Lipids

The first evidence for the existence of ether lipids was published in 1909, in which the presence of a nonsaponifiable lipid fraction in

TABLE 1 | Milestones in plasmalogen research [expanded on the basis of Snyder (1999)].

Year	Milestone	Citation
1909	Nonsaponifiable lipid isolates from starfish	Dorée (1909)
1924	Condensation of a long-chain fatty alcohol and glycerol forms an ether bond	Toyama (1924)
1924	First detection of plasmalogens	Feulgen and Voit (1924)
1928	Presence of an *O*-alkyl bond	Heilbron and Owens (1928)
1933	*O*-Alkyl moiety located at the *sn*-1 position	Davies et al. (1933)
1941	Stereochemistry of ether lipids	Baer and Fischer (1941)
1957	*O*-Alk-1′-enyl moiety of plasmalogens	Rapport et al. (1957); Debuch (1958)
1958	Presence of PE ether lipids in egg yolk	Carter et al. (1958)
1960	First intact isolate of the glyceryl ethers	Mangold and Malins (1960)
1960	Choline and ethanolamine phosphotransferases catalyze the transfer of CDP-choline and CDP-ethanolamine to *O*-alk-1′-enyl-acylglycerols	Kiyasu and Kennedy (1960)
1961	Isolation of ether lipids from bovine erythrocytes	Hanahan and Watts (1961)
1962	*cis*-nature of plasmalogen double bond	Norton et al. (1962); Warner and Lands (1963)
1963	Double bond position in the *O*-alkyl chain of selachyl alcohol at carbons 9 and 10	Hanahan et al. (1963)
1969	Cell-free synthesis of *O*-alkyl bond	Snyder et al. (1969)
1969	Alkyl-DHAP synthase forms ether lipids from glycerone-phosphate and a fatty alcohol	Hajra (1969); Wykle and Snyder (1969)
1979	Discovery of the chemical structure of platelet-activating factor (PAF)	Benveniste et al. (1979); Blank et al. (1979); Demopoulos et al. (1979)
1985	Plasmalogens are the major phospholipid constituent of the cardiac sarcoplasmic reticulum	Gross (1985)
1988	Plasmalogen bond protects against cell death	Zoeller et al. (1988)
1993	Choline plasmalogens are mainly derived from the ethanolamine plasmalogens	Blank et al. (1993)
1997	Identification of *AGPS*	de Vet et al. (1997)
1997/1998	Identification of *GNPAT*	Thai et al. (1997); Ofman et al. (1998)
2004	Identification of *FAR1* and *FAR2*	Cheng and Russell (2004)
2010	FAR1 is the rate-limiting enzyme in ether lipid biosynthesis	Honsho et al. (2010)
2012	Identification of *DHRS7b*	Lodhi et al. (2012)
2017	Identification of *EPT1* (*SELENOI*)	Ahmed et al. (2017)
2018	Role of *SELENOI* for plasmalogen biosynthesis	Horibata et al. (2018)
2019/2021	Identification of *PEDS1*	Gallego-García et al. (2019); Werner et al. (2020); Wainberg et al. (2021)
2020/2021	Role of ether lipids in ferroptosis	Zou et al. (2020); Cui et al. (2021)
2021	Plasmalogen synthase in anaerobic bacteria	Jackson et al. (2021)

isolates from starfish was established (Dorée, 1909). In the more than 100 years that followed, a whole series of breakthroughs led to our current understanding of ether lipids and plasmalogens, a selection of which is represented in **Figure 2** (for references, **Table 1**). Fred Snyder, without a doubt one of the most central figures in the advancement of the field, provided a detailed personal and historical perspective on many of these developments up to the turn of the millennium (Snyder, 1999). Until the 1970s, a majority of the research activities relating to plasmalogens focused on the elucidation of their fundamental structure and composition. Later on, important further discoveries were made, such as solving the exact chemical structure of the platelet-activating factor (PAF) in 1979 (Benveniste et al., 1979; Blank et al., 1979; Demopoulos et al., 1979). In parallel, but especially starting from the late 1950s, increasing attention was paid to the natural occurrence of ether lipids and plasmalogens in a wide variety of species, tissues, and other diverse biological sources (Carter et al., 1958; Hanahan and Watts, 1961; Gross, 1985). The growing understanding of plasmalogens and ether lipids triggered an era of research on their metabolism, biochemistry, and biological functions. The first signs of this change in research focus appeared in the 1960s (Kiyasu and Kennedy, 1960; Wykle and Snyder, 1969; Zoeller et al., 1988; Blank et al., 1993), a strong intensification of efforts was especially noticeable from the late 1980s onward. However, many research questions still remain unanswered, particularly regarding the enzymology of the metabolic network related to ether lipids and plasmalogens. Surprisingly, for a long time, it was not possible to identify the genes for many of the enzymes involved in their metabolism, even after the human genome had been deciphered. For example, only recently the genes coding for important functions such as the catabolism of plasmalogens (Wu et al., 2011), the *sn*-1 cleavage of plasmanyl lipids (Watschinger et al., 2010), and the core enzyme responsible for plasmalogen biosynthesis were identified (Gallego-García et al., 2019; Werner et al., 2020; Wainberg et al., 2021). In ether lipid metabolism other orphan enzymes might be present, but it is unclear so far whether the respective ester metabolizing enzymes that are already known also accept the ether analogs as substrates.

3.2 The Role of Novel Analytical Techniques

A major driving force behind the scientific progress in ether lipid and plasmalogen research was (and is) the different accessible analytical technologies. Importantly, the analytical tools available at the respective time also had a decisive influence on the trajectory of the research activities (and *vice versa*). Several methods for quantifying plasmalogen concentrations rely on the cleavage of the vinyl ether double bond in the presence of an acid, and the detection of the liberated aldehyde, frequently as

an acetal or hydrazone derivative (**Figure 2** and **Table 1**). While the special reactivity of plasmalogens increases their specificity, information on the remaining structure of the molecule, that is, the residues at *sn*-2 and *sn*-3 of the glycerolipids, is lost. In addition, proper controls need to be included to subtract the amounts of free aldehydes present in the sample before acidic liberation of the aldehyde at *sn*-1. This can be done by using hydrochloric acid to cleave the vinyl ether double bond and running an additional reaction with acetic acid instead of hydrochloric acid in parallel, which leaves the vinyl double bond intact and therefore represents the free aldehyde content only (Werner et al., 2018). However, in the selected mouse tissues investigated so far, the amount of free aldehydes was always below 1% as compared to the amount of plasmalogens (Werner et al., 2018). An additional drawback of these methods is that they fail to quantify ether lipids without the vinyl ether double bond, that is, plasmanyl lipids.

Already the very first detection of plasmalogens in 1924 relied on such a reaction, the formation of an adduct of aldehydes liberated from plasmalogens with fuchsin in sulfuric acid (Feulgen and Voit, 1924). A related procedure allowed high-throughput screening for bacterial colonies lacking plasmalogen formation in the search for genes responsible for plasmalogen formation in anaerobic bacteria (Jackson et al., 2021). The formation of dimethyl acetals by cleavage in acidic methanol (Gray, 1969) is still frequently used to quantify plasmalogens by gas chromatography–mass spectrometry (GC-MS) and liquid chromatography–mass spectrometry (LC-MS) methods (Ingrand et al., 2000; Moraitou et al., 2008; Brites et al., 2009; Bueno et al., 2012; Gallego-García et al., 2019). Other methods used 2, 4-dinitrophenyl hydrazine and thin layer chromatography (Rhee et al., 1967), or staining of thin-layer chromatograms with 4-amino-5-hydrazino-1,2,4-triazole-3-thiol sprays (Rahn and Schlenk, 1973). Derivatization with (pentafluorobenzyl) hydroxylamine hydrochloride allowed analysis using GC-MS (Ingrand et al., 2000). We developed a method to measure plasmalogens using dansylhydrazine as a derivatization agent and reversed-phase HPLC with fluorescence detection for quantification (Werner et al., 2018). This method was essential for independent measurement of total plasmalogen in mice deficient in PEDS1 (Werner et al., 2020), enabling the validation of LC-MS methods for the unequivocal discrimination between plasmanyl and plasmenyl lipids (Koch et al., 2020; Werner et al., 2020).

Besides the aforementioned thin layer chromatographic techniques with varying detection reagents and principles for the semi-quantitative analysis of ether lipids and plasmalogens (Schmid et al., 1975; Shantha and Napolitano, 1998), and other chromatographic approaches (Christie and Han, 2012), a diversity of analytical approaches has been developed (Messias et al., 2018). A series of assays based on radiolabeled substrates have been established, often to study the respective metabolic pathway structures and enzymology in a targeted manner (Paltauf, 1972; Wykle et al., 1972; Blank and Snyder, 1992). Furthermore, also ^{1}H, ^{13}C, and especially ^{31}P nuclear magnetic resonance (NMR) approaches have been employed to quantify PC and PE plasmalogens on the basis of the characteristic chemical shifts that vinyl ether double bonds cause (Meneses and Glonek, 1988; Sacchi et al., 1995), a technology that provides new scientific insights (Kimura et al., 2018; Bozelli et al., 2020). A major disadvantage of many of these methods, is that only little or no information about the respective molecular species, especially the chemical structure of their side chains, is extractable. In addition, the methods used often either do not allow a clear distinction between plasmalogens and other ether lipids or can solely quantify plasmalogens. Overcoming this often requires a laborious combination of different methods, such as the saponification of previously extracted and pre-separated ether lipids followed by GC-MS analysis of the fatty acids released (Maulik et al., 1993). For this reason, the analysis of ether lipids by means of LC-MS/MS is increasingly pursued in light of the rapidly improving instrumental performance in the field of mass spectrometry. LC-MS/MS-based approaches are highly attractive due to the abundance of extractable information, but of course, they come along with their specific challenges and problems, especially in regard to the reliable identification of plasmanyl and plasmenyl species, which are summarized in **Section 4**.

3.3 Implications for the Pathophysiological Knowledge About Ether Lipids

These and other conceptual and technical advances have of course had a major impact on our understanding of the role of plasmanyl and plasmenyl lipids in health and disease. A detailed summary would go far beyond the scope of this work and is already part of excellent reviews such as Braverman and Moser (2012) and Dean and Lodhi (2018). The functional involvement of ether lipids has been discussed in many pathologies. These include inherited peroxisomal disorders, often caused by mutations in one of the 14 different *peroxin* (*PEX*) genes (Berger et al., 2016) that lead to different manifestations of the Zellweger syndrome, as well as in the case of *PEX7* to rhizomelic chondrodysplasia punctata (RCDP) (Waterham and Ebberink, 2012). Additionally, reduced plasmalogen levels have been associated with neurodegenerative diseases such as Alzheimer's disease (Dorninger et al., 2020) and are discussed as a potential treatment target (Fujino et al., 2017). Furthermore, plasmalogens were recognized for their protective role against oxidative stress (Zoeller et al., 1988) and have been shown to inhibit apoptosis (Yamashita et al., 2015). However, this behavior has been reported to be cell-type specific, as plasmalogens play an important role in the apoptotic behavior of mouse neuroblastoma-derived cells but not in astrocyte-derived cells (Hossain et al., 2013).

4 MASS SPECTROMETRY-BASED ETHER LIPID ANALYSIS

Historically, characterizing the composition of alkyl and alkenyl lipids with reliable molecular subspecies resolution has been a highly laborious and tedious task, as detailed in the previous

section. With the advent of omics technologies and related bioinformatics capabilities, each of which is entangled with the developments in mass spectrometry (MS) instrumentation, the discriminative power and data quality were propelled forward. This is also related to the generation of large, information-rich data sets, where reliable data analysis strategies play a crucial role in systematically deciphering complex lipid compositions. There are a broad range of possibilities and different setups, where MS is used as the core detection principle for the quantification of plasmalogens and other ether lipids. Vítová et al. have recently provided a comprehensive overview on plasmalogen analysis methods and how they are used to study these lipids in various species (Vítová et al., 2021). There are both targeted and untargeted mass spectrometric approaches, and both have their specific advantages and disadvantages in terms of reliability, reproducibility, and information content. These are based on either direct infusion (shotgun) lipidomics (Han and Gross, 2005; Surma et al., 2021) or mass spectrometric detection after different types of pre-separation, including gas or liquid chromatography (Mawatari et al., 2007; Fauland et al., 2011; Lísa et al., 2017), capillary electrophoresis (Zhang et al., 2017; Ly et al., 2021), ion mobility separation (Vasilopoulou et al., 2020; Kirkwood et al., 2022), and supercritical fluid chromatography (Lísa et al., 2017; Schoeny et al., 2020). In this section, we will focus on how to tackle the analytical challenge to discriminate between plasmanyl and plasmenyl lipids. This differentiation is of great importance as introduction of a vinyl ether double bond in ether lipids severely alters the physicochemical properties of the molecule (e.g., its oxidizability) and therefore defines the respective functional roles.

4.1 Ether Lipid Identification by Mass Spectrometry

In general, a distinction must be made between high-resolution mass spectrometers, where the instrument can determine masses with an accuracy of as low as 0.1 mDa in relation to the exact mass, and low-resolution mass spectrometers that are only accurate to approximately 1 Da (Wallace and McCord, 2020, 254). In the molecular context of lipids, this implies that distinguishing between isobaric lipids such as the pair PE P-36:2 (plasmenyl) and PE 35:3 with respective mass-to-charge ratios (m/z) of 726.5443 and 726.5079 m/z in electrospray ionization (ESI) negative mode is possible only with high-resolution instruments, while the isomeric counterpart PE O-36:3 (plasmanyl, 726.5443 m/z) cannot be readily differentiated from PE P-36:2 even with highest resolution instruments (Keller, 2021). A further challenge is that such non-resolvable mass overlaps also occur between pairs of lipid species with a nominal mass difference of 2 m/z, as is the case for plasmenyl and plasmanyl species with identical side-chain substitution; that is, the M+2 isotopologue of a plasmenyl species interferes with the M+0 peak of the corresponding plasmanyl lipid (type-II isotopic effect) (Höring et al., 2021). This effect is particularly important when significantly larger amounts of plasmenyl species are present, which is often the case with PE ether lipids (Koch et al., 2020). In addition, the possible distortion due to mass overlaps scales with increasing numbers of non-most abundant (natural) isotopes contained within a lipid, which are responsible for changing isotopic intensity distributions (type-I isotopic effect) (Han and Gross, 2001). In other words, with increasing numbers of, for example, carbon atoms, the natural isotope prevalence causes changes in the isotopic distribution from (M+0) to (M+1) and higher isotopes, thus increasing the problem of interference due to signal interference. A type-II isotopic effect, if lipids differ by one double bond, can be (at least theoretically) circumvented when reaching very high mass resolutions (R > 200,000 for PE O-36:2/PE P-36:2); however, a correction using suitable deconvolution approaches during data analysis is possible. In contrast, this is not the case for the aforementioned overlap between isomers, which can only be resolved through combination with additional complementary analytical techniques.

4.2 Mass Spectrometry-Based Fragmentation and Derivatization Approaches

Several powerful possibilities to discriminate between plasmanyl and plasmenyl lipids arise from the fragmentation capabilities that many mass spectrometers provide. However, pure MS/MS fragment spectra in the negative ESI mode are not sufficient to achieve a clear assignment of plasmalogens and other ether lipids (Koch et al., 2020). A more advanced approach is the generation of unique fragmentation signatures obtained via repeated collision dissociations of lithiated ether lipid precursor ions in positive ESI mode [$(M + Li)^+$, $(M-H + 2Li)^+$, and $(M-2H + 3Li)^+$] (Hsu and Turk, 2008) restricted to mainly PE and PC, while in negative mode distinction for all major glycerophospholipid classes can be achieved by multistage fragmentation (Hsu and Turk, 2007; Hsu et al., 2014). However, those approaches are limited to mass spectrometers with MS^n ($n > 2$), and therefore intrinsically limited in their applicability (Hsu and Turk, 2008). In another method, silver ion adducts of phosphatidylethanolamine plasmalogens enabled their detection *via* neutral loss scans in the positive ESI mode. In the presence of Ag+ ions, a characteristic neutral loss of 141 Da is also predominantly observed for plasmenylethanolamines, and quantification is enabled by differential analysis (Kim et al., 2012). A further possible workflow includes the combination of ozone-induced dissociation (OzID) in the MS^1 dimension with additional collision-induced dissociation (CID) fragment spectra (MS^2) acquired in direct infusion (shotgun) workflows boosting lipidome coverage via a higher number of duty cycles (Deeley et al., 2009; Marshall et al., 2019). Depending on the combinations of CID and OzID, the *sn* position of each fatty acyl (FA) (CID/OzID), the double bond positions in the *sn*-1 FA (CID/$OzID^2$), and a full characterization (all double bond positions and chain lengths of *sn*-1 and *sn*-2 FA) are possible with $(CID/OzID)^2$ (Pham et al., 2014).

Also, derivatization strategies, for example, with iodine/methanol derivatized plasmenyl lipids, enable the differentiation between plasmanyl and plasmenyl species, and in combination with $^{13}C_1$–*S*, *S*′-dimethylthiobutanoyl-*N*-hydroxysuccinimide ester derivatization of aminophospholipids, this method can also resolve

type-I isotopic effects (Fhaner et al., 2013). Quite recently, a new application was published where the acquisition of fragmentation spectra at three different higher collision energy settings allowed an established computational model to correct and deconvolute different isobaric and isomeric features with different structural compositions (Schuhmann et al., 2019). Theoretically, this approach could also be able to distinguish between plasmanyl and plasmenyl lipids, but this was not discussed by the authors. A general discussion of the various derivatization strategies applied for MS-coupled lipidomics can be found in Hu et al. (2019). Furthermore, when primarily focusing on the quantification of plasmalogens, a distinct fragmentation behavior of plasmenyl PE lipids in the positive ESI mode can be exploited for their structure-specific quantification (Tsugawa et al., 2020; Morel et al., 2021).

4.3 Exploiting Different Chromatographic Properties of Plasmanyl and Plasmenyl Lipids

In addition, but also as an alternative to more complex MS^n methods, the combination of MS with chromatographic separation methods can in principle be used for the discrimination of plasmanyl and plasmenyl lipids. Generally, normal phase chromatography and hydrophilic interaction liquid chromatography (HILIC) separate lipids in a lipid class-dependent manner, while in reversed-phase chromatography a lipid species-specific separation behavior is facilitated. Both principles are widely applied in lipidomic studies as described by Harrieder et al. (2022), while promising methods utilizing supercritical fluid chromatography for separation are under development (Wolrab et al., 2020; Le Faouder et al., 2021) that should enable class-wise separation of plasmanyl and plasmenyl lipid species, which in comparison with strategies refined for DI methods (necessary to correct for type-II isotopic effects) should allow high-throughput lipidomics with plasmalogen resolution on a whole lipidome scale.

A major limiting factor for the systematic characterization of the separation properties of plasmalogens and other ether lipids is the lack of commercially available standards in sufficient numbers and variety. Pairs of plasmanyl/plasmenyl species rarely occur together in the same sample, precluding mutual relative referencing (Koch et al., 2020). However, with the help of a plasmalogen-deficient mouse model (Werner et al., 2020), it was possible to comprehensively describe that reversed-phase gradients allow for distinguishing between plasmanyl and plasmenyl lipids by a characteristic retention time offset (Koch et al., 2020). Furthermore, this retention time behavior is systematic (in addition to the contributions of double bond content and carbon atom number within fatty acyl side chains) and allows for building predictive models for the retention time behavior of plasmanyl and plasmenyl lipids in a lipid class-wise manner (Vaňková et al., 2022). This allows the challenging mass spectrometric problem of deconvoluting isomeric and isobaric ether lipids to be transformed into a much easier solvable chromatographic and data analysis issue. Even type-II isotopic effects can be readily resolved with baseline separation (Lange and Fedorova, 2020; Vaňková et al., 2022). This principle is also implemented in several targeted multiple reaction monitoring (MRM) and selective reaction monitoring (SRM) assays (Benjamin et al., 2013; Lee et al., 2021), which can be expanded and improved with an increasing variety of commercial standards. In contrast, in HILIC-based methods, the respective lipid class-wise elution behavior (Buré et al., 2013) reduces the potential to separate plasmanyl and plasmenyl species, although they elute prior to the diacyl lipids (Otoki et al., 2017). With such a separation method entirely focusing on the goal to distinguish plasmalogens, it is possible to achieve a clear separation also with HILIC; however, simultaneously there is a tradeoff in respect to the applicability of the method to characterize the general lipidome (Morel et al., 2021), which diminishes general feasibility of HILIC for detailed lipidomics (Lange and Fedorova, 2020).

4.4 Correctly Reporting the Level of Structural Identification

Different identification and quantification strategies for the analysis of plasmalogens and other ether lipids result from the current set of utilized LC-MS/MS-based approaches. Since, as discussed earlier, a differentiation between plasmanyl and plasmenyl species cannot be automatically assumed, this must be taken into account for both identification and lipid species nomenclature. When following good practice rules (Köfeler et al., 2021), it is clearly important to consider the level at which identifications take place, which in turn should be reflected in the name of the lipids (Liebisch et al., 2013, 2020). Depending on how conscientiously this is implemented, this leads to lipidomic studies in which a clear assignment of plasmalogens and other ether lipids 1) is not regarded at all, 2) is based on educated guesses, 3) is honestly reflecting the level of identification, or 4) is explicitly executed with one of the approaches detailed previously. Many general lipidomic studies that are based on reversed-phase HPLC separation do not (yet) distinguish between plasmanyl and plasmenyl lipids. Thus, it is advisable to fully utilize the existing analytical potential of untargeted LC-MS/MS-based lipidomics approaches, as already in standard workflows the combined information of exact masses, fragmentation behavior, and a well-characterized retention time behavior would be sufficient to correctly assign the otherwise tricky plasmanyl and plasmenyl isomers.

5 FUTURE PERSPECTIVES

PE, PC, and DG are the main lipid classes for which ether lipid and plasmalogen analogs have been described and are currently studied. However, ether-linked lipid species have also been found in a range of different other lipid classes, including phosphatidylinositol, phosphatidic acid, phosphatidylserine, and phosphatidylthreonines (Ivanova et al., 2010). Although these occur in comparatively small amounts, they must still be taken into account as part of the lipidome. However, since commercially available standards are already limited for the main lipid classes, this problem is even more pronounced for rarer ether lipid variants.

Likewise, much of the current research focus related to plasmalogens and other ether lipids relies on a relatively small subset of model organisms. Nevertheless, it has been shown that ether lipids can be much more complex in other organisms such as archaea (Albers et al., 2000; Pineda De Castro et al., 2016; Vítová et al., 2021). For example, while in mammals it can be assumed by default that the ether bond is located at the *sn*-1 position, this is far from set in stone in other species (Grossi et al., 2015) and can also become relevant in the analysis of plasmalogens in food (Yamashita et al., 2016). This circumstance must be explicitly taken into account in ether lipid and plasmalogen analytics.

Plasmanyl and plasmenyl ether lipids are increasingly being associated with diseases other than specific inherited metabolic diseases involving peroxisomes (Ferreira et al., 2021). In addition to Alzheimer's (Han et al., 2001; Igarashi et al., 2011; Kling et al., 2020), Down syndrome (Murphy et al., 2000), and Parkinson's disease (Dragonas et al., 2009), these also include abnormalities in the plasma of colorectal cancer patients (Liu et al., 2020). However, the use of plasmalogens as early diagnostic biomarkers places particularly strict demands on the performance of the analytical approaches used.

From the point of view of ether lipid and plasmalogen analytics, there are a number of important measures that should be taken in light of these developments. 1) Above all, it is important that the research field focuses on truthfully reporting the exact structural level of analysis of ether lipids, which should also be reflected in the respectively used lipid nomenclature (Liebisch et al., 2013, 2020) and thereby render them compatible with unified computational naming approaches like Goslin (Kopczynski et al., 2020). This aspect should not only be implemented "in-house" but also urged for, for example, in reviewing activities. 2) A further step is to utilize the structural information that is already available in the raw data more comprehensively, to differentiate between plasmanyl and plasmenyl lipids whenever applicable. 3) With increasing demand, it would be a welcome development if a greater diversity of commercial ether lipid and plasmalogen standard substances becomes available. In this regard, the recent identification of the gene that encodes for a key enzyme in plasmalogen biosynthesis can be of great help (Gallego-García et al., 2019; Werner et al., 2020; Wainberg et al., 2021). 4) Last but not least, it can be highly rewarding to continue working on the development and combination of new technologies. Within certain limits, a further increase in the mass resolution of new mass spectrometers can still have positive effects (type-II isotopic effects). There is strong potential for improvement in data analysis, for example, in terms of the utilization of already existing information and by means of sophisticated deconvolution methods. A promising approach could be the integration of techniques such as ion mobility, which for lipids produces a separation behavior similar to that of reversed-phase chromatography in lipids.

As the history of plasmalogen analysis shows, the continuous development of analytical possibilities has resulted in ever greater insights into the chemistry, biochemistry, and physiology of ether lipids. Nevertheless, the precise physiological functions of these lipids are only superficially understood. Particularly, this applies to the delimitation of the functional spectrum between lipid species that contain plasmenyl and plasmanyl residues, respectively. The intensification of research activities in this field, which is also reflected by this special issue, conveys a highly optimistic perspective about possible upcoming breakthroughs, to which plasmalogen analytics will most likely have a significant contribution.

AUTHOR CONTRIBUTIONS

JK and MK conceived the review. JK, KW, EW, and MK wrote the manuscript and revised the literature. All authors approved the submitted version of the manuscript.

FUNDING

This work was supported by the Austrian Science Fund (FWF) project P33333 (to MK) and projects P30800 and P34723 (to KW) and by the Austrian Academy of Sciences (ÖAW) with a DOC-Fellowship (to JK).

REFERENCES

Ahmed, M. Y., Al-Khayat, A., Al-Murshedi, F., Al-Futaisi, A., Chioza, B. A., and Pedro Fernandez-Murray, J. (2017). A Mutation of EPT1 (SELENOI) Underlies a New Disorder of Kennedy Pathway Phospholipid Biosynthesis. *Brain* 140, 547–554. doi:10.1093/brain/aww318

Albers, S. V., van de Vossenberg, J. L., Driessen, A. J., and Konings, W. N. (2000). Adaptations of the Archaeal Cell Membrane to Heat Stress. *Front. Biosci.* 5, 813–820. doi:10.2741/albers

Arthur, G., Mock, T., Zaborniak, C., and Choy, P. C. (1985). The Distribution and Acyl Composition of Plasmalogens in guinea Pig Heart. *Lipids* 20, 693–698. doi:10.1007/bf02534389

Baer, E., and Fischer, H. O. L. (1941). Studies on Acetone-Glyceraldehyde, and Optically Active Glycerides. *J. Biol. Chem.* 140, 397–410. doi:10.1016/s0021-9258(18)51328-4

Benjamin, D. I., Cozzo, A., Ji, X., Roberts, L. S., Louie, S. M., Mulvihill, M. M., et al. (2013). Ether Lipid Generating Enzyme AGPS Alters the Balance of Structural and Signaling Lipids to Fuel Cancer Pathogenicity. *Proc. Natl. Acad. Sci. U. S. A.* 110, 14912–14917. doi:10.1073/pnas.1310894110

Benveniste, J., Tencé, M., Varenne, P., Bidault, J., Boullet, C., and Polonsky, J. (1979). Semi-synthesis and Proposed Structure of Platelet-Activating Factor (P.A.F.): PAF-Acether an Alkyl Ether Analog of Lysophosphatidylcholine. *C. R. Seances Acad. Sci. D* 289, 1037–1040.

Berger, J., Dorninger, F., Forss-Petter, S., and Kunze, M. (2016). Peroxisomes in Brain Development and Function. *Biochim. Biophys. Acta* 1863, 934–955. doi:10.1016/j.bbamcr.2015.12.005

Beyene, H. B., Olshansky, G., Giles, C., Huynh, K., Cinel, M., Mellett, N. A., et al. (2021). Lipidomic Signatures of Changes in Adiposity: A Large Prospective Study of 5849 Adults from the Australian Diabetes, Obesity and Lifestyle Study. *Metabolites* 11, 646. doi:10.3390/metabo11090646

Blank, M. L., Fitzgerald, V., Lee, T.-C., and Snyder, F. (1993). Evidence for Biosynthesis of Plasmenylcholine from Plasmenylethanolamine in HL-60 Cells. *Biochim. Biophys. Acta* 1166, 309–312. doi:10.1016/0005-2760(93)90112-m

Blank, M. L., Snyder, F., Byers, L. W., Brooks, B., and Muirhead, E. E. (1979). Antihypertensive Activity of an Alkyl Ether Analog of Phosphatidylcholine.

Biochem. Biophys. Res. Commun. 90, 1194–1200. doi:10.1016/0006-291x(79)91163-x

Blank, M. L., and Snyder, F. (1992). Plasmanylethanolamine delta 1-desaturase. *Methods Enzymol.* 209, 390–396. doi:10.1016/0076-6879(92)09048-8

Bozelli, J. C., Jr, Lu, D., Atilla-Gokcumen, G. E., and Epand, R. M. (2020). Promotion of Plasmalogen Biosynthesis Reverse Lipid Changes in a Barth Syndrome Cell Model. *Biochim. Biophys. Acta Mol. Cel Biol. Lipids* 1865, 158677. doi:10.1016/j.bbalip.2020.158677

Braverman, N. E., and Moser, A. B. (2012). Functions of Plasmalogen Lipids in Health and Disease. *Biochim. Biophys. Acta* 1822, 1442–1452. doi:10.1016/j.bbadis.2012.05.008

Brites, P., Mooyer, P. A. W., El Mrabet, L., Waterham, H. R., and Wanders, R. J. A. (2009). Plasmalogens Participate in Very-Long-Chain Fatty Acid-Induced Pathology. *Brain* 132, 482–492. doi:10.1093/brain/awn295

Brites, P., Waterham, H. R., and Wanders, R. J. A. (2004). Functions and Biosynthesis of Plasmalogens in Health and Disease. *Biochim. Biophys. Acta* 1636, 219–231. doi:10.1016/j.bbalip.2003.12.010

Broniec, A., Klosinski, R., Pawlak, A., Wrona-Krol, M., Thompson, D., and Sarna, T. (2011). Interactions of Plasmalogens and Their Diacyl Analogs with Singlet Oxygen in Selected Model Systems. *Free Radic. Biol. Med.* 50, 892–898. doi:10.1016/j.freeradbiomed.2011.01.002

Bueno, A. A., Ghebremeskel, K., Bakheit, K. H., Elbashir, M. I., and Adam, I. (2012). Dimethyl Acetals, an Indirect Marker of the Endogenous Antioxidant Plasmalogen Level, Are Reduced in Blood Lipids of Sudanese Pre-eclamptic Subjects Whose Background Diet Is High in Carbohydrate. *J. Obstet. Gynaecol.* 32, 241–246. doi:10.3109/01443615.2011.641622

Buré, C., Ayciriex, S., Testet, E., and Schmitter, J.-M. (2013). A Single Run LC-MS/MS Method for Phospholipidomics. *Anal. Bioanal. Chem.* 405, 203–213. doi:10.1007/s00216-012-6466-9

Carter, H. E., Smith, D. B., and Jones, D. N. (1958). A New Ethanolamine-Containing Lipide from Egg Yolk. *J. Biol. Chem.* 232, 681–694. doi:10.1016/s0021-9258(19)77388-8

Cheng, J. B., and Russell, D. W. (2004). Mammalian Wax Biosynthesis. I. Identification of Two Fatty Acyl-Coenzyme A Reductases with Different Substrate Specificities and Tissue Distributions. *J. Biol. Chem.* 279, 37789–37797. doi:10.1074/jbc.m406225200

Christie, W. W., and Han, X. (2012). "Chromatographic Analysis of Phospholipids and Glycosyldiacylglycerols," in *Lipid Analysis* (Elsevier), 91–124. doi:10.1533/9780857097866.91

Cui, W., Liu, D., Gu, W., and Chu, B. (2021). Peroxisome-driven Ether-Linked Phospholipids Biosynthesis Is Essential for Ferroptosis. *Cell Death Differ* 28, 2536–2551. doi:10.1038/s41418-021-00769-0

Davies, W. H., Heilbron, I. M., and Jones, W. E. (1933). The Unsaponifiable Matter from the Oils of Elasmobranch Fish. Part IX. The Structure of Batyl and Selachyl Alcohols. *J. Chem. Soc.* 49165, 1.

de Vet, E. C., Zomer, A. W., Lahaut, G. J., and van den Bosch, H. (1997). Polymerase Chain Reaction-Based Cloning of Alkyl-Dihydroxyacetonephosphate Synthase Complementary DNA from guinea Pig Liver. *J. Biol. Chem.* 272, 798–803. doi:10.1074/jbc.272.2.798

Dean, J. M., and Lodhi, I. J. (2018). Structural and Functional Roles of Ether Lipids. *Protein Cell* 9, 196–206. doi:10.1007/s13238-017-0423-5

Debuch, H. (1958). Nature of the Linkage of the Aldehyde Residue of Natural Plasmalogens. *J. Neurochem.* 2, 243–248. doi:10.1111/j.1471-4159.1958.tb12370.x

Deeley, J. M., Thomas, M. C., Truscott, R. J. W., Mitchell, T. W., and Blanksby, S. J. (2009). Identification of Abundant Alkyl Ether Glycerophospholipids in the Human Lens by Tandem Mass Spectrometry Techniques. *Anal. Chem.* 81, 1920–1930. doi:10.1021/ac802395d

Demopoulos, C. A., Pinckard, R. N., and Hanahan, D. J. (1979). Platelet-activating Factor. Evidence for 1-O-Alkyl-2-Acetyl-Sn-Glyceryl-3-Phosphorylcholine as the Active Component (A New Class of Lipid Chemical Mediators). *J. Biol. Chem.* 254, 9355–9358. doi:10.1016/s0021-9258(19)83523-8

Dorée, C. (1909). The Occurrence and Distribution of Cholesterol and Allied Bodies in the Animal Kingdom. *Biochem. J.* 4, 72–106. doi:10.1042/bj0040072

Dorninger, F., Forss-Petter, S., Wimmer, I., and Berger, J. (2020). Plasmalogens, Platelet-Activating Factor and beyond - Ether Lipids in Signaling and Neurodegeneration. *Neurobiol. Dis.* 145, 105061. doi:10.1016/j.nbd.2020.105061

Dragonas, C., Bertsch, T., Sieber, C. C., and Brosche, T. (2009). Plasmalogens as a Marker of Elevated Systemic Oxidative Stress in Parkinson's Disease. *Clin. Chem. Lab. Med.* 47, 894–897. doi:10.1515/CCLM.2009.205

Draijer, L. G., Froon-Torenstra, D., van Weeghel, M., Vaz, F. M., Bohte, A. E., Holleboom, A. G., et al. (2020). Lipidomics in Nonalcoholic Fatty Liver Disease: Exploring Serum Lipids as Biomarkers for Pediatric Nonalcoholic Fatty Liver Disease. *J. Pediatr. Gastroenterol. Nutr.* 71, 433–439. doi:10.1097/mpg.0000000000002875

Engelmann, B. (2004). Plasmalogens: Targets for Oxidants and Major Lipophilic Antioxidants. *Biochem. Soc. Trans.* 32, 147–150. doi:10.1042/bst0320147

Fauland, A., Köfeler, H., Trötzmüller, M., Knopf, A., Hartler, J., Eberl, A., et al. (2011). A Comprehensive Method for Lipid Profiling by Liquid Chromatography-Ion Cyclotron Resonance Mass Spectrometry. *J. Lipid Res.* 52, 2314–2322. doi:10.1194/jlr.d016550

Felde, R., and Spiteller, G. (1994). Search for Plasmalogens in Plants. *Chem. Phys. Lipids* 71, 109–113. doi:10.1016/0009-3084(94)02305-0

Ferdinandusse, S., McWalter, K., Te Brinke, H., IJlst, L., Mooijer, P. M., Ruiter, J. P. N., et al. (2021). An Autosomal Dominant Neurological Disorder Caused by De Novo Variants in FAR1 Resulting in Uncontrolled Synthesis of Ether Lipids. *Genet. Med.* 23, 740–750. doi:10.1038/s41436-020-01027-3

Ferreira, C. R., Rahman, S., Keller, M., and Zschocke, J.ICIMD Advisory Group (2021). An International Classification of Inherited Metabolic Disorders (ICIMD). *J. Inherit. Metab. Dis.* 44, 164–177. doi:10.1002/jimd.12348

Feulgen, R., and Voit, K. (1924). Über einen weitverbreiteten festen Aldehyd. *Pflugers Arch.* 206, 389–410. doi:10.1007/bf01722779

Fhaner, C. J., Liu, S., Zhou, X., and Reid, G. E. (2013). Functional Group Selective Derivatization and Gas-phase Fragmentation Reactions of Plasmalogen Glycerophospholipids. *Mass. Spectrom.* 2, S0015. doi:10.5702/massspectrometry.s0015

Fujino, T., Yamada, T., Asada, T., Tsuboi, Y., Wakana, C., Mawatari, S., et al. (2017). Efficacy and Blood Plasmalogen Changes by Oral Administration of Plasmalogen in Patients with Mild Alzheimer's Disease and Mild Cognitive Impairment: A Multicenter, Randomized, Double-Blind, Placebo-Controlled Trial. *EBioMedicine* 17, 199–205. doi:10.1016/j.ebiom.2017.02.012

Gallego-García, A., Monera-Girona, A. J., Pajares-Martínez, E., Bastida-Martínez, E., Pérez-Castaño, R., Iniesta, A. A., et al. (2019). A Bacterial Light Response Reveals an Orphan Desaturase for Human Plasmalogen Synthesis. *Science* 366, 128–132. doi:10.1126/science.aay1436

Goldfine, H. (2010). The Appearance, Disappearance and Reappearance of Plasmalogens in Evolution. *Prog. Lipid Res.* 49, 493–498. doi:10.1016/j.plipres.2010.07.003

Goto-Inoue, N., Hayasaka, T., Zaima, N., and Setou, M. (2009). The Specific Localization of Seminolipid Molecular Species on Mouse Testis during Testicular Maturation Revealed by Imaging Mass Spectrometry. *Glycobiology* 19, 950–957. doi:10.1093/glycob/cwp089

Gray, G. M. (1969). "[65] the Preparation and Assay of Long-Chain Fatty Aldehydes," in Methods In Enzymology *Methods in Enzymology* (Elsevier), 678–684. doi:10.1016/s0076-6879(69)14068-9

Gross, R. W. (1985). Identification of Plasmalogen as the Major Phospholipid Constituent of Cardiac Sarcoplasmic Reticulum. *Biochemistry* 24, 1662–1668. doi:10.1021/bi00328a014

Grossi, V., Mollex, D., Vinçon-Laugier, A., Hakil, F., Pacton, M., and Cravo-Laureau, C. (2015). Mono- and Dialkyl Glycerol Ether Lipids in Anaerobic Bacteria: Biosynthetic Insights from the Mesophilic Sulfate Reducer Desulfatibacillum Alkenivorans PF2803T. *Appl. Environ. Microbiol.* 81, 3157–3168. doi:10.1128/aem.03794-14

Hajra, A. K. (1969). Biosynthesis of Alkyl-Ether Containing Lipid from Dihydroxyacetone Phosphate. *Biochem. Biophys. Res. Commun.* 37, 486–492. doi:10.1016/0006-291x(69)90941-3

Han, X., and Gross, R. W. (2001). Quantitative Analysis and Molecular Species Fingerprinting of Triacylglyceride Molecular Species Directly from Lipid Extracts of Biological Samples by Electrospray Ionization Tandem Mass Spectrometry. *Anal. Biochem.* 295, 88–100. doi:10.1006/abio.2001.5178

Han, X., and Gross, R. W. (2005). Shotgun Lipidomics: Electrospray Ionization Mass Spectrometric Analysis and Quantitation of Cellular Lipidomes Directly from Crude Extracts of Biological Samples. *Mass Spectrom. Rev.* 24, 367–412. doi:10.1002/mas.20023

Han, X., Holtzman, D. M., and McKeel, D. W., Jr (2001). Plasmalogen Deficiency in Early Alzheimer's Disease Subjects and in Animal Models: Molecular Characterization Using Electrospray Ionization Mass Spectrometry. *J. Neurochem.* 77, 1168–1180. doi:10.1046/j.1471-4159.2001.00332.x

Hanahan, D. J., Ekholm, J., and Jackson, C. M. (1963). Studies on the Structure of Glyceryl Ethers and the Glyceryl Ether Phospholipids of Bovine Erythrocytes. *Biochemistry* 2, 630–641. doi:10.1021/bi00904a002

Hanahan, D. J., and Watts, R. (1961). The Isolation of an α′-Alkoxy-β-acyl-α-glycerophosphorylethanolamine from Bovine Erythrocytes. *J. Biol. Chem.* 236, PC59–PC60. doi:10.1016/s0021-9258(18)64040-2

Harayama, T., and Riezman, H. (2018). Understanding the Diversity of Membrane Lipid Composition. *Nat. Rev. Mol. Cel Biol.* 19, 281–296. doi:10.1038/nrm.2017.138

Harrieder, E.-M., Kretschmer, F., Böcker, S., and Witting, M. (2022). Current State-Of-The-Art of Separation Methods Used in LC-MS Based Metabolomics and Lipidomics. *J. Chromatogr. B Analyt. Technol. Biomed. Life Sci.* 1188, 123069. doi:10.1016/j.jchromb.2021.123069

Heilbron, I. M., and Owens, W. M. (1928). CXXIV.—The Unsaponifiable Matter from the Oils of Elasmobranch Fish. Part IV. The Establishment of the Structure of Selachyl and Batyl Alcohols as Monoglyceryl Ethers. *J. Chem. Soc.* 0, 942–947. doi:10.1039/jr9280000942

Honsho, M., Asaoku, S., and Fujiki, Y. (2010). Posttranslational Regulation of Fatty Acyl-CoA Reductase 1, Far1, Controls Ether Glycerophospholipid Synthesis. *J. Biol. Chem.* 285, 8537–8542. doi:10.1074/jbc.m109.083311

Horibata, Y., Elpeleg, O., Eran, A., Hirabayashi, Y., Savitzki, D., Tal, G., et al. (2018). EPT1 (Selenoprotein I) Is Critical for the Neural Development and Maintenance of Plasmalogen in Humans. *J. Lipid Res.* 59, 1015–1026. doi:10.1194/jlr.p081620

Höring, M., Ejsing, C. S., Krautbauer, S., Ertl, V. M., Burkhardt, R., and Liebisch, G. (2021). Accurate Quantification of Lipid Species Affected by Isobaric Overlap in Fourier-Transform Mass Spectrometry. *J. Lipid Res.* 62, 100050. doi:10.1016/j.jlr.2021.100050

Horrocks, L. A., and Sharma, M. (1982). "Chapter 2 Plasmalogens and O-Alkyl Glycerophospholipids," in New Comprehensive Biochemistry *New Comprehensive Biochemistry* (Elsevier), 51–93. doi:10.1016/s0167-7306(08)60006-x

Hossain, M. S., Ifuku, M., Take, S., Kawamura, J., Miake, K., and Katafuchi, T. (2013). Plasmalogens rescue Neuronal Cell Death through an Activation of AKT and ERK Survival Signaling. *PLoS One* 8, e83508. doi:10.1371/journal.pone.0083508

Hsu, F.-F., Lodhi, I. J., Turk, J., and Semenkovich, C. F. (2014). Structural Distinction of Diacyl-, Alkylacyl, and Alk-1-Enylacyl Glycerophosphocholines as $[M - 15]^-$ Ions by Multiple-Stage Linear Ion-Trap Mass Spectrometry with Electrospray Ionization. *J. Am. Soc. Mass. Spectrom.* 25, 1412–1420. doi:10.1007/s13361-014-0908-x

Hsu, F.-F., and Turk, J. (2007). Differentiation of 1-O-Alk-1'-Enyl-2-Acyl and 1-O-Alkyl-2-Acyl Glycerophospholipids by Multiple-Stage Linear Ion-Trap Mass Spectrometry with Electrospray Ionization. *J. Am. Soc. Mass. Spectrom.* 18, 2065–2073. doi:10.1016/j.jasms.2007.08.019

Hsu, F.-F., and Turk, J. (2008). Structural Characterization of Unsaturated Glycerophospholipids by Multiple-Stage Linear Ion-Trap Mass Spectrometry with Electrospray Ionization. *J. Am. Soc. Mass. Spectrom.* 19, 1681–1691. doi:10.1016/j.jasms.2008.07.023

Hu, C., Wang, C., He, L., and Han, X. (2019). Novel Strategies for Enhancing Shotgun Lipidomics for Comprehensive Analysis of Cellular Lipidomes. *Trends Analyt. Chem.* 120, 115330. doi:10.1016/j.trac.2018.11.028

Igarashi, M., Ma, K., Gao, F., Kim, H.-W., Rapoport, S. I., and Rao, J. S. (2011). Disturbed Choline Plasmalogen and Phospholipid Fatty Acid Concentrations in Alzheimer's Disease Prefrontal Cortex. *J. Alzheimers. Dis.* 24, 507–517. doi:10.3233/jad-2011-101608

Ingrand, S. S., Wahl, A., Favrelière, S., Barbot, F., and Tallineau, C. (2000). Quantification of Long-Chain Aldehydes by Gas Chromatography Coupled to Mass Spectrometry as a Tool for Simultaneous Measurement of Plasmalogens and Their Aldehydic Breakdown Products. *Anal. Biochem.* 280, 65–72. doi:10.1006/abio.2000.4477

Ivanova, P. T., Milne, S. B., and Brown, H. A. (2010). Identification of Atypical Ether-Linked Glycerophospholipid Species in Macrophages by Mass Spectrometry. *J. Lipid Res.* 51, 1581–1590. doi:10.1194/jlr.d003715

Jackson, D. R., Cassilly, C. D., Plichta, D. R., Vlamakis, H., Liu, H., Melville, S. B., et al. (2021). Plasmalogen Biosynthesis by Anaerobic Bacteria: Identification of a Two-Gene Operon Responsible for Plasmalogen Production in. *ACS Chem. Biol.* 16, 6–13. doi:10.1021/acschembio.0c00673

Jain, S., Caforio, A., and Driessen, A. J. M. (2014). Biosynthesis of Archaeal Membrane Ether Lipids. *Front. Microbiol.* 5, 641. doi:10.3389/fmicb.2014.00641

Jenkins, C. M., Yang, K., Liu, G., Moon, S. H., Dilthey, B. G., and Gross, R. W. (2018). Cytochrome Is an Oxidative Stress-Activated Plasmalogenase that Cleaves Plasmenylcholine and Plasmenylethanolamine at the -1 Vinyl Ether Linkage. *J. Biol. Chem.* 293, 8693–8709. doi:10.1074/jbc.ra117.001629

Jiménez-Rojo, N., and Riezman, H. (2019). On the Road to Unraveling the Molecular Functions of Ether Lipids. *FEBS Lett.* 593, 2378–2389. doi:10.1002/1873-3468.13465

Kamio, Y., Kanegasaki, S., and Takahashi, H. (1969). Occurrence of Plasmalogens in Anaerobic Bacteria. *J. Gen. Appl. Microbiol.* 15, 439–451. doi:10.2323/jgam.15.439

Keller, M. A. (2021). Interpreting Phospholipid and Cardiolipin Profiles in Rare Mitochondrial Diseases. *Curr. Opin. Syst. Biol.* 28, 100383. doi:10.1016/j.coisb.2021.100383

Keller, M. A., Watschinger, K., Lange, K., Golderer, G., Werner-Felmayer, G., Hermetter, A., et al. (2012). Studying Fatty Aldehyde Metabolism in Living Cells with Pyrene-Labeled Compounds. *J. Lipid Res.* 53, 1410–1416. doi:10.1194/jlr.d025650

Keller, M. A., Zander, U., Fuchs, J. E., Kreutz, C., Watschinger, K., Mueller, T., et al. (2014). A Gatekeeper helix Determines the Substrate Specificity of Sjögren-Larsson Syndrome Enzyme Fatty Aldehyde Dehydrogenase. *Nat. Commun.* 5. doi:10.1038/ncomms5439

Kim, S. J., Kim, N., Koh, E. H., and Yoo, H. J. (2012). Identification of Ethanolamine Plasmalogens from Complex Lipid Mixtures by MS/MS and Ag Adduction. *Anal. Sci.* 28, 1207–1212. doi:10.2116/analsci.28.1207

Kimura, T., Kimura, A. K., Ren, M., Berno, B., Xu, Y., Schlame, M., et al. (2018). Substantial Decrease in Plasmalogen in the Heart Associated with Tafazzin Deficiency. *Biochemistry* 57, 2162–2175. doi:10.1021/acs.biochem.8b00042

Kirkwood, K. I., Christopher, M. W., Burgess, J. L., Littau, S. R., Foster, K., Richey, K., et al. (2022). Development and Application of Multidimensional Lipid Libraries to Investigate Lipidomic Dysregulation Related to Smoke Inhalation Injury Severity. *J. Proteome Res.* 21, 232–242. doi:10.1021/acs.jproteome.1c00820

Kiyasu, J. Y., and Kennedy, E. P. (1960). The Enzymatic Synthesis of Plasmalogens. *J. Biol. Chem.* 235, 2590–2594. doi:10.1016/s0021-9258(19)76919-1

Kling, M. A., Goodenowe, D. B., Senanayake, V., MahmoudianDehkordi, S., Arnold, M., Massaro, T. J., et al. (2020). Circulating Ethanolamine Plasmalogen Indices in Alzheimer's Disease: Relation to Diagnosis, Cognition, and CSF Tau. *Alzheimers. Dement.* 16, 1234–1247. doi:10.1002/alz.12110

Koch, J., Lackner, K., Wohlfarter, Y., Sailer, S., Zschocke, J., Werner, E. R., et al. (2020). Unequivocal Mapping of Molecular Ether Lipid Species by LC-MS/MS in Plasmalogen-Deficient Mice. *Anal. Chem.* 92, 11268–11276. doi:10.1021/acs.analchem.0c01933

Köfeler, H. C., Ahrends, R., Baker, E. S., Ekroos, K., Han, X., Hoffmann, N., et al. (2021). Recommendations for Good Practice in MS-based Lipidomics. *J. Lipid Res.* 62, 100138. doi:10.1016/j.jlr.2021.100138

Kopczynski, D., Hoffmann, N., Peng, B., and Ahrends, R. (2020). Goslin: A Grammar of Succinct Lipid Nomenclature. *Anal. Chem.* 92, 10957–10960. doi:10.1021/acs.analchem.0c01690

Kuerschner, L., Richter, D., Hannibal-Bach, H. K., Gaebler, A., Shevchenko, A., Ejsing, C. S., et al. (2012). Exogenous Ether Lipids Predominantly Target Mitochondria. *PLoS One* 7, e31342. doi:10.1371/journal.pone.0031342

Lange, M., and Fedorova, M. (2020). Evaluation of Lipid Quantification Accuracy Using HILIC and RPLC MS on the Example of NIST® SRM® 1950 Metabolites in Human Plasma. *Anal. Bioanal. Chem.* 412, 3573–3584. doi:10.1007/s00216-020-02576-x

Le Faouder, P., Soullier, J., Tremblay-Franco, M., Tournadre, A., Martin, J.-F., Guitton, Y., et al. (2021). Untargeted Lipidomic Profiling of Dry Blood Spots Using SFC-HRMS. *Metabolites* 11, 305. doi:10.3390/metabo11050305

Lee, C.-H., Tang, S.-C., and Kuo, C.-H. (2021). Differentiating Ether Phosphatidylcholines with a Collision Energy-Optimized MRM Method by

RPLC-MS/MS and its Application to Studying Ischemia-Neuronal Injury. *Anal. Chim. Acta* 1184, 339014. doi:10.1016/j.aca.2021.339014

Liebisch, G., Fahy, E., Aoki, J., Dennis, E. A., Durand, T., Ejsing, C. S., et al. (2020). Update on LIPID MAPS Classification, Nomenclature, and Shorthand Notation for MS-derived Lipid Structures. *J. Lipid Res.* 61, 1539–1555. doi:10.1194/jlr.s120001025

Liebisch, G., Vizcaíno, J. A., Köfeler, H., Trötzmüller, M., Griffiths, W. J., Schmitz, G., et al. (2013). Shorthand Notation for Lipid Structures Derived from Mass Spectrometry. *J. Lipid Res.* 54, 1523–1530. doi:10.1194/jlr.m033506

Lin, H. J., Jie, L. K., Lee, C. L., and Lee, D. H. (1977). Composition of O-Alkyl and O-Alk-1-Enyl Moieties in the Glycerolipids of the Human Adrenal. *Lipids* 12, 620–625. doi:10.1007/bf02533392

Lísa, M., Cífková, E., Khalikova, M., Ovčačíková, M., and Holčapek, M. (2017). Lipidomic Analysis of Biological Samples: Comparison of Liquid Chromatography, Supercritical Fluid Chromatography and Direct Infusion Mass Spectrometry Methods. *J. Chromatogr. A.* 1525, 96–108. doi:10.1016/j.chroma.2017.10.022

Liu, T., Tan, Z., Yu, J., Peng, F., Guo, J., Meng, W., et al. (2020). A Conjunctive Lipidomic Approach Reveals Plasma Ethanolamine Plasmalogens and Fatty Acids as Early Diagnostic Biomarkers for Colorectal Cancer Patients. *Expert Rev. Proteomics* 17, 233–242. doi:10.1080/14789450.2020.1757443

Lodhi, I. J., Yin, L., Jensen-Urstad, A. P. L., Funai, K., Coleman, T., Baird, J. H., et al. (2012). Inhibiting Adipose Tissue Lipogenesis Reprograms Thermogenesis and PPARγ Activation to Decrease Diet-Induced Obesity. *Cell Metab* 16, 189–201. doi:10.1016/j.cmet.2012.06.013

Lordan, R., Tsoupras, A., Zabetakis, I., and Demopoulos, C. A. (2019). Forty Years since the Structural Elucidation of Platelet-Activating Factor (PAF): Historical, Current, and Future Research Perspectives. *Molecules* 24, 4414. doi:10.3390/molecules24234414

Ly, R., Ly, N., Sasaki, K., Suzuki, M., Kami, K., Ohashi, Y., et al. (2021). Nontargeted Serum Lipid Profiling of Nonalcoholic Steatohepatitis by Multisegment Injection-Nonaqueous Capillary Electrophoresis-Mass Spectrometry: A Multiplexed Separation Platform for Resolving Ionic Lipids. *J. Proteome Res.* 21, 768–777. doi:10.1021/acs.jproteome.1c00682

Mangold, H. K., and Malins, D. C. (1960). Fractionation of Fats, Oils, and Waxes on Thin Layers of Silicic Acid. *J. Am. Oil Chem. Soc.* 37, 383–385. doi:10.1007/bf02672641

Marinetti, G. V., and Erbland, J. (1957). The Structure of Pig Heart Plasmalogen. *Biochim. Biophys. Acta* 26, 429–430. doi:10.1016/0006-3002(57)90028-8

Marshall, D. L., Criscuolo, A., Young, R. S. E., Poad, B. L. J., Zeller, M., Reid, G. E., et al. (2019). Mapping Unsaturation in Human Plasma Lipids by Data-independent Ozone-Induced Dissociation. *J. Am. Soc. Mass. Spectrom.* 30, 1621–1630. doi:10.1007/s13361-019-02261-z

Maulik, N., Bagchi, D., Jones, R., Cordis, G., and Das, D. K. (1993). Identification and Characterization of Plasmalogen Fatty Acids in Swine Heart. *J. Pharm. Biomed. Anal.* 11, 1151–1156. doi:10.1016/0731-7085(93)80097-k

Mawatari, S., Okuma, Y., and Fujino, T. (2007). Separation of Intact Plasmalogens and All Other Phospholipids by a Single Run of High-Performance Liquid Chromatography. *Anal. Biochem.* 370, 54–59. doi:10.1016/j.ab.2007.05.020

Meletis, C. D. (2020). Alkyl-Acylglycerols and the Important Clinical Ramifications of Raising Plasmalogens in Dementia and Alzheimer's Disease. *Integr. Med.* 19, 12–16.

Meneses, P., and Glonek, T. (1988). High Resolution 31P NMR of Extracted Phospholipids. *J. Lipid Res.* 29, 679–689. doi:10.1016/s0022-2275(20)38513-8

Messias, M. C. F., Mecatti, G. C., Priolli, D. G., and de Oliveira Carvalho, P. (2018). Plasmalogen Lipids: Functional Mechanism and Their Involvement in Gastrointestinal Cancer. *Lipids Health Dis.* 17, 41. doi:10.1186/s12944-018-0685-9

Moraitou, M., Dimitriou, E., Zafeiriou, D., Reppa, C., Marinakis, T., Sarafidou, J., et al. (2008). Plasmalogen Levels in Gaucher Disease. *Blood Cell Mol. Dis.* 41, 196–199. doi:10.1016/j.bcmd.2008.03.007

Morel, Y., Hegdekar, N., Sarkar, C., Lipinski, M. M., Kane, M. A., and Jones, J. W. (2021). Structure-specific, Accurate Quantitation of Plasmalogen Glycerophosphoethanolamine. *Anal. Chim. Acta* 1186, 339088. doi:10.1016/j.aca.2021.339088

Murphy, E. J., Schapiro, M. B., Rapoport, S. I., and Shetty, H. U. (2000). Phospholipid Composition and Levels Are Altered in Down Syndrome Brain. *Brain Res.* 867, 9–18. doi:10.1016/s0006-8993(00)02205-8

Nagan, N., and Zoeller, R. A. (2001). Plasmalogens: Biosynthesis and Functions. *Prog. Lipid Res.* 40, 199–229. doi:10.1016/s0163-7827(01)00003-0

Norton, W. T., Gottfried, E. L., and Rapport, M. M. (1962). The Structure of Plasmalogens: VI. Configuration of the Double Bond in the α,β-unsaturated Ether Linkage of Phosphatidal Choline. *J. Lipid Res.* 3, 456–459. doi:10.1016/s0022-2275(20)40391-8

Ofman, R., Hettema, E. H., Hogenhout, E. M., Caruso, U., Muijsers, A. O., and Wanders, R. J. (1998). Acyl-CoA:dihydroxyacetonephosphate Acyltransferase: Cloning of the Human cDNA and Resolution of the Molecular Basis in Rhizomelic Chondrodysplasia Punctata Type 2. *Hum. Mol. Genet.* 7, 847–853. doi:10.1093/hmg/7.5.847

Otoki, Y., Kato, S., Kimura, F., Furukawa, K., Yamashita, S., Arai, H., et al. (2017). Accurate Quantitation of Choline and Ethanolamine Plasmalogen Molecular Species in Human Plasma by Liquid Chromatography-Tandem Mass Spectrometry. *J. Pharm. Biomed. Anal.* 134, 77–85. doi:10.1016/j.jpba.2016.11.019

Paltauf, F. (1972). Plasmalogen Biosynthesis in a Cell-free System. Enzymic Desaturation of 1-O-Alkyl (2-acyl) Glycerophosphoryl Ethanolamine. *FEBS Lett.* 20, 79–82. doi:10.1016/0014-5793(72)80021-8

Paulick, M. G., and Bertozzi, C. R. (2008). The Glycosylphosphatidylinositol Anchor: a Complex Membrane-Anchoring Structure for Proteins. *Biochemistry* 47, 6991–7000. doi:10.1021/bi8006324

Pham, H. T., Maccarone, A. T., Thomas, M. C., Campbell, J. L., Mitchell, T. W., and Blanksby, S. J. (2014). Structural Characterization of Glycerophospholipids by Combinations of Ozone- and Collision-Induced Dissociation Mass Spectrometry: the Next Step towards "Top-down" Lipidomics. *Analyst* 139, 204–214. doi:10.1039/c3an01712e

Pineda De Castro, L. F., Dopson, M., and Friedman, R. (2016). Biological Membranes in Extreme Conditions: Simulations of Anionic Archaeal Tetraether Lipid Membranes. *PLoS One* 11, e0155287. doi:10.1371/journal.pone.0155287

Rahn, C. H., and Schlenk, H. (1973). Detection of Aldehydes with 4-Amino-5-Hydrazino-1,2,4-Triazole-3-Thiol as spray Reagent. *Lipids* 8, 612–616. doi:10.1007/bf02533143

Rapport, M. M., Lerner, B., Alonzo, N., and Franzl, R. E. (1957). The Structure of Plasmalogens. *J. Biol. Chem.* 225, 859–867. doi:10.1016/s0021-9258(18)64884-7

Řezanka, T., Křesinová, Z., Kolouchová, I., and Sigler, K. (2012). Lipidomic Analysis of Bacterial Plasmalogens. *Folia Microbiol.* 57, 463–472.

Rhee, K. S., Del Rosario, R. R., and Dugan, L. R., Jr (1967). Determination of Plasmalogens after Treating with a 2,4-Dinitrophenylhydrazine-Phosphoric Acid Reagent. *Lipids* 2, 334–338. doi:10.1007/bf02532121

Rizzo, W. B., and Craft, D. A. (2000). Sjögren-Larsson Syndrome: Accumulation of Free Fatty Alcohols in Cultured Fibroblasts and Plasma. *J. Lipid Res.* 41, 1077–1081. doi:10.1016/s0022-2275(20)32012-5

Sacchi, R., Medina, I., and Paolillo, L. (1995). One- and Two-Dimensional NMR Studies of Plasmalogens (Alk- L -Enyl-Phosphatidylethanolamine). *Chem. Phys. Lipids* 76, 201–209. doi:10.1016/0009-3084(95)02444-n

Schievano, E., Morelato, E., Facchin, C., and Mammi, S. (2013). Characterization of Markers of Botanical Origin and Other Compounds Extracted from Unifloral Honeys. *J. Agric. Food Chem.* 61, 1747–1755. doi:10.1021/jf302798d

Schmid, H. H., Bandi, P. C., and Su, K. L. (1975). Analysis and Quantification of Ether Lipids by Chromatographic Methods. *J. Chromatogr. Sci.* 13, 478–486. doi:10.1093/chromsci/13.10.478

Schmid, H. H., Tuna, N., and Mangold, H. K. (1967). The Composition of O-Alk-1-Enyl Diglycerides and O-Alkyl Diglycerides of Human Subcutaneous Adipose Tissue. *Hoppe Seylers Z. Physiol. Chem.* 348, 730–732.

Schoeny, H., Rampler, E., Hermann, G., Grienke, U., Rollinger, J. M., and Koellensperger, G. (2020). Preparative Supercritical Fluid Chromatography for Lipid Class Fractionation-A Novel Strategy in High-Resolution Mass Spectrometry Based Lipidomics. *Anal. Bioanal. Chem.* 412, 2365–2374. doi:10.1007/s00216-020-02463-5

Schuhmann, K., Moon, H., Thomas, H., Ackerman, J. M., Groessl, M., Wagner, N., et al. (2019). Quantitative Fragmentation Model for Bottom-Up Shotgun Lipidomics. *Anal. Chem.* 91, 12085–12093. doi:10.1021/acs.analchem.9b03270

Shantha, N. C., and Napolitano, G. E. (1998). in *Journal of Chromatography Library Journal of Chromatography Library* (Elsevier), 371–402. doi:10.1016/s0301-4770(08)60307-3*Analysis of Lipids by Thin-Layer Chromatography*

Snyder, F., Malone, B., and Wykle, R. L. (1969). The Biosynthesis of Alkyl Ether Bonds in Lipids by a Cell-free System. *Biochem. Biophys. Res. Commun.* 34, 40–47. doi:10.1016/0006-291x(69)90525-7

Snyder, F. (1999). The Ether Lipid Trail: a Historical Perspective. *Biochim. Biophys. Acta* 1436, 265–278. doi:10.1016/s0005-2760(98)00172-6

Snyder, F., and Wood, R. (1968). The Occurrence and Metabolism of Alkyl and Alk-1-Enyl Ethers of Glycerol in Transplantable Rat and Mouse Tumors. *Cancer Res.* 28, 972–978.

Staps, P., Rizzo, W. B., Vaz, F. M., Bugiani, M., Giera, M., Heijs, B., et al. (2020). Disturbed Brain Ether Lipid Metabolism and Histology in Sjögren-Larsson Syndrome. *J. Inherit. Metab. Dis.* 43, 1265–1278. doi:10.1002/jimd.12275

Sun, G. Y. (1973). Phospholipids and Acyl Groups in Subcellular Fractions from Human Cerebral Cortex. *J. Lipid Res.* 14, 656–663. doi:10.1016/s0022-2275(20)36847-4

Surma, M. A., Gerl, M. J., Herzog, R., Helppi, J., Simons, K., and Klose, C. (2021). Mouse Lipidomics Reveals Inherent Flexibility of a Mammalian Lipidome. *Sci. Rep.* 11, 19364. doi:10.1038/s41598-021-98702-5

Thai, T. P., Heid, H., Rackwitz, H. R., Hunziker, A., Gorgas, K., and Just, W. W. (1997). Ether Lipid Biosynthesis: Isolation and Molecular Characterization of Human Dihydroxyacetonephosphate Acyltransferase. *FEBS Lett.* 420, 205–211. doi:10.1016/s0014-5793(97)01495-6

Toyama, Y. (1924). Ueber die unverseifbaren Bestandteile (höheren Alkohole) der Haifisch- und Rochenleberöle. III. *Chemische Umschau auf dem Gebiet der Fette, Oele, Wachse und Harze* 31, 61–67. doi:10.1002/lipi.19240311302

Tsugawa, H., Ikeda, K., Takahashi, M., Satoh, A., Mori, Y., Uchino, H., et al. (2020). A Lipidome Atlas in MS-DIAL 4. *Nat. Biotechnol.* 38, 1159–1163. doi:10.1038/s41587-020-0531-2

Vaňková, Z., Peterka, O., Chocholoušková, M., Wolrab, D., Jirásko, R., and Holčapek, M. (2022). Retention Dependences Support Highly Confident Identification of Lipid Species in Human Plasma by Reversed-phase UHPLC/MS. *Anal. Bioanal. Chem.* 414, 319–331. doi:10.1007/s00216-021-03492-4

Vasilopoulou, C. G., Sulek, K., Brunner, A.-D., Meitei, N. S., Schweiger-Hufnagel, U., Meyer, S. W., et al. (2020). Trapped Ion Mobility Spectrometry and PASEF Enable In-Depth Lipidomics from Minimal Sample Amounts. *Nat. Commun.* 11, 331. doi:10.1038/s41467-019-14044-x

Vítová, M., Palyzová, A., and Řezanka, T. (2021). Plasmalogens - Ubiquitous Molecules Occurring Widely, from Anaerobic Bacteria to Humans. *Prog. Lipid Res.* 83, 101111. doi:10.1016/j.plipres.2021.101111

Wainberg, M., Kamber, R. A., Balsubramani, A., Meyers, R. M., Sinnott-Armstrong, N., Hornburg, D., et al. (2021). A Genome-wide Atlas of Co-essential Modules Assigns Function to Uncharacterized Genes. *Nat. Genet.* 53, 638–649. doi:10.1038/s41588-021-00840-z

Wallace, M. A. G., and McCord, J. P. (2020). "High-resolution Mass Spectrometry," in *Breathborne Biomarkers and the Human Volatilome* (Elsevier), 253–270. doi:10.1016/b978-0-12-819967-1.00016-5

Wanders, R. J. A., and Brites, P. (2010). Biosynthesis of Ether-Phospholipids Including Plasmalogens, Peroxisomes and Human Disease: New Insights into an Old Problem. *Clin. Lipidol.* 5, 379–386. doi:10.2217/clp.10.16

Wang, C., Wang, J., Qin, C., and Han, X. (2020). Analysis of Monohexosyl Alkyl (Alkenyl)-acyl Glycerol in Brain Samples by Shotgun Lipidomics. *Anal. Chim. Acta* 1129, 143–149. doi:10.1016/j.aca.2020.07.016

Warner, H. R., and Lands, W. E. M. (1963). The Configuration of the Double Bond in Naturally-Occurring Alkenyl Ethers. *J. Am. Chem. Soc.* 85, 60–64. doi:10.1021/ja00884a012

Warner, H. R., and Lands, W. E. (1961). The Metabolism of Plasmalogen: Enzymatic Hydrolysis of the Vinyl Ether. *J. Biol. Chem.* 236, 2404–2409. doi:10.1016/s0021-9258(18)64011-6

Waterham, H. R., and Ebberink, M. S. (2012). Genetics and Molecular Basis of Human Peroxisome Biogenesis Disorders. *Biochim. Biophys. Acta* 1822, 1430–1441. doi:10.1016/j.bbadis.2012.04.006

Watschinger, K., Keller, M. A., Golderer, G., Hermann, M., Maglione, M., Sarg, B., et al. (2010). Identification of the Gene Encoding Alkylglycerol Monooxygenase Defines a Third Class of Tetrahydrobiopterin-dependent Enzymes. *Proc. Natl. Acad. Sci. U. S. A.* 107, 13672–13677. doi:10.1073/pnas.1002404107

Werner, E. R., Keller, M. A., Sailer, S., Lackner, K., Koch, J., Hermann, M., et al. (2020). The TMEM189 Gene Encodes Plasmanylethanolamine Desaturase Which Introduces the Characteristic Vinyl Ether Double Bond into Plasmalogens. *Proc. Natl. Acad. Sci. U. S. A.* 117, 7792–7798. doi:10.1073/pnas.1917461117

Werner, E. R., Keller, M. A., Sailer, S., Seppi, D., Golderer, G., Werner-Felmayer, G., et al. (2018). A Novel Assay for the Introduction of the Vinyl Ether Double Bond into Plasmalogens Using Pyrene-Labeled Substrates. *J. Lipid Res.* 59, 901–909. doi:10.1194/jlr.d080283

Weustenfeld, M., Eidelpes, R., Schmuth, M., Rizzo, W. B., Zschocke, J., and Keller, M. A. (2019). Genotype and Phenotype Variability in Sjögren-Larsson Syndrome. *Hum. Mutat.* 40, 177–186. doi:10.1002/humu.23679

Wolrab, D., Chocholoušková, M., Jirásko, R., Peterka, O., and Holčapek, M. (2020). Validation of Lipidomic Analysis of Human Plasma and Serum by Supercritical Fluid Chromatography-Mass Spectrometry and Hydrophilic Interaction Liquid Chromatography-Mass Spectrometry. *Anal. Bioanal. Chem.* 412, 2375–2388. doi:10.1007/s00216-020-02473-3

Wu, L.-C., Pfeiffer, D. R., Calhoon, E. A., Madiai, F., Marcucci, G., Liu, S., et al. (2011). Purification, Identification, and Cloning of Lysoplasmalogenase, the Enzyme that Catalyzes Hydrolysis of the Vinyl Ether Bond of Lysoplasmalogen. *J. Biol. Chem.* 286, 24916–24930. doi:10.1074/jbc.m111.247163

Wykle, R. L., Blank, M. L., Malone, B., and Snyder, F. (1972). Evidence for a Mixed Function Oxidase in the Biosynthesis of Ethanolamine Plasmalogens from 1-Alkyl-2-Acyl-Sn-Glycero-3-Phosphorylethanolamine. *J. Biol. Chem.* 247, 5442–5447. doi:10.1016/s0021-9258(20)81125-9

Wykle, R. L., and Snyder, F. (1969). The Glycerol Source for the Biosynthesis of Alkyl Glycerol Ethers. *Biochem. Biophys. Res. Commun.* 37, 658–662. doi:10.1016/0006-291x(69)90861-4

Yamashita, S., Kanno, S., Honjo, A., Otoki, Y., Nakagawa, K., Kinoshita, M., et al. (2016). Analysis of Plasmalogen Species in Foodstuffs. *Lipids* 51, 199–210. doi:10.1007/s11745-015-4112-y

Yamashita, S., Kanno, S., Nakagawa, K., Kinoshita, M., and Miyazawa, T. (2015). Extrinsic Plasmalogens Suppress Neuronal Apoptosis in Mouse Neuroblastoma Neuro-2A Cells: Importance of Plasmalogen Molecular Species. *RSC Adv.* 5, 61012–61020. doi:10.1039/c5ra00632e

Zhang, W., Hankemeier, T., and Ramautar, R. (2017). Next-generation Capillary Electrophoresis-Mass Spectrometry Approaches in Metabolomics. *Curr. Opin. Biotechnol.* 43, 1–7. doi:10.1016/j.copbio.2016.07.002

Zoeller, R. A., Morand, O. H., and Raetz, C. R. (1988). A Possible Role for Plasmalogens in Protecting Animal Cells against Photosensitized Killing. *J. Biol. Chem.* 263, 11590–11596. doi:10.1016/s0021-9258(18)38000-1

Zou, Y., Henry, W. S., Ricq, E. L., Graham, E. T., Phadnis, V. V., Maretich, P., et al. (2020). Plasticity of Ether Lipids Promotes Ferroptosis Susceptibility and Evasion. *Nature* 585, 603–608. doi:10.1038/s41586-020-2732-8

Conflict of Interest: The authors declare that the research was conducted in the absence of any commercial or financial relationships that could be construed as a potential conflict of interest.

frontiers | Frontiers in Cell and Developmental Biology

REVIEW
published: 11 May 2022
doi: 10.3389/fcell.2022.884689

Plasmalogens and Photooxidative Stress Signaling in Myxobacteria, and How it Unmasked CarF/TMEM189 as the Δ1′-Desaturase PEDS1 for Human Plasmalogen Biosynthesis

S. Padmanabhan[1], Antonio J. Monera-Girona[2], Elena Pajares-Martínez[2], Eva Bastida-Martínez[2], Irene del Rey Navalón[2], Ricardo Pérez-Castaño[2], María Luisa Galbis-Martínez[2], Marta Fontes[2] and Montserrat Elías-Arnanz[2]**

[1]Instituto de Química Física "Rocasolano", Consejo Superior de Investigaciones Científicas, Madrid, Spain, [2]Departamento de Genética y Microbiología, Área de Genética (Unidad Asociada al IQFR-CSIC), Facultad de Biología, Universidad de Murcia, Murcia, Spain

OPEN ACCESS

Edited by:
Fabian Dorninger,
Medical University of Vienna, Austria

Reviewed by:
Katrin Watschinger,
Medical University of Innsbruck, Austria
Steve Holly,
Campbell University, United States

***Correspondence:**
S. Padmanabhan
padhu@iqfr.csic.es
Montserrat Elías-Arnanz
melias@um.es

Specialty section:
This article was submitted to Cellular Biochemistry, a section of the journal Frontiers in Cell and Developmental Biology

Received: 26 February 2022
Accepted: 25 April 2022
Published: 11 May 2022

Citation:
Padmanabhan S, Monera-Girona AJ, Pajares-Martínez E, Bastida-Martínez E, del Rey Navalón I, Pérez-Castaño R, Galbis-Martínez ML, Fontes M and Elías-Arnanz M (2022) Plasmalogens and Photooxidative Stress Signaling in Myxobacteria, and How it Unmasked CarF/TMEM189 as the Δ1′-Desaturase PEDS1 for Human Plasmalogen Biosynthesis. Front. Cell Dev. Biol. 10:884689. doi: 10.3389/fcell.2022.884689

Plasmalogens are glycerophospholipids with a hallmark *sn*-1 vinyl ether bond that endows them with unique physical-chemical properties. They have proposed biological roles in membrane organization, fluidity, signaling, and antioxidative functions, and abnormal plasmalogen levels correlate with various human pathologies, including cancer and Alzheimer's disease. The presence of plasmalogens in animals and in anaerobic bacteria, but not in plants and fungi, is well-documented. However, their occurrence in the obligately aerobic myxobacteria, exceptional among aerobic bacteria, is often overlooked. Tellingly, discovery of the key desaturase indispensable for vinyl ether bond formation, and therefore fundamental in plasmalogen biogenesis, emerged from delving into how the soil myxobacterium *Myxococcus xanthus* responds to light. A recent pioneering study unmasked myxobacterial CarF and its human ortholog TMEM189 as the long-sought plasmanylethanolamine desaturase (PEDS1), thus opening a crucial door to study plasmalogen biogenesis, functions, and roles in disease. The findings demonstrated the broad evolutionary sweep of the enzyme and also firmly established a specific signaling role for plasmalogens in a photooxidative stress response. Here, we will recount our take on this fascinating story and its implications, and review the current state of knowledge on plasmalogens, their biosynthesis and functions in the aerobic myxobacteria.

Keywords: plasmalogens, *Myxococcus xanthus*, CarF, lipid signaling, singlet oxygen, photoregulation, TMEM189, PEDS1

INTRODUCTION

Membranes are vital barriers between a living cell and its environment, and between subcellular compartments, which ensure selective trafficking of substances, signal sensing and transduction, energy generation, and enable many other functions indispensable for cell viability (Harayama and Riezman, 2018). Their basic and predominant components are lipids of highly diverse chemical structures, composition, and distribution, depending on the organism, cell type or organelle. Lipids affect membrane properties, like rigidity and fluidity, and serve as platforms for other crucial

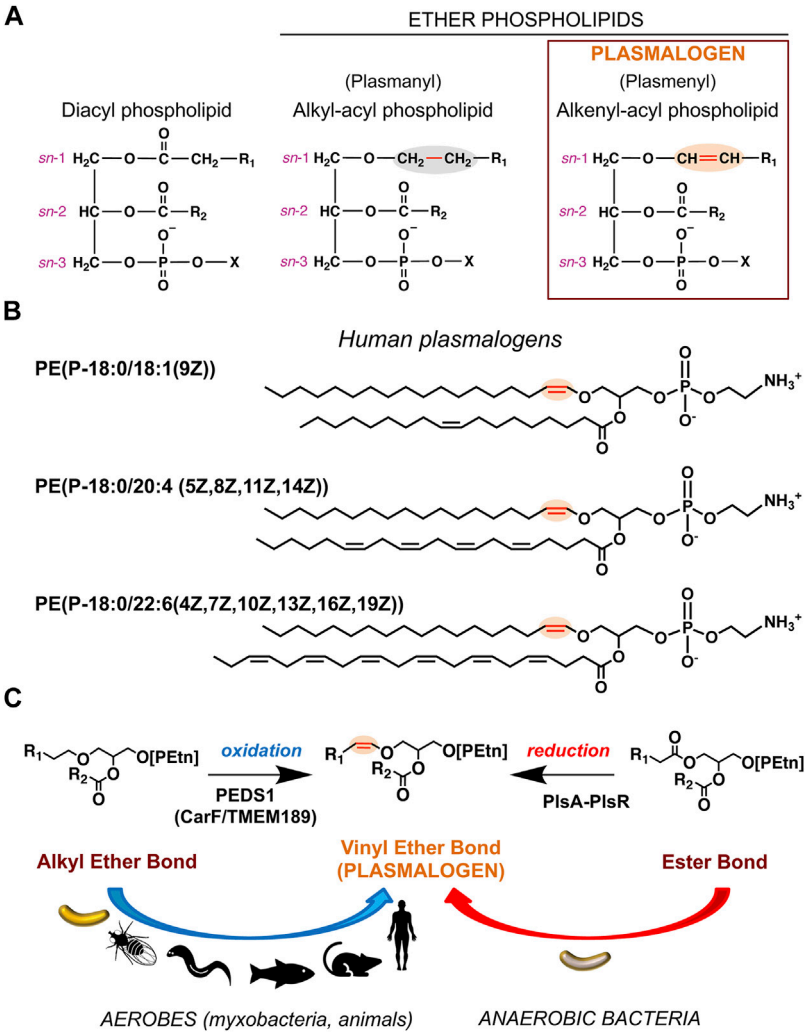

FIGURE 1 | Chemical structures of plasmalogens and generation of the hallmark vinyl ether bond. **(A)** Chemical structures represented as Fischer projections of the ester-linked diacyl glycerophospholipids (left), alkyl ether lipids (middle), and vinyl ether lipids or plasmalogens (right). The vinyl ether and its precursor alkyl ether bond are highlighted in red and shaded orange and grey, respectively; *sn* positions are indicated; R_1 and R_2 represent hydrocarbon chains at the *sn*-1 and *sn*-2 positions, respectively; X = ethanolamine (Etn) or choline (Cho) moiety. **(B)** Representative human plasmalogens. PE (P-18:0/18:1 (9Z)) or 1-(1Z-octadecenyl)-2-(9Z-octadecenoyl)-sn-glycero-3-phosphoethanolamine; PE (P-18:0/20:4 (5Z,8Z,11Z,14Z)) or 1-(1Z-octadecenyl)-2-(5Z,8Z,11Z,14Z-eicosatetraenoyl)-sn-glycero-3-phosphoethanolamine (5Z,8Z,11Z,14Z-eicosatetraenoyl = arachidonyl); PE (P-18:0/22:6 (4Z,7Z,10Z,13Z,16Z,19Z)) or 1-(1Z-octadecenyl)-2-(4Z,7Z,10Z,13Z,16Z,19Z-docosahexaenoyl)-sn-glycero-3-phosphoethanolamine. LIPID MAPS Structure Database (https://www.lipidmaps.org/databases/lmsd) common and systematic names are used. **(C)** Vinyl ether bond formation in plasmalogens by the aerobic (oxidative) pathway in myxobacteria and animals and the anaerobic (reductive) route in anaerobic bacteria.

biomolecules, like proteins and carbohydrates. Lipids are classified into eight categories based on the chemically functional backbone and further divided into classes and subclasses depending on their alkyl/acyl unit size, number and position(s) of double bond(s), hydroxylation, presence/type of polar headgroups, and presence of ester or ether bonds (Fahy et al., 2009). Plasmalogens, the theme of the current Research Topic, belong to a major membrane lipid category known as glycerophospholipids (GPs), defined by a glycerol backbone, one of whose hydroxyl groups is esterified to a phosphate (or phosphonate (Metcalf and van der Donk, 2009; Horsman and Zechel, 2017)) group at the *sn*-3 position (*sn*, stereospecific numbering). Typical GPs (or diacyl GPs) have both remaining hydroxyl groups linked through ester bonds to long-chain fatty acids, whereas ether GPs have an ether bonded alkyl chain at *sn*-1 and an ester bonded fatty acid at *sn*-2 (**Figure 1A**). Variants with a second ether-linked alkyl group at *sn*-2 reportedly occur in some bacteria (Caillon et al., 1983). The alkyl chains, especially in mammals, are 16 or 18 carbon atoms long, usually saturated (**Figure 1B**) or monounsaturated, while in bacteria they often have odd number of carbon atoms and can be saturated, unsaturated, and iso-branched (Kaneda, 1991; Rezanka and Sigler, 2009; Sohlenkamp and Geiger, 2016). Among ether lipids with an *sn*-2 fatty acyl group, plasmanyl GPs contain an

sn-1 alkyl group (1-*O*-alkyl, linked by an ether bond), while plasmenyl GPs contain an *sn*-1 alkenyl group (1-*O*-alk-1′-enyl, with a double bond adjacent to the ether linkage or vinyl ether bond) and are known as plasmalogens (**Figure 1A**).

Plasmalogens were identified a century ago and so named as the source of "plasmal", the aldehyde produced by acid treated cell plasma (Feulgen and Voit, 1924; Snyder, 1999). Their presence in animals and anaerobic bacteria is well established, as also their absence (save some stray reports) in plants and fungi (Braverman and Moser, 2012; Goldfine, 2017; Zhou et al., 2020; Vítová et al., 2021). Obligate or facultative aerobic bacteria are often described as lacking plasmalogens but this ignores a striking exception, the obligately aerobic myxobacteria, where the presence of plasmalogens was first reported 50 years ago (Kleinig, 1972) and confirmed in subsequent studies (Stein and Budzikiewicz, 1987; Curtis et al., 2006; Ring et al., 2006; Lorenzen et al., 2014a; Lorenzen et al., 2014b; Gallego-García et al., 2019). When present, plasmalogens often exceed other ether lipids in abundance and can constitute as much as a fifth of the mammalian phospholipidome (Braverman and Moser, 2012). Their composition varies with organisms, organelles, and cell types. Enriched in the brain, heart, kidney, lung, skeletal muscle, and neutrophils but low in the liver, plasmalogens occur in almost all subcellular membranes except in peroxisomes, the site of the early steps in their biosynthesis (Braverman and Moser, 2012). Their levels fluctuate with age, growth, and environmental conditions and reflect a balance between biosynthesis and degradation. In mammals, the first step in their biosynthesis, the generation of a fatty alcohol by FAR1, a peroxisome-associated fatty alcohol reductase that preferentially reduces C16 and C18 fatty acyl-CoAs (see below), is proposed to be rate-limiting. Plasmalogen levels appear to modulate feedback regulation as well as degradation of FAR1, but the underlying molecular mechanisms for sensing, signaling and spatiotemporal regulation remain undetermined (Honsho and Fujiki, 2017). Moreover, crosstalk and co-regulation of ether lipids and plasmalogens with other lipid classes form an important part of the complex interconnections in membrane lipid metabolism and homeostasis networks (Jiménez-Rojo and Riezman, 2019). In bacteria, lipids and their compositions also vary with species, growth and environmental conditions (Sohlenkamp and Geiger, 2016). For example, in the aerobic plasmalogen-producing soil myxobacterium *Myxococcus xanthus*, large shifts in lipid composition accompany the starvation-induced development of vegetatively growing cells into multicellular spore-filled fruiting bodies (Lorenzen et al., 2014b; Ahrendt et al., 2015).

Abnormalities and deficiencies in ether lipid/plasmalogen levels have been linked to various human pathologies ranging from rare genetic disorders (Rhizomelic chondrodysplasia punctata, Zellweger syndrome) to cancer, neurodegenerative diseases like Alzheimer's disease, and metabolic disorders (Braverman and Moser, 2012; Dean and Lodhi, 2018; Paul et al., 2019). Recently, plasmalogens were implicated in cell fitness under hypoxia (low oxygen) conditions (Jain et al., 2020) and in ferroptosis (Zou et al., 2020; Cui et al., 2021). The special physicochemical attributes of the plasmalogen vinyl ether bond can affect membrane fluidity, signaling and function (Braverman and Moser, 2012; Jiménez-Rojo and Riezman, 2019), and its susceptibility to cleavage by reactive oxygen species (ROS) such as singlet oxygen ($^1O_2$) yields products that may act as second messengers (Morand et al., 1988; Zoeller et al., 1988; Stadelmann-Ingrand et al., 2001; Jenkins et al., 2018; Gallego-García et al., 2019). Membrane microdomain platforms called lipid rafts, proposed to recruit and activate signaling proteins, are enriched in plasmalogens (Pike et al., 2002; Braverman and Moser, 2012; Dean and Lodhi, 2018). Hence, plasmalogens have been associated with antioxidative and signaling mechanisms. Yet, despite their abundance, links to disease and distinctive properties, studies on plasmalogens, although rising in recent years, remain modest when compared to other lipid classes, and their exact biological functions and the molecular basis of their actions continue to be enigmatic.

Multistep pathways have been charted for the aerobic plasmalogen biosynthesis in mammals and for a different oxygen-independent route in anaerobic bacteria, with enzymes for most of the proposed steps identified (Braverman and Moser, 2012; Goldfine, 2017; Vítová et al., 2021). Even so, the key enzymes that generate the characteristic plasmalogen vinyl ether bond in the final steps of both pathways remained unknown and were discovered only very recently (**Figure 1C**). A year ago, one study identified a two-gene bacterial operon encoding a multidomain complex for the anaerobic reduction-dehydration that converts the *sn*-1 ester bond of a diacyl lipid into a vinyl ether one (Jackson et al., 2021). It also reported that diverse facultative anaerobic bacteria, including many human gut microbes, can and do make plasmalogens, not just obligate anaerobes as suggested earlier (Goldfine, 2010). Two years ago, work on photooxidative stress signaling in the obligately aerobic *M. xanthus* led to the discovery that the oxygen-dependent desaturase for plasmalogen biosynthesis is a membrane protein called CarF, and that this protein is functionally conserved in sequence homologues denoted TMEM189 in human, mouse, zebrafish, fruit fly or nematodes (Gallego-García et al., 2019). The unmasking of this mammalian enzyme, now named PEDS1 and sought for five decades, was reinforced further in two subsequent reports (Werner et al., 2020; Wainberg et al., 2021). Besides revealing the identity of a key enzyme for aerobic plasmalogen biogenesis and its remarkable evolutionary conservation from bacteria to humans, the study in *M. xanthus* unearthed a specific signaling role for plasmalogens in directing a response to $^1O_2$ and photooxidative stress. We discuss below these aspects of aerobic plasmalogen biosynthesis and signaling roles in myxobacteria.

Myxococcus xanthus AND MYXOBACTERIA- AN OVERVIEW

M. xanthus is a Gram-negative soil bacterium and the best studied member of myxobacteria. These constitute the order Myxococcales, currently in the Deltaproteobacteria class of the phylum Proteobacteria, but recently proposed for reclassification as a new phylum named Myxococcota, with the order comprising three suborders (Cystobacterineae,

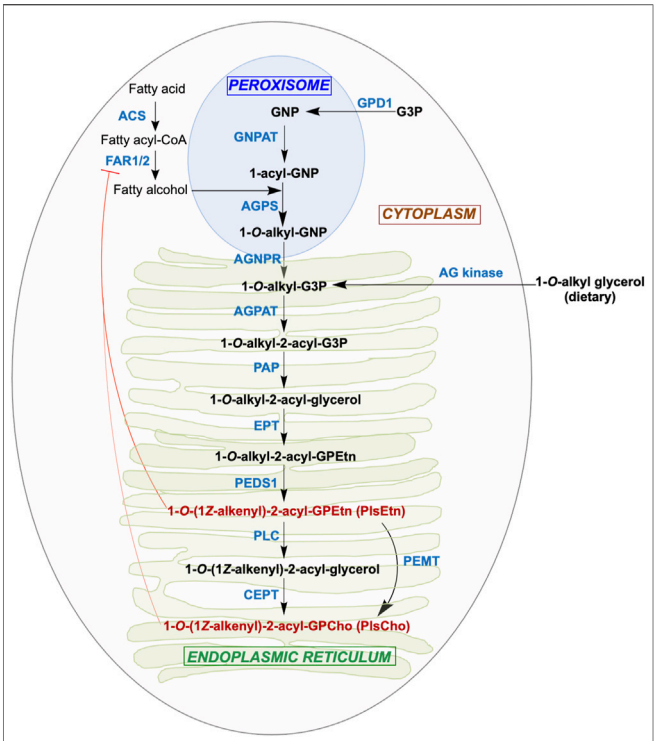

FIGURE 2 | Aerobic plasmalogen biosynthesis pathway in mammals. Synthesis of the major ethanolamine form of the plasmalogen (PlsEtn) begins in the peroxisomes and ends in the ER, followed by transport to post-Golgi compartments. The substrate and product (black boldface), abbreviated enzyme names (blue boldface; see text for full names and Enzyme Comission numbers), the organelle where each step takes place, and feedback regulation of FAR1 by plasmalogens (red blunt ended arrow) are shown.

Sorangiineae, Nannocystineae) and 10 families (Mohr, 2018; Vos, 2021; Pérez-Castaño et al., 2022). Widely distributed, most myxobacteria are soil-dwelling, though examples in aquatic environments are also known, and all are obligate aerobes except for the facultative anaerobic genus *Anaeromyxobacter*. Their GC-rich (66–75%) genomes are among the largest in bacteria (~9–16 Mb; 9.14 Mb and around 7,500 genes in *M. xanthus*) but reduced with extensive gene loss in *Anaeromyxobacter* (~4.4 Mb) and *Vulgatibacter incomptus* (~5 Mb). They are an important source, albeit not fully tapped, of many unique bioactive compounds and secondary metabolites that are often drug leads for pharmaceutical applications (Bader et al., 2020). Myxobacteria are striking in their complex lifestyles, with some traits usually attributed to eukaryotes, like multicellular development, social cooperative behavior, kin recognition, predation, motility and, pertinent to this review, biosynthesis of specialized lipids and steroids (Muñoz-Dorado et al., 2016; Cao and Wall, 2019; Gallego-García et al., 2019; Hoshino and Gaucher, 2021). These aspects have been investigated in *Myxococcus xanthus* that, as a model bacterial system to study light sensing and response, has uncovered new photosensory transduction and gene regulation paradigms (Elías-Arnanz et al., 2011; Padmanabhan et al., 2021), including the aforementioned conserved desaturase for plasmalogen biosynthesis (Gallego-García et al., 2019).

MAMMALIAN AEROBIC PLASMALOGEN BIOSYNTHESIS

An obligate aerobe with the same enzyme PEDS1 for a key late step in plasmalogen biogenesis as in animals, *M. xanthus* may share other parallels with the mammalian pathway. The latter (**Figure 2**), which has been reviewed elsewhere (Nagan and Zoeller, 2001; Braverman and Moser, 2012; Dean and Lodhi, 2018; Zhou et al., 2020; Vítová et al., 2021), begins in the peroxisome and ends in the endoplasmic reticulum (ER). The earliest steps in the peroxisomal lumen use as substrates: 1) imported dihydroxyacetone phosphate (DHAP) or glycerone phosphate (GNP), derived from glycerol 3-phosphate (G3P), possibly catalyzed by glycerol 3-phosphate dehydrogenase 1 (GPD1; Enzyme Comission number EC 1.1.1.8); 2) long-chain (C16, C18) fatty alcohols generated by the action of fatty acyl-CoA reductase (FAR1 or the less broadly distributed FAR2; EC 1.2.1.84) on fatty acyl-CoA, produced from fatty acid by acyl-CoA synthase (ACS; EC 6.2.1.3). FAR1 is tail anchored to the peroxisome membrane cytosolic face and is also found in lipid droplets (Exner et al., 2019). Glycerone phosphate *O*-acyltransferase (GNPAT; EC 2.3.1.42) converts GNP to 1-acyl-GNP, whose acyl chain is then replaced by a fatty alcohol to yield 1-*O*-alkyl-GNP (AGP) in a reaction catalysed by alkylglycerone-phosphate synthase (AGPS; EC 2.5.1.26). GNPAT and AGPS function as a complex to optimize substrate channeling and catalytic efficiency. In the next step, the acylglycerone-phosphate reductase (AGNPR or PexRAP, for peroxisomal reductase activating PPARγ; EC 1.1.1.101), localized in the ER and peroxisomal membranes (Lodhi et al., 2012; Honsho et al., 2020), reduces 1-*O*-alkyl-GNP to 1-*O*-alkyl-G3P, which can also be supplied by phosphorylation of dietary 1-*O*-alkylglycerol (AG) by alkylglycerol kinase (AG kinase; EC 2.7.1.93) (Snyder, 1992). Exchange of 1-*O*-alkyl-G3P and other lipids between peroxisomes and the ER is mediated by peroxisome-ER tethering, which relies on the interactions of the peroxisomal membrane protein ACBD5 (acyl-CoA binding domain containing 5) with cytosolic regions of the ER-resident VAMP-associated proteins VAPA and VAPB (Hua et al., 2017).

The remaining steps in the ER to produce plasmalogens mirror those for ester-linked diacyl GP biosynthesis from diacyl-G3P. Acylation at the *sn*-2 position of 1-*O*-alkyl-G3P by an alkylglycerolphosphate 2-*O*-acyltransferase (AGPAT; EC 2.3.1.-) yields 1-*O*-alkyl-2-acyl-G3P, whose phosphate group removal by phosphatidate phosphatase (PAP; EC 3.1.3.4) produces 1-*O*-alkyl-2-acyl-glycerol. To this, ethanolamine (Etn) phosphotransferase (EPT; EC 2.7.8.1) adds a phospho-Etn group from cytidine diphosphate ethanolamine to produce 1-*O*-alkyl-2-acyl-GPEtn. This alkyl ether (plasmanyl) lipid is the substrate for the oxygen and cytochrome *b5*-dependent TMEM189 or plasmanylethanolamine desaturase (PEDS1; EC 1.14.19.77), which generates the vinyl ether bond in PlsEtn, the

Etn plasmalogen. Conversion of PlsEtn to the choline (Cho) form, PlsCho, is achieved either by phosphatidylethanolamine N-methyltransferase (PEMT; EC 2.1.1.17) or by removal of phospho-Etn by phospholipase C (PLC; EC 3.1.4.3) and phospho-Cho addition by choline/ethanolamine phosphotransferase 1 (CEPT; EC 2.7.8.2). In most mammalian tissues, PlsEtn generally predominates and is longer-lived than PlsCho (Braverman and Moser, 2012; Messias et al., 2018). Although the above enzymatic steps were established early on, some of the actual enzymes involved were unknown and described as "orphan" (Watschinger and Werner, 2013). The identities of some of these, like TMEM189, or the exact roles and cellular locations of others, like EPT/CEPT, were established just recently (Horibata et al., 2020), which presages that new players with possibly new roles may emerge in future studies.

Regulation of plasmalogen biosynthesis and metabolism would be expected at several levels, given the multiple enzymes involved, the need for coordinated transport of precursors and products to target organelles and membranes, and links to degradation and turnover. Feedback regulation and degradation of FAR1 (hence, fatty alcohol substrate availability) by cellular plasmalogen levels, and crosstalk and co-regulation of ether lipids/plasmalogens and some other lipid classes, have been mentioned (Honsho and Fujiki, 2017; Jiménez-Rojo and Riezman, 2019). But in contrast to many other lipid classes, transcriptional and post-translational regulatory mechanisms in plasmalogen biosynthesis remain largely unknown. The plasmalogen vinyl ether bond can be cleaved by plasmalogenase activity of cytochrome *c* in the presence of cardiolipin, O_2 and H_2O_2, or oxidized cardiolipin and O_2, to produce 2-acyl-lysophospholipids and α-hydroxy fatty aldehydes; or by acidic HOCl or HOBr generated by leukocyte myeloperoxidase to yield α-haloaldehydes (Jenkins et al., 2018; Ebenezer et al., 2020). The vinyl ether bond in lysoplasmalogen, lacking the *sn*-2 acyl group, is reportedly targeted by lysoplasmalogenase (TMEM86B), which is localized at the cytoplasmic membrane (Wu et al., 2011). On the other hand, ER membrane-localized alkylglycerol monooxygenase (AGMO or TMEM195) cleaves the alkyl (not vinyl) ether bond in alkylglycerols or lyso-alkylGPs to generate a fatty aldehyde and the corresponding glycerol derivative (Watschinger et al., 2010). Although there is evidence that these degradation products may act as signaling molecules or second messengers, many questions remain, including their possible links to plasmalogen biosynthesis (Dorninger et al., 2020; Ebenezer et al., 2020). In short, regulation of plasmalogen biosynthesis may occur at multiple levels but most of the mechanisms involved remain to be elucidated.

AEROBIC PLASMALOGEN BIOSYNTHESIS IN MYXOBACTERIA

Compared to mammals, far less is known about ether lipid or plasmalogen biosynthesis in aerobic myxobacteria. In the best-studied *M. xanthus*, a complete data set for molecular lipid species was reported less than a decade ago (Lorenzen et al., 2014a; Lorenzen et al., 2014b) and culminated preceding studies (Curtis et al., 2006; Ring et al., 2006; Hoiczyk et al., 2009). The predominance of iso-branched fatty acids (FAs) in *M. xanthus* and some other myxobacteria was described 50 years ago (Ware and Dworkin, 1973), as also the presence of alkyl-acyl and alk-1′-enyl-acyl phosphoglycerides (Kleinig, 1972), with the latter shown to correspond to plasmalogens over a decade later (Stein and Budzikiewicz, 1987). The principal plasmalogen, denoted MxVEPE, and the corresponding alkyl ether plasmanyl form (MxAEPE) are both Etn GPs (*M. xanthus* is devoid of Cho GPs) with iso-branched C15 (i15:0) chains at both the *sn*-1 and *sn*-2 positions, although low levels of i17:0 can be found at *sn*-2 (**Figure 3A**). Under both vegetative and starvation conditions, MxVEPE far exceeds MxAEPE (Lorenzen et al., 2014a; Lorenzen et al., 2014b). Moreover, during starvation, which induces fruiting body formation, neutral ether lipids like 1-*O*-alkyl-*sn*-glycerol, 1-*O*-alkyl-2-acyl-*sn*-glycerol and, primarily, 1-*O*-alkyl-2,3-diacyl-*sn*-glycerol (TG-1; **Figure 3A**), accumulate in lipid bodies (Ring et al., 2006; Hoiczyk et al., 2009). TG-1, rare in nature like other diacylglycerol ether lipids, is a reported signal for *M. xanthus* fruiting body development (Bhat et al., 2014a).

Even though the identity of the Δ1′-desaturase required for aerobic plasmalogen synthesis was first unmasked in *M. xanthus* (Gallego-García et al., 2019), most other steps and relevant enzymes in the pathway remain uncharacterized. A feature of the mammalian pathway is the distribution of defined steps among organelles. This is unlikely in a prokaryote like *M. xanthus*, but there is increasing evidence that microcompartments or organelles in bacteria, including myxobacteria, can sequester and control specific metabolic pathways (Kerfeld et al., 2018; Greening and Lithgow, 2020). The formation of iso-branched FAs required early in *M. xanthus* plasmalogen biosynthesis (**Figure 3B**), which has been studied in some detail, occurs through two-carbon extensions of the starting unit isovaleryl-CoA to full length via the fatty acid synthase cycle and several proposed enzymes (Bhat et al., 2014b). Two distinct pathways generate isovaleryl-CoA, whose levels fall drastically when both routes are disrupted. One is the standard pathway for leucine degradation (also for valine or isoleucine) by the multisubunit branched-chain α-keto acid dehydrogenase (Bkd; or Esg, from E-signal) complex (Toal et al., 1995). A two-gene operon encodes the E1α and E1β α-ketoacid dehydrogenase subunits, while two proximal genes at another genomic locus encode the E2 dihydrolipoamide acetyl transacylase and E3 dihydrolipoamide dehydrogenase subunits. Transcription of these genes, which would be important in the regulation of branched-chain fatty acid synthesis, and thereby of ether lipids, depends on the growth medium (Bartholomeusz et al., 1998), but the molecular mechanisms involved remain unresolved. The alternative isovaleryl-CoA biosynthesis (Aib) pathway is an offshoot, possibly unique to myxobacteria, of the well-known mevalonate pathway for isoprenoid biosynthesis. It involves a gene for a 3-hydroxy-3-methylglutaryl coenzyme A dehydratase (LiuC) and a five-gene Aib operon. The latter operon encodes a transcriptional

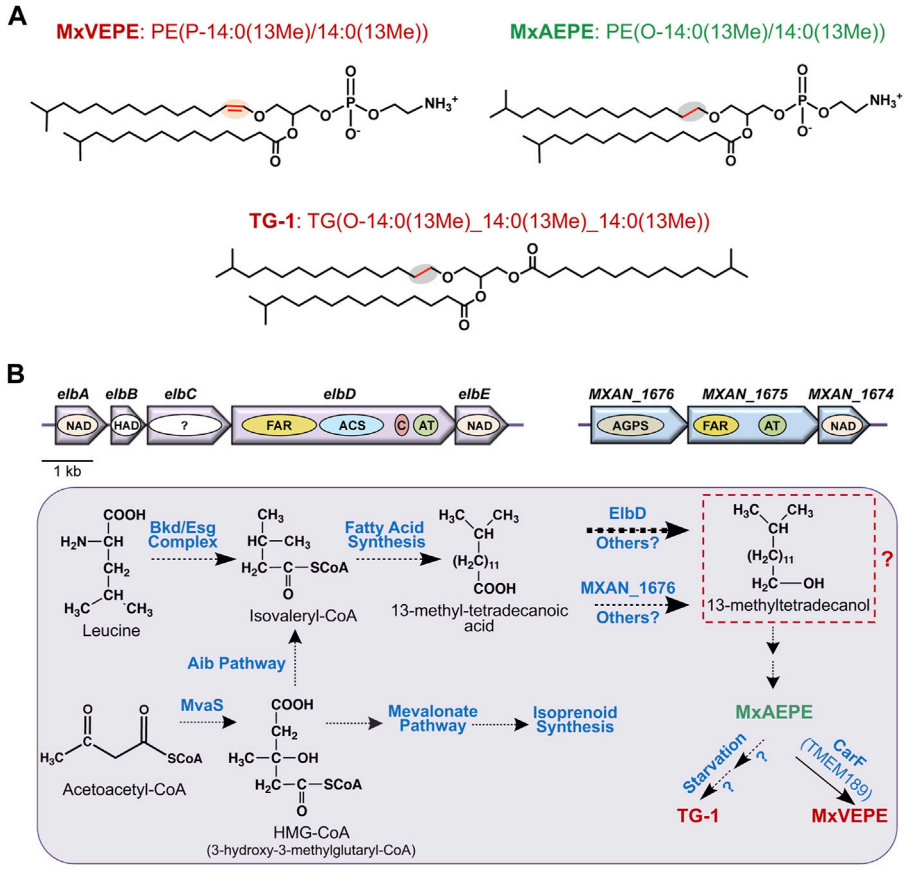

FIGURE 3 | *M. xanthus* alkyl ether lipids, plasmalogens and their biosynthesis. **(A)** *M. xanthus* plasmalogen MxVEPE: 1-(13-methyl-1Z-tetradecenyl)-2-(13-methyl-tetradecanonyl)-sn-glycero-3-phosphoethanolamine; its alkyl ether (plasmanyl) precursor MxAEPE: 1-(13-methyl-tetradecanyl)-2-(13-methyl-tetradecanoyl)-sn-glycero-3-phosphoethanolamine; and the alkyldiacylglycerol ether lipid TG-1: rac1,2-di-(13-methyltetradecanoyl)-3-(13-methyltetradecyl)-glycerol. LIPID MAPS Structure Database (https://www.lipidmaps.org/databases/lmsd) systematic and common names are used. **(B)** Plasmalogen biosynthesis pathway in *M. xanthus* highlighting known and proposed steps. Top: The *elbA-elbE* and the *MXAN_1676-MXAN_1674* operons. Arrows indicate genes and the ovals inside depict proteins or putative domains. AGPS, FAR, and ACS are as in **Figure 2**, AT is acyltransferase (AGPAT/GNPAT-like); C is acyl-carrier protein or ACP; NAD is an NAD-dependent epimerase/dehydratase family protein; "?" is a protein domain of unknown function. Bottom: Proposed and known steps in *M. xanthus* plasmalogen biosynthesis. Broken arrows indicate multiple steps involved, and the thick arrow for ElbD indicates this pathway is predominant. Steps from the iso-branched fatty acid to the alkyl ether lipid MxAEPE are unknown and may involve hypothetical conversion to a fatty alcohol (red dashed box) as in the mammalian aerobic plasmalogen biosynthesis pathway.

regulator (AibR), the 3-hydroxy-3-methylglutaryl coenzyme A synthase (MvaS), two subunits of a novel type of decarboxylase (AibA and AibB), and a medium-chain reductase-dehydrogenase (AibC). AibR, when bound to isovaleryl-CoA, downregulates the Aib operon and a gene encoding a putative acetyl-CoA acetyltransferase that likely catalyzes formation of the MvaS substrate acetoacetyl-CoA (Mahmud et al., 2002; Bode et al., 2006; Bode et al., 2009; Li et al., 2013; Bock et al., 2016; Bock et al., 2017a; Bock et al., 2017b). Interestingly, Aib pathway genes are upregulated upon starvation (when Bkd pathway genes are downregulated), and also in *bkd* mutants (Bode et al., 2009; Bhat et al., 2014b; Muñoz-Dorado et al., 2019), presumably to ensure supply of isovaleryl-CoA for iso-branched fatty acid synthesis-homeostasis under different conditions.

The pathway from iso-branched fatty acids to plasmalogens and the enzymes involved are unknown, except for the final steps, which emerged from two key recent studies. The first (Lorenzen et al., 2014a) described a multidomain protein, ElbD, encoded in a five-gene ether lipid biosynthesis *elb* operon (**Figure 3B**). Its study stemmed from examining the *M. xanthus* genome for genes encoding enzymes akin to ones known in plasmalogen biosynthesis. Thus, ElbD was annotated as a putative long-chain-fatty-acid CoA ligase with an N-terminal domain similar to FAR1, which generates fatty alcohol from fatty acid early in the mammalian pathway, and domains for ACS, which produces the FAR1 substrate, for acyl–carrier protein (ACP) and for an AGPAT-like acyltransferase (**Figures 2**, **3B**). The *elbD* gene is flanked by *elbC*, which encodes a protein of unknown function, and by *elbE*, which encodes an NAD-dependent epimerase/dehydratase family protein, as does *elbA*. The fifth gene in the operon, *elbB,* encodes a protein of the haloacid dehalogenase (HAD)-like phosphohydrolase superfamily, whose members have diverse functions. The *M. xanthus* genome also revealed a three-gene operon (**Figure 3B**) comprising: 1) *MXAN_1676*,

whose product is ~42% identical (92% coverage) in sequence to human AGPS, which acts in the second peroxisomal step of ether lipid biosynthesis (**Figure 2**); 2) *MXAN_1675*, encoding a protein with an N-terminal FAR1-like domain and a C-terminal GNPAT-like acyltransferase domain; 3) *MXAN_1674,* encoding a putative NAD-dependent epimerase/dehydratase family protein, like ElbA and ElbE. The similarities of MXAN_1675 and MXAN_1676 to eukaryotic enzymes and their possible implication in *M. xanthus* ether lipid biosynthesis had been noted and suggested, but not established, in an earlier study (Curtis et al., 2006). Disrupting *MXAN_1676*, however, caused only a minor reduction in ether lipids, suggesting an alternative pathway that was shown to depend on ElbD (Lorenzen et al., 2014a).

Insertion mutagenesis of *elbD* was found to strongly reduce vinyl and alkyl ether lipid content under both vegetative and starvation conditions and was rescued by complementation with *elbD* (Lorenzen et al., 2014a). Since insertions in *elbA* had no effects, ElbA was considered to be uninvolved in ether lipid synthesis. Insertions in *elbB* reduced vinyl and alkyl ether lipid levels, though not as much as in *elbD* mutants, and was partially restored by expression of *elbD*. This was attributed to polar effects of the *elbB* disruption. Finally, inactivating *elbE* decreased ether lipid formation and was not complemented by an extra copy of *elbD*. The study thus concluded that ElbD, and possibly ElbE, were important in *M. xanthus* ether lipid and plasmalogen biosynthesis. ElbD and a truncated form lacking the N-terminal putative FAR1-like domain could be purified as soluble proteins, which suggests ElbD is cytosolic. Analysis *in vitro* confirmed the ACP and ACS activities for these two ElbD domains, but the FAR1 and AGPAT domains could not be evaluated since no acyltransferase protein activity was detected with isolated ElbD, and fatty alcohols linked to FAR activity were undetected (Lorenzen et al., 2014a). Because an i15:0 aldehyde could be identified in wild-type strains but not in *elbD* mutants, it was proposed that the ElbD acyl-CoA reductase activity was to reduce CoA-bound fatty acid to the aldehyde, and that this was somehow involved in vinyl ether bond formation. Since only alkenyl and not alkyl Etn GPs were detectable in *M. xanthus* under vegetative and developmental conditions, a "reductive" ether lipid formation pathway was considered, with conversion of MxVEPE to MxAEPE to TG-1 (Ring et al., 2006; Lorenzen et al., 2014a). Such a route, which drew upon clues from the anaerobic pathway, would be unprecedented and is now implausible in light of the discovery that CarF drives aerobic oxidation of MxAEPE to MxVEPE (**Figure 1C**).

Lipid profiles along the *M. xanthus* life cycle have indicated that alkyl ether lipids accumulate only during development, when TG-1 reaches high levels while MxVEPE decreases gradually from ~10% relative abundance in vegetative cells to ~4% in mature fruiting bodies (Lorenzen et al., 2014a; Lorenzen et al., 2014b; Ahrendt et al., 2015). By comparison, the most abundant diacyl Etn GP decreases far more sharply, to 5% of the vegetative levels. Ether lipid metabolism has thus been inferred to exhibit differences in regulation and biosynthesis from the other lipids. Conclusive data are, however, needed regarding if and how the *elb* and *MXAN_1676* operons are regulated and what layers of regulation beyond transcription come into play. Identification of ElbD as a key player in *M. xanthus* alkyl ether lipid and plasmalogen biosynthesis provided a crucial launch point for further investigations, but many questions persist on the exact functions and biochemical mechanisms of ElbD and on the other players mentioned above. The recent finding that none of these generate the vinyl ether bond and that this task falls on CarF was therefore an important breakthrough.

PHOTOSENSORY SIGNALING IN *M. xanthus* CAROTENOID SYNTHESIS, CarF AND ITS EARLY CHARACTERIZATION

The surprising road to unmasking CarF in *M. xanthus* and its homologue TMEM189 in metazoa as the conserved Δ1′-desaturase for plasmalogen formation was paved in studies that examined how *M. xanthus* responds to light by synthesizing carotenoids, which quench $^1O_2$ produced upon illumination and thereby protect cells against photooxidative damage (Padmanabhan et al., 2021). Carotenoids are lipophilic isoprenoid pigments with extended, all-trans, conjugated polyene chains (usually C40, sometimes C50, C45 and C30 terpenes) with acyclic, monocyclic, or bicyclic ends. Their synthesis in *M. xanthus* is visibly reflected by cells that are yellow in the dark (due to noncarotenoid pigments) turning to an orange-red color upon exposure to light (**Figure 4A**).

Two modes of light sensing and signaling operate in *M. xanthus* to trigger a transcriptional response leading to carotenoid biosynthesis (Padmanabhan et al., 2021; Pérez-Castaño et al., 2022). In one, the photoreceptor protein CarH, with coenzyme B_{12} as its chromophore, directly senses UV, blue or green light and turns on transcription of genes encoding enzymes required for carotenogenesis (Ortiz-Guerrero et al., 2011; Jost et al., 2015; Padmanabhan et al., 2017; Padmanabhan et al., 2019; Padmanabhan et al., 2022). In the other mechanism (**Figure 4B**), blue light excites the iron-free heme precursor protoporphyrin IX or PPIX, a hydrophobic cyclic tetrapyrrole and photosensitizer that accumulates in the *M. xanthus* cell membrane especially during stationary phase (Burchard and Dworkin, 1966; Galbis-Martínez et al., 2012). PPIX photoexcitation generates the high-energy ^{3}PPIX triplet state, which can transfer energy to molecular oxygen yielding the extremely reactive and cytotoxic $^1O_2$, a relatively long-lived and diffusible ROS in membrane environments (Ziegelhoffer and Donohue, 2009; Glaeser et al., 2011). This photoinduced $^1O_2$ inactivates CarR (with six transmembrane helices) by an unknown mechanism to liberate CarQ, which is sequestered specifically at the membrane via its physical interaction with CarR. Free CarQ, in complex with RNA polymerase, activates transcription of genes for carotenoid synthesis. CarR belongs to a class of bacterial regulators known as anti-σ factors, which negatively control cognate factors known as extracytoplasmic function or ECF *σ* factors. Generally, specific signals inactivate a given anti-σ to liberate its cognate ECF *σ*, which associates with RNA polymerase to recognize defined promoters and initiate transcription of the corresponding genes (de Dios et al., 2021).

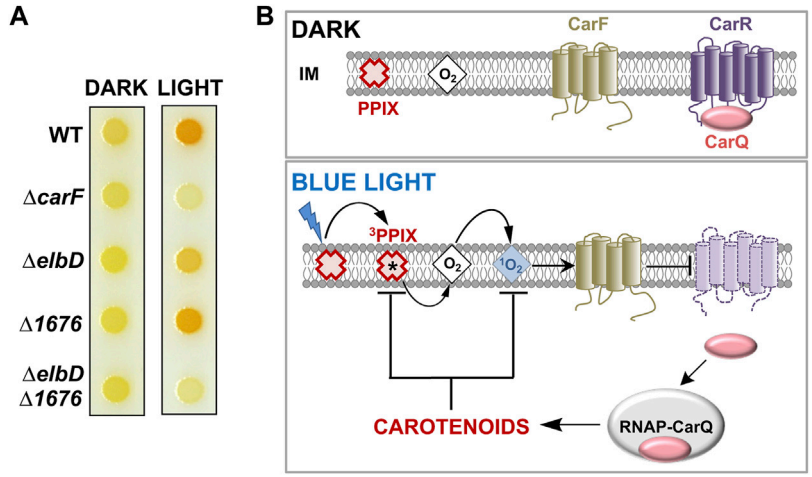

FIGURE 4 | Light response in *M. xanthus*. **(A)** *M. xanthus* colony color in the dark and in the light in the wild-type strain (WT) and with various indicated deletions (adapted from (Gallego-García et al., 2019)). **(B)** Simplified model for the blue light-PPIX-$^1O_2$ signal transduction pathway in *M. xanthus*. In the dark, an inner membrane (IM) anti-σ factor (CarR) with a six transmembrane-helix topology sequesters its cognate σ factor (CarQ). Blue light excites protoporphyrin IX (PPIX), the iron-free heme precursor and photosensitizer, to the high-energy ^{3}PPIX state, from which energy transfer to O_2 generates highly reactive $^1O_2$, which requires CarF to inactivate CarR by an unknown mechanism. This leads to the release of CarQ, which associates with RNA polymerase (RNAP) to activate specific genes enabling the synthesis of carotenoids to quench reactive $^1O_2$ and ^{3}PPIX and limit photooxidative damage (black arrows: activation; blunt-ended arrows: inactivation).

The quest to elucidate how light and $^1O_2$ cause inactivation of CarR led to the discovery of CarF.

The *carF* gene was identified two decades ago (Fontes et al., 2003) by genetic analysis of *M. xanthus* mutants devoid of light-induced carotenogenesis (hence the *car* nomenclature). Strains with *carF* disrupted or deleted (Δ*carF*) failed to produce carotenoids and therefore did not acquire the characteristic orange-red color in the light (**Figure 4A**). Moderate and steady levels of expression of *carF* over a wide range of conditions (dark or light, vegetative or stationary phase) were observed, and epistatic analysis established that CarF acted earlier than CarR in the signaling cascade (Fontes et al., 2003). The 281-amino acid CarF sequence was found to lack significant similarity to any bacterial or archaeal protein. But it strongly resembled (46% sequence identity, 59% similarity over a 237-residue stretch) a human protein of unknown function at the time that was named Kua (Thomson et al., 2000), but is now better known as TMEM189. CarF/Kua homologues were found in mouse (*Mus musculus*), zebrafish (*Danio rerio*), fruit fly (*Drosophila melanogaster*), worm (*Caenorhabditis elegans*), protozoa (*Leishmania*), and plants (*Arabidopsis thaliana*). The human gene for Kua/TMEM189 lies adjacent to *UEV1*, which encodes an inactive variant of E2 ubiquitin-conjugating enzymes. *Kua* and *UEV1* were found to be expressed as separate transcripts for the individual Kua and UEV1 proteins, but also as a rare hybrid transcript for a two-domain Kua-UEV1 fusion protein. The fusion product was also observed in rhesus monkey and chimpanzee but not in mice or non-mammals like *C. elegans* or *D. melanogaster* (Thomson et al., 2000; Duex et al., 2010). The Kua and CarF protein sequences suggested that they would be membrane proteins, with several histidines (see below) distributed in a pattern reminiscent of diiron histidine-rich motifs found on the luminal side of membrane fatty acid desaturases and hydroxylases (Shanklin et al., 2009). Interest in human Kua was, however, more centered on this rare inactive UEV fusion. Indeed, Kua homologues figured only as a UEV1 localization domain in a protein family PF10520 described as Kua-UEV1_localn; and their true function remained elusive even after a *Tmem189* knockout mouse was generated in a large-scale international mouse phenotyping consortium and several associated phenotypes, such as decreased body mass, and eye, bone and blood abnormalities were described (White et al., 2013).

What role CarF played in light-regulated carotenogenesis also remained enigmatic. It was demonstrated experimentally that CarF is a four-transmembrane helix topology protein that self-interacted and was essential in mediating the transmission of the $^1O_2$ signal in the trajectory from blue light to CarR inactivation (**Figure 4B**) (Galbis-Martínez et al., 2008; Galbis-Martínez et al., 2012). Nevertheless, the molecular interplay between CarF and $^1O_2$, whether it was direct or it involved one or more intermediary molecules still remained unanswered. How this was addressed and uncovered CarF function is described next.

UNMASKING CarF/TMEM189 AS THE CONSERVED Δ1′-DESATURASE FOR VINYL ETHER BOND FORMATION IN PLASMALOGEN BIOSYNTHESIS

An extensive search for homologues across a wide range of organisms revealed that CarF was confined to very few bacteria, mainly myxobacteria and a few *Leptospira* and Alphaproteobacteria, and that it was absent in archaea (Gallego-García et al., 2019). By contrast, CarF homologues

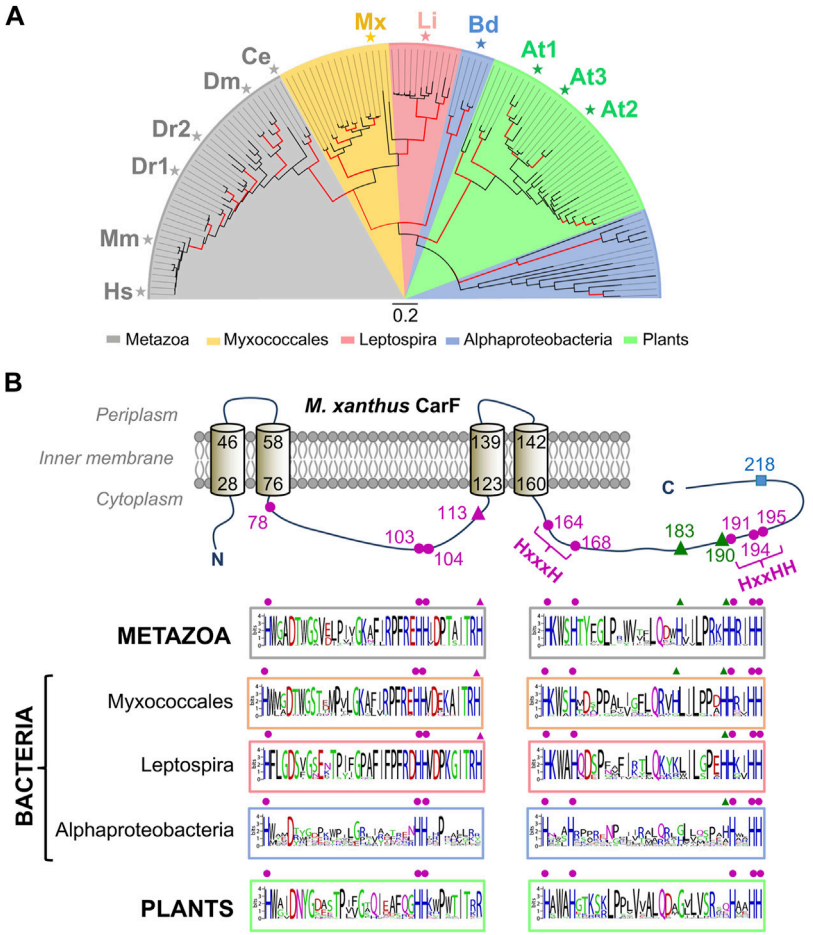

FIGURE 5 | Phylogenetic distribution and conserved histidines of CarF homologues. **(A)** Phylogenetic tree for CarF homologues in metazoa, bacteria and plants (maximum-likelihood with red branches for ≥ 75% confidence from 200 bootstrap replicates; scale bar, number of substitutions per residue; key below for colored sectors; adapted from (Padmanabhan et al., 2021). Homologues that were tested for CarF function in *M. xanthus* are indicated: Hs, *Homo sapiens*; Mm, *M. musculus*; Dr, *D. rerio* (two homologues); Dm, *D. melanogaster*; Ce, *C. elegans*; Mx, *M. xanthus*; Li, *Leptospira interrogans*; Bd, *Bradyrhizobium diazoefficiens*; At, *A. thaliana* (three homologues). **(B)** Top: *M. xanthus* CarF cartoon representation with its experimentally established four transmembrane-helix topology (helix delimiting residues numbered) and twelve histidines (all cytoplasmic and numbered). CarF histidines conserved in all homologues, whose mutation abolishes function, are depicted by the magenta dots; the one histidine in CarF present in homologues from metazoa, myxobacteria and *Leptospira* and also essential for function is depicted by the magenta triangle; the two histidines conserved only in some homologues (primarily, from metazoa and myxobacteria), whose mutation has no effect, are depicted as green triangles; the non-conserved and non-essential CarF histidine (H218) is depicted as a cyan square. Bottom: sequence logos for segments containing the conserved and semi-conserved histidines in CarF homologues from metazoa, bacteria and plants (histidines are aligned with the equivalent ones in the CarF cartoon and marked using the same symbols; adapted from (Gallego-García et al., 2019)).

were very prevalent among eukaryotes, invertebrate or vertebrate animal species, and also in plants, but very rare in fungi. Phylogenetic analysis based on more than a hundred homologues suggested that myxobacterial and *Leptospira* CarF homologues are more closely related to those in animals (TMEM189) than to those in Alphaproteobacteria and plants (**Figure 5A**). Most species have a single copy of the gene, with exceptions like zebrafish (with two copies at distinct loci; DR1 and DR2) or *A. thaliana* (with three copies; At1, At2, At3). Interestingly, within myxobacteria, CarF is largely restricted to the suborder Cystobacterineae, as are the counterparts to all of the known factors of the *M. xanthus* blue light-PPIX-$^1O_2$-CarR signaling pathway (Pérez-Castaño et al., 2022). Sequence analysis of CarF homologues and mutational analysis revealed that out of the twelve histidines in *M. xanthus* CarF, all of which would be in the cytoplasm (**Figure 5B**): 1) the eight that are conserved in all homologues, five of which are arranged as in motifs typically found in membrane fatty acid desaturases and hydroxylases, are essential for function (the orange-red colony color in the light, when cells have a functional CarF, provided a simple and valuable visual tool to assess function); 2) the one histidine (H113) present in homologues from metazoa, myxobacteria and *Leptospira*, but not in those from plants (where it is usually an arginine) or from Alphaproteobacteria, is also essential for function; 3) the remaining three histidines are not essential for function. One of the three homologues in *A. thaliana*, At3, turned out to be an elusive desaturase found in chloroplasts, named FAD4, which is the founding member of a

novel class of plant fatty acid desaturases that generate an unusual *trans* double bond between carbons 3 and 4 from the carboxyl end of the *sn*-2 acyl chain of a specific type of phosphatidylglycerol (Gao et al., 2009; Horn et al., 2020). These observations hinted that CarF could be a special type of desaturase, as was indeed demonstrated.

Lipid analysis of wild-type versus a Δ*carF* strain, and of the latter complemented with an inducible *carF* copy in *trans*, all pointed to CarF as essential in the formation of the *M. xanthus* plasmalogen MxVEPE (Gallego-García et al., 2019). Moreover, MxVEPE was produced when purified CarF was added to cell extracts of the Δ*carF* strain together with NADPH (nicotinamide adenine dinucleotide phosphate), a required cofactor for the Δ1′-desaturase activity (Blank and Snyder, 1992). How CarF function was linked to ElbD and MXAN_1676, implicated in *M. xanthus* alkyl ether lipid and plasmalogen biosynthesis, was evaluated by comparing the response to light and the lipid profiles of the Δ*carF* strain versus strains with a single in-frame deletion of *elbD* (Δ*elbD*) or *MXAN_1676* (Δ*1676*), or with the double Δ*elbD* Δ*1676* deletion (**Figure 4A**). Altogether, the data indicated that whereas ElbD and to a minor degree MXAN_1676 were required for MxAEPE formation, CarF was indispensable for MxVEPE formation (Gallego-García et al., 2019). Remarkably, *M. xanthus* light-induced carotenogenesis could be chemically complemented in strains lacking MxVEPE by feeding the cells with any of three human plasmalogens tested, whose moieties at *sn*-1 and *sn*-2 (**Figure 1B**) differ from those in MxVEPE (**Figure 3A**). Furthermore, so long as CarF was present, a human alkyl ether lipid precursor could also restore the response to light, via its conversion intracellularly into the corresponding plasmalogen (Gallego-García et al., 2019). These findings firmly established that CarF is the PEDS1 desaturase, whose principal specificity determinant appears to be the alkyl ether linkage, with the type or length of the alkyl and acyl chains in the plasmanyl precursor being less crucial. They also demonstrated that plasmalogens, and not their precursors, are specifically required in the blue light-PPIX-$^1O_2$ signaling pathway leading to CarR inactivation in the *M. xanthus* carotenogenic response.

Consistent with the phylogenetic analysis of CarF homologues, those from human, mouse, zebrafish, fruit fly and worm, as well as from the animal pathogen *Leptospira*, could complement lack of CarF in *M. xanthus* (Gallego-García et al., 2019), demonstrating that these were genuine functional homologues of CarF, whereas the three plant homologues in *A. thaliana* or that from Alphaproteobacteria were not. Moreover, knocking out TMEM189 in a human cell line was shown to produce loss of plasmalogens, which were restored by supplying TMEM189 in *trans*; and mutational analysis revealed that the nine histidines equivalent to those required for CarF function were also essential for human TMEM189 to function in *M. xanthus* (Gallego-García et al., 2019). In sum, CarF PEDS1 activity was shared by its animal homologues but not by those in plants, which accords with the presence of plasmalogens in animals but not in plants, as well as with *A. thaliana* FAD4 having a different desaturase activity. Importantly, it revealed the identity of the elusive desaturase for human plasmalogen synthesis, which was substantiated soon after by two other studies demonstrating the same *via* completely different approaches (Werner et al., 2020; Wainberg et al., 2021). In one study (Wainberg et al., 2021), a statistical method to identify gene co-essentiality and predict functions of uncharacterized genes inferred TMEM189 to be PEDS1, and experimentally demonstrated it by the marked decrease in plasmalogen levels observed upon targeting *TMEM189* expression in human cell lines, as well as by the decrease in TMEM189 protein levels in a plasmalogen-deficient cell line with deficient PEDS1 activity. In the other study (Werner et al., 2020), TMEM189 emerged as the candidate by comparing gene expression data and PEDS1 activity in various human cell lines and mouse tissues, and using the criterion that PEDS1 is a probable membrane protein present only in animals (since these, but not plants or fungi, synthesize plasmalogens) with histidine motifs of the type found in lipid desaturases. This study experimentally demonstrated loss of plasmalogen and PEDS1 activity by knocking out or silencing *TMEM189* in human cell lines (and recovery by specifically expressing *TMEM189*) as well as by showing lack of plasmalogen/PEDS1 activity in mice with inactivated *TMEM189*. It further demonstrated that the same nine histidines mentioned above as crucial for CarF and human TMEM189 were also required for PEDS1 activity of the murine homologue, in which mutating H131 (the CarF H113 counterpart) strongly reduced, but did not eliminate, plasmalogen production. Besides these histidines, an aspartate (D100) and a phenylalanine (F118) conserved in CarF/TMEM189 homologues (D99 and F117, respectively, in human TMEM189) were recently shown to be required for PEDS1 activity (Werner et al., 2022).

High-resolution structures of CarF or TMEM189 can provide valuable molecular insights into how PEDS1 generates the characteristic vinyl ether bond. These studies require pure proteins but, to our knowledge, only *M. xanthus* CarF has been purified as detergent-solubilized protein, which exhibited some PEDS1 activity and appeared oligomeric with two equivalents of bound iron (Gallego-García et al., 2019). CarF thus shares the reported features of many lipid desaturases, which use a diiron center to bind and activate molecular oxygen and have an oligomeric nature proposed to be important for activity (Shanklin et al., 2009; Liu et al., 2015). Because stable expression and purification of integral membrane desaturases is generally a formidable challenge, few high-resolution structures of these proteins have been resolved. One is that of the quintessential mammalian stearoyl-CoA desaturase (SCD), which catalyzes double bond formation on saturated acyl-CoA as substrate. Interestingly, like TMEM189, the also ER-localized SCD appears to be an oligomer (Zhang et al., 2005) and its regio- and stereo-specific activity requires NADPH, cytochrome b_5 reductase and cytochrome b_5. The reported SCD structures are, however, monomers with four transmembrane helices and a diiron center with nine coordinating histidines and a water molecule, that is, hydrogen bonded to an asparagine residue in the cytosolic domain (**Figure 6**) (Bai et al., 2015; Wang et al., 2015; Shen et al., 2020). In the absence of experimentally determined structures, the single-chain AlphaFold2 structure

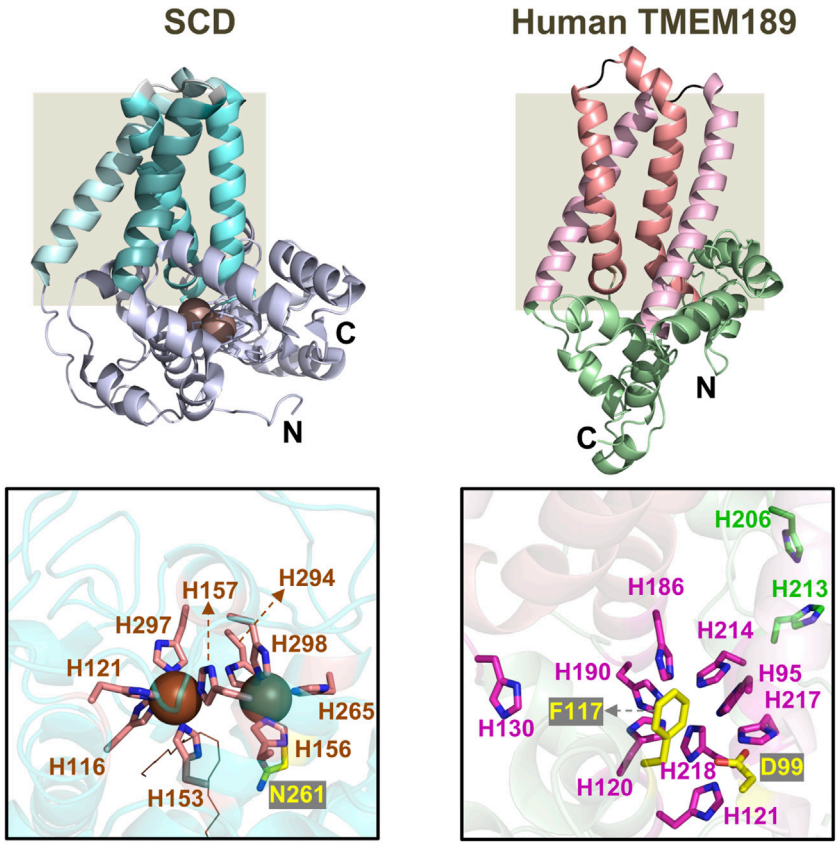

FIGURE 6 | The AlphaFold2 predicted structure of human TMEM189 compared to the crystal structure of SCD. Left: Crystal structure determined for mouse stearoyl-CoA desaturase/SCD (PDB accession code; 6WF2). Right: Single-chain AlphaFold2 structure of human TMEM189 (https://alphafold.ebi.ac.uk/entry/A5PLL7). The grey box highlights the transmembrane region with four helices in each structure. Shown below are close-ups of: (left) the diiron centre (dark spheres) and the nine coordinating His and one Asn (through a water molecule) in the SCD structure (a portion of the substrate in the active site is shown by thin lines); (right) the conserved His (magenta), Asp and Phe (both yellow) essential for function, and two conserved histidines (green) not required for activity in human TMEM189 (see text).

of human TMEM189 (**Figure 6**) publicly available for nearly a year now (Tunyasuvunakool et al., 2021), reveals the four transmembrane helix topology experimentally demonstrated for CarF (Galbis-Martínez et al., 2008) and a spatial arrangement of the nine histidines, the aspartate and the phenylalanine required for PEDS1 activity, all of which are likely retained in the functionally equivalent CarF. This predicted fold will aid future experimental structure determinations and structure-based functional analyses of CarF/TMEM189 and their mutants.

LIPID AND PLASMALOGEN SIGNALING IN *M. xanthus*

One of the clearest and most striking examples of signaling mediated specifically by plasmalogens is in the *M. xanthus* response to photooxidative stress (Gallego-García et al., 2019). It represents a new example of lipid signaling in *M. xanthus*, adding to those reported in gliding motility, chemotaxis, and the development of fruiting bodies and mature spores. Specific phosphatidylethanolamine (PE) lipids were described as chemoattractants in *M. xanthus* over 20 years ago (Kearns and Shimkets, 1998). They acted with two chemotaxis systems (Dif and Frz) that direct cell movements required for predation and fruiting body/spore formation of *M. xanthus*, a motile bacterium lacking flagella that glides slowly over solid surfaces (Kearns and Shimkets, 2001; Bonner and Shimkets, 2006; Zusman et al., 2007). Two specific PEs signaling this chemotactic response were dilauroyl (C12:0) and dioleoyl (C18:1 ω9c) PEs, which are absent in *M. xanthus* but occur in many of its prey bacteria and may be important in prey recognition. On the other hand, di [11-*Z*-hexadecenoyl] (C16:1ω5c), the third PE, is rare in bacteria but abundant in *M. xanthus* and may have roles in self-recognition (Curtis et al., 2006; Zusman et al., 2007). The two *M. xanthus* chemotaxis systems responded to these PEs via parallel, competing sensory pathways, albeit with some interdependence, to control motility (Kearns and Shimkets, 2001; Bonner and Shimkets, 2006; Zusman et al., 2007; Xu et al., 2008). Chemoreceptors present in fibrils, the extracellular appendages composed of a polysaccharide matrix and decorated with proteins of unknown function, were proposed for dilauroyl PE (Kearns and Shimkets, 2001), but those for the other two PEs are unknown. Whether PE plasmalogens also

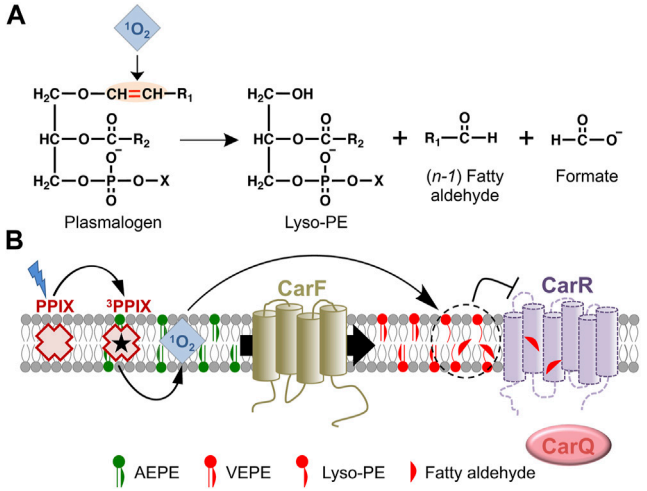

FIGURE 7 | Plasmalogen signaling in the *M. xanthus* response to photooxidative stress. **(A)** Cleavage by $^1O_2$ of the plasmalogen vinyl ether bond and its products. **(B)** Model for the plasmalogen-based signal transduction pathway leading to CarR inactivation in *M. xanthus* (arrows for activation; blunt ended for inactivation). As the PEDS1 desaturase, CarF converts (both in the dark and in the light) the plasmanyl precursor (AEPE) to plasmalogen (VEPE), which is absolutely required in the response to blue light. Generation of $^1O_2$ upon photoexcitation of PPIX provokes cleavage of VEPE at the vinyl ether bond, generating a fatty aldehyde and lyso-PE. This may inactivate CarR directly by adduct formation with the reactive fatty aldehyde or by lipid remodeling and perturbation of the local membrane structure around CarR, leading to a conformational change and/or degradation of CarR. As a consequence, CarQ is liberated, associates with RNA polymerase (RNAP), and activates specific genes leading to carotenoid synthesis.

participate, and details of the molecular mechanisms by which these systems affect taxis to PE remain to be elucidated.

An essential signal (the E-signal) in the cell-cell communication/signaling required to express many genes for production of multicellular fruiting bodies and myxospores was genetically mapped to the *esg* or *bkd* loci, linking the process to branched-chain fatty acid metabolism, as mentioned earlier (Downard and Toal, 1995; Toal et al., 1995). Subsequent studies focused on the rare TG-1 alkyl ether lipid (**Figure 3A**), with its i15:0 *O*-alkylglycerol moiety, as important in signaling this *M. xanthus* developmental process (Bhat et al., 2014a; Ahrendt et al., 2016). Mutants in the Bkd and Aib pathway that block synthesis of the starting isovaleryl-CoA unit and, thereby, of i15:0 FA, were incapable of forming fruiting body aggregates or viable myxospores and were rescued by feeding isovalerate or i15:0 FA (Bode et al., 2009), besides TG-1 (Bhat et al., 2014a). The Elb pathway mutants, with impaired ether lipid and TG-1 formation, were delayed in fruiting body development, produced defective spores (Lorenzen et al., 2014a), and were rescued by ether lipids (Ahrendt et al., 2016). These studies thus emphasized that the i15:0 FA and the ether linkage, both present in TG-1, are important structural determinants in signaling by this alkyl ether lipid. Nonetheless, the exact identity of the ether lipid signal, whether it is TG-1 or a related lipid, has to be unequivocally established, as also the mechanisms by which this signal is detected, what its targets are, and how it is integrated into the complex cell differentiation and developmental process.

Plasmalogen-specific signaling in the *M. xanthus* photooxidative stress response is triggered by production of $^1O_2$ (Galbis-Martínez et al., 2012; Gallego-García et al., 2019), with protein CarR as the candidate molecular target. Remarkably, both the natural *M. xanthus* plasmalogen, with *sn*-1 vinyl ether-linked and *sn*-2 ester-linked i15:0 moieties, as well as different human plasmalogens tested (bearing *sn*-1 vinyl ether-linked C18 moieties and a variety of *sn*-2 ester-linked straight chains), can signal the response (Gallego-García et al., 2019). The vinyl ether bond is therefore the crucial structural determinant required, with little or no dependence on the nature of the *sn*-1 and *sn*-2 chains. Since this photooxidative stress response leads to synthesis of carotenoids, whose role as antioxidants against $^1O_2$ and other ROS is well-established, the part played by plasmalogens can be readily attributed to signaling rather than as antioxidant. An antioxidant role for plasmalogens, though speculative and debated (Dorninger et al., 2020; Vítová et al., 2021), is often invoked based on early findings showing the vinyl ether bond to interact with and being cleaved by ROS (Morand et al., 1988; Zoeller et al., 1988; Stadelmann-Ingrand et al., 2001).

The molecular basis for how plasmalogens signal the presence of $^1O_2$ in *M. xanthus* is still an open question. Reasonable conjectures can be made based on the known properties of plasmalogens, whose vinyl ether bond is susceptible of cleavage by $^1O_2$ to yield a fatty aldehyde and a 2-acyl lyso-PE, with an *sn*-1 OH group, as illustrated in **Figure 7A** (Morand et al., 1988; Stadelmann-Ingrand et al., 2001). Both these cleavage products have been proposed as signaling molecules or second messengers, and their possible modes of action have been reviewed elsewhere (Jenkins et al., 2018; Dorninger et al., 2020; Ebenezer et al., 2020; Rangholia et al., 2021). Fatty aldehydes are frequent intermediates in fatty acid-fatty alcohol interconversions and are usually present at low cellular levels. They are also highly reactive and can form adducts with biomolecules such as proteins, through their cysteine, histidine or lysine residues, and these post-translational modifications may modulate cellular signaling and adaptive stress responses. Thus, an attractive hypothesis for how the *M. xanthus* photooxidative stress response may be signaled through plasmalogens is that $^1O_2$-mediated cleavage of their vinyl ether bond produces CarR inactivation through adduct formation with the fatty aldehyde product, which may cause a CarR conformational change or trigger its degradation (**Figure 7B**). Nonetheless, other mechanisms cannot yet be ruled out, such as that CarR inactivation results from local perturbation of membrane structure and properties caused by plasmalogen cleavage, or more unlikely, that signaling proceeds without cleavage of the vinyl ether bond. Moreover, even though CarR is the probable direct target, the possibility of still unidentified intermediate players cannot be excluded. Future studies that exploit state-of-the-art lipidomics and click chemistry methods, combined with genetic and functional analyses, should provide the answer, and reveal the molecular intricacies underlying the *M. xanthus* plasmalogen-based signaling mechanism, designed to alert the cells that they are exposed to photooxidative stress stemming from generation of the harmful $^1O_2$.

EVOLUTIONARY IMPLICATIONS OF PLASMALOGEN AND CarF DISTRIBUTION ACROSS THE TREE OF LIFE

The unusual distribution of plasmalogens, with their presence in strictly anaerobic bacteria and in animals (vertebrates and invertebrates), and their absence in nearly all aerobic or facultatively anaerobic bacteria, fungi, or plants, led to the hypothesis that they first evolved in anaerobic bacteria, were lost in facultative and aerobic species with the advent of increasing oxygen on earth, and reappeared in animals (Goldfine, 2010). The loss in aerobes and facultative anaerobes was ascribed to adverse lipid and cell damage resulting from the increased breakdown of plasmalogens by $^1O_2$ and other ROS with rising oxygen levels. Their reappearance in animals (with mitochondria, respiration, and molecular oxygen dependence) was attributed to the emergence of a new pathway for aerobic plasmalogen biosynthesis, distinct from the anaerobic one, and the ability to deal with cell damage from the breakdown of plasmalogens as well as to exploit their unique properties in signaling, in modulating membrane properties, and as antioxidants. Why plants lack plasmalogens was, however, unexplained, other than the aerobic pathway simply did not evolve in them. On the other hand, plasmalogen occurrence in aerobic myxobacteria was either overlooked or considered in the context of that known in anaerobic bacteria. Admittedly, at the time of the hypothesis, identifying species that made plasmalogens to gain evolutionary insights was hampered by the unknown identities of PEDS1 and of the genes for anaerobic plasmalogen biosynthesis (Goldfine, 2010). But this has now changed with the knowledge of PEDS1 identity and its remarkable conservation across a vast evolutionary distance from the aerobic myxobacteria to animals (Gallego-García et al., 2019). Moreover, the anaerobic counterpart for plasmalogen vinyl ether bond generation was also recently identified and it was found that facultative anaerobic bacteria can make plasmalogens (Jackson et al., 2021), contrary to earlier thinking that this was confined to obligate anaerobes (Goldfine, 2010). These developments and the presence in plants of PEDS1 sequence homologues with a distinct and unusual desaturase activity (Gao et al., 2009) warrant a fresh look at plasmalogen biosynthesis, distribution and evolution.

In addition to the stark difference in how the signature vinyl ether bond is created in the aerobic versus the anaerobic pathways for plasmalogen biosynthesis (**Figure 1C**), a crucial dividing line between the two mechanisms is the use of GNP in the aerobic route (Goldfine, 2010). In the aerobic animal ether lipid/plasmalogen biosynthesis, except for vinyl ether bond formation catalyzed by the oxygen-dependent PEDS1 in a key late step, the other ER-localized reactions mirror those for ester-linked diacyl GP, and it is in the earliest steps in the peroxisome that the specialized FAR1, GNPAT and AGPS enzymes ensure formation of the defining *O*-alkyl ether linkage from GNP (**Figure 2**). Whether similar mechanisms operate in the aerobic myxobacterial pathway is therefore an important question. This is likely given the putative FAR1, GNPAT and AGPS domains in ElbD, MXAN_1676 (both shown to participate in alkyl ether lipid synthesis), and/or MXAN_1675 (**Figure 3B**), although these and other steps and enzymes need to be fully characterized (Lorenzen et al., 2014a; Gallego-García et al., 2019). Strikingly, CarF homologues are found in just one myxobacterial suborder, the Cystobacterineae (Pérez-Castaño et al., 2022), but *elbD* and *elbE* (forming a cluster with *elbB* and *elbC*, or unlinked to them) are found in all three suborders (Lorenzen et al., 2014a). Consequently, alkyl ether lipids may be common across myxobacteria, but plasmalogens are most likely restricted to a single suborder. Interestingly, beyond myxobacteria, true CarF homologues have been reported only in *Leptospira* (Gallego-García et al., 2019), and the genome of *L. interrogans*, a Gram-negative obligately aerobic animal pathogen, reveals an annotated AGPS but no FAR1. Whether it is capable of *ab initio* plasmalogen biosynthesis or requires the animal host for suitable precursors or plasmalogens is unknown. On the other hand, some bacteria from other phyla that lack CarF and are anaerobes, animal pathogens, or extremophiles possess ElbD-like homologues, but almost all of these lack a FAR1 domain (Lorenzen et al., 2014a), and little or no lipid analysis is available for these bacteria.

Generally, the chemistry and composition of eukaryotic membrane lipids are far more like those in bacteria than in archaea (Lombard et al., 2012; López-García and Moreira, 2020; Hoshino and Gaucher, 2021). Myxobacteria, in particular, stand out as a singular group among prokaryotes, with several typically "eukaryotic" lipids that include phosphatidylinositol, sphingolipids and steroids (or their molecular surrogates called hopanoids) besides, of course, ether lipids/plasmalogens (Ring et al., 2009; Lorenzen et al., 2014a; Lorenzen et al., 2014b; Sohlenkamp and Geiger, 2016; Gallego-García et al., 2019; Hoshino and Gaucher, 2021). Notably, counterparts to both the eukaryotic oxygen-dependent steroid and its isoprenoid precursor mevalonate biosynthesis pathways are near exclusive to aerobic myxobacteria (Hoshino and Gaucher, 2021; Pérez-Castaño et al., 2022). Thus, rather than an anomaly, animal-like aerobic plasmalogen biosynthesis in myxobacteria constitutes yet another candidate to add to a growing list of eukaryotic-like factors and traits. This list has led to the hypothesis that symbiosis or syntrophy of an ancestral host myxobacterium, an Asgard-like archaeon as future nucleus, and an alpha-proteobacterium as future mitochondrion may have been a crucial early event in the origin of eukaryotes (López-García and Moreira, 2020; Hoshino and Gaucher, 2021). If so, it would point to a myxobacterial source in the beginnings of aerobic plasmalogen biosynthesis. Studies to further elucidate the pathway in myxobacteria may therefore reinforce such conjectures on its origins and provide evolutionary insights into extant mechanisms.

CONCLUDING REMARKS

Unmasking the identity of the long-elusive oxygen-dependent PEDS1 and its largely unanticipated occurrence in bacteria is arguably a turning point and a thrust to studies on the biosynthesis, functions, origins, evolution, and roles in disease of the enigmatic plasmalogens. It may also provide a valuable synthetic biological tool for aerobic plasmalogen synthesis. Strikingly, discovery of myxobacterial PEDS1 simultaneously uncovered a novel and specific role of

plasmalogens as exquisitely sensitive signaling molecules acting with $^1O_2$ in a photooxidative stress response. Deciphering the complete pathway(s) in the biosynthesis of plasmalogens, how they signal, and what their target molecules and processes are in myxobacteria may reveal novel molecular mechanisms. These may be universal, perhaps extensible, to other cell types, notably mammalian, and shed light on conserved as well as evolutionary aspects of plasmalogens in prokaryotes and eukaryotes.

AUTHOR CONTRIBUTIONS

SP and ME-A conceived and wrote the original draft of the manuscript, revised it and acquired funding. All authors contributed to the work, and in revising, discussing, and commenting on the manuscript.

FUNDING

This work was supported by the Ministerio de Ciencia, Innovación y Universidades (MCIU)/Agencia Estatal de Investigación (AEI)/European Regional Development Fund (ERDF) grants PGC 2018-094635-B-C21 to ME-A and PGC 2018-094635-B-C22 to SP, both funded by MCIU/AEI 10.13039/501100011033 and by "ERDF A way of making Europe"; and the Fundación Séneca (Murcia)-Spain grant 20992/PI/18 to ME-A.

ACKNOWLEDGMENTS

We thank past members of the group for their contributions, and J.A. Madrid and V. López-Egea (Universidad de Murcia-Spain) for technical support.

REFERENCES

Ahrendt, T., Dauth, C., and Bode, H. B. (2016). An Iso-15 : 0 O-Alkylglycerol Moiety Is the Key Structure of the E-Signal in *Myxococcus xanthus*. *Microbiology* 162, 138–144. doi:10.1099/mic.0.000169

Ahrendt, T., Wolff, H., and Bode, H. B. (2015). Neutral and Phospholipids of the *Myxococcus xanthus* Lipodome during Fruiting Body Formation and Germination. *Appl. Environ. Microbiol.* 81, 6538–6547. doi:10.1128/aem.01537-15

Bader, C. D., Panter, F., and Müller, R. (2020). In Depth Natural Product Discovery - Myxobacterial Strains that provided Multiple Secondary Metabolites. *Biotechnol. Adv.* 39, 107480. doi:10.1016/j.biotechadv.2019.107480

Bai, Y., McCoy, J. G., Levin, E. J., Sobrado, P., Rajashankar, K. R., and Fox, B. G. (1998). X-Ray Structure of a Mammalian Stearoyl-CoA Desaturase. *Nature* 524, 252–256. doi:10.1038/nature14549

Bartholomeusz, G., Zhu, Y., and Downard, J. (1998). Growth Medium-dependent Regulation of *Myxococcus xanthus* Fatty Acid Content Is Controlled by the *esg* Locus. *J. Bacteriol.* 180, 5269–5272. doi:10.1128/jb.180.19.5269-5272.1998

Bhat, S., Ahrendt, T., Dauth, C., Bode, H. B., and Shimkets, L. J. (2014a). Two Lipid Signals Guide Fruiting Body Development of *Myxococcus xanthus*. *mBio* 5, e00939–13. doi:10.1128/mBio.00939-13

Bhat, S., Boynton, T. O., Pham, D., and Shimkets, L. J. (2014b). Fatty Acids from Membrane Lipids Become Incorporated into Lipid Bodies during *Myxococcus xanthus* Differentiation. *PLoS One* 9, e99622. doi:10.1371/journal.pone.0099622

Blank, M. L., and Snyder, F. (1992). Plasmanylethanolamine Δ1-desaturase. *Methods Enzymol.* 209, 390–396. doi:10.1016/0076-6879(92)09048-8

Bock, T., Luxenburger, E., Hoffmann, J., Schütza, V., Feiler, C., Müller, R., et al. (2017a). AibA/AibB Induces an Intramolecular Decarboxylation in Isovalerate Biosynthesis by *Myxococcus xanthus*. *Angew. Chem. Int. Ed.* 56, 9986–9989. doi:10.1002/anie.201701992

Bock, T., Reichelt, J., Müller, R., and Blankenfeldt, W. (2016). The Structure of LiuC, a 3-Hydroxy-3-Methylglutaconyl CoA Dehydratase Involved in Isovaleryl-CoA Biosynthesis in *Myxococcus xanthus*, Reveals Insights into Specificity and Catalysis. *Chembiochem* 17, 1658–1664. doi:10.1002/cbic.201600225

Bock, T., Volz, C., Hering, V., Scrima, A., Müller, R., and Blankenfeldt, W. (2017b). The AibR-Isovaleryl Coenzyme A Regulator and its DNA Binding Site - a Model for the Regulation of Alternative De Novo Isovaleryl Coenzyme A Biosynthesis in *Myxococcus xanthus*. *Nucleic Acids Res.* 45, 2166–2178. doi:10.1093/nar/gkw1238

Bode, H. B., Ring, M. W., Schwär, G., Altmeyer, M. O., Kegler, C., Jose, I. R., et al. (2009). Identification of Additional Players in the Alternative Biosynthesis Pathway to Isovaleryl-CoA in the Myxobacterium *Myxococcus xanthus*. *Chembiochem* 10, 128–140. doi:10.1002/cbic.200800219

Bode, H. B., Ring, M. W., Schwär, G., Kroppenstedt, R. M., Kaiser, D., and Müller, R. (2006). 3-Hydroxy-3-methylglutaryl-coenzyme A (CoA) Synthase Is Involved in Biosynthesis of Isovaleryl-CoA in the Myxobacterium *Myxococcus xanthus* during Fruiting Body Formation. *J. Bacteriol.* 188, 6524–6528. doi:10.1128/jb.00825-06

Bonner, P. J., and Shimkets, L. J. (2006). Phospholipid Directed Motility of Surface-Motile Bacteria. *Mol. Microbiol.* 61, 1101–1109. doi:10.1111/j.1365-2958.2006.05314.x

Braverman, N. E., and Moser, A. B. (2012). Functions of Plasmalogen Lipids in Health and Disease. *Biochimica Biophysica Acta (BBA) - Mol. Basis Dis.* 1822, 1442–1452. doi:10.1016/j.bbadis.2012.05.008

Burchard, R. P., and Dworkin, M. (1966). Light-induced Lysis and Carotenogenesis in *Myxococcus xanthus*. *J. Bacteriol.* 91, 535–545. doi:10.1128/jb.91.2.535-545.1966

Caillon, E., Lubochinsky, B., and Rigomier, D. (1983). Occurrence of Dialkyl Ether Phospholipids in *Stigmatella aurantiaca* DW4. *J. Bacteriol.* 153, 1348–1351. doi:10.1128/jb.153.3.1348-1351.1983

Cao, P., and Wall, D. (2019). Direct Visualization of a Molecular Handshake that Governs Kin Recognition and Tissue Formation in Myxobacteria. *Nat. Commun.* 10, 3073. doi:10.1038/s41467-019-11108-w

Cui, W., Liu, D., Gu, W., and Chu, B. (2021). Peroxisome-driven Ether-Linked Phospholipids Biosynthesis Is Essential for Ferroptosis. *Cell Death Differ.* 28, 2536–2551. doi:10.1038/s41418-021-00769-0

Curtis, P. D., Geyer, R., White, D. C., and Shimkets, L. J. (2006). Novel Lipids in *Myxococcus xanthus* and Their Role in Chemotaxis. *Environ. Microbiol.* 8, 1935–1949. doi:10.1111/j.1462-2920.2006.01073.x

de Dios, R., Santero, E., and Reyes-Ramírez, F. (2021). Extracytoplasmic Function σ Factors as Tools for Coordinating Stress Responses. *Int. J. Mol. Sci.* 22. doi:10.3390/ijms22083900

Dean, J. M., and Lodhi, I. J. (2018). Structural and Functional Roles of Ether Lipids. *Protein Cell* 9, 196–206. doi:10.1007/s13238-017-0423-5

Dorninger, F., Forss-Petter, S., Wimmer, I., and Berger, J. (2020). Plasmalogens, Platelet-Activating Factor and beyond - Ether Lipids in Signaling and Neurodegeneration. *Neurobiol. Dis.* 145, 105061. doi:10.1016/j.nbd.2020.105061

Downard, J., and Toal, D. (1995). Branched-chain Fatty Acids: the Case for a Novel Form of Cell-Cell Signalling during *Myxococcus xanthus* Development. *Mol. Microbiol.* 16, 171–175. doi:10.1111/j.1365-2958.1995.tb02290.x

Duex, J. E., Mullins, M. R., and Sorkin, A. (2010). Recruitment of Uev1B to Hrs-Containing Endosomes and its Effect on Endosomal Trafficking. *Exp. Cell Res.* 316, 2136–2151. doi:10.1016/j.yexcr.2010.04.017

Ebenezer, D. L., Fu, P., Ramchandran, R., Ha, A. W., Putherickal, V., Sudhadevi, T., et al. (2020). S1P and Plasmalogen Derived Fatty Aldehydes in Cellular Signaling and Functions. *Biochimica Biophysica Acta (BBA) - Mol. Cell Biol. Lipids* 1865, 158681. doi:10.1016/j.bbalip.2020.158681

Elías-Arnanz, M., Padmanabhan, S., and Murillo, F. J. (2011). Light-dependent Gene Regulation in Nonphototrophic Bacteria. *Curr. Opin. Microbiol.* 14, 128–135.

Exner, T., Romero-Brey, I., Yifrach, E., Rivera-Monroy, J., Schrul, B., Zouboulis, C. C., et al. (2019). An Alternative Membrane Topology Permits Lipid Droplet Localization of Peroxisomal Fatty Acyl-CoA Reductase 1. *J. Cell Sci.* 132. doi:10.1242/jcs.223016

Fahy, E., Subramaniam, S., Murphy, R. C., Nishijima, M., Raetz, C. R. H., Shimizu, T., et al. (2009). Update of the LIPID MAPS Comprehensive Classification System for Lipids. *J. Lipid Res.* 50 (Suppl. l), S9–S14. doi:10.1194/jlr.r800095-jlr200

Feulgen, R., and Voit, K. (1924). Über einen weitverbreiteten festen Aldehyd. *Pflügers Arch.* 206, 389–410. doi:10.1007/bf01722779

Fontes, M., Galbis-Martínez, L., and Murillo, F. J. (2003). A Novel Regulatory Gene for Light-Induced Carotenoid Synthesis in the Bacterium *Myxococcus xanthus*. *Mol. Microbiol.* 47, 561–571. doi:10.1046/j.1365-2958.2003.03319.x

Galbis-Martínez, L., Galbis-Martínez, M., Murillo, F. J., and Fontes, M. (2008). An Anti-antisigma Factor in the Response of the Bacterium *Myxococcus xanthus* to Blue Light. *Microbiol* 154, 895–904.

Galbis-Martínez, M., Padmanabhan, S., Murillo, F. J., and Elías-Arnanz, M. (2012). CarF Mediates Signaling by Singlet Oxygen, Generated via Photoexcited Protoporphyrin IX, in *Myxococcus xanthus* Light-Induced Carotenogenesis. *J. Bacteriol.* 194, 1427–1436.

Gallego-García, A., Monera-Girona, A. J., Pajares-Martínez, E., Bastida-Martínez, E., Pérez-Castaño, R., Iniesta, A. A., et al. (2019). A Bacterial Light Response Reveals an Orphan Desaturase for Human Plasmalogen Synthesis. *Science* 366, 128–132.

Gao, J., Ajjawi, I., Manoli, A., Sawin, A., Xu, C., Froehlich, J. E., et al. (2009). FATTY ACID DESATURASE4 of *Arabidopsis* Encodes a Protein Distinct from Characterized Fatty Acid Desaturases. *Plant J.* 60, 832–839. doi:10.1111/j.1365-313x.2009.04001.x

Glaeser, J., Nuss, A. M., Berghoff, B. A., and Klug, G. (2011). Singlet Oxygen Stress in Microorganisms. *Adv. Microb. Physiol.* 58, 141–173. doi:10.1016/b978-0-12-381043-4.00004-0

Goldfine, H. (2017). The Anaerobic Biosynthesis of Plasmalogens. *FEBS Lett.* 591, 2714–2719. doi:10.1002/1873-3468.12714

Goldfine, H. (2010). The Appearance, Disappearance and Reappearance of Plasmalogens in Evolution. *Prog. Lipid Res.* 49, 493–498. doi:10.1016/j.plipres.2010.07.003

Greening, C., and Lithgow, T. (2020). Formation and Function of Bacterial Organelles. *Nat. Rev. Microbiol.* 18, 677–689. doi:10.1038/s41579-020-0413-0

Harayama, T., and Riezman, H. (2018). Understanding the Diversity of Membrane Lipid Composition. *Nat. Rev. Mol. Cell Biol.* 19, 281–296. doi:10.1038/nrm.2017.138

Hoiczyk, E., Ring, M. W., Mchugh, C. A., Schwär, G., Bode, E., Krug, D., et al. (2009). Lipid Body Formation Plays a Central Role in Cell Fate Determination during Developmental Differentiation of *Myxococcus xanthus*. *Mol. Microbiol.* 74, 497–517. doi:10.1111/j.1365-2958.2009.06879.x

Honsho, M., and Fujiki, Y. (2017). Plasmalogen Homeostasis - Regulation of Plasmalogen Biosynthesis and its Physiological Consequence in Mammals. *FEBS Lett.* 591, 2720–2729. doi:10.1002/1873-3468.12743

Honsho, M., Tanaka, M., Zoeller, R. A., and Fujiki, Y. (2020). Distinct Functions of Acyl/alkyl Dihydroxyacetonephosphate Reductase in Peroxisomes and Endoplasmic Reticulum. *Front. Cell Dev. Biol.* 8, 855. doi:10.3389/fcell.2020.00855

Horibata, Y., Ando, H., and Sugimoto, H. (2020). Locations and Contributions of the Phosphotransferases EPT1 and CEPT1 to the Biosynthesis of Ethanolamine Phospholipids. *J. Lipid Res.* 61, 1221–1231. doi:10.1194/jlr.ra120000898

Horn, P. J., Smith, M. D., Clark, T. R., Froehlich, J. E., and Benning, C. (2020). PEROXIREDOXIN Q Stimulates the Activity of the Chloroplast 16:1 Δ3trans FATTY ACID DESATURASE4. *Plant J.* 102, 718–729. doi:10.1111/tpj.14657

Horsman, G. P., and Zechel, D. L. (2017). Phosphonate Biochemistry. *Chem. Rev.* 117, 5704–5783. doi:10.1021/acs.chemrev.6b00536

Hoshino, Y., and Gaucher, E. A. (2021). Evolution of Bacterial Steroid Biosynthesis and its Impact on Eukaryogenesis. *Proc. Natl. Acad. Sci. U. S. A.* 118, e2101276118. doi:10.1073/pnas.2101276118

Hua, R., Cheng, D., Coyaud, É., Freeman, S., Di Pietro, E., Wang, Y., et al. (2017). VAPs and ACBD5 Tether Peroxisomes to the ER for Peroxisome Maintenance and Lipid Homeostasis. *J. Cell Biol.* 216, 367–377. doi:10.1083/jcb.201608128

Jackson, D. R., Cassilly, C. D., Plichta, D. R., Vlamakis, H., Liu, H., Melville, S. B., et al. (2021). Plasmalogen Biosynthesis by Anaerobic Bacteria: Identification of a Two-Gene Operon Responsible for Plasmalogen Production in *Clostridium perfringens*. *ACS Chem. Biol.* 16, 6–13. doi:10.1021/acschembio.0c00673

Jain, I. H., Calvo, S. E., Markhard, A. L., Skinner, O. S., To, T.-L., Ast, T., et al. (2020). Genetic Screen for Cell Fitness in High or Low Oxygen Highlights Mitochondrial and Lipid Metabolism. *Cell* 181, 716–727. e711. doi:10.1016/j.cell.2020.03.029

Jenkins, C. M., Yang, K., Liu, G., Moon, S. H., Dilthey, B. G., and Gross, R. W. (2018). Cytochrome C Is an Oxidative Stress-Activated Plasmalogenase that Cleaves Plasmenylcholine and Plasmenylethanolamine at the *sn*-1 Vinyl Ether Linkage. *J. Biol. Chem.* 293, 8693–8709. doi:10.1074/jbc.ra117.001629

Jiménez-Rojo, N., and Riezman, H. (2019). On the Road to Unraveling the Molecular Functions of Ether Lipids. *FEBS Lett.* 593, 2378–2389.

Jost, M., Fernández-Zapata, J., Polanco, M. C., Ortiz-Guerrero, J. M., Chen, P. Y.-T., Kang, G., et al. (2015). Structural Basis for Gene Regulation by a B_{12}-dependent Photoreceptor. *Nature* 526, 536–541. doi:10.1038/nature14950

Kaneda, T. (1991). Iso- and Anteiso-Fatty Acids in Bacteria: Biosynthesis, Function, and Taxonomic Significance. *Microbiol. Rev.* 55, 288–302. doi:10.1128/mr.55.2.288-302.1991

Kearns, D. B., and Shimkets, L. J. (1998). Chemotaxis in a Gliding Bacterium. *Proc. Natl. Acad. Sci. U.S.A.* 95, 11957–11962. doi:10.1073/pnas.95.20.11957

Kearns, D. B., and Shimkets, L. J. (2001). Lipid Chemotaxis and Signal Transduction in *Myxococcus xanthus*. *Trends Microbiol.* 9, 126–129. doi:10.1016/s0966-842x(01)01948-5

Kerfeld, C. A., Aussignargues, C., Zarzycki, J., Cai, F., and Sutter, M. (2018). Bacterial Microcompartments. *Nat. Rev. Microbiol.* 16, 277–290. doi:10.1038/nrmicro.2018.10

Kleinig, H. (1972). Membranes from *Myxococcus fulvus* (Myxobacterales) Containing Carotenoid Glucosides. *Biochimica Biophysica Acta (BBA) - Biomembr.* 274, 489–498. doi:10.1016/0005-2736(72)90194-0

Li, Y., Luxenburger, E., and Müller, R. (2013). An Alternative Isovaleryl CoA Biosynthetic Pathway Involving a Previously Unknown 3-methylglutaconyl CoA Decarboxylase. *Angew. Chem. Int. Ed.* 52, 1304–1308. doi:10.1002/anie.201207984

Liu, Q., Chai, J., Moche, M., Guy, J., Lindqvist, Y., and Shanklin, J. (2015). Half-of-the-Sites Reactivity of the Castor Δ9-18:0-Acyl Carrier Protein Desaturase. *Plant Physiol.* 169, 432–441. doi:10.1104/pp.15.00622

Lodhi, I. J., Yin, L., Jensen-Urstad, A. P. L., Funai, K., Coleman, T., Baird, J. H., et al. (2012). Inhibiting Adipose Tissue Lipogenesis Reprograms Thermogenesis and PPARγ Activation to Decrease Diet-Induced Obesity. *Cell Metab.* 16, 189–201. doi:10.1016/j.cmet.2012.06.013

Lombard, J., López-García, P., and Moreira, D. (2012). The Early Evolution of Lipid Membranes and the Three Domains of Life. *Nat. Rev. Microbiol.* 10, 507–515. doi:10.1038/nrmicro2815

López-García, P., and Moreira, D. (2020). The Syntrophy Hypothesis for the Origin of Eukaryotes Revisited. *Nat. Microbiol.* 5, 655–667.

Lorenzen, W., Ahrendt, T., Bozhüyük, K. A. J., and Bode, H. B. (2014a). A Multifunctional Enzyme Is Involved in Bacterial Ether Lipid Biosynthesis. *Nat. Chem. Biol.* 10, 425–427. doi:10.1038/nchembio.1526

Lorenzen, W., Bozhüyük, K. A. J., Cortina, N. S., and Bode, H. B. (2014b). A Comprehensive Insight into the Lipid Composition of *Myxococcus xanthus* by UPLC-ESI-MS. *J. Lipid Res.* 55, 2620–2633. doi:10.1194/jlr.m054593

Mahmud, T., Bode, H. B. r., Silakowski, B., Kroppenstedt, R. M., Xu, M., Nordhoff, S., et al. (2002). A Novel Biosynthetic Pathway Providing Precursors for Fatty Acid Biosynthesis and Secondary Metabolite Formation in Myxobacteria. *J. Biol. Chem.* 277, 32768–32774. doi:10.1074/jbc.m205222200

Messias, M. C. F., Mecatti, G. C., Priolli, D. G., and De Oliveira Carvalho, P. (2018). Plasmalogen Lipids: Functional Mechanism and Their Involvement in Gastrointestinal Cancer. *Lipids Health Dis.* 17, 41. doi:10.1186/s12944-018-0685-9

Metcalf, W. W., and van der Donk, W. A. (2009). Biosynthesis of Phosphonic and Phosphinic Acid Natural Products. *Annu. Rev. Biochem.* 78, 65–94. doi:10.1146/annurev.biochem.78.091707.100215

Mohr, K. I. (2018). Diversity of Myxobacteria-We Only See the Tip of the Iceberg. *Microorganisms* 6. doi:10.3390/microorganisms6030084

Morand, O. H., Zoeller, R. A., and Raetz, C. R. (1988). Disappearance of Plasmalogens from Membranes of Animal Cells Subjected to Photosensitized Oxidation. *J. Biol. Chem.* 263, 11597–11606. doi:10.1016/s0021-9258(18)38001-3

Muñoz-Dorado, J., Marcos-Torres, F. J., García-Bravo, E., Moraleda-Muñoz, A., and Pérez, J. (2016). Myxobacteria: Moving, Killing, Feeding, and Surviving Together. *Front. Microbiol.* 7, 781.

Muñoz-Dorado, J., Moraleda-Muñoz, A., Marcos-Torres, F. J., Contreras-Moreno, F. J., Martin-Cuadrado, A. B., Schrader, J. M., et al. (2019). Transcriptome Dynamics of the *Myxococcus xanthus* Multicellular Developmental Program. *Elife* 8.

Nagan, N., and Zoeller, R. A. (2001). Plasmalogens: Biosynthesis and Functions. *Prog. Lipid Res.* 40, 199–229. doi:10.1016/s0163-7827(01)00003-0

Ortiz-Guerrero, J. M., Polanco, M. C., Murillo, F. J., Padmanabhan, S., and Elías-Arnanz, M. (2011). Light-dependent Gene Regulation by a Coenzyme B_{12} -based Photoreceptor. *Proc. Natl. Acad. Sci. U.S.A.* 108, 7565–7570. doi:10.1073/pnas.1018972108

Padmanabhan, S., Jost, M., Drennan, C. L., and Elías-Arnanz, M. (2017). A New Facet of Vitamin B_{12}: Gene Regulation by Cobalamin-Based Photoreceptors. *Annu. Rev. Biochem.* 86, 485–514. doi:10.1146/annurev-biochem-061516-044500

Padmanabhan, S., Monera-Girona, A. J., Pérez-Castaño, R., Bastida-Martínez, E., Pajares-Martínez, E., Bernal-Bernal, D., et al. (2021). Light-triggered Carotenogenesis in *Myxococcus xanthus*: New Paradigms in Photosensory Signaling, Transduction and Gene Regulation. *Microorganisms* 9, 1067. doi:10.3390/microorganisms9051067

Padmanabhan, S., Pérez-Castaño, R., and Elías-Arnanz, M. (2019). B_{12}-based Photoreceptors: from Structure and Function to Applications in Optogenetics and Synthetic Biology. *Curr. Opin. Struct. Biol.* 57, 47–55. doi:10.1016/j.sbi.2019.01.020

Padmanabhan, S., Pérez-Castaño, R., Osete-Alcaraz, L., Polanco, M. C., and Elías-Arnanz, M. (2022). Vitamin B_{12} Photoreceptors. *Vitam. Horm.* 119, 149–184. doi:10.1016/bs.vh.2022.01.007

Paul, S., Lancaster, G. I., and Meikle, P. J. (2019). Plasmalogens: A Potential Therapeutic Target for Neurodegenerative and Cardiometabolic Disease. *Prog. Lipid Res.* 74, 186–195. doi:10.1016/j.plipres.2019.04.003

Pérez-Castaño, R., Bastida-Martínez, E., Fernández Zapata, J., Polanco, M. D. C., Galbis-Martínez, M. L., Iniesta, A. A., et al. (2022). Coenzyme B_{12}-dependent and Independent Photoregulation of Carotenogenesis across Myxococcales. *Environ. Microbiol.* 24, 1865-1886. doi:10.1111/1462-2920.15895

Pike, L. J., Han, X., Chung, K.-N., and Gross, R. W. (2002). Lipid Rafts Are Enriched in Arachidonic Acid and Plasmenylethanolamine and Their Composition Is Independent of Caveolin-1 Expression: a Quantitative Electrospray Ionization/mass Spectrometric Analysis. *Biochemistry* 41, 2075–2088. doi:10.1021/bi0156557

Rangholia, N., Leisner, T. M., and Holly, S. P. (2021). Bioactive Ether Lipids: Primordial Modulators of Cellular Signaling. *Metabolites* 11. doi:10.3390/metabo11010041

Rezanka, T., and Sigler, K. (2009). Odd-numbered Very-Long-Chain Fatty Acids from the Microbial, Animal and Plant Kingdoms. *Prog. Lipid Res.* 48, 206–238. doi:10.1016/j.plipres.2009.03.003

Ring, M. W., Schwär, G., and Bode, H. B. (2009). Biosynthesis of 2-Hydroxy and Iso-even Fatty Acids Is Connected to Sphingolipid Formation in Myxobacteria. *Chembiochem* 10, 2003–2010. doi:10.1002/cbic.200900164

Ring, M. W., Schwär, G., Thiel, V., Dickschat, J. S., Kroppenstedt, R. M., Schulz, S., et al. (2006). Novel Iso-Branched Ether Lipids as Specific Markers of Developmental Sporulation in the Myxobacterium *Myxococcus xanthus*. *J. Biol. Chem.* 281, 36691–36700. doi:10.1074/jbc.m607616200

Shanklin, J., Guy, J. E., Mishra, G., and Lindqvist, Y. (2009). Desaturases: Emerging Models for Understanding Functional Diversification of Diiron-Containing Enzymes. *J. Biol. Chem.* 284, 18559–18563. doi:10.1074/jbc.r900009200

Shen, J., Wu, G., Tsai, A. L., and Zhou, M. (2020). Structure and Mechanism of a Unique Diiron Center in Mammalian Stearoyl-CoA Desaturase. *J. Mol. Biol.* 432, 5152–5161. doi:10.1016/j.jmb.2020.05.017

Snyder, F. (1992). Alkylglycerol Phosphotransferase. *Methods Enzymol.* 209, 211–215. doi:10.1016/0076-6879(92)09025-x

Snyder, F. (1999). The Ether Lipid Trail: a Historical perspective. *Biochimica Biophysica Acta (BBA) - Mol. Cell Biol. Lipids* 1436, 265–278. doi:10.1016/s0005-2760(98)00172-6

Sohlenkamp, C., and Geiger, O. (2016). Bacterial Membrane Lipids: Diversity in Structures and Pathways. *FEMS Microbiol. Rev.* 40, 133–159. doi:10.1093/femsre/fuv008

Stadelmann-Ingrand, S., Favreliere, S., Fauconneau, B., Mauco, G., and Tallineau, C. (2001). Plasmalogen Degradation by Oxidative Stress: Production and Disappearance of Specific Fatty Aldehydes and Fatty α-hydroxyaldehydes. *Free Radic. Biol. Med.* 31, 1263–1271. doi:10.1016/s0891-5849(01)00720-1

Stein, J., and Budzikiewicz, H. (1987). 1-O-(13-Methyl-1-Z-tetradecenyl)-2-O-(13-methyltetradecanoyl)- glycero-3-phospho-ethanolamin, ein plasmalogen aus *Myxococcus stipitatus*/1-O-(13-Methyl-1-Z-tetradecenyl)-2-O-(13-methyltetradecanoyl)-glycero-3-phosphoethanolamine, a plasmalogen from *Myxococcus stipitatus*. *Z. für Naturforsch. B* 42, 1017–1020. doi:10.1515/znb-1987-0815

Thomson, T. M., Lozano, J. J., Loukili, N., Carrio, R., Serras, F., Cormand, B., et al. (2000). Fusion of the Human Gene for the Polyubiquitination Coeffector UEV1 with *Kua*, a Newly Identified Gene. *Genome Res.* 10, 1743–1756. doi:10.1101/gr.gr-1405r

Toal, D. R., Clifton, S. W., Roe, B. A., and Downard, J. (1995). The Esg Locus of *Myxococcus xanthus* Encodes the E1α and E1β Subunits of a Branched-Chain Keto Acid Dehydrogenase. *Mol. Microbiol.* 16, 177–189. doi:10.1111/j.1365-2958.1995.tb02291.x

Tunyasuvunakool, K., Adler, J., Wu, Z., Green, T., Zielinski, M., Žídek, A., et al. (2021). Highly Accurate Protein Structure Prediction for the Human Proteome. *Nature* 596, 590–596. doi:10.1038/s41586-021-03828-1

Vítová, M., Palyzová, A., and Řezanka, T. (2021). Plasmalogens - Ubiquitous Molecules Occurring Widely, from Anaerobic Bacteria to Humans. *Prog. Lipid Res.* 83, 101111.

Vos, M. (2021). *Myxococcus xanthus*. *Trends Microbiol.* 29, 562–563. doi:10.1016/j.tim.2021.03.006

Wainberg, M., Kamber, R. A., Balsubramani, A., Meyers, R. M., Sinnott-Armstrong, N., Hornburg, D., et al. (2021). A Genome-wide Atlas of Co-essential Modules Assigns Function to Uncharacterized Genes. *Nat. Genet.* 53, 638–649. doi:10.1038/s41588-021-00840-z

Wang, H., Klein, M. G., Zou, H., Lane, W., Snell, G., Levin, I., et al. (2015). Crystal Structure of Human Stearoyl-Coenzyme A Desaturase in Complex with Substrate. *Nat. Struct. Mol. Biol.* 22, 581–585. doi:10.1038/nsmb.3049

Ware, J. C., and Dworkin, M. (1973). Fatty Acids of *Myxococcus xanthus*. *J. Bacteriol.* 115, 253–261. doi:10.1128/jb.115.1.253-261.1973

Watschinger, K., Keller, M. A., Golderer, G., Hermann, M., Maglione, M., Sarg, B., et al. (2010). Identification of the Gene Encoding Alkylglycerol Monooxygenase Defines a Third Class of Tetrahydrobiopterin-dependent Enzymes. *Proc. Natl. Acad. Sci. U.S.A.* 107, 13672–13677. doi:10.1073/pnas.1002404107

Watschinger, K., and Werner, E. R. (2013). Orphan Enzymes in Ether Lipid Metabolism. *Biochimie* 95, 59–65. doi:10.1016/j.biochi.2012.06.027

Werner, E. R., Fernández-Quintero, M. L., Hulo, N., Golderer, G., Sailer, S., Lackner, K., et al. (2022). Essential Role of a Conserved Aspartate for the Enzymatic Activity of Plasmanylethanolamine Desaturase. *Cell Mol. Life Sci.* 79, 214. doi:10.1007/s00018-022-04238-w

Werner, E. R., Keller, M. A., Sailer, S., Lackner, K., Koch, J., Hermann, M., et al. (2020). The *TMEM189* Gene Encodes Plasmanylethanolamine Desaturase Which Introduces the Characteristic Vinyl Ether Double Bond into Plasmalogens. *Proc. Natl. Acad. Sci. U.S.A.* 117, 7792–7798. doi:10.1073/pnas.1917461117

White, J. K., Gerdin, A.-K., Karp, N. A., Ryder, E., Buljan, M., Bussell, J. N., et al. (2013). Genome-wide Generation and Systematic Phenotyping of Knockout Mice Reveals New Roles for Many Genes. *Cell* 154, 452–464. doi:10.1016/j.cell.2013.06.022

Wu, L.-C., Pfeiffer, D. R., Calhoon, E. A., Madiai, F., Marcucci, G., Liu, S., et al. (2011). Purification, Identification, and Cloning of Lysoplasmalogenase, the Enzyme that Catalyzes Hydrolysis of the Vinyl Ether Bond of Lysoplasmalogen. *J. Biol. Chem.* 286, 24916–24930. doi:10.1074/jbc.m111.247163

Xu, Q., Black, W. P., Cadieux, C. L., and Yang, Z. (2008). Independence and Interdependence of Dif and Frz Chemosensory Pathways in *Myxococcus xanthus* chemotaxis. *Mol. Microbiol.* 69, 714–723. doi:10.1111/j.1365-2958.2008.06322.x

Zhang, S., Yang, Y., and Shi, Y. (2005). Characterization of Human SCD2, an Oligomeric Desaturase with Improved Stability and Enzyme Activity by Cross-Linking in Intact Cells. *Biochem. J.* 388, 135–142. doi:10.1042/bj20041554

Zhou, Y., Yu, N., Zhao, J., Xie, Z., Yang, Z., and Tian, B. (2020). Advances in the Biosynthetic Pathways and Application Potential of Plasmalogens in Medicine. *Front. Cell Dev. Biol.* 8, 765. doi:10.3389/fcell.2020.00765

Ziegelhoffer, E. C., and Donohue, T. J. (2009). Bacterial Responses to Photo-Oxidative Stress. *Nat. Rev. Microbiol.* 7, 856–863. doi:10.1038/nrmicro2237

Zoeller, R. A., Morand, O. H., and Raetz, C. R. (1988). A Possible Role for Plasmalogens in Protecting Animal Cells against Photosensitized Killing. *J. Biol. Chem.* 263, 11590–11596. doi:10.1016/s0021-9258(18)38000-1

Zou, Y., Henry, W. S., Ricq, E. L., Graham, E. T., Phadnis, V. V., Maretich, P., et al. (2020). Plasticity of Ether Lipids Promotes Ferroptosis Susceptibility and Evasion. *Nature* 585, 603–608. doi:10.1038/s41586-020-2732-8

Zusman, D. R., Scott, A. E., Yang, Z., and Kirby, J. R. (2007). Chemosensory Pathways, Motility and Development in *Myxococcus xanthus*. *Nat. Rev. Microbiol.* 5, 862–872. doi:10.1038/nrmicro1770

Conflict of Interest: The authors declare that the research was conducted in the absence of any commercial or financial relationships that could be construed as a potential conflict of interest.

Publisher's Note: All claims expressed in this article are solely those of the authors and do not necessarily represent those of their affiliated organizations, or those of the publisher, the editors and the reviewers. Any product that may be evaluated in this article, or claim that may be made by its manufacturer, is not guaranteed or endorsed by the publisher.

frontiers | Frontiers in Cell and Developmental Biology

ORIGINAL RESEARCH
published: 02 June 2022
doi: 10.3389/fcell.2022.894734

Orally Administered Plasmalogens Alleviate Negative Mood States and Enhance Mental Concentration: A Randomized, Double-Blind, Placebo-Controlled Trial

*Minoru Fujino[1], Jun Fukuda[2], Hirohisa Isogai[2], Tetsuro Ogaki[2], Shiro Mawatari[3], Atsushi Takaki[4], Chikako Wakana[1] and Takehiko Fujino[3,5]**

[1]BOOCS Clinic Fukuoka, Fukuoka, Japan, [2]Faculty of Human Sciences, Kyushu Sangyo University, Fukuoka, Japan, [3]Institute of Rheological Functions of Food, Fukuoka, Japan, [4]Department of Integrative Physiology, Kyushu University Graduate School of Medical Sciences, Fukuoka, Japan, [5]The Japanese Plasmalogen Society, Fukuoka, Japan

OPEN ACCESS

Edited by:
Johannes Berger,
Medical University of Vienna, Austria

Reviewed by:
Shawn M. Talbott,
Amare Global, United States
Angelina Angelova,
UMR8612 Institut Galien Paris Sud (IGPS), France

***Correspondence:**
Takehiko Fujino
fujino-t@boocsclinic.com

Specialty section:
This article was submitted to Cellular Biochemistry, a section of the journal Frontiers in Cell and Developmental Biology

Received: *12 March 2022*
Accepted: *21 April 2022*
Published: *02 June 2022*

Citation:
Fujino M, Fukuda J, Isogai H, Ogaki T, Mawatari S, Takaki A, Wakana C and Fujino T (2022) Orally Administered Plasmalogens Alleviate Negative Mood States and Enhance Mental Concentration: A Randomized, Double-Blind, Placebo-Controlled Trial. Front. Cell Dev. Biol. 10:894734. doi: 10.3389/fcell.2022.894734

Background: Plasmalogens have been shown to improve neurodegenerative pathology and cognitive function. We hypothesized that plasmalogens work in small amounts as a kind of hormone interacting with a G protein-coupled receptor, and then explored the effects of scallop-derived purified plasmalogens on psychobehavioral conditions in a randomized placebo-controlled trial of college athletes in Japan.

Methods and materials: Eligible participants were male students aged 18–22 years who belonged to university athletic clubs. They were randomly allocated to either plasmalogen (2 mg per day) or placebo treatment of 4 weeks' duration. The primary outcome was the T-score of the Profile of Mood States (POMS) 2–Adult Short, and the secondary outcomes included the seven individual scales of the POMS 2, other psychobehavioral measures, physical performance, and laboratory measurements. The trial was registered at the Japan Registry of Clinical Trials (jRCTs071190028).

Results: Forty participants (20 in the plasmalogen group and 20 in the placebo group) completed the 4-week treatment. The Total Mood Disturbance (TMD) score of the plasmalogen group showed a greater decrease at 4 weeks than that of the placebo group while the between-group difference was marginally significant ($p = 0.07$). The anger-hostility and fatigue-inertia scores of the POMS 2 decreased significantly in the plasmalogen group, but not in the placebo group, at 4 weeks. Between-group differences in those scores were highly significant ($p = 0.003$ for anger-hostility and $p = 0.005$ for fatigue-inertia). The plasmalogen group showed a slight decrease in the Athens Insomnia Scale at 2 weeks, and the between-group difference was near-significant ($p = 0.07$). The elapsed time in minute patterns on the Uchida-Kraepelin test, which is a marker of mental concentration, revealed significantly greater performance in the plasmalogen group than in the placebo group. There were no between-group differences in physical and laboratory measurements.

Conclusion: It is suggested that orally administered plasmalogens alleviate negative mood states and sleep problems, and also enhance mental concentration.

Keywords: plasmalogen, scallop-derived, psychobehavioral effect, sleep, mental concentration, athlete, randomized placebo-controlled trial

1 INTRODUCTION

Plasmalogens are a class of glycerophospholipids containing a vinyl ether bond at the sn-1 position of the glycerol backbone and polyunsaturated fatty acids (PUFA) at the sn-2 position, being produced by the multistep process in peroxisome and endoplasmic reticulum. In humans, plasmalogens exist mainly in the forms of phosphatidyl ethanolamine plasmalogen (PlsPE) and phosphatidyl choline plasmalogen (PlsPC), of which the former is predominant in human tissues, especially in the brain (Farooqui and Horrocks, 2001; Braverman and Moser, 2012). The levels of plasmalogens have been reported to be decreased in the postmortem brain of Alzheimer's disease (AD) and in the blood of AD patients (Ginsberg et al., 1995; Guan et al., 1999; Han et al., 2001; Goodenowe et al., 2007; Wood et al., 2010; Oma et al., 2012; Wood et al., 2015; Yamashita et al., 2016; Zarrouk et al., 2018). Several recent reviews have suggested that plasmalogen supplementation may improve cognitive function and neurodegenerative pathology (Farooqui and Horrocks, 2001; Braverman and Moser, 2012; Lizard et al., 2012; Dorninger et al., 2017; Su et al., 2019). Moreover, a simple method was developed to extract a large number of plasmalogens from animals (Mawatari et al., 2007; Mawatari et al., 2009), which enabled research on plasmalogen treatment. In mice, plasmalogen administration not only suppressed inflammation-induced activation of microglia, amyloid formation, and neuronal cell death in the brain but also improved cognitive function (Ifuku et al., 2012; Katafuchi et al., 2012; Hossain et al., 2013; Hossain et al., 2018; Gu et al., 2022; Hossain et al., 2022). A randomized controlled trial demonstrated that scallop-derived purified plasmalogens improved cognitive function in patients with mild AD or mild cognitive impairment (Fujino et al., 2017; Fujino et al., 2018). Improvement in cognitive function associated with plasmalogen supplementation was also observed in patients with moderate to severe AD (Fujino et al., 2019) and Parkinson's disease (Mawatari et al., 2020).

Plasmalogens may also be potentially beneficial with respect to psychobehavioral aspects other than cognition. However, the effects of plasmalogen supplementation on psychological states have not been investigated while psychological distress is very common in free-living populations and affects mental and physical health (Brandt et al., 2017). Training and participation in competitive sport may affect athletes' mood and sleep, which in turn may influence their daily life and competition performance (Weerakkody et al., 2021). We explored the effects of scallop-derived purified plasmalogens on psychobehavioral conditions of college athletes in a randomized placebo-controlled trial. The Profile of Mood States (POMS) Version 2 (Heuchert and McNair, 2012), other psychobehavioral parameters, physical performance, and laboratory measurements were used in the present study.

2 METHODS AND MATERIALS

2.1 Participants

Eligible participants were unmarried male students aged 18–22 years who belonged to the athletic clubs of Kyushu Sangyo University. Those were excluded if they had regular medical treatment or follow-up in hospitals or clinics; if they participated in any other clinical trials; or if they had an allergy to shellfish. Furthermore, students were not admitted to the trial if a principal physician investigator (MF) or an organizing professor of the University (TO) deemed them ineligible to participate.

2.2 Design and Procedures

Study participants were recruited at the University campus *via* posters, brochures, and internet advertisements from October to November 2019. All participants gave written informed consent, and their guardians also gave consent in the case of students under 20 years of age. Eligible students were randomly allocated to either plasmalogen (2 mg per day) or placebo treatment of 4 weeks' duration and ingested two capsules of 0.5 mg plasmalogen or placebo twice daily. Allocation was made at the baseline examination according to the sequence of a randomization list. A computer-generated list of randomizations was prepared by an independent statistician (MedStat Corporation, Fukuoka) using the permuted block method with a block size of four containing equal assignments to the two groups. The plasmalogen and placebo capsules were prepared by a manufacturer (B&S Corporation, Tokyo). Packages of plasmalogen or placebo capsules were numbered according to the list of randomizations and were transferred to the study site. The central management center confirmed the eligibility of each participant and monitored the enrollment. The list of random allocation was kept confidential until the completion of the electric data files used for the statistical analysis.

Participants visited the study site at the university campus at 0, 2, and 4 weeks for assessment of efficacy parameters and adverse events. Laboratory measurements were performed at 0 and 4 weeks of the treatment. The baseline measurements were taken on November 9–19, 2019, and the 4-week measurements were on December 9–19, 2019. Compliance with the treatment was assessed by counting the number of remaining capsules.

The primary efficacy outcome was the Total Mood Disturbance (TMD) T-score of POMS 2–Adult Short (Heuchert and McNair, 2012). Secondary outcomes included the seven individual scales of POMS 2, other psychobehavioral measures (Athens Insomnia Scale and Uchida-Kraepelin test), physical performance test (shuttle run, grip muscle strength, and standing long jump), plasmalogen levels in plasma and erythrocytes, plasma levels of brain-derived neurotrophic factor (BDNF), urinary 8-hydroxy-2′-deoxyguanosine (8-OHdG), body mass index, and percent body

fat. Adverse events were captured by self-report and in-person interview if needed and by means of laboratory measurements at 4 weeks (serum biochemistry and blood cell counts).

2.3 Measurements

2.3.1 Psychological Assessment

The POMS 2–Adult Short is a mood inventory consisting of 35 items rated on a 5-point scale from 0 (not-at-all) to 4 (extremely) to capture the seven scales measuring anger-hostility, confusion-bewilderment, depression-dejection, fatigue-inertia, tension-anxiety, vigor-activity, and friendliness during the past 1 week. The TMD was obtained by summation of the six-scale scores other than the friendliness score (Heuchert and McNair, 2012). The Japanese version of POMS 2 is commercially available (Yokoyama, 2015). We used the T-scores of the TMD and seven scales, which are standardized so that the distribution has a mean of 50 points and SD of 10 points based on a survey of Japanese adults (Yokoyama, 2015).

The Athens Insomnia Scale is a self-administered questionnaire asking eight questions rated on a 4-point scale from 0 (no problem) to 3 (severe problem) in response (Soldatos et al., 2000; Okajima et al., 2013). While the prototype is designed to assess insomnia over the past 1 month, the present study used the past 1 week as a reference period.

The Uchida-Kraepelin test is a psychodiagnostic test derived from the Kraepelin's work curve (Kashiwagi, 1962; Seiwa, 1971), and has been used to measure work performance, and to assess occupational aptitude and mental arithmetic stressors (Sugimoto et al., 2009; Yoto et al., 2018). The standard test sheets were purchased (Japan Psychiatric Technology Institute, Inc., Tokyo). A test sheet contains an array of 17 lines of 116 random single-digit numbers per line. The task is a consecutive summation of two adjacent digits per line in one minute, the answers being written down below the line. Examinees are requested to perform calculations as quickly and accurately as possible and to move sequentially to the next line on the examiner's cue. While the test is usually performed in two 15 min sessions with a 5 min rest, the task in the present study was one 10 min session using the first 10 lines. The number of attained calculations and incorrect answers were counted per line. Total and line-specific percentages of correct calculations were used as indices of task performance.

2.3.2 Anthropometric Measurements

Height (in 0.1 cm) was measured in an upright position, and body weight (in 0.1 kg) was measured with underwear on. Body mass index (kg/m^2) was calculated. Percent body fat was measured by the impedance method using a commercial apparatus (In Body 770, In Body Japan Co., Tokyo).

2.3.3 Physical Performance Test

Physical performance was measured with respect to grip strength, standing long jump, and 20 m shuttle run test in accordance with the Manual for the New Physical Fitness Tests (age of 20–64 years) of the Japanese Ministry of Education, Culture, Sports, Science and Technology ["Ministry of Education Culture Sports Science and Technology. Manual for the New Physical Fitness Tests (Age of 20-64 Years)," 1999]. The number of repeats in the shuttle run test was transformed to VO_2 max by using the conversion table of the Manual.

TABLE 1 | Lipid composition of purified ether phospholipid from scallop.

Lipid	(mg/g)
Ethanolamine plasmalogen	39.7
Ethanolamine alkyl phospholipid	2.9
Choline plasmalogen	1.6
Choline alkyl phospholipid	32.6
Cholesterol	11.5
Ceramide aminoethyl phosphonate	10.6

2.3.4 Laboratory Measurements

Venous blood was drawn after an overnight fast, and urine sample was collected before blood sampling. Plasmalogen levels in plasma and erythrocyte membrane were determined at the Institute of Rheological Functions of Food (Hisayama-machi, Fukuoka) according to the method described elsewhere (Mawatari et al., 2007; Mawatari et al., 2016). Plasma BDNF and urinary 8-OHdG and deoxyguanosine (dG) were determined at the Department of Integrative Physiology, Kyushu University Graduate School of Medical Sciences. Plasma BDNF was determined by the ELISA method (Tiekou Lorinczova et al., 2020) using a commercial kit (biosensis, Adelaide). Urinary 8-OHdG and dG were measured using a commercial kit by the TAS system (TAS Project Co., Ltd., Fukuoka) (Matsuoka et al., 2010). 8-OHdG and dG were detected by electrochemical and UV detector at 254 nm followed by HPLC, using the same sample. Hereby, 8-OHdG/dG ratio indicating biological oxidation was calculated. Routine biochemical measurements and blood cell counting were carried out at an external laboratory (BML, Tokyo). Adverse events in laboratory measurements were defined in accordance with the Common Terminology Criteria Adverse Events (CTCAE) version 5.0 ("U.S. Department of Health and Human Service. Common Terminology Criteria for Adverse Events (Ctcae) Version 5.0 Published: November 27, 2017").

2.4 Materials

The lipid composition of purified ether phospholipids from scallop is shown in **Table 1**. One capsule, used in this study, contained 0.48 mg of ethanolamine plasmalogen and 0.02 mg of choline plasmalogen.

2.5 Statistical Analysis

The sample size was determined to be 20 in each group. On the basis of the results from randomized and non-randomized trials of psychobehavioral therapy or supplementation on POMS (Katsuki et al., 2013; Okuyama et al., 2018; Irie et al., 2019), we assumed a 20% greater improvement in the POMS T-score for the plasmalogen group than for the placebo group. The SD of the TMD T-score is 10, and the SD of the change in the T-score is 10 if the correlation between the T-scores before and after treatment

TABLE 2 | Background characteristics of the study participants.

Variable	Plasmalogen (n = 20)	Placebo (n = 20)	p*
Age (year), mean ± SD	19.6 ± 0.7	19.3 ± 0.9	0.23
Current smoking, n (%)	0 (0.0)	2 (10.0)	0.49
Alcohol use (≥1/week), n (%)	0 (0.0)	3 (15.0)	0.23
Food allergy, n (%)	2 (10.0)	2 (10.0)	1.00
Height (cm), means ± SD	170.3 ± 5.2	171.5 ± 5.0	0.47
Body weight (kg), means ± SD	66.8 ± 9.2	68.1 ± 5.6	0.59

SD: standard deviation.

**Unpaired t-test for continuous variables and Fisher's exact test for dichotomous variables.*

is assumed to be 0.50 (Follmann et al., 1992). Under the conditions of a two-sided significance level of 0.05 and detection power of 0.80, the required sample size was calculated as 17 for each group. The target number was set to be 20 for each as a precaution against dropouts.

The safety analysis population consisted of all randomized participants who received at least one dose of treatment and completed both baseline and follow-up assessments regarding adverse events. The efficacy analysis population comprised those in the safety analysis population for whom efficacy data were available.

Mean and standard deviation (SD) were presented for continuous variables, and proportion was used for dichotomous variables. The changes from baseline at 2 and 4 weeks were compared between the two groups. The magnitude of the between-group difference in the change from baseline was expressed by mean difference and 95% confidence interval (CI). The between-group difference was assessed by unpaired t-test for continuous variables and by Fisher's exact probability for dichotomous variables. Statistical significance of the change from baseline in each group was assessed by paired t-test. The interaction between baseline value and treatment was evaluated by using multiple regression analysis. The analysis on the interaction had not been specified in the protocol; however, it was adopted because it was naturally conceivable that improvement, if any, could be expected in men having a poor state of the outcome at baseline. The effects on daily physical and mental conditions were examined by the mixed-model regression analysis, in which days of assessment were nested in individuals. Statistical significance was declared if the two-sided p was <0.05. Statistical analyses were carried out by Stata Statistical Software Release 13 (StataCorp, College Station, TX).

3 RESULTS

A total of 42 participants were randomly allocated to either plasmalogen (n = 21) or placebo (n = 21) treatment, all of which completed the 4-week treatment. All the participants consumed more than 80% of the capsules containing the test substance in each group. However, the efficacy analysis included 40 participants (20 in the plasmalogen group and 20 in the placebo group) because the Review Board recommended that the analysis should exclude the two last-enrolled students who exceeded the target number specified in the protocol.

3.1 Baseline Characteristics

There was no measurable between-group difference with respect to background characteristics of the study participants such as age, smoking, alcohol drinking, and anthropometric measurements (**Table 2**). None of the primary and secondary outcome variables showed an appreciable difference between the two groups at baseline (**Table 3**). Mean T-scores for the scales of vigor-activity and friendliness were approximately 60 points while mean T-scores were not more than 50 points for the TMD and the other five individual scales.

3.2 Effects on POMS 2

Table 4 shows the changes from baseline in T-scores of the TMD and the seven scales of POMS 2 at 2 and 4 weeks. Notable changes were not observed for these scores at 2 weeks. The TMD T-score at 4 weeks decreased statistically significantly in the plasmalogen group ($p < 10^{-3}$) and decreased near-significantly in the placebo group (p = 0.07), resulting in a greater decrease in the former group than in the latter. While the overall between-group difference in the decrease was not statistically significant (p = 0.07), the decrease in the plasmalogen group was more evident in those with higher baseline scores (interaction p = 0.048), as illustrated in **Figure 1**.

The scores of anger-hostility and fatigue-inertia decreased significantly in the plasmalogen group, but not in the placebo group, at 4 weeks. The decreases were statistically significantly greater in the plasmalogen group than in the placebo group (p = 0.003 for anger-hostility and p = 0.005 for fatigue-inertia). The vigor-activity score also showed a statistically significant difference in the 4-week change between the two groups (p = 0.04) whereas the within-group change was not statistically significant in either group; the T-score tended to decrease in the plasmalogen group and to increase in the placebo group. There was no measurable difference in the changes in the other scales between the two groups.

P values for the interactions between baseline score and treatment on the changes in the T-scores at 4 weeks were as follows: anger-hostility 0.03, confusion-bewilderment 0.12, depression-dejection 0.24, fatigue-inertia 0.07, tension-anxiety 0.19, vigor-activity 0.11, and friendliness 0.74. The decreases in the scores of anger-hostility and fatigue-inertia in the plasmalogen group were greater when the baseline scores were higher (**Figure 2**).

TABLE 3 | Primary and secondary outcomes at baseline lightfaced (means ± SD).

Variable	Plasmalogen (n = 20)	Placebo (n = 20)	p^a
POMS2 T-score[b]			
Total mood disturbance	46.4 ± 7.6	44.3 ± 7.5	0.39
Anger-hostility	46.8 ± 8.8	43.5 ± 6.3	0.17
Confusion-bewilderment	49.3 ± 8.8	48.4 ± 7.0	0.72
Depression-dejection	47.6 ± 6.5	46.1 ± 6.8	0.49
Fatigue-inertia	48.4 ± 7.1	46.4 ± 6.5	0.36
Tension-anxiety	47.1 ± 8.6	46.4 ± 8.9	0.79
Vigor-activity	57.2 ± 7.7	58.0 ± 7.7	0.73
Friendliness	59.7 ± 10.5	59.6 ± 11.2	0.97
Other psychological tests			
Athens Insomnia Scale[b]	3.3 ± 2.5	3.1 ± 2.4	0.73
Uchida-Kraepelin Test	47.6 ± 11.8	43.0 ± 13.3	0.26
Physical fitness test			
Grip strength (kg)	43.7 ± 8.5	44.9 ± 6.4	0.60
Standing long jump (cm)	234 ± 19	224 ± 29	0.22
VO_2max (ml/kg/min)	49.0 ± 4.0	49.0 ± 3.2	0.99
Obesity-related measurement			
Body mass index (kg/m^2)	23.0 ± 2.7	23.2 ± 2.0	0.81
Percent body fat (%)	14.8 ± 5.1	14.3 ± 6.0	0.79
Laboratory measurement			
Plasma PlsPE (mg/dl)	5.15 ± 1.32	5.27 ± 2.06	0.83
Erythrocyte PlsPE (%)	8.54 ± 0.87	8.54 ± 0.75	0.99
Plasma BDNF (ng/ml)	8.52 ± 3.74	7.81 ± 2.41	0.48
Urinary 8-OHdG (ng/ml)	39.4 ± 24.1	58.7 ± 85.7	0.34
Urinary 8-OHdG/dG (%)	2.98 ± 2.46	2.91 ± 3.20	0.94

BDNF, brain-derived neurotrophic factor; dG, deoxyguanosine; 8-OHdG, 8-hydoroxy deoxyguanosine; PlsPE, phosphatidyl ethanolamine plasmalogen; SD, standard deviation.
[a]*Unpaired t-test.*
[b]n = *19 in the plasmalogen group.*

TABLE 4 | Changes of POMS 2 T-scores from baseline at 2 and 4 weeks in plasmalogen and placebo groups.

Scale	Plasmalogen		Placebo		Difference		
	Mean ± SD	p^a	Mean ± SD	p^a	Mean	95% CI	p^b
2 weeks	(n = 18)		(n = 19)				
Total mood disturbance	−1.5 ± 3.8	0.12	−0.6 ± 5.2	0.60	−0.9	−3.9, 2.2	0.57
Anger-hostility	−2.4 ± 5.0	0.06	0.5 ± 6.1	0.71	−2.9	−6.7, 0.8	0.12
Confusion-bewilderment	−2.8 ± 6.0	0.07	−1.0 ± 7.7	0.58	−1.8	−6.4, 2.8	0.44
Depression-dejection	−0.1 ± 4.8	0.92	0.3 ± 5.3	0.80	−0.4	−3.8, 3.0	0.80
Fatigue-inertia	−0.6 ± 5.7	0.65	1.1 ± 6.8	0.49	−1.7	−5.9, 2.5	0.41
Tension-anxiety	−2.6 ± 4.6	0.03	−1.8 ± 5.5	0.17	−0.8	−4.2, 2.6	0.63
Vigor-activity	−1.4 ± 7.1	0.42	2.6 ± 7.7	0.16	−4.0	−9.0, 0.9	0.11
Friendliness	−3.5 ± 10.5	0.17	1.4 ± 7.0	0.39	−0.9	−10.8, 1.0	0.10
4 weeks	(n = 19)		(n = 20)				
Total mood disturbance	−4.2 ± 4.3	$<10^{-3}$	−1.8 ± 4.0	0.07	−2.5	−5.2, 0.2	0.07
Anger-hostility	−4.0 ± 4.3	$<10^{-3}$	0.3 ± 4.1	0.75	−4.3	−7.0, −1.6	0.003
Confusion-bewilderment	−4.9 ± 6.9	0.006	−2.0 ± 5.5	0.13	−3.0	−7.0, 1.0	0.14
Depression-dejection	−1.8 ± 5.9	0.19	−0.2 ± 3.1	0.77	−1.6	−4.7, 1.4	0.28
Fatigue-inertia	−6.4 ± 6.1	$<10^{-3}$	−0.9 ± 5.4	0.49	−5.5	−9.2, −1.8	0.005
Tension-anxiety	−6.0 ± 5.6	$<10^{-3}$	−3.4 ± 6.1	0.02	−2.6	−6.4, 1.2	0.17
Vigor-activity	−3.7 ± 8.8	0.09	2.5 ± 9.4	0.26	−6.1	−12.1, −0.2	0.04
Friendliness	−6.4 ± 14.2	0.07	0.4 ± 7.5	0.81	−6.8	−14.1, 0.5	0.07

CI: confidence interval; SD: standard deviation.
[a]*Paired* t*-test for the within-group comparison.*
[b]*Unpaired* t*-test for the between-group comparison.*

3.3 Effects on Other Psychological Parameters

Table 5 summarizes the results of the Athens Insomnia Scale and Uchida-Kraepelin test. The Plasmalogen group showed small, but statistically significant decreases in the Athens Insomnia Scale score at both 2 and 4 weeks whereas no such decreases were noted in the placebo group; the between-group difference in the decrease was nearly

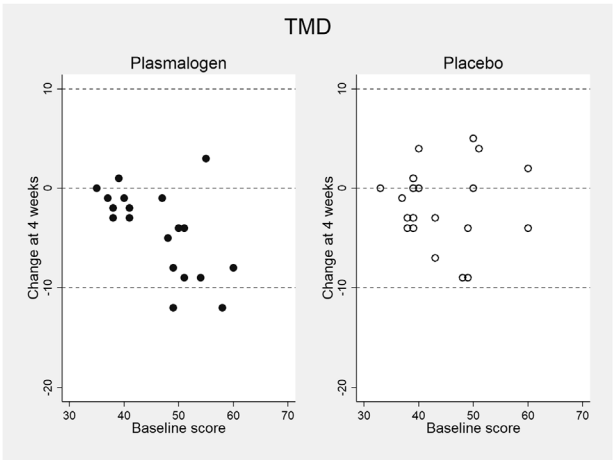

FIGURE 1 | Change in total mood disturbance (TMD) T-score of POMS 2 at 4 weeks versus baseline score in plasmalogen and placebo groups.

significant at 2 weeks ($p = 0.07$), but not at 4 weeks ($p = 0.26$). However, the decrease in the plasmalogen group was more pronounced in those with higher baseline scores at 2 weeks (interaction $p = 0.02$) and 4 weeks (interaction $p = 0.004$).

A highly significant improvement in the Uchida-Kraepelin test was observed at 2 and 4 weeks in both groups. The improvement seemed to be slightly greater in the plasmalogen group than in the placebo group, but the between-group difference was not significant at 2 and 4 weeks, respectively. The baseline values did not affect the treatment effect either at 2 weeks (interaction $p = 0.85$) or at 4 weeks (interaction $p = 0.65$). The post-hoc analysis showed a significant interaction between treatment and elapsed time in minute on the Uchida-Kraepelin test ($p < 0.01$). The Plasmalogen group showed a significantly increased performance in the middle (5 and 6 min) and toward the end of the 10 min task compared with the placebo group (**Figure 3**).

3.4 Physical Performance and Obesity-Related Measures

There was no measurable effect of plasmalogen supplementation on either physical performance or obesity-related measures (**Table 6**).

3.5 Laboratory Outcomes

Plasma PlsPE levels significantly decreased in the plasmalogen group ($p < 10^{-3}$) and non-significantly in the placebo group ($p = 0.11$), and the decrease did not differ by treatment group (**Table 6**). On the other hand, erythrocyte PlsPE increased to almost the same magnitude in the plasmalogen ($p < 10^{-4}$) and the placebo ($p < 10^{-5}$) groups, with no between-group difference in the change of PlsPE. Plasma BNDF, urinary 8-OHdG, and urinary 8-OHdG/dG did not change differentially in the plasmalogen and placebo groups. Nor did body mass index and percent body fat.

3.6 Adverse Events

Clinical adverse events were reported by three participants (common cold, acute gastroenteritis, and calcaneal fracture) in the plasmalogen group and by one participant (common cold) in the placebo group ($p = 0.61$). Laboratory adverse events were noted in 14 men (66.7%) in the plasmalogen group and in 13 men (61.9%) in the placebo group ($p = 1.00$). The average numbers of the laboratory adverse events were 1.1 (SD 1.0) in the plasmalogen group and 1.3 (SD 1.5) in the placebo group ($p = 0.63$). Details of laboratory adverse events are described in **Supplementary Table S1**. Almost all of the laboratory adverse

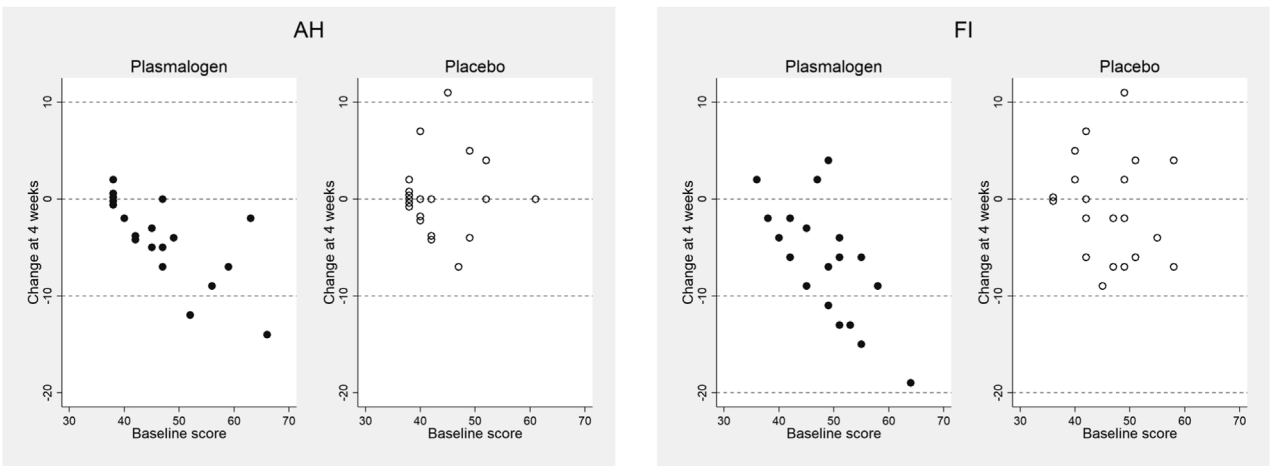

FIGURE 2 | Changes in anger-hostility (AH) and fatigue-inertia (FI) T-scores of POMS 2 at 4 weeks versus baseline scores in plasmalogen and placebo groups. Points of identical values in the two dimensions are minimally shifted along the vertical direction and are displayed as aggregated circles.

TABLE 5 | Changes from baseline in Athens Insomnia Score and Uchida-Kraepelin Test (achievement percentage) at 2 and 4 weeks.

Scale	Plasmalogen		Placebo		Difference		
	Mean ± SD (*n*)	p^a	Mean ± SD (*n*)	p^a	Mean	95% CI	p^b
2 weeks							
Athens Insomnia Score	−1.4 ± 2.1 (19)	0.009	−0.2 ± 1.9 (20)	0.64	−1.2	−2.5, 0.1	0.07
Uchida-Kraepelin Test	9.5 ± 4.9 (20)	$<10^{-7}$	7.2 ± 4.9 (20)	$<10^{-5}$	2.3	−0.9, 5.5	0.15
4 weeks							
Athens Insomnia Score	−1.3 ± 2.4 (19)	0.03	−0.5 ± 1.7 (20)	0.21	−0.8	−2.1, 0.6	0.26
Uchida-Kraepelin Test	11.8 ± 6.7 (20)	$<10^{-6}$	8.9 ± 5.4 (20)	$<10^{-6}$	2.9	−1.0, 6.8	0.14

CI: confidence interval; SD: standard deviation.
[a]*Paired* t*-test for the within-group comparison.*
[b]*Unpaired* t*-test for the between-group comparison.*

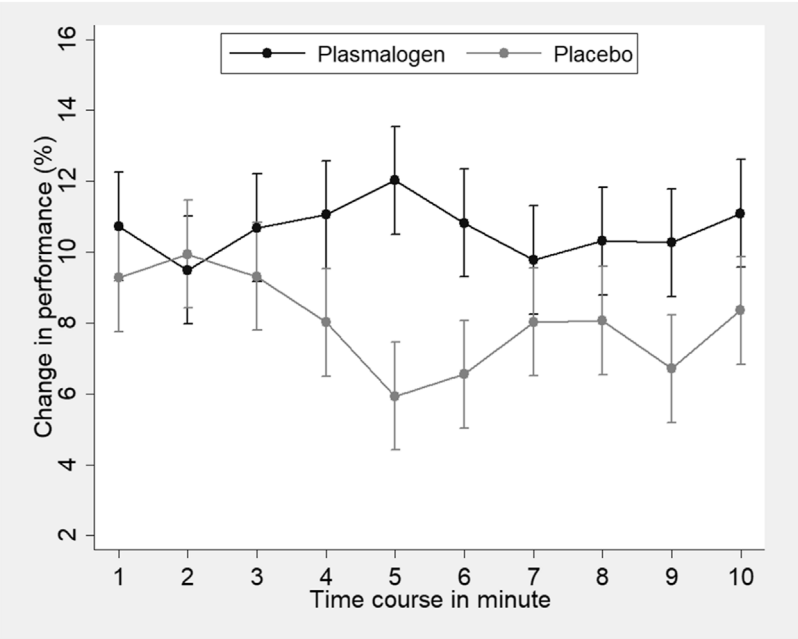

FIGURE 3 | Change in the Uchida-Kraepelin test performance according to time-course minutes of the task in plasmalogen and placebo groups. Based on repeated measures analysis of variance with weeks of treatment (2 points) and elapsed minutes (10 points) specified as repeated measures. Vertical bars represent 95% confidence intervals of marginal means. Interaction for treatment and elapsed minutes was statistically significant ($p < 0.01$, corrected by the Greenhouse-Geisser method).

events were grade 1. The most common one was an elevation in serum creatine phosphokinase (CPK).

4 DISCUSSION

In male college athletes, a 4-week supplementation with plasmalogens improved the T-scores of anger-hostility and fatigue-inertia more greatly than with placebo and also tended to alleviate the overall mood disturbance. The findings suggest that plasmalogens may mitigate a mood state of anger-hostility and enhance the perception of recovery from fatigue-inertia. It is of particular interest that the effects of plasmalogens on the TMD and the scales of anger-hostility and fatigue-inertia were greater in those with worse scores at baseline. These interactions further support the beneficial effect of plasmalogens on mood state.

The finding on the vigor-activity score was an unexpected one. The vigor-activity score decreased by 3.7 points in the plasmalogen group and increased by 2.5 points in the placebo group. While these changes were not statistically significant in either group, the plasmalogen group statistically significantly deteriorated the vigor-activity scale in comparison with the placebo group. The vigor-activity scale represents a positive mood state and seems to be the opposite mood of fatigue-inertia. The vigor-activity scale represents the degree of being "lively," "active," "energetic," "vigorous" and "enthusiastic,"

TABLE 6 | Changes in physical fitness, laboratory measurements, and obesity-related measures at 2 and 4 weeks from baseline.

	Plasmalogen (n = 20)		Placebo (n = 20)		Difference		
	Mean ± SD	p^a	Mean ± SD	p^a	Mean	95% CI	p^b
Physical fitness test							
Grip strength (kg)	−0.8 ± 3.1	0.27	−1.4 ± 2.1	0.01	0.6	−1.1, 2.3	0.51
Standing long jump (cm)	−3.4 ± 10.2	0.16	5.7 ± 19.6	0.21	−9.1	−19.3, 1.1	0.08
VO_2max (ml/kg/min)	0.5 ± 2.6	0.40	0.0 ± 2.2	0.95	0.5	−1.1, 2.1	0.53
Laboratory measurement							
Plasma PlsPE (mg/dl)	−0.84 ± 0.89	$<10^{-3}$	−0.62 ± 1.66	0.11	−0.22	−1.07, 0.64	0.61
Erythrocyte PlsPE (%)	0.64 ± 0.57	$<10^{-4}$	0.76 ± 0.57	$<10^{-5}$	−0.12	−0.48, 0.25	0.52
Plasma BDNF (ng/ml)	0.01 ± 4.32	0.99	0.14 ± 3.80	0.87	−0.13	−2.73, 2.48	0.92
Urinary 8-OHdG (ng/ml)[c]	−0.171 ± 0.656	0.26	0.005 ± 1.054	0.98	−0.176	−0.738, 0.386	0.53
Urinary 8-OHdG/dG[c]	−0.430 ± 0.875	0.04	−0.080 ± 0.900	0.69	−0.350	−0.918, 0.219	0.22
Obesity-related measure							
Body mass index (kg/m^2)	0.22 ± 0.41	0.03	0.18 ± 0.35	0.04	0.05	−0.20, 0.29	0.71
Percent body fat (%)	0.93 ± 1.42	0.008	0.83 ± 1.57	0.03	0.10	−0.86, 1.06	0.83

CI: confidence interval; SD: standard deviation.
[a]*Paired* t*-test for the within-group comparison.*
[b]*Unpaired* t*-test for the between-group comparison.*
[c]*Measurements were transformed to the natural logarithm scale.*

whereas the fatigue-inertia scale measures the degree of being "worn out," "fatigued," "exhausted," "weary" and "drained" (Heuchert and McNair, 2012). In a previous study of government employees in the United States (Travis et al., 2018), a psychological intervention of meditation resulted in an increase in the POMS vigor-activity score and consistent decreases in the five other negative scales. In that study, the Pearson correlation coefficient for the 4-month changes in the scores between the vigor-activity and fatigue-inertia scales was −0.52 (Travis et al., 2018). In the present study, the vigor-activity score was weakly correlated with the fatigue-inertia score negatively at baseline and in a positive direction longitudinally (r = −0.13 for the baseline score and r = 0.17 for the change at 4 weeks). The decrease in the vigor-activity score may not necessarily indicate an unfavorable effect on the present study population. It deserves to be mentioned that the vigor-activity scores were within normal limits at both baseline and 4 weeks. A small decrease of four points in the vigor-activity score may have reflected a change toward mental calmness and composedness or weakening of aggressiveness and offensiveness in the young athletes with a relatively high score at baseline.

The findings regarding the Athens Insomnia Scale suggest that plasmalogens may alleviate sleep problems. It is noteworthy that the effect of plasmalogens decreasing the score of the Athens Insomnia Scale was greater in those with higher baseline scores, consistently at 2 and 4 weeks. It is also notable that the effect of plasmalogens was observable even at 2 weeks of treatment.

A learning or practice effect has been documented in the Uchida-Kraepelin test, particularly when the test is repeated at short intervals (Seiwa, 1971). It is thus likely that the successive increases in the performance at 2 and 4 weeks are ascribed to a learning effect. It is known that the performance decreases with the passage of time in a session of the Uchida-Kraepelin test (Kashiwagi, 1962). It is thus of interest to examine the treatment effect on minute-specific performance. Increased performance in the plasmalogen group was more notable in the middle (5 and 6 min) and toward the end of the 10-min task (**Figure 3**). To our knowledge, none of the previous intervention studies have addressed the effect on the minute-specific performance in the Uchida-Kraepelin test (Ataka et al., 2008; Johnson et al., 2016; Takanari et al., 2016; Saito et al., 2018). It could be argued that plasmalogens may maintain the performance in the middle of work, elicit the so-called last spurt in work performance, and increase mental concentration. The present findings are compatible with the abovementioned effect of plasmalogens improving the POMS fatigue-inertia score.

It seems strange that a small dose (2 mg per day) of plasmalogens showed the prominent improvement and enhancement in brain function as mentioned above although the same small dose of plasmalogens also revealed the significant efficacy on cognitive function in AD, mild cognitive impairment, and Parkinson's disease. One of the major mechanisms for such effects is that plasmalogens may be the ligand of G protein-coupled receptors and thus may act as a hormone. More detailed mechanisms have been discussed in the previous report (Fujino et al., 2017; Fujino et al., 2020).

In this study, all participants were young athletes and there was no improvement in physical performance measured by grip strength, standing long jump, and 20 m shuttle run. However, some improvement in competition performance might be expected because it is well known that competition performance is strongly affected by such negative mood states, sleep disorders, and mental concentration (Mah et al., 2011; Brandt et al., 2017; Weerakkody et al., 2021) as improved in this study. Further research is required to determine a positive correlation between plasmalogens and competition performance.

Despite the abovementioned significant improvement in psychobehavioral measures in the plasmalogen group, plasmalogen blood levels (plasma PlsPE and erythrocyte PlsPE) showed no significant difference between the two groups. The reason for that is not clear. However, it might be partly due to the fact that

the study period was as short as 1 month, considering that there was no significant between-group difference in plasmalogen blood levels during the first 2 months after administration shown in the previous study (Fujino et al., 2017).

Recent studies have demonstrated that oxidative stress-induced neuroinflammation impairs brain function including cognitive function. However, the present study did not find a significant change in urinary 8-OHdG, known to reflect oxidative stress (Valavanidis et al., 2009; Urbaniak et al., 2020). Moreover, no statistically significant change was observed in blood BDNF although plasmalogens are assumed to improve brain function by increasing BDNF (Hossain et al., 2022). These results suggest that neither urinary 8-OHdG nor blood BDNF may reflect a minute change in the brain.

This study strongly suggests that oral administration of plasmalogens alleviates negative mood states and sleep disorders, and enhances mental concentration. These effects may be responsible for the suppression effects of plasmalogens on oxidative stress-induced neuroinflammation (Ifuku et al., 2012; Hossain et al., 2018). Yet, the fact also remains that most of the neuroinflammation-suppression effects observed in animal studies were achieved using mouse hippocampus, providing no direct evidence of suppression effects in the amygdala or neocortex related to the abovementioned symptoms and function. As another potential mechanism for these effects, it may be suggested that plasmalogens improved sleep conditions, resulting in the enhancement of mental concentration.

There are several weaknesses to be noted in this study although random allocation, use of placebo, and high compliance to test substances are among the strengths of the present study. The 4 week treatment period may have been relatively short, and the number of study participants was too small to detect an observed between-group difference in terms of the TMD score (the primary outcome) which turned out to be much smaller than expected. Further studies are needed to corroborate the observed effects of plasmalogens on negative mood states of the POMS 2, sleep disorders, and mental concentration in large and different populations such as insomnia and depression.

DATA AVAILABILITY STATEMENT

The raw data supporting the conclusion of this article will be made available by the authors, without undue reservation.

ETHICS STATEMENT

The studies involving human participants were reviewed and approved by the Human Subjects Research Ethics Review Committee of Kyushu Sangyo University and the Clinical Research Network Fukuoka Certified Review Board. The patients/participants provided their written informed consent to participate in this study.

AUTHOR CONTRIBUTIONS

Conceptualization, TF and TO. Methodology, TF. Software, HI. Validation, TF and TO. Formal analysis, MF and CW. Investigation, MF, CW, TO, JF, HI, AT, and SM. Resources, JF, HI, and TO. Data curation, MF and CW. Writing–original draft preparation, MF. Writing–review and editing, TF. Visualization, CW. Supervision, TF. Project administration, TO and CW. Funding acquisition, TF. All authors have read and agreed to the published version of the manuscript.

FUNDING

This study was financially supported by the Japanese Plasmalogen Society.

ACKNOWLEDGMENTS

The authors are grateful to the students participating in the study; B&S Corporation for the provision of test substance; Suminori Kono at MedStat Corporation for his technical support; and Chizuko Kanemaru for her support in preparing the manuscript.

SUPPLEMENTARY MATERIAL

The Supplementary Material for this article can be found online at: https://www.frontiersin.org/articles/10.3389/fcell.2022.894734/full#supplementary-material

Supplementary Table S1 | Laboratory adverse effects in plasmalogen and placebo groups.

REFERENCES

Ataka, S., Tanaka, M., Nozaki, S., Mizuma, H., Mizuno, K., Tahara, T., et al. (2008). Effects of Oral Administration of Caffeine and D-Ribose on Mental Fatigue. *Nutrition* 24, 233–238. doi:10.1016/j.nut.2007.12.002

Brandt, R., Bevilacqua, G. G., and Andrade, A. (2017). Perceived Sleep Quality, Mood States, and Their Relationship with Performance Among Brazilian Elite Athletes During a Competitive Period. *J. Strength Cond. Res.* 31, 1033–1039. doi:10.1519/jsc.0000000000001551

Braverman, N. E., and Moser, A. B. (2012). Functions of Plasmalogen Lipids in Health and Disease. *Biochimica Biophysica Acta (BBA) - Mol. Basis Dis.* 1822, 1442–1452. doi:10.1016/j.bbadis.2012.05.008

Dorninger, F., Forss-Petter, S., and Berger, J. (2017). From Peroxisomal Disorders to Common Neurodegenerative Diseases - the Role of Ether Phospholipids in the Nervous System. *FEBS Lett.* 591, 2761–2788. doi:10.1002/1873-3468.12788

Farooqui, A. A., and Horrocks, L. A. (2001). Book Review: Plasmalogens: Workhorse Lipids of Membranes in Normal and Injured Neurons and Glia. *Neuroscientist* 7, 232–245. doi:10.1177/107385840100700308

Follmann, D., Elliott, P., Suh, I., and Cutler, J. (1992). Variance Imputation for Overviews of Clinical Trials with Continuous Response. *J. Clin. Epidemiol.* 45, 769–773. doi:10.1016/0895-4356(92)90054-q

Fujino, T., Hossain, M. S., and Mawatari, S. (2020). Therapeutic Efficacy of Plasmalogens for Alzheimer's Disease, Mild Cognitive Impairment, and Parkinson's Disease in Conjunction with a New Hypothesis for the Etiology of Alzheimer's Disease. *Adv. Exp. Med. Biol.* 1299, 195–212. doi:10.1007/978-3-030-60204-8_14

Fujino, T., Yamada, T., Asada, T., Ichimaru, M., Tsuboi, Y., Wakana, C., et al. (2018). Effects of Plasmalogen on Patients with Mild Cognitive Impairment: A Randomized, Placebo-Controlled Trial in Japan. *J. Alzheimers Dis. Park.* 08, 419. doi:10.4172/2161-0460.1000419

Fujino, T., Yamada, T., Asada, T., Tsuboi, Y., Wakana, C., Mawatari, S., et al. (2017). Efficacy and Blood Plasmalogen Changes by Oral Administration of Plasmalogen in Patients with Mild Alzheimer's Disease and Mild Cognitive Impairment: A Multicenter, Randomized, Double-Blind, Placebo-Controlled Trial. *EBioMedicine* 17, 199–205. doi:10.1016/j.ebiom.2017.02.012

Fujino, T., Yamada, T., Mawatari, S., Shinfuku, N., Tsuboi, Y., Wakana, C., et al. (2019). Effects of Plasmalogen on Patients with Moderate-To-Severe Alzheimer's Disease and Blood Plasmalogen Changes: A Multi-Center, Open-Label Study. *J. Alzheimer's Dis. Park.* 9, 474.

Ginsberg, L., Rafique, S., Xuereb, J. H., Rapoport, S. I., and Gershfeld, N. L. (1995). Disease and Anatomic Specificity of Ethanolamine Plasmalogen Deficiency in Alzheimer's Disease Brain. *Brain Res.* 698, 223–226. doi:10.1016/0006-8993(95)00931-f

Goodenowe, D. B., Cook, L. L., Liu, J., Lu, Y., Jayasinghe, D. A., Ahiahonu, P. W. K., et al. (2007). Peripheral Ethanolamine Plasmalogen Deficiency: A Logical Causative Factor in Alzheimer's Disease and Dementia. *J. Lipid Res.* 48, 2485–2498. doi:10.1194/jlr.P700023-JLR200

Gu, J., Chen, L., Sun, R., Wang, J.-L., Wang, J., Lin, Y., et al. (2022). Plasmalogens Eliminate Aging-Associated Synaptic Defects and Microglia-Mediated Neuroinflammation in Mice. *Front. Mol. Biosci.* 9. doi:10.3389/fmolb.2022.815320

Guan, Z., Wang, Y., Cairns, N. J., Lantos, P. L., Dallner, G., and Sindelar, P. J. (1999). Decrease and Structural Modifications of Phosphatidylethanolamine Plasmalogen in the Brain with Alzheimer Disease. *J. Neuropathology Exp. Neurology* 58, 740–747. doi:10.1097/00005072-199907000-00008

Han, X., Holtzman, D. M., and McKeel, D. W., Jr. (2001). Plasmalogen Deficiency in Early Alzheimer's Disease Subjects and in Animal Models: Molecular Characterization Using Electrospray Ionization Mass Spectrometry. *J. Neurochem.* 77, 1168–1180. doi:10.1046/j.1471-4159.2001.00332.x

Heuchert, J. P., and McNair, D. M. (2012). *Profile of Mood States 2*. Toronto: Multi-Health Systems (MHS).

Hossain, M. S., Ifuku, M., Take, S., Kawamura, J., Miake, K., and Katafuchi, T. (2013). Plasmalogens Rescue Neuronal Cell Death Through an Activation of Akt and Erk Survival Signaling. *PLoS One* 8, e83508. doi:10.1371/journal.pone.0083508

Hossain, M. S., Mawatari, S., and Fujino, T. (2022). Plasmalogens, the Vinyl Ether-Linked Glycerophospholipids, Enhance Learning and Memory by Regulating Brain-Derived Neurotrophic Factor. *Front. Cell Dev. Biol.* 10, 828282. doi:10.3389/fcell.2022.828282

Hossain, M. S., Tajima, A., Kotoura, S., and Katafuchi, T. (2018). Oral Ingestion of Plasmalogens Can Attenuate the Lps-Induced Memory Loss and Microglial Activation. *Biochem. Biophysical Res. Commun.* 496, 1033–1039. doi:10.1016/j.bbrc.2018.01.078

Ifuku, M., Katafuchi, T., Mawatari, S., Noda, M., Miake, K., Sugiyama, M., et al. (2012). Anti-Inflammatory/Anti-Amyloidogenic Effects of Plasmalogens in Lipopolysaccharide-Induced Neuroinflammation in Adult Mice. *J. Neuroinflammation.* 9, 197. doi:10.1186/1742-2094-9-197

Irie, T., Kawamura, A., Aoki, S., Yokomitsu, K., and Sakano, Y. (2019). The Effectiveness of Group Acceptance and Commitment Therapy on Mental Health Among College Students: A Non-Randomized Pilot Trial. *Jpn. J. Assoc. Behav. Cogn. Ther.* 45, 1–12.

Johnson, M., Hassinger, L., Davis, J., Devor, S. T., and DiSilvestro, R. A. (2016). A Randomized, Double Blind, Placebo Controlled Study of Spirulina Supplementation on Indices of Mental and Physical Fatigue in Men. *Int. J. Food Sci. Nutr.* 67, 203–206. doi:10.3109/09637486.2016.1144719

Kashiwagi, S. (1962). Studies on the Work Curve of Uchida-Kraepelin. *Shinrigaku Kenkyu Jpn. J. Psychol.* 33, 36–38. doi:10.4992/jjpsy.33.98

Katafuchi, T., Ifuku, M., Mawatari, S., Noda, M., Miake, K., Sugiyama, M., et al. (2012). Effects of Plasmalogens on Systemic Lipopolysaccharide-Induced Glial Activation and β-Amyloid Accumulation in Adult Mice. *Ann. N.Y. Acad. Sci.* 1262, 85–92. doi:10.1111/j.1749-6632.2012.06641.x

Katsuki, F., Sugimatus, T., Koyano, H., and Takaoka, M. (2013). The Effectiveness of a Stress Management-Empowerment Program for Psychiatric Nurses: A Randomized Controlled Trial. *J. Jpn. Acad. Psychiatr. Ment. Helath Nurs.* 22, 1–10.

Lizard, G., Rouaud, O., Demarquoy, J., Cherkaoui-Malki, M., and Iuliano, L. (2012). Potential Roles of Peroxisomes in Alzheimer's Disease and in Dementia of the Alzheimer's Type. *Jad* 29, 241–254. doi:10.3233/JAD-2011-111163

Mah, C. D., Mah, K. E., Kezirian, E. J., and Dement, W. C. (2011). The Effects of Sleep Extension on the Athletic Performance of Collegiate Basketball Players. *Sleep* 34, 943–950. doi:10.5665/sleep.1132

Matsuoka, T., Takaki, A., Ohtaki, H., and Shioda, S. (2010). Early Changes to Oxidative Stress Levels Following Exposure to Formaldehyde in Icr Mice. *J. Toxicol. Sci.* 35, 721–730. doi:10.2131/jts.35.721

Mawatari, S., Hazeyama, S., and Fujino, T. (2016). Measurement of Ether Phospholipids in Human Plasma with HPLC-ELSD and LC/ESI-MS After Hydrolysis of Plasma with Phospholipase A1. *Lipids* 51, 997–1006. doi:10.1007/s11745-016-4170-9

Mawatari, S., Ohara, S., Taniwaki, Y., Tsuboi, Y., Maruyama, T., and Fujino, T. (2020). Improvement of Blood Plasmalogens and Clinical Symptoms in Parkinson's Disease by Oral Administration of Ether Phospholipids: A Preliminary Report. *Parkinson's Dis.* 2020, 1–7. doi:10.1155/2020/2671070

Mawatari, S., Okuma, Y., and Fujino, T. (2007). Separation of Intact Plasmalogens and All Other Phospholipids by a Single Run of High-Performance Liquid Chromatography. *Anal. Biochem.* 370, 54–59. doi:10.1016/j.ab.2007.05.020

Mawatari, S., Yunoki, K., Sugiyama, M., and Fujino, T. (2009). Simultaneous Preparation of Purified Plasmalogens and Sphingomyelin in Human Erythrocytes with Phospholipase A1 from Aspergillus Orizae. *Biosci. Biotechnol. Biochem.* 73, 2621–2625. doi:10.1271/bbb.90455

Ministry of Education Culture Sports Science and Technology (1999). Manual for the New Physical Fitness Tests (Age of 20-64 Years). Available at https://www.mext.go.jp/a_menu/sports/stamina/03040901.htm.

Okajima, I., Nakajima, S., Kobayashi, M., and Inoue, Y. (2013). Development and Validation of the Japanese Version of the Athens Insomnia Scale. *Psychiatry Clin. Neurosci.* 67, 420–425. doi:10.1111/pcn.12073

Okuyama, T., Fujita, S., Isaka, T., Okumura, T., and Nishizawa, M. (2018). The Ameliorative Effect of the Oligomerized-Polyphenol from Litchi Chinensis Fruit Extract (Oplfe) on Temporary Physical Fatigue for University Track and Field Athletes. *Jpn. Pharmacol. Ther.* 46, 1425–1431.

Oma, S., Mawatari, S., Saito, K., Wakana, C., Tsuboi, Y., Yamada, T., et al. (2012). Changes in Phospholipid Composition of Erythrocyte Membrane in Alzheimer's Disease. *Dement. Geriatr. Cogn. Disord. Extra* 2, 298–303. doi:10.1159/000341603

Saito, Y., Murata, N., Noma, T., Itoh, H., Kayano, M., Nakamura, K., et al. (2018). Relationship of a Special Acidified Milk Protein Drink with Cognitive Performance: A Randomized, Double-Blind, Placebo-Controlled, Crossover Study in Healthy Young Adults. *Nutrients* 10, 574. doi:10.3390/nu10050574

Seiwa, H. (1971). A Basic Study of the Uchida Kraepelin Psychodiagnostic Test: An Effect of Test-Repetitions Upon the Change of the U-K Curve: An Effect of Test-Repetitions Upon the Change of the U-K Curve. *Jpn. J. Psychol.* 42, 152–164. doi:10.4992/jjpsy.42.152

Soldatos, C. R., Dikeos, D. G., and Paparrigopoulos, T. J. (2000). Athens Insomnia Scale: Validation of an Instrument Based on Icd-10 Criteria. *J. Psychosomatic Res.* 48, 555–560. doi:10.1016/s0022-3999(00)00095-7

Su, X. Q., Wang, J., and Sinclair, A. J. (2019). Plasmalogens and Alzheimer's Disease: A Review. *Lipids Health Dis.* 18, 100. doi:10.1186/s12944-019-1044-1

Sugimoto, K., Kanai, A., and Shoji, N. (2009). The Effectiveness of the Uchida-Kraepelin Test for Psychological Stress: An Analysis of Plasma and Salivary Stress Substances. *Biopsychosoc. Med.* 3, 5. doi:10.1186/1751-0759-3-5

Takanari, J., Nakahigashi, J., Sato, A., Waki, H., Miyazaki, S., Uebaba, K., et al. (2016). Effect of Enzyme-Treated Asparagus Extract (Etas) on Psychological

Stress in Healthy Individuals. *J. Nutr. Sci. Vitaminol.* 62, 198–205. doi:10.3177/jnsv.62.198

Tiekou Lorinczova, H., Fitzsimons, O., Mursaleen, L., Renshaw, D., Begum, G., and Zariwala, M. G. (2020). Co-Administration of Iron and a Bioavailable Curcumin Supplement Increases Serum Bdnf Levels in Healthy Adults. *Antioxidants* 9, 645. doi:10.3390/antiox9080645

Travis, F., Valosek, L., Konrad, A., Link, J., Salerno, J., Scheller, R., et al. (2018). Effect of Meditation on Psychological Distress and Brain Functioning: A Randomized Controlled Study. *Brain Cognition* 125, 100–105. doi:10.1016/j.bandc.2018.03.011

Urbaniak, S. K., Boguszewska, K., Szewczuk, M., Kaźmierczak-Barańska, J., and Karwowski, B. T. (2020). 8-Oxo-7,2028-Oxo-7,8-Dihydro-2′-Deoxyguanosine (8-OxodG) and 8-Hydroxy-2′-Deoxyguanosine (8-OHdG) as a Potential Biomarker for Gestational Diabetes Mellitus (GDM) Development. *Molecules* 25. doi:10.3390/molecules25010202

U.S. Department of Health and Human Service. Available at: https://ctep.cancer.gov/protocoldevelopment/electronic_applications/docs/ctcae_v5_quick_reference_8.5x11.pdf (Accessed on November 27, 2017). Common Terminology Criteria for Adverse Events (Ctcae) Version 5.0 Published.

Valavanidis, A., Vlachogianni, T., and Fiotakis, C. (2009). 8-Hydroxy-2′-Deoxyguanosine (8-OHdG): A Critical Biomarker of Oxidative Stress and Carcinogenesis. *J. Environ. Sci. Health, Part C* 27, 120–139. doi:10.1080/10590500902885684

Weerakkody, N. S., Taylor, C. J., Bulmer, C. L., Hamilton, D. B., Gloury, J., O'Brien, N. J., et al. (2021). The Effect of Mental Fatigue on the Performance of Australian Football Specific Skills Amongst Amateur Athletes. *J. Sci. Med. Sport* 24, 592–596. doi:10.1016/j.jsams.2020.12.003

Wood, P. L., Barnette, B. L., Kaye, J. A., Quinn, J. F., and Woltjer, R. L. (2015). Non-Targeted Lipidomics of Csf and Frontal Cortex Grey and White Matter in Control, Mild Cognitive Impairment, and Alzheimer's Disease Subjects. *Acta Neuropsychiatr.* 27, 270–278. doi:10.1017/neu.2015.18

Wood, P. L., Mankidy, R., Ritchie, S., Heath, D., Wood, J. A., Flax, J., et al. (2010). Circulating Plasmalogen Levels and Alzheimer Disease Assessment Scale-Cognitive Scores in Alzheimer Patients. *Jpn* 35, 59–62. doi:10.1503/jpn.090059

Yamashita, S., Kiko, T., Fujiwara, H., Hashimoto, M., Nakagawa, K., Kinoshita, M., et al. (2015). Alterations in the Levels of Amyloid-β, Phospholipid Hydroperoxide, and Plasmalogen in the Blood of Patients with Alzheimer's Disease: Possible Interactions Between Amyloid-β and These Lipids. *Jad* 50, 527–537. doi:10.3233/jad-150640

Yokoyama, K. (2015). *Translation Supervisor, Profile of Mood States Second Edition Poms2, Manual of Japanese Version.* Tokyo: Kaneko Shobou. *(in Japanese).*

Yoto, A., Fukui, N., Kaneda, C., Torita, S., Goto, K., Nanjo, F., et al. (2018). Black Tea Aroma Inhibited Increase of Salivary Chromogranin-A After Arithmetic Tasks. *J. Physiol. Anthropol.* 37, 3. doi:10.1186/s40101-018-0163-0

Zarrouk, A., Debbabi, M., Bezine, M., Karym, E. M., Badreddine, A., Rouaud, O., et al. (2018). Lipid Biomarkers in Alzheimer's Disease. *Car* 15, 303–312. doi:10.2174/1567205014666170505101426

Conflict of Interest: The authors declare that the research was conducted in the absence of any commercial or financial relationships that could be construed as a potential conflict of interest.

Publisher's Note: All claims expressed in this article are solely those of the authors and do not necessarily represent those of their affiliated organizations, or those of the publisher, the editors, and the reviewers. Any product that may be evaluated in this article, or claim that may be made by its manufacturer, is not guaranteed or endorsed by the publisher.

frontiers | Frontiers in Cell and Developmental Biology

ORIGINAL RESEARCH
published: 06 June 2022
doi: 10.3389/fcell.2022.912880

Plasmalogen Loss in Sepsis and SARS-CoV-2 Infection

*Daniel P. Pike[1,2], Reagan M. McGuffee[1,2], Elizabeth Geerling[3], Carolyn J. Albert[1,2], Daniel F. Hoft[3,4], Michael G. S. Shashaty[5,6], Nuala J. Meyer[5,6], Amelia K. Pinto[3] and David A. Ford[1,2]**

[1]Edward A. Doisy Department of Biochemistry and Molecular Biology, Saint Louis University School of Medicine, St. Louis, MO, United States, [2]Center for Cardiovascular Research, Saint Louis University School of Medicine, St. Louis, MO, United States, [3]Department of Molecular Microbiology and Immunology, Saint Louis University School of Medicine, St. Louis, MO, United States, [4]Department of Internal Medicine, Division of Infectious Diseases, Allergy and Immunology, Saint Louis University School of Medicine, St. Louis, MO, United States, [5]Pulmonary, Allergy, and Critical Care Division, University of Pennsylvania Perelman School of Medicine, Philadelphia, PA, United States, [6]Center for Translational Lung Biology, University of Pennsylvania Perelman School of Medicine, Philadelphia, PA, United States

Plasmalogens are plasma-borne antioxidant phospholipid species that provide protection as cellular lipid components during cellular oxidative stress. In this study we investigated plasma plasmalogen levels in human sepsis as well as in rodent models of infection. In humans, levels of multiple plasmenylethanolamine molecular species were decreased in septic patient plasma compared to control subject plasma as well as an age-aligned control subject cohort. Additionally, lysoplasmenylcholine levels were significantly decreased in septic patients compared to the control cohorts. In contrast, plasma diacyl phosphatidylethanolamine and phosphatidylcholine levels were elevated in septic patients. Lipid changes were also determined in rats subjected to cecal slurry sepsis. Plasma plasmenylcholine, plasmenylethanolamine, and lysoplasmenylcholine levels were decreased while diacyl phosphatidylethanolamine levels were increased in septic rats compared to control treated rats. Kidney levels of lysoplasmenylcholine as well as plasmenylethanolamine molecular species were decreased in septic rats. Interestingly, liver plasmenylcholine and plasmenylethanolamine levels were increased in septic rats. Since COVID-19 is associated with sepsis-like acute respiratory distress syndrome and oxidative stress, plasmalogen levels were also determined in a mouse model of COVID-19 (intranasal inoculation of K18 mice with SARS-CoV-2). 3 days following infection, lung infection was confirmed as well as cytokine expression in the lung. Multiple molecular species of lung plasmenylcholine and plasmenylethanolamine were decreased in infected mice. In contrast, the predominant lung phospholipid, dipalmitoyl phosphatidylcholine, was not decreased following SARS-CoV-2 infection. Additionally total plasmenylcholine levels were decreased in the plasma of SARS-CoV-2 infected mice. Collectively, these data demonstrate the loss of plasmalogens during both sepsis and SARS-CoV-2 infection. This study also indicates plasma plasmalogens should be considered in future studies as biomarkers of infection and as prognostic indicators for sepsis and COVID-19 outcomes.

Keywords: sepsis, SARS-CoV-2, plasmalogen, infection, inflammation, lipidomics

OPEN ACCESS

Edited by:
Fabian Dorninger, Medical University of Vienna, Austria

Reviewed by:
Christine Des Rosiers, Université de Montréal, Canada
Jesús Balsinde, Instituto de Biología y Genética Molecular (CSIC), Spain

****Correspondence:***
David A. Ford
david.ford@health.slu.edu

Specialty section:
This article was submitted to Cellular Biochemistry, a section of the journal Frontiers in Cell and Developmental Biology

Received: *05 April 2022*
Accepted: *23 May 2022*
Published: *06 June 2022*

Citation:
Pike DP, McGuffee RM, Geerling E, Albert CJ, Hoft DF, Shashaty MGS, Meyer NJ, Pinto AK and Ford DA (2022) Plasmalogen Loss in Sepsis and SARS-CoV-2 Infection. Front. Cell Dev. Biol. 10:912880. doi: 10.3389/fcell.2022.912880

INTRODUCTION

Sepsis has been a major threat to global health over the past several decades. In the United States, approximately one million individuals are diagnosed with sepsis annually, with mortality estimated between 12 and 25 percent (Mayr et al., 2014; Paoli et al., 2018). An estimated 20 percent of all deaths globally were attributed to sepsis (Rudd et al., 2020). The more severe septic shock has an estimated 38 percent mortality, and half of all Americans who die in the hospital are diagnosed with sepsis (Liu et al., 2014; Vincent et al., 2019). Sepsis occurs when an infection triggers a dysregulated host immune response, leading to systemic microcirculatory and immune dysfunction. This dysregulated inflammatory response in the microvasculature leads to direct damage of cells from reactive oxygen species and other inflammatory mediators, activation of the coagulation cascade, vasodilation, and tissue hypoxia with subsequent mitochondrial dysfunction. This complex system culminates in life-threatening organ injury and metabolic derangements (Chuang et al., 2006; Robertson and Coopersmith, 2006; Galley, 2011; Angus and van der Poll, 2013; Delano and Ward, 2016; Singer et al., 2016; Prauchner, 2017). Lipids and lipid-related signaling pathways have been investigated as mediators, potentially at the blood-endothelial interface during sepsis (Amunugama et al., 2021a). Specific lipids may also have prognostic value as biomarkers in sepsis (Meyer et al., 2017; Mecatti et al., 2018; Mecatti et al., 2020; Wang et al., 2020; Amunugama et al., 2021a). Additionally, a major cause of COVID-19 mortality is sepsis-associated acute respiratory distress syndrome (ARDS). Similar to sepsis, lipids have been investigated as important mediators and biomarkers in COVID-19 (Tanner et al., 2014; Aktepe et al., 2015; Villareal et al., 2015; Jean Beltran et al., 2018; Fernández-Oliva et al., 2019; Sviridov et al., 2020; Casari et al., 2021; Mesquita et al., 2021; Theken et al., 2021).

Plasmalogens comprise a significant fraction of the lipid content in the plasma, immune cells, and endothelium (Chilton and Murphy, 1986; Chilton and Connell, 1988; Kayganich and Murphy, 1992; Murphy et al., 1992; Bräutigam et al., 1996). There is considerable diversity in plasmalogen molecular species. In general, plasmalogens contain either phosphocholine or phosphoethanolamine at the *sn*-3 position of the glycerol backbone. The vinyl ether aliphatic group attached to the glycerol backbone predominantly contains sixteen and eighteen carbon groups. Recently we have also shown neutrophil plasmalogens contain vinyl ether groups that are greater than twenty carbons in length (Amunugama et al., 2021b). Plasmalogens have been suggested to have important roles in biological membranes, which are due, in part, to their unique packing in membranes compared to diacyl phospholipids (Han and Gross, 1990; Han and Gross, 1991). Plasmalogens have been shown to have roles in synaptic fusion, cholesterol efflux, lipid rafts, and transmembrane protein function (Glaser and Gross, 1994; Ford and Hale, 1996; Mandel et al., 1998; Pike et al., 2002). Plasmalogens likely have key roles in inflammation at several levels. Plasmalogens are plasma-borne antioxidants and have been shown to protect endothelium from oxidative stress (Vance, 1990; Zoeller et al., 1999). The vinyl ether bond of plasmalogens is susceptible to attack by reactive species, and this propensity suggests that these lipids can protect cells by scavenging reactive oxygen species (Zoeller et al., 1988; Reiss et al., 1997; Zoeller et al., 1999; Zoeller et al., 2002; Dean and Lodhi, 2018). Additionally, plasmalogens have been shown to have a key role in macrophage phagocytosis (Rubio et al., 2018). Furthermore, plasmalogens are enriched with arachidonic acid and docosahexaenoic acid at the *sn*-2 position, and their metabolism by phospholipases leads to the mobilization of these fatty acids and their subsequent oxidation to bioactive eicosanoids and resolvins (Paul et al., 2019). Collectively, the roles of plasmalogens in membrane molecular dynamics, as antioxidants, and as precursors of bioactive lipids indicate they may be important in inflammation associated with disease and infection.

Plasma plasmalogen levels have been shown to decrease during inflammation such as during endotoxemia (Ifuku et al., 2012), Parkinson's disease (Dragonas et al., 2009; Fabelo et al., 2011), and lupus (Hu et al., 2016). Several of these previous studies (Dragonas et al., 2009; Hu et al., 2016) have suggested the loss of plasmalogens during Parkinson's disease and lupus is due to the associated oxidative stress. Surprisingly only one study has investigated plasmalogen loss during human sepsis, which also attributed plasmalogen loss to oxidative stress (Brosche et al., 2013). This study was limited to measuring dimethyl acetals as a measure of plasmalogen levels and was performed in a limited number of geriatric septic patients. In addition to sepsis, several investigations have emerged over the past 2 years demonstrating plasma plasmalogen levels in humans with severe COVID-19 are decreased (Schwarz et al., 2021; Snider et al., 2021). The loss of plasmalogens and other phospholipids enriched with arachidonic acid and docosahexaenoic acid as well as increased secretory phospholipase A_2 (Snider et al., 2021) in COVID-19 patients support an important role for plasmalogens as precursors of oxylipids.

We have previously shown the plasmalogen vinyl ether bond is targeted by neutrophil-derived HOCl (a product of myeloperoxidase activity) resulting in 2-chlorofatty aldehyde and 2-chlorofatty acid production (Albert et al., 2001; Thukkani et al., 2002; Anbukumar et al., 2010). Furthermore, increased 2-chlorofatty acid plasma levels associate with ARDS-caused mortality in human sepsis (Meyer et al., 2017). 2-Chlorofatty acids are also elevated in the plasma and several organs in rats subjected to cecal slurry sepsis (Pike et al., 2020). Since plasmalogens are the precursors of chlorinated lipid production during sepsis and since limited molecular detail is known about human plasma plasmalogen loss during sepsis, in the present study we have investigated plasma plasmalogen levels in human sepsis patients. Furthermore, we have employed the rat cecal slurry sepsis model to identify both plasma plasmalogen loss as well as changes in liver and kidney plasmalogen levels during sepsis. Lastly, we examined changes in plasmalogen levels in plasma and lung in mice challenged with SARS-CoV-2. Collectively, these studies show the loss of plasmalogens during sepsis and SARS-CoV-2 infection with new detail into changes in plasma molecular species, as well as changes in organs in rodent models of sepsis and COVID-19.

MATERIALS AND METHODS

Human Plasma Specimens and Analysis

Sepsis plasma samples were obtained from subjects admitted to the intensive care unit (ICU) with suspected infection and acute organ dysfunction (sepsis) at day 7 in the ICU. The cohort has been previously described (Reilly et al., 2018). The cohort study is approved by the University of Pennsylvania institutional review board (IRB protocol #808542), and all subjects or their proxies provided informed consent to participate. Control healthy plasma samples were obtained at Saint Louis University under IRB protocol 26646. Plasma samples were stored in aliquots to minimize freeze thaw cycles to two times or less.

Rat Cecal Slurry Studies

Rats were supplied from Envigo (Harlan—Indianapolis, IN, United States). All rats were young adult male Sprague-Dawley weighing between 270–330 g (8–12 weeks old). All animals were maintained in a temperature and humidity-controlled room with a 12 h light/dark cycle and unrestricted access to chow and water. Upon arrival to Saint Louis University, rats were acclimated to the environment for at least a week prior to experiments. All animal experiments were conducted with the approval of the Institutional Animal Care and Use Committee at Saint Louis University. Cecal slurry (CS) was prepared from cecal contents of donor male Sprague-Dawley rats as previously detailed (Pike et al., 2020). Prior to ip CS administration for sepsis studies, aliquots of CS were thawed quickly in warm water. Rats were administered 15 ml/kg CS or 15% glycerol vehicle control (ip) in a total volume of 20 ml/kg, with the remaining 5 ml/kg being sterile saline (B Braun Medical, Bethlehem, PA, United States). At the time of CS administration, animals were administered a concurrent 30 ml/kg dose of subcutaneous sterile saline. Eight hours following CS treatment, 25 mg/kg ceftriaxone (Hospira) in sterile saline was administered intramuscularly in the hind limb in a 1 ml/kg volume. A second subcutaneous 30 ml/kg dose of sterile saline was administered concurrently with the ceftriaxone in order to simulate treatment of human sepsis with crystalloid and antibiotics. 20 h following CS injection, rats were euthanized, and organs were collected, which were immediately frozen on dry ice. Blood was collected *via* cardiac puncture, and plasma was immediately prepared and then stored at −80°C. Plasma preparation and storage was achieved within 30–45 min of the blood draw. Plasma samples were stored in aliquots to minimize freeze thaw cycles to two times or less. Rats were euthanized by injecting 0.5 ml Somnasol (390 mg/ml sodium pentobarbital and 50 mg/ml phenytoin sodium), ip followed by thoracotomy.

Mouse SARS-CoV-2 Infection Studies

K18 mice (JAX strain 034860, human angiotensin converting enzyme 2 (hACE2 transgenic)) were supplied from the Jackson Laboratory (Bar Harbor, MA, United States). All mice were young adult females weighing between 25–30 g (~9 weeks old). All animals were maintained in a temperature and humidity-controlled room with a 12 h light/dark cycle and unrestricted access to chow and water. Upon arrival to Saint Louis University, mice were acclimated to the ABSL-3 environment for at least a week prior to experiments. All animal experiments were conducted with the approval of the Institutional Animal Care and Use Committee at Saint Louis University. K18 mice were either mock infected or infected with 1×10^4 focus forming units (FFU) of the beta variant B.1.351 of SARS-CoV-2 intranasally (20 µl). The beta variant B.1.351 of SARS-CoV-2 was obtained from BEI Resources (#NR55282). Tissues and plasma were collected from euthanized mice three- or 4-days following infection. Tissue homogenates were prepared for analyses of either viral burden, cytokine mRNA, or lipids. SARS-CoV-2 viral burden was measured by focus forming assays (FFAs) using Vero E6 cells transfected with hACE2 and TMPRSS2 as we have previously described (Geerling et al., 2022). Inflammatory cytokine levels were measured *via* qRT-PCR using Taqman primer and probe sets from IDT as previously described (Geerling et al., 2021).

Lipid Analysis

Tissue and plasma lipids were extracted in the presence of internal standards (see **Supplementary Table S1**) by a modified Bligh-Dyer extraction as previously described (Bligh and Dyer, 1959; Maner-Smith et al., 2020; Pike et al., 2020; Amunugama et al., 2021b). Individual choline and ethanolamine glycerophosphospholipids were detected using selected reaction monitoring (see **Supplementary Table S1** for transitions) with an Altis TSQ mass spectrometer equipped with a Vanquish UHPLC System (Thermo Scientific) with isotopomer corrections for each target molecular species compared to the respective internal standard. Lipids were separated on an Accucore™ C30 column 2.1 mm × 150 mm (Thermo Scientific) with mobile phase A comprised of 60% acetonitrile, 40% water, 10 mM ammonium formate, and 0.1% formic acid and mobile phase B comprised of 90% isopropanol, 10% acetonitrile with 2 mM ammonium formate, and 0.02% formic acid. Initial conditions were 30% B with a discontinuous gradient to 100% B at a flow rate of 0.260 ml/min. Plasmalogen molecular species were identified by acid lability and fatty acid aliphatic group identification under identical conditions employed using the TSQ mass spectrometer but using a Q-Exactive mass spectrometer with choline glycerophospholipids detected in negative ion mode.

Statistics

Student's t-test was used to compare two groups in rat CS and K18 mouse SARS-CoV-2 infection studies. Plasma concentrations were compared between healthy control subjects and sepsis subjects by Wilcoxon rank sum test.

RESULTS

Alterations in Plasma Plasmalogen and Diacyl Phospholipids in Human Sepsis

Human geriatric septic patients have previously been shown to have decreased plasma plasmalogen levels as determined by assessing dimethyl acetals of plasmalogens by gas chromatography. These analyses did not identify the lipid class

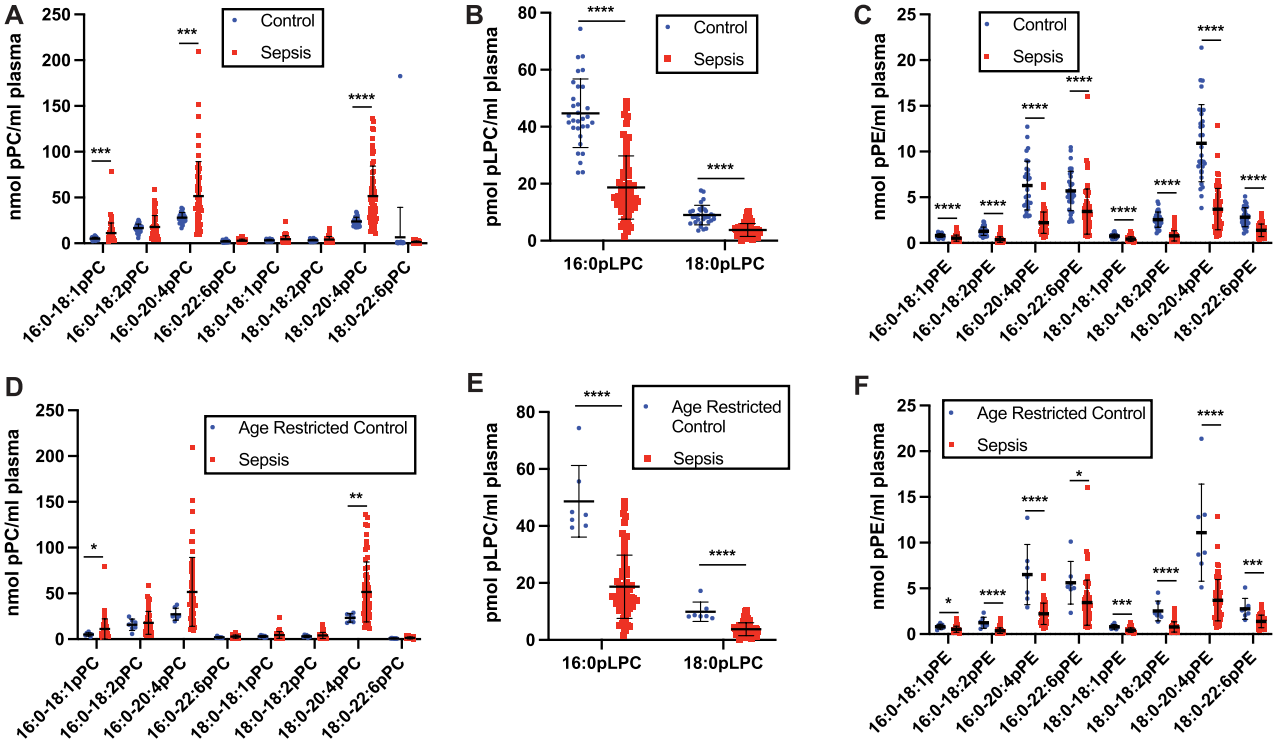

FIGURE 1 | Loss of plasma plasmenylethanolamine (pPE) and lysoplasmenylcholine (pLPC) in human sepsis. Plasma was collected from 31 healthy humans (control) and 63 ICU patients with sepsis following 7 days in the ICU. Lipids were extracted and plasmalogen levels were quantitated as described in "Materials and Methods." Plasma plasmenylcholine (pPC) **(A,D)**, pLPC **(B,E)**, and pPE **(C,F)** are compared between the control and sepsis cohorts **(A–C)** and an age restricted control and sepsis cohorts **(D–F)**. *, **, ***, and **** indicate $p < 0.05$, 0.01, 0.001, and 0.0001, respectively, for comparisons between cohorts. Mean and standard deviation values are indicated for each molecular species and condition.

TABLE 1 | Clinical characteristics of the sepsis and control population.

	Sepsis (*n* = 63)	Controls (*n* = 31)	Age restricted controls (*n* = 7)
Age, years	59.8 ± 12.7	38.2 ± 15.1	56.6 ± 8.4
Female sex (N, %)	25, 39.6%	Not available	Not available
APACHE III score[a]	85 (68, 107)	—	—
Diabetes (N, %)	19, 30.2%		
Solid organ malignancy (N, %)	12, 19%		
Hematologic malignancy (N, %)	20, 31.7%		
Mortality at 30 days (N, %)	17, 27%		

[a]*The acute physiology and chronic health examination (APACHE) III score is displayed as median (interquartile range) due to a skewed distribution.*

(choline or ethanolamine) of the plasmalogen pool or the molecular species that decrease during sepsis. Additionally, we have previously shown plasma 2-chloropalmitic acid levels are increased in human sepsis and associate with ARDS-caused mortality (Meyer et al., 2017). 2-Chloropalmitic acid is derived from 2-chloropalmitaldehyde produced by the action of HOCl targeting the vinyl ether bond of plasmalogens (Albert et al., 2001; Thukkani et al., 2002; Anbukumar et al., 2010). Accordingly, we performed a detailed study of plasma plasmalogens in septic humans. The plasma specimens of patients in this study are from septic patients collected following 7 days in the ICU. The average age of these patients is 59.8 years. Interestingly, data shown in **Figure 1A** show levels of plasma plasmenylcholine (pPC) molecular species either were unchanged or increased in septic patients compared to control subjects. Since the control cohort age was younger than the sepsis group (**Table 1**), we also compared changes in plasma pPC levels between the sepsis cohort and an age restricted subgroup of the control subjects to test a cohort that was more closely aligned in age with the sepsis cohort (**Figure 1D**). A similar pattern of either increased or unchanged levels of pPC was observed in the septic patients compared to the age restricted controls to sepsis. The two pPC

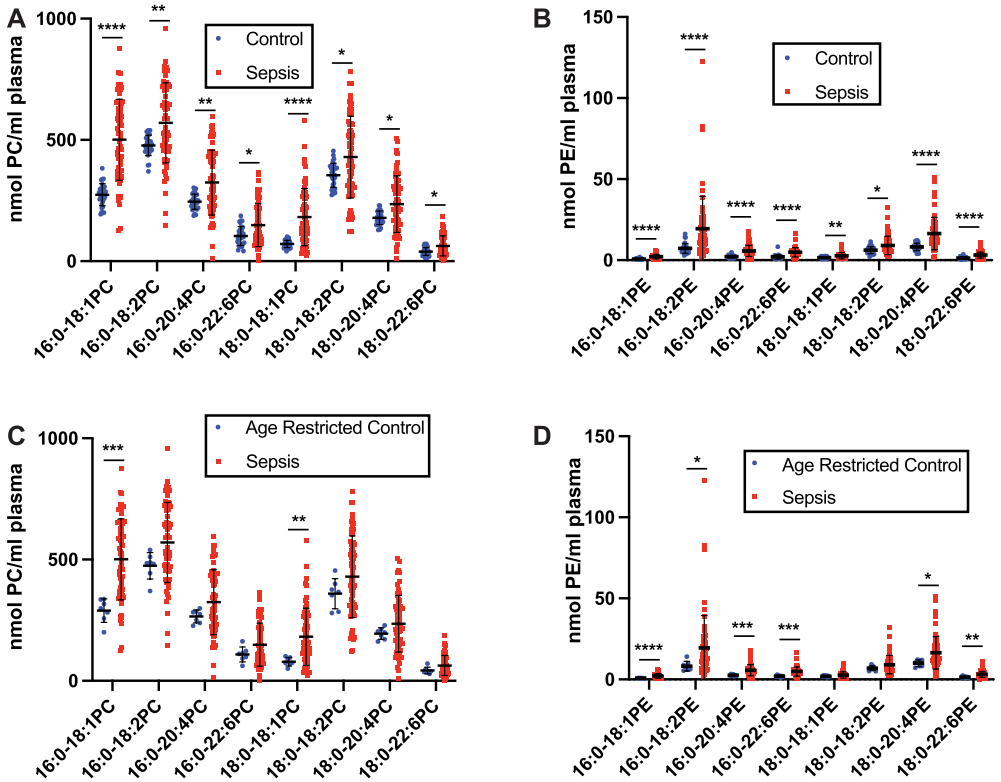

FIGURE 2 | Increases in plasma phosphatidylcholine (PC) and phosphatidylethanolamine (PE) in human sepsis. Plasma was collected from 31 healthy humans (control) and 63 ICU patients with sepsis following 7 days in the ICU. Lipids were extracted and plasmalogen levels were quantitated as described in "Materials and Methods." Plasma PC **(A,C)** and PE **(B,D)** are compared between the control and sepsis cohorts **(A,B)** and an age restricted control and sepsis cohorts **(C,D)**. *, **, ***, and **** indicate $p < 0.05$, 0.01, 0.001, and 0.0001, respectively, for comparisons between cohorts. Mean and standard deviation values are indicated for each molecular species and condition.

molecular species elevated in sepsis were 16:0-18:1 pPC and 18:0-20:4 pPC (x:y-x:y where x# of carbons and y# of double bonds in aliphatic groups at the *sn*-1 and *sn*-2 position, respectively). In contrast, significant decreases were observed with plasma 16:0 and 18:0 lysoplasmenylcholine (pLPC) in septic subjects with comparisons to both the unrestricted control group **(Figure 1B)**, as well as the age restricted control group (**Figure 1E**). Furthermore, all plasma plasmenylethanolamine (pPE) molecular species in our targeted analyses were significantly decreased in the septic patient cohort in comparison to both the unrestricted control group (**Figure 1C**), as well as the age restricted control group (**Figure 1F**). In contrast to pPE, plasma levels of diacyl phosphatidylethanolamine (PE), as well as phosphatidylcholine (PC), were increased in the sepsis cohort in comparisons to both the unrestricted and age restricted cohorts **(Figures 2A–D)**.

Alterations in Plasmalogen and Diacyl Phospholipids in Rodent Sepsis

To gain further insights into alterations in plasmalogens, as well as diacyl phospholipids, during sepsis we examined both plasma and tissue changes in these phospholipids in the cecal slurry (CS) rodent model of sepsis. Previous studies have demonstrated under the CS infection conditions followed by antibiotic treatment 8 h post infection employed in these studies, rats survive at least 20 h and have increased plasma 2-chlorofatty acid levels in comparison to vehicle treated rats (Pike et al., 2020). pPC was identified as the most abundant plasmalogen class in both control and sepsis rat plasma compared to pPE. (**Figures 3A,C**). Plasma plasmalogen loss was observed in CS treated rats compared to vehicle injected rats. Plasma 16:0-18:2, 18:0-18:2, and 18:0-18:1 pPC levels were decreased in septic rats 20 h post infection (**Figure 3A**). Similar to human sepsis, both 16:0 and 18:0 pLPC levels were decreased in septic rats in comparison to control vehicle-treated rats (**Figure 3B**). In contrast to human sepsis, the predominant species of plasma pPE levels were not significantly decreased in rat sepsis, however less abundant species such as 16:0-18:2, 18:0-18:2, and 18:0-18:1 pPE did significantly decrease (**Figure 3C**). For the diacyl species, sepsis resulted in a decrease of only 16:0-20:4 PC in rat plasma (**Figure 3D**). In stark contrast to the drop in plasma pPE levels, all diacyl PE levels were significantly increased (**Figure 3E**).

Previously in this rodent model we identified the kidney and liver as primary sites of organ failure based on loss of permeability barrier function as assessed by Evans blue extravasation (Pike et al., 2020). Additionally, both liver and kidney levels of 2-

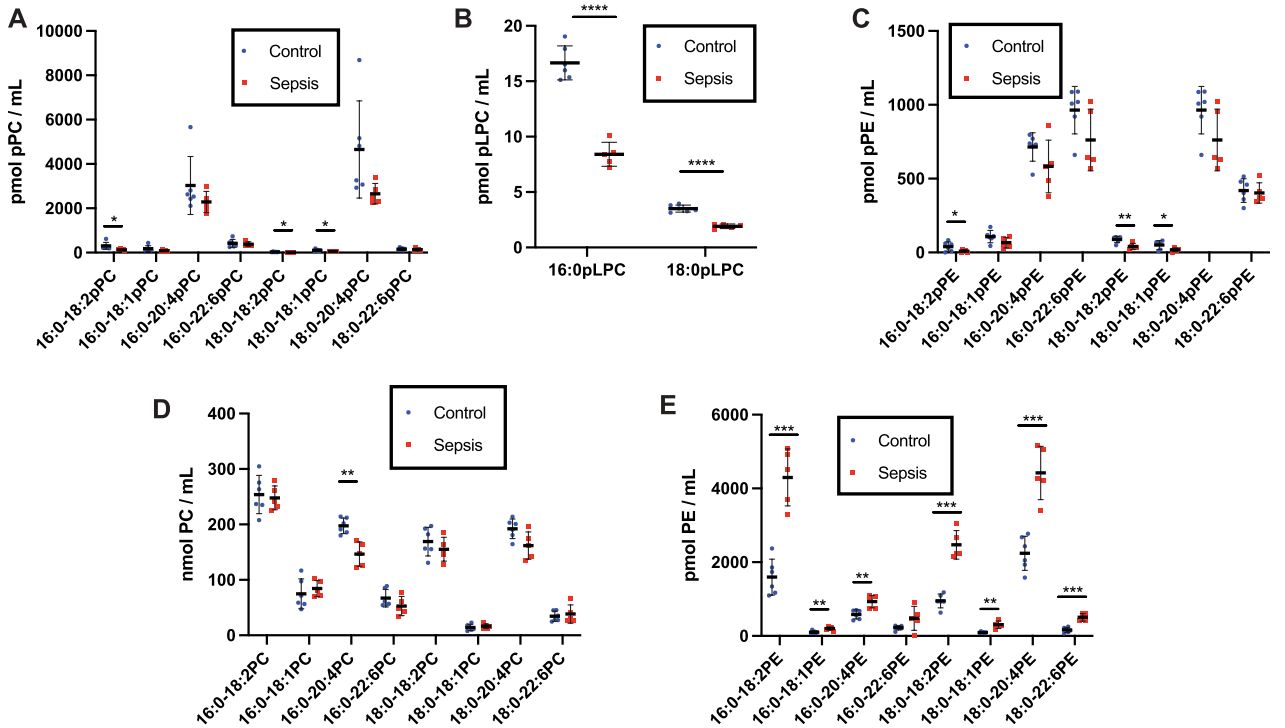

FIGURE 3 | Loss of plasma plasmalogens and increases in diacyl PC and PE in septic rats. Rats were injected with cecal slurry (sepsis) ($n = 5$) or vehicle (control) ($n = 6$) and were subsequently treated with fluid replacement and ceftriaxone 8 h following cecal slurry injection as described in "Materials and Methods." Plasma was collected 20 h following cecal slurry or vehicle treatment, and lipids were extracted. Plasmalogen levels were quantitated as described in "Materials and Methods." Plasma pPC, pLPC, pPE, PC, and PE are shown in **(A–E)**, respectively. *, **, ***, and **** indicate $p < 0.05$, 0.01, 0.001, and 0.0001, respectively, for comparisons between control and septic rats. Mean and standard deviation values are indicated for each molecular species and condition.

chlorofatty acids were previously shown to be increased in this sepsis model (Pike et al., 2020). 2-Chlorofatty acids are produced as a result of neutrophil-derived HOCl targeting plasmalogens (Thukkani et al., 2002; Anbukumar et al., 2010). Accordingly, we examined plasmalogen levels in the kidney and liver of CS infected rats. In contrast to plasma, pPE is the predominant plasmalogen class in both rat kidney and liver compared to pPC (**Figures 4**, **5**). Multiple pPE molecular species in the rat kidney were significantly decreased in septic rats, including the predominant 16:0-20:4 and 18:0-20:4 pPE species (**Figure 4C**). Renal 16:0 pLPC was also significantly decreased in sepsis (**Figure 4B**). Meanwhile, some less predominant renal pPC levels were increased (**Figure 4A**). In contrast to changes in rat plasma and kidney plasmalogens, as well as in human plasma, several liver plasmalogens increased during rat sepsis. All pPC species significantly increased, including the predominant 16:0-20:4 pPC and 18:0-20:4 pPC species, in livers of CS elicited septic rats (**Figure 5A**). 16:0-20:4 pPE and 18:0-20:4 pPE, among others, also were significantly increased in livers from septic rats compared to control rats (**Figure 5C**). Further in contrast to changes in the plasma and kidney, there was no significant difference in pLPC levels in livers from septic rats compared to those of control rats (**Figure 5B**). Diacyl species were measured in the kidney and liver as well. In the kidney, multiple species of diacyl PC and PE were significantly decreased (**Figures 4D,E**). While in the liver, CS-elicited sepsis resulted in increases in both diacyl PC and PE (**Figures 5D,E**).

Plasmalogens in SARS-CoV-2 Infected K18 Mice

Since plasmalogens have been shown to decrease in the plasma of humans with severe COVID-19 (Schwarz et al., 2021; Snider et al., 2021) and SARS-CoV-2 infection leads to a form of sepsis-associated ARDS, we investigated the role of airway infection with SARS-CoV-2 in K18-hACE2 transgenic mice. The human keratin 18 promoter (K18) in K18 mice directs human ACE2 expression in the epithelium, which is important as SARS-CoV-2 infections tend to begin in airway epithelia. Three days following nasal inoculation with SARS-CoV-2 a robust viral burden was observed in the lung (**Figure 6A**), which is similar to findings by others (Zheng et al., 2021). The associated cytokine storm of SARS-CoV-2 infection was confirmed with increases in interleukin-1β (IL-1B), interleukin-6 (IL-6) and tumor necrosis factor-α (TNF-α) mRNA expression in lung tissue (**Figure 6B**). These cytokine mRNAs were not detected in mock-infected lung (data not shown). 16:0-20:4 pPC and 18:0-20:4 pPC levels in the lung were selectively decreased in SARS-CoV-2 infected K18 mice (**Figure 6C**). Additionally, both 16:0-20:4 pPE and 18:0-20:4 pPE, as well as 18:0-22:6 pPE, were decreased in the lung of SARS-

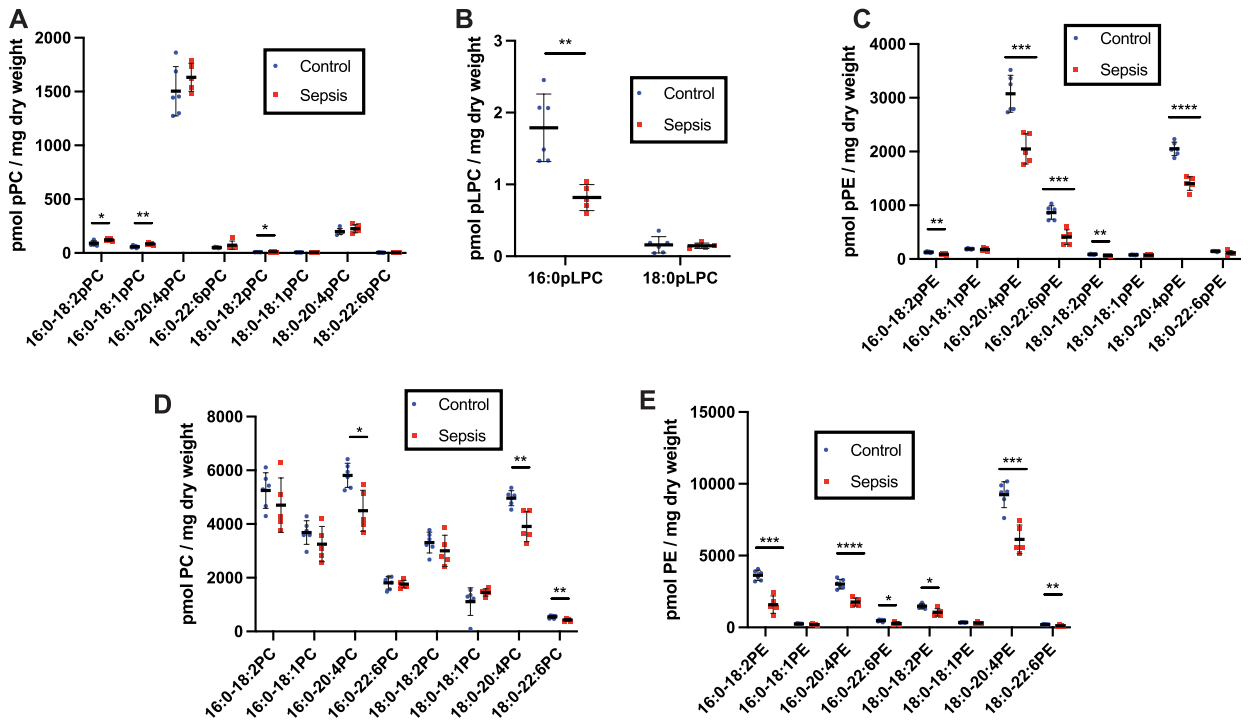

FIGURE 4 | Alterations in kidney diacyl and plasmalogen phospholipids during rat sepsis. Rats were injected with cecal slurry (sepsis) ($n = 5$) or vehicle (control) ($n = 6$) as described in **Figure 3**. Kidneys were collected 20 h following cecal slurry or vehicle treatment, and lipids were extracted. Plasmalogen levels were quantitated as described in "Materials and Methods." Kidney pPC, pLPC, pPE, PC, and PE are shown in **(A–E)**, respectively. *, **, ***, and **** indicate $p < 0.05$, 0.01, 0.001, and 0.0001, respectively, for comparisons between control and septic rats. Mean and standard deviation values are indicated for each molecular species and condition.

CoV-2 mice (**Figure 6D**). As in rat tissues, pPE levels were higher than that of pPC in the mouse lung. We also assessed the major lung lipid, 1,2-dipalmitoyl-*sn*-glycero-3-phosphocholine (DPPC) in the lungs, which is the major phospholipid component of surfactant. Lung DPPC levels were not altered in SARS-CoV-2 infected mice (**Figure 6E**). Changes in plasma plasmalogen levels were only modestly decreased in SARS-CoV-2 infected mice (**Figure 6F**).

DISCUSSION

Plasmalogens are a lipid subclass characterized by a vinyl ether linked aliphatic group attached to the *sn*-1 position of glycerol, a fatty acid esterified at the *sn*-2 position and, in general, either phosphoethanolamine or phosphocholine at the *sn*-3 position. The *sn*-2 fatty acid of plasmalogens is enriched with arachidonic acid in many mammalian tissues and thus one role of plasmalogens has been described as a storage depot for arachidonic acid that is released during inflammation (Chilton and Connell, 1988; Ford and Gross, 1989; Braverman and Moser, 2012). The *sn*-1 vinyl ether is a target for reactive oxygen species leading to the release of free fatty aldehydes that subsequently can be metabolized to free fatty acids (Khaselev and Murphy, 1999; Stadelmann-Ingrand et al., 2001). The reaction of reactive oxygen species with the vinyl ether is a terminal event for ROS and thus is considered an antioxidant activity. Multiple studies have shown plasmalogens protect tissues and cells from reactive oxygen species and oxidative stress. Cells deficient in plasmalogens are susceptible to free radical-mediated toxicity (Morand et al., 1988; Zoeller et al., 1988). Furthermore, supplementing cells with precursors to plasmalogens has been shown to protect cells from reactive oxygen species including during hypoxic damage to endothelial cells (Zoeller et al., 1999). Collectively, the abundance of arachidonic acid esterified to plasmalogens that can be mobilized for eicosanoid production and the susceptibility of the vinyl ether to oxidative stress suggest plasmalogens may have important roles in infection and inflammation. Plasma plasmalogen depletion has also been demonstrated in humans with Parkinson's disease, Alzheimer's disease, lupus and endotoxemia (Dragonas et al., 2009; Fabelo et al., 2011; Ifuku et al., 2012; Hu et al., 2016; Su et al., 2019). In the present study we provide further support for the involvement of plasmalogens in inflammation by providing molecular detail to changes in plasmalogen levels both in plasma and in organs during sepsis as well as SARS-CoV-2 infection.

Previous studies showed the 16:0 dimethyl acetal derivative of plasmalogens containing a sixteen-carbon vinyl ether aliphatic group bound to the glycerol backbone are decreased 55% in plasma of twenty geriatric septic patients compared to age-matched healthy subjects (Brosche et al., 2013). In this previous study, data for 18:0 dimethyl acetals were not reported and changes in 16:0 dimethyl acetal were from patient plasma collected within 24 h of severe sepsis diagnosis.

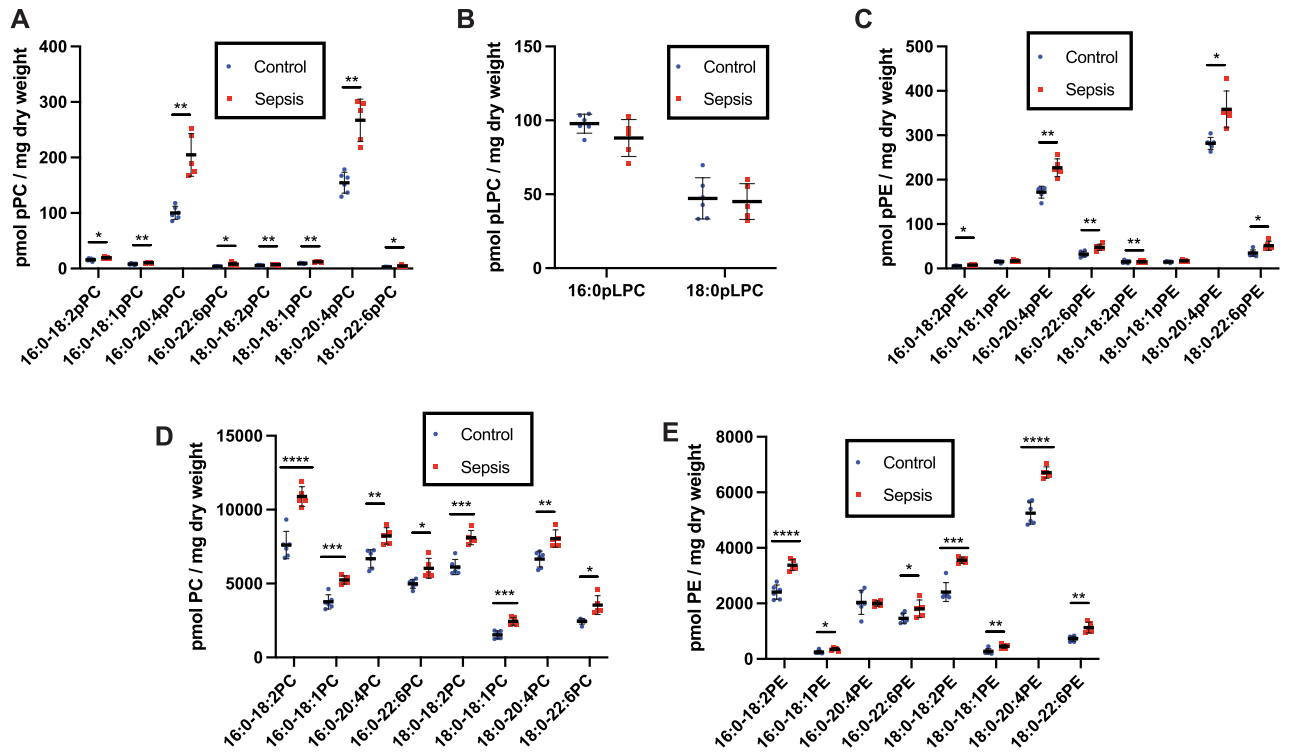

FIGURE 5 | Alterations in liver diacyl and plasmalogen phospholipids during rat sepsis. Rats were injected with cecal slurry (sepsis) ($n = 5$) or vehicle (control) ($n = 6$) as described in **Figure 3**. Liver was collected 20 h following cecal slurry or vehicle treatment, and lipids were extracted. Plasmalogen levels were quantitated as described in "Materials and Methods." Liver pPC, pLPC, pPE, PC, and PE are shown in **(A–E)**, respectively. *, **, ***, and **** indicate $p < 0.05$, 0.01, 0.001, and 0.0001, respectively, for comparisons between control and septic rats. Mean and standard deviation values are indicated for each molecular species and condition.

Human plasma pPC levels are ~8–10 fold greater than pPE levels, and pPC is highly enriched in molecular species containing a sixteen-carbon vinyl ether aliphatic group bound to the glycerol backbone, suggesting the plasma plasmalogens that decreased in geriatric sepsis patients (Brosche et al., 2013) are from pPC pools. In contrast to this previous study, our findings from the MESSI cohort were from patient plasma collected 7d following ICU admission for sepsis. This difference in time for plasma collection prevents direct comparisons to the previously reported study (Brosche et al., 2013). However, in the present studies pPE molecular species containing 16:0 vinyl ether groups, as well as 16:0 pLPC, were decreased in the human sepsis cohort. Plasma pPE species containing 18:0 vinyl ether groups were also significantly decreased in septic subjects investigated in our study. Future studies should be directed at determining details of plasmalogen loss at 24 h and examine longitudinal changes in plasmalogen loss. It will also be interesting to compare changes in human plasmalogen molecular species at 24 h to the changes we observed in the rat plasma plasmalogen molecular species that changed 20 h post CS injection. Interestingly with rat sepsis, plasma plasmalogen loss at 20 h decreased in several pPC and pPE species as well as pLPC. A summary of levels of plasmalogen and diacyl species shows a general downward trend in plasmalogen levels in sepsis, excluding livers from of septic rats (**Figure 7**). In particular, this summary highlights the many differences in changes elicited during sepsis between plasmalogen and diacyl phospholipid levels depending on the tissue and particular phospholipid class. One of the more striking observations is the loss of pPE in plasma in contrast to increases in diacyl PE during sepsis in both humans and rats.

The mechanisms responsible for plasma pLPC and pPE loss during sepsis are not known, but several mechanisms seem likely. One mechanism is that loss of plasmalogen is due to oxidative stress during sepsis. We have previously shown plasma 2-chlorofatty acid levels are elevated in human sepsis (Meyer et al., 2017; Amunugama et al., 2021b). Furthermore, in this rat sepsis model there are increased levels of 2-chlorofatty acid levels (Pike et al., 2020), which is derived from plasmalogens (Albert et al., 2001; Thukkani et al., 2002; Amunugama et al., 2021b). During sepsis the tissue plasmalogen pool or the specific plasmalogen molecular species targeted by HOCl has not been determined. In this respect it could be speculated that the impressive loss of plasma pLPC, which is overall a small pool of the total plasmalogen, could be responsible for the nanomolar levels of 2-chlorofatty acid observed during sepsis. It is also possible that the loss of plasmalogens is due to the activation of phospholipases. It has been suggested that phospholipase A_2-mediated release of arachidonic acid from plasmalogens is important in the production of oxylipids in COVID-19

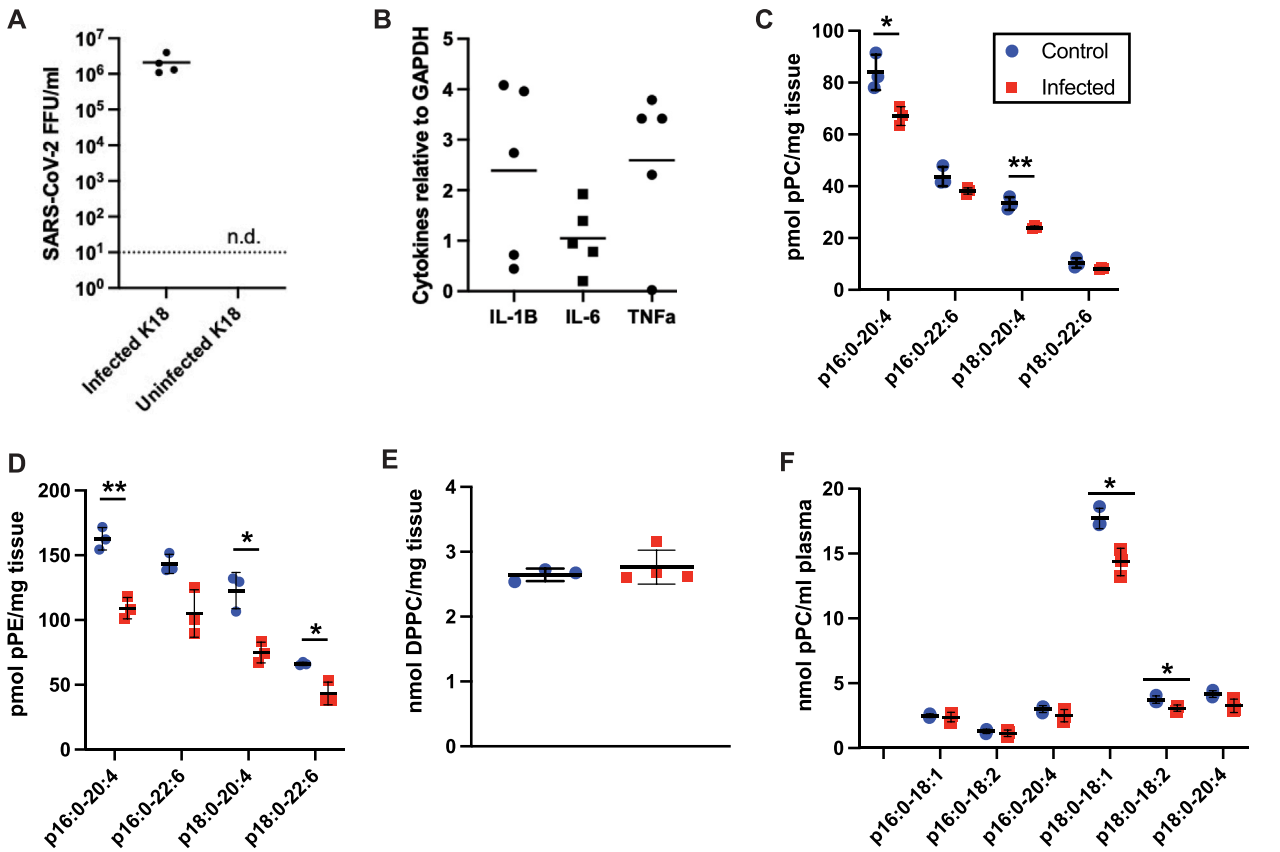

FIGURE 6 | Plasmalogen changes in K18 mice infected with the beta B.1.351 SARS-CoV-2 variant. K18 mice were either mock infected (blue circles) or infected (red squares) with 10^4 FFU of SARS-CoV-2, 20 ul, IN. 3 days post infection, lungs **(C–E)** and plasma **(F)** were collected for lipidomics analyses ($n = 3$ for both conditions). *, **, and *** indicate $p < 0.05$, 0.01, and 0.001, respectively, for comparisons between mock and virus infected mice. **(A)** SARS-CoV-2 titers in lungs of infected ($n = 4$) and uninfected ($n = 4$) mice from this study. N.d. indicates titers were not observed in the uninfected lungs. **(B)** Pro-inflammatory cytokine mRNA was detected in the infected lungs ($n = 4$ or 5) but were not detected in the uninfected lungs. Mean and standard deviation values are indicated for each molecular species and condition.

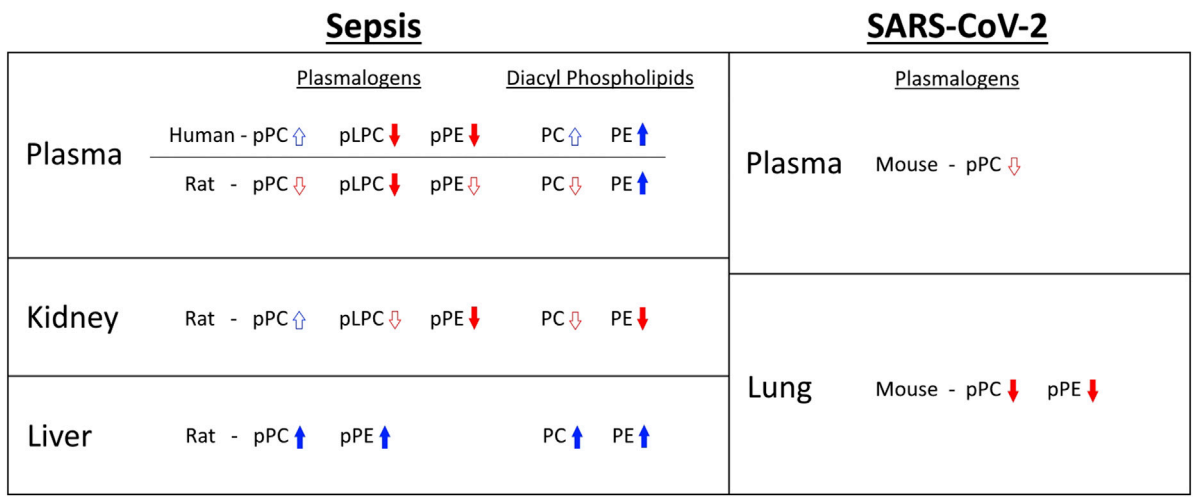

FIGURE 7 | Summary of plasmalogen and diacyl phospholipid changes observed in sepsis and SARS-CoV-2 infection. Arrow outlines indicate that fewer than half of reported species show statistically significant increase or decrease. Solid arrows indicate that at least half of reported species show statistically significant increase or decrease. For human sepsis, only trends in age restricted data are shown.

(Schwarz et al., 2021; Snider et al., 2021). The phospholipase A_2 mechanisms may be directly responsible for pPE loss. It is also possible pLPC loss is due to either accelerated use as an acceptor by acyltransferases leading to conserved levels of pPC despite putative oxidative loss or tissue uptake during sepsis. Another possibility is pPE and pLPC decrease as a result of reduced release from the liver and vascular endothelium. In human sepsis, HDL-cholesterol decreases (Vavrova et al., 2016; Tanaka et al., 2019), which may also be due to decreased secretion from the liver. Decreased plasma plasmalogens and increased liver plasmalogens during sepsis are similar to plasmalogen changes in *H-Lrpprc* mice, a mouse model of the monogenic form of the mitochondrial disease, Leigh syndrome (Ruiz et al., 2019). In *H-Lrpprc* mice, hepatic *Far1* and *Agps* are also elevated suggesting decreased plasma plasmalogen levels mediate a feedback system to increase liver plasmalogen biosynthesis. Such a feedback system may also be responsible for elevated liver plasmalogen levels in livers during sepsis. It will be interesting in future studies to examine *Agps* and *Far1* as well as differences in the levels of the plasmalogen precursors, alkyl ether lipids, in the livers from septic and control rats.

The possibility that pLPC is a circulating precursor to enrich plasmalogens in endothelium is intriguing. Plasmalogen enhancement in isolated cell studies protects cells from oxidative stress (Zoeller et al., 1999). Additionally, several studies have investigated plasmalogen precursors as a potential treatment in inflammatory diseases (Bozelli and Epand, 2021; Paul et al., 2021). Enhancing plasmalogen levels is difficult since dietary consumption of plasmalogens is reduced due to the acidic environment of the gastrointestinal tract. Using acid-stable precursors such as alkyl ether lipids will raise plasmalogen levels over time following desaturation of the alkyl ether bond to the vinyl ether. However, under acute conditions such as sepsis, the conversion of an alkyl ether to plasmalogens likely will be very slow. On the other hand, circulating pLPC already has the vinyl ether bond and lysolipids are rapidly incorporated into cells. It will be important in the future to determine the source of circulating pLPC under physiological conditions as well as during sepsis. It could be envisaged that pLPC is a product of lipoprotein-associated pPC hydrolysis by either secretory phospholipase A_2 or lipoprotein lipase. During sepsis pLPC levels potentially are dependent on a combination of oxidation of pPC or pLPC and pPC hydrolysis. Finally, the role of pLPC during sepsis needs to be further considered as a biomarker of outcomes. Similarly, the role of other plasmalogens, as well as the relationship of plasma plasmalogen levels with changes in plasma 2-chlorofatty acid levels, need to be considered as outcome predictors. The relationship of plasmalogen and chlorinated lipid levels may also allow distinction of changes in these lipids with greater specificity to infection compared to other disease states associated with only decreased plasma plasmalogen levels with the exception of lupus (Dragonas et al., 2009; Fabelo et al., 2011; Ifuku et al., 2012; Mahieu et al., 2014; Hu et al., 2016; Paul et al., 2019; Su et al., 2019).

The studies herein show plasmalogen loss during sepsis. However, there are several limitations to these studies. In the human studies we analyzed differences between septic humans and healthy control humans. Our healthy cohort average age was thirty-eight while the sepsis group was sixty. To overcome this limitation, we selected the oldest individuals ($n = 7$) in the healthy group and assessed differences in this control subset compared to the larger group of septic subjects (**Figures 1D–F**, **2**; **Table 1**). These additional analyses indicated plasma pLPC and pPE levels were reduced in the sepsis cohort when compared to this age-aligned control subgroup. Another limitation is that we have no data on the sex of individuals in our healthy cohort, while our sepsis cohort was comprised of 40% females. Our rat studies focused on changes occurring only in male rats and 20 h following cecal slurry injection. Thus, comparisons of rat specimens to human specimens were collected at different times and sex differences were not a parameter in the rat studies. It should also be appreciated that plasma levels of plasmalogens were considerably different in healthy controls due to the inherent differences in plasmalogen levels in man versus rat. Nevertheless, both human and rat sepsis led to decreases in plasma plasmalogen levels, and the rat studies afforded the opportunity to investigate changes in plasmalogen levels in the liver and kidney during sepsis. There were also limitations to the SARS-CoV-2 infection studies when comparisons are made to the rat and human sepsis studies. The SARS-CoV-2 infection studies were a viral infection elicited by airway inoculation to transgenic mice expressing the hACE2 receptor in all epithelial cells. Humans do not express ACE2 in all epithelial cells. Furthermore, these studies were performed only in female mice due to availability of genotyped mice for this study. Future studies are needed to consider sex as a parameter in both SARS-CoV-2 infected mice and rat cecal slurry sepsis. Compared to the unknown time for human sepsis beginning and the known time for CS injection, mouse infections with SARS-CoV-2 leading to pulmonary inflammation require time for viral replication to elicit injury which is typically 3–5 days. While our human and rat sepsis studies involved systemic infection, SARS-CoV-2 infection of K18 mice initially was primarily localized to infection of the respiratory tree. Infection led to robust increases in the expression of pro-inflammatory cytokines. The loss of plasmalogen in the lung during SARS-CoV-2 infection likely is the result of oxidative stress. We did not observe a loss in DPPC in the lung of infected mice. The chemical makeup of plasmalogens compared to DPPC provides a contrast in susceptibility to oxidative stress. The plasmalogen vinyl ether bond is a target for oxidation while the saturated fatty acids of DPPC are very stable under oxidative stress. Similar to findings with severe COVID-19 patients (Schwarz et al., 2021; Snider et al., 2021) we detected decreases in plasma plasmalogens in infected K18 mice.

This is the first demonstration of the loss of plasmalogens at a molecular species level in human sepsis. Furthermore, we show pLPC loss in both human and rodent sepsis. It is possible that plasma pLPC is a critical lipid to maintain endothelial plasmalogen levels under oxidative stress associated with sepsis. The demonstration of plasmalogen loss during SARS-CoV-2 further highlights the nature of plasmalogen loss during oxidative stress associated with infectious disease. The role of plasmalogens as biomarkers of outcomes in

sepsis and COVID-19 need to be explored as well as the potential protective role of plasmalogens during infectious disease.

DATA AVAILABILITY STATEMENT

The original contributions presented in the study are included in the article/**Supplementary Material**, further inquiries can be directed to the corresponding author.

ETHICS STATEMENT

The studies involving human participants were reviewed and approved by the University of Pennsylvania institutional review board and Saint Louis University institutional review board. The patients/participants provided their written informed consent to participate in this study. The animal study was reviewed and approved by the Institutional Animal Care and Use Committee at Saint Louis University.

AUTHOR CONTRIBUTIONS

DP performed experimental studies and data analysis and prepared the manuscript. RM performed experimental studies and data analysis and contributed to final manuscript preparation. EG performed experimental studies and data analysis and contributed to final manuscript preparation. CA performed experimental studies and data analysis and contributed to final manuscript preparation. DH contributed specimen collection and final manuscript preparation. MS contributed clinical study data collection, statistical analyses, and final manuscript preparation. NM contributed clinical study data collection, statistical analyses, and final manuscript preparation. AP performed data analysis and contributed to final manuscript preparation. DF was responsible for oversight of all aspects of studies, manuscript preparation, and final manuscript.

FUNDING

This study was supported (in part) by research funding from the National Institutes of Health R01 GM-115553 and S10OD025246 to DF. Clinical samples and patient phenotyping were funded by NIH HL137006 and HL137915 to NM.

SUPPLEMENTARY MATERIAL

The Supplementary Material for this article can be found online at: https://www.frontiersin.org/articles/10.3389/fcell.2022.912880/full#supplementary-material

REFERENCES

Aktepe, T. E., Pham, H., and Mackenzie, J. M. (2015). Differential Utilisation of Ceramide during Replication of the Flaviviruses West Nile and Dengue Virus. *Virology* 484, 241–250. doi:10.1016/j.virol.2015.06.015

Albert, C. J., Crowley, J. R., Hsu, F.-F., Thukkani, A. K., and Ford, D. A. (2001). Reactive Chlorinating Species Produced by Myeloperoxidase Target the Vinyl Ether Bond of Plasmalogens: Identification of 2-chlorohexadecanal. *J. Biol. Chem.* 276 (26), 23733–23741. doi:10.1074/jbc.m101447200

Amunugama, K., Jellinek, M. J., Kilroy, M. P., Albert, C. J., Rasi, V., Hoft, D. F., et al. (2021). Identification of Novel Neutrophil Very Long Chain Plasmalogen Molecular Species and Their Myeloperoxidase Mediated Oxidation Products in Human Sepsis. *Redox Biol.* 48, 102208. doi:10.1016/j.redox.2021.102208

Amunugama, K., Pike, D. P., and Ford, D. A. (2021). The Lipid Biology of Sepsis. *J. Lipid Res.* 62, 100090. doi:10.1016/j.jlr.2021.100090

Anbukumar, D. S., Shornick, L. P., Albert, C. J., Steward, M. M., Zoeller, R. A., Neumann, W. L., et al. (2010). Chlorinated Lipid Species in Activated Human Neutrophils: Lipid Metabolites of 2-chlorohexadecanal. *J. Lipid Res.* 51 (5), 1085–1092. doi:10.1194/jlr.m003673

Angus, D. C., and van der Poll, T. (2013). Severe Sepsis and Septic Shock. *N. Engl. J. Med.* 369 (9), 840–851. doi:10.1056/nejmra1208623

Bligh, E. G., and Dyer, W. J. (1959). A Rapid Method of Total Lipid Extraction and Purification. *Can. J. Biochem. Physiol.* 37, 911–917. doi:10.1139/o59-099

Bozelli, J. C., Jr., and Epand, R. M. (2021). Plasmalogen Replacement Therapy. *Membr. (Basel)* 11 (11), 838. doi:10.3390/membranes11110838

Bräutigam, C., Engelmann, B., Reiss, D., Reinhardt, U., Thiery, J., Richter, W. O., et al. (1996). Plasmalogen Phospholipids in Plasma Lipoproteins of Normolipidemic Donors and Patients with Hypercholesterolemia Treated by LDL Apheresis. *Atherosclerosis* 119 (1), 77–88. doi:10.1016/0021-9150(95)05632-7

Braverman, N. E., and Moser, A. B. (2012). Functions of Plasmalogen Lipids in Health and Disease. *Biochimica Biophysica Acta (BBA) - Mol. Basis Dis.* 1822 (9), 1442–1452. doi:10.1016/j.bbadis.2012.05.008

Brosche, T., Bertsch, T., Sieber, C. C., and Hoffmann, U. (2013). Reduced Plasmalogen Concentration as a Surrogate Marker of Oxidative Stress in Elderly Septic Patients. *Archives gerontology geriatrics* 57, 66–69. doi:10.1016/j.archger.2013.02.007

Casari, I., Manfredi, M., Metharom, P., and Falasca, M. (2021). Dissecting Lipid Metabolism Alterations in SARS-CoV-2. *Prog. Lipid Res.* 82, 101092. doi:10.1016/j.plipres.2021.101092

Chilton, F. H., and Connell, T. R. (1988). 1-ether-linked Phosphoglycerides. Major Endogenous Sources of Arachidonate in the Human Neutrophil. *J. Biol. Chem.* 263 (11), 5260–5265. doi:10.1016/s0021-9258(18)60709-4

Chilton, F. H., and Murphy, R. C. (1986). Remodeling of Arachidonate-Containing Phosphoglycerides within the Human Neutrophil. *J. Biol. Chem.* 261 (17), 7771–7777. doi:10.1016/s0021-9258(19)57467-1

Chuang, C.-C., Shiesh, S.-C., Chi, C.-H., Tu, Y.-F., Hor, L.-I., Shieh, C.-C., et al. (2006). Serum Total Antioxidant Capacity Reflects Severity of Illness in Patients with Severe Sepsis. *Crit. Care* 10 (1), R36. doi:10.1186/cc4826

Dean, J. M., and Lodhi, I. J. (2018). Structural and Functional Roles of Ether Lipids. *Protein Cell* 9 (2), 196–206. doi:10.1007/s13238-017-0423-5

Delano, M. J., and Ward, P. A. (2016). The Immune System's Role in Sepsis Progression, Resolution, and Long-Term Outcome. *Immunol. Rev.* 274 (1), 330–353. doi:10.1111/imr.12499

Dragonas, C., Bertsch, T., Sieber, C. C., and Brosche, T. (2009). Plasmalogens as a Marker of Elevated Systemic Oxidative Stress in Parkinson's Disease. *Clin. Chem. Lab. Med.* 47 (7), 894–897. doi:10.1515/CCLM.2009.205

Fabelo, N., Martín, V., Santpere, G., Marín, R., Torrent, L., Ferrer, I., et al. (2011). Severe Alterations in Lipid Composition of Frontal Cortex Lipid Rafts from Parkinson's Disease and Incidental Parkinson's Disease. *Mol. Med.* 17 (9-10), 1107–1118. doi:10.2119/molmed.2011.00119

Fernández-Oliva, A., Ortega-González, P., and Risco, C. (2019). Targeting Host Lipid Flows: Exploring New Antiviral and Antibiotic Strategies. *Cell. Microbiol.* 21 (3), e12996. doi:10.1111/cmi.12996

Ford, D. A., and Gross, R. W. (1989). Plasmenylethanolamine Is the Major Storage Depot for Arachidonic Acid in Rabbit Vascular Smooth Muscle and Is Rapidly

Hydrolyzed after Angiotensin II Stimulation. *Proc. Natl. Acad. Sci. U.S.A.* 86 (10), 3479–3483. doi:10.1073/pnas.86.10.3479

Ford, D. A., and Hale, C. C. (1996). Plasmalogen and Anionic Phospholipid Dependence of the Cardiac Sarcolemmal Sodium-Calcium Exchanger. *FEBS Lett.* 394 (1), 99–102. doi:10.1016/0014-5793(96)00930-1

Galley, H. F. (2011). Oxidative Stress and Mitochondrial Dysfunction in Sepsis. *Br. J. Anaesth.* 107 (1), 57–64. doi:10.1093/bja/aer093

Geerling, E., Pinski, A. N., Stone, T. E., DiPaolo, R. J., Zulu, M. Z., Maroney, K. J., et al. (2022). Roles of Antiviral Sensing and Type I Interferon Signaling in the Restriction of SARS-CoV-2 Replication. *iScience* 25 (1), 103553. doi:10.1016/j.isci.2021.103553

Geerling, E., Stone, E. T., Steffen, T. L., Hassert, M., Brien, J. D., and Pinto, A. K. (2021). Obesity Enhances Disease Severity in Female Mice Following West Nile Virus Infection. *Front. Immunol.* 12, 739025. doi:10.3389/fimmu.2021.739025

Glaser, P. E., and Gross, R. W. (1994). Plasmenylethanolamine Facilitates Rapid Membrane Fusion: a Stopped-Flow Kinetic Investigation Correlating the Propensity of a Major Plasma Membrane Constituent to Adopt an HII Phase with its Ability to Promote Membrane Fusion. *Biochemistry* 33 (19), 5805–5812. doi:10.1021/bi00185a019

Han, X., and Gross, R. W. (1990). Plasmenylcholine and Phosphatidylcholine Membrane Bilayers Possess Distinct Conformational Motifs. *Biochemistry* 29 (20), 4992–4996. doi:10.1021/bi00472a032

Han, X., and Gross, R. W. (1991). Proton Nuclear Magnetic Resonance Studies on the Molecular Dynamics of Plasmenylcholine/cholesterol and Phosphatidylcholine/cholesterol Bilayers. *Biochimica Biophysica Acta (BBA) - Biomembr.* 1063 (1), 129–136. doi:10.1016/0005-2736(91)90362-c

Hu, C., Zhou, J., Yang, S., Li, H., Wang, C., Fang, X., et al. (2016). Oxidative Stress Leads to Reduction of Plasmalogen Serving as a Novel Biomarker for Systemic Lupus Erythematosus. *Free Radic. Biol. Med.* 101, 475–481. doi:10.1016/j.freeradbiomed.2016.11.006

Ifuku, M., Katafuchi, T., Mawatari, S., Noda, M., Miake, K., Sugiyama, M., et al. (2012). Anti-inflammatory/anti-amyloidogenic Effects of Plasmalogens in Lipopolysaccharide-Induced Neuroinflammation in Adult Mice. *J. Neuroinflammation* 9, 197. doi:10.1186/1742-2094-9-197

Jean Beltran, P. M., Cook, K. C., Hashimoto, Y., Galitzine, C., Murray, L. A., Vitek, O., et al. (2018). Infection-Induced Peroxisome Biogenesis Is a Metabolic Strategy for Herpesvirus Replication. *Cell Host Microbe* 24 (4), 526–541. doi:10.1016/j.chom.2018.09.002

Kayganich, K. A., and Murphy, R. C. (1992). Fast Atom Bombardment Tandem Mass Spectrometric Identification of Diacyl, Alkylacyl, and Alk-1-Enylacyl Molecular Species of Glycerophosphoethanolamine in Human Polymorphonuclear Leukocytes. *Anal. Chem.* 64 (23), 2965–2971. doi:10.1021/ac00047a015

Khaselev, N., and Murphy, R. C. (1999). Susceptibility of Plasmenyl Glycerophosphoethanolamine Lipids Containing Arachidonate to Oxidative Degradation. *Free Radic. Biol. Med.* 26 (3-4), 275–284. doi:10.1016/s0891-5849(98)00211-1

Liu, V., Escobar, G. J., Greene, J. D., Soule, J., Whippy, A., Angus, D. C., et al. (2014). Hospital Deaths in Patients with Sepsis from 2 Independent Cohorts. *Jama* 312 (1), 90–92. doi:10.1001/jama.2014.5804

Mahieu, M. A., Guild, C. P., Albert, C. J., Kondos, G. T., Carr, J. J., Edmundowicz, D., et al. (2014). Alpha-chlorofatty Acid and Coronary Artery or Aorta Calcium Scores in Women with Systemic Lupus Erythematosus. A Pilot Study. *J. Rheumatol.* 41 (9), 1834–1842. doi:10.3899/jrheum.131361

Mandel, H., Sharf, R., Berant, M., Wanders, R. J. A., Vreken, P., and Aviram, M. (1998). Plasmalogen Phospholipids Are Involved in HDL-Mediated Cholesterol Efflux: Insights from Investigations with Plasmalogen-Deficient Cells. *Biochem. Biophysical Res. Commun.* 250 (2), 369–373. doi:10.1006/bbrc.1998.9321

Maner-Smith, K. M., Goll, J. B., Khadka, M., Jensen, T. L., Colucci, J. K., Gelber, C. E., et al. (2020). Alterations in the Human Plasma Lipidome in Response to Tularemia Vaccination. *Vaccines* 8 (3), 414. doi:10.3390/vaccines8030414

Mayr, F. B., Yende, S., and Angus, D. C. (2014). Epidemiology of Severe Sepsis. *Virulence* 5 (1), 4–11. doi:10.4161/viru.27372

Mecatti, G. C., Fernandes Messias, M. C., Sant'Anna Paiola, R. M., Figueiredo Angolini, C. F., da Silva Cunha, I. B., Eberlin, M. N., et al. (2018). Lipidomic Profiling of Plasma and Erythrocytes from Septic Patients Reveals Potential Biomarker Candidates. *Biomark. Insights* 13, 1177271918765137. doi:10.1177/1177271918765137

Mecatti, G. C., Messias, M. C. F., and de Oliveira Carvalho, P. (2020). Lipidomic Profile and Candidate Biomarkers in Septic Patients. *Lipids Health Dis.* 19 (1), 68. doi:10.1186/s12944-020-01246-2

Mesquita, F. S., Abrami, L., Sergeeva, O., Turelli, P., Kunz, B., Raclot, C., et al. (2021). S-acylation Controls ARS-Cov-2 Membrane Lipid Organization and Enhances Infectivity. *Dev Cell* 56, 2790. doi:10.1016/j.devcel.2021.09.016

Meyer, N. J., Reilly, J. P., Feng, R., Christie, J. D., Hazen, S. L., Albert, C. J., et al. (2017). Myeloperoxidase-derived 2-chlorofatty Acids Contribute to Human Sepsis Mortality via Acute Respiratory Distress Syndrome. *JCI Insight* 2. e96432. doi:10.1172/jci.insight.96432

Morand, O. H., Zoeller, R. A., and Raetz, C. R. (1988). Disappearance of Plasmalogens from Membranes of Animal Cells Subjected to Photosensitized Oxidation. *J. Biol. Chem.* 263 (23), 11597–11606. doi:10.1016/s0021-9258(18)38001-3

Murphy, E. J., Joseph, L., Stephens, R., and Horrocks, L. A. (1992). Phospholipid Composition of Cultured Human Endothelial Cells. *Lipids* 27 (2), 150–153. doi:10.1007/bf02535816

Paoli, C. J., Reynolds, M. A., Sinha, M., Gitlin, M., and Crouser, E. (2018). Epidemiology and Costs of Sepsis in the United States-An Analysis Based on Timing of Diagnosis and Severity Level*. *Crit. care Med.* 46 (12), 1889–1897. doi:10.1097/ccm.0000000000003342

Paul, S., Lancaster, G. I., and Meikle, P. J. (2019). Plasmalogens: A Potential Therapeutic Target for Neurodegenerative and Cardiometabolic Disease. *Prog. Lipid Res.* 74, 186–195. doi:10.1016/j.plipres.2019.04.003

Paul, S., Smith, A. A. T., Culham, K., Gunawan, K. A., Weir, J. M., Cinel, M. A., et al. (2021). Shark Liver Oil Supplementation Enriches Endogenous Plasmalogens and Reduces Markers of Dyslipidemia and Inflammation. *J. Lipid Res.* 62, 100092. doi:10.1016/j.jlr.2021.100092

Pike, D. P., Vogel, M. J., McHowat, J., Mikuzis, P. A., Schulte, K. A., and Ford, D. A. (2020). 2-Chlorofatty Acids Are Biomarkers of Sepsis Mortality and Mediators of Barrier Dysfunction in Rats. *J. Lipid Res.* 61 (7), 1115–1127. doi:10.1194/jlr.ra120000829

Pike, L. J., Han, X., Chung, K.-N., and Gross, R. W. (2002). Lipid Rafts Are Enriched in Arachidonic Acid and Plasmenylethanolamine and Their Composition Is Independent of Caveolin-1 Expression: a Quantitative Electrospray Ionization/mass Spectrometric Analysis. *Biochemistry* 41, 2075–2088. doi:10.1021/bi0156557

Prauchner, C. A. (2017). Oxidative Stress in Sepsis: Pathophysiological Implications Justifying Antioxidant Co-therapy. *Burns* 43 (3), 471–485. doi:10.1016/j.burns.2016.09.023

Reilly, J. P., Wang, F., Jones, T. K., Palakshappa, J. A., Anderson, B. J., Shashaty, M. G. S., et al. (2018). Plasma Angiopoietin-2 as a Potential Causal Marker in Sepsis-Associated ARDS Development: Evidence from Mendelian Randomization and Mediation Analysis. *Intensive Care Med.* 44 (11), 1849–1858. doi:10.1007/s00134-018-5328-0

Reiss, D., Beyer, K., and Engelmann, B. (1997). Delayed Oxidative Degradation of Polyunsaturated Diacyl Phospholipids in the Presence of Plasmalogen Phospholipids *In Vitro*. *Biochem. J.* 323 (Pt 3Pt 3), 807–14. doi:10.1042/bj3230807

Robertson, C. M., and Coopersmith, C. M. (2006). The Systemic Inflammatory Response Syndrome. *Microbes Infect.* 8 (5), 1382–1389. doi:10.1016/j.micinf.2005.12.016

Rubio, J. M., Astudillo, A. M., Casas, J., Balboa, M. A., and Balsinde, J. (2018). Regulation of Phagocytosis in Macrophages by Membrane Ethanolamine Plasmalogens. *Front. Immunol.* 9, 1723. doi:10.3389/fimmu.2018.01723

Rudd, K. E., Johnson, S. C., Agesa, K. M., Shackelford, K. A., Tsoi, D., Kievlan, D. R., et al. (2020). Global, Regional, and National Sepsis Incidence and Mortality, 1990-2017: Analysis for the Global Burden of Disease Study. *Lancet* 395 (10219), 200–211. doi:10.1016/s0140-6736(19)32989-7

Ruiz, M., Cuillerier, A., Daneault, C., Deschênes, S., Frayne, I. R., Bouchard, B., et al. (2019). Lipidomics Unveils Lipid Dyshomeostasis and Low Circulating Plasmalogens as Biomarkers in a Monogenic Mitochondrial Disorder. *JCI Insight* 4 (14), e123231. doi:10.1172/jci.insight.123231

Schwarz, B., Sharma, L., Roberts, L., Peng, X., Bermejo, S., Leighton, I., et al. (2021). Cutting Edge: Severe SARS-CoV-2 Infection in Humans Is Defined by a Shift in the Serum Lipidome, Resulting in Dysregulation of Eicosanoid Immune Mediators. *J. Immunol.* 206 (2), 329–334. doi:10.4049/jimmunol.2001025

Singer, M., Deutschman, C. S., Seymour, C. W., Shankar-Hari, M., Annane, D., Bauer, M., et al. (2016). The Third International Consensus Definitions for Sepsis and Septic Shock (Sepsis-3). *JAMA* 315 (8), 801–10. doi:10.1001/jama.2016.0287

Snider, J. M., You, J. K., Wang, X., Snider, A. J., Hallmark, B., Zec, M. M., et al. (2021). Group IIA Secreted Phospholipase A2 Is Associated with the Pathobiology Leading to COVID-19 Mortality. *J. Clin. Invest.* 131 (19), e149236. doi:10.1172/JCI149236

Stadelmann-Ingrand, S., Favreliere, S., Fauconneau, B., Mauco, G., and Tallineau, C. (2001). Plasmalogen Degradation by Oxidative Stress: Production and Disappearance of Specific Fatty Aldehydes and Fatty α-hydroxyaldehydes. *Free Radic. Biol. Med.* 31, 1263–1271. doi:10.1016/s0891-5849(01)00720-1

Su, X. Q., Wang, J., and Sinclair, A. J. (2019). Plasmalogens and Alzheimer's Disease: a Review. *Lipids Health Dis.* 18 (1), 100. doi:10.1186/s12944-019-1044-1

Sviridov, D., Miller, Y. I., Ballout, R. A., Remaley, A. T., and Bukrinsky, M. (2020). Targeting Lipid Rafts-A Potential Therapy for COVID-19. *Front. Immunol.* 11, 574508. doi:10.3389/fimmu.2020.574508

Tanaka, S., Diallo, D., Delbosc, S., Genève, C., Zappella, N., Yong-Sang, J., et al. (2019). High-density Lipoprotein (HDL) Particle Size and Concentration Changes in Septic Shock Patients. *Ann. Intensive Care* 9 (1), 68. doi:10.1186/s13613-019-0541-8

Tanner, L. B., Chng, C., Guan, X. L., Lei, Z., Rozen, S. G., and Wenk, M. R. (2014). Lipidomics Identifies a Requirement for Peroxisomal Function during Influenza Virus Replication. *J. Lipid Res.* 55 (7), 1357–1365. doi:10.1194/jlr.m049148

Theken, K. N., Tang, S. Y., Sengupta, S., and FitzGerald, G. A. (2021). The Roles of Lipids in SARS-CoV-2 Viral Replication and the Host Immune Response. *J. Lipid Res.* 62, 100129. doi:10.1016/j.jlr.2021.100129

Thukkani, A. K., Hsu, F.-F., Crowley, J. R., Wysolmerski, R. B., Albert, C. J., and Ford, D. A. (2002). Reactive Chlorinating Species Produced during Neutrophil Activation Target Tissue Plasmalogens: Production of the Chemoattractant, 2-chlorohexadecanal. *J. Biol. Chem.* 277 (6), 3842–3849. doi:10.1074/jbc.m109489200

Vance, J. E. (1990). Lipoproteins Secreted by Cultured Rat Hepatocytes Contain the Antioxidant 1-Alk-1-Enyl-2-Acylglycerophosphoethanolamine. *Biochimica Biophysica Acta (BBA) - Lipids Lipid Metabolism* 1045 (2), 128–134. doi:10.1016/0005-2760(90)90141-j

Vavrova, L., Rychlikova, J., Mrackova, M., Novakova, O., Zak, A., and Novak, F. (2016). Increased Inflammatory Markers with Altered Antioxidant Status Persist after Clinical Recovery from Severe Sepsis: a Correlation with Low HDL Cholesterol and Albumin. *Clin. Exp. Med.* 16 (4), 557–569. doi:10.1007/s10238-015-0390-1

Villareal, V. A., Rodgers, M. A., Costello, D. A., and Yang, P. L. (2015). Targeting Host Lipid Synthesis and Metabolism to Inhibit Dengue and Hepatitis C Viruses. *Antivir. Res.* 124, 110–121. doi:10.1016/j.antiviral.2015.10.013

Vincent, J.-L., Jones, G., David, S., Olariu, E., and Cadwell, K. K. (2019). Frequency and Mortality of Septic Shock in Europe and North America: a Systematic Review and Meta-Analysis. *Crit. Care* 23 (1), 196. doi:10.1186/s13054-019-2478-6

Wang, J., Sun, Y., Teng, S., and Li, K. (2020). Prediction of Sepsis Mortality Using Metabolite Biomarkers in the Blood: a Meta-Analysis of Death-Related Pathways and Prospective Validation. *BMC Med.* 18 (1), 83. doi:10.1186/s12916-020-01546-5

Zheng, J., Wong, L.-Y. R., Li, K., Verma, A. K., Ortiz, M. E., Wohlford-Lenane, C., et al. (2021). COVID-19 Treatments and Pathogenesis Including Anosmia in K18-hACE2 Mice. *Nature* 589 (7843), 603–607. doi:10.1038/s41586-020-2943-z

Zoeller, R. A., Lake, A. C., Nagan, N., Gaposchkin, D. P., Legner, M. A., and Lieberthal, W. (1999). Plasmalogens as Endogenous Antioxidants: Somatic Cell Mutants Reveal the Importance of the Vinyl Ether. *Biochem. J.* 338 (Pt 3), 769–76. doi:10.1042/bj3380769

Zoeller, R. A., Grazia, T. J., LaCamera, P., Park, J., Gaposchkin, D. P., and Farber, H. W. (2002). Increasing Plasmalogen Levels Protects Human Endothelial Cells during Hypoxia. *Am. J. Physiology-Heart Circulatory Physiology* 283 (2), H671–H679. doi:10.1152/ajpheart.00524.2001

Zoeller, R. A., Morand, O. H., and Raetz, C. R. (1988). A Possible Role for Plasmalogens in Protecting Animal Cells against Photosensitized Killing. *J. Biol. Chem.* 263 (23), 11590–11596. doi:10.1016/s0021-9258(18)38000-1

Author's Disclaimer: The content is solely the responsibility of the authors and does not necessarily represent the official views of the National Institutes of Health.

Conflict of Interest: The authors declare that the research was conducted in the absence of any commercial or financial relationships that could be construed as a potential conflict of interest.

Publisher's Note: All claims expressed in this article are solely those of the authors and do not necessarily represent those of their affiliated organizations, or those of the publisher, the editors and the reviewers. Any product that may be evaluated in this article, or claim that may be made by its manufacturer, is not guaranteed or endorsed by the publisher.

frontiers | Frontiers in Molecular Biosciences

ORIGINAL RESEARCH
published: 27 June 2022
doi: 10.3389/fmolb.2022.915457

ATP8B2-Mediated Asymmetric Distribution of Plasmalogens Regulates Plasmalogen Homeostasis and Plays a Role in Intracellular Signaling

Masanori Honsho[1,2]*, *Shiro Mawatari*[3] and *Yukio Fujiki*[2,4]*

[1]Department of Neuroinflammation and Brain Fatigue Science, Graduate School of Medical Sciences, Kyushu University, Fukuoka, Japan, [2]Institute of Rheological Functions of Food-Kyushu University Collaboration Program, Kyushu University, Fukuoka, Japan, [3]Institute of Rheological Functions of Food, Fukuoka, Japan, [4]Graduate School of Science, University of Hyogo, Hyogo, Japan

OPEN ACCESS

Edited by:
Marie-Pierre Golinelli, UPR2301 Institut de Chimie des Substances Naturelles (ICSN CNRS), France

Reviewed by:
Todd R. Graham, Vanderbilt University, United States
Pedro Brites, Universidade do Porto, Portugal
Takao Shimizu, National Center, Japan

***Correspondence:**
Masanori Honsho
honsho.masanori.707@m.kyushu-u.ac.jp
Yukio Fujiki
yfujiki@kyudai.jp

Specialty section:
This article was submitted to Cellular Biochemistry, a section of the journal Frontiers in Molecular Biosciences

Received: 08 April 2022
Accepted: 23 May 2022
Published: 27 June 2022

Citation:
Honsho M, Mawatari S and Fujiki Y (2022) ATP8B2-Mediated Asymmetric Distribution of Plasmalogens Regulates Plasmalogen Homeostasis and Plays a Role in Intracellular Signaling. Front. Mol. Biosci. 9:915457. doi: 10.3389/fmolb.2022.915457

Plasmalogens are a subclass of glycerophospholipid containing vinyl-ether bond at the *sn*-1 position of glycerol backbone. Ethanolamine-containing plasmalogens (plasmalogens) are major constituents of cellular membranes in mammalian cells and *de novo* synthesis of plasmalogens largely contributes to the homeostasis of plasmalogens. Plasmalogen biosynthesis is regulated by a feedback mechanism that senses the plasmalogen level in the inner leaflet of the plasma membrane and regulates the stability of fatty acyl-CoA reductase 1 (Far1), a rate-limiting enzyme for plasmalogen biosynthesis. However, the molecular mechanism underlying the localization of plasmalogens in cytoplasmic leaflet of plasma membrane remains unknown. To address this issue, we attempted to identify a potential transporter of plasmalogens from the outer to the inner leaflet of plasma membrane by focusing on phospholipid flippases, type-IV P-type adenosine triphosphatases (P4-ATPase), localized in the plasma membranes. We herein show that knockdown of *ATP8B2* belonging to the class-1 P4-ATPase enhances localization of plasmalogens but not phosphatidylethanolamine in the extracellular leaflet and impairs plasmalogen-dependent degradation of Far1. Furthermore, phosphorylation of protein kinase B (AKT) is downregulated by lowering the expression of *ATP8B2*, which leads to suppression of cell growth. Taken together, these results suggest that enrichment of plasmalogens in the cytoplasmic leaflet of plasma membranes is mediated by ATP8B2 and this asymmetric distribution of plasmalogens is required for sensing plasmalogens as well as phosphorylation of AKT.

Keywords: plasmalogen, sensing, asymmetric distribution, P4-ATPase, Akt, plasma membrane

INTRODUCTION

Alkenyl-ether glycerophospholipids characterized by the presence of a vinyl ether linkage at the *sn*-1 position are named plasmalogens, in which the head group of plasmalogens is commonly occupied by ethanolamine in mammals (Nagan and Zoeller, 2001; Braverman and Moser, 2012). Physiological roles of plasmalogens in the differentiation of Schwann cells, myelination of oligodendrocytes,

neuron excitability, and homeostasis of cholesterol and neurotransmitter have been explored from several *in vitro* and *in vivo* studies using plasmalogen-deficient cells and mice (da Silva et al., 2014; Dorninger et al., 2019; Honsho et al., 2019; Malheiro et al., 2019; da Silva et al., 2021). Defect of plasmalogen biosynthesis caused by the mutations in genes essential for plasmalogen biosynthesis leads to extremely reduced levels of plasmalogens and causes a human genetic disorder, rhizomelic chondrodysplasia punctata (RCDP) (Wanders et al., 1992; Wanders et al., 1994; Braverman et al., 1997; Motley et al., 1997; Purdue et al., 1997; Buchert et al., 2014; Barøy et al., 2015). The patients with RCDP manifest severe growth retardation, proximal shortening of the upper extremities, and congenital cataract (Braverman and Moser, 2012). Plasmalogen levels of peripheral tissues in the RCDP model mouse are restored by the administration of alkylglycerol, by which the progression of the pathology in peripheral tissues such as testis and adipose tissue are suppressed (Brites et al., 2011), hence suggesting a physiological importance of the plasmalogen homeostasis in the functions of animal tissues.

The finding of a severe defect of plasmalogens in several different tissues from a patient with RCDP highlights that *de novo* synthesis of plasmalogens plays a pivotal role in the homeostasis of plasmalogens in tissues (Malheiro et al., 2015). Furthermore, recent findings of the elevation of plasmalogen biosynthesis in the patient caused by the mutation of fatty acyl-CoA reductase 1 (Far1), a rate-limiting enzyme of plasmalogen biosynthesis (Honsho et al., 2010) and sharing neurological symptoms such as spastic features, seizures with the patients defective in plasmalogen synthesis further strengthen the physiological importance of the regulation of plasmalogen biosynthesis (Ferdinandusse et al., 2021). These studies indicate that regulation of plasmalogen biosynthesis greatly contributes to the homeostasis of plasmalogens in tissues.

Plasmalogen biosynthesis is initiated in peroxisome matrix by acylation of dihydroxyacetonephosphate (DHAP) catalyzed by glyceronephosphate O-acyltransferase (GNPAT). The acyl-DHAP is further converted to alkyl-DHAP by alkylglycerone phosphate synthase (AGPS) that replaces acyl-chain of acyl-DHAP with long chain fatty alcohol (Nagan and Zoeller, 2001; Braverman and Moser, 2012). Far1, a peroxisomal C-tail anchored protein catalyzes the generation of fatty alcohol by reducing fatty acyl-CoA (Cheng and Russell, 2004). Based on the findings that Far1 activity is upregulated in the absence of plasmalogens (Honsho et al., 2010; Wiese et al., 2012), whereas plasmalogen synthesis is downregulated by the elevation of cellular plasmalogens by suppressing the activity of Far1 through augmenting degradation of Far1 without altering a transcription level of *FAR1* (Honsho et al., 2010), we proposed that Far1 is a rate-limiting enzyme in the plasmalogen biosynthesis. Given these results together with the recent study by Ferdinandusse et al. (2021), it is now widely accepted that biosynthesis of plasmalogens is regulated by modulating the stability of Far1 *via* sensing cellular plasmalogen level (Honsho and Fujiki, 2017). However, precise mechanism of sensing the plasmalogen level remains largely unknown.

To address this issue, we focused on the plasmalogens asymmetrically enriched in the inner leaflet of plasma membranes (Kirschner and Ganser, 1982; Fellmann et al., 1993; Honsho et al., 2017). This asymmetric distribution of plasmalogens is likely established by the function of type-IV P4-ATPase(s) that drives the outer-to-inner translocation of phospholipids. As reported (Honsho et al., 2017), the localization of plasmalogens in the outer leaflet of plasma membrane is indeed augmented upon reducing the protein level of CDC50A, a β-subunit of type-IV P4-ATPases that is essential for localization of the most of P4-ATPases in plasma membrane. Interestingly, the impairment of asymmetric distribution of plasmalogens elevates Far1 protein level (Honsho et al., 2017), thereby suggesting that asymmetric distribution of plasmalogens contributes to the regulation of plasmalogen biosynthesis. In addition to these findings, the recruitment of protein kinase B (AKT), a master regulator of cellular metabolism, to the plasma membranes that is an essential step for the phosphorylation of AKT is impaired in the absence of plasmalogens in Schwann cells, mouse embryonic fibroblasts, and neurons (da Silva et al., 2014; da Silva et al., 2021). This suggests that the asymmetric distribution of plasmalogens is tightly linked to cellular metabolism.

In the present study, we attempted to identify potential P4-ATPase(s) involved in translocating plasmalogens from extracellular leaflet to cytoplasmic leaflet and explore its functional significance in the biosynthesis and cellular functions of plasmalogens.

MATERIALS AND METHODS

Cell Culture, DNA Transfection, and RNAi

HeLa cells were maintained in DMEM (Invitrogen) supplemented with 10% FBS (Sigma). All cell lines were cultured at 37°C under 5% CO_2.

siRNA-mediated knockdown was performed using predesigned Stealth™ siRNAs (Invitrogen) and MISSION siRNAs (Sigma), respectively. Cells were harvested at 72 h after the initial transfection using Lipofectamine 2000. The following siRNAs were used: MISSION® siRNA for human CDC50A (HS_TMEM30A_4522), ATP8B2#9 (SASI_Hs01_00037709), ATP8B2#13 (SASI_Hs01_00037913), ATP10D (SASI_Hs01_00069039), ATP11A (SASI_Hs01_00106358), ATP11B (SASI_Hs01_00045762), and Universal Negative Control#1. Stealth™ siRNAs for AGPS#30 (Agps-MSS213530) and AGPS#32 (AGPS-MSS213532). For counting cell numbers, cells were harvested at 48 and 72 h after transfection of siRNA and suspended in the equal volume of medium. An aliquot (30 μl) of the cell suspension was diluted with the equal volume of trypan blue (Fujifilm Wako Pure Chemical Corporation) and viable cells were counted with hemocytometer.

Antibodies

We used rabbit antisera to AGPS (Honsho et al., 2008) and Far1 (Honsho et al., 2010). Rabbit antibodies to phospho-AKT (S473), phospho-AKT (T308), AKT were purchased from Cell Signaling. Rabbit antibody to ATP8B2 (Abgent) and mouse antibodies to actin (Santa Cruz) and GAPDH (Santa Cruz) were used.

RT-PCR

Total RNA was isolated from HeLa cells using a TRIzol reagent (Ambion) and synthesis first-strand cDNA was performed using the PrimeScript RT reagent Kit (Takara Bio). Quantitative real-time RT-PCR was performed in an ABI7500 Real Time System (Applied Biosystem) using SYBR Premix Ex TaqTM II (Ti RNaseH Plus) (Takara Bio). Primers used were as follows: human ATP8B2 sense: ATP8B2Fw. 5′-TCCTCCTTTCCAGCA GTGAG-3′ antisense: ATP8B2Rv. 5′-ACTTCACCGTCAAAC TTGGC-3′, human ATP10D sense: ATP10DFw. 5′-ACAGTC AGTGGTTCCCTCAG-3′ antisense: ATP10DRv. 5′-ACTGGC TCCTTCTCCACTTC-3′, human ATP11A sense: ATP11AFw. 5′-GGCTCCGAACTTTGTGTGTT-3′ antisense: ATP11ARv. 5′-TCTCTCGATCTTGAAGGGCC-3′, and human ATP11B sense: ATP11BFw. 5′-GACTCCATGTGCTGTTTCCC-3′ antisense: ATP11BRv. 5′-ATCTGCTGATGTGGGTTGGA-3’.

Immunoblotting

Protein samples were separated by SDS-PAGE and electrotransferred to a nitrocellulose membrane (Bio-Rad). After blocking for 1 h in TBST (10 mM Tris-HCl pH 7.4, 200 mM NaCl, and 0.05% Tween-20) containing 5% non-fat dry milk, blots were subjected to immunoblotting with primary antibodies overnight at 4°C, followed by incubating with a secondary antibody for 2 h at room temperature. Immunoblots were developed with Clarity™ Western ECL Substrate (Bio-Rad) and scanned with an ImageQuant LAS 4010 imager (GE Healthcare). For antibody reprobing, membranes were incubated three times for 10 min in a mild membrane stripping buffer (Abcam), extensively washed with TBST, and incubated with antibody. The intensity of bands was quantified by ImageJ software (National Institutes of Health).

Lipid Analysis

Distribution of plasmalogens in plasma membranes was assessed as described (Honsho et al., 2017). In brief, cells were metabolically labeled for 18 h with 0.1 μCi of ^{14}C-ethanolamine (Moravek), washed with ice-cold SHT buffer (0.25 M sucrose, 10 mM Hepes-KOH, pH 8.5) containing 1 μg/ml taxol (Sigma), incubated on ice for 5 min, and further treated with 10 mM 2,4,6-trinitrobenzene sulfonic acid (TNBS) (Wako) dissolved in SHT buffer on ice for 30 min in the dark. Excess TNBS was quenched for 15 min with 50 mM Tris-HCl, pH 8.0. Equal aliquots (100 μg protein) of cell lysates were treated with 5% of trichloroacetic acid for 10 min at room temperature and precipitated by centrifugation at 20,000 × g for 1 min, followed by lipid extraction by the Bligh and Dyer method (Bligh and Dyer, 1959). Lipids were analyzed on thin layer chromatography plates (silica gel 60, Merck) with chloroform/methanol/acetic acid solution (v/v/v: 65/25/10) (Honsho et al., 2008). ^{14}C-labeled lipids were detected by autoradiography using a FLA-5000 imaging analyzer (Fuji Film) and quantified using an image analyzer software (Multi Gauge, Fuji Film).

Cellular plasmalogen level was determined by liquid chromatography connected to tandem mass spectrometry (LC-MS/MS) with modification of the method described by Abe et al. (2014). Total cellular lipids were extracted by the Bligh and Dyer method (Bligh and Dyer, 1959). Briefly, cell lysates containing 50 μg of total cellular proteins were dissolved in methanol/chloroform/water (v/v/v: 2:1:0.8) and 50 pmol internal standard (1-heptadecanoyl-sn-glycero-3-phosphocholine, 1, 2-didodecanoyl-sn-glycero-3-phosphocholine and 1, 2-didodecanoyl-sn-glycero-3-phosphoethanolamine). After 5 min, 1 ml each of water and chloroform was added and the whole mixtures were centrifuged to collect the lower organic phase. One ml chloroform was added again to re-extract the lipids. Collected organic phase was then evaporated under the nitrogen stream and suspended in pure methanol. LC-MS assay was performed using a Xevo TQ-S micro with ACQUITY UPLC System (Waters). Samples were injected into an ACQUIRY UPLC BEH C18 column and then directly subjected to ESI-MS/MS analysis. A 10-μl aliquot of each sample was directly introduced by autosampler injector and the samples were separated by step-gradient elution with mobile phase A (acetonitrile:methanol: water at 2:2:1 (v/v/v), 0.1% formic acid and 0.028% ammonium) and mobile phase B (isopropanol, 0.1% formic acid and 0.028% ammonium) at the ratios: 100:0 (for 0–5 min), 70:30 (5–20 min), 45:55 (20–40 min), and 100:0 (40–51 min), with a flow rate (70 μl/min at 35°C) and source temperature (150°C). Ethanolamine plasmalogens (PlsEtns) were detected at positive ion mode and the method used to detect plasmalogens is listed in **Supplementary Table S1**. The data were analyzed and quantified using the TargetLynx (Waters).

Statistical Analysis and Data Presentation

Statistical analysis was performed using one-tailed Student's t-tests unless otherwise described in figure legends. A $p < 0.05$ was considered statistically significant. Quantitative data were shown as means ± SD.

RESULTS

Identification of P4-ATPase Responsible for Topogenesis of Plasmalogens

We earlier showed that asymmetric distribution of plasmalogens in HeLa cells is compromised upon knocking down of CDC50A, a β-subunit of P4-ATPases (Takatsu et al., 2011), resulting in the elevation of Far1 protein level (Honsho et al., 2017). Given these results together with the fact that several P4-ATPases require the association with CDC50A protein for their exit from the endoplasmic reticulum (Bryde et al., 2010; Paulusma and Elferink, 2010; van der Velden et al., 2010), we hypothesized that asymmetric distribution of plasmalogens in plasma membrane is established by the function of P4-ATPase(s). Therefore, we attempted to identify the P4-ATPase(s) responsible for topogenesis of plasmalogens by focusing on P4-ATPases expressed in HeLa cells.

Of the eleven P4-ATPase that are expressed in HeLa cells (Takatsu et al., 2011), we selected four P4-ATPases (ATP8B2, ATP10D, ATP11A, and ATP11B) that associate with CDC50A (Shin and Takatsu, 2019) and present on plasma membranes (Andersen et al., 2016), whereas ATP8B1 and ATP11C were not considered here from potential P4-ATPases for plasmalogens because of their functions in transport of phosphatidylcholine (PC) and phosphatidylserine (PS), respectively (Takatsu et al., 2014; Takada et al., 2015; Hayashi et al., 2018).

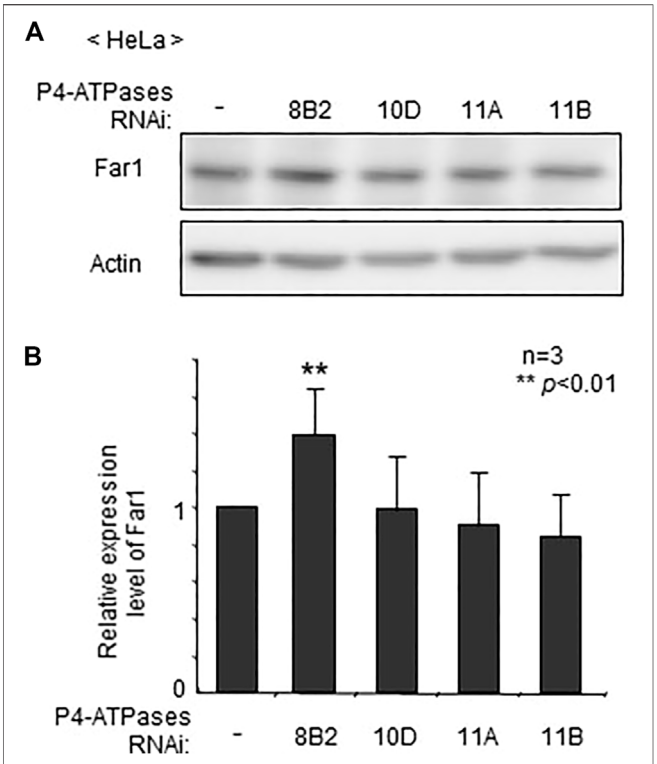

FIGURE 1 | Elevated protein level of Far1 by knockdown of *ATP8B2*. **(A)** HeLa cells were transfected with dsRNA against *ATP8B2* (8B2), *ATP10D* (10D), *ATP11A* (11A), or *ATP11B* (11B) and cultured for 72 h. Protein level of Far1 and actin (Actin) was analyzed by immunoblotting with respective antibodies as indicated. Actin was used as a loading control. **(B)** The amount of Far1 was normalized by the actin level in respective transfectants and presented relative to that in non-transfected cells (-) (n = 3). Data indicate means ± SD. $^{**}p < 0.01$ by Student's t-test.

To assess whether localization of plasmalogens in the inner leaflet of plasma membranes is mediated by any of these four P4-ATPases, we verified protein level of Far1 in HeLa cells that had been treated for knocking down of P4-ATPases. The transfection of siRNAs against four P4-ATPases successfully reduced the expression of the target genes as assessed at mRNA level (**Supplementary Figure S1**). The elevation of Far1 protein levels was detected upon transfection of siRNA against *ATP8B2* but not other *P4-ATPases* (**Figure 1**). These results suggest that the plasmalogen-sensing mechanism regulating the levels of Far1 is affected by the downregulation of ATP8B2.

We next studied distribution of plasmalogens at the outer leaflet in *ATP8B2*-knocked down HeLa cells with a membrane impermeable amine-reactive reagent TNBS, by which phosphatidylethanolamine (PE) and plasmalogens localizing at the outer leaflet of plasma membranes are converted to TNBS-PE and TNBS-plasmalogens distinguishable from PE and plasmalogens (Kobayashi and Pagano, 1989; Honsho et al., 2017). By acid hydrolysis of vinyl-ether bond of plasmalogens, TNBS-plasmalogens and plasmalogens are converted to TNBS-2-acyl-glycerophosphoethanolamine (GPE) and 2-acyl-GPE, respectively, thereby allowing separation of PE, plasmalogens, and two TNBS-modified ethanolamine glycerophospholipids by thin layer chromatography (Honsho et al., 2017). As anticipated, the amount of TNBS-plasmalogens but not TNBS-PE was indeed elevated in *ATP8B2*-knocked down HeLa cells, whereas distribution of plasmalogens and PE was not altered in *ATP11B*-knocked down cells (**Figure 2**). Taken together, these results suggested that ATP8B2 flips plasmalogens from the exoplasmic to the cytosolic leaflet at the plasma membranes and a less mount of plasmalogens in the inner leaflet of plasma membrane induces the elevation of Far1 protein due to the impairment of sensing plasmalogens.

Plasmalogens Are Required for the Phosphorylation of AKT

The physiological roles of plasmalogens localized in the inner leaflet of plasma membranes remain largely unknown. The fact that recruitment of AKT to the plasma membranes, a critical step in its phosphorylation by phosphoinositide-dependent protein kinase one and mammalian TOR complex 2 (Vivanco and Sawyers, 2002; Bozulic and Hemmings, 2009; Gao et al., 2011) is impaired in the absence of plasmalogens in mouse embryonic fibroblasts, Schwan cells, and neurons derived from *Gnpat*$^{-/-}$ mice (da Silva et al., 2014; da Silva et al., 2021), suggests the link of asymmetric distribution of plasmalogens and cellular metabolism.

To assess whether plasmalogens are required for the phosphorylation of AKT in other types of cells, we verified phosphorylation state of AKT by lowering the level of plasmalogens in HeLa cells. Upon knocking down *AGPS* with two different double-strand RNAs, AGPS protein was lowered to about 60–70% of that in mock-treated cells (**Figures 3A,B**) and plasmalogen level was reduced by nearly 30% (**Figure 3B**). Under these conditions, phosphorylation of AKT at both threonine 308 (T308) in the kinase domain and at serine 473 (S473) in the C-terminal regulatory domain was suppressed (**Figures 3C,D**). These results are consistent with the previous study showing the impaired AKT-activation in plasmalogen-deficient cells and mouse (da Silva et al., 2014; da Silva et al., 2021) and further reveal the importance of plasmalogen homeostasis in the AKT activation.

Phosphorylation of AKT is Suppressed by a Reduced Expression of ATP8B2

We next investigated whether plasmalogens in the cytoplasmic leaflet of plasma membranes are required for the activation of AKT. To this end, we verified the effect of the knocking down of *ATP8B2* on the phosphorylation level of AKT. Phosphorylation of AKT at both threonine 308 and serine 473 was reduced upon transfection of siRNA#9 against *ATP8B2* (**Figure 4**), presumably giving rise to an impaired asymmetric distribution of plasmalogens (**Figure 2**). Likewise, phosphorylation of AKT was significantly less efficient in HeLa cells transfected with other *ATP8B2* siRNA#13 (**Supplementary Figure S2**), implying an impaired phosphorylation of AKT caused by mislocalization of plasmalogen from the inner leaflet of plasma membrane. Collectively, these results strongly suggest that ATP8B2-mediated localization of plasmalogens in the inner leaflet of plasma membrane linked to phosphorylation of AKT.

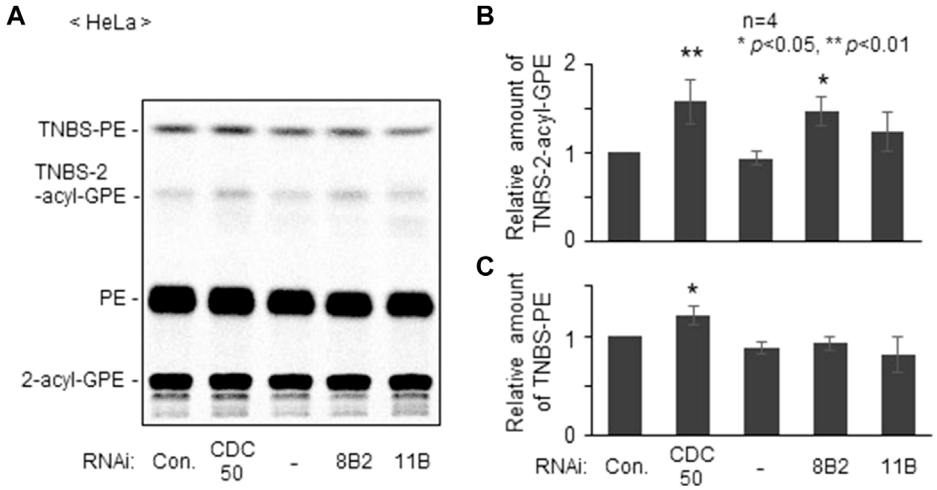

FIGURE 2 | Knockdown of *ATP8B2* elevates plasmalogens localization in outer leaflet of plasma membranes. **(A)** HeLa cells were transfected for 54 h with control dsRNA (Con.) and dsRNA against *CDC50A* (CDC50), *ATP8B2* (8B2), or *ATP11B* (11B), and further cultured in the presence of ^{14}C-ethanolamine for 18 h. Cells were incubated with TNBS, a membrane impermeable amine-reactive reagent. Total cellular lipids were extracted from equal aliquots of respective cell proteins after treatment of trichloroacetic acid to cleave vinyl-ether bond of plasmalogens and analyzed by TLC. Note that plasmalogens and TNBS-modified plasmalogens are converted to 2-acyl-GPE and TNBS-2-acyl-GPE, respectively, upon trichloroacetic acid treatment. **(B,C)** Relative amounts of TNBS-modified plasmalogens **(B)** and TNBS-modified PE **(C)** were represented by taking as one those in HeLa cells transfected with control dsRNA (Con.) ($n = 4$). Data indicate means ± SD. $^{*}p < 0.05$, $^{**}p < 0.01$, by one-way ANOVA with Dunnett's post hoc test as compared with control dsRNA-transfected HeLa cells (Con.).

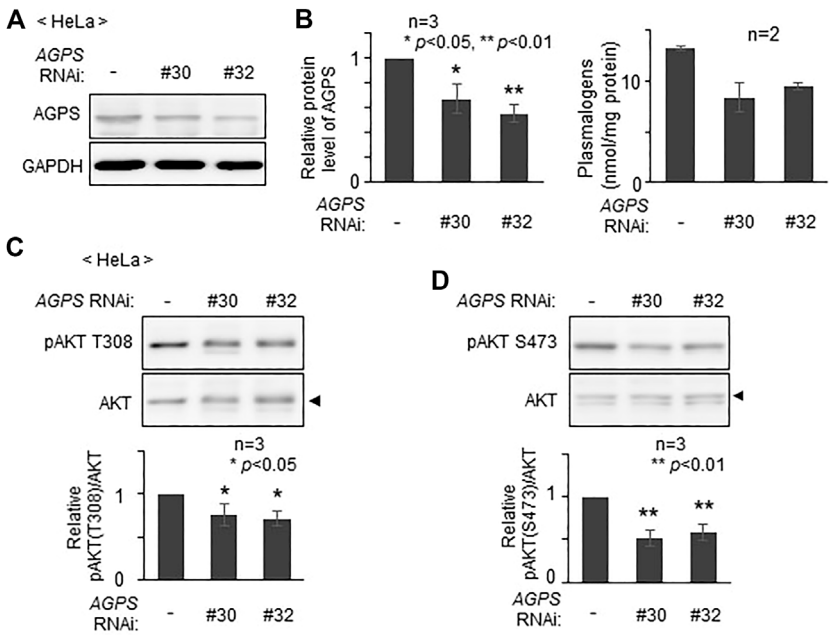

FIGURE 3 | Reduction of AKT activity by lowering plasmalogens. **(A)** HeLa cells were transfected with two different dsRNAs (#30 and #32) against *AGPS* and cultured for 72 h. Protein level of AGPS was analyzed by immunoblotting. GAPDH was used as a loading control. **(B)** Protein level of AGPS (*left*) and plasmalogen level (*right*) were represented by taking as one that in non-transfected HeLa cells. **(C,D)** Phosphorylation of AKT was analyzed by immunoblotting using antibodies specific for the phosphorylated T308 **(C)** and S473 **(D)** and total unmodified AKT (arrowhead). The amounts of pAKT T308 **(C)** and pAKT S473 **(D)** relative to total AKT were represented (*lower panels*). Data indicate means ± SD ($n = 3$). $^{*}p < 0.05$ and $^{*}p < 0.01$, by one-way ANOVA with Dunnett's post hoc test as compared with HeLa cells (-).

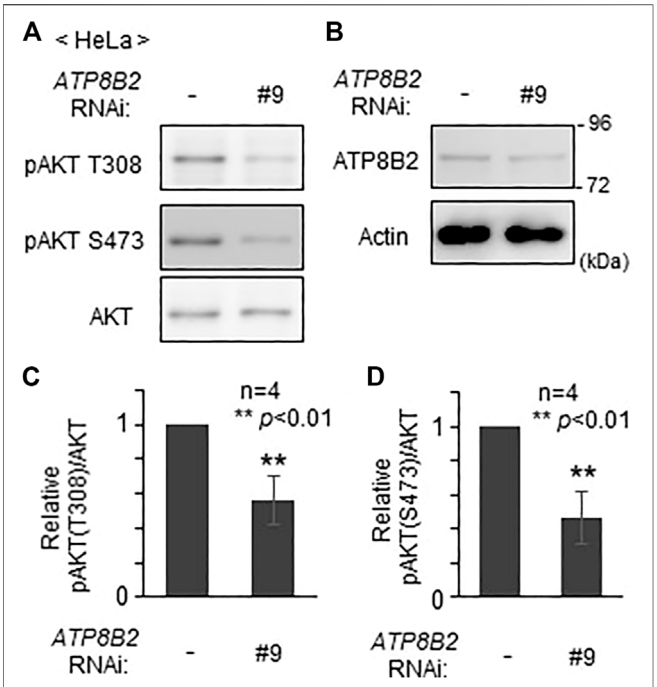

FIGURE 4 | Reduction of AKT activity by lowering ATP8B2 expression. **(A,B)** HeLa cells were transfected with siRNA (#9) against *ATP8B2* and cultured for 72 h. Phosphorylation of AKT **(A)** and expression of ATP8B2 **(B)** were verified by immunoblot using the indicated antibodies. Actin was a loading control. **(C,D)** The amounts of pAKT T308 **(C)** and pAKT S473 **(D)** relative to total AKT were represented ($n = 4$). Data indicate means ± SD. $^{**}p < 0.01$, by Student's *t*-test.

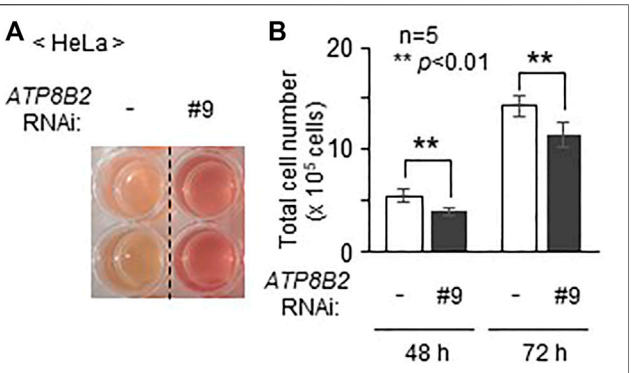

FIGURE 5 | Suppression of cell growth upon lowering the expression of *ATP8B2*. **(A)** Mock transfected HeLa cells (-) or HeLa cells transfected with siRNA against *ATP8B2* (#9) were cultured for 72 h. Acidification of the culture medium was monitored by visual-checking the color of the medium. **(B)** Total number of cells cultured as in **(A)** was counted at the indicated time after transfection with the respective siRNA ($n = 5$). Data indicate means ± SD. $^{**}p < 0.01$, by Student's *t*-test.

Knockdown of ATP8B2 Suppresses Cell Growth

Inhibition of AKT activity in several cancer cell lines induces cell death (Kostaras et al., 2020). In addition, suppression of AGPS activity in cancer cells such as MDA-MB-231 expressing a higher level of AGPS reduces cell proliferation, although the precise mechanism underlying the suppression of cell growth by the inhibition of AGPS activity remains unknown (Stazi et al., 2019). Moreover, we frequently observed less acidification of the culture medium in cells transfected with siRNA against *ATP8B2* expression as compared with control cells (**Figure 5A**), suggesting the reduced cell growth by lowering *ATP8B2* expression. Consistent with this result, total number of the *ATP8B2* siRNA-transfected cells was less than that in control siRNA-treated cells (**Figure 5B**). Taken together, these results suggest that the reduced expression of ATP8B2 lowers plasmalogens in the cytoplasmic leaflet of plasma membranes, thereby reducing the cell growth *via* suppressing AKT activation.

DISCUSSION

Asymmetric distribution of plasmalogens in the plasma membrane has been reported in red blood, myelin, and cultured cells (Kirschner and Ganser, 1982; Fellmann et al., 1993; Honsho et al., 2017). We earlier showed that asymmetric distribution of plasmalogens is important for the regulation of plasmalogen synthesis, where plasmalogens enriched in the inner leaflet of plasma membranes are sensed by yet unknown mechanism (Honsho et al., 2017). We here provide several lines of evidence that asymmetric distribution of plasmalogens is mediated by ATP8B2, a type-IV P4-ATPase (**Figure 2**). Furthermore, we demonstrated a role of plasmalogens enriched in the cytoplasmic leaflet of plasma membranes by showing the reduced activation of AKT in cells upon transfection of siRNA against *ATP8B2* (**Figure 4**; **Supplementary Figure S2**).

In the human protein atlas (https://www.proteinatlas.org/), ATP8B2 is described to be expressed in a wide range of tissues including brain, kidney, and lung where plasmalogens are enriched (Braverman and Moser, 2012). These data and the findings reporting an elevated protein level of Far1 in the kidney of plasmalogen-deficient *PEX7* knockout mouse (Wiese et al., 2012) and the cerebellum of plasmalogen-deficient *GNPAT* knockout mouse (Honsho et al., 2019) suggest that ATP8B2 is involved in the regulation of plasmalogen synthesis in these tissues.

ATP8B2 is reported to have flippase activity toward PC with a substrate, a fluorescent PC analogue, 1-oleoyl-2-{6-[(7-nitro-2-,3-benzoxadiazol-4-yl)amino]hexanoyl}-*sn*-glycero-3-phosphocholine (Takatsu et al., 2014), although its PC flippase activity is lower than that of ATP8B1 and ATP10A (Takatsu et al., 2014; Naito et al., 2015). Substrate specificity of ATP8B2 was assessed with several fluorescent phospholipids (Takatsu et al., 2014). However, no fluorescent-conjugated plasmalogen is commercially available, thus the topogenesis of plasmalogens has not been addressed despite being one of the major glycerophospholipids in mammalian cells. We here show that ATP8B2 functions as a flippase of plasmalogens by assessing the topology of chemically modified plasmalogens in the extracellular leaflet of plasma membranes (**Figure 2**). Clearly, developing a

plasmalogen analogue such as fluorescent-conjugated plasmalogen is required for further investigation of the mechanistic insight to ATP8B2-mediated topogenesis of plasmalogens and identification of other P4-ATPases acting as another plasmalogen flippase, if any.

Physiological importance of plasmalogens enriched in the cytoplasmic leaflet of plasma membranes is not fully understood. We earlier proposed that topogenesis of plasmalogens is important for sensing plasmalogens from the finding that knockdown of *CDC50A* elevates the protein level of Far1 by compromising asymmetric distribution of plasmalogens (Honsho et al., 2017). This notion is further supported in the present study by the finding that a reduced expression of ATP8B2 induces the elevation of plasmalogens localized at the extracellular leaflet of plasma membranes, thereby increasing the Far1 protein level (**Figures 1**, **2**).

Synthesis of plasmalogen can be augmented by expression of the mutant Far1 harboring a mutation in the regulatory region that is essential for the plasmalogen-induced degradation (Ferdinandusse et al., 2021) or by ectopic expression of wild-type Far1 but not GNPAT (Hajra et al., 2000; Honsho et al., 2010; Liu et al., 2005). Elevation of plasmalogens has been shown in several cancer cells (Albert and Anderson, 1977; Roos and Choppin, 1984; Snyder and Wood, 1969), which is likely associated with the pathogenicity of tumors because an inhibitor of AGPS lowers the plasmalogen levels and suppresses the pathogenicity of various types of cancer cells *in vitro* (Piano et al., 2015). According to the data from GEPIA 2 (http://gepia2.cancer-pku.cn/), expression of *TMEM189* encoding plasmanylethanolamine desaturase that introduces the vinyl ether double-bond into plasmanylethanolamine (Gallego-García et al., 2019; Werner et al., 2020) is upregulated in most of the human cancers, although higher expression of TMEM189 reduces the protein level of Far1 (Cui et al., 2021). In contrast to the upregulated expression of *TMEM189*, *ATP8B2* expression is reduced in most of those human cancers as searched in the GEPIA 2. Based on these facts, it is tempting to speculate that elevation of plasmalogens in human cancers is achieved by escaping from the plasmalogen-sensing step *via* reducing the plasmalogens in the cytoplasmic leaflet of plasma membrane. The higher level of plasmalogens augments the sensitivity of cancer cells to ferroptosis (Cui et al., 2021). Nevertheless, several different cancer cells get sensitized to evasion from ferroptosis by lowering plasmalogens where expression of *ATP8B2* mRNA is increased, though both protein and mRNA expressions of AGPS and TMEM189 are reduced (Zou et al., 2020). These results suggest that ATP8B2 is involved in the downregulation of plasmalogens by lowering the protein level of Far1 under pathophysiological condition together with the reduction in the expression of enzymes catalyzing plasmalogen biosynthesis.

AKT activation is reduced by lowering expression of ATP8B2 (**Figure 4**; **Supplementary Figure S2**), consistent with the earlier report indicating the impaired AKT activation in plasmalogen-deficient mouse embryonic fibroblasts, Schwann cells, and neurons (da Silva et al., 2014; da Silva et al., 2021). In our assay, PE was not exposed to the extracellular leaflet in *ATP8B2*-knocked down cells (**Figure 2**), which may be due to the compensatory function of other P4-ATPases such as ATP11A and ATP11C, both with a higher PE flipping activity than ATP8B2 (Segawa et al., 2016). In contrast, the exposure of PE in the extracellular leaflet was evident upon knocking down of *CDC50A* expression consistent with the earlier studies (Honsho et al., 2017; Kato et al., 2013) (**Figure 2**), which is likely due to the inactivation of several P4-ATPases simultaneously acting as PE flippase. Similarly, three P4-ATPases, ATP8B1, ATP10A, and ATP8B2, are a flippase towards PC in HeLa cells (Takatsu et al., 2011; Takatsu et al., 2014; Naito et al., 2015), of which the former two are suspected to compensate the PC flippase activity in cells reduced in the expression of ATP8B2. In a very recent study, PS is revealed as the most favored substrate for ATP8B1 (Cheng et al., 2022). Based on these facts together with a higher similarity of amino acid sequence between ATP8B2 and ATP8B1, ATP8B2 has a potential activity to transfer PS across membrane. The reduced activity of ATP8B2 toward PS might suppress AKT phosphorylation because PS is known to activate AKT (Huang et al., 2011). However, PS exposure in extracellular leaflet is unlikely in *ATP8B2*-knocked down cells, because plasma membrane-localized ATP11A and ATP11C, both have much higher PS-flipping activity as compared with ATP8B2 (Segawa et al., 2016), are expressed in HeLa cells as well as several human and mouse tissues (Takatsu et al., 2011). Taken together, these findings strongly suggest that the lower activation of AKT in *ATP8B2*-knocked down HeLa cells is most likely caused by the impaired asymmetric distribution of plasmalogens, hence strengthening the physiological consequence of asymmetrically distributed plasmalogens in cellular metabolism.

The possible link between ATP8B2 and Parkinson's disease (PD) progression has been addressed by a genome-wide association study on PD progression using more than three thousand patients with PD (Tan et al., 2021). Noteworthily, the abrogated AKT activation is detectable in postmortem tissue from the substantia nigra of PD patients (Malagelada et al., 2008; Timmons et al., 2009), whereas the expression of constitutive active form of AKT blocks apoptosis of dopamine neurons of substantia nigra in a neurotoxin mouse model of Parkinsonism upon injecting 6-hydroxydopamine, an endogenous metabolite of dopamine (Ries et al., 2006). Based on these studies, we hypothesize that impairment of asymmetric distribution of plasmalogens mediated by ATP8B2 in dopamine neuron is a potential cause of the PD pathogenesis. Nevertheless, further investigations to address plasmalogen homeostasis, including the activity and expression levels of proteins involved in the regulation of plasmalogen biosynthesis, are required to understand how abnormalities in plasmalogen homeostasis are responsible for the pathogenesis of PD.

DATA AVAILABILITY STATEMENT

The original contributions presented in the study are included in the article/**Supplementary Material**, further inquiries can be directed to the corresponding authors.

AUTHOR CONTRIBUTIONS

MH conceived, designed the study, and performed experiments. SM performed LC-ESI-MS/MS analysis. MH and YF interpreted the data, wrote, and edited the manuscript. All authors contributed to the article and approved the submitted version.

FUNDING

This work was supported in part by the JSPS Grants-in Aid for Scientific Research Grant Nos. JP17K07337 and JP21K06839 (to MH), JP26116007, JP17H03675 (to YF); grants (to YF) from the Takeda Science Foundation, the Naito Foundation, and the Novartis Foundation (Japan) for the Promotion of Science.

ACKNOWLEDGMENTS

We are especially grateful to Dr. Yuichi Abe (Kyushu Univ.) for his efforts in setting up the mass-spectrometric experimental system. We thank A. Tajima, S. Maeda, and Y. Nanri for technical assistance, Y. Toyohama and K. Tanaka for preparing figures. We appreciate the technical assistance from The Research Support Center, Research Center for Human Disease Modeling, Kyushu University Graduate School of Medical Sciences.

SUPPLEMENTARY MATERIAL

The Supplementary Material for this article can be found online at: https://www.frontiersin.org/articles/10.3389/fmolb.2022.915457/full#supplementary-material

REFERENCES

Abe, Y., Honsho, M., Nakanishi, H., Taguchi, R., and Fujiki, Y. (2014). Very-Long-Chain Polyunsaturated Fatty Acids Accumulate in Phosphatidylcholine of Fibroblasts from Patients with Zellweger Syndrome and Acyl-CoA Oxidase1 Deficiency. *Biochim. Biophys. Acta-Mol. Cell Biol. Lipids.* 1841, 610–619. doi:10.1016/j.bbalip.2014.01.001

Albert, D. H., and Anderson, C. E. (1977). Ether-Linked Glycerolipids in Human Brain Tumors. *Lipids* 12, 188–192. doi:10.1007/bf02533292

Andersen, J. P., Vestergaard, A. L., Mikkelsen, S. A., Mogensen, L. S., Chalat, M., and Molday, R. S. (2016). P4-ATPases as Phospholipid Flippases-Structure, Function, and Enigmas. *Front. Physiol.* 7, 275. doi:10.3389/fphys.2016.00275

Barøy, T., Koster, J., Strømme, P., Ebberink, M. S., Misceo, D., Ferdinandusse, S., et al. (2015). A Novel Type of Rhizomelic Chondrodysplasia Punctata, RCDP5, is Caused by Loss of the PEX5 Long Isoform. *Hum. Mol. Genet.* 24, 5845–5854. doi:10.1093/hmg/ddv305

Bligh, E. G., and Dyer, W. J. (1959). A Rapid Method of Total Lipid Extraction and Purification. *Can. J. Biochem. Physiol.* 37, 911–917. doi:10.1139/o59-099

Bozulic, L., and Hemmings, B. A. (2009). PIKKing on PKB: Regulation of PKB Activity by Phosphorylation. *Curr. Opin. Cell Bio.* 21, 256–261. doi:10.1016/j.ceb.2009.02.002

Braverman, N. E., and Moser, A. B. (2012). Functions of Plasmalogen Lipids in Health and Disease. *Biochim. Biophys. Acta.* 1822, 1442–1452. doi:10.1016/j.bbadis.2012.05.008

Braverman, N., Steel, G., Obie, C., Moser, A., Moser, H., Gould, S. J., et al. (1997). Human *PEX7* Encodes the Peroxisomal PTS2 Receptor and is Responsible for Rhizomelic Chondrodysplasia Punctata. *Nat. Genet.* 15, 369–376. doi:10.1038/ng0497-369

Brites, P., Ferreira, A. S., Ferreira da Silva, T., Sousa, V. F., Malheiro, A. R., Duran, M., et al. (2011). Alkyl-Glycerol Rescues Plasmalogen Levels and Pathology of Ether-Phospholipid Deficient Mice. *PLoS One* 6, e28539. doi:10.1371/journal.pone.0028539

Bryde, S., Hennrich, H., Verhulst, P. M., Devaux, P. F., Lenoir, G., and Holthuis, J. C. M. (2010). CDC50 Proteins are Critical Components of the Human Class-1 P_4-ATPase Transport Machinery. *J. Biol. Chem.* 285, 40562–40572. doi:10.1074/jbc.m110.139543

Buchert, R., Tawamie, H., Smith, C., Uebe, S., Innes, A. M., Al Hallak, B., et al. (2014). A Peroxisomal Disorder of Severe Intellectual Disability, Epilepsy, and Cataracts Due to Fatty Acyl-CoA Reductase 1 Deficiency. *Am. J. Hum. Genet.* 95, 602–610. doi:10.1016/j.ajhg.2014.10.003

Cheng, J. B., and Russell, D. W. (2004). Mammalian Wax Biosynthesis. I. Identification of Two Fatty Acyl-Coenzyme A Reductases with Different Substrate Specificities and Tissue Distributions. *J. Biol. Chem.* 279, 37789–37797. doi:10.1074/jbc.m406225200

Cheng, M. T., Chen, Y., Chen, Z. P., Liu, X., Zhang, Z., Chen, Y., et al. (2022). Structural Insights into the Activation of Autoinhibited Human Lipid Flippase ATP8B1 upon Substrate Binding. *Proc. Natl. Acad. Sci. USA* 119, e2118656119. doi:10.1073/pnas.2118656119

Cui, W., Liu, D., Gu, W., and Chu, B. (2021). Peroxisome-Driven Ether-Linked Phospholipids Biosynthesis is Essential for Ferroptosis. *Cell Death Differ.* 28, 2536–2551. doi:10.1038/s41418-021-00769-0

da Silva, T. F., Eira, J., Lopes, A. T., Malheiro, A. R., Sousa, V., Luoma, A., et al. (2014). Peripheral Nervous System Plasmalogens Regulate Schwann Cell Differentiation and Myelination. *J. Clin. Invest.* 124, 2560–2570. doi:10.1172/jci72063

da Silva, T. F., Granadeiro, L. S., Bessa-Neto, D., Luz, L. L., Safronov, B. V., and Brites, P. (2021). Plasmalogens Regulate the AKT-ULK1 Signaling Pathway to Control the Position of the Axon Initial Segment. *Prog. Neurobiol.* 205, 102123. doi:10.1016/j.pneurobio.2021.102123

Dorninger, F., König, T., Scholze, P., Berger, M. L., Zeitler, G., Wiesinger, C., et al. (2019). Disturbed Neurotransmitter Homeostasis in Ether Lipid Deficiency. *Hum. Mol. Genet.* 28, 2046–2061. doi:10.1093/hmg/ddz040

Fellmann, P., Hervé, P., and Devaux, P. F. (1993). Transmembrane Distribution and Translocation of Spin-Labeled Plasmalogens in Human Red Blood Cells. *Chem. Phys. Lipids.* 66, 225–230. doi:10.1016/0009-3084(93)90010-z

Ferdinandusse, S., McWalter, K., te Brinke, H., IJlst, L., Mooijer, P. M., Ruiter, J. P. N., et al. (2021). An Autosomal Dominant Neurological Disorder Caused by De Novo Variants in FAR1 Resulting in Uncontrolled Synthesis of Ether Lipids. *Genet. Med.* 23, 740–750. doi:10.1038/s41436-020-01027-3

Gallego-García, A., Monera-Girona, A. J., Pajares-Martínez, E., Bastida-Martínez, E., Pérez-Castaño, R., Iniesta, A. A., et al. (2019). A Bacterial Light Response Reveals an Orphan Desaturase for Human Plasmalogen Synthesis. *Science* 366, 128–132. doi:10.1126/science.aay1436

Gao, X., Lowry, P. R., Zhou, X., Depry, C., Wei, Z., Wong, G. W., et al. (2011). PI3K/Akt Signaling Requires Spatial Compartmentalization in Plasma Membrane Microdomains. *Proc. Natl. Acad. Sci. USA.* 108, 14509–14514. doi:10.1073/pnas.1019386108

Hajra, A. K., Larkins, L. K., Das, A. K., Hemati, N., Erickson, R. L., and MacDougald, O. A. (2000). Induction of the Peroxisomal Glycerolipid-Synthesizing Enzymes during Differentiation of 3T3-L1 Adipocytes. *J. Biol. Chem.* 275, 9441–9446. doi:10.1074/jbc.275.13.9441

Hayashi, H., Naoi, S., Togawa, T., Hirose, Y., Kondou, H., Hasegawa, Y., et al. (2018). Assessment of ATP8B1 Deficiency in Pediatric Patients with Cholestasis Using Peripheral Blood Monocyte-Derived Macrophages. *EBioMedicine* 27, 187–199. doi:10.1016/j.ebiom.2017.10.007

Honsho, M., Abe, Y., and Fujiki, Y. (2017). Plasmalogen Biosynthesis Is Spatiotemporally Regulated by Sensing Plasmalogens in the Inner Leaflet of Plasma Membranes. *Sci. Rep.* 7, 43936. doi:10.1038/srep43936

Honsho, M., Asaoku, S., and Fujiki, Y. (2010). Posttranslational Regulation of Fatty Acyl-CoA Reductase 1, Far1, Controls Ether Glycerophospholipid Synthesis. *J. Biol. Chem.* 285, 8537–8542. doi:10.1074/jbc.m109.083311

Honsho, M., Dorninger, F., Abe, Y., Setoyama, D., Ohgi, R., Uchiumi, T., et al. (2019). Impaired Plasmalogen Synthesis Dysregulates Liver X Receptor-Dependent Transcription in Cerebellum. *J. Biochem.* 166, 353–361. doi:10.1093/jb/mvz043

Honsho, M., and Fujiki, Y. (2017). Plasmalogen Homeostasis - Regulation of Plasmalogen Biosynthesis and its Physiological Consequence in Mammals. *FEBS Lett.* 591, 2720–2729. doi:10.1002/1873-3468.12743

Honsho, M., Yagita, Y., Kinoshita, N., and Fujiki, Y. (2008). Isolation and Characterization of Mutant Animal Cell Line Defective in Alkyl-Dihydroxyacetonephosphate Synthase: Localization and Transport of Plasmalogens to Post-Golgi Compartments. *Biochim. Biophys. Acta.* 1783, 1857–1865. doi:10.1016/j.bbamcr.2008.05.018

Huang, B. X., Akbar, M., Kevala, K., and Kim, H.-Y. (2011). Phosphatidylserine is a Critical Modulator for Akt Activation. *J. Cell Biol.* 192, 979–992. doi:10.1083/jcb.201005100

Kato, U., Inadome, H., Yamamoto, M., Emoto, K., Kobayashi, T., and Umeda, M. (2013). Role for Phospholipid Flippase Complex of ATP8A1 and CDC50A Proteins in Cell Migration. *J. Biol. Chem.* 288, 4922–4934. doi:10.1074/jbc.m112.402701

Kirschner, D. A., and Ganser, A. L. (1982). Myelin Labeled with Mercuric Chloride. Asymmetric Localization of Phosphatidylethanolamine Plasmalogen. *J. Mol. Biol.* 157, 635–658. doi:10.1016/0022-2836(82)90503-4

Kobayashi, T., and Pagano, R. E. (1989). Lipid Transport during Mitosis. Alternative Pathways for Delivery of Newly Synthesized Lipids to the Cell Surface. *J. Biol. Chem.* 264, 5966–5973. doi:10.1016/s0021-9258(18)83644-4

Kostaras, E., Kaserer, T., Lazaro, G., Heuss, S. F., Hussain, A., Casado, P., et al. (2020). A Systematic Molecular and Pharmacologic Evaluation of AKT Inhibitors Reveals New Insight into Their Biological Activity. *Br. J. Cancer.* 123, 542–555. doi:10.1038/s41416-020-0889-4

Liu, D., Nagan, N., Just, W. W., Rodemer, C., Thai, T.-P., and Zoeller, R. A. (2005). Role of Dihydroxyacetonephosphate Acyltransferase in the Biosynthesis of Plasmalogens and Nonether Glycerolipids. *J. Lipid Res.* 46, 727–735. doi:10.1194/jlr.m400364-jlr200

Malagelada, C., Jin, Z. H., and Greene, L. A. (2008). RTP801 Is Induced in Parkinson's Disease and Mediates Neuron Death by Inhibiting Akt Phosphorylation/Activation. *J. Neurosci.* 28, 14363–14371. doi:10.1523/jneurosci.3928-08.2008

Malheiro, A. R., Correia, B., Ferreira da Silva, T., Bessa-Neto, D., Van Veldhoven, P. P., and Brites, P. (2019). Leukodystrophy Caused by Plasmalogen Deficiency Rescued by Glyceryl 1-myristyl Ether Treatment. *Brain Pathol.* 29, 622–639. doi:10.1111/bpa.12710

Malheiro, A. R., da Silva, T. F., and Brites, P. (2015). Plasmalogens and Fatty Alcohols in Rhizomelic Chondrodysplasia Punctata and Sjögren-Larsson Syndrome. *J. Inherit. Metab. Dis.* 38, 111–121. doi:10.1007/s10545-014-9795-3

Motley, A. M., Hettema, E. H., Hogenhout, E. M., Brites, P., ten Asbroek, A. L. M. A., Wijburg, F. A., et al. (1997). Rhizomelic Chondrodysplasia Punctata is a Peroxisomal Protein Targeting Disease Caused by a Non-Functional PTS2 Receptor. *Nat. Genet.* 15, 377–380. doi:10.1038/ng0497-377

Nagan, N., and Zoeller, R. A. (2001). Plasmalogens: Biosynthesis and Functions. *Prog. Lipid Res.* 40, 199–229. doi:10.1016/s0163-7827(01)00003-0

Naito, T., Takatsu, H., Miyano, R., Takada, N., Nakayama, K., and Shin, H.-W. (2015). Phospholipid Flippase ATP10A Translocates Phosphatidylcholine and is Involved in Plasma Membrane Dynamics. *J. Biol. Chem.* 290, 15004–15017. doi:10.1074/jbc.m115.655191

Paulusma, C. C., and Elferink, R. P. (2010). P4 ATPases - The Physiological Relevance of Lipid Flipping Transporters. *FEBS Lett.* 584, 2708–2716. doi:10.1016/j.febslet.2010.04.071

Piano, V., Benjamin, D. I., Valente, S., Nenci, S., Marrocco, B., Mai, A., et al. (2015). Discovery of Inhibitors for the Ether Lipid-Generating Enzyme AGPS as Anti-Cancer Agents. *ACS Chem. Biol.* 10, 2589–2597. doi:10.1021/acschembio.5b00466

Purdue, P. E., Zhang, J. W., Skoneczny, M., and Lazarow, P. B. (1997). Rhizomelic Chondrodysplasia Punctata is Caused by Deficiency of Human *PEX7*, a Homologue of the Yeast PTS2 Receptor. *Nat. Genet.* 15, 381–384. doi:10.1038/ng0497-381

Ries, V., Henchcliffe, C., Kareva, T., Rzhetskaya, M., Bland, R., During, M. J., et al. (2006). Oncoprotein Akt/PKB Induces Trophic Effects in Murine Models of Parkinson's Disease. *Proc. Natl. Acad. Sci. USA* 103, 18757–18762. doi:10.1073/pnas.0606401103

Roos, D. S., and Choppin, P. W. (1984). Tumorigenicity of Cell Lines with Altered Lipid Composition. *Proc. Natl. Acad. Sci. USA.* 81, 7622–7626. doi:10.1073/pnas.81.23.7622

Segawa, K., Kurata, S., and Nagata, S. (2016). Human Type IV P-Type ATPases That Work as Plasma Membrane Phospholipid Flippases and Their Regulation by Caspase and Calcium. *J. Biol. Chem.* 291, 762–772. doi:10.1074/jbc.m115.690727

Shin, H.-W., and Takatsu, H. (2019). Substrates of P4-ATPases: Beyond Aminophospholipids (Phosphatidylserine and Phosphatidylethanolamine). *FASEB J.* 33, 3087–3096. doi:10.1096/fj.201801873r

Snyder, F., and Wood, R. (1969). Alkyl and Alk-1-Enyl Ethers of Glycerol in Lipids from Normal and Neoplastic Human Tissues. *Cancer Res.* 29, 251–257.

Stazi, G., Battistelli, C., Piano, V., Mazzone, R., Marrocco, B., Marchese, S., et al. (2019). Development of Alkyl Glycerone Phosphate Synthase Inhibitors: Structure-Activity Relationship and Effects on Ether Lipids and Epithelial-Mesenchymal Transition in Cancer Cells. *Eur. J. Med. Chem.* 163, 722–735. doi:10.1016/j.ejmech.2018.11.050

Takada, N., Takatsu, H., Miyano, R., Nakayama, K., and Shin, H.-W. (2015). ATP11C Mutation Is Responsible for the Defect in Phosphatidylserine Uptake in UPS-1 Cells. *J. Lipid Res.* 56, 2151–2157. doi:10.1194/jlr.m062547

Takatsu, H., Baba, K., Shima, T., Umino, H., Kato, U., Umeda, M., et al. (2011). ATP9B, a P4-ATPase (A Putative Aminophospholipid Translocase), Localizes to the *Trans*-Golgi Network in a CDC50 Protein-independent Manner. *J. Biol. Chem.* 286, 38159–38167. doi:10.1074/jbc.m111.281006

Takatsu, H., Tanaka, G., Segawa, K., Suzuki, J., Nagata, S., Nakayama, K., et al. (2014). Phospholipid Flippase Activities and Substrate Specificities of Human Type IV P-type ATPases Localized to the Plasma Membrane. *J. Biol. Chem.* 289, 33543–33556. doi:10.1074/jbc.m114.593012

Tan, M. M. X., Lawton, M. A., Jabbari, E., Reynolds, R. H., Iwaki, H., Blauwendraat, C., et al. (2021). Genome-Wide Association Studies of Cognitive and Motor Progression in Parkinson's Disease. *Mov. Disord.* 36, 424–433. doi:10.1002/mds.28342

Timmons, S., Coakley, M. F., Moloney, A. M., and O' Neill, C. (2009). Akt Signal Transduction Dysfunction in Parkinson's Disease. *Neurosci. Lett.* 467, 30–35. doi:10.1016/j.neulet.2009.09.055

van der Velden, L. M., Wichers, C. G. K., van Breevoort, A. E. D., Coleman, J. A., Molday, R. S., Berger, R., et al. (2010). Heteromeric Interactions Required for Abundance and Subcellular Localization of Human CDC50 Proteins and Class 1 P_4-ATPases. *J. Biol. Chem.* 285, 40088–40096. doi:10.1074/jbc.m110.139006

Vivanco, I., and Sawyers, C. L. (2002). The Phosphatidylinositol 3-Kinase-AKT Pathway in Human Cancer. *Nat. Rev. Cancer.* 2, 489–501. doi:10.1038/nrc839

Wanders, R. J. A., Dekker, C., Hovarth, V. A. P., Schutgens, R. B. H., Tager, J. M., van Laer, P., et al. (1994). Human Alkyldihydroxyacetonephosphate Synthase Deficiency: A New Peroxisomal Disorder. *J. Inherit. Metab. Dis.* 17, 315–318. doi:10.1007/bf00711817

Wanders, R. J. A., Schumacher, H., Heikoop, J., Schutgens, R. B. H., and Tager, J. M. (1992). Human Dihydroxyacetonephosphate Acyltransferase Deficiency: A New Peroxisomal Disorder. *J. Inher. Metab. Dis.* 15, 389–391. doi:10.1007/bf02435984

Werner, E. R., Keller, M. A., Sailer, S., Lackner, K., Koch, J., Hermann, M., et al. (2020). The *TMEM189* Gene Encodes Plasmanylethanolamine Desaturase Which Introduces the Characteristic Vinyl Ether Double Bond into Plasmalogens. *Proc. Natl. Acad. Sci. USA* 117, 7792–7798. doi:10.1073/pnas.1917461117

Wiese, S., Gronemeyer, T., Brites, P., Ofman, R., Bunse, C., Renz, C., et al. (2012). Comparative Profiling of the Peroxisomal Proteome of Wildtype and *Pex7* Knockout Mice by Quantitative Mass Spectrometry. *Int. J. Mass Spectrom.* 312, 30–40. doi:10.1016/j.ijms.2011.09.005

Zou, Y., Henry, W. S., Ricq, E. L., Graham, E. T., Phadnis, V. V., Maretich, P., et al. (2020). Plasticity of Ether Lipids Promotes Ferroptosis Susceptibility and Evasion. *Nature* 585, 603–608. doi:10.1038/s41586-020-2732-8

Conflict of Interest: MH and SM are inventors of a patent application that covers the screening methods for anticancer agents.

The remaining authors declare that the research was conducted in the absence of any commercial or financial relationships that could be construed as a potential conflict of interest.

Publisher's Note: All claims expressed in this article are solely those of the authors and do not necessarily represent those of their affiliated organizations, or those of the publisher, the editors and the reviewers. Any product that may be evaluated in this article, or claim that may be made by its manufacturer, is not guaranteed or endorsed by the publisher.

frontiers | Frontiers in Cell and Developmental Biology

ORIGINAL RESEARCH
published: 06 July 2022
doi: 10.3389/fcell.2022.864842

Targeted Plasmalogen Supplementation: Effects on Blood Plasmalogens, Oxidative Stress Biomarkers, Cognition, and Mobility in Cognitively Impaired Persons

Dayan B. Goodenowe[1], Jonathan Haroon[2], Mitchel A. Kling[3,4,5], Margaret Zielinski[2], Kennedy Mahdavi[2], Barshen Habelhah[2], Leah Shtilkind[1] and Sheldon Jordan[2]*

[1]Prodrome Services USA LLC, Temecula, CA, United States, [2]The Regenesis Project, Santa Monica, CA, United States, [3]Pereleman School of Medicine, University of Pennsylvania, Philadelphia, PA, United States, [4]Crescenz VA Medical Center, Philadelphia, PA, United States, [5]New Jersey Institute for Successful Aging, Department of Geriatrics and Gerontology, Rowan School of Osteopathic Medicine, Stratford, NJ, United States

OPEN ACCESS

Edited by:
Fabian Dorninger,
Medical University of Vienna, Austria

Reviewed by:
Md.Shamim Hossain,
Institute of Rheological Functions of Food, Japan
Sonja Forss-Petter,
Medical University of Vienna, Austria

***Correspondence:**
Dayan B. Goodenowe
d.goodenowe@prodromesciences.com

Specialty section:
This article was submitted to Cellular Biochemistry, a section of the journal Frontiers in Cell and Developmental Biology

Received: 28 January 2022
Accepted: 18 May 2022
Published: 06 July 2022

Citation:
Goodenowe DB, Haroon J, Kling MA, Zielinski M, Mahdavi K, Habelhah B, Shtilkind L and Jordan S (2022) Targeted Plasmalogen Supplementation: Effects on Blood Plasmalogens, Oxidative Stress Biomarkers, Cognition, and Mobility in Cognitively Impaired Persons. Front. Cell Dev. Biol. 10:864842. doi: 10.3389/fcell.2022.864842

Plasmalogens are a specific type of glycerophospholipid found in especially high levels in neuronal membranes. Decreased blood and brain levels of docosahexaenoic acid (DHA) containing plasmalogens are associated with decreased cognition and neuromuscular function in humans. Administration of 1-O-alkyl-2-acylglycerol (AAG) plasmalogen precursors containing DHA at the sn-2 position dose-dependently increase blood DHA plasmalogens and are neuroprotective in animal models of neurodegeneration at doses between 10 and 50 mg/kg. We conducted an investigational clinical trial in 22 cognitively impaired persons to evaluate the effects of an escalating oral dosing regimen of DHA-AAG from 900 to 3,600 mg/day over a 4-month period on blood serum plasmalogen and non-plasmalogen phospholipids and oxidative stress biomarkers. Safety, tolerability and therapeutic effects on cognition and mobility were also evaluated. DHA plasmalogen levels increased with increasing dose and remained significantly elevated at all treatment doses and durations. DHA plasmalogen levels were positively associated with catalase activity and negatively associated with malondialdehyde (MDA) levels. DHA-AAG supplementation normalized catalase activity in persons with low baseline catalase activity, normalized MDA levels in persons with high baseline MDA levels, and normalized superoxide dismutase activity in persons with high baseline SOD activity. Cognition improved in nine participants, was unchanged in nine, and declined in four. Mobility improved in twelve, was unchanged in five and declined in four participants. Changes in cognition and mobility were statistically significant versus a random outcome. Baseline DHA-plasmalogen levels were not predictive of clinical response. DHA-AAG was well tolerated at all dosages and no adverse reactions were observed.

Keywords: plasmalogen, sarcopenia, dementia, oxidative stress, catalase, malondiadehyde, superoxide dismutase, alkylglycerol (AKG)

INTRODUCTION

A 2021 survey of 1,221 adults in the US revealed that cognitive decline and the loss of mobility were the two most feared health outcomes (Author Anonymous, 2021). The prevalence of dementia in persons with sarcopenia is approximately three times higher than in persons without sarcopenia (Pacifico et al., 2020) and reduced muscle function is associated with increased risk of incident dementia and a faster rate of cognitive decline (Beeri et al., 2021). Reduced cognition and reduced mobility are comorbid. Reduced cognition and reduced mobility are also associated with plasmalogen deficiency. In humans, the association between low blood and brain plasmalogen levels and reduced cognition is robust and reproducible (Ginsberg et al., 1995; Ginsberg et al., 1998; Guan et al., 1999; Han et al., 2001; Han, 2005; Goodenowe et al., 2007; Wood et al., 2010; Wood et al., 2011a; Goodenowe and Senanayake, 2019; Senanayake and Goodenowe, 2019; Kling et al., 2020; Lim et al., 2020; Goodenowe, 2021). In animal models of plasmalogen deficiency, neuromuscular junction defects (Dorninger et al., 2017a; Dorninger et al., 2017b) have been reported and the selective knockout of oligodendrocyte peroxisomes cause white matter plasmalogen defects, morphology and symptomology similar to multiple sclerosis (Kassmann et al., 2007). These observations imply that impaired or insufficient plasmalogen related functions may represent a putative common link between dementia and sarcopenia.

A core component of human physiology is the compartmentalization of specific and distinct functions at both the intra- and intercellular level. The integrity and maintenance of function of these compartments are dependent upon efficient communication and transport of materials between compartments. This biochemical compartmentalization of function is dependent upon the physical and operational integrity of the biological membranes that separate cells from one another and divide intracellular space into various organelles and cytoplasm. These membranes are mostly comprised of glycerol phospholipids and cholesterol. The ability of cells and subcellular organelles to maintain optimal membrane functionality is dependent upon the cell's ability to regulate its membrane composition. Membrane composition regulation, in turn, is dependent upon a complex interdependent mix of genetics, environment, and nutrition.

The backbone of most phospholipids is glycerol—a simple three carbon molecule with a single free alcohol on each carbon. The three carbons are commonly referred to as sn-1, -2, or -3. Glycerol phospholipids contain a polar phosphate-linked head group at sn-3. Phospho-ethanolamine or phospho-choline are the most abundant and ubiquitous phospholipid head groups in the human body. The sn-1 position is comprised of either a fatty alcohol (plasmalogen) or fatty acid (phosphatidyl). The sn-1 bond type and the type of fatty acid at sn-2 are the key determiners of the effect of membrane phospholipid composition on membrane structure and cellular function (Mankidy et al., 2010; Wood et al., 2011a). When alkyl-acylglycerols (AAG) are converted to ethanolamine plasmalogens (PL) the PL species retains the sn-2 fatty acid of the AAG. *In vitro* studies have shown that increasing membrane levels of DHA-plasmalogens using DHA-AAG dose-dependently increases the non-amyloidogenic processing of amyloid precursor protein (APP) *via* an upregulation of the alpha-secretase pathway resulting in an equally dose dependent increase in secreted APP-alpha and a dose-dependent decrease in $A\beta_{1\text{-}42}$ (Wood et al., 2011a). In addition, increasing membrane DHA plasmalogen levels increases HDL-mediated cholesterol transport by dose-dependently increasing cholesterol esterification *via* acetyl-CoA acetyltransferase (ACAT) and dose-dependently decreases the level of free cholesterol in membranes (Mankidy et al., 2010). DHA-AAG plasmalogen precursor also blocks the increase in $A\beta_{1\text{-}42}$ caused by cholesterol loading (Wood et al., 2011a).

There has been an increasing interest in plasmalogens as a potential therapeutic agent for age-related cognitive decline and neurodegenerative conditions, given the growing understanding of their involvement in key cellular functions as well as the clinical trends observed when plasmalogen levels are depleted. In addition to supporting the structural integrity of membranes, plasmalogens are also involved in a variety of critically important cell functions: membrane fusion, ion transport, vesicle formation, cholesterol and amyloid regulation, and oxidation-reduction (Glaser and Gross, 1994; Glaser and Gross, 1995; Sindelar et al., 1999; Zoeller et al., 1999; Farooqui et al., 2000; Munn et al., 2003; Mankidy et al., 2010; Wood et al., 2011b; Wood et al., 2011c; Stables and Gilroy, 2011; Messias et al., 2018). In addition, recent research has shown that oral, DHA-enriched plasmalogen supplementation in mice increased hippocampal plasmalogen levels, improved learning and memory, and modulated various cell signaling pathways. In particular, research results suggested that the observed effect of oral plasmalogens on memory and learning were due, in part, to enhanced brain derived neurotrophic factor (BDNF) expression (Hossain et al., 2022). These observations are consistent with the detailed post-mortem examination of plasmalogen and phosphatidyl ethanolamine species, neuropathology and premortem cognition in human (Goodenowe and Senanayake, in press). Epidemiologically, it has been demonstrated that plasmalogen levels in the brain increase up to 30–40 years of age, and then significantly decrease by around 70 years of age (Rouser and Yamamoto, 1968; Goodenowe, 2021) and plasmalogen supplementation has been reported to improve cognition in humans (Fujino et al., 2017; Fujino et al., 2018).

Aging-related neurological and muscular degeneration lack accessible and effective therapeutic interventions. A possible treatment approach would involve a supplementation regimen of a plasmalogen precursor, such as the DHA-AAG plasmalogen precursor investigated in this study.

MATERIALS AND METHODS

Study Participants

Twenty-two persons diagnosed with cognitive impairment were enrolled. Eleven were male and eleven were female and their ages

ranged from 37 to 84 (average = 67). Cognitive impairment ranged from mild/questionable cognitive impairment (n = 14), to mild dementia (n = 4), to moderate dementia (n = 4) according to the Clinical Dementia Rating Scale (CDR). No biomarker analyses were performed prior to enrollment and no pre-selection occurred. 29 persons were screened, four were excluded due to non-compliance, and three dropped out due to non-trial related reasons. All participants signed informed consent forms and the trial registration number was NCT04484454.

Study Materials

The DHA-AAG (Prodrome Sciences United States LLC) used was a synthetic alkyl-acylglycerol comprised of C16 and C18 alkylglycerol backbone (chimyl and batyl alcohol) with DHA covalently bound to the sn-2 and sn-3 positions. The relative proportion of C16 and C18 plasmalogen backbone was 1:1 and the relative proportion of the fatty acids at sn-2 and sn-3 were >95% DHA, 2–5% docosapentaenoic acid (DPA) and <2% eicosapentaenoic acid (EPA). The DHA was purified from an algae source. The average density of the final product was 0.9 g/ml which corresponded to 900 mg of active product per ml. Product purity was >98%. A 1-month supply of DHA-AAG was provided to participants after each visit. Participants were instructed to take DHA-AAG each morning at the following dosages: 1.0 ml/day (Month 1, M1); 2.0 ml/day (Months 2 + 3, M2, M3); 4.0 ml/day (Month 4, M4); 0 mg/day (Month 5, M5).

Clinical Assessments

Cognition and mobility assessments were administered at baseline and the end of each month of the study. The primary outcome for cognitive status was change in Clinical Dementia Rating level (CDR) derived using the Quick Dementia Rating System (QDRS). The QDRS is a 10-item questionnaire completed by an informed third party to the participant (caregiver, spouse, etc.,). Scores range from 0 to 30 with higher scores representing greater cognitive impairment in a corresponding CDR level. The CDR rates cognitive function in six categories (memory, orientation, judgment and problem solving, and performance in community affairs, home and hobbies, and personal care). A CDR level of 0 indicates no dementia; CDR 0.5 represents MCI or very mild dementia; CDR 1, 2, or three corresponds to mild, moderate, or severe dementia respectively (Galvin, 2015).

The primary mobility outcome was the 30-s Sit/Stand test. Participants were given 30 s to fully stand and sit for as many repetitions as possible within the time window. The Sit/Stand test has been found to be both reliable and valid in assessing the functional mobility in older adults, and has also been shown to be sensitive to change (McAllister and Palombaro, 2020).

A clinically relevant change in cognition or mobility was defined as a change in CDR of one or more units or a change in two or more sit/stands, respectively. The monthly CDR and sit/stand performance of each participant were evaluated to determine the relative cognitive and mobility status of each participant at the end of months four and five relative to their baseline assessment. Each participant was rated as either exhibiting functional improvement, no change, or decline.

At the end of the study, each participant was asked to evaluate the treatment regimen using an 11-point Global Rating of Change scale from −5 to +5 in which the participant rates the overall change in their health. No change is rated as "0", improved health from minor "+1" to significant "+5", and reduced health from minor "−1" to significant "−5" (Kamper et al., 2009). The individual participant results are presented in **Table 4**.

Blood Serum Collection

Blood was drawn by trained nurses in an on-site surgical center. Venous blood was collected in a 10 ml redtop vacutainer tube and allowed to clot for 45–120 min. Serum was separated from the whole blood sample *via* centrifugation and stored at −80°C until processing.

Plasmalogen Extraction and Analysis

Serum samples were extracted using a modified version of the protocol described by Goodenowe et al. (Goodenowe et al., 2007). Briefly, 10 μL of serum was diluted with 50 μL of 0.1% formic acid and subjected to extraction three times with 1.0 ml of acidified ethyl acetate (98:2 ethyl acetate: 0.1% formic acid). Extracts were directly injected into a Thermo Fisher Scientific LTQ Orbitrap mass spectrometer (Thermo Fisher Scientific, MA, United States) in both positive and negative ionization electrospray modes at a flow rate of 200 μL/min. Full scan mass spectral data were collected for masses of 150–1,200 amu at maximum resolution. A common pooled reference serum sample was prepared before the study and aliquots of this pooled serum were extracted with each batch of study samples and run on the mass spectrometer at the beginning, middle, and end of each run batch to monitor and correct for batch-to-batch variance throughout the study. Phospholipid species of interest were identified based upon their (M-H)− or (M) or (M + H)+ accurate masses (mass accuracy <1 ppm). Only accurate mass species represented by single Gaussian peaks subjected to baseline resolution from any surrounding mass peaks were included in the analyses. The intensity of each species was determined by averaging 20 contiguous scans.

Serological Analyses

Catalase activity capacity (ThermoFisher Scientific), superoxide dismutase activity capacity (Cayman Chemical Company), and malondialdehyde levels (Northwest Life Science Specialties) were measured according to the manufacturer's specifications.

Statistical Analyses

Stata (version 14.2) was used for all statistical analyses.

RESULTS

Pharmacokinetic Evaluation of DHA-AAG on Serum Levels of Omega-3 and Omega-6 Containing Ethanolamine Phospholipids.

To evaluate the dose effects of DHA-AAG administration on serum ethanolamine phospholipid levels, four composite indices representative of the key serum omega-6 [linoleic acid (LA) and arachidonic acid (AA)] and omega-3 (DHA) phosphatidylethanolamine (PE) and ethanolamine plasmalogen

TABLE 1 | Ethanolamine phospholipid indices.

Index	Species	Molecular formula	[M-H]-
(LA + AA)-PE	PtdEtn 18:0/18:2	$C_{41}H_{78}NO_8P$	742.5392
PE Omega-6 Index	PtdEtn 16:0/20:4	$C_{41}H_{74}NO_8P$	738.5079
	PtdEtn 18:0/20:4	$C_{43}H_{78}NO_8P$	766.5392
DHA-PE	PtdEtn 16:0/22:6	$C_{43}H_{74}NO_8P$	762.5079
PE Omega-3 Index	PtdEtn 18:0/22:6	$C_{45}H_{78}NO_8P$	790.5392
(LA + AA)-PL	PlsEtn 18:0/18:2	$C_{41}H_{78}NO_7P$	726.5443
PL Omega-6 Index	PlsEtn 16:0/20:4	$C_{41}H_{74}NO_7P$	722.5130
	PlsEtn 18:0/20:4	$C_{43}H_{78}NO_7P$	750.5443
DHA-PL	PlsEtn 16:0/22:6	$C_{43}H_{74}NO_7P$	746.5130
PL Omega-3 Index	PlsEtn 18:0/22:6	$C_{45}H_{78}NO_7P$	774.5443

(PL) species were created (**Table 1**). From these four composite indices, three omega-3/6 ratio indices were created: DHA-PE/(LA + AA)-PE, DHA-PL/(LA + AA)-PL and DHA-PL/(LA + AA)-PE. These seven indices were then used to evaluate the absolute and relative effects of an escalating DHA-AAG dose on serum ethanolamine phospholipid levels (**Figures 1A,B**, **Supplementaray Table S1**). The serum level of each index for each participant at all time points was normalized to the respective baseline group mean of that index.

Since DHA-AAG is comprised of a plasmalogen backbone with DHA covalently bound at sn-2 it is a direct precursor to DHA-PL; an indirect precursor to DHA-PE and (LA + AA)-PL; and is biochemically unrelated to (LA + AA)-PE. **Figure 1A** illustrates that the plasmalogen precursor DHA-AAG dose-dependently elevated both direct and indirect target species [DHA-PL, DHA-PE, and (LA + AA)-PL] and had no effect on the levels of the biochemically unrelated PE species index (LA + AA)-PE. DHA-AAG had a greater elevating effect on its direct target, DHA-PL than its indirect targets. The 1-month washout

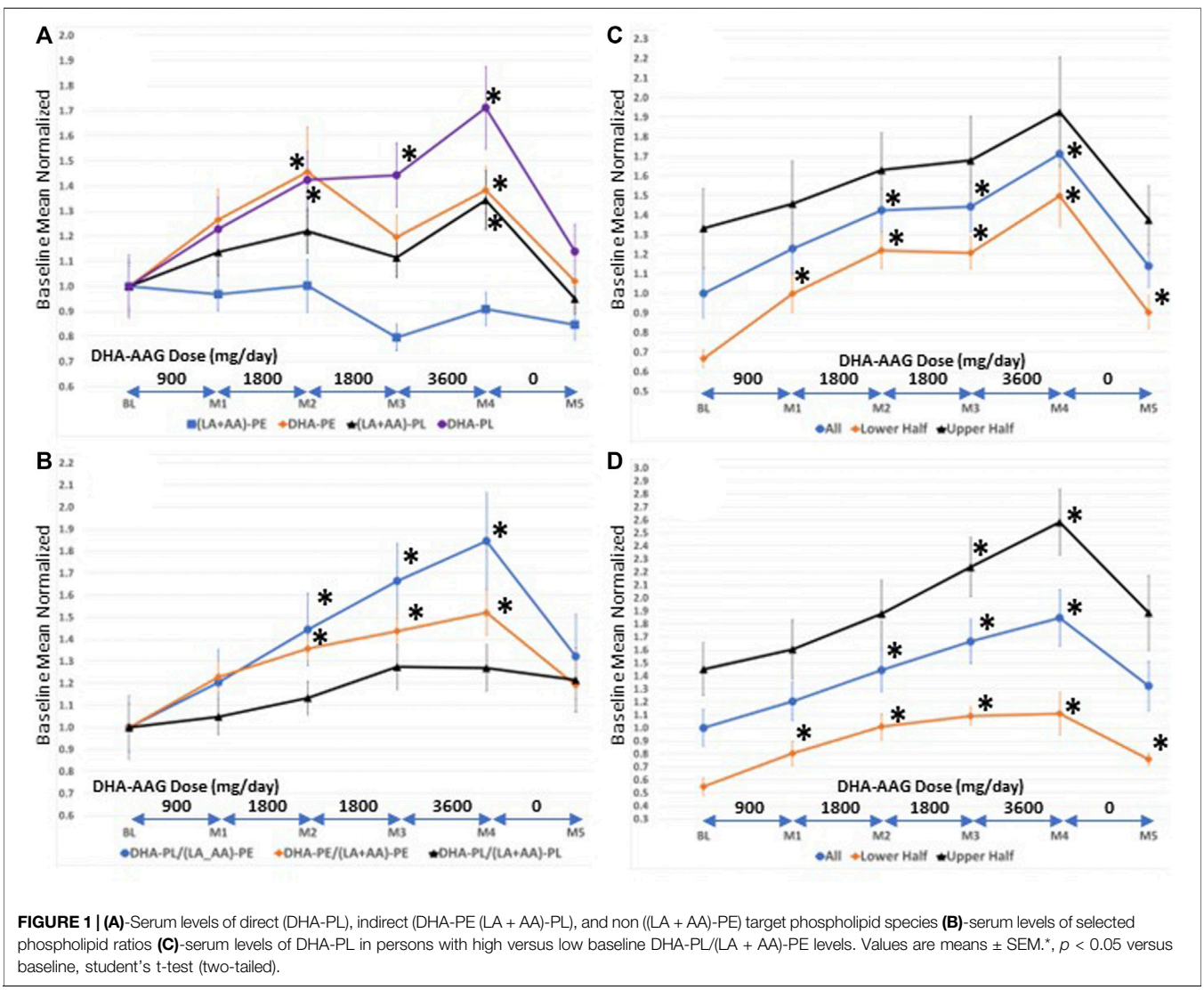

FIGURE 1 | (A)-Serum levels of direct (DHA-PL), indirect (DHA-PE (LA + AA)-PL), and non ((LA + AA)-PE) target phospholipid species **(B)**-serum levels of selected phospholipid ratios **(C)**-serum levels of DHA-PL in persons with high versus low baseline DHA-PL/(LA + AA)-PE levels. Values are means ± SEM.*, $p < 0.05$ versus baseline, student's t-test (two-tailed).

period resulted in decreased levels of both the direct and indirect target species and no effect on the unrelated PE species.

To more precisely evaluate the effects of DHA-AAG on the levels of the direct, indirect, and unrelated ethanolamine phospholipid species, internal ratios of the omega-3 and omega-6 indices were evaluated in each subject over the course of the study as illustrated in **Figure 1B**. The relative ratio of the direct target DHA-PL to the unrelated (LA + AA)-PE was observed to exhibit the greatest elevation with dose and time. The relative ratio of the indirect DHA-PE to the unrelated (LA + AA)-PE exhibited the second greatest dose and time elevation and the relative ratio of the direct DHA-PL to the indirect (LA + AA)-PL exhibited the smallest dose and time effect. **Figures 1A,B** illustrate that DHA-AAG is converted to its direct and indirect target species in humans as predicted from animal studies on similar AAG plasmalogen precursors (Wood et al., 2011d).

Participants were not evaluated for DHA-PL levels prior to enrollment. To evaluate the effect of baseline DHA-PL levels on DHA-AAG pharmacokinetics, the participants were divided into either lower or upper halves based upon their baseline DHA-PL (**Figure 1C**) or their DHA-PL/(LA + AA)-PE (**Figure 1D**) levels. As illustrated in **Figures 1C,D**, DHA-AAG elevated target species levels regardless of baseline DHA plasmalogen levels. However, participants with low baseline DHA-PL or DHA-PL/(LA + AA)-PE ratios experienced a greater relative improvement due to their low baseline levels and this relative improvement persisted even after the 1-month washout. Each participant's baseline mean-normalized DHA-PL/(LA + AA)-PE ratio at baseline, end of month 4, and the maximum ratio observed is presented in **Table 4**.

Higher age was associated with lower levels of DHA-PL (LA + AA)-PL, higher levels of (LA + AA)-PE and lower levels of DHA-PL/(LA + AA)-PE and DHA-PE/(LA + AA)-PE (**Supplementary Table S1**). These data are consistent with previously published results in a large random population cohort (Wood et al., 2011a). Male sex was associated with lower levels of DHA-PE and (LA + AA)-PE (**Supplementary Table S1**). Lower levels of DHA-PE in males is consistent with previously published results in a large elderly cohort (Goodenowe and Senanayake, 2019).

Pharmacodynamic Evaluation of DHA-AAG on Serum Malondialdehyde, Catalase, and Superoxide Dismutase

The vinyl ether bond of the target ethanolamine plasmalogen species chemically reacts with reactive oxygen species to neutralize and prevent peroxidation of polyunsaturated fatty acids (Sindelar et al., 1999; Stadelmann-Ingrand et al., 2001). To determine if the DHA-PL elevating effect of DHA-AAG had a pharmacodynamic effect, levels of malondialdehyde (MDA), catalase (CAT), and superoxide dismutase (SOD) were measured at baseline, and at end of months 3, 4, and 5. MDA is a final end-product of lipid peroxidation of LA and AA. Penultimate to lipid peroxidation of all polyunsaturated fatty acids such as LA and AA is the insufficient neutralization of hydrogen peroxide. Excess hydrogen peroxide in the presence of superoxide anion can undergo conversion to the hydroxyl radical, which can then react with polyunsaturated fatty acids *via* a series of free radical reactions to form lipid peroxides. The superoxide anion is neutralized by SOD into molecular oxygen and hydrogen peroxide. Accordingly, SOD is the main producer of hydrogen peroxide. Catalase is a ubiquitous enzyme that neutralizes the hydrogen peroxide produced by SOD into water and molecular oxygen. Both SOD and CAT are potent inhibitors of lipid peroxidation (Gutteridge, 1984). SOD is a self-inducing enzyme in that the product of its activity (hydrogen peroxide) induces SOD synthesis (Yoo et al., 1999). In contrast, catalase is inactivated by hydrogen peroxide (Kokkaliari et al., 1992), and in an animal model of sarcopenia, increased superoxide anion is associated with increased SOD, increased hydrogen peroxide and decreased catalase (Sullivan-Gunn and Lewandowski, 2013).

Linear regression analysis of the seven phospholipid indices, MDA, CAT, and SOD is presented in **Table 2**. MDA is derived from the lipid peroxidation of LA or AA, so MDA levels are presumed to be influenced by both total LA + AA levels and overall peroxidation load. Interestingly (LA + AA)-PE, but not (LA + AA)-PL was positively associated with MDA levels. This observation indicates that the PL vinyl ether bond is likely protecting the PL bound AA from peroxidation *in vivo* as predicted by previous *in vitro* studies (Sindelar et al., 1999) thereby disassociating (LA + AA)-PL from MDA formation. Although both DHA-PL and DHA-PE levels were elevated by DHA-AAG treatment, only DHA-PL was observed to be negatively associated with MDA levels indicating that it is the PL vinyl ether bond, not DHA that is responsible for the negative association with MDA levels. All three omega-3/6 ratio indices were negatively associated with MDA levels. Catalase activity was negatively associated with MDA levels and DHA-PL was both positively associated with catalase activity and negatively associated with MDA.

Since it is unclear from the binary associations in **Table 2** as to the dominance, independence, or relative contributions of the serological biomarkers to MDA and CAT levels, multivariate linear regression analysis was performed using multiple models (**Table 3**). This analysis showed that (LA + AA)-PE was the dominant predictor MDA levels. CAT had a strong negative association with MDA levels (Model 5), but this association was lost when PL species were included (Model 7). The increase in R-squared value when CAT was added to the PL model (Model 7 vs. 2) was minimal indicating that the effect of CAT on MDA levels was being caused by the effect of the PL species on CAT. This is clearly observed by comparing Model 9 vs. 14 wherein the PL species exhibited the strongest association with CAT (Model 9) which was minimally affected by the addition of MDA (Model 14). Collectively, these data indicate that the elevation of DHA-PL by DHA-AAG was independently associated with an increase in (LA + AA)-PL, CAT, and a decrease in MDA (Model 15).

To investigate potential ceiling or floor effects on MDA, CAT, and SOD, participants were grouped based upon their

TABLE 2 | Relationship between key serological indices.

Variable	MDA (coef, *p*)		CAT (coef, *p*)		SOD (*p*)	PE (LA + AA) (Coef, *p*)		PE (DHA) (Coef, *p*)	
(LA + AA)-PE	0.718	1.5e-07	-	NS	NS	-	-	-	-
DHA-PE	-	NS	-	NS	NS	0.503	1.1E-14	-	-
DHA/(LA + AA)-PE	–0.427	5.7e-04	0.596	4.3e-03	NS	-	-	-	-
(LA + AA)-PL	-	NS	-	NS	NS	0.254	2.4E-03	0.260	1.1e-02
DHA-PL	–0.233	3.3e-02	0.549	2.2e-03	NS		NS	0.431	1.7e-07
DHA/(LA + AA)-PL	–0.372	8.9e-04	0.736	6.1e-05	NS	–0.298	7.3E-05	0.291	1.6e-03
PL Omega-3/PE Omega-6	–0.349	6.4e-06	0.397	2.9e-03	NS	-	-	-	NS
MDA	-	-	–0.474	7.9e-03	NS	-	-	-	-
CAT	-	-	-	-	NS	-	-	-	-

All variables were mean normalized and log10 transformed prior to linear regression analysis. Abbreviations: MDA = Malondialdehyde, CAT = Catalase, SOD = Superoxide Dismutase. For description of PE and PL species and indices see ***Table 1****.*

TABLE 3 | Multivariate analyses of selected serological markers associated with catalase and malondialdehyde.

Model	Outcome	Variables	Coef	*p*	R-squared
1	MDA	DHA-PE (LA + AA)-PE	–0.225 0.846	5.4e-02 3.8e-08	0.313
2	MDA	DHA-PL (LA + AA)-PL	–0.368 0.380	2.1e-03 1.1e-02	0.124
3	MDA	DHA-PL (LA + AA)-PE	–0.146 0.685	1.3e-01 5.6e-07	0.301
4 5	MDA MDA	DHA-PL CAT	–0.233 –0.474	3.3e-02 7.9e-03	0.053 0.081
6	MDA	DHA-PL CAT	–0.156 –0.141	1.6e-01 3.6e-02	0.102
7	MDA	DHA-PL (LA + AA)-PL CAT	–0.290 0.316 –0.101	2.5e-02 4.1e-02 1.4e-01	0.147
8	CAT	DHA-PE (LA + AA)-PE	0.577 –0.634	1.0e-02 2.0e-02	0.094
9	CAT	DHA-PL (LA + AA)-PL	0.776 –0.639	8.3e-05 8.4e-03	0.179
10	CAT	DHA-PL (LA + AA)-PE	0.525 –0.187	3.9e-03 4.3e-01	0.113
11	CAT	DHA-PL	0.549	2.2e-03	0.106
12	CAT	MDA	–0.474	7.9e-03	0.081
13	CAT	DHA-PL MDA	0.463 –0.368	9.7e-03 3.6e-02	0.153
14	CAT	DHA-PL (LA + AA)-PL MDA	0.680 –0.540 –0.262	8.9e-04 3.0e-02 1.4e-01	0.200
15	DHA-PL	(LA + AA)-PL CAT MDA	0.639 0.186 –0.207	1.5e-07 8.9e-04 2.5e-02	0.378
16	DHA-PL	DHA-PE (LA + AA)-PE	0.807 –0.716	1.2e-15 7.0e-10	0.403

All variables were mean normalized and log10 transformed prior to linear regression analysis. Abbreviations: MDA = Malondialdehyde, CAT = Catalase, SOD = Superoxide Dismutase. For description of PE and PL species and indices see ***Table 1****.*

baseline levels and the effect of DHA-AAG treatment evaluated in the lower and upper halves of each (**Figure 2**). This analysis revealed that DHA-AAG treatment normalized MDA in persons with high baseline MDA levels, SOD activity in persons with high baseline SOD activity, and CAT activity in persons with low baseline CAT activity.

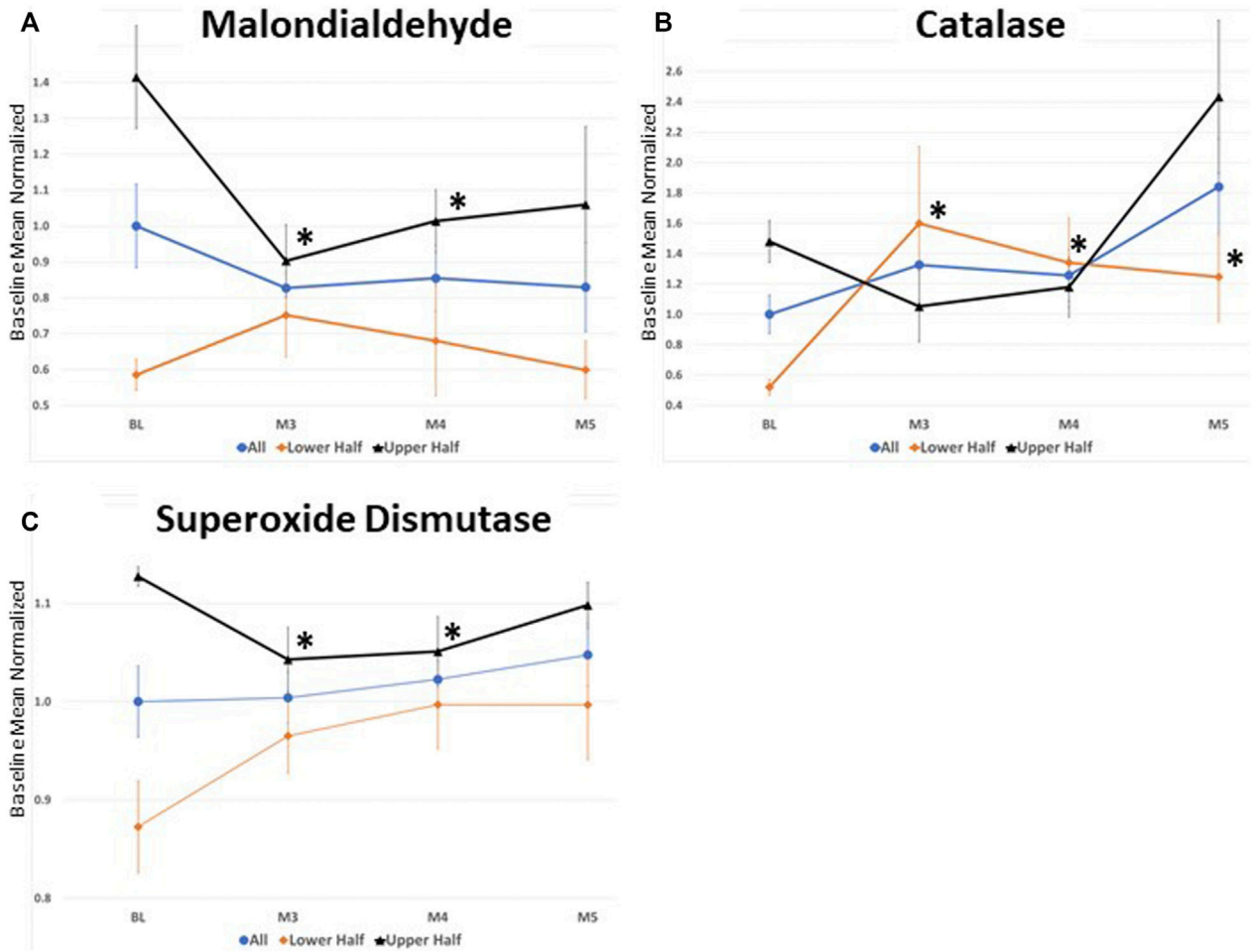

FIGURE 2 | (A) serum Malondialdehyde levels **(B)** Catalase capacity, and **(C)** superoxide Dismutase capacity. All values where normalized to the total baseline average. values represent the mean ± SEM. *,$p < 0.05$ versus baseline of that cohort subset, student's t-test (two-tailed).

Clinical Evaluation of DHA-AAG on Cognition and Mobility

Of the 22 participants who completed the study, cognition improved in 9 (41%), declined in 4 (18%) and remained stable in 9 (41%) during the 4-months treatment period (**Table 4**). No relationship between baseline DHA-PL levels and response or lack of response was observed (5 in lower half and four in upper half). However, a higher proportion of persons with more severe baseline cognitive impairment improved than persons with mild cognitive impairment (3/4 subjects with baseline CDR of 2; 2/4 subjects with baseline CDR of 1, and 4/14 subjects with baseline CDR = 0.5). Mobility improved in 12 participants (55%), remained stable in 5 (23%) and declined in 4 (18%). Using a random non-response based upon the observed decline rate as the predictor, the observed response rates were significant for both cognition and mobility (**Table 5**). At the end of the trial each participant was asked to self-evaluate the overall effect of the DHA-AAG treatment using the Global Rating of Change scale (Kamper et al., 2009). Of the eighteen participants who completed the GRC, twelve reported that their health improved over the 4-month trial and six reported no change. No participant reported a negative change. The individual participant responses are included in **Table 4**.

DISCUSSION

This open-label investigational study evaluated the clinical and serological effects of an escalating dose of DHA-AAG (900 mg/day—3,600 mg/day) in cognitively impaired persons. Each dose was administered for at least 1 month and a 1-month washout at the end of the trial was used. Pharmacokinetic, pharmacodynamic, and clinical outcomes were monitored.

The key pharmacological observation was that the plasmalogen precursor DHA-AAG exhibited a dose-dependent and species-selective elevating effect on serum ethanolamine phospholipids. Specifically, DHA-containing PL species were preferentially elevated. Non-DHA containing PL species and DHA-containing PE species were also elevated, but to a lesser extent. Non-DHA PE species were unaffected by the DHA-AAG

TABLE 4 | Individual participant demographics and clinical responses.

Id	Age	Sex	CDR		S/S		CDR	S/S	DHA-PL/(LA + AA)-PE			GRC
			(BL)	(M4)	(BL)	(M4)	(+/-)	(+/-)	(BL)	(M4)	Max (month)	GRC
Group 1—Moderate Dementia (CDR = 2)												
16	78	F	2	3	16	14	-	-	0.29	0.48	0.90 (M3)	0
19	58	F	2	1	11	16	+	+	0.88	2.15	2.15 (M4)	0
1	81	M	2	1	11	15	+	+	0.90	1.65	1.65 (M4)	+5
29	63	F	2	0.5	30	34	+	+	1.26	2.56	2.69 (M5)	+2
Group 2—Mild Dementia (CDR = 1)												
12	75	M	1	1	15	21	0	+	2.72	3.03	3.03 (M4)	+2
18	80	M	1	1	21	16	0	-	0.69	0.90	1.35 (M2)	0
8	84	M	1	0.5	12	15	+	+	0.57	0.64	0.74 (M3)	NA
21	48	M	1	0.5	14	14	+	0	1.04	1.78	2.38 (M2)	+1
Group 3—Mild Cognitive Impairment (CDR = 0.5)												
11	69	F	0.5	2	NA	NA	-	NA	1.03	2.44	2.44 (M4)	+1
24	66	F	0.5	2	13	16	-	+	0.36	1.96	1.96 (M4)	NA
7	81	F	0.5	1	15	16	-	0	0.87	1.57	1.57 (M4)	0
3	74	F	0.5	0.5	13	17	0	+	0.41	1.33	1.33 (M4)	0
6	74	M	0.5	0.5	12	14	0	+	0.91	2.69	2.69 (M4)	+1
10	81	M	0.5	0.5	19	22	0	+	0.87	0.87	1.17 (M2)	+2
20	78	M	0.5	0.5	11	8	0	-	0.44	0.62	1.10 (M3)	0
22	63	F	0.5	0.5	13	12	0	0	2.27	3.88	4.04 (M3)	NA
23	64	F	0.5	0.5	10	12	0	+	0.40	1.79	1.79 (M4)	+4
28	67	F	0.5	0.5	12	14	0	+	2.38	3.94	3.94 (M4)	NA
2	37	M	0.5	0	13	14	+	0	0.79	1.54	1.54 (M4)	+1
14	59	M	0.5	0	14	12	+	-	1.24	2.92	2.92 (M4)	+1
15	64	M	0.5	0	21	22	+	0	1.33	1.36	2.73 (M5)	+1
17	77	F	0.5	0	11	14	+	+	0.34	0.51	1.16 (M3)	+4

BL-baseline, M4—Month 4, S/S—Sit/Stand, GRC, Global Rating of Change, NA-Not Available.

TABLE 5 | Categorical treatment response summary.

Clinical Observation	CDR (observed)	CDR (predicted)	Sit/Stand (observed)	Sit/Stand (predicted)
Improvement	9	4	12	4
No Change	9	14	5	13
Decline	4	4	4	4
Chi Squared *p*-value	1.8e-02		2.9e-05	

Predicted responses were based upon an assumed random non-response rate based upon the observed decline rate for each outcome.

administration. These observations are consistent with the previously proposed metabolic fate of AAG (Mankidy et al., 2010; Wood et al., 2011a; Wood et al., 2011d) and summarized in **Figure 3**. In brief, 1-O-alkyl, 2,3-diacylglycerols are metabolized by gut lipases to 1-O-alkyl, 2-acylglycerol which is absorbed into the blood stream and then converted to 1-O-alkyl-2-acylglycerophosphoethanolamine which is then desaturated to the final vinyl ether ethanolamine plasmalogen in endoplasmic reticulum of the cells of the body. Since no peroxisome-specific biochemical steps are required to convert AAG plasmalogen precursors into vinyl ether plasmalogens, AAG plasmalogen precursors bypass the obligate rate-limiting peroxisomal enzymes necessary for endogenous plasmalogen biosynthesis.

Several key pharmacodynamic observations and interpretations were made. First, serum MDA levels exhibited a strong positive correlation with serum levels of AA and LA containing PE species, but serum levels of AA and LA containing PL species were not correlated with MDA levels. It is hypothesized that, consistent with *in vitro* observations (Sindelar et al., 1999), the sn-1 vinyl ether bond of plasmalogens protects the sn-2 AA and LA from peroxidation and thus blocks the formation of MDA from AA and LA containing PL species. A higher level of serum DHA-PL was associated with a lower MDA level independent of LA and AA PE levels indicating a direct anti-peroxidation effect of serum DHA-PL. Secondly, MDA was negatively and DHA-PL was positively associated with serum CAT capacity. Detailed multivariate statistical analyses revealed that the positive association between serum DHA-PL levels and CAT capacity was independent of the MDA lowering effect of DHA-PL which is suggestive of a more generalized improvement in peroxisomal function following DHA-AAG supplementation—perhaps due to reduced endogenous

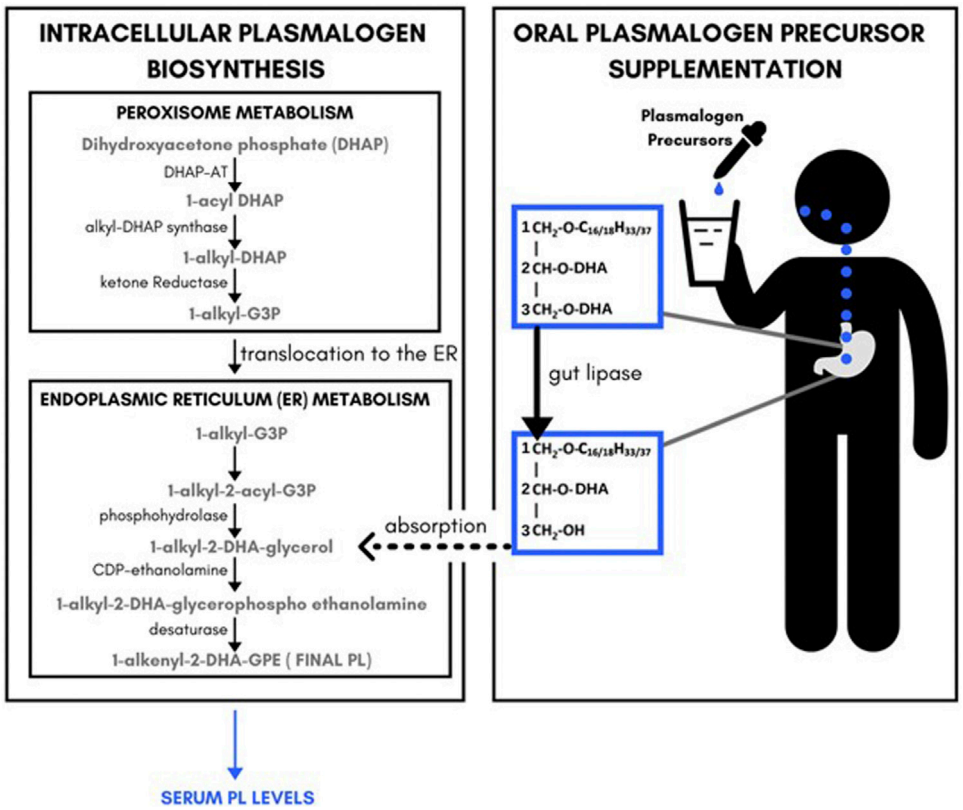

FIGURE 3 | Relationship between endogenous plasmalogeon biosynthesis pathways, plasmalogeon precursor supplement administration and serum plasmalogeon levels.

plasmalogen synthesis demand. Thirdly, the effect of DHA-AAG on SOD activity appeared more complicated and less clear. Since SOD is inducible as well as degradable, we looked at the effect of DHA-AAG administration on persons with high or low SOD. DHA-AAG normalized both groups of participants. Further investigation is needed to confirm this observation, however it is possible that persons with a robust SOD biosynthesis capacity exhibit elevated SOD in the presence of excess hydrogen peroxide, which is alleviated by DHA-AAG whereas persons with a weak SOD biosynthesis capacity exhibit decreased SOD, which is enhanced by DHA-AAG.

Due to the small investigational nature of the study, cognition, as measured by QDRS and sarcopenia, as measured by the sit-stand test were evaluated as preliminary indices of potential clinical benefit from DHA-AAG supplementation. Despite the small number of participants, a clear participant benefit was observed. Participants self-reported increased energy, clarity of thought, and fluidity of movement. Two-thirds of the participants reported an increase in their global rating of change evaluation and one-third reported no change. None reported a decline (**Table 4**). QDRS is an objective evaluation of a person (the trial participant) by a third-party witness with intimate knowledge of the daily activities of the person. According to such third person observation, 9 (41%) of the participants displayed significant cognitive improvement, nine remained stable and 4 declined. Participants with the most severe cognitive impairment at baseline were observed to preferentially benefit from the DHA-AAG therapy in that three of the four participants with moderate dementia (CDR = 2) exhibited clinically meaningful improvement and two of the four participants with mild dementia (CDR = 1) exhibited clinically meaningful improvement. Improved mobility, as measured by the sit-stand test was more generally observed. Only one participant exhibited a decline in both cognition and mobility, whereas five participants exhibited improvements in both cognition and mobility and ten exhibited improvements in either cognition or mobility.

SUMMARY AND CONCLUSION

The study has several obvious attributes and limitations. It was designed to investigate the pharmacokinetic and pharmacodynamic effects of an escalating oral dose of DHA-AAG. It was not designed to critically evaluate clinical response. The pharmacokinetic (dose dependent increase in serum levels of the target DHA-PL species) and pharmacodynamic (increased CAT activity and decreased MDA levels) are robust and consistent with previous research results in animal models and *in vitro* studies. The DHA-AAG was well tolerated at the doses and durations administered. The small number of participants (22), short duration (4-months), and the lack of a sufficient placebo control or cross-over design are obvious limitations as to the interpretation of the positive clinical effects on

cognition and mobility observed. Clinical response data should be interpreted with caution. However, it is clear that subsequent clinical trials designed to more critically evaluate the clinical utility of DHA-AAG in dementia and sarcopenia are warranted.

Impact Statement

The study presented is the first targeted plasmalogen precursor treatment evaluation in humans. Numerous epidemiological and post-mortem studies have described structure-specific associations between plasmalogen deficiencies and reduced cognition and mobility. Numerous preclinical studies have similarly described structure-specific biological activities of plasmalogens. An escalating dose of a DHA-specific plasmalogen precursor (DHA-AAG) was administered to cognitively impaired persons and the pharmacokinetic, pharmacodynamic, and clinical effects evaluated. A dose-dependent elevation in DHA-plasmalogen levels was observed. Oxidative stress biomarkers (malondialdehyde, catalase, superoxide dismutase) improved and this improvement was correlated with higher DHA-plasmalogen levels. A statistically significant improvement in cognition and mobility was observed. The research results establish that blood levels of structurally specific plasmalogen species can be preferentially targeted and modulated and that this is a therapeutically viable approach worthy of further investigation and optimization for the treatment of plasmalogen deficiency mediated diseases.

DATA AVAILABILITY STATEMENT

The raw data supporting the conclusions of this article will be made available by the authors, without undue reservation.

ETHICS STATEMENT

The studies involving human participants were reviewed and approved by the Sterling IRB. The patients/participants provided their written informed consent to participate in this study.

AUTHOR CONTRIBUTIONS

DBG designed the DHA-AAG plasmalogen precursor and oversaw the manufacturing. DBG prepared the manuscript. DBG, MAK, and SJ designed the trial. LS oversaw analytical testing. SJ oversaw the execution of the clinical trial. JH, KM, MZ, and BH generated the clinical data.

SUPPLEMENTARY MATERIAL

The Supplementary Material for this article can be found online at: https://www.frontiersin.org/articles/10.3389/fcell.2022.864842/full#supplementary-material

REFERENCES

Author Anonymous (2021). *The Top 5 Most Feared Health Conditions in 2021*. medicare advantage. https://www.medicareadvantage.com/news/.

Beeri, M. S., Leugrans, S. E., Delbono, O., Bennett, D. A., and Buchman, A. S. (2021). Sarcopenia Is Associated with Incident Alzheimer's Dementia, M Ild Cognitive Impairment, and Cognitive Decline. *J. Am. Geriatr. Soc.* 69, 1826–1835. doi:10.1111/jgs.17206

Dorninger, F., Forss-Petter, S., and Berger, J. (2017). From Peroxisomal Disorders to Common Neurodegenerative Diseases - the Role of Ether Phospholipids in the Nervous System. *FEBS Lett.* 591, 2761–2788. doi:10.1002/1873-3468.12788

Dorninger, F., Herbst, R., Kravic, B., Camurdanoglu, B. Z., Macinkovic, I., Zeitler, G., et al. (2017). Reduced Muscle Strength in Ether Lipid-Deficient Mice Is Accompanied by Altered Development and Function of the Neuromuscular Junction. *J. Neurochem.* 143, 569–583. doi:10.1111/jnc.14082

Farooqui, A. A., Horrocks, L. A., and Farooqui, T. (2000). Glycerophospholipids in Brain: Their Metabolism, Incorporation into Membranes, Functions, and Involvement in Neurological Disorders. *Chem. Phys. lipids* 106, 1–29. doi:10.1016/s0009-3084(00)00128-6

Fujino, T., Yamada, T., Asada, T., Ichimaru, M., Tsuboi, Y., Wakana, C., et al. (2018). Effects of Plasmalogen on Patients with Mild Cognitive Impairment: A Randomized, Placebo-Controlled Trial in Japan. *J. Alzheimers Dis. Park.* 8. doi:10.4172/2161-0460.1000419

Fujino, T., Yamada, T., Asada, T., Tsuboi, Y., Wakana, C., Mawatari, S., et al. (2017). Efficacy and Blood Plasmalogen Changes by Oral Administration of Plasmalogen in Patients with Mild Alzheimer's Disease and Mild Cognitive Impairment: A Multicenter, Randomized, Double-Blind, Placebo-Controlled Trial. *EBioMedicine* 17, 199–205. doi:10.1016/j.ebiom.2017.02.012

Galvin, J. E. (2015). The Quick Dementia Rating System (Qdrs): A Rapid Dementia Staging Tool. *Alzheimer's & Dement. Diagn. Assess. & Dis. Monit.* 1, 249–259. doi:10.1016/j.dadm.2015.03.003

Ginsberg, L., Xuereb, J. H., and Gershfeld, N. L. (1998). Membrane Instability, Plasmalogen Content, and Alzheimer's Disease. *J. Neurochem.* 70, 2533–2538. doi:10.1046/j.1471-4159.1998.70062533.x

Ginsberg, L., Rafique, S., Xuereb, J. H., Rapoport, S. I., and Gershfeld, N. L. (1995). Disease and Anatomic Specificity of Ethanolamine Plasmalogen Deficiency in Alzheimer's Disease Brain. *Brain Res.* 698, 223–226. doi:10.1016/0006-8993(95)00931-f

Glaser, P. E., and Gross, R. W. (1994). Plasmenylethanolamine Facilitates Rapid Membrane Fusion: a Stopped-Flow Kinetic Investigation Correlating the Propensity of a Major Plasma Membrane Constituent to Adopt an HII Phase with its Ability to Promote Membrane Fusion. *Biochemistry* 33, 5805–5812. doi:10.1021/bi00185a019

Glaser, P. E., and Gross, R. W. (1995). Rapid Plasmenylethanolamine-Selective Fusion of Membrane Bilayers Catalyzed by an Isoform of Glyceraldehyde-3-Phosphate Dehydrogenase: Discrimination between Glycolytic and Fusogenic Roles of Individual Isoforms. *Biochemistry* 34, 12193–12203. doi:10.1021/bi00038a013

Goodenowe, D. B., and Senanayake, V. (2019). Relation of Serum Plasmalogens and APOE Genotype to Cognition and Dementia in Older Persons in a Cross-Sectional Study. *Brain Sci.* 9. doi:10.3390/brainsci9040092

Goodenowe, D. B., Cook, L. L., Liu, J., Lu, Y., Jayasinghe, D. A., Ahiahonu, P. W. K., et al. (2007). Peripheral Ethanolamine Plasmalogen Deficiency: a Logical Causative Factor in Alzheimer's Disease and Dementia. *J. lipid Res.* 48, 2485–2498. doi:10.1194/jlr.p700023-jlr200

Goodenowe, D. (2021). *Breaking Alzheimer's - A 15 Year Crusade to Expose the Cause and Deliver the Cure*. USA: Dayan Goodenowe.

Guan, Z., Wang, Y., Cairns, N. J., Lantos, P. L., Dallner, G., and Sindelar, P. J. (1999). Decrease and Structural Modifications of Phosphatidylethanolamine Plasmalogen in the Brain with Alzheimer Disease. *J. Neuropathology Exp. Neurology* 58, 740–747. doi:10.1097/00005072-199907000-00008

Gutteridge, J. M. C. (1984). Lipid Peroxidation Initiated by Superoxide-dependent Hydroxyl Radicals Using Complexed Iron and Hydrogen Peroxide. *FEBS Lett.* 172, 245–249. doi:10.1016/0014-5793(84)81134-5

Han, X., Holtzman, D. M., and McKeel, D. W., Jr. (2001). Plasmalogen Deficiency in Early Alzheimer's Disease Subjects and in Animal Models: Molecular Characterization Using Electrospray Ionization Mass Spectrometry. *J. Neurochem.* 77, 1168–1180. doi:10.1046/j.1471-4159.2001.00332.x

Han, X. (2005). Lipid Alterations in the Earliest Clinically Recognizable Stage of Alzheimers Disease: Implication of the Role of Lipids in the Pathogenesis of Alzheimers Disease. *Car* 2, 65–77. doi:10.2174/1567205052772786

Hossain, M. S., Mawatari, S., and Fujino, T. (2022). Plasmalogens, the Vinyl Ether-Linked Glycerophospholipids, Enhance Learning and Memory by Regulating Brain-Derived Neurotrophic Factor. *Front. Cell. Dev. Biol.* 10, 828282. doi:10.3389/fcell.2022.828282

Kamper, S. J., Maher, C. G., and Mackay, G. (2009). Global Rating of Change Scales: a Review of Strengths and Weaknesses and Considerations for Design. *J. Man. Manip. Ther.* 17, 163–170. doi:10.1179/jmt.2009.17.3.163

Kassmann, C. M., Lappe-Siefke, C., Baes, M., Brügger, B., Mildner, A., Werner, H. B., et al. (2007). Axonal Loss and Neuroinflammation Caused by Peroxisome-Deficient Oligodendrocytes. *Nat. Genet.* 39, 969–976. doi:10.1038/ng2070

Kling, M. A., Goodenowe, D. B., Senanayake, V., MahmoudianDehkordi, S., Arnold, M., Massaro, T. J., et al. (2020). Circulating Ethanolamine Plasmalogen Indices in Alzheimer's Disease: Relation to Diagnosis, Cognition, and CSF Tau. *Alzheimer's & Dement.* 16, 1234–1247. doi:10.1002/alz.12110

Kokkaliari, M., Fawibe, O., Berry, H., and Baum, H. (1992). Serum Catalase as the Protective Agent against Inactivation of Alpha 1-proteinase Inhibitor by Hydrogen Peroxide; Comparison between Normal and Rheumatoid Sera. *Biochem. Int.* 28, 219–227.

Lim, W. L. F., Huynh, K., Chatterjee, P., Martins, I., Jayawardana, K. S., Giles, C., et al. (2020). Relationships between Plasma Lipids Species, Gender, Risk Factors, and Alzheimer's Disease. *Jad* 76, 303–315. doi:10.3233/jad-191304

Mankidy, R., Ahiahonu, P. W., Ma, H., Jayasinghe, D., Ritchie, S. A., Khan, M. A., et al. (2010). Membrane Plasmalogen Composition and Cellular Cholesterol Regulation: a Structure Activity Study. *Lipids Health Dis.* 9, 62. doi:10.1186/1476-511x-9-62

McAllister, L. S., and Palombaro, K. M. (2020). Modified 30-Second Sit-To-Stand Test: Reliability and Validity in Older Adults Unable to Complete Traditional Sit-To-Stand Testing. *J. Geriatr. Phys. Ther.* 43, 153–158. doi:10.1519/jpt.0000000000000227

Messias, M. C. F., Mecatti, G. C., Priolli, D. G., and de Oliveira Carvalho, P. (2018). Plasmalogen Lipids: Functional Mechanism and Their Involvement in Gastrointestinal Cancer. *Lipids Health Dis.* 17, 41. doi:10.1186/s12944-018-0685-9

Munn, N. J., Arnio, E., Liu, D., Zoeller, R. A., and Liscum, L. (2003). Deficiency in Ethanolamine Plasmalogen Leads to Altered Cholesterol Transport. *J. lipid Res.* 44, 182–192. doi:10.1194/jlr.m200363-jlr200

Pacifico, J., Geerlings, M. A. J., Reijnierse, E. M., Phassouliotis, C., Lim, W. K., and Maier, A. B. (2020). Prevalence of Sarcopenia as a Comorbid Disease: A Systematic Review and Meta-Analysis. *Exp. Gerontol.* 131, 110801. doi:10.1016/j.exger.2019.110801

Rouser, G., and Yamamoto, A. (1968). Curvilinear Regression Course of Human Brain Lipid Composition Changes with Age. *Lipids* 3, 284–287. doi:10.1007/bf02531202

Senanayake, V., and Goodenowe, D. B. (2019). Plasmalogen Deficiency and Neuropathology in Alzheimer's Disease: Causation or Coincidence? *Alzheimer's & Dementia Transl. Res. & Clin. Interventions* 5, 524–532. doi:10.1016/j.trci.2019.08.003

Sindelar, P. J., Guan, Z., Dallner, G., and Ernster, L. (1999). The Protective Role of Plasmalogens in Iron-Induced Lipid Peroxidation. *Free Radic. Biol. Med.* 26, 318–324. doi:10.1016/s0891-5849(98)00221-4

Stables, M. J., and Gilroy, D. W. (2011). Old and New Generation Lipid Mediators in Acute Inflammation and Resolution. *Prog. Lipid Res.* 50, 35–51. doi:10.1016/j.plipres.2010.07.005

Stadelmann-Ingrand, S., Favreliere, S., Fauconneau, B., Mauco, G., and Tallineau, C. (2001). Plasmalogen Degradation by Oxidative Stress: Production and Disappearance of Specific Fatty Aldehydes and Fatty α-hydroxyaldehydes. *Free Radic. Biol. Med.* 31, 1263–1271. doi:10.1016/s0891-5849(01)00720-1

Sullivan-Gunn, M. J., and Lewandowski, P. A. (2013). Elevated Hydrogen Peroxide and Decreased Catalase and Glutathione Peroxidase Protection Are Associated with Aging Sarcopenia. *BMC Geriatr.* 13, 104. doi:10.1186/1471-2318-13-104

Wood, P. L., Khan, A. M., Mankidy, R., Smith, T., and Goodenowe, D. (2011). "Plasmalogen Deficit: A New and Testable Hypothesis for the Etiology of Alzheimer's Disease," in *Alzheimer's Disease Pathogenesis-Core Concepts, Shifting Paradigms and Therapeutic Targets*. Editor S. De la Monte (London: InTech).

Wood, P. L., Khan, M., Smith, T., and Goodenowe, D. B. (2011). Cellular Diamine Levels in Cancer Chemoprevention: Modulation by Ibuprofen and Membrane Plasmalogens. *Lipids Health Dis.* 10, 214. doi:10.1186/1476-511x-10-214

Wood, P. L., Mankidy, R., Ritchie, S., Heath, D., Wood, J. A., Flax, J., et al. (2010). Circulating Plasmalogen Levels and Alzheimer Disease Assessment Scale-Cognitive Scores in Alzheimer Patients. *jpn* 35, 59–62. doi:10.1503/jpn.090059

Wood, P. L., Smith, T., Lane, N., Khan, M. A., Ehrmantraut, G., and Goodenowe, D. B. (2011). Oral Bioavailability of the Ether Lipid Plasmalogen Precursor, PPI-1011, in the Rabbit: a New Therapeutic Strategy for Alzheimer's Disease. *Lipids Health Dis.* 10, 227. doi:10.1186/1476-511x-10-227

Wood, P. L., Smith, T., Pelzer, L., and Goodenowe, D. B. (2011). Targeted Metabolomic Analyses of Cellular Models of Pelizaeus-Merzbacher Disease Reveal Plasmalogen and Myo-Inositol Solute Carrier Dysfunction. *Lipids Health Dis.* 10, 102. doi:10.1186/1476-511x-10-102

Yoo, H. Y., Chang, M. S., and Rho, H. M. (1999). The Activation of the Rat Copper/zinc Superoxide Dismutase Gene by Hydrogen Peroxide through the Hydrogen Peroxide-Responsive Element and by Paraquat and Heat Shock through the Same Heat Shock Element. *J. Biol. Chem.* 274, 23887–23892. doi:10.1074/jbc.274.34.23887

Zoeller, R. A., Lake, A. C., Nagan, N., Gaposchkin, D. P., Legner, M. A., and Lieberthal, W. (1999). Plasmalogens as Endogenous Antioxidants: Somatic Cell Mutants Reveal the Importance of the Vinyl Ether. *Biochem. J.* 338 (Pt 3) (Pt 3), 769–776. doi:10.1042/bj3380769

Conflict of Interest: Author DBG was a shareholder and employee of Prodrome Sciences USA LLC. LS was employed by the company Prodrome Sciences United States LLC.

The remaining authors declare that the research was conducted in the absence of any commercial or financial relationship that could be construed as a potential conflict of interest.

Publisher's Note: All claims expressed in this article are solely those of the authors and do not necessarily represent those of their affiliated organizations, or those of the publisher, the editors and the reviewers. Any product that may be evaluated in this article, or claim that may be made by its manufacturer, is not guaranteed or endorsed by the publisher.

frontiers | Frontiers in Cell and Developmental Biology

ORIGINAL RESEARCH
published: 11 July 2022
doi: 10.3389/fcell.2022.886316

A *Pex7* Deficient Mouse Series Correlates Biochemical and Neurobehavioral Markers to Genotype Severity—Implications for the Disease Spectrum of Rhizomelic Chondrodysplasia Punctata Type 1

Wedad Fallatah[1,2]*, *Wei Cui*[3], *Erminia Di Pietro*[3], *Grace T. Carter*[3], *Brittany Pounder*[3], *Fabian Dorninger*[4], *Christian Pifl*[5], *Ann B. Moser*[6], *Johannes Berger*[4] and *Nancy E. Braverman*[1,3]*

[1]Department of Human Genetics, McGill University, Montreal, QC, Canada, [2]Department of Medical Genetics, King Abdul-Aziz University, Jeddah, Saudi Arabia, [3]Child Health and Human Development Program, Peroxisome Disease Laboratory, Research Institute of the McGill University Health Centre, Montreal, QC, Canada, [4]Department of Pathobiology of the Nervous System, Center for Brain Research, Medical University of Vienna, Vienna, Austria, [5]Department of Molecular Neurosciences, Center for Brain Research, Medical University of Vienna, Vienna, Austria, [6]Hugo W Moser Research Institute, Kennedy Krieger Institute, Baltimore, MD, United States

OPEN ACCESS

Edited by:
Venkaiah Betapudi,
United States Department of Health and Human Services, United States

Reviewed by:
Karolina M Stepien,
Salford Royal NHS Foundation Trust, United Kingdom
Karen Malone,
Leiden Analytics, Netherlands

***Correspondence:**
Wedad Fallatah
wedad.fallatah@mail.mcgill.ca
Nancy E. Braverman
nancy.braverman@mcgill.ca

Specialty section:
This article was submitted to Cellular Biochemistry, a section of the journal Frontiers in Cell and Developmental Biology

Received: 28 February 2022
Accepted: 19 May 2022
Published: 11 July 2022

Citation:
Fallatah W, Cui W, Di Pietro E, Carter GT, Pounder B, Dorninger F, Pifl C, Moser AB, Berger J and Braverman NE (2022) A Pex7 Deficient Mouse Series Correlates Biochemical and Neurobehavioral Markers to Genotype Severity—Implications for the Disease Spectrum of Rhizomelic Chondrodysplasia Punctata Type 1. Front. Cell Dev. Biol. 10:886316. doi: 10.3389/fcell.2022.886316

Rhizomelic chondrodysplasia punctata type 1 (RCDP1) is a peroxisome biogenesis disorder caused by defects in *PEX7* leading to impairment in plasmalogen (Pls) biosynthesis and phytanic acid (PA) oxidation. Pls deficiency is the main pathogenic factor that determines the severity of RCDP. Severe (classic) RCDP patients have negligible Pls levels, congenital cataracts, skeletal dysplasia, growth and neurodevelopmental deficits, and cerebral hypomyelination and cerebellar atrophy on brain MRI. Individuals with milder or nonclassic RCDP have higher Pls levels, better growth and cognitive outcomes. To better understand the pathophysiology of RCDP disorders, we generated an allelic series of *Pex7* mice either homozygous for the hypomorphic allele, compound heterozygous for the hypomorphic and null alleles or homozygous for the null allele. Pex7 transcript and protein were almost undetectable in the hypomorphic model, and negligible in the compound heterozygous and null mice. *Pex7* deficient mice showed a graded reduction in Pls and increases in C26:0-LPC and PA in plasma and brain according to genotype. Neuropathological evaluation showed significant loss of cerebellar Purkinje cells over time and a decrease in brain myelin basic protein (MBP) content in *Pex7* deficient models, with more severe effects correlating with *Pex7* genotype. All *Pex7* deficient mice exhibited a hyperactive behavior in the open field environment. Brain neurotransmitters analysis of *Pex7* deficient mice showed a significant reduction in levels of dopamine, norepinephrine, serotonin and GABA. Also, a significant correlation was found between brain neurotransmitter levels, the hyperactivity phenotype, Pls level and the severity of *Pex7* genotype. In conclusion, our study showed evidence of a genotype-phenotype correlation between the severity of *Pex7* deficiency and several clinical and neurobiochemical

phenotypes in RCDP1 mouse models. We propose that PA accumulation may underlie the cerebellar atrophy seen in older RCDP1 patients, as even relatively low tissue levels were strongly associated with Purkinje cells loss over time in the murine models. Also, our data demonstrate the interrelation between Pls, brain neurotransmitter deficiencies and the neurobehavioral phenotype, which could be further used as a valuable clinical endpoint for therapeutic interventions. Finally, these models show that incremental increases in *Pex7* levels result in dramatic improvements in phenotype.

Keywords: rhizomelic chondrodysplasia punctata (RCDP), peroxisome biogenesis disorders, PEX7 gene, adult Refsum's disease, neurobehavioral phenotypes, plasmalogens, phytanic acid, very long chain fatty acid (VLCFA)

1 INTRODUCTION

Rhizomelic chondrodysplasia punctata type 1 (RCDP1) is a distinct peroxisome biogenesis disorder caused by defects in *PEX7* that impair the peroxisomal pathways of plasmalogen (Pls) synthesis and phytanic acid (PA) oxidation. Clinically, there is a spectrum of phenotype severity that can be distinguished by the degree of Pls deficiency. Although the majority of patients have classic (severe) RCDP, there are patients with non-classic (mild) RCDP.

Classic (severe) RCDP is characterized by congenital cataracts, proximal limb shortening (rhizomelia) and the radiographic finding of punctate calcifications in the epiphyseal cartilages (chondrodysplasia punctata, CDP). Most patients have congenital cardiac defects. The clinical course involves dramatic postnatal growth deficiency and profound global cognitive and developmental disabilities [Braverman et al., 2001 November 16 (Updated 30 January 2020)]. Most patients also develop seizures, frequent pulmonary infections, feeding and swallowing disorders (White et al., 2003; Bams-Mengerink et al., 2013; Huffnagel et al., 2013; Duker et al., 2016). Hypomyelination and cerebellar atrophy has been observed on brain magnetic resonance imaging (MRI) (Bams-Mengerink et al., 2006). Classic RCDP has a 55% mortality rate by age 12 years and death usually results from respiratory complications (Duker et al., 2019). The biochemical profile of classic RCDP1 includes markedly reduced erythrocyte Pls and high plasma PA levels (if not under dietary restriction) with essentially normal plasma very long chain fatty acids (VLCFA).

Nonclassic (mild) RCDP1 is characterized by congenital cataracts, variable skeletal defects and neurobehavioral issues (Braverman et al., 2002; Bams-Mengerink et al., 2013; Yu et al., 2013; Fallatah et al., 2020). A recent survival analysis and natural history study showed that 91% of mild RCDP1 individuals survive to adulthood and have better growth and developmental outcomes (Braverman et al., 2002; Bams-Mengerink et al., 2013; Yu et al., 2013; Duker et al., 2019; Fallatah et al., 2020). Their biochemical profile shows reduced erythrocyte Pls levels that were higher than classical RCDP, and up to 43% of healthy controls (Fallatah et al., 2020). These individuals can accumulate high PA levels on unrestricted diets.

Additionally, mild *PEX7* deficiency can result in a phenotype like Adult Refsum disease (ARD), a disorder caused by isolated accumulation of PA due to mutations in the peroxisomal enzyme, PHYH (van den Brink et al., 2003). PA is a saturated methyl-branched-chain fatty acid that is exclusively of dietary origin, obtained mainly from fat of ruminant animals that can release phytol from chlorophyll. ARD presents with retinitis pigmentosa, anosmia, peripheral neuropathy, cerebellar ataxia and hearing loss in early adulthood due to gradual accumulation of dietary PA [Wanders et al., 2006 March 20 [Updated 11 June 2015)]. Patients with ARD due to *PEX7* defects might present earlier with sensorimotor neuropathy and cataract, an overlapping feature of RCDP. These individuals usually have near normal erythrocyte Pls levels and minimal impairment in Pls synthesis but have significant elevation in plasma PA levels that could be within the range of classic ARD patients (van den Brink et al., 2003; Horn et al., 2007).

Genotype-phenotype correlations have shown that the common *PEX7* allele, p. L292X, is a founder allele in individuals of northern European descent (Braverman et al., 2000). It is a nonfunctional protein and homozygosity is associated with the classic RCDP phenotype (Braverman et al., 2002). In contrast, unique hypomorphic variants were solely linked to a milder RCDP or ARD phenotype and could be associated to residual PEX7 protein activity (Braverman et al., 2000; Braverman et al., 2002; Motley et al., 2002; Fallatah et al., 2020). There is evidence that a few of these *PEX7* hypomorphic alleles result from residual amounts of normal *PEX7* transcript and protein possibly "leaking" through splice site or 5' UTR mutations (Braverman et al., 2002).

The overall estimated RCDP prevalence rates are between 0.5 and 0.7 cases per 100,000 births in the US and Europe, respectively (Luisman et al., 2021). RCDP can be caused by defects in 5 peroxisomal genes that result in Pls deficiency. RCDP1 accounts for 90% of cases and is caused by mutations in *PEX7,* encoding the cytosolic receptor for peroxisomal matrix proteins carrying the Peroxisomal Targeting Signal 2 (PTS2). PEX7 receptor defects impair peroxisomal import of the three known PTS2-enzymes: alkylglycerone-phosphate synthase (AGPS), phytanoyl-CoA hydroxylase (PHYH) and 3-oxoacyl-CoA thiolase or acetyl-CoA acyltransferase (ACAA1) (Braverman et al., 1997; Motley et al., 1997; Purdue et al., 1997). Consequently, PEX7 deficiency results in reduced Pls synthesis (due to AGPS deficiency) and PA degradation (due to PHYH deficiency). Peroxisomal thiolase (ACAA1) deficiency does not impair the oxidation of VLCFA in humans, presumably due to availability of sterol carrier protein X (SCPx), a PTS1-

enzyme with thiolase activity (Seedorf et al., 1994; Wanders et al., 1997). The RCDP phenotype results also from isolated deficiency in peroxisomal enzymes Glyceronephosphate O-acyltransferase (GNPAT) (Wanders et al., 1992; Barr et al., 1993), AGPS (Wanders et al., 1994) and fatty acyl-CoA reductase 1 (FAR1) (Buchert et al., 2014), causing RCDP2-4 respectively. RCDP5 is caused by defects in a specific domain of the peroxisomal matrix enzyme co-transporter, PEX5, that binds to PEX7 (Baroy et al., 2015).

The unique deficiency of Pls phospholipids in RCDP highlights their importance in the development and homeostasis of multiple organ systems. Acquired Pls deficiency has also been reported in common disorders including neurodegenerative, respiratory, cardiovascular and metabolic diseases that highlight the important role of Pls in a wide range of physiological functions (Braverman and Moser, 2012; Dorninger et al., 2017a; Paul, Lancaster and Meikle, 2019). Pls are ether phospholipids typically characterized by the presence of a C16:0, C18:0 or C18:1 fatty alcohol with a vinyl ether linkage at the sn-1 position, an ester bond linking mainly to polyunsaturated fatty acids (such as arachidonic acid (AA) or docosahexaenoic acid (DHA)) at the sn-2 position, and polar head groups of phospho-ethanolamine (most abundant form in the brain and many tissues) or phospho-choline at the sn-3 position of the glycerol backbone. Pls bring unique structural and functional features to membranes, and are critical components of myelin sheaths, synaptic vesicles in neuronal junctions as well as the pulmonary surfactant barrier (Brites et al., 2004; Braverman and Moser, 2012). Pls have antioxidant effects (Luoma et al., 2015; Wu et al., 2019) and are considered a valuable source of the polyunsaturated omega-3 fatty acid DHA (C22:6 n−3), an essential structural component of the human brain and retina (Hishikawa et al., 2017). Pls play a significant role in modulating cellular signaling, cholesterol biosynthesis, innate immunity and macrophage phagocytosis (Pike et al., 2002; Brodde et al., 2012; Honsho, Abe and Fujiki, 2015; Di Cara et al., 2017; Rubio et al., 2018).

Studying the neurological aspects of RCDP in terms of pathology and function is critical to understand the pathophysiological consequences of Pls deficiency in the nervous system and for determining endpoints in pre-clinical therapeutic trials. Previous *in-vivo* nervous system studies of *Pex7* null (RCDP1) and *Gnpat* null (RCDP2) mouse models showed abnormal myelination in central and peripheral nervous systems, impairment in cerebellar Purkinje cells foliation and innervation, and deficits in brain neurotransmitters and nerve conduction velocity (Brites et al., 2003; da Silva et al., 2014; Malheiro et al., 2019; Rodemer et al., 2003; Teigler et al., 2009; Dorninger et al., 2019b). *Gnpat* null mice exhibited hyperactive and stereotypic behavioral patterns, social interaction impairment as well as defects in neuromuscular transmission and neuromotor function (Dorninger et al., 2017b; Dorninger et al., 2019a; Dorninger et al., 2019b).

We previously reported the initial characterization of a hypomorphic *Pex7* mouse model that resembled a mild RCDP1 phenotype and showed early cataracts, abnormalities of lens epithelial cells and delayed skeletal ossification (Braverman et al., 2010). Full length Pex7 transcript was reduced to <5% of control due to the intronic insertion of a neo cassette. Here we used these mice to generate and characterize a *Pex7* deficient allelic mouse series representing the severe ($Pex7^{null/null}$) and milder RCDP1 phenotypes ($Pex7^{hypo/null}$ and $Pex7^{hypo/hypo}$). These *Pex7* deficient mice show graded changes in growth, survival and biochemical profiles including Pls, VLCFA, and PA levels that reflected the degree of *Pex7* deficiency. Histological assessment showed myelin reduction and Purkinje cells loss. All *Pex7* deficient mice reveal increased activity levels in the open field environment. These models help to correlate biochemical changes with disease severity, including the correlation between Pls reduction and neurotransmitter levels, and show a potential role for PA accumulation in the cerebellar phenotype. Finally, the marked reduction observed in *Pex7* transcript and protein levels in the hypomorphic mice suggest that small increases in *Pex7* transcript and protein result in large improvement in the RCDP phenotype and are useful for pre-clinical trial planning.

2 MATERIALS AND METHODS

2.1 Generation, Care and Tissue Collection of *Pex7* Deficient Mouse Series

We used the previously reported *Pex7* hypomorphic mouse model (Braverman et al., 2010) B6;129S6-$Pex7^{tm2.0Brav}$ (named here as $Pex7^{hypo/hypo}$), to generate an allelic series, (B6;129S6-$Pex7^{tm2.2Brav}$) referred as $Pex7^{null/null}$ and (B6;129S6-$Pex7^{tm2.3Brav}$) referred to as $Pex7^{hypo/null}$. The *Pex7* null allele was generated by breeding CMV-driven Cre recombinase deleter mice, B6.C-Tg(CMV-cre)1Cgn/J, with $Pex7^{hypo/hypo}$ mice, in which loxP sites flanked exon 3. Four different primer sets were used to distinguish the $Pex7^{hypo}$, $Pex7^{null}$ and $Pex7^{WT}$ alleles; unique primer combinations distinguished each genotype (see **Supplementary Table S1** for primer list). $Pex7^{WT/null}$ mice were bred to obtain $Pex7^{null/null}$ mice. $Pex7^{WT/null}$ females were bred with $Pex7^{hypo/hypo}$ males to generate the intermediate $Pex7^{hypo/null}$ mouse model. SNP genotyping showed a stable 87% 129S6/SvEvTac and 13% C57BL/6NCrl strain background (MaxBax, Charles River, Wilmington, MA). For PCR genotyping, ear notches were collected in 75 µl of alkaline lysis buffer (25 mM NaOH/ 0.2 mM Na_2EDTA) at 95°C × 30 min for digestion followed by neutralization with 250 µl of 40 mM Tris-HCl. *Gnpat* null mice ($Gnpat^{tm1Just}$, MGI: 2670462) (Rodemer et al., 2003) were maintained on an outbred C57BL/6 × CD1 background. Experimental cohorts with $Gnpat^{null/null}$ and $Gnpat^{WT/WT}$ littermates were obtained by breeding $Gnpat^{null/WT}$ animals; genotypes were determined by PCR as described (Rodemer et al., 2003). Mice were housed in the animal facility at the RI-MUHC and the local animal facility of the Medical University of Vienna with 12 h of dark and light cycles. Animals were fed a commercial laboratory rodent diet [Teklad Global 18% Protein, Envigo, Canada (that does not have sources of PA listed)] and had free access to water. For all experiments, we used both males and females at ages 1, 4, and 12 months. Control groups were

Pex7$^{WT/WT}$ and *Pex7*$^{WT/hypo}$ littermates for experiments involving *Pex7*-deficient mice and *Gnpat*$^{WT/WT}$ littermates for experiments involving *Gnpat*$^{null/null}$ mice. Euthanasia was performed by CO_2 preceded by 5% isoflurane anesthesia. For gene expression, protein studies and biochemical analysis, tissues (cerebral cortex, cerebellum, heart, liver, lung, and kidney) were collected, snap frozen in liquid nitrogen and stored at −80°C until analysis. Blood samples and separation of plasma from erythrocytes was prepared as described (Fallatah et al., 2019). For histology, whole brain tissue was harvested and fixed in 10% neutral buffered formalin at 4°C × 48 h, then transferred to 70% ethanol and processed for paraffin embedding. This study was conducted under a McGill University animal care committee approved protocol (#5538) or a license by the Austrian Federal Ministry of Science and Research (BMBWF-66.009/0174-V/3b/2019).

2.2 Quantitative Real-Time PCR (qPCR)

Total RNA was extracted from ~20 mg of cerebral cortex or cerebellum using TRIZOL™ (Invitrogen). For cDNA synthesis, we used 1 µg of RNA and OneScript® Plus cDNA Synthesis SuperMix reverse transcriptase (Abm, G453), and qPCR with EvaGreen 2X qPCR Kit (Abm™ II) and CFX96 Touch Real-Time PCR Detection System (Bio-Rad). *Pex7* gene expression was normalized to murine hypoxanthine guanine phosphoribosyltransferase (*Hprt*) using Bio Rad software (Bio-Rad CFX Maestro). qPCR experiments were performed twice per sample; in each experiment, we used 3 biological and 2 technical replicates per genotype. Primer sets are listed in **Supplementary Table S1**.

2.3 Immunohistochemistry (IHC)/ Immunofluorescence (IF)

Paraffin embedded brain sections were sagittally sectioned (7 µm) and used for protein detection. We used stainless-steel brain matrices to obtain uniform sagittal sections across different animals. Allen Mouse Brain reference Sagittal Atlas version 1, 2008 (Sunkin et al., 2013) was used as a reference to match levels of cerebral cortex sections and all sections were between levels 15–16 (0.875–1.10 mm lateral to midline). Brain sections were deparaffinized with xylene and rehydrated with decreasing concentrations of ethanol and rinsed in 1X phosphate-buffered saline (PBS). Following antigen retrieval and serum blocking, sections were incubated overnight with primary antibody. Secondary antibodies were applied, and sections processed by fluorescent labeling and mounting using ProLong Gold antifade reagent with DAPI (Invitrogen, Carlsbad, CA) for IF staining, or DAB following a Vectorstain Elite ABC kit (Vector Laboratories) and hematoxylin counterstaining for IHC staining. Images were detected using a Leica DM6000B microscope with DFC345FX camera and LASX software (Richmond Hill, Canada). Primary antibodies and concentrations used were: mouse monoclonal anti-msCalbindin-D-28K (1:200, C9848, Sigma Aldrich), rat monoclonal anti-Myelin Basic Protein antibody "MBP" (1:1000, ab7349, Abcam) and rabbit polyclonal anti-hsPEX7 (1:200, Abcam, ab167036). Secondary antibodies were: goat anti-Mouse IgG (H + L) Alexa Fluor Plus 488 (1:200, A32723, Invitrogen), Goat Anti-Rat IgG H&L HRP conjugated (1:200, ab205720, Abcam).

2.4 Quantification of Cerebellar Purkinje Cells

To calculate the numbers of calbindin-D28K-positive Purkinje cells, mid-sagittal cerebellar sections (0.875–1.10 mm lateral to midline) from 3-4 independent samples per genotype were analyzed. Purkinje cells were counted in three to four cerebellar slices in entirety per mouse genotype at 1, 4, and 12 months of age by two independent researchers using the cell counter plugin from ImageJ software (Schneider et al., 2012).

2.5 Immunoblotting

Cerebral cortex and cerebellar tissues from *Pex7* deficient mice were homogenized using TissueLyser II (QIAGEN, cat#:85300) in RIPA buffer as previously described (Argyriou et al., 2019). Primary antibodies used were: rabbit polyclonal anti-beta-Tubulin (1:17,000, Abcam, ab6046), and rabbit monoclonal anti-PEX7 (1:1000 Abcam, ab134962). Visualization of membrane was performed using an Amersham 600 gel imager. Immunoblotting and densitometric analyses were performed as previously described (Argyriou et al., 2019; Fallatah et al., 2020).

2.6 Behavioral Tests

2.6.1 Open Field Test

The open field test was used to assess the general locomotor activity in *Pex7* deficient mice as described (Fallatah et al., 2019). For activity measures, we evaluated the total distance traveled in meters and activity time in 300 s. These parameters were analyzed using Any-Maze software (Stoelting Co., IL, United States).

2.6.2 Noldus CatWalk Gait Analysis

To evaluate gait patterns of *Pex7* deficient mice, we utilized the CatWalk gait analysis system (Noldus information technology). The mice were allowed to freely cross the pressure-sensitive plate of the CatWalk. Paw prints were labeled [right-fore (RF), right-hind (RH), left-fore (LF), left-hind (LH)] and analyzed using CatWalk software. The mice were trained the first day followed by 3 days of experimental sessions. Gait parameters were recorded and averaged over the 4 successful trials per session per day. A successful complete trial was defined as uninterrupted tracks with at least 4 cycles of complete steps and with speed variation less than 25% between the mice. Any mouse that did not complete 4 cycles in 15 min was excluded from the analysis.

2.6.3 Forced Alternation Test (Y-Maze)

Forced alternation tests were performed using a symmetrical Y-maze containing three identical arms and made of a grey acrylic bottom and walls (Stoelting Co., Wood Dale, IL). Each Y-maze arm was 50 cm long, 10 cm wide, and 20 cm high. The mice were trained for 3 days followed by 3 days of the experimental test. The test used a 5-min sample trial (first test) followed by a 5-min retrieval trial (second test). In the first test, the mouse was placed at the end of the start arm, facing

the wall and away from the center. The mouse was then allowed to freely explore only two arms of the Y-maze, while entry into the third arm was blocked. After the sample trial, the mouse was returned to its home cage for 30 min. In the second test, the block in arm 3 was removed; the mouse was again placed in the start arm and allowed to explore all three arms of the maze. An arm entry was recorded when 90% of a mouse's body entered the arm. Both tests were recorded by an overhead USB camera (model 60531, Stoelting CO., Wood Dale, IL, United States). Footage was analyzed by an automated tracking system (Any-maze Video Tracking Software, Stoelting CO. Wood Dale, IL, United States) for the number of entries and the percentage of time spent in each arm. A successful response considered to be correct when the number of entries and the time spent in the novel arm are significantly higher than other arms. Each mouse was subjected to 5 consecutive trials in a session per day. Any mouse with less than three arm entries in the first minute of the second test was excluded from the analysis.

2.7 LC-MS/MS Analysis for PlsEtn and C26:0-LPC Levels

Reagents used were authentic Pls standards, tetradeuterated internal standards 26:0-D4 lysoPC (Avanti Polar Lipids, Alabaster, Alabama), 16:0-D4 lyso PAF (Cayman Chemical Company, Ann Arbor, Michigan) and HPLC grade solvents (methanol, acetonitrile, chloroform, water) (Fisher Scientific, Waltham, MA), formic acid (Honeywell Fluka), ammonium formate (Sigma-Aldrich), and PBS (Thermo Fisher Scientific, Waltham, MA). LC-MS/MS analysis was performed in blood and tissues from *Pex7* deficient mice as previously described (Fallatah et al., 2019). PlsEtn were detected by multiple reaction monitoring (MRM) transitions representing fragmentation of [M + H] + species to m/z 339, 361, 385, 389, and 313 for compounds with 18:1, 20:4.22:6, 22:4, and 16:0, at the sn-2 position, respectively. Lysophosphatidyl choline (LPC) species were detected by MRM transitions representing fragmentation of [M + H] + species to m/z 104.

2.8 GC/MS Analysis for PA and DHA

Analysis was done in plasma, cerebral cortex and cerebellum from *Pex7* and *Gnpat* deficient mice as well as rodent chow using standard methods in the Peroxisome Disease Laboratory, Kennedy Krieger Institute, Baltimore Maryland (Dacremont et al., 1995; Dacremont and Vincent, 1995; Krauß et al., 2017).

2.9 High-Performance Liquid Chromatography Analysis for Brain Neurotransmitters

Analysis was performed on mice half cerebrum tissues without cerebellum using High-Performance Liquid Chromatography (HPLC) with electrochemical detection (monoamines) or fluorometric detection (amino acids) as previously reported (Hörtnagl et al., 1991; Peneder et al., 2011; Dorninger et al., 2019b).

2.10 Statistical Analysis

Data analysis was done using the GraphPad Prism software package (version 9.0) (GraphPad Software, La Jolla, United States). Statistical analysis was performed using one way or two-way analysis of variance (ANOVA) followed by appropriate correction tests for multiple comparisons. Simple linear regression was performed for correlation analysis between specific variables. Data are shown as the mean ± SD and statistical significance was set at $p < 0.05$. Since we did not observe any significant differences between male and female animals in biochemical and behavioral results, the data obtained from both genders were combined in the final statistical analysis.

3 RESULTS

In this study, an allelic series of *Pex7* deficient mice were generated to investigate the broad phenotypic spectrum of RCDP1. These mice include 2 hypomorphic models: a previously reported homozygous, $Pex7^{hypo/hypo}$ (Braverman et al., 2010) and a novel compound heterozygous, $Pex7^{hypo/null}$, resembling milder RCDP1. The third model, $Pex7^{null/null}$ represents severe RCDP1.

3.1 *Pex7* Transcript and Protein Levels are Extremely Reduced in Brain Tissues From *Pex7* Deficient Mice

The *Pex7* hypomorphic mouse model contains a *neo* cassette in reverse orientation in intron 2 and lox sites flanking exon 3 (Braverman et al., 2010). The intronic neo cassette reduces full length transcript levels and the lox sites were used to generate the null allele; thus all mice were generated from the same construct (Meyers et al., 1998). To determine *Pex7* transcript levels in our *Pex7* deficient mouse series, we performed quantitative RT-PCR analysis in cerebral cortex, cerebellum, liver, lung and kidney tissues. The average *Pex7* gene expression levels for $Pex7^{hypo/hypo}$ and $Pex7^{hypo/null}$, were 0.394 ± 0.3% and 0.174 ± 0.1% of wild type *Pex7* transcript, respectively. Pex7 transcript was not detected in any tissues from $Pex7^{null/null}$ (**Table 1**).

To investigate the endogenous amounts of PEX7 protein in *Pex7* deficient mice, immunoblot analysis using PEX7 antiserum was performed on brain tissue homogenates. PEX7 protein could not be detected in the brain tissue homogenates from $Pex7^{hypo/null}$ or $Pex7^{null/null}$ mice. However, with higher protein quantity and longer exposure, traces of PEX7 protein were detected in $Pex7^{hypo/hypo}$ mice (**Figure 1**).

3.2 PEX7 Expression Is Reduced in the Cerebellar Tissue From *Pex7* Deficient Mice

The distribution of PEX7 was determined by IHC. PEX7 expression was markedly localized to cerebellar Purkinje cells. Evaluation of cerebellar tissue sections of $Pex7^{hypo/hypo}$ and $Pex7^{hypo/null}$ at 1 month of age revealed a global reduction in PEX7 expression within Purkinje cells. PEX7 expression was completely undetectable in cerebellar Purkinje cells of the

TABLE 1 | *Pex7* transcript levels according to the genotype severity of *Pex7* deficient mice.

Pex7 genotype	*Pex7*				*Hprt*			
	WT/WT	hypo/hypo	hypo/null	null/null	WT/WT	hypo/hypo	hypo/null	null/null
				Cerebral cortex				
Relative expression[a] (SEM)[b]	100.0 (32.61)	0.061 (0.015)	0.016 (0.011)	–	–	–	–	–
Mean Cq[c] (SEM)	23.21 (0.286)	33.37 (0.311)	35.35 (0.885)	–	18.77 (0.373)	18.26 (0.15416)	18.28 (0.495)	18.71 (0.411)
				Cerebellum				
Relative expression (SEM)	100.0 (17.49)	0.181 (0.030)	0.081 (0.039)	–	–	–	–	–
Mean Cq (SEM)	23.85 (0.186)	32.64 (0.166)	35.10 (0.669)	–	17.95 (0.232)	17.59 (0.348)	19.16 (0.235)	18.51 (0.189)
				Liver				
Relative expression (SEM)	100.0 (43.98)	0.529 (0.179)	0.245 (0.096)	–	–	–	–	–
Mean Cq (SEM)	24.09 (0.459)	32.04 (0.321)	33.98 (0.422)	–	20.22 (0.438)	20.60 (0.368)	21.43 (0.372)	21.06 (0.244)
				Lung				
Relative expression (SEM)	100.0 (16.97)	0.566 (0.193)	0.273 (0.076)	–	–	–	–	–
Mean Cq (SEM)	26.14 (0.191)	33.91 (0.305)	36.95 (0.342)	–	20.68 (0.155)	20.90 (0.137)	22.51 (0.204)	21.19 (0.531)
				Kidney				
Relative expression (SEM)	100.0 (23.89)	0.633 (0.134)	0.257 (0.056)	–	–	–	–	–
Mean Cq (SEM)	25.26 (0.227)	33.11 (0.204)	33.77 (0.196)	–	22.96 (0.259)	23.49 (0.225)	22.86 (0.248)	22.81 (0.275)

[a]*Relative expression of Pex7 to Hprt is reported as the percentage of Pex7 wild type expression. Each tissue and genotype represent the means of 3 mice performed in duplicates.*
[b]*SEM (the standard error of mean) which is used as a measure of precision for the estimated mean.*
[c]*Cq (the quantification cycle value of an amplification reaction) is defined as the fractional number of cycles that were needed for the fluorescence to reach a quantification threshold.*

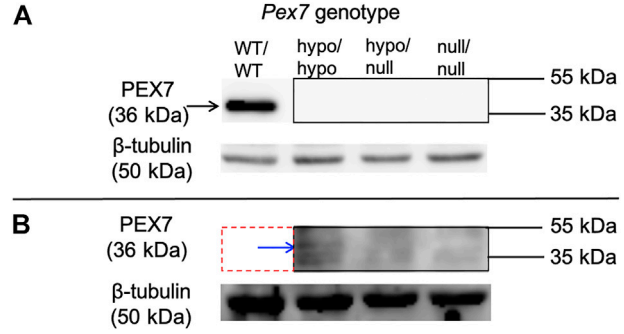

FIGURE 1 | PEX7 protein levels in the brain are undetectable in *Pex7*$^{null/null}$ or *Pex7*$^{hypo/null}$ and barely detectable in *Pex7*$^{hypo/hypo}$ mice. Immunoblotting of the cerebral cortex tissue lysates showing that PEX7 protein is not detected in any of the *Pex7* deficient models at the amount of 40 µg of protein and 10 min exposure time **(A)**. However, at protein quantity of 100 µg and exposure time of 20 min, small amounts of PEX7 protein are only detected in *Pex7*$^{hypo/hypo}$ mice (blue arrow) **(B)**, the red dotted line represents the omitted *Pex7*$^{WT/WT}$ lane due to overexposure. β-tubulin was used as a loading control.

Pex7$^{null/null}$ mice (**Figure 2**). These observations suggested that PEX7 is highly expressed in Purkinje cells and thus could be critical to their normal physiological function.

3.3 *Pex7* Genotype Correlates With Survival Rate and Weight Gain

Survival data of *Pex7* deficient mice showed survival rates of 100% and 91.2% in *Pex7*$^{hypo/hypo}$ and *Pex7*$^{hypo/null}$, respectively, over the 150 days observation period. However, only 22.7% of the *Pex7*$^{null/null}$ mice survived beyond 21 days. Around 45% of *Pex7*$^{null/null}$ pups died within the first 3 days of life and 32% died before weaning (**Figure 3A**). Close observation of the latter showed poor weight gain in general and reduced activity a few days before death; the exact cause of death remains unknown. The *Pex7*$^{hypo/hypo}$ and *Pex7*$^{hypo/null}$ animals weighed 70%–80% and 67%–78% of their control littermates respectively. However, the *Pex7*$^{null/null}$ mice weighed only 47%–53% of littermate controls. Measurements were performed at 1, 4 and 12 months of age (**Figure 3B**). Although body length was not measured, the mice appeared smaller in size, and their length appeared proportional to the reduction in weight.

3.4 *Pex7* Genotype Correlates With Peroxisome Metabolite Levels

3.4.1 Phosphatidylethanolamine Plasmalogens (PlsEtn) Levels

We measured PlsEtn that contain C16:0, C18:0, and C18:1 fatty alcohols at sn-1 in plasma, erythrocytes and tissues (cerebral cortex, cerebellum, lung, heart, liver and kidney) from the *Pex7* deficient mouse series using LC-MS/MS. In *Pex7*$^{hypo/hypo}$ and *Pex7*$^{hypo/null}$, the total PlsEtn levels were reduced to 30%–69% and 20%–50% of wild type controls, respectively. PlsEtn were undetectable in cortical or cerebellar brain regions of *Pex7*$^{null/null}$ mice, and markedly decreased in blood and peripheral tissues to 5%–15% of wild type littermates (**Figure 4**). Pls species containing DHA (C22:6) at *sn-2* showed graded and profound deficiency in all tissues evaluated according to genotype severity.

In control mice (*Pex7*$^{WT/WT}$ and *Pex7*$^{WT/hypo}$), we observed that distribution and quantity of PlsEtn subspecies were tissue dependent. The highest amount of Pls was found in the brain followed by heart, lung, erythrocyte and kidney while the lowest Pls quantity was observed in liver and plasma (**Supplementary Figure S1**). Among PlsEtn species, C18:0 was the most abundant subclass in all tissues examined except lung which was enriched in C16:0. In contrast, C18:1 was the least abundant Pls subspecies in all peripheral tissues evaluated except lung in *Pex7* deficient mice.

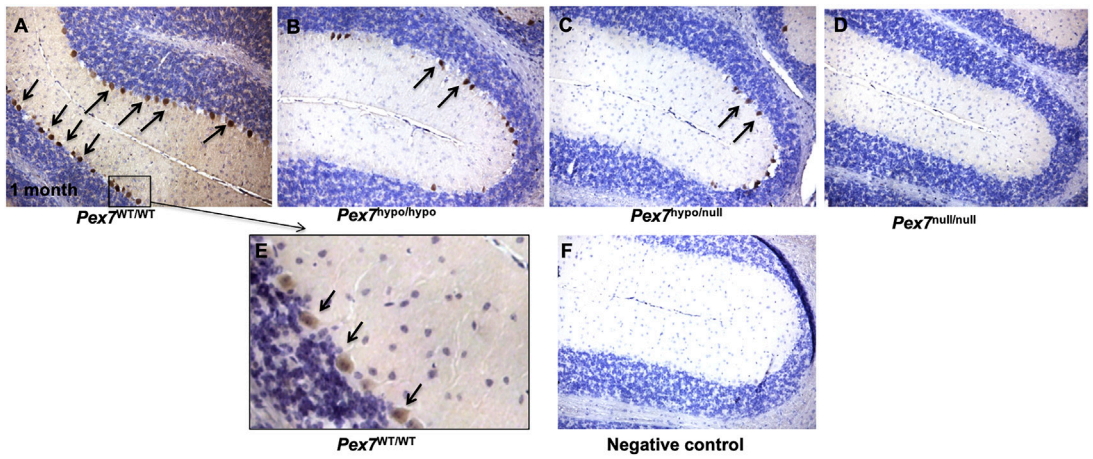

FIGURE 2 | PEX7 protein expression in cerebellar tissues from 1 month old *Pex7* deficient mice. A highly concentrated PEX7 expression was observed in the cerebellar Purkinje cells of $Pex7^{WT/WT}$ **(A, E)** higher magnification). However, the cerebellar Purkinje cell sections from $Pex7^{hypo/hypo}$ $Pex7^{hypo/null}$ **(B, C)** display a reduction in PEX7 expression. PEX7 expression was entirely absent in the cerebellar Purkinje cells of $Pex7^{null/null}$ **(D)**. Negative control includes $Pex7^{WT/WT}$ section without primary PEX7 antibody **(F)**. Slides were counterstained with hematoxylin (Scale bar = 100 μm), ($n = 3$ per genotype). Sections from the same mice at 1 month of age were stained with anti-Calbindin to determine cerebellar Purkinje cells number (see **Figure 8**).

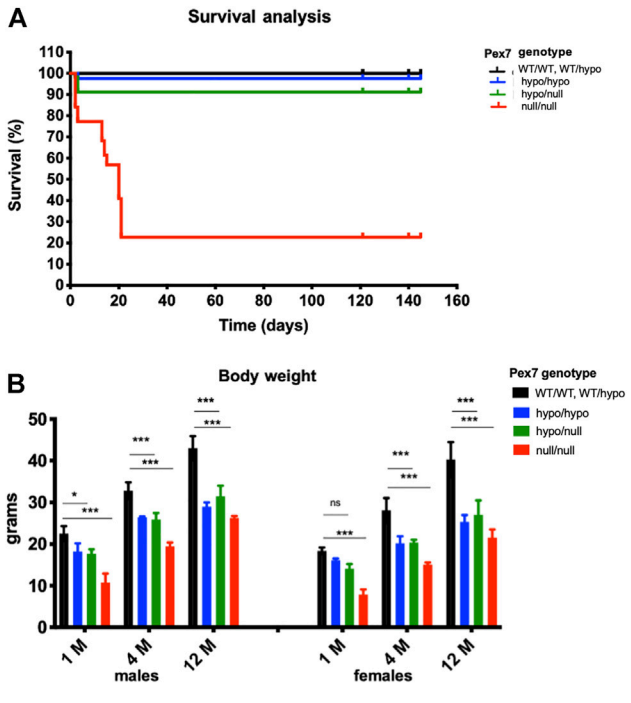

FIGURE 3 | *Pex7* genotype correlates with survival rates and weight gain. Kaplan–Meier plots showing the percentage of survival of *Pex7* deficient mice ($n = 41$–60 per genotype). Analyzing the survival data by log rank tests showed significant differences between genotypes ($p < 0.001$) in accordance to the severity of *Pex7* genotype **(A)**. Graded and significant reduction in body weight according to *Pex7* genotype severity is found in *Pex7* mutants compared to controls at 1, 4, and 12 months (M) of age ($n = 10$–12 per genotype) **(B)**. ns: nonsignificant, $^{*}p < 0.05$, $^{**}p < 0.01$, $^{***}p < 0.001$, $^{****}p < 0.0001$.

There were no significant differences in terms of distribution or quantity of total Pls between the two control groups, $Pex7^{WT/WT}$ and $Pex7^{WT/hypo}$ (**Supplementary Figure S1**).

3.4.2 C26:0-LPC Levels

We examined the levels of C26:0-LPC, a sensitive measure of the VLCFA C26:0 content, in blood and tissues from *Pex7* deficient models using LC-MS/MS. Interestingly, these results showed tissue dependent elevations in C26:0-LPC and a direct correlation between *Pex7* genotype and C26:0-LPC levels. C26:0-LPC levels were highest in lung, but also increased in blood and peripheral tissues (kidney, liver, heart). In contrast, C26:0-LPC levels were normal in cerebral cortex. Specifically, $Pex7^{hypo/hypo}$ showed a 2-7-fold increase in C26:0-LPC levels over *Pex7* controls in lung, liver and blood, whereas $Pex7^{hypo/null}$ exhibited a 2–9-fold increase in all peripheral tissues. However, $Pex7^{null/null}$ mice displayed a more marked elevation of 2–11-fold change over *Pex7* wild type controls in all peripheral tissues as well as the cerebellar region of the brain (**Figure 5**).

3.4.3 Phytanic Acid Levels

Phytanic Acid (PA) levels were examined by GC/MS in plasma, cerebral cortex and cerebellar tissues from the *Pex7* deficient mice at 1, 4, and 12 months of age. While PA was not elevated in plasma or brain tissues from $Pex7^{hypo/hypo}$ mice, a minor and significant elevation of PA levels was found in $Pex7^{hypo/null}$ mice only at 12 months of age. A much higher accumulation of PA was detected in the $Pex7^{null/null}$ mice with the highest elevation observed in plasma compared to brain tissues (**Figure 6**). There is a small amount of PA (0.373 mg/100 g) detected in standard mouse chow. The total free and esterified phytol in standard mouse chow is 1.87 mg/100 g weight of mouse chow.

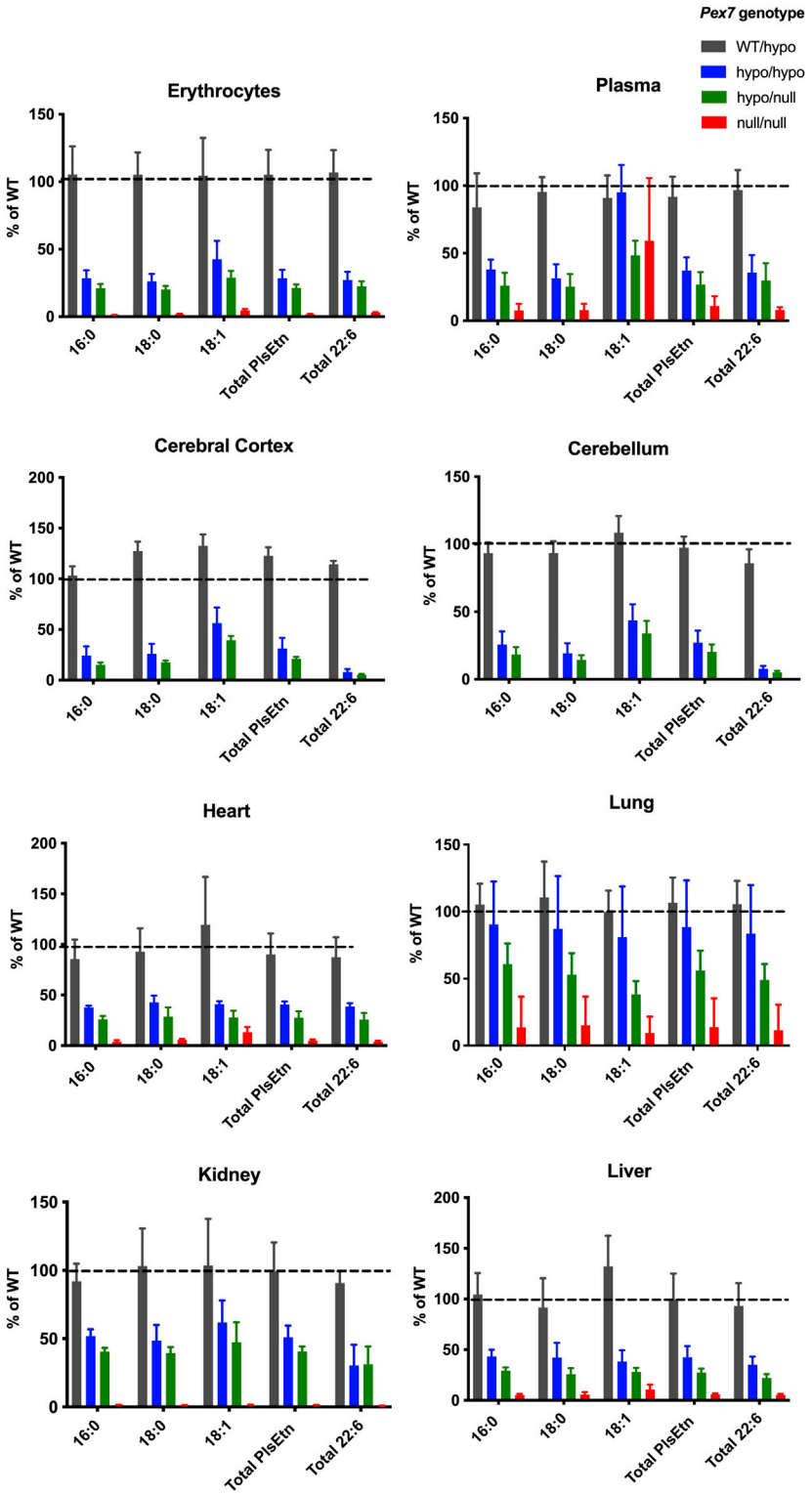

FIGURE 4 | *Pex7* genotype correlates with PlsEtn levels. Pls levels [reported as the percentage of wild type (% of WT)] are significantly decreased in all tissues studied in accordance to the severity of the genotype of *Pex7* deficient mice ($p < 0.0001$, $n = 4$–6 per genotype). The C16:0, C18:0, and C18:1 represent the sum of individual measurements of the PlsEtn species with C16:0, C18:0, or C18:1 fatty alcohol at the *sn*-1 position. Total PlsEtn refers to the sum of these species and the total C22:6 represents the sum of C16:0, C18:0, and C18:1 Pls containing C22:6 fatty acid side chains at the *sn*-2 position.

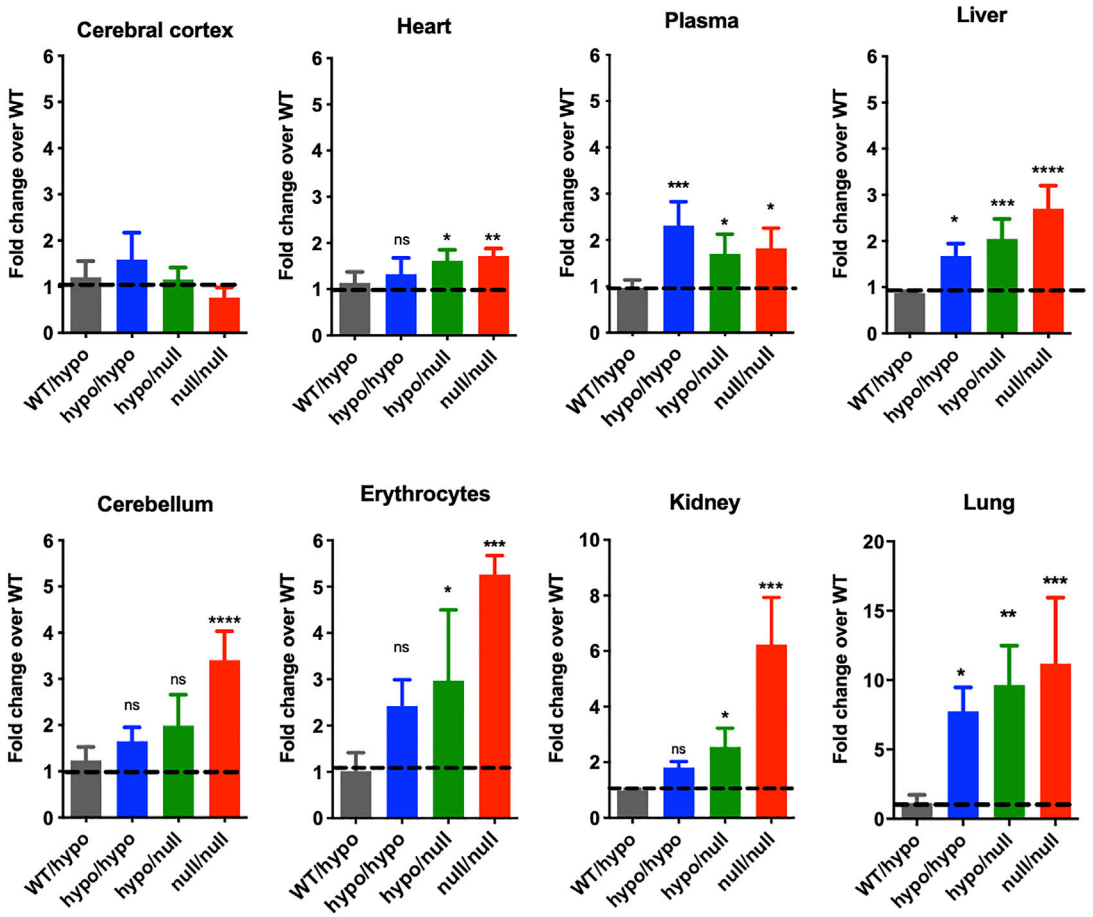

FIGURE 5 | *Pex7* genotype correlates with C26:0-LPC (VLCFA) levels. Elevations in C26:0-LPC represented as fold change over wild-type (WT) are detected in the blood and several tissues of 4-month-old *Pex7* deficient mice. No significant increase in C26:0-LPC levels was found in the cerebral cortex of *Pex7* deficient mice ($n = 4–6$ per genotype). The dotted line represents the C26:0-LPC levels in $Pex7^{WT/WT}$ mice. ns: nonsignificant, $^{*}p < 0.05$, $^{**}p < 0.01$, $^{***}p < 0.001$, $^{****}p < 0.0001$.

Additionally, there is very little phytol in the chlorophyll fraction of mouse chow. We concluded that even these small amounts of PA in rodent diet could lead to PA toxicity over time in *Pex7* deficient mice.

3.5 Peroxisome Metabolites in *Gnpat*$^{null/null}$ Mice

Pex7 deficiency results in a complex biochemical phenotype of Pls and DHA deficiencies in addition to elevations in VLCFA and PA (Brites et al., 2003; Brites et al., 2009; Braverman et al., 2010). To determine whether these biochemical phenotypes were specific for RCDP1 due *Pex7* deficiency or associated with other RCDP types, we concurrently examined the biochemical profiles of plasma and brain tissues from 4-month-old $Gnpat^{null/null}$ mice. We found that $Gnpat^{null/null}$ mice were deficient in total PlsEtn and DHA levels. No accumulation of either C26:0-LPC or PA levels was found in plasma or brain tissues from $Gnpat^{null/null}$ mice compared to their littermate controls (**Supplementary Figure S2**).

3.6 Histopathology of Cortical and Cerebellar Brain Regions of *Pex7* Deficient Mice

Hematoxylin and eosin staining of cortical brain sagittal sections did not show any gross anatomical differences between *Pex7* deficient mice and their littermate controls at 4 months of age (data not shown). However, a reduction in the number of Purkinje cells on cerebellar sagittal sections was observed in $Pex7^{null/null}$ mice and investigated further.

3.6.1 Cerebellar Purkinje Cells Number and Morphology

To further examine and quantify Purkinje cells, we performed IHC using an antibody directed to Purkinje cells (Calbindin-D28K) in the cerebellar tissues from *Pex7* deficient mice at 1, 4, and 12 months of age (**Figure 7**). We observed normal Purkinje cells morphology with reduced intensity of Calbindin staining in *Pex7* deficient mice. At 1 month of age, there were no differences in Purkinje cells quantity between *Pex7* deficient mice and their littermate controls (**Figure**

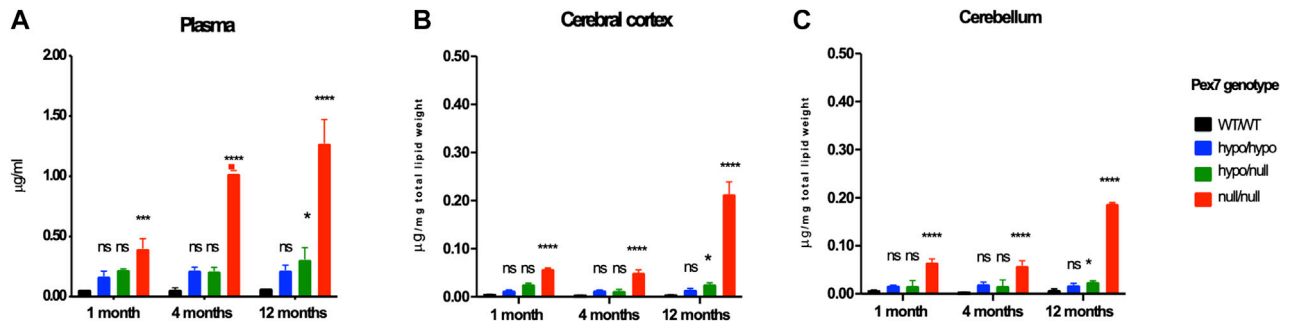

FIGURE 6 | *Pex7* genotype correlates with PA levels. Graded accumulation of PA levels is detected in the plasma **(A)**, cerebral cortex **(B)** and cerebellum **(C)** of *Pex7* deficient mouse models compared to WT controls. (n = 2–4 per genotype). ns: nonsignificant, *p < 0.05, **p < 0.01, ***p < 0.001, ****p < 0.0001.

7A–D). As early as 4 months of age, *Pex7*$^{null/null}$ mice showed a significant loss of Purkinje cells (**Figure 7E–H**). In contrast, *Pex7*$^{hypo/hypo}$ and *Pex7*$^{hypo/null}$ animals had a significant reduction in Purkinje cells number only at 12 months of age (**Figure 7I–L**). In order to determine whether Purkinje cells loss is due to Pls deficiency, accumulated PA [since Purkinje cells loss was documented in the ARD mice fed with 0.1% and 0.25% phytol diet (Ferdinandusse et al., 2008)] or a combination of both, we evaluated cerebellar samples from the *Gnpat*$^{null/null}$ mice at 4 months of age. There was no significant difference in the number of Purkinje cells in *Gnpat*$^{null/null}$ mice compared to their wild-type controls (**Figure 7M,N**). These results suggested that Purkinje cells loss in *Pex7* deficient mice is due to either PA accumulation alone, or the combination of Pls deficiency and elevated PA in this model.

3.6.2 Myelin Content

Since Pls is a critical component of myelin and myelin deficits were previously reported in *Gnpat*$^{null/null}$ mice (Rodemer et al., 2003; Teigler et al., 2009; Malheiro et al., 2019), we evaluated myelin content by IHC using MBP antibody. At 4 months of age, *Pex7*$^{hypo/hypo}$ and *Pex7*$^{hypo/null}$ mice had normal myelination in the corpus callosum and cerebellum, however, reduced MBP staining was observed in cerebellar white matter and corpus callosum in the *Pex7*$^{null/null}$ (data not shown). At 12 months of age, there was a slight reduction in MBP in the corpus callosum and cerebellar white matter of *Pex7*$^{hypo/hypo}$ and *Pex7*$^{hypo/null}$ mice, and an even more pronounced reduction in *Pex7*$^{null/null}$ mice (**Figures 8A–J**). The MBP protein levels of 12-month-old *Pex7* deficient mice were also decreased by immunoblot analysis in a graded fashion according to the genotype (**Figures 8K,L**).

3.7 Behavioral Assessments in *Pex7* Deficient Mice

3.7.1 Increased Baseline Locomotor Activity of *Pex7* Deficient Mice in the Open Field Environment

We performed the open field test to assess the baseline locomotive function of *Pex7* deficient mice in response to a novel environment. In comparison to littermate controls, all *Pex7* deficient mice exhibited increased activity levels in the open field measured by increased total distance traveled and movement (activity) time. This hyperactive behavior was persistent at 1, 4, and 12 months of age in the *Pex7* deficient mouse series and the overall data trended towards a negative correlation between severity of *Pex7* genotype and activity. In fact, the *Pex7*$^{null/null}$ showed the highest activity levels compared to *Pex7* hypomorphic models (**Figure 9**).

3.7.2 Late Onset Cerebellar Ataxia was Only Evident in the *Pex7*$^{null/null}$

PA accumulation and Purkinje cells loss within the cerebellum are often associated with the clinical finding of gait ataxia (Ferdinandusse et al., 2008). We have identified both cerebellar Purkinje cells drop out and increases in plasma and brain PA levels in *Pex7* deficient mice. However, only *Pex7*$^{null/null}$ mice displayed unsteady gait that was clinically evident at the age of 12 months. Considering these findings, we further analyzed the gait pattern and parameters in *Pex7* deficient mice using the CatWalk XT gait analysis system. The 12-month-old *Pex7*$^{null/null}$ mice showed abnormal gait parameters in the form of reduced base of support of the hind paws. No significant differences were found in any of the gait parameters analyzed in the *Pex7* $^{hypo/null}$ model compared to their littermate controls (**Supplementary Figure S3A**).

3.7.3 Working Memory and Exploratory Behavior Were Unaffected in *Pex7* Deficient Mice

To evaluate working memory and exploration of new environment in *Pex7* deficient mice, we performed the forced alternation of a 3-arm Y maze test that consists of 2 test trials with a 30-min interval between the 2 trials. We measured the number of entries of each arm and percent time spent in the novel arm. No significant difference was observed between *Pex7* deficient mice and their littermate controls in the percent of time spent in the novel arm. However, *Pex7* deficient mice showed increased number of entries into each arm compared to littermate controls, which reflects the higher activity levels in these mice that also shown in the open field test (**Supplementary Figures S3B-D**).

3.8 Reduced Brain Neurotransmitter Levels in *Pex7* Deficient Mice

HPLC analysis was performed to examine the levels of the major monoamine neurotransmitters dopamine (DA), norepinephrine (NE)

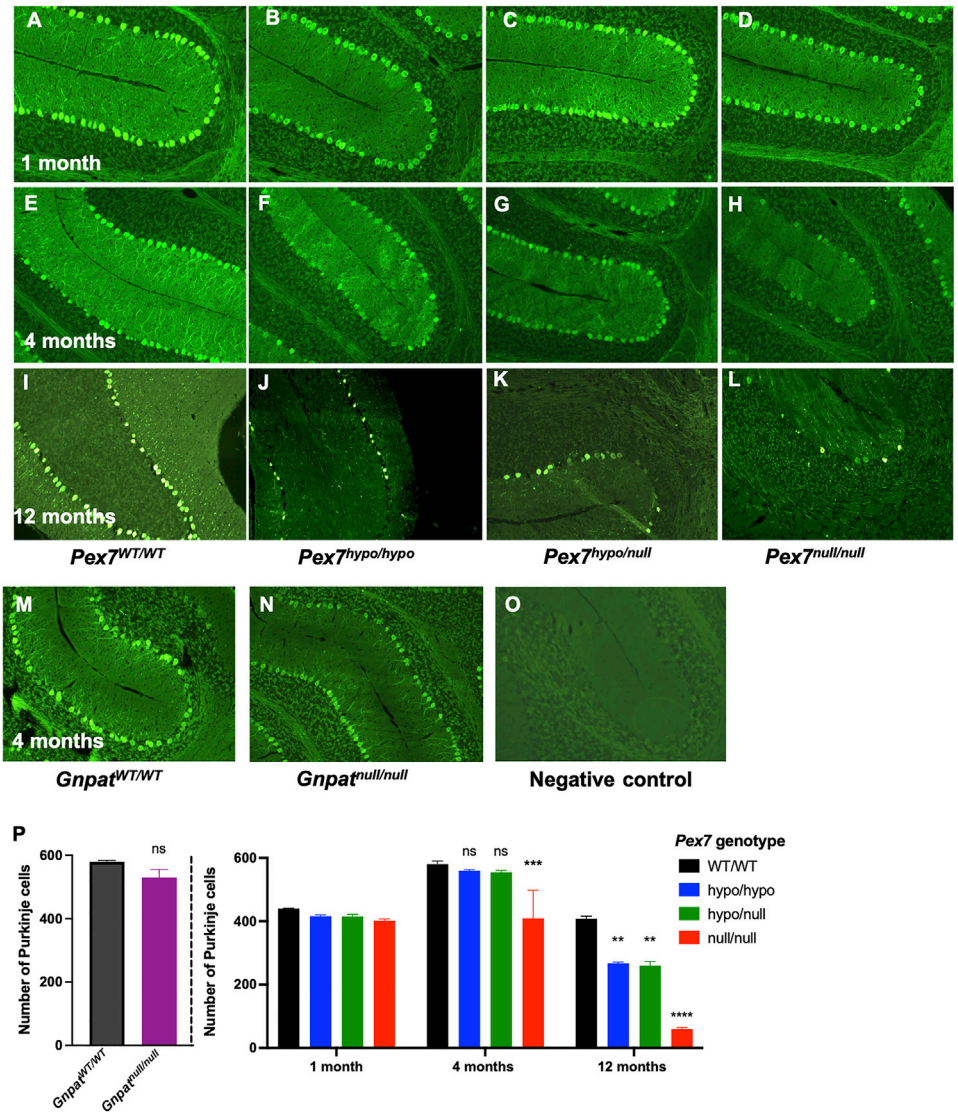

FIGURE 7 | Progressive cerebellar Purkinje cells loss over time in *Pex7* deficient mice. Sagittal sections of cerebellum showed loss of Purkinje cells in the cerebellum of *Pex7* deficient mice at 4 **(E–H)** and 12 months of age **(I–L)** using anti-Calbindin Immunofluorescence staining Negative control includes $Pex7^{WT/WT}$ section without primary Calbindin antibody **(O)**. No loss of Purkinje cells in *Pex7* deficient mice at 1 month of age **(A–D)** or in $Gnpat^{null/null}$ mice **(M, N)**. Quantification of Purkinje cells in *Pex7* and *Gnpat* deficient mice in comparison to their littermate controls revealed significant decrease in Purkinje cells number in *Pex7* deficient mice **(P)**. The severe model ($Pex7^{null/null}$ mice) showed the most significant decrease in Purkinje cells numbers, with the lowest number of Purkinje cells at 12 months of age using anti-Calbindin Immunofluorescence staining. $^{*}p < 0.05$, $^{**}p < 0.01$, $^{***}p < 0.001$ (Scale bar = 100 μm), (n = 3-4 per genotype).

and serotonin (5-hydroxytryptamine; 5-HT) in addition to the amino acid neurotransmitter gamma aminobutyric acid (GABA) in whole brain tissue homogenates from *Pex7* deficient mice. Overall, we found a trend toward reduction in the mean levels of brain neurotransmitters across all genotypes of the *Pex7* deficient mouse series. The deficiency in DA and 5-HT levels was robust and significant in all *Pex7* deficient mice and the reduction of NE and GABA was significant in $Pex7^{hypo/null}$ and $Pex7^{null/null}$ mice. We also observed a tendency toward gradual decrease in the levels of NE and 5-HT from mild to severe *Pex7* deficient mice (**Figure 10B**).

Additionally, we measured the baseline levels of metabolites derived from monoamine neurotransmitters in whole brain tissue homogenates from *Pex7* deficient mice and calculated the ratio of the metabolite to its respective transmitter. This ratio reflects the turnover of monoamine neurotransmitters. No significant differences were observed between *Pex7* deficient mice and their littermate controls for the following metabolites: 5-hydroxyindoleacetic acid (5-HIAA), the main metabolite of 5-HT, 3,4-dihydroxyphenylacetic acid (DOPAC) and homovanillic acid (HVA), the primary metabolites for DA. Investigation of the ratio of the metabolites for the monoamine neurotransmitters revealed a significantly higher DOPAC/DA and 5-HIAA/5-HT ratios in $Pex7^{hypo/hypo}$ and $Pex7^{null/null}$ while the HVA/DA ratio was significantly higher only in $Pex7^{hypo/hypo}$ mouse model. This increase in the metabolite/

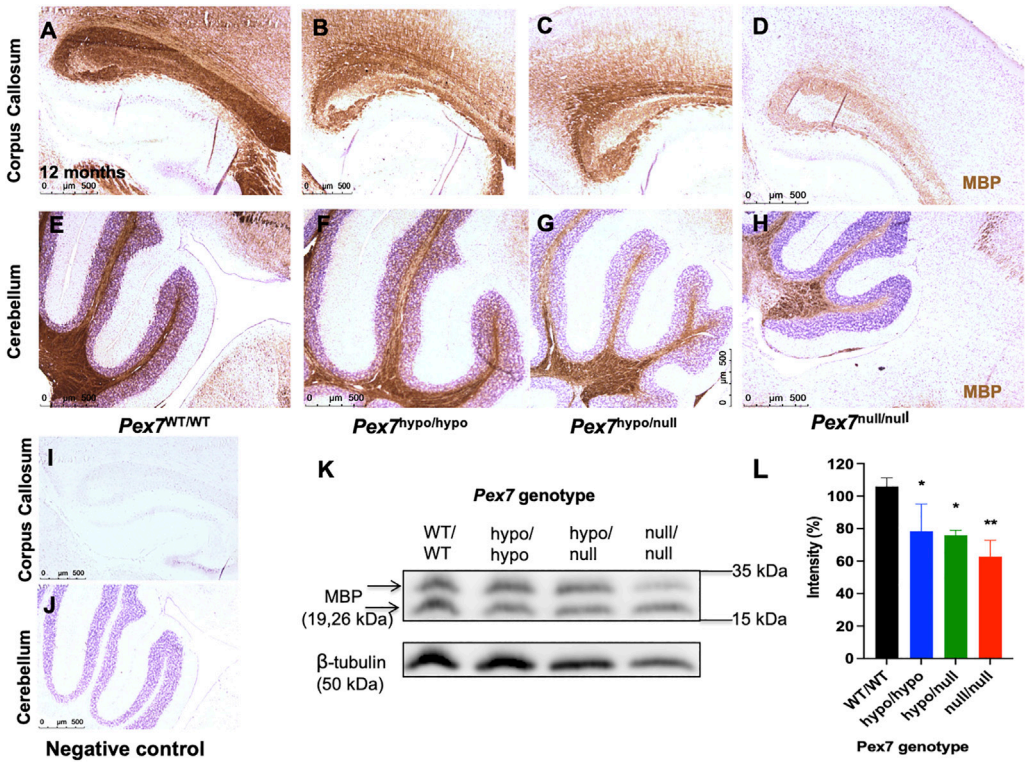

FIGURE 8 | *Pex7* genotype correlates with the myelin content in brain tissues from 12-month-old *Pex7* deficient mice. Sagittal sections of brain tissues: corpus callosum **(A–D)** and cerebellum **(E–H)** show graded reduction in the levels of anti-MBP immunohistochemical staining in 12-month-old *Pex7* deficient mice compared to their littermate controls. Slides were counterstained with hematoxylin **(I, J)** (Scale bar = 500 μm). Graded reduction in the amount of MBP protein levels was found in the immunoblot and densitometric analysis of cerebellar homogenates from *Pex7* deficient mice at 12 months of age **(K, L)**. (*n* = 3 per genotype).

neurotransmitter ratios mainly results from the significant reduction in the levels of neurotransmitters without alteration in their corresponding metabolites (**Supplementary Figure S4**).

3.9 An Association Between the Hyperactive Behavior, Brain Neurotransmitters and Pls Levels in *Pex7* Deficient Mice

We repeated the open field test to evaluate the baseline activity levels in a subgroup of adult *Pex7* deficient mice prior to brain neurotransmitter analysis. Our results confirmed the hyperactive behavior in the *Pex7* hypomorphic mouse series compared to littermate controls (**Figure 10A**). Following the neurotransmitter analysis, a statistical correlation analysis was made to investigate the relation between the neurotransmitter deficits in cerebral cortex and activity levels. We found that the hyperactivity phenotype in *Pex7* deficient mice is inversely correlated with DA, NE, 5-HT, and GABA levels in cortical brain tissues (**Figure 10C**). Additionally, we observed a significant inverse correlation between hyperactivity and PlsEtn levels in plasma and cerebral cortex of *Pex7* deficient mice (**Figure 10D**).

3.10 Brain Neurotransmitter Deficits are Strongly Linked to Cerebral Cortex and Plasma Pls Levels in *Pex7* Deficient Mice

We further investigated the interrelation between brain neurotransmitter measurements and total PlsEtn levels in the cerebral cortex and plasma samples from *Pex7* deficient mice. We found that brain neurotransmitters deficits are positively and significantly correlated with the degree of Pls deficiency in cerebral cortex and plasma from *Pex7* deficient mice (**Figure 11**).

4 DISCUSSION

We generated and evaluated an allelic series of *Pex7* hypomorphic mice to reflect the spectrum of human RCDP1 phenotypes. A comparative analysis of behavioral, biochemical, histological profiles of the nervous system was performed to highlight the effect of Pls deficiency particularly in the milder form of RCDP1. Furthermore, insight into disease pathophysiology can help to improve RCDP1 patient care.

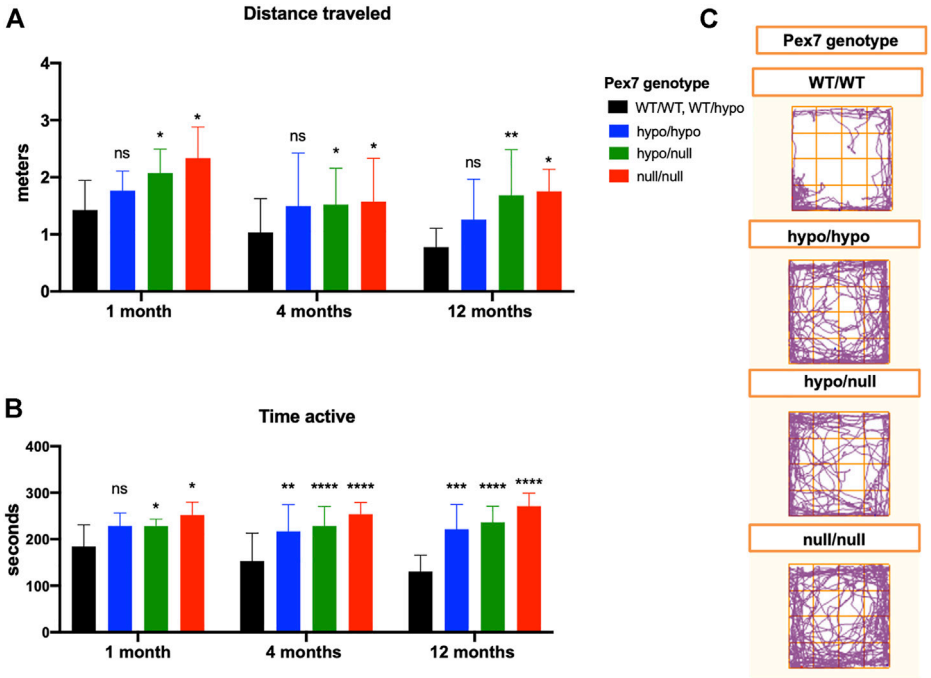

FIGURE 9 | The hyperactivity behavior of *Pex7* deficient mice in the open field environment. *Pex7* deficient mice showed significant increase in activity levels measured by distance traveled **(A)** and activity time **(B)** at different ages in comparison to controls ($Pex7^{WT/WT}$ and $Pex7^{WT/hypo}$). Representative images of track blots recorded during the open field test of *Pex7* deficient mice and their littermate controls **(C)**. Bars represent group means ± SD. ns: nonsignificant, $^{*}p < 0.05$, $^{**}p < 0.01$, $^{***}p < 0.001$, $^{****}p < 0.0001$ (n = 12–36 per genotype).

4.1 Small Increases in *Pex7* Transcript and Protein Levels can Dramatically Improve Phenotypes

Gene expression studies of $Pex7^{hypo/hypo}$ and $Pex7^{hypol/null}$ revealed extremely low levels (<1%) of *Pex7* transcript in all tissues evaluated and undetectable *Pex7* transcript in $Pex7^{null/null}$. However, the high cycle quantification (Cq) values associated with *Pex7* relative expression (above 30) in the *Pex7* hypomorphic models, suggests that *Pex7* transcript levels were extremely low and could be beyond the limit of detection in qPCR analysis (Taylor et al., 2010). Consistent with the reduced transcript levels observed, PEX7 protein levels were very low in tissues from the $Pex7^{hypo/hypo}$ mice, and undetectable by immunoblotting in either $Pex7^{hypo/null}$ or $Pex7^{null/null}$. Although *Pex7* hypomorphic mice exhibited very low *Pex7* transcript and protein levels, the phenotypic manifestations were dramatically improved in comparison to $Pex7^{null/null}$. Overall, these data suggest that small increases in *Pex7* transcript and/or protein can markedly improve the clinical phenotype, which might be substantially beneficial to accelerate future therapeutic interventions.

4.2 Correlations Between *Pex7* Genotype Severity and Phenotypes

4.2.1 Survival

The $Pex7^{null/null}$ had the highest mortality rate of 77% within the first 3 weeks of life, similar to the previously reported $Pex7^{null/null}$ model (Brites et al., 2003). The mortality rate in human patients with classic RCDP was 55% at the age 12 years (Duker et al., 2019). In individuals with mild (nonclassic) RCDP, the estimated mortality rate was only 9% by the end of childhood stage (Duker et al., 2019), similar to the 10% mortality rate that was observed in *Pex7* hypomorphic mice.

4.2.2 Pls Levels

The concept that Pls deficiency plays a key role in determining the degree of phenotype severity in RCDP was first introduced in the initial genotype-phenotype correlation of human RCDP1 patients (Braverman et al., 2002). Accordingly, in previously reported RCDP mouse models, Pls levels were undetectable in $Gnpat^{null/null}$ and severely reduced levels to 5% in erythrocyte and 0.05% in brain tissues from $Pex7^{null/null}$ (Brites et al., 2003; Rodemer et al., 2003). We observed graded reduction of Pls levels in *Pex7* deficient mice according to the severity of RCDP.

4.2.3 C26:0-LPC Levels as a Reflection of VLCFA Levels

Human RCDP1 patients typically do not show elevated VLCFA levels in plasma or have a measurable impairment in peroxisomal fatty acid β-oxidation in cultured skin fibroblasts. However in one study of 20 RCDP patients, a 2-fold increase in C26:0-LPC over controls in blood cells was observed, with normal levels in plasma and fibroblasts (Schutgens et al., 1993). We reported a transient elevation in C26:0-LPC with 1.5-fold increase over controls in erythrocytes from 4 mild RCDP patients (Fallatah et al., 2020). Transient VLCFA elevation was also reported in liver and brain

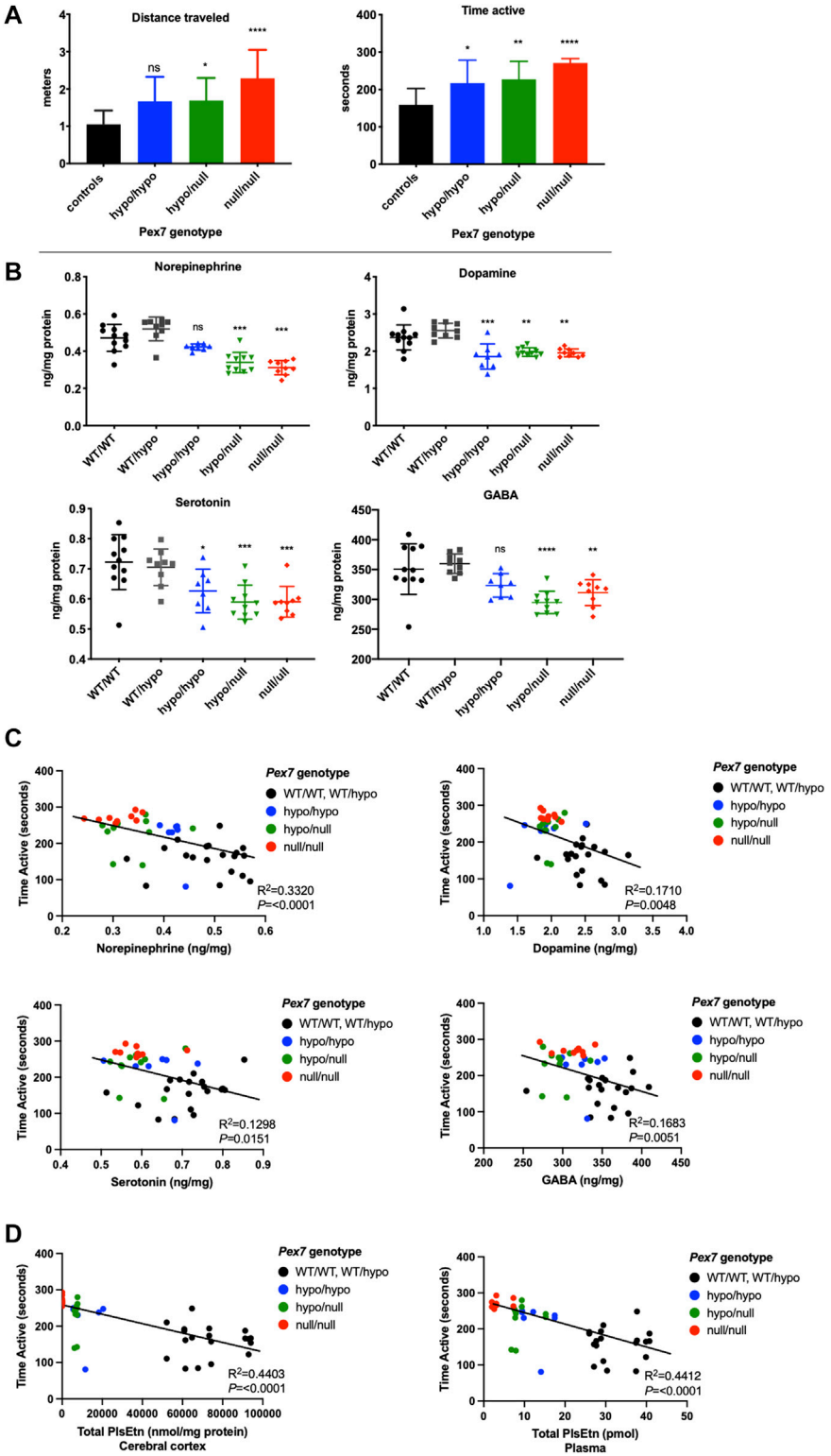

FIGURE 10 | Brain neurotransmitter deficits correlate with activity levels in *Pex7* deficient mice. A significant increase in activity levels of a subset of *Pex7* deficient mice is confirmed before neurotransmitters analysis **(A)**. A significant reduction in dopamine, serotonin, norepinephrine and GABA neurotransmitters is observed in cortical brain tissues from *Pex7* deficient mice compared to littermate controls ($Pex7^{WT/WT}$ and $Pex7^{WT/hypo}$) **(B)**. The hyperactive phenotype in *Pex7* deficient mice is inversely correlated with brain neurotransmitter levels **(C)** and total PlsEtn levels in cerebral cortex as well as plasma **(D)**. Bars represent group means ± SD. ns: nonsignificant, $*p < 0.05$, $**p < 0.01$, $***p < 0.001$, $****p < 0.0001$ (n = 8–10 per genotype).

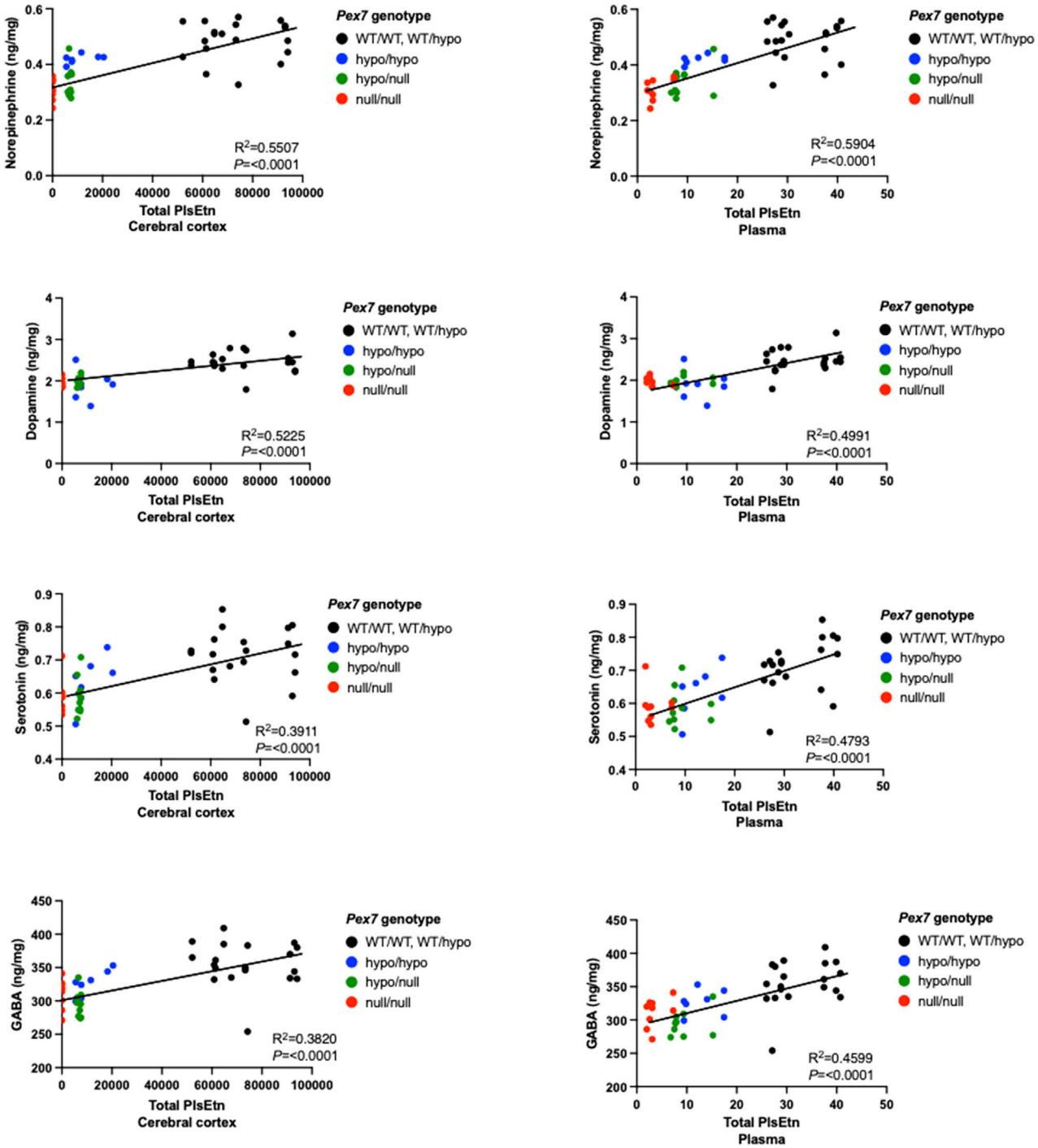

FIGURE 11 | Brain neurotransmitter deficits correlate with total Pls levels in plasma and cerebral cortex samples from *Pex7* deficient mice. A significant positive correlation was found between the brain neurotransmitter levels and total PlsEtn measurements in plasma and cerebral cortex tissue from *Pex7* deficient mice. Total PlsEtn in cerebral cortex was measured as (nmol/mg protein) and in plasma was measured as (pmol). ****$p < 0.0001$ (n = 8–10 per genotype).

tissues from *Pex7* null mice at birth, but normalized by age 2 months (Brites et al., 2003). In the current study, we showed that C26:0-LPC levels were elevated in accordance to genotype severity in *Pex7* deficient mice at 4 months of age. The extent of C26:0 elevation was variable between examined tissues and showed a range of 2- to 11-fold increase over WT in sampled

peripheral tissues. Surprisingly, no accumulation of C26:0-LPC was found in cerebral cortex. We compared C26:0-LPC levels in our *Pex7* deficient mice to a previously reported mouse model of the peroxisome biogenesis disorder Zellweger Spectrum disorder (*Pex5* KO) and the peroxisomal enzyme/transporter deficiency X-linked adrenoleukodystrophy (*Abcd1* KO). *Pex5* KO mice showed a range of 3- to 9-fold increase over WT in C26:0 VLCFA in plasma and brain tissues at 3 months of age (Baes et al., 1997; Baes et al., 2002). *Abcd1* KO mice displayed 4- to 5-fold C26:0 increase over WT in brain, spinal cord, liver, spleen, kidney and testis at 6 months of age (Brites et al., 2009). Thus, the elevation of VLCFA in *Pex7* deficiency is distinguished by being absent in the cerebral cortex making it unlikely to contribute to the cortical phenotype in *Pex7* deficient mice. Tissue elevation is most likely due to the absence of ACAA1 thiolase without full compensation from SCPx, which is imported by PEX5. Tissue specific differences in VLCFA levels in the *Pex7* deficient mice could reflect tissue specific availability of the SCPx protein.

4.2.4 PA Levels

To determine the significance of elevated PA, we compared levels in plasma and brain tissues from our *Pex7* deficient mice and previously reported ARD mouse model ($Phyh^{null/null}$ mice) with isolated defects in PA oxidation. To make the comparison of PA levels between *Pex7* deficient mice and ARD mice, we used fold change over WT which would adjust and correct for unit differences and make the comparison between studies possible. Seven-week-old ARD mice on standard chow showed an 80-fold increase over control in plasma with undetectable levels in cerebellar tissues (Ferdinandusse et al., 2008). We have shown that $Pex7^{null/null}$ have a gradual and significant accumulation of PA, with 6-fold increase at 1 month and 18-fold increase at 12 months of age compared to $Pex7^{WT/WT}$ in plasma, and 12- to 67-fold increase compared to $Pex7^{WT/WT}$ in brain. In plasma and brain tissues from $Pex7^{hypo/null}$ mice, there was a 3- and 5-fold increase respectively over $Pex7^{WT/WT}$ at 12 months of age. Thus, plasma PA levels accumulate in Pex7 deficiency and partially correlate to genotype but are higher in the ARD mouse model.

We found a small amount of PA (0.373 mg/100 g) in standard mouse chow. The total free and esterified phytol in standard mouse chow was 1.87 mg/100 g weight of mouse chow. If a mouse eats 4 g of chow per day, then they are getting around 80 μg of phytol/esters plus PA, equal to 96 μg per day. We concluded that even these small amounts of PA in rodent chow could lead to PA toxicity over time in *Pex7* deficient mice. The 6-fold–67-fold elevation over wild type (that is dependent on age and tissue) observed in our mice corresponds to the 20–100-fold elevation that can be seen in ARD patients on regular diets (Baldwin et al., 2010). The tolerable daily intake for ARD patients is less than 10 mg of phytol per day (Krauß et al., 2017). Also, PA levels in liver and brain tissue from 8-week-old *Pex1* hypomorphic mice on standard mouse chow were 100-fold and 7-fold elevated respectively compared to wild type mice (Moser et al. unpublished data). Thus, it is apparent that significant amounts of phytol are in standard mouse chow, and depending on the mice ability to degrade this, can accumulate in tissues.

The pathological consequences of elevated PA were investigated in ARD mice supplemented with 0.1%–0.25% phytol diet for 3–6 weeks (Ferdinandusse et al., 2008). Phytol-treated ARD mice exhibited unsteady gait with reduced base of support for the hind paws in the CatWalk system (ataxia), delayed motor nerve conduction velocity (peripheral neuropathy) and loss of cerebellar Purkinje cells. The authors of the study (Ferdinandusse et al., 2008) suggested that Purkinje cells loss could be a result of elevated PA and lead to the ataxia. We found that $Pex7^{null/null}$ mice displayed significant Purkinje cells loss by 4 months of age which was more prominent and associated with ataxia at age 12 months, as well as a significant elevation of PA. $Pex7^{hypo/hypo}$ and $Pex7^{hypo/null}$ mice had lower PA levels in cerebellum, a milder reduction in the number of cerebellar Purkinje cells and no gait abnormalities at age of 12 months. These data also suggest that PA accumulation to critical levels could result in Purkinje cells loss and clinical manifestation of cerebellar ataxia. In the ARD mouse model Purkinje cell loss occurred only after phytol supplementation and without the effect of Pls deficiency. In our *Pex7* deficient series, which did not receive phytol supplementation but did receive small amounts from standard chow, we proposed that Pls deficiency might exacerbate the effect of PA accumulation and subsequently lead to Purkinje cell loss as well as ataxic gait. Similarly, a previous report showed that Pls deficiency can aggravate the pathology of elevated VLCFA (Brites et al., 2009). We think that the comparison of PA levels between *Pex7* deficient mice and the ARD mouse model is a crucial step for clinical significance as it provides insight into the threshold at which PA levels could lead to neuropathological manifestation of Purkinje cell loss and clinical presentation of ataxia. PA levels could be a valuable clinical tool to manage in order to prevent the clinical manifestation of ataxia and Purkinje cell loss overtime particularly in patients with milder form of PEX7 deficiency.

Purkinje cell loss was previously reported in postmortem examinations of 3 patients with classic (severe) RCDP and it was suggested to be the causative factor of cerebellar atrophy found in RCDP patients although the levels of PA in 2 cases were not provided and mentioned to be high only in a single patient (Powers and Moser, 1998; Powers et al., 1999). It is possible that the development of cerebellar atrophy could be preventable by applying a PA-restricted diet.

4.3 Behavioral Abnormalities and Neurotransmitter Defects are Linked to Pls Deficiency

Neurobehavioral disorders including autism spectrum disorder (ASD) and attention deficit hyperactivity disorder (ADHD) were reported in patients with milder forms of RCDP (Bams-Mengerink et al., 2013; Yu et al., 2013). In addition, we found that 56% of mild RCDP individuals have behavioral abnormalities (Fallatah et al., 2020). Our results revealed that *Pex7* deficient mice displayed a hyperactive behavior, which also matches the previous report of a hyperactivity phenotype in the $Gnpat^{null/null}$ (RCDP2) mouse model (Dorninger et al., 2019b). Pls deficiency could be a contributing factor in the development

of this hyperactive behavior through the role of PLs in regulating brain neurotransmitter homeostasis.

In this study we detected significant deficiencies in major brain neurotransmitters including DA, 5-HT, NE, and GABA in brain homogenates from *Pex7* deficient mice with a significant correlation to activity levels. Also, we found that deficits in NE and 5-HT were strongly correlated with Pls levels and thus the severity of Pex7 genotype. Similar neurotransmitter deficits were reported in *Gnpat*$^{null/null}$ mice and were proposed to be caused by defects in presynaptic neurotransmitter release and an impairment in vesicular uptake (Dorninger et al., 2019b). Brodde et al., (2012) showed an impairment in presynaptic release of glutamate and acetylcholine neurotransmitters in murine nerve terminals (synaptosomes) isolated from *Gnpat*$^{null/null}$ mice with reduction in exocytosis of endogenous acetylcholine and glutamate by 50%—60% of normal control synaptosomes. Additionally, *in vitro* radiolabeled neurotransmitter release studies of slices from hippocampus and parietal cortex of *Gnpat*$^{null/null}$ mice showed 22%–30% reduction in [^{3}H] norepinephrine release upon chemical and electrical stimuli. Decreased levels of vesicular monoamine transporter type 2 (VMAT2) were observed in striatum from *Gnpat*$^{null/null}$ mice. VMAT2 is responsible for transporting monoamines from the cytosol to presynaptic vesicles and its reduction could affect the transport of neurotransmitters into synaptic vesicles therefore causing the depletion in monoamine neurotransmitters in Pls deficient mice (Dorninger et al., 2019b). Additionally, the hyperactive phenotype was previously reported in non-peroxisomal mouse models with deficiency in brain neurotransmitters including dopamine (Giros et al., 1996), 5-HT (Whitney et al., 2016) and GABA (Chen et al., 2015), which further supports the hypothesis of a direct role of brain neurotransmitter deficits in the manifestation of hyperactivity. For the future, it is possible to investigate RCDP patients for neurotransmitter deficits - urine, plasma or CSF can be analyzed for 5-HT, DA, NE as well as neurotransmitter metabolites (5-HIAA, HVA).

In the nervous system, Pls are considered as a critical source of the polyunsaturated omega-3 essential fatty acid DHA (22:6 n−3) that plays a crucial role in brain development, myelination and function (Hishikawa et al., 2017). In a prior cross-sectional study of 53 school age children with ADHD and age-matched normal controls, a lower proportion of plasma levels of DHA 22:6 *n*−3 was found in ADHD group (Burgess et al., 2000). Additionally, a deficiency of DHA in rhesus monkeys was associated with a stereotyped behavior (Reisbick et al., 1994). Also, previous studies indicated a deficiency of DHA in brain tissues and erythrocytes from *Gnpat*$^{null/null}$ (Rodemer et al., 2003) and hypomorphic *Pex7* mice (Braverman et al., 2010). In the current project, we show a reduction in all Pls in addition to DHA-containing Pls in brain tissues from *Pex7* deficient mice using LC-MS/MS. We propose that DHA deficiency might contribute to the development of the hyperactivity phenotype observed in *Pex7* deficient mice.

To summarize, we engineered an allelic series of Pex7 deficient mice based on reductions of a normal Pex7 transcript, that mimics the human RCDP1 spectrum. *Pex7* deficient mice showed genotype-phenotype correlations in terms of survival, body weight, peroxisome metabolites (Pls, C26:0-LPC, and PA) neurochemical, neuroanatomical and neurobehavioral (neurotransmitter levels, myelination, Purkinje cells numbers, and activity levels) manifestations. This graded genotype-phenotype correlation provided a type of "dose response" that strengthened the association of the phenotypes with *Pex7* deficiency. The marked improvement in survival and body weight with only marginal changes in *Pex7* transcript and PEX7 protein levels from the null to the hypomorphic model should facilitate the efficacy of any future molecular therapies in RCDP.

Our results of the hyperactivity behavior in *Pex7* deficient mice suggest that reduced Pls levels play a significant role in the development of behavioral dysfunction associated with RCDP. This hyperactivity is sensitive to small reductions in Pls levels and could represent the neurobehavioral phenotype observed in mild (nonclassic) RCDP patients. We recently showed that oral supplementation of a mature synthetic Pls improved Pls levels in plasma, erythrocyte, heart, liver, small intestine and skeletal muscle tissues from *Pex7*$^{hypo/null}$ mice (Fallatah et al., 2019). Although we did not observe an augmentation in Pls levels in the cerebral cortex and cerebellum, mature Pls effectively normalized the hyperactive behavioral phenotype in *Pex7* deficient mice.

Our data highlight the significant correlation that was observed in *Pex7* deficient mice between the hyperactivity, brain neurotransmitter deficits and Pls deficiency. These key findings emphasize the mechanistic role of Pls deficiency in regulating brain function and behavior. While the underlying mechanisms of PEX7 defects as well as Pls deficiency in complex brain behavior is still unknown, we speculate that Pls deficiency results in altered membrane lipid composition that could directly influence the basic physiological function of cellular membranes in the nervous system. Additionally, Pls deficiency might affect the overall cellular signaling as well as intracellular pathways and synaptic release and transmission, which might lead to impairments in brain function.

DATA AVAILABILITY STATEMENT

The original contributions presented in the study are included in the article/**Supplementary Material**, further inquiries can be directed to the corresponding authors.

ETHICS STATEMENT

The animal study was reviewed and approved by the Institutional Animal Care Committee of McGill University, Canada (protocol #5538) and the Austrian Federal Ministry of Science and Research (BMBWF-66.009/0174-V/3b/2019) as well as the Institutional Animal Care and Use Committee of the Medical University of Vienna, Austria.

AUTHOR CONTRIBUTIONS

WF designed the experiments, collected and processed tissues, performed all *Pex7* deficient mouse–related experiments, carried out data analyses and interpretations and wrote the manuscript. WC established the *Pex7* deficient mice colony, breeding scheme, and genotyping protocols, generated and maintained the *Pex7* hypomorphic mice, and designed primers for qPCR experiments. EP designed, performed and interpreted data from LC-MSMS lipid analysis. GC and BP assisted with histology, genotyping and behavioral experiments. FD collected tissues from *Gnpat* deficient mice. FD, CP, and JB designed, performed, and interpreted data from HPLC analysis for brain neurotransmitters levels. AM designed, performed, and interpreted data from GC-MSMS analysis for branched-chain fatty acids. NB designed and supervised the experiments, contributed to the interpretation of results and wrote the manuscript. All authors critically reviewed the manuscript before submission.

FUNDING

This project was supported by E-Rare-3 Joint Translational Call (2015) supported by Canadian Institute of Health Research and Fonds de Recherche du Quebec Sante (NB) (E-Rare # ERT-144213 and #34575) and the Austrian Science Fund, FWF (JB; I2738-B26), and a scholarship from King AbdulAziz University to WF. Additional support to JB and FD was provided by the FWF (P34723, P24843-B24, P31082-B21) and RhizoKids International.

ACKNOWLEDGMENTS

We would like to thank the managers Anna Choy, Joshua Ejdelman and the staff of the animal resources division at the RI-MUHC for animal care and behavioral room support, and Mathieu Simard the Platform manager of McGill Small Animal Imaging Labs for his help with the CatWalk gait analysis. Also, we would like to thank members of Guillaume Sébire, Rima Rozen, Loydie Jerome-Majewska, Myriam Baes, and Stacey Rizzo laboratories for guidance and assistance with behavioral tests and IHC/IF staining techniques. In addition, we want to credit Harald Reither and Gerhard Zeitler for excellent technical support. We give special thanks to RhizoKids International for inspiring this project.

SUPPLEMENTARY MATERIAL

The Supplementary Material for this article can be found online at: https://www.frontiersin.org/articles/10.3389/fcell.2022.886316/full#supplementary-material

REFERENCES

Argyriou, C., Polosa, A., Cecyre, B., Hsieh, M., Di Pietro, E., Cui, W., et al. (2019). A Longitudinal Study of Retinopathy in the PEX1-Gly844Asp Mouse Model for Mild Zellweger Spectrum Disorder. *Exp. Eye Res.* 186, 107713. doi:10.1016/j.exer.2019.107713

Baes, M., Gressens, P., Baumgart, E., Carmeliet, P., Casteels, M., Fransen, M., et al. (1997). A Mouse Model for Zellweger Syndrome. *Nat. Genet.* 17 (1), 49–57. doi:10.1038/ng0997-49

Baes, M., Dewerchin, M., Janssen, A., Collen, D., and Carmeliet, P. (2002). Generation ofPex5-loxP Mice Allowing the Conditional Elimination of Peroxisomes. *Genesis* 32 (2), 177–178. doi:10.1002/gene.10047

Baldwin, E. J., Gibberd, F. B., Harley, C., Sidey, M. C., Feher, M. D., and Wierzbicki, A. S. (2010). The Effectiveness of Long-Term Dietary Therapy in the Treatment of Adult Refsum Disease. *J. Neurol. Neurosurg. Psychiatry* 81 (9), 954–957. doi:10.1136/jnnp.2008.161059

Bams-Mengerink, A. M., Majoie, C. B. L. M., Duran, M., Wanders, R. J. A., Van Hove, J., Scheurer, C. D., et al. (2006). MRI of the Brain and Cervical Spinal Cord in Rhizomelic Chondrodysplasia Punctata. *Neurology* 66 (6), 798–803. discussion 789. doi:10.1212/01.wnl.0000205594.34647.d0

Bams-Mengerink, A. M., Koelman, J. H., Waterham, H., Barth, P. G., and Poll-The, B. T. (2013). The Neurology of Rhizomelic Chondrodysplasia Punctata. *Orphanet J. Rare Dis.* 8, 174. doi:10.1186/1750-1172-8-174

Baroy, T., Koster, J., Strømme, P., Ebberink, M. S., Misceo, D., Ferdinandusse, S., et al. (2015). A Novel Type of Rhizomelic Chondrodysplasia Punctata, RCDP5, Is Caused by Loss of the PEX5 Long Isoform. *Hum. Mol. Genet.* 24 (20), 5845–5854. doi:10.1093/hmg/ddv305

Barr, D. G., Kirk, J. M., al Howasi, M., Wanders, R. J., and Schutgens, R. B. (1993). Rhizomelic Chondrodysplasia Punctata with Isolated DHAP-AT Deficiency. *Archives Dis. Child.* 68 (3), 415–417. doi:10.1136/adc.68.3.415

Braverman, N. E., and Moser, A. B. (2012). Functions of Plasmalogen Lipids in Health and Disease. *Biochim. Biophys. Acta (BBA) - Mol. Basis Dis.* 1822 (9), 1442–1452. doi:10.1016/j.bbadis.2012.05.008

Braverman, N., Steel, G., Obie, C., Moser, A., Moser, H., Gould, S. J., et al. (1997). Human PEX7 Encodes the Peroxisomal PTS2 Receptor and Is Responsible for Rhizomelic Chondrodysplasia Punctata. *Nat. Genet.* 15 (4), 369–376. doi:10.1038/ng0497-369

Braverman, N., Steel, G., Lin, P., Moser, A., Moser, H., and Valle, D. (2000). PEX7 Gene Structure, Alternative Transcripts, and Evidence for a Founder Haplotype for the Frequent RCDP Allele, L292ter. *Genomics* 63 (2), 181–192. doi:10.1006/geno.1999.6080

Braverman, N. E., Steinberg, S. J., Fallatah, W., Duker, A., and Bober, M. (2001). "Rhizomelic Chondrodysplasia Punctata Type 1,". [Internet] in Gene*Reviews*®. Editors R. A. Pagon, Ardinger, and e.a. HH (Seattle (WA)Seattle: University of Washington), 1993–2020. Updated 2020 Jan 30.

Braverman, N., Chen, L., Lin, P., Obie, C., Steel, G., Douglas, P., et al. (2002). Mutation Analysis of PEX7 in 60 Probands with Rhizomelic Chondrodysplasia Punctata and Functional Correlations of Genotype with Phenotype. *Hum. Mutat.* 20 (4), 284–297. doi:10.1002/humu.10124

Braverman, N., Zhang, R., Chen, L., Nimmo, G., Scheper, S., Tran, T., et al. (2010). A Pex7 Hypomorphic Mouse Model for Plasmalogen Deficiency Affecting the Lens and Skeleton. *Mol. Genet. Metabolism* 99 (4), 408–416. doi:10.1016/j.ymgme.2009.12.005

Brites, P., Motley, A. M., Gressens, P., Mooyer, P. A., Ploegaert, I., Everts, V., et al. (2003). Impaired Neuronal Migration and Endochondral Ossification in Pex7 Knockout Mice: a Model for Rhizomelic Chondrodysplasia Punctata. *Hum. Mol. Genet.* 12 (18), 2255–2267. doi:10.1093/hmg/ddg236

Brites, P., Waterham, H. R., and Wanders, R. J. (2004). Functions and Biosynthesis of Plasmalogens in Health and Disease. *Biochim. Biophys. Acta* 1636 (2-3), 219–231. doi:10.1016/j.bbalip.2003.12.010

Brites, P., Mooyer, P. A., El Mrabet, L., Waterham, H. R., and Wanders, R. J. (2009). Plasmalogens Participate in Very-Long-Chain Fatty Acid-Induced Pathology. *Brain* 132 (Pt 2), 482–492. doi:10.1093/brain/awn295

Brodde, A., Teigler, A., Brugger, B., Lehmann, W. D., Wieland, F., Berger, J., et al. (2012). Impaired Neurotransmission in Ether Lipid-Deficient Nerve Terminals. *Hum. Mol. Genet.* 21 (12), 2713–2724. doi:10.1093/hmg/dds097

Buchert, R., Tawamie, H., Smith, C., Uebe, S., Innes, A. M., Al Hallak, B., et al. (2014). A Peroxisomal Disorder of Severe Intellectual Disability, Epilepsy, and

Cataracts Due to Fatty Acyl-CoA Reductase 1 Deficiency. *Am. J. Hum. Genet.* 95 (5), 602–610. doi:10.1016/j.ajhg.2014.10.003

Burgess, J. R., Stevens, L., Zhang, W., and Peck, L. (2000). Long-chain Polyunsaturated Fatty Acids in Children with Attention-Deficit Hyperactivity Disorder. *Am. J. Clin. Nutr.* 71 (1 Suppl. l), 327S–30S. doi:10.1093/ajcn/71.1.327S

Chen, L., Yang, X., Zhou, X., Wang, C., Gong, X., Chen, B., et al. (2015). Hyperactivity and Impaired Attention in Gamma Aminobutyric Acid Transporter Subtype 1 Gene Knockout Mice. *Acta Neuropsychiatr.* 27 (6), 368–374. doi:10.1017/neu.2015.37

da Silva, T. F., Eira, J., Lopes, A. T., Malheiro, A. R., Sousa, V., Luoma, A., et al. (2014). Peripheral Nervous System Plasmalogens Regulate Schwann Cell Differentiation and Myelination. *J. Clin.* . 124 (6), 2560–2570. doi:10.1172/jci72063

Dacremont, G., and Vincent, G. (1995). Assay of Plasmalogens and Polyunsaturated Fatty Acids (PUFA) in Erythrocytes and Fibroblasts. *J. Inherit. Metab. Dis.* 18 (Suppl. 1), 84–89. doi:10.1007/978-94-011-9635-2_7

Dacremont, G., Cocquyt, G., and Vincent, G. (1995). Measurement of Very Long-Chain Fatty Acids, Phytanic and Pristanic Acid in Plasma and Cultured Fibroblasts by Gas Chromatography. *J. Inherit. Metab. Dis.* 18 (Suppl. 1), 76–83. doi:10.1007/978-94-011-9635-2_6

Di Cara, F., Sheshachalam, A., Braverman, N. E., Rachubinski, R. A., and Simmonds, A. J. (2017). Peroxisome-Mediated Metabolism Is Required for Immune Response to Microbial Infection. *Immunity* 47 (1), 93–106.e7. doi:10.1016/j.immuni.2017.06.016

Dorninger, F., Forss-Petter, S., and Berger, J. (2017a). From Peroxisomal Disorders to Common Neurodegenerative Diseases - the Role of Ether Phospholipids in the Nervous System. *FEBS Lett.* 591 (18), 2761–2788. doi:10.1002/1873-3468.12788

Dorninger, F., Herbst, R., Kravic, B., Camurdanoglu, B. Z., Macinkovic, I., Zeitler, G., et al. (2017b). Reduced Muscle Strength in Ether Lipid-Deficient Mice Is Accompanied by Altered Development and Function of the Neuromuscular Junction. *J. Neurochem.* 143 (5), 569–583. doi:10.1111/jnc.14082

Dorninger, F., Gundacker, A., Zeitler, G., Pollak, D. D., and Berger, J. (2019a). Ether Lipid Deficiency in Mice Produces a Complex Behavioral Phenotype Mimicking Aspects of Human Psychiatric Disorders. *Int. J. Mol. Sci.* 20 (16), 3929. doi:10.3390/ijms20163929

Dorninger, F., König, T., Scholze, P., Berger, M. L., Zeitler, G., Wiesinger, C., et al. (2019b). Disturbed Neurotransmitter Homeostasis in Ether Lipid Deficiency. *Hum. Mol. Genet.* 28 (1), 2046–2061. doi:10.1093/hmg/ddz040

Duker, A. L., Eldridge, G., Braverman, N. E., and Bober, M. B. (2016). Congenital Heart Defects Common in Rhizomelic Chondrodysplasia Punctata. *Am. J. Med. Genet.* 170 (1), 270–272. doi:10.1002/ajmg.a.37404

Duker, A. L., Niiler, T., Kinderman, D., Schouten, M., Poll-The, B. T., Braverman, N., et al. (2019). Rhizomelic Chondrodysplasia Punctata Morbidity and Mortality, an Update. *Am. J. Med. Genet. A* 182 (3), 579–583. doi:10.1002/ajmg.a.61413

Fallatah, W., Smith, T., Cui, W., Jayasinghe, D., Di Pietro, E., Ritchie, S. A., et al. (2019). Oral Administration of a Synthetic Vinyl-Ether Plasmalogen Normalizes Open Field Activity in a Mouse Model of Rhizomelic Chondrodysplasia Punctata. *Dis. Model Mech.* 13 (1), dmm042499. doi:10.1242/dmm.042499

Fallatah, W., Schouten, M., Yergeau, C., Di Pietro, E., Engelen, M., Waterham, H. R., et al. (2020). Clinical, Biochemical, and Molecular Characterization of Mild (Nonclassic) Rhizomelic Chondrodysplasia Punctata. *J. Inherit. Metab. Dis.* 44 (4), 1021–1038. doi:10.1002/jimd.12349

Ferdinandusse, S., Zomer, A. W. M., Komen, J. C., van den Brink, C. E., Thanos, M., Hamers, F. P. T., et al. (2008). Ataxia with Loss of Purkinje Cells in a Mouse Model for Refsum Disease. *Proc. Natl. Acad. Sci. U.S.A.* 105 (46), 17712–17717. doi:10.1073/pnas.0806066105

Giros, B., Jaber, M., Jones, S. R., Wightman, R. M., and Caron, M. G. (1996). Hyperlocomotion and Indifference to Cocaine and Amphetamine in Mice Lacking the Dopamine Transporter. *Nature* 379 (6566), 606–612. doi:10.1038/379606a0

Hishikawa, D., Valentine, W. J., Iizuka-Hishikawa, Y., Shindou, H., and Shimizu, T. (2017). Metabolism and Functions of Docosahexaenoic Acid-Containing Membrane Glycerophospholipids. *FEBS Lett.* 591 (18), 2730–2744. doi:10.1002/1873-3468.12825

Hörtnagl, H., Berger, M. L., Sperk, G., and Pifl, C. (1991). Regional Heterogeneity in the Distribution of Neurotransmitter Markers in the Rat hippocampus. *Neuroscience* 45 (2), 261–272. doi:10.1016/0306-4522(91)90224-c

Honsho, M., Abe, Y., and Fujiki, Y. (2015). Dysregulation of Plasmalogen Homeostasis Impairs Cholesterol Biosynthesis. *J. Biol. Chem.* 290 (48), 28822–28833. doi:10.1074/jbc.m115.656983

Horn, M. A., van den Brink, D. M., Wanders, R. J. A., Duran, M., Poll-The, B. T., Tallaksen, C. M. E., et al. (2007). Phenotype of Adult Refsum Disease Due to a Defect in Peroxin 7. *Neurology* 68 (9), 698–700. doi:10.1212/01.wnl.0000255960.01644.39

Huffnagel, I. C., Clur, S.-A. B., Bams-Mengerink, A. M., Blom, N. A., Wanders, R. J. A., Waterham, H. R., et al. (2013). Rhizomelic Chondrodysplasia Punctata and Cardiac Pathology. *J. Med. Genet.* 50 (7), 419–424. doi:10.1136/jmedgenet-2013-101536

Krauß, S., Michaelis, L., and Vetter, W. (2017). Phytyl Fatty Acid Esters in Vegetables Pose a Risk for Patients Suffering from Refsum's Disease. *PLoS One* 12 (11), e0188035. doi:10.1371/journal.pone.0188035

Luisman, T., Smith, T., Ritchie, S., and Malone, K. E. (2021). Genetic Epidemiology Approach to Estimating Birth Incidence and Current Disease Prevalence for Rhizomelic Chondrodysplasia Punctata. *Orphanet J. Rare Dis.* 16 (1), 300. doi:10.1186/s13023-021-01889-z

Luoma, A. M., Kuo, F., Cakici, O., Crowther, M. N., Denninger, A. R., Avila, R. L., et al. (2015). Plasmalogen Phospholipids Protect Internodal Myelin from Oxidative Damage. *Free Radic. Biol. Med.* 84, 296–310. doi:10.1016/j.freeradbiomed.2015.03.012

Malheiro, A. R., Correia, B., Ferreira da Silva, T., Bessa-Neto, D., Van Veldhoven, P. P., and Brites, P. (2019). Leukodystrophy Caused by Plasmalogen Deficiency Rescued by Glyceryl 1-myristyl Ether Treatment. *Brain Pathol.* 29 (5), 622–639. doi:10.1111/bpa.12710

Meyers, E. N., Lewandoski, M., and Martin, G. R. (1998). An Fgf8 Mutant Allelic Series Generated by Cre- and Flp-Mediated Recombination. *Nat. Genet.* 18 (2), 136–141. doi:10.1038/ng0298-136

Motley, A. M., Hettema, E. H., Hogenhout, E. M., Brites, P., ten Asbroek, A. L. M. A., Wijburg, F. A., et al. (1997). Rhizomelic Chondrodysplasia Punctata Is a Peroxisomal Protein Targeting Disease Caused by a Non-functional PTS2 Receptor. *Nat. Genet.* 15 (4), 377–380. doi:10.1038/ng0497-377

Motley, A. M., Brites, P., Gerez, L., Hogenhout, E., Haasjes, J., Benne, R., et al. (2002). Mutational Spectrum in the PEX7 Gene and Functional Analysis of Mutant Alleles in 78 Patients with Rhizomelic Chondrodysplasia Punctata Type 1. *Am. J. Hum. Genet.* 70 (3), 612–624. doi:10.1086/338998

Paul, S., Lancaster, G. I., and Meikle, P. J. (2019). Plasmalogens: A Potential Therapeutic Target for Neurodegenerative and Cardiometabolic Disease. *Prog. Lipid Res.* 74, 186–195. doi:10.1016/j.plipres.2019.04.003

Peneder, T. M., Scholze, P., Berger, M. L., Reither, H., Heinze, G., Bertl, J., et al. (2011). Chronic Exposure to Manganese Decreases Striatal Dopamine Turnover in Human Alpha-Synuclein Transgenic Mice. *Neuroscience* 180, 280–292. doi:10.1016/j.neuroscience.2011.02.017

Pike, L. J., Han, X., Chung, K.-N., and Gross, R. W. (2002). Lipid Rafts Are Enriched in Arachidonic Acid and Plasmenylethanolamine and Their Composition Is Independent of Caveolin-1 Expression: a Quantitative Electrospray Ionization/mass Spectrometric Analysis. *Biochemistry* 41 (6), 2075–2088. doi:10.1021/bi0156557

Powers, J. M., and Moser, H. W. (1998). Peroxisomal Disorders: Genotype, Phenotype, Major Neuropathologic Lesions, and Pathogenesis. *Brain Pathol.* 8 (1), 101–120. doi:10.1111/j.1750-3639.1998.tb00139.x

Powers, J. M., Kenjarski, T. P., Moser, A. B., and Moser, H. W. (1999). Cerebellar Atrophy in Chronic Rhizomelic Chondrodysplasia Punctata: a Potential Role for Phytanic Acid and Calcium in the Death of its Purkinje Cells. *Acta Neuropathol.* 98 (2), 129–134. doi:10.1007/s004010051060

Purdue, P. E., Zhang, J. W., Skoneczny, M., and Lazarow, P. B. (1997). Rhizomelic Chondrodysplasia Punctata Is Caused by Deficiency of Human PEX7, a Homologue of the Yeast PTS2 Receptor. *Nat. Genet.* 15 (4), 381–384. doi:10.1038/ng0497-381

Reisbick, S., Neuringer, M., Hasnain, R., and Connor, W. E. (1994). Home Cage Behavior of Rhesus Monkeys with Long-Term Deficiency of Omega-3 Fatty

Acids. *Physiology Behav.* 55 (2), 231–239. doi:10.1016/0031-9384(94)90128-7

Rodemer, C., Thai, T.-P., Brugger, B., Kaercher, T., Werner, H., Nave, K.-A., et al. (2003). Inactivation of Ether Lipid Biosynthesis Causes Male Infertility, Defects in Eye Development and Optic Nerve Hypoplasia in Mice. *Hum. Mol. Genet.* 12 (15), 1881–1895. doi:10.1093/hmg/ddg191

Rubio, J. M., Astudillo, A. M., Casas, J., Balboa, M. A., and Balsinde, J. (2018). Regulation of Phagocytosis in Macrophages by Membrane Ethanolamine Plasmalogens. *Front. Immunol.* 9, 1723. doi:10.3389/fimmu.2018.01723

Schneider, C. A., Rasband, W. S., and Eliceiri, K. W. (2012). NIH Image to ImageJ: 25 Years of Image Analysis. *Nat. Methods* 9 (7), 671–675. doi:10.1038/nmeth.2089

Schutgens, R. B., Bouman, I. W., Nijenhuis, A. A., Wanders, R. J., and Frumau, M. E. (1993). Profiles of Very-Long-Chain Fatty Acids in Plasma, Fibroblasts, and Blood Cells in Zellweger Syndrome, X-Linked Adrenoleukodystrophy, and Rhizomelic Chondrodysplasia Punctata. *Clin. Chem.* 39 (8), 1632–1637. doi:10.1093/clinchem/39.8.1632

Seedorf, U., Brysch, P., Engel, T., Schrage, K., and Assmann, G. (1994). Sterol Carrier Protein X Is Peroxisomal 3-oxoacyl Coenzyme A Thiolase with Intrinsic Sterol Carrier and Lipid Transfer Activity. *J. Biol. Chem.* 269 (33), 21277–21283. doi:10.1016/s0021-9258(17)31960-9

Sunkin, S. M., Ng, L., Lau, C., Dolbeare, T., Gilbert, T. L., Thompson, C. L., et al. (2013). Allen Brain Atlas: an Integrated Spatio-Temporal Portal for Exploring the Central Nervous System. *Nucleic Acids Res.* 41 (Database issue), D996–D1008. doi:10.1093/nar/gks1042

Taylor, S., Wakem, M., Dijkman, G., Alsarraj, M., and Nguyen, M. (2010). A Practical Approach to RT-qPCR-Publishing Data that Conform to the MIQE Guidelines. *Methods* 50 (4), S1–S5. doi:10.1016/j.ymeth.2010.01.005

Teigler, A., Komljenovic, D., Draguhn, A., Gorgas, K., and Just, W. W. (2009). Defects in Myelination, Paranode Organization and Purkinje Cell Innervation in the Ether Lipid-Deficient Mouse Cerebellum. *Hum. Mol. Genet.* 18 (11), 1897–1908. doi:10.1093/hmg/ddp110

van den Brink, D. M., Brites, P., Haasjes, J., Wierzbicki, A. S., Mitchell, J., Lambert-Hamill, M., et al. (2003). Identification of PEX7 as the Second Gene Involved in Refsum Disease. *Am. J. Hum. Genet.* 72 (2), 471–477. doi:10.1086/346093

Wanders, R. J. A., Schumacher, H., Heikoop, J., Schutgens, R. B. H., and Tager, J. M. (1992). Human Dihydroxyacetonephosphate Acyltransferase Deficiency: a New Peroxisomal Disorder. *J. Inherit. Metab. Dis.* 15 (3), 389–391. doi:10.1007/bf02435984

Wanders, R. J. A., Dekker, C., Hovarth, V. A. P., Schutgens, R. B. H., Tager, J. M., Van Laer, P., et al. (1994). Human Alkyldihydroxyacetonephosphate Synthase Deficiency: a New Peroxisomal Disorder. *J. Inherit. Metab. Dis.* 17 (3), 315–318. doi:10.1007/bf00711817

Wanders, R. J. A., Denis, S., Wouters, F., Wirtz, K. W. A., and Seedorf, U. (1997). Sterol Carrier Protein X (SCPx) Is a Peroxisomal Branched-Chain Beta-Ketothiolase Specifically Reacting with 3-Oxo-Pristanoyl-CoA: a New, Unique Role for SCPx in Branched-Chain Fatty Acid Metabolism in Peroxisomes. *Biochem. Biophys. Res. Commun.* 236 (3), 565–569. doi:10.1006/bbrc.1997.7007

Wanders, R. J. A., Waterham, H. R., and Bp, L. (2006). "Refsum Disease,". [Internet] in *GeneReviews®*. Editors M.P. Adam, H.H. Ardinger, R.A. Pagon, S.E. Wallace, L.J.H. Bean, K. Stephens, et al. (Seattle: University of Washington). Updated 2015 Jun 11.

White, A. L., Modaff, P., Holland-Morris, F., and Pauli, R. M. (2003). Natural History of Rhizomelic Chondrodysplasia Punctata. *Am. J. Med. Genet.* 118A (4), 332–342. doi:10.1002/ajmg.a.20009

Whitney, M. S., Shemery, A. M., Yaw, A. M., Donovan, L. J., Glass, J. D., and Deneris, E. S. (2016). Adult Brain Serotonin Deficiency Causes Hyperactivity, Circadian Disruption, and Elimination of Siestas. *J. Neurosci.* 36 (38), 9828–9842. doi:10.1523/jneurosci.1469-16.2016

Wu, Y., Chen, Z., Darwish, W. S., Terada, K., Chiba, H., and Hui, S.-P. (2019). Choline and Ethanolamine Plasmalogens Prevent Lead-Induced Cytotoxicity and Lipid Oxidation in HepG2 Cells. *J. Agric. Food Chem.* 67 (27), 7716–7725. doi:10.1021/acs.jafc.9b02485

Yu, T. W., Chahrour, M. H., Coulter, M. E., Jiralerspong, S., Okamura-Ikeda, K., Ataman, B., et al. (2013). Using Whole-Exome Sequencing to Identify Inherited Causes of Autism. *Neuron* 77 (2), 259–273. doi:10.1016/j.neuron.2012.11.002

Conflict of Interest: The authors declare that the research was conducted in the absence of any commercial or financial relationships that could be construed as a potential conflict of interest.

Publisher's Note: All claims expressed in this article are solely those of the authors and do not necessarily represent those of their affiliated organizations, or those of the publisher, the editors and the reviewers. Any product that may be evaluated in this article, or claim that may be made by its manufacturer, is not guaranteed or endorsed by the publisher.

frontiers | Frontiers in Cell and Developmental Biology

TYPE Original Research
PUBLISHED 24 August 2022
DOI 10.3389/fcell.2022.866156

OPEN ACCESS

EDITED BY
Fabian Dorninger,
Medical University of Vienna, Austria

REVIEWED BY
Danni Li,
University of Minnesota Twin Cities, United States
Atsushi Nagai,
Shimane University, Japan

*CORRESPONDENCE
Dayan B. Goodenowe,
d.goodenowe@prodromesciences.com

SPECIALTY SECTION
This article was submitted to Cellular Biochemistry, a section of the journal Frontiers in Cell and Developmental Biology

RECEIVED 30 January 2022
ACCEPTED 11 July 2022
PUBLISHED 24 August 2022

CITATION
Goodenowe DB and Senanayake V (2022), Brain ethanolamine phospholipids, neuropathology and cognition: A comparative post-mortem analysis of structurally specific plasmalogen and phosphatidyl species. *Front. Cell Dev. Biol.* 10:866156. doi: 10.3389/fcell.2022.866156

Brain ethanolamine phospholipids, neuropathology and cognition: A comparative post-mortem analysis of structurally specific plasmalogen and phosphatidyl species

Dayan B. Goodenowe* and Vijitha Senanayake

Prodrome Sciences USA LLC, Temecula, CA, United States

Reduced cognition in the elderly is associated with low levels of plasmalogens and high levels of lipid rafts, amyloid plaques, and neurofibrillary tangles in the temporal cortex. A systematic integrative analysis of key indices of these pathologies to determine their collective and independent contributions to cognition was performed. Levels of four phosphatidylethanolamines (PE) and four ethanolamine plasmalogens (PL) of identical sn-1 carbon length and desaturation (stearic, 18:0) and identical sn-2 fatty acid compositions of varying side chain lengths and degrees of unsaturation (oleic, 18:1; linoleic, 18:2; arachidonic, 20:4; docosahexaenoic, 22:6), flotillin-1 expression and amyloid plaque and neurofibrillary tangle densities were measured in inferior temporal cortex tissue from 100 elderly subjects (Rush University Memory and Aging Project, 88.5 $\pm$ 5.8 years old). Subjects were evenly distributed with respect to gender (52/48, F/M) and cognitive status (38/24/38, no cognitive impairment/mild cognitive impairment/Alzheimer's dementia) proximate to death. Multivariate logistic regression analyses were used to determine the relative and collective associations of the neuropathological indices with cognition. Higher levels of tangles, amyloid, or flotillin and lower levels of PL 18:0/22:6 were significantly associated with lower cognition in the base model (adjusted for age, sex, education). Multivariate analysis revealed that only PL 18:0/22:6 ($\beta = 0.506$; $p < 0.00001$), tangles (–0.307; $p < 0.01$), and flotillin (–0.2027; $p < 0.05$) were independently associated with reduced cognition. PL 18:0/22:6 and PE 18:0/22:6 levels were independently associated with cognition in the presence of tangles, amyloid, and flotillin, but only PL 18:0/22:6 retained its association with cognition when both PL and PE 18:0/22:6 were included in the model indicating that PE 18:0/22:6 levels were associated with PL 18:0/22:6, not cognition. Only high brain levels of PL 18:0/22:6 (>mean+1SD) was predictive of normal cognition (coef = 1.67, $p < 0.05$) and non-demented state (coef = –2.73, $p < 0.001$), whereas low levels of PL 18:0/22:6 and high levels of tangles or flotillin were predictive of dementia. The association of high brain polyunsaturated (PUFA)-PL levels with better cognition was independent of amyloid plaque, neurofibrillary tangle, PE, and flotillin-1 expression. Maintenance or augmentation of brain docosahexaenoic (DHA)-PL levels

warrants further investigation as a target for preventing cognitive decline or improving cognition in the elderly, respectively.

KEYWORDS

plasmalogen, amyloid, neurofibrillary tangle, flotillin, docosahexaenic acid, cognition, Alzheimer's, brain

Introduction

Neurodegeneration leading to dementia and death is emerging as the most important age-related disease of our time. The average time to death from a diagnosis of dementia is only 4.5 years (Xie et al., 2008) and Alzheimer's disease (AD) is the predominant form of dementia in the elderly. The economic and health cost of dementia is enormous and growing due to an increasingly aged population (Alzheimer's Association, 2018). Dementia in the elderly is a neuropathological disease. Amyloid plaques and neurofibrillary tangles are pathological hallmarks of AD and were once thought to be not just biomarkers of neuropathological decline, but causative of neuropathological and functional decline in the elderly (Hardy and Selkoe, 2002). However, recent clinical trials have cast doubt on the putative causative roles of these well-established neuropathological markers on cognitive decline (Kozin et al., 2018). The presence of high amyloid plaque densities in cognitively normal persons illustrates that there must be other neuropathological features that modulate the associations of these historical pathologies with cognition (Negash et al., 2011) and which are more proximate to the biochemical mechanisms that are required for normal cognitive function.

Changes in neuronal membrane composition are directly implicated as potential causative mechanisms involved in the pathological accumulation of amyloid (Nitsch et al., 1992) and reduced neuronal synaptic activity (Wurtman, 1992). A higher density of cholesterol-rich lipid raft regions are associated with increased β-secretase activity and increased $A\beta_{1\text{-}42}$ production (Kojro et al., 2001; Cordy et al., 2003) and a higher density of polyunsaturated plasmalogen rich regions is associated with increased α-secretase activity and decreased $A\beta_{1\text{-}42}$ production (Wood et al., 2011a). Membrane fusion dynamics, the biophysical process through which neurotransmitters are released into the synapse, is dependent upon membrane levels of polyunsaturated fatty acid (PUFA) containing ethanolamine plasmalogens (PL) (Glaser and Gross, 1995). PL is emerging as both a diagnostic and therapeutic target for neuropathological decline and dementia (Goodenowe et al., 2007). Brain PL levels are lower in AD than age-matched controls (Ginsberg et al., 1995; Han et al., 2001; Wood et al., 2011a; Igarashi et al., 2011; Otoki et al., 2021) and low brain levels correlate with low serum levels (Wood et al., 2011a). Serum PL levels correlate with cognition in subjects diagnosed with probable AD, in AD subjects at diagnosis who were later confirmed by autopsy, and in serum samples collected at time of death in subjects with post-mortem AD pathology (Goodenowe et al., 2007). Reductions in metabolic pathways involved in PL biosynthesis are associated with lower cognition (Astarita et al., 2010). Relation of PL and other phospholipid species in the brain in individuals with different cognitive categories (Clinical Dementia Rating) has been previously studied (Han et al., 2001).

Studying the effects of plasmalogen supplementation is challenging due to the complex distribution of molecular species in mammalian tissues (Han et al., 2001) which renders measuring the effects of a single type of plasmalogen difficult using animal extracts. Their extensive gut metabolism and acid degradation during oral administration (Fallatah et al., 2020) creates additional scientific challenges. To overcome these issues, 1-O-alkyl-2-acylglycerols were developed as metabolic precursors to plasmalogens. These precursors can be synthetized to contain specific sn-1 alcohols and specific sn-2 fatty acid side chains. They are stable, orally bioavailable, and dose-dependently elevate PL levels *in vitro* and *in vivo* corresponding to the sn-1 fatty alcohol and sn-2 fatty acid of the precursor (Mankidy et al., 2010; Wood et al., 2011a; Wood et al., 2011b). These precursors enable researchers to precisely assess the effects of plasmalogen supplementation. These plasmalogen precursors are neuroprotective in animal models of Parkinson's (Miville-Godbout et al., 2016) and multiple sclerosis (Wood et al., 2011a) and improve neurological function in neurologically compromised animals (Gregoire et al., 2015).

The extent to which PL interact with and modulate the association of pathology with cognition in the human brain are not known. We therefore sought to investigate in greater detail the associations between cognition, canonical neuropathology and a series of structurally specific membrane phospholipids known to be altered in persons with AD pathology or reduced cognition. All neurological functions are dependent upon the presynaptic release of neurotransmitters and the subsequent postsynaptic interaction of these neurotransmitters on postsynaptic receivers/receptors. Cognition is dependent upon cholinergic neuron integrity and function (Blusztajn and Wurtman, 1983; Wurtman et al., 1985; Wurtman, 1992). Presynaptic cholinergic axon terminals are unique among neurons in that both the release of its neurotransmitter, acetylcholine, and the reabsorption of the neurotransmitter precursor, choline, is dependent upon membrane fusion due to the unique cellular location of the re-uptake protein. The choline high affinity transporter (CHT) is not constituently expressed on the presynaptic membrane like the

neurotransmitter uptake proteins of other neuron types, but instead is expressed only on the presynaptic vesicles and only transiently expressed on the presynaptic membrane during neurotransmitter release (Ferguson et al., 2003). Pharmacological inhibition of CHT with hemicholinium-3 reduces acetylcholine release (Maire and Wurtman, 1985) and choline starvation causes membrane depletion of equimolar levels of both phosphatidylethanolamine (PE) and phosphatidylcholine (PC) phospholipids (Ulus et al., 1989). Glaser and Gross (Glaser and Gross, 1995) convincingly demonstrated that membrane fusion is selectively dependent upon sufficient levels of PL, but not PE phospholipids. Specifically, sufficient levels of PL containing a polyunsaturated fatty acid at the sn-2 position (arachidonic acid, AA) but not PL containing a monounsaturated fatty acid (oleic acid, OA) or phosphatidylethanolamine (PE) containing either AA or OA at the sn-2 position was an obligate requirement for membrane fusion activity. Han et al. (Han et al., 2001) performed a comprehensive analysis of PE and PL phospholipids in both gray and white matter of different brain regions, including temporal cortex, of persons with varying degree of cognitive impairment. White matter demonstrated a preponderant loss of PL containing a monounsaturated fatty acid at sn-2 and gray matter demonstrated a preponderant loss of PL containing a polyunsaturated fatty acid at sn-2 (AA and docosahexaenoic acid, DHA).

The temporal cortex was selected as a representative brain region of interest due the previous detailed characterization of PL and PE species by Han et al. (Han et al., 2001); the observation that this brain region exhibits early loss of synaptic density (Scheff et al., 2011); the association between amyloid and tau accumulation in this region and early dysfunction in AD (Halawa et al., 2019); and its early association with aging and cognitive decline (Braak and Braak, 1991; Bancher et al., 1993; Braak et al., 1996; Braak and Braak, 1997). A representative and matched series of PE and PL species containing the same carbon number at sn-1 (stearic, 18:0) and identical sn-2 fatty acids [OA (18:1), linoleic, LA (18:2); AA (20:4); DHA (22:6)] were chosen such that differential associations between cognition and pathology and sn-1 composition (plasmenyl vs. phosphatidyl) and sn-2 composition [side chain length (18, 20, 22) and unsaturation (1,2,4,6)] could be evaluated. Accordingly, the only difference between the two series of phospholipids investigated is that the sn-1 stearic (18:0) moiety in the PL species is connected to the glycerol backbone *via* a fatty alcohol vinyl ether bond and sn-1 stearic (18:0) moiety in the PE species is connected to the glycerol backbone *via* a fatty acid ester bond. The chemical compositions and structures of the two phospholipid series are identical in all other aspects.

Materials and methods

Brain samples

One hundred inferior temporal cortex brain samples were obtained from the Rush University Memory and Aging Project (MAP). Rush MAP is a community-based study that enrolls older persons without known dementia who agreed to annual clinical and cognitive evaluations and to donate their brains after death (Bennett et al., 2012; Yu et al., 2017). Brain samples were fractioned and immediately frozen and stored at −80° until analysis (average post-mortem interval of approximately 8 h). All participant samples were processed under the same protocol and no significant differences in sample collection times were observed (Table 1). At the last clinical visit prior to the death and subsequent autopsies of the donors, 38 had no cognitive impairment (NCI), 44 had mild cognitive impairment (MCI) and 38 had dementia of the Alzheimer's type (AD). Genders of the study participants were equally distributed (52 females and 48 males) and the average age was 88.5 ± 5.8 years old. A uniform structured clinical evaluation was performed to document the level of cognition and the presence of AD, MCI, and other causes of cognitive impairment. Neuropsychological indices of cognition were summarized as a global measure of cognition (Gcog) based on the average z-score of 19 tests in each study, using the means and standard deviations from the baseline visit. Participant characteristics and the number of people in each clinical category is given in Table 1.

Neuropathological measurements

Global cortical amyloid load and PHF-tangle density were assessed separately using immunohistochemical methods (Yu et al., 2017). Braak staging and CERAD scoring were based on blinded assessment by a trained neuropathologist (Yu et al., 2013). Braak Stage is a semiquantitative measure of severity of neurofibrillary tangle (NFT) pathology (range 1–6; 6 = severe neocortical involvement). CERAD score is a semiquantitative measure of neuritic plaques (range: 1–4; 1 = definite AD; 4 = No AD). Flotillin-1 (FLOT1) mRNA expression was measured by qPCR. Total messenger RNA was extracted from cells using TRIzol™ following the manufacturer's instructions (ThermoFisher). qPCR was conducted using a Nanodrop 1000 (ThermoFisher). The primers used were as follows: forward: 5′-CCCATCTCAGTCACTGGCATT-3′ and reverse: 5′-CCGCCA ACATCTCCTTGTTC-3′ for FLOT1 and β-actin was used as an internal reference.

TABLE 1 Demographic, clinical and biochemical summary of the study cohort.

Variable	NCI[a]	MCI	AD		Cognitively normal	Non-cognitively normal		Non-demented	Demented	*p*-value
	Mean (SD)	Mean (SD)	Mean (SD)	*p*-value	Mean (SD)	Mean (SD)	*p*-value	Mean (SD)	Mean (SD)	
Gender										
Male (*n*)	18	11	19	9.5e−1	18	30	9.2e−1	29	19	7.5e−1
Female (*n*)	20	13	19		20	32		33	19	
Age (SD)	86.7 (6.16)	88.6 (5.66)	90.2 (5.01)	2.6e−2*	86.7 (6.16)	89.6 (5.29)	1.4e−2*	87.4 (5.99)	90.2 (5.01)	1.7e−2*
Education (SD)	14.2 (2.79)	14.7 (2.16)	14.8 (3.20)	1.5Ee−1	14.2 (2.79)	14.7 (2.82)	3.4e−2*	14.4 (2.55)	14.8 (3.19)	4.7e−1
Post-mortem Interval (min)	369.4 (136.3)	492.5 (320.2)	394.2 (272.0)	5.3e−1	369.4 (136.3)	431.3 (292.4)	2.3e−1	416.6 (230.7)	394.2 (272.0)	6.6e−1
MMSE	28.4 (1.59)	25.6 (2.99)	12.0 (8.05)	<1.0e−5*	28.4 (1.59)	17.4 (9.32)	<1.0e−5*	27.3 (2.61)	12.0 (8.04)	<1.0e−5*
Gcog	0.213 (0.421)	−0.436 (0.33)	−1.91 (1.01)	<1.0e−5*	0.213 (0.42)	−1.33 (1.08)	<1.0e−5	−0.04 (0.50)	−1.91 (1.01)	<1.0e−*
Braak	*n*	*n*	*n*	*p*-value	*n*	*n*	*p*-value	*n*	*n*	*p*-value
I/II	13	6	2	<1.0e−3*	13	8	<1.0e−3*	19	2	<1.0e−3*
III	14	7	5		14	12		21	5	
IV	11	5	12		11	17		16	12	
V/VI	0	6	19		0	25		6	19	
Cerad	*n*	*n*	*n*	*p*-value	*n*	*n*	*p*-value	*n*	*n*	*p*-value
1	6	4	25	<1.0e−3*	6	29	8.0e−3*	10	25	<1.0e−3*
2	12	7	9		12	16		19	9	
3	5	5	2		5	7		10	2	
4	15	8	2		15	10		23	2	
Tangles	3.13 (3.92)	7.03 (8.39)	13.8 (13.7)	<1.0e−5*	4.45 (3.92)	11.1 (12.3)	2.0e−4*	4.64 (6.29)	13.8 (13.7)	<1.0e−5*
Amyloid	2.62 (2.95)	3.52 (4.33)	5.03 (3.20)	1.1e−2*	2.62 (2.95)	4.44 (3.72)	1.3e−2*	2.97 (3.55)	5.02 (3.20)	4.5e−3*
PE 18:0/18:1	0.037 (0.085)	−0.001 (0.087)	−0.074 (0.127)	<1.0e−5*	0.04 (0.09)	−0.05 (0.12)	3.0e−4*	0.02 (0.09)	−0.07 (0.13)	<1.0e−5*
PE 18:0/18:2	0.052 (0.131)	−0.031 (0.132)	−0.089 (0.117)	<1.0e−5*	0.05 (0.13)	−0.07 (0.12)	<1.0e−5*	0.02 (0.13)	−0.09 (0.12)	1.0e−4*
PE 18:0/20:4	0.034 (0.076)	0.012 (0.084)	−0.074 (0.119)	<1.0e−5*	0.03 (0.08)	−0.04 (0.11)	6.0e−4*	0.03 (0.08)	−0.07 (0.12)	<1.0e−5*
PE 18:0/22:6	0.034 (0.070)	0.017 (0.079)	−0.072 (0.105)	<1.0e−5*	0.03 (0.07)	−0.04 (0.11)	3.0e−4*	0.03 (0.07)	−0.07 (0.11)	<1.0e−5*
PL 18:0/18:1	−0.073 (0.239)	−0.084 (0.242)	−0.078 (0.236)	9.9e−1	−0.08 (0.24)	−0.08 (0.24)	8.8e−1	−0.08 (0.24)	−0.08 (0.24)	9.8e−1
PL 18:0/18:2	0.014 (0.120)	−0.032 (0.116)	−0.039 (0..117)	1.2e−1	0.01 (0.12)	−0.04 (0.12)	4.0e−2*	−0.004 (0.13)	−0.04 (0.12)	1.5e−1
PL 18:0/20:4	0.019 (0.064)	0.009 (0.074)	−0.051 (0.114)	2.0e−3*	0.02 (0.06)	−0.03 (0.10)	1.5e−2*	0.02 (0.07)	−0.05 (0.11)	4.0e−4*
PL 18:0/22:6	0.032 (0.071)	0.004 (0.055)	−0.054 (0.088)	<1.0e−5*	0.03 (0.07)	−0.03 (0.08)	1.0e−4*	0.02 (0.07)	−0.05 (0.09)	<1.0e−5*
Flotillin	0.039 (0.015)	0.037 (0.012)	0.052 (0.020)	4.0e−4*	0.04 (0.02)	0.05 (0.02)	7.9e−2	0.04 (0.01)	0.05 (0.02)	1.0e−4*

NCI, No cognitive impairment; MCI, Mild Cognitive Impairment; AD, Alzheimer's Disease; SD, Standard Deviation. *$p < 0.05$.
[a]Clinical and biochemical differences between clinical entities were compared using analysis of variance.

Tissue ethanolamine phospholipid measurements

Brain samples were processed essentially as described in a previous publication (Miville-Godbout et al., 2016). Briefly, brain samples were randomized prior to processing and then homogenized and ground to a fine powder in liquid nitrogen. Tissue samples were aliquoted (1 mg), water (200 µl) was added and samples were sonicated in an ice bath. After adding 600 µl of EtOAc, samples were shaken at 2000 rpm for 15 min followed by a 10 min centrifugation at 2851 *g*. An aliquot of the upper organic layer (36 µl) was then diluted with 420 µl of a solution of 0.5%

TABLE 2 MRM transitions used for ethanolamine phospholipid.

Phosphatidylethanolamines (PE)			Ethanolamine plasmalogens (PL)		
Analyte	Molecular Formula	MRM Transition	Analyte	Molecular Formula	MRM Transition
^{13}C-PE 16:0/22:6	$C_{24}{}^{13}C_{19}H_{74}NO_8P$	781.5/327.2	^{13}C-PL 16:0/22:6	$C_{37}{}^{13}C_6H_{74}NO_7P$	752.5/327.2
PE 18:0/18:1	$C_{41}H_{80}NO_8P$	744.5/283.2	PL 18:0/18:1	$C_{41}H_{80}NO_7P$	728.5/281.2
PE 18:0/18:2	$C_{41}H_{78}NO_8P$	742.5/283.2	PL 18:0/18:2	$C_{41}H_{78}NO_7P$	726.5/279.2
PE 18:0/20:4	$C_{43}H_{78}NO_8P$	766.5/283.2	PL 18:0/20:4	$C_{43}H_{78}NO_7P$	750.6/303.2
PE 18:0/22:6	$C_{45}H_{78}NO_8P$	790.5/283.2	PL 18:0/22:6	$C_{45}H_{78}NO_7P$	774.5/327.2

MRM, Multiple reaction monitoring.

water in EtOAc containing labeled internal standards [1 μg/ml ^{13}C-PL ($C_{37}{}^{13}C_6H_{74}NO_7P$) and 1 μg/ml of ^{13}C-PE ($C_{24}{}^{13}C_{19}H_{74}NO_8P$)]. Samples were again shaken at 2000 rpm for 15 min followed by a 2 min centrifugation at 2851 *g* from which a 100 μl aliquot was analyzed by flow injection LC-MS/MS as described previously (Goodenowe et al., 2007; Miville-Godbout et al., 2016). Briefly, the speciation of the ethanolamine phospholipids of interest were analyzed using multiple reaction monitoring (MRM) of one parent/fragment transition for the ion pairs (Table 2) on an API4000™ mass spectrometer equipped with a TurboV™ source in the negative ionization atmospheric pressure chemical ionization mode. Negatively charged PE and PL parent ion species fragment under collision induced dissociation. The negative charge of the parent ion is retained on the sn-2 fatty acid fragment in PL species and either the sn-1 or sn-2 fatty acid fragment in PE species. Therefore the combination of the [M-H]- parent ion and the sn-1 or sn-2 [R]- ion uniquely identifies the PE or PL species of interest (Goodenowe et al., 2007). Similarly, negative ion MS/MS analysis of phosphatidylcholine species enables speciation determination (Ritchie et al., 2016). Stable isotope ratios for each analyte were calculated and used for all analyses.

Statistical analyses

In descriptive analyses, demographic and clinico-pathological parameters among diagnostic categories (NCI, MCI and AD) were compared using chi-square or Fishers's exact tests for categorical variables and analysis of variance for continuous variables. PL and PE analytes were first mean normalized and then log transformed to reduce skewness.

For continuous outcomes such as Gcog, we first screened potential predictors by examining correlations with the outcome and then fit multiple linear regression models including variables of interest and terms to adjust for age, sex and education. For continuous predictors, associations are shown per SD of the predictor. Stata 15.0 was used to perform statistical analyses; statistical significance is $p < 0{\cdot}05$ in all analyses.

Results

Key associations with study outcomes

First, we examined the age, education, genotype, post-mortem interval, Mini-Mental State Examination (MMSE) score, Gcog, Braak stage, CERAD score, tangle density, amyloid density, brain levels of selected PL and PE phospholipids and flotillin-1 expression differences between the diagnostic categories (Table 1). The age, MMSE score, Gcog, Braak stage, Cerad score, tangle density, amyloid density, flotillin-1 expression, each of the PE and two of the PL species (PL 18:0/20:4 and 18:0/22:6) differed significantly between the diagnostic categories.

We also examined how these variables differed between cognitively unimpaired persons (NCI) and cognitively impaired persons (MCI and AD), and between non-demented (NCI and MCI) and demented (Alzheimer's dementia) persons. Age and education were higher ($p < 0.05$) in cognitively impaired persons compared to cognitively unimpaired persons (Table 1). Demented persons were older ($p < 0.05$) than non-demented persons. As expected, MMSE and Gcog were lower ($p < 0.05$) in cognitively impaired persons and in demented persons compared to cognitively unimpaired and non-demented persons respectively. Similarly, there were more individuals with higher Braak staging, increased tangle density, increased amyloid density and lower Cerad scoring ($p < 0.05$) in cognitively impaired and demented groups than their respective cognitively unimpaired and non-demented counterparts. Each of the PE species and PL 18:0/20:4 and PL 18:0/22:6 was significantly lower in the brain of individuals belonging to the cognitively impaired and demented categories compared to cognitively unimpaired and non-demented categories respectively. PL 18:0/18:2 brain levels were significantly lower in cognitively impaired persons compared to cognitively unimpaired persons and levels of this species was similar between non-demented and demented. Flotillin-1 gene expression was significantly higher in demented persons than non-demented persons (Table 1).

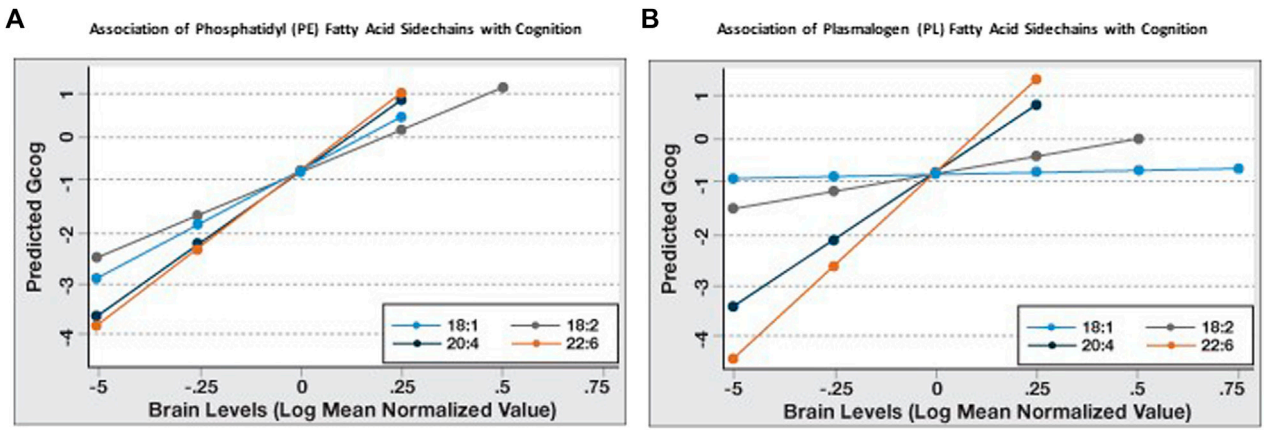

FIGURE 1
Sn-2 fatty acid sidechain-specific associations of phosphatidyl (PE) and plasmalogen ethanolamines (PL) with cognitive function (Gcog). Regression analyses were conducted with Gcog as the outcome variable and respective phospholipid species with different sn-2 fatty acid side chains as the independent variable. Four separate models for each phospholipid species, adjusted for age, sex and education, were constructed and postestimation predicted value of the outcome variable by brain levels of respective phospholipid were plotted in a single graph for comparison. **(A)** Effect of phosphatidyl ethanolamine (PE) species with different sn-2 fatty acid side chains on cognition; **(B)** Effect of plasmalogen ethanolamine (PL) species with different sn-2 fatty acid side chains on cognition.

Association of degree of unsaturation and chain length of PL and PE with cognition

We examined the association between brain levels of monounsaturated fatty acid (MUFA) and PUFA-containing (at sn-2) PE and PL with Gcog and found that higher levels of each PE species predicted higher Gcog irrespective of the level of unsaturation at the sn-2 position. However, only higher levels of highly unsaturated AA (20:4, n-6) or DHA (22:6, n-3)-containing PL was associated with higher Gcog.

Since it appeared that the coefficient of association of PL and PE species with Gcog was affected by the degree of unsaturation and chain length of the sn-2 sidechains, we further examined the association of the change in sn-2 chain length (18 carbon to 22 carbon) and the degree of unsaturation (one double bond to six double bonds) with cognition in each phospholipid type. We observed that for PE, the predicted Gcog values after adjusting for age, sex and education changed little based on the sn-2 side chains (Figure 1A). However, for PL, the regression slopes increased incrementally with increasing sn-2 chain length and unsaturation (Figure 1B). As expected, pathological markers were negatively associated with cognition (Table 3).

Similarly, the strength of the association (β-coefficient) increased with increasing sn-2 unsaturation and chain length in both phospholipid types and DHA-containing PL and PE had the strongest association with Gcog (Table 3). Since our objective was to examine how phospholipids modulate the association of brain pathology with cognition, we limited further statistical analyses to these two phospholipids.

TABLE 3 Association of clinical and biological variables with cognition.

Variable[a]		Gcog		
	n	Coef[b]	*p*	Adj R^2
PE18:0/18:1	99	0.4950	6.0e−06*	0.2346
PE18:0/18:2	99	0.4882	1.7e−05*	0.2180
PE18:0/20:4	99	0.5983	4.1e−08*	0.3095
PE18:0/22:6	99	0.5989	2.4e−08*	0.3174
PL 18:0/18:1	99	0.0380	7.4e−01	0.0483
PL 18:0/18:2	99	0.1692	1.4e−01	0.0691
PL 18:0/20:4	99	0.4981	9.0e−06*	0.2283
PL 18:0/22:6	99	0.6191	9.6e−09*	0.3300
Amyloid	98	−0.3901	5.7e−04*	0.1499
Tangles	99	−0.5510	6.7e−07*	0.2685
Flotillin	94	−0.2601	3.4e−02*	0.0879

[a]Multiple regression analysis with phospholipids or pathological parameters as the independent variable and Gcog as the dependent variable. Gcog represents a composite measure of cognitive function assessed by a battery of cognitive tests.
[b]Coefficients for continuous variables expressed per Standard Deviation; Models were adjusted for age, education, and gender. *$p < 0.05$.

Multivariate associations of brain pathology, membrane markers and phospholipids with cognition

We then examined the association of amyloid and tangles with Gcog. As expected, both amyloid and tangle density, which are hallmarks of AD-related brain pathology, predicted lower Gcog

TABLE 4 Association of amyloid, tangles, flotillin and phospholipids with cognition.

Variable	Gcog[a]			
	Base model	Model A	Model B	Final model
PL 18:0/22:6 (Coef[b])	Not Included	Not Included	0.5194*	0.5058***
PE 18:0/22:6 (Coef)	Not Included	Not Included	−0.0520	Not Included
Amyloid (Coef)	−0.2435*	−0.2315*	−0.1267	Not Included
Tangles (Coef)	−0.4792***	−0.4569***	−0.2815*	−0.3069 **
Flotillin (Coef)	Not Included	−0.1605	−0.2029	−0.2027*
Age (Coef)	−0.2168*	−0.1574	−0.2145	−0.2109*
Education (Coef)	0.1803	0.1501	0.0622	0.0628
Male sex (Coef)	−0.0811	−0.0700	−0.0005	−0.0053
F	9.18***	7.71***	9.39***	12.84***
Adjusted R^2	0.2965	0.3045	0.4219	0.4331
N	98	93	93	94

Independent multivariate regression models with Gcog as the outcome and phospholipids and pathological parameters as variables.
[a]Gcog (Global Cognition) represents a composite measure of cognitive function assessed by a battery of cognitive tests.
[b]Coef (Coefficient of association) for continuous variables expressed per Standard Deviation; Base Model: demographics + amyloid and tangles; Model A: Base Model + Flotillin; Base Model + Flotillin and DHA ethanolamine phospholipids; Final Model: only demographics and variables independently associated with Gcog after multivariate assessment ($p < 0.05$). *$p < 0.05$; **$p < 0.01$, ***$p < 0.00001$.

(Base Model, Table 4). We then examined whether the expression of flotillin-1, which is a marker of lipid rafts, modulate the association of amyloid and tangles with Gcog in the Base Model. Flotillin-1 was not significantly associated with cognition when amyloid and tangles were in the model and the associations of amyloid and tangles with Gcog remained intact after the addition of flotillin-1 to the model (Model A, Table 4), indicating the independence of the association of amyloid and tangles with Gcog. We then added both PE 18:0/22:6 and PL 18:0/22:6, the phospholipids most associated with Gcog from Table 3, to the model and found that these phospholipids reduced the strength of the association of amyloid and tangles with Gcog and increased the association of flotillin-1 with Gcog ($p = 0.053$) (Model B, Table 4). The strengths of the associations (as determined by the β-coefficient) of these pathological markers with cognition weakened in relation to the base model (adjusted only for age, sex and education; Table 3) when PE and PL 18:0/22:6 were added to the model, indicating that the brain levels of these phospholipids contribute to the variability explained by these pathological markers (Model B, Table 4).

However, the association of PE 18:0/22:6 with Gcog observed in Table 3 disappeared under multivariate analysis that included PL 18:0/22:6 (Model B, Table 4). Therefore, to derive the final model, we removed PE 18:0/22:6 and other variables that were not associated with Gcog under multivariate conditions. Removal of these variables resulted in an increase in the variance in cognition explained by the model (Final Model, Table 4). The Final Model resulted in an improvement of the association of flotillin-1 with Gcog ($p < 0.05$). Brain amyloid levels were not associated with Gcog under multivariate analysis (Model B, Final Model, Table 4). When compared to the model without PL 18:0/22:6, inclusion of PL 18:0/22:6 in the model strengthened the association of flotillin-1 with Gcog.

Modulation of the association between cognition and PE 18:0/22:6 by PL 18:0/22:6

When the association between cognition and PE 18:0/22:6 in Table 3 is compared to Model B, Table 4 the addition of PL 18:0/22:6 was observed to affect this association. To investigate the relative and interactive associations of these two similar phospholipids on cognition, four predictive models were created (Figure 2). Figure 2A illustrates the association between PE 18:0/22:6 and cognition with and without PL 18:0/22:6 as a covariate. Inclusion of PL 18:0/22:6 completely neutralized the association between PE 18:0/22:6 and cognition. Figure 2B illustrates the association between PL 18:0/22:6 and cognition with and without PE 18:0/22:6 as a covariate. Inclusion of PE 18:0/22:6 had no effect on the association between PL 18:0/22:6 and cognition. These results indicate that cognition is directly associated with the level of PL 18:0/22:6 not PE 18:0/22:6.

Modulation of the association between cognition and amyloid, tangles and flotillin by PL 18:0/22:6

When the associations between cognition and amyloid, tangles and flotillin-1 in Table 3 and Table 4 (Model A) are compared, the association between cognition and tangles is minimally affected by amyloid and flotillin (−0.55 to −0.46), but the association between amyloid and cognition is reduced

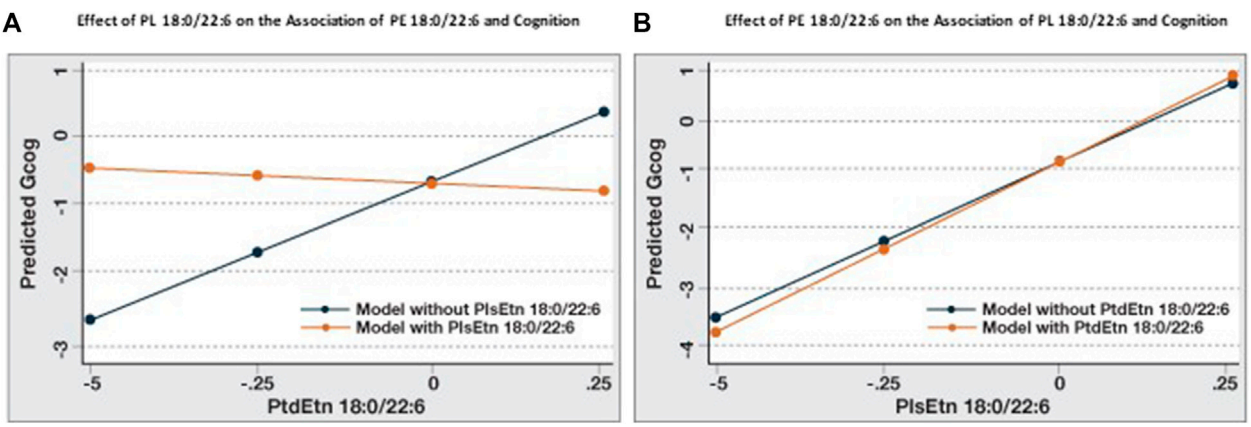

FIGURE 2
Association of PE 18:0/22:6 with cognition is modulated by PL 18:0/22:6. Regression analyses were conducted with Gcog as the outcome variable and PE 18:0/22:6 or PL 18:0/22:6 as the independent variable. Two separate models for each phospholipid, with or without the counterpart phospholipid in the model, were constructed. All models were adjusted for age, sex and education. Postestimation predicted value of the outcome variable by brain levels of the phospholipid were plotted in a single graph for comparison. **(A)** Effect of PE 18:0/22:6 on cognition with or without PL 18:0/22:6 in the model; **(B)** Effect of PL 18:0/22:6 on cognition with or without PE 18:0/22:6 in the model.

almost in half (−0.39 to −0.23). When brain phospholipids are subsequently included (Model B), the association between tangles and cognition drops from −0.46 to −0.28 and the association between amyloid and cognition becomes insignificant (−0.23 to −0.13). To illustrate the effect of PL 18:0/22:6 on these associations, six predictive models were created to compare the associations between each of these pathologies and cognition with and without PL 18:0/22:6 in the model (Figure 3). Figure 3A illustrates the flattening of the association between tangles and cognition by PL 18:0/22:6. Figure 3B illustrates the flattening of the association between amyloid and cognition by PL 18:0/22:6. Amyloid is not associated with cognition when PL 18:0/22:6 is a covariate. Figure 3C illustrates that PL 18:0/22:6 has no modulatory effect on the association between flotillin-1 and cognition. What is illustrated in Figures 2, 3 which is not discernible from the data in Tables 3, 4 is the variance in cognition observed across the range of measured values of tangles, amyloid, flotillin-1 and PL 18:0/22:6. Gcog values ranged from just over 0 in persons with the lowest level of tangles to just under -1 in persons with the highest level of tangle density for a total variance in cognition of just under 2 Gcog units across the range of measured brain tangle density. The total variance in Gcog across the measured range of amyloid levels was approximately 0.5 Gcog units and the total variance of cognition across the range of flotillin-1 values was approximately 1.5 Gcog units. Whereas in Figure 2, the total variance in cognition across the range of PL 18:0/22:6 values was approximately 5 Gcog units (from −4 in persons with the lowest brain PL 18:0/22:6 levels to +1 in persons with the highest brain PL 18:0/22:6 levels).

Association of brain pathology, flotillin and PL 18:0/22:6 with normal cognition and dementia

Multivariate regression analyses identified brain levels of PL 18:0/22:6, tangles and flotillin-1 as key predictors of cognition. To understand the nature of these associations across the full range of their measured values, we categorized the levels of these variables into low (<mean-1SD), median (mean ± 1SD) and high (>mean+1SD) and used logistic regression to determine the associations of these categories with different ends of the measurable cognition range. The terms “no cognitive impairment, NCI” and “cognitively normal, CN” are not synonymous with high cognitive function. In fact, the range of cognitive performance in individual neuropsychometric tests in persons determined, clinically, to be NCI or CN represents a distribution with an equal number of persons above normal and an equal number of persons below normal, but above cognitive impairment (Bennett et al., 2006). Likewise, there is a distribution of cognition in persons determined, clinically, to be demented ranging from mild to severe dementia, but lower than a determination of questionable or mild cognitive impairment (MCI). Therefore, the prediction of CN from non-CN (MCI + dementia) and demented from non-demented (CN + MCI) is not an equal but opposite analysis. The lack of a negative association is not the same as the presence of a positive association. We reasoned that with these analyses, we would

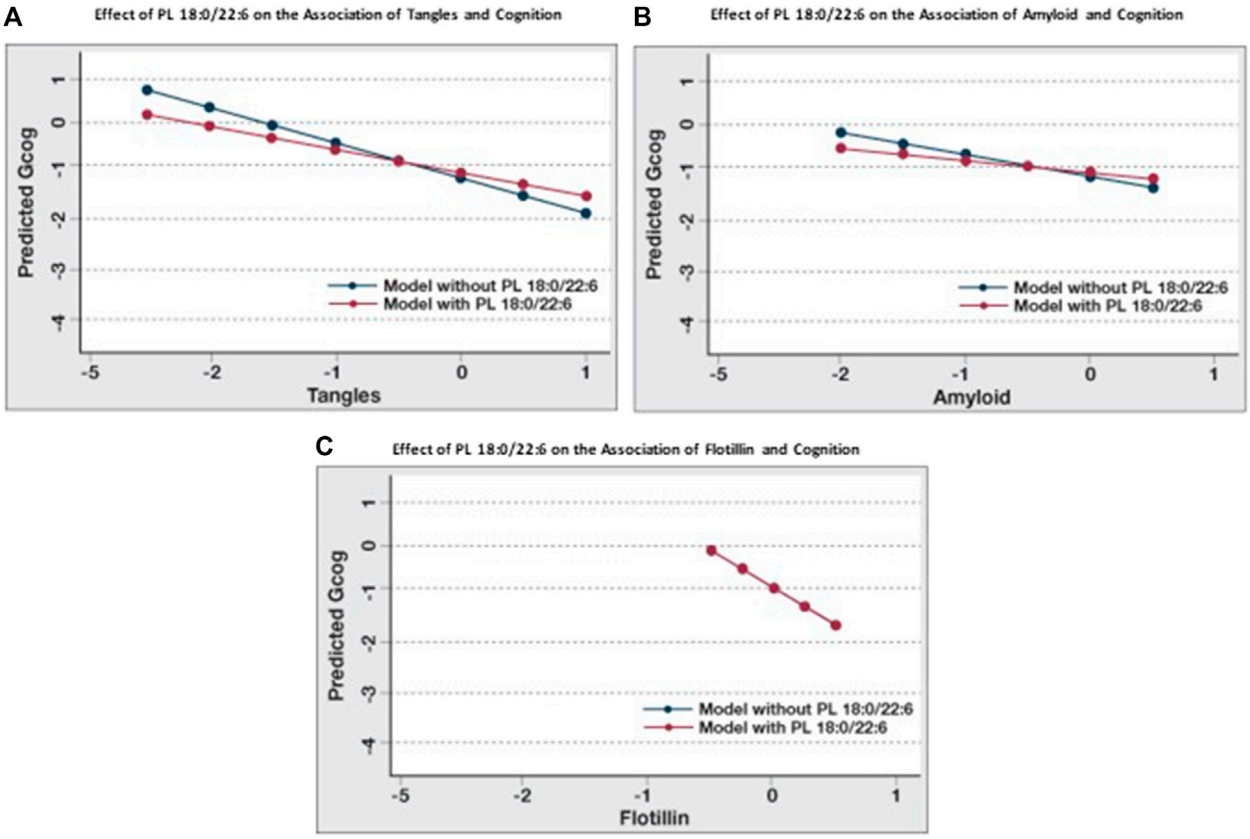

FIGURE 3
Modulation of the effects of pathological parameters on cognition by PL 18:0/22:6. Regression analyses were conducted with Gcog as the outcome variable and tangles, amyloid or flotillin respectively as the independent variable. Two separate models for each pathological parameter, with or without PL 18:0/22:6 in the model, were constructed. All models were adjusted for age, sex and education. Postestimation predicted value of the outcome variable by brain levels of the respective pathological parameter were plotted in a single graph for comparison. **(A)** Effect of tangles on cognition with or without PL 18:0/22:6 in the model; **(B)** Effect of amyloid on cognition with or without PL 18:0/22:6 in the model; **(C)** Effect of flotillin on cognition with or without PL 18:0/22:6 in the model (blue and red lines are superimposed).

be able to determine and compare the strength of the positive and negative associations of lower and higher levels of these variables with cognition.

The analysis results indicated that high brain PL 18:0/22:6 (>mean+1SD) predicted normal cognition and non-demented state, but low tangle, flotillin-1 or amyloid levels did not (Table 5). However, low brain PL 18:0/22:6 (<mean-1SD) and high levels of tangles and flotillin-1 (>mean+1SD) and intermediate levels of amyloid (mean ± 1SD) predicted dementia (Table 5).

Discussion

In our previous studies, we demonstrated that serum plasmalogen levels were associated with cognitive outcomes (Goodenowe et al., 2007; Wood et al., 2010; Goodenowe and Senanayake, 2019). We have also demonstrated neuroprotective effects of exogenous supplementation of plasmalogen precursors in animal models (Wood et al., 2011a; Gregoire et al., 2015; Miville-Godbout et al., 2016) and in a preliminary 4-month, escalating dose, open label study of a targeted equimolar formulation of PL 16:0/22:6 and PL 18:0/22:6 plasmalogen precursors in 22 cognitively impaired persons, blood levels of PL 16:0/22:6 and PL 18:0/22:6 were elevated by approximately 70% from baseline and this increase was associated with decreased malondialdehyde levels and increased catalase enzymatic capacity. Improved cognition and mobility were also reported (Goodenowe et al., 2022). Low brain and circulating serum plasmalogen levels in neurodegenerative diseases such as Alzheimer's disease have been observed by multiple independent researchers and these

TABLE 5 Association of low, medium and high levels of PL 18:0/22:6, amyloid, tangles and flotillin with normal cognition and Dementia.

Variable[a]	Cognitively	Non-demented vs. demented
	Abnormal vs. NCI	
	Coefficient (95% CI)	Coefficient (95% CI)
PL 18:0/22:6		
<Mean-1SD	Ref	2.73 (1.00 to 4.46)**
Mean ± 1SD	0.56 (−0.82 to 1.95)	1.52 (0.06 to 2.99)
>Mean+1SD	1.67 (0.27 to 3.06)*	Ref
Tangles		
<Mean-1SD	17.1 (−4108.5 to 4142.6)	Ref
Mean ± 1SD	16.8 (−4108.8 to 4142.4)	0.62 (−1.38 to 2.61)
>Mean+1SD	Ref	4.85 (1.44 to 8.26)**
Flotillin		
<Mean-1SD	0.74 (−0.93 to 2.41)	Ref
Mean ± 1SD	−0.13 (−1.38 to 1.12)	1.65 (−0.35 to 3.65)
>Mean+1SD	Ref	2.27 (0.012 to 4.52)*
Amyloid		
<Mean-1SD	0.62 (−1.41 to 2.66)	Ref
Mean ± 1SD	0.43 (−1.51 to 2.37)	2.87 (0.57 to 5.17)*
>Mean+1SD	Ref	1.53 (−1.15 to 4.20)

[a]Logistic regression analysis to determine the effects of low, medium and high levels of phospholipids and pathological parameters on cognitively normal state (NCI) and dementia diagnosis. Dummy variables were created from continuous variables of these parameters to derive categories representing low, medium and high levels. Each model was adjusted for age, sex and education in addition to PL 18:0/22:6, tangles, flotillin as continuous variables, when the corresponding categorical variable is not included in the model. NCI, No cognitive impairment. *$p < 0.05$; **$p < 0.01$.

deficiencies are thought to contribute to defects in cellular membrane function (Ginsberg et al., 1995; Farooqui et al., 1997; Han et al., 2001; Dorninger et al., 2015). In this study, we sought to examine a specific class of brain membrane lipids (ethanolamine phospholipids) based upon their known high abundance in neuronal membranes (Han, 2005), diverse sn-1 and sn-2 speciation (Han et al., 2001), and their direct physiological role in membrane fusion/neurotransmitter release (Glaser and Gross, 1995). Similarly, we selected the temporal cortex, a brain region known to exhibit pathological (Braak and Braak, 1997; Scheff et al., 2011), morphological (Braak and Braak, 1991) and functional (Halawa et al., 2019) changes at the earliest clinically detectable stages of cognitive impairment and dementia as a relevant brain region of interest.

The major findings of this study are: *1*) The association between brain levels of PL and cognition was observed to be dependent on the chain-length and the degree of unsaturation of the sn-2 fatty acid side chain. *2*) The associations between PE species and cognition were observed to be indirect and mediated *via* their association with PL 18:0/22:6. *3*) High levels (>mean+1SD) of PL 18:0/22:6 predicted normal cognition and low levels (<mean-1SD) predicted reduced cognition and dementia. In contrast, a high density of neurofibrillary tangles or high flotillin-1 expression was observed to be predictive of reduced cognition, but low levels were not predictive of normal cognition. *4*) PL 18:0/22:6 modulated the associations between cognition and PE 18:0/22:6, tangles and amyloid. *5*) Brain amyloid density was not predictive of cognition after correcting for tangle density, PL 18:0/22:6 levels, and flotillin-1 expression.

A higher age is a primary epidemiological variable associated with lower cognition and our data confirm this association (Table 1). As expected, cognitive status (Gcog), neurofibrillary tangle density, amyloid plaque density, Braak Stage (V/VI), and CERAD score significantly differed between the diagnostic subgroups (Table 1). Each of the PE species and the two PUFA-containing PL species (18:0/20:4 and 18:0/22:6) significantly differed between the diagnostic categories indicating that a global loss in brain ethanolamine phospholipid species is associated with reduced cognition. Flotillin-1 expression was significantly higher in demented

individuals, which is consistent with previously published results (Girardot et al., 2003).

We observed that more double bonds (6>4>2>1) and higher carbon chain length (22>20>18) in the sn-2 fatty acid strengthened the association of PL species with cognition but had a minimal effect on the association between PE species levels and cognition. Neurotransmission involves both biophysical and biochemical processes. Prior to a putative neurotransmission event, neurotransmitter molecules are stored in presynaptic membrane-bound vesicles which isolate them from the intracellular metabolism of the presynaptic neuron. Upon receipt of a depolarizing action potential, the vesicles migrate to the outer presynaptic membrane where they fuse with and release the neurotransmitters into the extracellular synaptic cleft where they subsequently interact with protein receptors on the postsynaptic membrane of the adjacent neuron. Sufficient membrane levels of PUFA PL are required for this membrane fusion process to occur (Lohner, 1996). Efficient fusion of cellular membranes is required for effective neurotransmission (Yang et al., 2017). Membrane fusion efficiency was observed to be dependent on the amount of PL in the membrane as well as the structural composition of the PL. A longer chain length and higher degree of unsaturation of the sn-2 PL sidechain incrementally increased membrane fusion events. A direct comparison of PL and PE species of identical side chain compositions further illustrated the dependence of membrane fusion on membrane PL levels (Glaser and Gross, 1995). This is a plausible biophysical mechanism for the differential trends in the associations between PL and PE sn-2 sidechains with cognition observed in this study. Although brain plasmalogens have been shown to be lower in brain regions with AD-related pathology and the association of low serum PL levels with brain pathology have been demonstrated by us and others (Ginsberg et al., 1995; Farooqui et al., 1997; Han et al., 2001; Dorninger et al., 2015), to our knowledge this is the first direct demonstration of the compositional specificity of the PL association with cognition. Brain levels of PL with sn-2 fatty acids with longer chain length and a higher degree of unsaturation were associated with cognition whereas PL with sn-2 fatty acids with shorter chain length and a lower degree of unsaturation were not.

We examined whether the levels of PL 18:0/22:6 in the brain altered the associations between amyloid and tangles, the hallmarks of AD pathology, with cognition. Our data indicate that higher brain PL 18:0/22:6 levels decrease the strength of the association (β-coefficient) between amyloid and tangles with cognition, indicating that the association between brain pathology and cognition is affected by the level of PL 18:0/22:6 levels in the brain. These observations are consistent with the findings that amyloid and tangles do not correlate directly with cognition nor do they explain the variance of cognition in AD (Negash et al., 2011). Inclusion of PL 18:0/22:6 in the model, along with amyloid and tangles, increased the explained variance when cognition was the outcome of interest. Furthermore, when the variance in cognitive status across the full measured ranges of amyloid plaque density, neurofibrillary tangle density, flotillin-1 expression and PL 18:0/22:6 in temporal cortex were compared (Figures 1, 2) the cognitive status associated with highest versus lowest levels of these biomarkers was observed to be dramatically different. The variance in cognition across the range of amyloid density was about 0.5 Gcog units, and about 1.5 for tangles and flotillin-1, but was about 5 units for PL 18:0/22:6.

The association of PL 18:0/20:6 with cognition remained unchanged when adjusted for brain pathology (amyloid and tangles) and the increased explained variance in this model indicates that the amount of PL 18:0/20:6 in the brain is an independent contributor to cognition. Similarly, when adjusted for PL 18:0/22:6 levels, the association of PE 18:0/22:6 with cognition disappeared, while adjustment for PE 18:0/22:6 levels did not change the association of PL 18:0/22:6 with cognition. These findings suggest that PL 18:0/22:6 is an independent predictor of cognition and the association of PE 18:0/22:6 with cognition is spurious, and probably reflects the homeostatic adjustment of PE levels due to PL deficiency (Dorninger et al., 2015). Association of higher PL 18:0/22:6 levels (>mean+1SD) with normal cognition and the association of lower levels (<mean-1SD) with dementia is suggestive of protective effects at higher levels and deleterious effects at lower brain levels.

Flotillin is a marker of lipid rafts in the brain (Dermine et al., 2001). Lipid rafts are cholesterol and sphingolipid-enriched areas in the membrane that help sequester certain proteins. Lipid rafts are known to be associated with gamma-secretase that generate amyloid β-protein (Aβ) and thought to promote the interaction of the amyloid precursor protein (APP) with gamma-secretase (Matsumura et al., 2014). The apparent enhancement of the negative association of flotillin with cognition by PL 18:0/22:6 probably indicate modification of membrane structure by PL 18:0/22:6. In fact, it has been shown that increasing membrane DHA-PL levels dose dependently increased soluble APPα and decreased gamma-secretase expression (Wood et al., 2011a).

Recent research findings suggest that the onset of AD neuropathological changes occur years prior to the appearance of clinical symptoms (Sperling et al., 2014). Exploring biochemical changes associated with early pathophysiological events is crucial to finding modifiable risk factors that can be used for primary and secondary prevention (Sperling et al., 2011). PL deficiency in the brain is one such biochemical change reported to be associated with brain pathology and cognition (Ginsberg et al., 1995; Han et al., 2001; Goodenowe et al., 2007; Wood et al., 2010; Goodenowe and Senanayake, 2019). We recently reported that higher levels of serum plasmalogens weaken or nullify the associations between age and APOE e4 allele status and AD and

cognition (Goodenowe and Senanayake, 2019) and that increasing circulating DHA plasmalogen levels using a plasmalogen precursor had positive effects on cognition and mobility (Goodenowe et al., 2022).

Glycerophospholipids containing a vinyl ether bond at sn-1 are called plasmalogens. They are synthetized *via* a single non-redundant biochemical pathway in intracellular organelles called peroxisomes (Brites et al., 2004). A decline in peroxisomal function due to aging leads to low PL levels in the membranes and lipoproteins in the brain causing defective membrane function (Farooqui et al., 1997) and aberrations in brain cholesterol metabolism (Goodenowe and Senanayake, 2019). These two factors lead to suboptimal cholinergic neuron function (Blusztajn and Wurtman, 1983) and atrophy and defects in amyloid clearance respectively (Sun et al., 2015), presumably leading to brain pathology characteristic of AD. PL predominates in the body over choline plasmalogens (Farooqui and Horrocks, 2001) and they play a significant role in maintaining optimal brain function (Rouser and Yamamoto, 1968; Farooqui et al., 2008). These phospholipids are associated with cellular membranes in the brain and are involved in multiple brain functions including cholesterol metabolism, synaptic function, and APP processing (Farooqui and Horrocks, 2001; Brites et al., 2004; Rothhaar et al., 2012). Alteration of membrane function is hypothesized to be mechanistically linked to the pathology and clinical symptoms observed in AD (Glaser and Gross, 1995; Askarova et al., 2011).

The study has several limitations. First it was designed to focus on a single class of lipids in a single brain region to investigate specific membrane structural changes with pathology and cognition. Extrapolation of the results to other lipid classes or brain regions or the contributions of other brain regions or other pathologies or other phospholipids to cognition was not investigated. Upstream (impaired peroxisomal function) or downstream (high levels of inflammation/oxidative stress) causal factors that may simultaneously influence PL levels and cognition was not investigated. Future studies are needed to further explore and define the roles of additional contributing factors such as these in the outcomes observed and reported in this study.

This is the first reported evidence of a potential modifiable risk factor that can modulate the effects of brain pathology on cognition possibly through membrane alterations. This report also demonstrates the spurious association of DHA-phosphatide with cognition and unequivocally demonstrates the significance of DHA-plasmalogens on cognition. Increasing DHA-plasmalogen levels in the brain might have the potential to modify the neurodegenerative pathways responsible for cognitive deficits.

Data availability statement

The raw data supporting the conclusions of this article will be made available by the authors, without undue reservation.

Ethics statement

The studies involving human participants were reviewed and approved by Rush University. The patients/participants provided their written informed consent to participate in this study.

Author contributions

DG and VS equally contributed to the data analysis and preparation of the initial draft manuscript. DG was responsible for the design of the study, final interpretation of the results and final manuscript revisions.

Acknowledgments

We wish to thank David A. Bennett and Sue E. Leurgans for critical discussions and review of the statistical results their valuable suggestions. We acknowledge and thank Rush University Alzheimer's Disease Center for providing the brain samples.

Conflict of interest

The corresponding author is the CEO and President of Prodrome Sciences USA LLC. Second author was an employee of Prodrome Sciences USA LLC.

The remaining author declares that the research was conducted in the absence of any commercial or financial relationships that could be construed as a potential conflict of interest.

Publisher's note

All claims expressed in this article are solely those of the authors and do not necessarily represent those of their affiliated organizations, or those of the publisher, the editors and the reviewers. Any product that may be evaluated in this article, or claim that may be made by its manufacturer, is not guaranteed or endorsed by the publisher.

References

Alzheimer's Association (2018). Alzheimer's Disease Facts and Figures. *Alzheimers Dement.* 14 (3), 367–429.

Askarova, S., Yang, X., and Lee, J. C. (2011). Impacts of membrane biophysics in alzheimer's disease: From amyloid precursor protein processing to aβ peptide-induced membrane changes. *Int. J. Alzheimers Dis.* 2011, 134971. doi:10.4061/2011/134971

Astarita, G., Jung, K. M., Berchtold, N. C., Nguyen, V. Q., Gillen, D. L., Head, E., et al. (2010). Deficient liver biosynthesis of docosahexaenoic acid correlates with cognitive impairment in Alzheimer's disease. *PLoS ONE* 5, 0012538. doi:10.1371/journal.pone.0012538

Bancher, C., Braak, H., Fischer, P., and Jellinger, K. A. (1993). Neuropathological staging of Alzheimer lesions and intellectual status in Alzheimer's and Parkinson's disease patients. *Neurosci. Lett.* 162, 179–182. doi:10.1016/0304-3940(93)90590-h

Bennett, D. A., Schneider, J. A., Arvanitakis, Z., Kelly, J. F., Aggarwal, N. T., Shah, R. C., et al. (2006). Neuropathology of older persons without cognitive impairment from two community-based studies. *Neurology* 66, 1837–1844. doi:10.1212/01.wnl.0000219668.47116.e6

Bennett, D. A., Schneider, J. A., Buchman, A. S., Barnes, L. L., Boyle, P. A., Wilson, R. S., et al. (2012). Overview and findings from the rush memory and aging Project. *Curr. Alzheimer Res.* 9, 646–663. doi:10.2174/156720512801322663

Blusztajn, J. K., and Wurtman, R. J. (1983). Choline and cholinergic neurons. *Science* 221, 614–620. doi:10.1126/science.6867732

Braak, H., and Braak, E. (1997). Frequency of stages of Alzheimer-related lesions in different age categories. *Neurobiol. Aging* 18, 351–357. doi:10.1016/s0197-4580(97)00056-0

Braak, H., and Braak, E. (1991). Neuropathological stageing of Alzheimer-related changes. *Acta Neuropathol.* 82, 239–259. doi:10.1007/BF00308809

Braak, H., Braak, E., Yilmazer, D., de Vos, R. A., Jansen, E. N., Bohl, J., et al. (1996). Pattern of brain destruction in Parkinson's and Alzheimer's diseases. *J. Neural Transm.* 103, 455–490. doi:10.1007/BF01276421

Brites, P., Waterham, H. R., and Wanders, R. J. (2004). Functions and biosynthesis of plasmalogens in health and disease. *Biochim. Biophys. Acta* 1636, 219–231. doi:10.1016/j.bbalip.2003.12.010

Cordy, J. M., Hussain, I., Dingwall, C., Hooper, N. M., and Turner, A. J. (2003). Exclusively targeting beta-secretase to lipid rafts by GPI-anchor addition up-regulates beta-site processing of the amyloid precursor protein. *Proc. Natl. Acad. Sci. U. S. A.* 100, 11735–11740. doi:10.1073/pnas.1635130100

Dermine, J. F., Duclos, S., Garin, J., St-Louis, F., Rea, S., Parton, R. G., et al. (2001). Flotillin-1-enriched lipid raft domains accumulate on maturing phagosomes. *J. Biol. Chem.* 276, 18507–18512. doi:10.1074/jbc.M101113200

Dorninger, F., Brodde, A., Braverman, N. E., Moser, A. B., Just, W. W., Forss-Petter, S., et al. (2015). Homeostasis of phospholipids - the level of phosphatidylethanolamine tightly adapts to changes in ethanolamine plasmalogens. *Biochim. Biophys. Acta* 1851, 117–128. doi:10.1016/j.bbalip.2014.11.005

Fallatah, W., Smith, T., Cui, W., Jayasinghe, D., Di Pietro, E., Ritchie, S. A., et al. (2020). Oral administration of a synthetic vinyl-ether plasmalogen normalizes open field activity in a mouse model of rhizomelic chondrodysplasia punctata. *Dis. Model. Mech.* 13, dmm042499. doi:10.1242/dmm.042499

Farooqui, A. A., Farooqui, T., and Horrocks, L. A. (2008). *Metabolism and functions of bioactive ether lipids in the brain*. New York: Springer Science + Business Media, LLC.

Farooqui, A. A., and Horrocks, L. A. (2001). Plasmalogens: Workhorse lipids of membranes in normal and injured neurons and glia. *Neuroscientist* 7, 232–245. doi:10.1177/107385840100700308

Farooqui, A. A., Rapoport, S. I., and Horrocks, L. A. (1997). Membrane phospholipid alterations in alzheimer's disease: Deficiency of ethanolamine plasmalogens. *Neurochem. Res.* 22, 523–527. doi:10.1023/a:1027380331807

Ferguson, S. M., Savchenko, V., Apparsundaram, S., Zwick, M., Wright, J., Heilman, C. J., et al. (2003). Vesicular localization and activity-dependent trafficking of presynaptic choline transporters. *J. Neurosci.* 23, 9697–9709. doi:10.1523/jneurosci.23-30-09697.2003

Ginsberg, L., Rafique, S., Xuereb, J. H., Rapoport, S. I., and Gershfeld, N. L. (1995). Disease and anatomic specificity of ethanolamine plasmalogen deficiency in Alzheimer's disease brain. *Brain Res.* 698, 223–226. doi:10.1016/0006-8993(95)00931-f

Girardot, N., Allinquant, B., Langui, D., Laquerriere, A., Dubois, B., Hauw, J. J., et al. (2003). Accumulation of flotillin-1 in tangle-bearing neurones of Alzheimer's disease. *Neuropathol. Appl. Neurobiol.* 29, 451–461. doi:10.1046/j.1365-2990.2003.00479.x

Glaser, P. E., and Gross, R. W. (1995). Rapid plasmenylethanolamine-selective fusion of membrane bilayers catalyzed by an isoform of glyceraldehyde-3-phosphate dehydrogenase: Discrimination between glycolytic and fusogenic roles of individual isoforms. *Biochemistry* 34, 12193–12203. doi:10.1021/bi00038a013

Goodenowe, D. B., Cook, L. L., Liu, J., Lu, Y., Jayasinghe, D. A., Ahiahonu, P. W., et al. (2007). Peripheral ethanolamine plasmalogen deficiency: A logical causative factor in alzheimer's disease and dementia. *J. Lipid Res.* 48, 2485–2498. doi:10.1194/jlr.P700023-JLR200

Goodenowe, D. B., and Senanayake, V. (2019). Relation of serum plasmalogens and APOE genotype to cognition and dementia in older persons in a cross-sectional study. *Brain Sci.* 9, E92. doi:10.3390/brainsci9040092

Goodenowe, D., Haroon, J., Kling, M. A., Z. M.Habelhah, B., Shtilkind, L., et al. (2022). Targeted plasmalogen supplementation: Effects on blood plasmalogens, oxidative stress biomarkers, cognition, and mobility in cognitively impaired persons. *Front. Cell. Dev. Biol.* 10, 864842. doi:10.3389/fcell.2022.864842

Gregoire, L., Smith, T., Senanayake, V., Mochizuki, A., Miville-Godbout, E., Goodenowe, D., et al. (2015). Plasmalogen precursor analog treatment reduces levodopa-induced dyskinesias in parkinsonian monkeys. *Behav. Brain Res.* 286, 328–337. doi:10.1016/j.bbr.2015.03.012

Halawa, O. A., Gatchel, J. R., Amariglio, R. E., Rentz, D. M., Sperling, R. A., Johnson, K. A., et al. (2019). Inferior and medial temporal tau and cortical amyloid are associated with daily functional impairment in Alzheimer's disease. *Alzheimers Res. Ther.* 11, 14. doi:10.1186/s13195-019-0471-6

Han, X., Holtzman, D. M., and McKeel, D. W., Jr. (2001). Plasmalogen deficiency in early alzheimer's disease subjects and in animal models: Molecular characterization using electrospray ionization mass spectrometry. *J. Neurochem.* 77, 1168–1180. doi:10.1046/j.1471-4159.2001.00332.x

Han, X. (2005). Lipid alterations in the earliest clinically recognizable stage of alzheimer's disease: Implication of the role of lipids in the pathogenesis of alzheimer's disease. *Curr. Alzheimer Res.* 2, 65–77. doi:10.2174/1567205052772786

Hardy, J., and Selkoe, D. J. (2002). The amyloid hypothesis of alzheimer's disease: Progress and problems on the road to therapeutics. *Science* 297, 353–356. doi:10.1126/science.1072994

Igarashi, M., Ma, K., Gao, F., Kim, H. W., Rapoport, S. I., Rao, J. S., et al. (2011). Disturbed choline plasmalogen and phospholipid fatty acid concentrations in Alzheimer's disease prefrontal cortex. *J. Alzheimers Dis.* 24, 507–517. doi:10.3233/JAD-2011-101608

Kojro, E., Gimpl, G., Lammich, S., Marz, W., and Fahrenholz, F. (2001). Low cholesterol stimulates the nonamyloidogenic pathway by its effect on the alpha -secretase ADAM 10. *Proc. Natl. Acad. Sci. U. S. A.* 98, 5815–5820. doi:10.1073/pnas.081612998

Kozin, S. A., Barykin, E. P., Mitkevich, V. A., and Makarov, A. A. (2018). Anti-amyloid therapy of alzheimer's disease: Current state and prospects. *Biochemistry.* 83, 1057–1067. doi:10.1134/S0006297918090079

Lohner, K. (1996). Is the high propensity of ethanolamine plasmalogens to form non-lamellar lipid structures manifested in the properties of biomembranes? *Chem. Phys. Lipids* 81, 167–184. doi:10.1016/0009-3084(96)02580-7

Maire, J. C., and Wurtman, R. J. (1985). Effects of electrical stimulation and choline availability on the release and contents of acetylcholine and choline in superfused slices from rat striatum. *J. Physiol.* 80, 189–195.

Mankidy, R., Ahiahonu, P. W., Ma, H., Jayasinghe, D., Ritchie, S. A., Khan, M. A., et al. (2010). Membrane plasmalogen composition and cellular cholesterol regulation: A structure activity study. *Lipids Health Dis.* 9, 62. doi:10.1186/1476-511X-9-62

Matsumura, N., Takami, M., Okochi, M., Wada-Kakuda, S., Fujiwara, H., Tagami, S., et al. (2014). γ-Secretase associated with lipid rafts: Multiple interactive pathways in the stepwise processing of β-carboxyl-terminal fragment. *J. Biol. Chem.* 289, 5109–5121. doi:10.1074/jbc.M113.510131

Miville-Godbout, E., Bourque, M., Morissette, M., Al-Sweidi, S., Smith, T., Mochizuki, A., et al. (2016). Plasmalogen augmentation reverses striatal dopamine loss in MPTP mice. *PLoS One* 11, e0151020. doi:10.1371/journal.pone.0151020

Negash, S., Bennett, D. A., Wilson, R. S., Schneider, J. A., and Arnold, S. E. (2011). Cognition and neuropathology in aging: Multidimensional perspectives from the rush religious orders study and rush memory and aging Project. *Curr. Alzheimer Res.* 8, 336–340. doi:10.2174/156720511795745302

Nitsch, R. M., Blusztajn, J. K., Pittas, A. G., Slack, B. E., Growdon, J. H., Wurtman, R. J., et al. (1992). Evidence for a membrane defect in Alzheimer disease brain. *Proc. Natl. Acad. Sci. U. S. A.* 89, 1671–1675. doi:10.1073/pnas.89.5.1671

Otoki, Y., Kato, S., Nakagawa, K., Harvey, D. J., Jin, L. W., Dugger, B. N., et al. (2021). Lipidomic analysis of postmortem prefrontal cortex phospholipids reveals changes in choline plasmalogen containing docosahexaenoic acid and stearic acid between cases with and without alzheimer's disease. *Neuromolecular Med.* 23, 161–175. doi:10.1007/s12017-020-08636-w

Ritchie, S. A., Jayasinge, D., Wang, L., and Goodenowe, D. B. (2016). Improved specificity of serum phosphatidylcholine detection based on side-chain losses during negative electrospray ionization tandem mass spectrometry. *Anal. Bioanal. Chem.* 408, 7811–7823. doi:10.1007/s00216-016-9884-2

Rothhaar, T. L., Grosgen, S., Haupenthal, V. J., Burg, V. K., Hundsdorfer, B., Mett, J., et al. (2012). Plasmalogens inhibit APP processing by directly affecting gamma-secretase activity in Alzheimer's disease. *ScientificWorldJournal.* 2012, 141240. doi:10.1100/2012/141240

Rouser, G., and Yamamoto, A. (1968). Curvilinear regression course of human brain lipid composition changes with age. *Lipids* 3, 284–287. doi:10.1007/BF02531202

Scheff, S. W., Price, D. A., Schmitt, F. A., Scheff, M. A., and Mufson, E. J. (2011). Synaptic loss in the inferior temporal gyrus in mild cognitive impairment and Alzheimer's disease. *J. Alzheimers Dis.* 24, 547–557. doi:10.3233/JAD-2011-101782

Sperling, R. A., Aisen, P. S., Beckett, L. A., Bennett, D. A., Craft, S., Fagan, A. M., et al. (2011). Toward defining the preclinical stages of alzheimer's disease: Recommendations from the national institute on aging-alzheimer's association workgroups on diagnostic guidelines for alzheimer's disease. *Alzheimers Dement.* 7, 280–292. doi:10.1016/j.jalz.2011.03.003

Sperling, R., Mormino, E., and Johnson, K. (2014). The evolution of preclinical alzheimer's disease: Implications for prevention trials. *Neuron* 84, 608–622. doi:10.1016/j.neuron.2014.10.038

Sun, J. H., Yu, J. T., and Tan, L. (2015). The role of cholesterol metabolism in Alzheimer's disease. *Mol. Neurobiol.* 51, 947–965. doi:10.1007/s12035-014-8749-y

Ulus, I. H., Wurtman, R. J., Mauron, C., and Blusztajn, J. K. (1989). Choline increases acetylcholine release and protects against the stimulation-induced decrease in phosphatide levels within membranes of rat corpus striatum. *Brain Res.* 484, 217–227. doi:10.1016/0006-8993(89)90364-8

Wood, P. L., Khan, A. M., Mankidy, R., Smith, T., and Goodenowe, D. (2011). "Plasmalogen deficit: A new and testable hypothesis for the etiology of Alzheimer's disease," in *Alzheimer's disease pathogenesis-core concepts, shifting paradigms and therapeutic targets*. Editor S. De la Monte (India: InTech).

Wood, P. L., Mankidy, R., Ritchie, S., Heath, D., Wood, J. A., Flax, J., et al. (2010). Circulating plasmalogen levels and alzheimer disease assessment scale-cognitive scores in alzheimer patients. *J. Psychiatry Neurosci.* 35, 59–62. doi:10.1503/jpn.090059

Wood, P. L., Smith, T., Lane, N., Khan, M. A., Ehrmantraut, G., Goodenowe, D. B., et al. (2011). Oral bioavailability of the ether lipid plasmalogen precursor, PPI-1011, in the rabbit: A new therapeutic strategy for alzheimer's disease. *Lipids Health Dis.* 10, 227. doi:10.1186/1476-511X-10-227

Wurtman, R. J., Blusztajn, J. K., and Maire, J.-C. (1985). "Autocannibalism" of choline-containing membrane phospholipids in the pathogenesis of Alzheimer's disease-A hypothesis. *Neurochem. Int.* 7, 369–372. doi:10.1016/0197-0186(85)90127-5

Wurtman, R. J. (1992). Choline metabolism as a basis for the selective vulnerability of cholinergic neurons. *Trends Neurosci.* 15, 117–122. doi:10.1016/0166-2236(92)90351-8

Xie, J., Brayne, C., Matthews, F. E., and Medical Research Council Cognitive, F. (2008). Survival times in people with dementia: Analysis from population based cohort study with 14 year follow-up. *BMJ* 336, 258–262. doi:10.1136/bmj.39433.616678.25

Yang, Z., Gou, L., Chen, S., Li, N., Zhang, S., Zhang, L., et al. (2017). Membrane fusion involved in neurotransmission: Glimpse from electron microscope and molecular simulation. *Front. Mol. Neurosci.* 10, 168. doi:10.3389/fnmol.2017.00168

Yu, L., Boyle, P., Schneider, J. A., Segawa, E., Wilson, R. S., Leurgans, S., et al. (2013). APOE ε4, Alzheimer's disease pathology, cerebrovascular disease, and cognitive change over the years prior to death. *Psychol. Aging* 28, 1015–1023. doi:10.1037/a0031642

Yu, L., Dawe, R. J., Boyle, P. A., Gaiteri, C., Yang, J., Buchman, A. S., et al. (2017). Association between brain gene expression, DNA methylation, and alteration of *ex vivo* magnetic resonance imaging transverse relaxation in late-life cognitive decline. *JAMA Neurol.* 74, 1473–1480. doi:10.1001/jamaneurol.2017.2807

frontiers | Frontiers in Cell and Developmental Biology

TYPE Review
PUBLISHED 31 August 2022
DOI 10.3389/fcell.2022.946393

OPEN ACCESS

EDITED BY
Richard M. Epand,
McMaster University, Canada

REVIEWED BY
Christoph Thiele,
University of Bonn, Germany
Neale David Ridgway,
Dalhousie University, Canada

*CORRESPONDENCE
Fabian Dorninger,
fabian.dorninger@meduniwien.ac.at
Katrin Watschinger,
katrin.watschinger@i-med.ac.at

SPECIALTY SECTION
This article was submitted to Cellular Biochemistry,
a section of the journal
Frontiers in Cell and Developmental Biology

RECEIVED 17 May 2022
ACCEPTED 25 July 2022
PUBLISHED 31 August 2022

CITATION
Dorninger F, Werner ER, Berger J and Watschinger K (2022), Regulation of plasmalogen metabolism and traffic in mammals: The fog begins to lift. *Front. Cell Dev. Biol.* 10:946393. doi: 10.3389/fcell.2022.946393

Regulation of plasmalogen metabolism and traffic in mammals: The fog begins to lift

Fabian Dorninger[1]*, Ernst R. Werner[2], Johannes Berger[1] and Katrin Watschinger[2]*

[1]Department of Pathobiology of the Nervous System, Center for Brain Research, Medical University of Vienna, Vienna, Austria, [2]Institute of Biological Chemistry, Biocenter, Medical University of Innsbruck, Innsbruck, Austria

Due to their unique chemical structure, plasmalogens do not only exhibit distinct biophysical and biochemical features, but require specialized pathways of biosynthesis and metabolization. Recently, major advances have been made in our understanding of these processes, for example by the attribution of the gene encoding the enzyme, which catalyzes the final desaturation step in plasmalogen biosynthesis, or by the identification of cytochrome C as plasmalogenase, which allows for the degradation of plasmalogens. Also, models have been presented that plausibly explain the maintenance of adequate cellular levels of plasmalogens. However, despite the progress, many aspects around the questions of how plasmalogen metabolism is regulated and how plasmalogens are distributed among organs and tissues in more complex organisms like mammals, remain unresolved. Here, we summarize and interpret current evidence on the regulation of the enzymes involved in plasmalogen biosynthesis and degradation as well as the turnover of plasmalogens. Finally, we focus on plasmalogen traffic across the mammalian body – a topic of major importance, when considering plasmalogen replacement therapies in human disorders, where deficiencies in these lipids have been reported. These involve not only inborn errors in plasmalogen metabolism, but also more common diseases including Alzheimer's disease and neurodevelopmental disorders.

KEYWORDS

phospholipid, precursor treatment, lipid traffic, plasmalogen degradation, plasmalogen remodeling, plasmalogen biosynthesis, ether lipids, lipid metabolism

Abbreviations: AGMO, alkylglycerol monooxygenase; AGPS, alkylglyceronephosphate synthase; CDP-[E], CDP-ethanolamine; DG[O], 1-*O*-alkyl-2-acyl-*sn*-glycerol; DG[P], 1-*O*-alkenyl-2-acyl-*sn*-glycerol; DMA, dimethylacetal; ER, endoplasmic reticulum; FAR, fatty acyl-CoA reductase; GNPAT, glyceronephosphate *O*-acyltransferase; LPA[O], alkyl lysophosphatidic acid; LPA[P], alkenyl lysophosphatidic acid; LPE[P], alkenyl lysophosphatidylethanolamine; MG[O], monoalkylglycerol; PAF, platelet-activating factor; PA[O], alkyl phosphatidic acid; PBD, peroxisome biogenesis disorders; PEDS1, plasmanylethanolamine desaturase; PC, phosphatidylcholine; PC[O], plasmanylcholine; PC[P], plasmenylcholine (choline plasmalogen); PE, phosphatidylethanolamine; PE[O], plasmanylethanolamine; PE[P], plasmenylethanolamine (ethanolamine plasmalogen); PEX, peroxin; PL, phospholipase; PUFA, polyunsaturated fatty acid; RCDP, rhizomelic chondrodysplasia punctata.

1 Introduction

The discovery of plasmalogens in 1924 as an unknown, aldehyde-releasing substance present in plasma (plasmal-ogen) was an accidental observation owed to Robert Feulgen's group preferring to spend a hot summer day off in the woods and on the next day - tired of the day before - forgetting to put the $HgCl_2$-stained tissue slices into fixative and acid before staining with fuchsin-sulfurous acid (Debuch and Seng, 1972). In contrast to obtaining the expected intense nuclear purple-staining of DNA-derived aldehydes forming a Schiff base with the colorless acidic fuchsin solution - a nuclear staining method established in the Feulgen lab - they found fuchsin-staining also in the cellular plasma. Further investigations then revealed that these aldehydes derived from lipids. Nowadays, it has emerged, that these accidentally identified lipids are important and intriguing because of their involvement in different disease spectra and their distinct biophysical properties distinguishing them from other membrane lipids.

Plasmalogens, which are also called plasmenyl lipids, belong to the group of ether phospholipids (or short only ether lipids). They are discriminated from their metabolic precursors, the plasmanyl lipids, by a cis vinyl ether double bond (Norton et al., 1962; Warner and Lands, 1963). If both plasmanyl and plasmenyl lipids are absent, like in the peroxisomal disorders rhizomelic chondrodysplasia punctata (RCDP) and Zellweger spectrum disorders, but also in knockout mouse models with deletion of one of the initial, peroxisomal steps of plasmanyl/plasmenyl lipid biosynthesis, symptoms of affected individuals include impaired growth and neurological development, cataracts, and bone phenotypes with mouse models being generally milder than the respective human disease (Berger et al., 2016), where most patients die during childhood (Duker et al., 2020). So far, it is, however, not possible to clearly attribute symptom development to either missing plasmanyl lipids or plasmalogens, a line of research we are currently following. Decreased levels of plasmalogens have also been associated with smoking-related lung disease (Braverman and Moser, 2012) and were found in brains of Alzheimer's (Kou et al., 2011) and Parkinson's (Fabelo et al., 2011) disease patients. It is, however, still not clear whether loss of plasmalogens is causative in the etiology of these diseases or a consequence of them.

Plasmalogens are present in animals but are missing in plants and fungi (Goldfine, 2010). Knowledge on the genetics of plasmalogen biosynthesis was only very recently expanded with *Tmem189* (transmembrane protein of unknown function 189) having been shown to code for plasmanylethanolamine desaturase (PEDS1), the enzyme that introduces the crucial vinyl ether double bond into plasmanylethanolamines (PE[O]) in animals and thereby gives rise to the lipid subclass of plasmalogens (Gallego-García et al., 2019; Werner et al., 2020; Wainberg et al., 2021). Some bacteria, especially anaerobes, can also synthesize plasmalogens, however, they lost this capacity upon increase of oxygen in the atmosphere, possibly due to the sensitivity of plasmalogens to O_2. Later in evolution, plasmalogen biosynthesis reappeared in bacteria and was introduced rapidly also in animals (Goldfine, 2010). A distinct metabolic pathway for plasmalogen biosynthesis in bacteria was recently discovered (Jackson et al., 2021).

About 20% of all phospholipids in a human body are plasmalogens, which carry almost exclusively ethanolamine or choline as head group (Braverman and Moser, 2012). Such high values suggest that they are not only storage molecules for inflammatory mediators and signaling precursors but that they are required for shaping the properties of biological membranes (Koivuniemi, 2017). In this regard, Horrocks and Sharma stated in 1982 that plasmalogens are more loosely packed than their diacyl counterparts thereby increasing membrane fluidity, and that they differ in their surface potential from other phospholipids (Horrocks and Sharma, 1982). In 1984, the Paltauf group in Graz showed that ethanolamine plasmalogens (plasmenylethanolamine; PE[P]) are more likely to adopt the inverted hexagonal phase because they have lower lamellar gel to liquid-crystalline and lamellar to inverse-hexagonal phase transition temperatures compared to their alkylacyl- and diacyl-homologues (Lohner et al., 1984). Presence of the vinyl ether double bond decreases hydrophilicity and leads to a perpendicular orientation of the acyl side chain at *sn*-2 relative to the membrane surface (Lohner, 1996). This intrinsic drive to form inverted hexagonal structures as well as their reduced transition temperature between lamellar and non-lamellar phase also make plasmalogens important determinants in membrane fusion (Lohner, 1996). However, this was only shown for PE[P] and not for choline plasmalogens (plasmenylcholine; PC[P]), which do not form non-bilayer structures at temperatures around 37°C (Lohner, 1996). In contrast to Horrocks' and Sharma's observation, a membrane-rigidifying effect was attributed to plasmalogens by studying membranes of Zellweger patients and comparing them to healthy individuals (Hermetter et al., 1989). This finding was validated by atomistic molecular dynamics simulation studies showing higher lipid membrane condensation and thickness in membranes consisting purely of PE[P] (Rog and Koivuniemi, 2016). So far, it is not clear which plasmalogen content is needed in biological membranes to make a significant impact on membrane properties.

Very recently, ether lipids including plasmalogens were shown to have pro-ferroptotic traits (Aldrovandi and Conrad, 2020; Zou et al., 2020). Ferroptosis is elicited by lipid peroxidation (Stockwell et al., 2017). The current hypothesis regarding ether lipids is that the high abundance of polyunsaturated fatty acids (PUFA) at the *sn*-2 position makes them prone to oxidation due to their chemical properties and therefore these lipids promote this form of orchestrated cell death (Zou et al., 2020). Also two enzymes of ether lipid metabolism

which are crucial for plasmalogen biosynthesis were shown to be important for evoking ferroptosis (Cui et al., 2021). The first is fatty acyl-CoA reductase 1 (FAR1), the rate-limiting enzyme responsible for providing the fatty alcohol needed for the formation of the ether bond in peroxisomes (Cheng and Russell, 2004) and which is regulated in a feedback loop by the cellular amount of plasmalogens (see chapter 3.1.1.1 *Peroxisomal steps* and chapter 3.1.2 *Regulation of plasmalogen biosynthesis*) (Honsho et al., 2010). The second enzyme implicated in ferroptosis is PEDS1, however, Zou and co-workers did not identify PEDS1 in their CRISPR-screen (Zou et al., 2020). Further research will determine the exact impact of PEDS1 on ferroptosis and whether an enzyme exists that specifically enriches PUFA at the *sn*-2 position of plasmalogens, by distinguishing between plasmenyl and plasmanyl ether lipids.

Based on previous excellent reviews on the topic (Lessig and Fuchs, 2009; Braverman and Moser, 2012; Honsho and Fujiki, 2017; Dean and Lodhi, 2018; Dorninger et al., 2020), in this review we give an update on the knowledge of plasmalogen metabolism in mammals with a particular focus on steady state levels in health and disease, on the regulation of biosynthesis and remodeling as well as of the different ways for degradation. Furthermore, we highlight recent developments on trafficking of these lipids from dietary intake or autonomous biosynthesis to the distribution across the various tissues.

2 Steady state levels of plasmalogens in health and disease

The results of quantitative plasmalogen analyses are snapshots of the amount of plasmalogens at the time of extraction. In some investigations, the data reflect a mixture of many different cell types providing an overview of the situation in an entire tissue at an individual time point. It has long been known that lipid turnover rates vary strongly with respect to lipid species and tissue. One classical example is myelin, where the lipid turnover rate is much lower than in other brain-derived cell membranes (cf. chapter 3.3.2 *Turnover of plasmalogens*). Within cell membranes, lipid composition can change rapidly in response to environmental changes or in response to pathogens. For instance, plasmalogen levels increase in macrophages after cytomegalovirus infection (Jean Beltran et al., 2018). However, different techniques of plasmalogen determination must be distinguished for correct interpretation of the lipid changes. For example, the quantification of dimethylacetals (DMA) provides the amount of plasmalogens irrespective of the head group and the *sn*-2 fatty acid, but differentiating between the *sn*-1 alkyl chains (e.g., the total amount of C16:0, C18:1, C18:0 and C20:0 DMA). Thus, the sum of the most abundant DMA species yields a broad overview of general plasmalogen changes, like those resulting from altered biosynthesis or degradation. In contrast, lipidome analysis can identify changes in individual plasmalogen species in spite of unchanged overall plasmalogen levels, for example due to remodeling (Koch et al., 2022). With this distinction in mind, for example the robust changes in individual plasmalogen species observed in macrophages 120 h post viral infection might be a result of remodeling of the *sn*-2 position rather than being caused by increased plasmalogen synthesis, as most common plasmalogen species remain unaltered (Jean Beltran et al., 2018). On the other hand, the abnormalities in brain tissue of patients with Alzheimer's disease seem to represent a general reduction of total plasmalogen levels, as proven by different methods (Guan et al., 1999; Han et al., 2001; Grimm et al., 2011b; Kou et al., 2011). The inverse correlation between plasmalogen levels and pathology markers can be observed by both the sum of the most abundant DMA species (C16:0, C18:1, and C18:0) and common as well as uncommon individual plasmalogen species (Kou et al., 2011). It is known that in cell culture and in entire tissues compensatory adaptive lipid changes occur in response to the reduction or increase by exogenous supplementation of plasmalogens keeping the overall levels of ethanolamine phospholipids constant (Dorninger et al., 2015). Whether or not the same tight compensatory mechanisms also apply to lipids with other head groups is currently not known, presumably due to former difficulties in the identification of PC[P] species.

When considering the biological relevance of plasmalogen alterations, the head group is of crucial importance. In particular, the asymmetric distribution of different plasmalogen subclasses between the cytofacial and exofacial leaflets of the plasma membrane is not only essential for physical membrane properties, but possibly also for the ability of PLA2 to release PUFA from the *sn*-2 position. These considerations are particularly relevant given the involvement of these important fatty acids in signaling (Bazinet and Layé, 2014). It has been demonstrated by Fellmann and others that PE[P], like its diacyl counterpart phosphatidylethanolamine (PE), diffuses rapidly from the outer to the inner leaflet, whereas only less than 20% of PC[P] molecules, comparably to phosphatidylcholine (PC), reach the interior face of the membrane after 4 h. Thus, plasmalogens behave as the corresponding diacyl lipids in this respect (Fellmann et al., 1993). PE[P] has been suggested to accumulate in lipid rafts (also termed membrane rafts) (Pike et al., 2002), membrane microdomains enriched in cholesterol and sphingolipids, which compartmentalize cellular processes. However, confirmatory follow-up data on this issue are lacking and the concept of lipid rafts has been in constant flux over the years (Levental et al., 2020), thus clouding the potential role of plasmalogens within these membrane compartments. Also other membrane subdomains, caveolae and clathrin-coated pits, which are important for endo- and exocytotic processes, are dependent on plasmalogens as indicated by the fact that their morphology is altered upon ether lipid deficiency (Thai et al., 2001), which is in line with the fusogenic properties ascribed to plasmalogens

(Glaser and Gross, 1995). Apart from their potential enrichment in lipid rafts, plasmalogens have an additional connection to cholesterol: the levels of plasmalogens have been reported to influence cholesterol biosynthesis by modulating the stability of one of the key enzymes in the pathway, squalene monooxygenase (Honsho and Fujiki, 2017; Honsho et al., 2019).

2.1 Plasmalogen levels in different tissues

The contribution of plasmalogens to the total amount of phospholipids differs strongly between mammalian tissues with the highest amount being present in the myelin sheath, where plasmalogens account for about 31%–37% of all phospholipids (Horrocks, 1972). In brain white matter, which contains large amounts of myelin, PE[P] makes up about 85 mol% of all ethanolamine phospholipid species. Also in human gray matter, the proportion of plasmalogens among total ethanolamine phospholipids is relatively high with about 55 mol%–60 mol% (Han et al., 2001). With regard to the head group, it is of importance that in the entire brain PE[P] is particularly abundant representing 58% of total ethanolamine phospholipids (20% of all phospholipids), whereas PC[P] accounts for only about 1% of total choline phospholipids (0.8% of total phospholipids) (Panganamala et al., 1971; Heymans et al., 1983). In the heart, a similar proportion of ethanolamine phospholipids is present in the plasmalogen form (about 53% of total ethanolamine phospholipids) but, contrasting the brain, 26% of all choline phospholipids are PC[P] (Panganamala et al., 1971; Heymans et al., 1983). Skeletal muscle is comparable to heart tissue in this respect with 48% PE[P] of total ethanolamine phospholipids and 19% PC[P] of total choline phospholipids. On the other hand, the distribution in the kidney more closely resembles that of brain tissue (46% of total ethanolamine phospholipids as PE[P] and 5% of total choline phospholipids as PC[P]). The lowest amounts of plasmalogens are found in the liver with PE[P] representing only 8% of total ethanolamine phospholipids and PC[P] making up 3% of total choline phospholipids (Panganamala et al., 1971; Heymans et al., 1983). Modern lipidome analysis mostly confirms these historical analyses and constitutes an ideal, reliable and valuable technical resource for the detection of changes when comparing different experimental conditions or genotypes. However, due to the differences in the analytical procedure between different lipid classes it can be problematic to compare between individual lipid classes. On the other hand, the use of state-of-the-art lipidomic techniques elucidated an increasing number of less abundant plasmalogen species. From that, it became evident that next to the most common alcohols used by the alkylglyceronephosphate synthase (AGPS)/glyceronephosphate *O*-acyltransferase (GNPAT) complex to form the ether bond, i.e., C16:0, C18:0 and C18:1, also C20:0 is relatively common and many others with chain lengths from 16 to 24 carbon atoms, either saturated or with one or two double bonds, can exist (Amunugama et al., 2021; Azad et al., 2021). Furthermore, recent studies have shown that, apart from the predominant head groups ethanolamine and choline, also serine and inositol can serve as head group (Acar et al., 2007), whereas the broad range of fatty acyl residues at *sn*-2 has long been known.

2.2 Plasmalogen levels in different age groups

Plasmalogen levels are not constant in humans but increase and decrease with age. As deficiencies in plasmalogens are associated with a broad spectrum of diseases (see below), it is particularly important to understand which levels are physiological at what age. During gestation, plasmalogen concentration in the cerebrum starts to rapidly increase around the 32nd week together with other important lipids e.g., gangliosides. This increase continues also postnatally until about 6 month of age. Levels in cerebella were described to be generally higher than in the forebrain and continued to rise until the age of 2 years in children (Martínez and Ballabriga, 1978). Another study measured plasmalogen levels in red blood cells of full term neonates showing that they were low and in the range of a peroxisomal biogenesis defect patient. In this study levels doubled in their total value up to the age of 1–5 years (Labadaridis et al., 2009). This strong increase in early childhood was also found by other authors (Rouser and Yamamoto, 1968). In the human central nervous system (CNS), the levels of plasmalogens are relatively low at birth, but rise strongly during early development (Altrock and Debuch, 1968), thus paralleling myelination (Balakrishnan et al., 1961). They were shown to reach a maximum during adulthood, even though the diverse studies come to different conclusions as to the exact age [30 years in (Rouser and Yamamoto, 1968) and 70 years in (Weisser et al., 1997)]. In centenarians, though, lower levels than those measured in a 6-month old embryo were found (Weisser et al., 1997). Another study showed that plasmalogen levels in serum in elderly (65.5 ± 12.0 years of age) were clearly reduced when compared to a younger control cohort (23.5 ± 3.6 years of age) (Maeba et al., 2007). However, in a study comprising 152 elderly people (75.68 ± 0.43 years), the plasma PC[P] levels significantly increased during 90 months of aging and this increase was comparable to that of lyso-PC and lyso-platelet-activating factor (lyso-PAF) (Dorninger et al., 2018).

2.3 Plasmalogen levels in disease

The steady state of plasmalogen levels has been described to be altered in many different disorders (Farooqui and Horrocks, 2001; Dorninger et al., 2017). As the initial steps of plasmalogen synthesis take place within peroxisomes, peroxisome biogenesis disorders (PBD; Mendelian Inheritance in Man (MIM) database #601539) including the Zellweger syndrome spectrum (Zellweger syndrome, neonatal adrenoleukodystrophy and infantile Refsum disease), which are caused by either the total absence of peroxisomes or the presence of only peroxisomal ghosts without any luminal enzymes due to impaired protein import, have severely reduced plasmalogen levels. Newborns with PBD are often hypotonic and feed poorly. Further disease characteristics include distinctive facies, congenital malformations, neuronal migration defects associated with neonatal-onset seizures, renal cysts, skeletal abnormalities (chondrodysplasia punctata, rhizomelia) and liver disease that can be severe. Infants with severe PBD are significantly impaired and typically die during the first year of life, usually without developmental progress (Steinberg et al., 2006). The Zellweger syndrome spectrum represents a clinical continuum due to residual import capacity of the affected proteins associated with less severe phenotypes. In Zellweger syndrome spectrum, plasmalogen deficiency contributes to the pathology but as other peroxisomal functions such as peroxisomal ß-oxidation and peroxisomal α-oxidation etc. are disturbed as well, it is difficult to attribute individual pathologies to a specific impaired biochemical pathway. In contrast, the clinical symptoms can solely be attributed to ether lipid deficiency in patients with single enzyme deficiencies affecting one of the genes related to ether lipid biosynthesis, namely the *GNPAT* and the *AGPS* genes (for details see chapter 3.1.1.1 *Peroxisomal steps*), which cause RCDP type 2 (MIM #222765) and RCDP type 3 (MIM #600121), respectively, both of which are inherited autosomal recessively. In patients with the most severe classical form of RCDP, rhizomelia and chondrodysplasia punctata can be detected as early as 18 weeks of gestation by routine ultrasound (Krakow et al., 2003). Patients present with profound rhizomelia, growth retardation, facial dysmorphia, congenital cataract, cardiac defects, seizures, developmental delay and contractures (Braverman and Moser, 2012). As in the Zellweger syndrome spectrum, also the clinical spectrum of RCDP can vary depending on the extent of residual ether lipid synthesis, which can then lead to atypical forms of RCDP without rhizomelia and with only mild growth retardation, subtle facial dysmorphia, congenital cataract and developmental delay (Fallatah et al., 2021). Mutations in the peroxisomal matrix protein import receptors peroxin (PEX) 7 and PEX5L, both required for the import of AGPS into the peroxisome, are the genetic causes for RCDP type 1 (MIM #215100) and RCDP type 5 (MIM #616716), respectively. In the severe form, RCDP types 1, 2, 3, and 5 are clinically indistinguishable. Inherited mutations in the *FAR1* gene causing reduction or complete loss of FAR1 activity result in peroxisomal FAR1 deficiency (MIM #616154, also referred to as RCDP type 4), which can be clinically distinguished from the other forms of RCDP by the absence of chondrodysplasia punctata or rhizomelia (Buchert et al., 2014; Alshenaifi et al., 2019).

While the molecular basis for the plasmalogen reduction is obvious for all these peroxisomal disorders, the observed reduction in non-peroxisomal disorders like Alzheimer's disease is still under investigation. Presumably, several components contribute to the observed changes in the plasmalogen levels. The causes may also differ depending on which disease and which tissue is investigated. In Alzheimer's disease, the most common neurodegenerative disease and cause of dementia worldwide, considerably reduced levels of PE[P] (Guan et al., 1999; Han et al., 2001; Kou et al., 2011; Wood et al., 2015) and PC[P] (Grimm et al., 2011a; Igarashi et al., 2011) have been observed in *post mortem* brain tissues. The findings are consistent and were observed in several brain areas as well as in gray and white matter tissues. Interestingly, Kou et al. could demonstrate that in the very same gray matter regions, where plasmalogens were decreased, also other peroxisomal parameters such as peroxisomal density in neurons were affected and an increased concentration of very long-chain fatty acids, which are normally degraded in peroxisomes, has been observed (Kou et al., 2011). Thus, it might well be that different parameters such as synaptic loss (changing lipid composition) as well as impaired peroxisomal functions are causative for the observed reduction in plasmalogens in tissues of patients with Alzheimer's disease. The amount of plasmalogen reduction in *post mortem* gray matter tissue correlates with the severity of the disease measured as cognitive decline (Han, 2005) or neuropathological staging (Kou et al., 2011). Also in two different mouse models of Alzheimer's disease, reduced levels of plasmalogens have been described (Fabelo et al., 2012; Tajima et al., 2013). Whereas in the brain tissues of Alzheimer's disease patients the majority of plasmalogen species are reduced, in blood of Alzheimer's disease patients only selected plasmalogen species are reduced (Goodenowe et al., 2007; Yamashita et al., 2016; Huynh et al., 2020). Moreover, some of these plasmalogen species, whose levels were observed to be altered, have been suggested as biomarkers for cognitive decline (Mapstone et al., 2014). Interestingly, a recent study also detected reductions of individual plasmanylcholine (PC[O]) and PE[O] species next to PC[P] and PE[P] (Huynh et al., 2020). Another longitudinal population-based birth cohort study demonstrated alterations in the plasma levels of specific choline phospholipids in Alzheimer's disease that mimic accelerated aging (Dorninger et al., 2018). Also in the plasma of autistic patients the levels of total plasmalogens were found to be reduced by about 15%–20% in two independent studies (Bell et al., 2004; Wiest et al., 2009) and PE[P] were decreased by about 15% in the brain of a rat

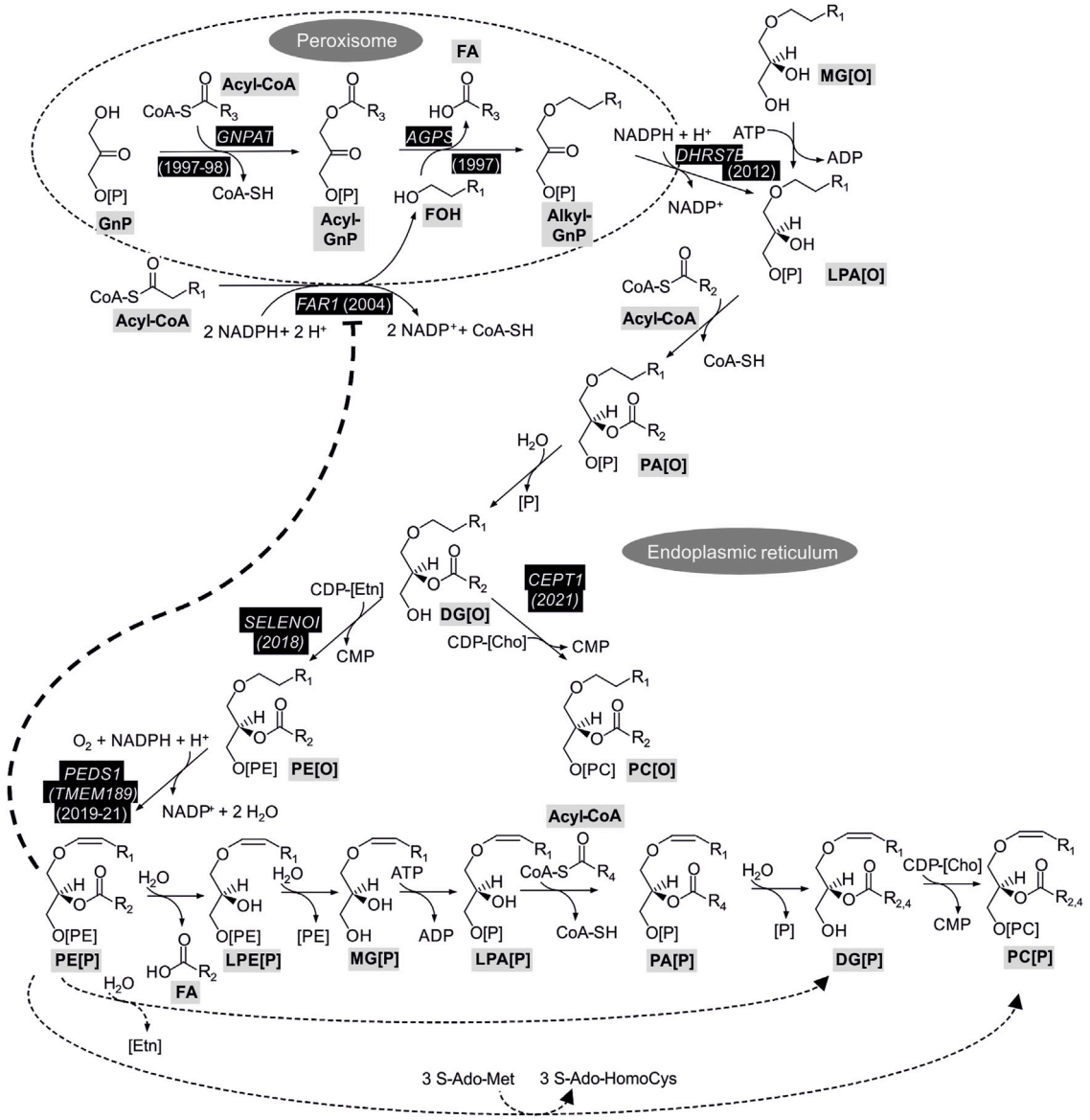

FIGURE 1
Enzymatic reactions and coding genes with confirmed role for plasmalogen biosynthesis. Gene symbols shown in white on black background indicate genes with experimental evidence for a role in plasmalogen biosynthesis with the year of publication of cloning or sequence assignment. For the steps without a gene assignment it is not clear to what extent genes catalyzing the reactions for ester (diacyl) lipids are also important for ether lipids. The bold dotted line indicates the feedback inhibition of plasmalogens on FAR1 protein stability which is detailed in a dedicated paragraph in chapter 3.1.2 *Regulation of plasmalogen biosynthesis*. The dotted lines in the bottom of the Figure represent routes of biosynthesis alternative to the main route connected by continuous lines. 1-O-Alkenyl-2-acyl-sn-glycerol (DG[P]) and PC[P] carry different side chains at sn-2 (R2 or R4) depending on the route taken from PE[P] (see text for details). The abbreviations of the metabolites follow the guidelines suggested for shorthand notation of mass spectrometry-derived lipid structures (Liebisch et al., 2020). Cho, choline; Etn, ethanolamine; FA, fatty acid; FOH, fatty alcohol; S-AdoMet, S-adenosyl-methionine; S-Ado-HomoCys, S-adenosyl-homocysteine.

model of autism (Thomas et al., 2010). In the case of autism spectrum disorders it is interesting to notice that mutations in the *PEX7* gene have been identified using whole exome sequencing (Yu et al., 2013) in agreement with the finding that RCDP patients with a milder (nonclassical) form often present with hyperactivity (Fallatah et al., 2021). Interestingly, also the mouse models for RCDP types 1 and 3 show hyperactive behavior as measured in the open field test (Dorninger et al., 2019b; Fallatah et al., 2020). Moreover, a detailed characterization of the *Gnpat*-deficient mouse model for RCDP type 3 revealed a complex behavioral phenotype mimicking several aspects of human psychiatric disorders (Dorninger et al., 2019a). In this context,

it is particularly remarkable that there is a direct correlation between plasmalogen levels and hyperactivity, as demonstrated in a mouse model series with varying degrees of Pex7 deficiency (Fallatah et al., 2022). Thus, there is growing evidence that reduced plasmalogen levels might be associated with hyperactivity in autism spectrum disorders but possibly also in Alzheimer's disease where hyperactivity is also a commonly observed feature.

Also in other disorders like Parkinson's disease (Hershkowitz and Adunsky, 1996; Dragonas et al., 2009; Fabelo et al., 2011) and Down syndrome (Murphy et al., 2000; Bueno et al., 2015), reduced levels of plasmalogens in plasma and gray matter have been described. Similarly, plasmalogen levels have been reported to be altered in schizophrenia. However, elevated levels of some PC[P] and PE[P] species have been described in the frontal cortex of patients (Wood et al., 2014), whereas reduced plasmalogen levels were detected in plasma (Kaddurah-Daouk et al., 2012).

3 Regulation of plasmalogens on the cellular level

3.1 Plasmalogen biosynthesis

3.1.1 Biosynthesis of plasmalogens

3.1.1.1 Peroxisomal steps

Enzymatic reactions of plasmalogen biosynthesis and their coding genes together with the year of gene assignment are shown in Figure 1. Biosynthesis of plasmalogens starts in peroxisomes and is completed at the endoplasmic reticulum (ER) (Nagan and Zoeller, 2001). In a first peroxisomal step, the glycolysis metabolite glycerone phosphate (GnP, previously called dihydroxyacetone phosphate) is acylated by GNPAT (EC 2.3.1.42; encoded by the *GNPAT* gene; (Thai et al., 1997; Ofman et al., 1998)) to yield acylglycerone phosphate (acyl-GnP). Subsequently, the acyl group is exchanged to an alkyl group by AGPS (E.C. 2.5.1.26; encoded by the *AGPS* gene; (de Vet et al., 1997)) by incorporation of a fatty alcohol to yield alkylglycerone phosphate (alkyl-GnP). The fatty alcohol is supplied by alcohol-forming FAR [E.C. 1.2.1.84; encoded by *FAR1* and *FAR2*; (Cheng and Russell, 2004)]. Due to its tissue distribution and enzymatic parameters, the *FAR1* gene product is considered to be more important for ether phospholipid biosynthesis (Cheng and Russell, 2004). Alkylglycerone phosphate is subsequently reduced to 1-*O*-alkyl-*sn*-glycero-3-phosphate (alkyl-lysophosphatidic acid, LPA[O]), which is the ether analog of lysophosphatidic acid (LPA), by the action of acylglycerone phosphate reductase [E.C. 1.1.1.101, previously called acyl/alkyl dihydroxyacetone phosphate reductase; encoded by *DHRS7B*; (Lodhi et al., 2012)]. The DHRS7B protein is associated with the peroxisomal membrane and the ER (Honsho et al., 2020) and the product is released to the ER.

3.1.1.2 Steps at the ER

The peroxisomal steps of plasmalogen biosynthesis can be bypassed by feeding of cells with (mono)alkylglycerol (MG[O]), which is phosphorylated to LPA[O]. At the ER the pathway proceeds downstream of LPA[O] similarly to the classical 1-*O*-acyl glycerophospholipids by acylation at *sn*-2 to alkyl phosphatidic acid (PA[O]) followed by cleavage of the phosphate from *sn*-3 to 1-*O*-alkyl-2-acyl-*sn*-glycerol (DG[O]). It is assumed that the respective enzymes for diacyl glycerophospholipids also act on the analogous ether lipids. DG[O] is then converted to PE[O] by ethanolamine phosphotransferase (E.C. 2.7.8.1) using CDP-ethanolamine (CDP-[E]). In contrast to the previous two steps, in this case the gene important for this step of plasmalogen synthesis is known, i.e., *SELENOI*. The underlying evidence comes from studying a rare inherited disease where this gene was affected, leading to severe complicated hereditary spastic paraplegia, sensorineural deafness, blindness and seizures (Horibata et al., 2018). Interestingly, the levels of PE[P] were more dramatically reduced in the patients' fibroblasts than that of the classical ester form PE. Due to the block in *SELENOI*, PC[O] (see Figure 1) was increased in the cells. The gene product of *SELENOI*, ethanolamine phosphotransferase 1, is not the only protein known to catalyze this reaction, it can also be supported by the product of *CEPT1* (choline/ethanolamine phosphotransferase 1), but patient data clearly show the prominent role of *SELENOI* for the biosynthesis of plasmalogens (Horibata et al., 2018). Knockout of *SELENOI* in human embryonic kidney (HEK293) cells confirmed its essential role for plasmalogen biosynthesis (Horibata et al., 2020). SELENOI showed a preference for synthesis of PE[O] with longer polyunsaturated side chains at *sn*-2 (Horibata et al., 2020). This may contribute to the preferential occurrence of these long polyunsaturated side chains at *sn*-2 in plasmalogens (Nagan and Zoeller, 2001). The enzyme encoded by *CEPT1*, on the other hand, has been shown to be the major enzyme responsible for the formation of PC[O] in HEK293 cells (Horibata and Sugimoto, 2021). The *CEPT1* gene product prefers shorter more saturated side chains (Horibata et al., 2020), which are also found at *sn*-2 of PC[O] in mouse tissues (Oemer et al., 2020). *CHPT1* is another gene encoding a choline phosphotransferase enzyme capable of attaching choline to DG[O] to form PC[O] like CEPT1. Although of minor importance in quantitative terms in HEK293 cells, the *CHPT1* gene product is remarkable in displaying a preference for the formation of PC[O] with longer unsaturated side chains (Horibata and Sugimoto 2021). Subsequent to *SELENOI*, PEDS1 (E.C. 1.14.19.77, former gene symbol: *TMEM189*) introduces the crucial vinyl ether bond to yield the first plasmalogen in the pathway, i.e., PE[P]. The *PEDS1* gene was recently assigned independently by three groups, one studying a bacterial light response (Gallego-García et al., 2019), one by a dedicated strategy to assign the gene

(Werner et al., 2020), and one with a systematic strategy to assign functions to genes with unknown function by looking for co-essentiality of genes in a dataset of 485 human cell lines (Wainberg et al., 2021). PC[P] cannot be formed directly from PC[O] by PEDS1-mediated desaturation, but is formed from PE[P] via several steps yielding the exchange of the phosphoethanolamine at *sn*-3 to phosphocholine (main route, connected by continuous lines in Figure 1) (Lee, 1998). Two further possibilities for the conversion of PE[P] to PC[P], which may also differ between tissues and physiological states of the cells (Nagan and Zoeller, 2001), are illustrated by dotted lines in Figure 1. The routes differ in the retention or exchange of the side chain at *sn*-2 (R_2 versus R_4). In the route indicated by a dotted line at the very bottom of the Figure, PE[P] is converted to PC[P] by the action of an N-methyltransferase (Mozzi et al., 1989). PE N-methyltransferase, however, has been found to occur mainly in the liver (Vance et al., 1997), an organ with very low plasmalogen content. Using radiolabeled precursors and HL-60 promyelocytic human cells (Blank et al., 1993) and Madin-Darby canine kidney (MDCK) cells (Strum and Daniel, 1993), it was suggested that a mixture of routes occurs in cultured cells, with only a minor contribution of the N-methylation pathway in neonatal rat myocytes (Lee et al., 1991). Alternatively to the routes shown in Figure 1, phospholipase (PL) D cleavage of alkenyl lysophosphatidylethanolamine (LPE[P]) to alkenyl lysophosphatidic acid (LPA[P], without the MG[P] intermediate) or direct head group alcohol exchange from PE[P] to PC[P] (without the DG[P] intermediate) have been suggested (Blank et al., 1993).

3.1.1.3 Specificity of enzymatic reactions for ether versus ester glycerolipid biosynthesis

With respect to the regulation of plasmalogen biosynthesis it is helpful to keep in mind that many enzymes along the pathway also have roles in the metabolism of diacyl glycerophospholipids. Acylation of glyceronephosphate by GNPAT followed by reduction of acylglyceronephosphate by acylglyceronephosphate reductase (the protein product of the *DHRS7B* gene, which can reduce both acylglycerone phosphate and alkylglycerone phosphate) has been shown by labeling experiments to be of major importance for triacylglycerol biosynthesis in the differentiation of 3T3-L1 adipocytes (Hajra et al., 2000). When calcineurin B homologous protein (CHP1) was inactivated in cells, this resulted in inactivation of glycerol-3-phosphate acyltransferase 4 (GPAT4), yielding a dependence of ester glycerolipid biosynthesis on GNPAT (Zhu et al., 2019). On the other hand, reconstituting a Chinese hamster ovary cell line with GNPAT deficiency by overexpressing GNPAT did not cause gross alterations in non-ether glycerophospholipid concentrations, showing that GNPAT does not normally contribute to non-ether glycerolipid biosynthesis (Liu et al., 2005). Analysis of lipids in cells with a specific deficiency in acylglyceronephosphate reductase suggested a role for this enzyme for ester in addition to ether glycerophospholipids (James et al., 1997). Overexpressing full length or N-terminally truncated acylglyceronephosphate reductase in this cell line altered the subcellular localization of the recombinant enzyme and the preference for restoration of ester versus ether lipids (Honsho et al., 2020). A cell line deficient in AGPS, in contrast, showed no impairment of ester glycerophospholipid biosynthesis (Nagan et al., 1997).

3.1.2 Regulation of plasmalogen biosynthesis

Regulation of plasmalogen biosynthesis has recently been reviewed by Honsho and Fujiki (Honsho and Fujiki, 2017), who have contributed seminal work to this topic. The key regulatory step of plasmalogen biosynthesis is FAR, which is encoded by two genes in man and mouse, i.e., *FAR1* and *FAR2* (Cheng and Russell, 2004). Of these, *FAR1* is of prime importance for plasmalogen synthesis, as it is more widespread in tissue distribution, has substrate specificities resembling the composition of plasmalogens at the *sn*-1 position, and leads to a severe inherited disease in humans with drastically lowered plasmalogen levels when inactivated (Buchert et al., 2014). *FAR2* has a more restricted expression pattern, other substrate specificities, i.e., a preference for saturated fatty acids, and has been suggested to be important for wax ester biosynthesis (Cheng and Russell, 2004). In work with cultured cells, Honsho and others could show that a sensing mechanism in the inner leaflet of the plasma membrane transmits a signal resulting in proteasomal degradation of FAR1 protein when plasmalogen levels are high (Honsho et al., 2010, 2017). This degradation of FAR1 protein can be triggered by PE[P], but not by PE. To which extent precursors or metabolic products of PE[P] can also trigger this regulatory mechanism, remains to be elucidated. A deficiency in the GNPAT or AGPS activities suppressed the formation of plasmalogens and led to an accumulation of fatty alcohols produced by FAR1 both in cultured cells (Honsho et al., 2010) and in plasma and cells from patients with inherited deficiencies in one of these steps (Rizzo et al., 1993). Recently, Ferdinandusse and others described an autosomal dominant disorder caused by *de novo* variants in *FAR1* resulting in uncontrolled ether lipid biosynthesis (Ferdinandusse et al., 2021). Apparently, the mutation inactivates the mechanism of FAR1 protein degradation in the presence of sufficient plasmalogens, leading to a fourfold increase of plasmalogen synthesis in patients' fibroblasts. Interestingly, the symptoms resemble in some aspects those of plasmalogen deficiency. For example, juvenile cataracts occur in both defective and uncontrolled synthesis of ether lipids. The regulation of plasmalogen biosynthesis by the described sensing of plasmalogens may also limit attempts to increase plasmalogen levels by administration of plasmalogens or precursors. To correct decreased plasmalogens, in murine models of cardiac

pathologies (Tham et al., 2018), batyl alcohol (1-*O*-octadecyl-*sn*-glycerol; MG[O] 18:0) was administered (Tham et al., 2018). This resulted in increased amounts of plasmalogens with a 18:0 side chain at *sn*-1, but also in a concomitant reduction of plasmalogens with 16:0 and 18:1 side chains at *sn*-1. Obviously, endogenous biosynthesis of plasmalogens had been downregulated as a result of the treatment, which also failed to correct the cardiac pathologies (Tham et al., 2018).

3.2 Plasmalogen remodeling

Plasmalogen remodeling can be discussed from two perspectives, i.e., side chain remodeling on the one hand and remodeling of the polar head group on the other hand.

3.2.1 Side chain remodeling

Side chain remodeling in plasmalogens is a fast process limited to the *sn*-2 position, as cleavage of the vinyl ether-bonded alkyl residue at the *sn*-1 position is an irreversible reaction. Remodeling at the *sn*-2 position consists of rapid deacylation-reacylation steps better known as the Land's cycle, which also occurs at both *sn*-1 and *sn*-2 in the ester analogues (Shindou et al., 2013; Wang and Tontonoz, 2019).

Deacylation at the *sn*-2 position is the first step in glycerophospholipid remodeling and is accomplished by the PLA_2 superfamily. This huge enzyme family is divided into six subfamilies, i.e., cytosolic PLA_2 ($cPLA_2$), calcium-independent PLA_2 ($iPLA_2$), secreted PLA_2 ($sPLA_2$), lysosomal PLA_2, PAF acetylhydrolases, and adipose-specific PLA_2 (Peng et al., 2021). The first three of these six subfamilies together comprise more than 20 different isoforms (Peng et al., 2021). The PLA_2 reaction results in a free fatty acid and a lysophospholipid. Besides being important for the remodeling itself, PLA_2-mediated release of arachidonic acid directly impacts inflammatory processes because it provides the precursor for many bioactive inflammatory mediators like eicosanoids. Arachidonic acid was shown to be specifically introduced into plasmalogens via the remodeling pathway and not by the *de novo* biosynthesis pathway (Ford and Gross, 1994; Yamashita et al., 1997).

Until now, involvement of the type of *sn*-1 chain linkage in determining PLA_2 selectivity was only scarcely investigated. Functioning of PAF, a pleiotropic factor in many cellular processes including inflammation and the best-described member of the PC[O] class (Demopoulos et al., 1979), is regulated by hydrolysis of the acetyl residue at *sn*-2 leading to its deactivation. It was shown that this specific deacetylation step is accomplished by PAF acetylhydrolase (also known as lipoprotein-associated PLA_2) (Tjoelker et al., 1995; Mouchlis et al., 2022). Also, 1-*O*-alkyl and 1-*O*-alkenyl ether phospholipids have been proposed to be remodeled by a CoA-independent transacylase, which specifically transfers polyunsaturated C20- and C22-fatty acids (Fleming and Hajra, 1977; Sugiura et al., 1987) explaining the finding that ether-linked phospholipid species specifically accumulate PUFA at their *sn*-2 position. The distribution pattern of this enzyme system, which is mainly located to microsomes of most tissues except liver, mirrors the distribution pattern of ether-linked phospholipids making it a likely candidate for ether phospholipid remodeling (Yamashita et al., 2014). However, no gene has been assigned so far to this proposed CoA-independent transacylase activity. Two additional studies also looked into the influence of the *sn*-1 bond type on substrate specificity of single PLA_2 enzymes. In 1992, Diez and others investigated a 14 kDa recombinant human synovial fluid PLA_2 and found a slight preference for acyl over alkyl residues at *sn*-1, whereas a 85 kDa cytosolic PLA_2 from monocytic cells (also named high molecular weight PLA_2) did not display a preference for a C16 ester- versus ether-bonded side chain at *sn*-1 (Diez et al., 1992). One year later, Hanel et al. also found that mammalian high molecular weight PLA_2 accepted 1-stearoyl-2-arachidonyl-*sn*-glycero-3-phosphocholine and 1-*O*-hexadec-1′-enyl-2-arachidonyl-*sn*-glycero-3-phosphocholine equally well as substrate (Hanel et al., 1993). Two calcium-independent PLA_2 with a preference for plasmalogens were described in the 1990s. The first one purified from canine myocardial tissue was shown to specifically hydrolyze PC[P] and arachidonylated glycerophospholipids (Hazen et al., 1990). The second one purified from bovine brain has a molecular mass of 39 kDa and was shown to preferentially cleave PE[P] (Hirashima et al., 1992). Two decades later, the same group also described a protocol for partial purification of a plasmalogen-selective PLA_2 from pig brain (Farooqui, 2010). Finally, very recently, a significant step forward was made in our understanding of how the *sn*-1 linkage impacts on PLA_2 selectivity. Hayashi and co-workers systematically assessed this issue by studying three different PLA_2 isoforms. They were able to show that for 1-*O*-alkyl ether phospholipids both group IVa $cPLA_2$ and group VIa $iPLA_2$ had about half the activity as for ester phospholipids (for group IVa $cPLA_2$ activity depended strongly on the *sn*-2 fatty acyl side chain, whereas group VIa $iPLA_2$ was more permissive in this regard). When testing 1-*O*-alkenyl ether phospholipids, however, preference of group IVa $cPLA_2$ was clearly on the side of the plasmalogens and not the ester-bonded lipids with a selectivity for PUFA at the *sn*-2 position, while group VIa $iPLA_2$ was equally active towards ester and plasmalogen phospholipids. In contrast to these two PLA_2 subtypes, the secreted isoform group V $sPLA_2$ clearly favors ester lipids over both alkyl and alkenyl ether phospholipids (Hayashi et al., 2022). These results indicate that the enzymes can distinguish between the various *sn*-1 bond types present in glycerophospholipids. Molecular modeling studies also revealed that the carbonyl oxygen in ester lipids interacts with a tryptophan in group V $sPLA_2$ allowing for precise accomodation of the ester glycerophospholipids in the

catalytic pocket and efficient hydrolysis of the acyl side chain (Hayashi et al., 2022).

The reacylation of ester and ether lysophospholipids is catalyzed by at least 14 different acyltransferases, which are known as acylglycerophosphate acyltransferases (AGPAT), membrane-bound *O*-acyltransferases (MBOAT), lysophosphocholine(ethanolamine) acyltransferases (LPC(E)AT) or more generally as lysophospholipid acyltransferases (LPLAT). As existing names were quite confusing, in part with multiple names for a single protein, a new nomenclature was recently proposed focusing on LPLAT only (Valentine et al., 2022). In the following paragraph we will focus on those isoforms known to impact on ether lipid, including plasmalogen, remodeling by using the updated nomenclature and providing former enzyme names in brackets.

Recently, it was found that LPLAT12 (LPCAT3)-deficient mice presented with disrupted plasmalogen homeostasis. A strong decrease was found in arachidonic (C20:4) and eicosapentaenoic (C20:5) acid *sn*-2 substitutions, which were compensated by other fatty acids (e.g., C22:4) leading to an overall balanced total amount of plasmalogens (Thomas et al., 2018). It is however not clear so far whether LPLAT12 (LPCAT3) contributes to the previously described CoA-independent transacylase system. In PAF remodeling, the acylation step consists of acetylation of lyso-PAF accomplished by LPLAT9 (LPCAT2), but also LPLAT8 (LPCAT1) (Shindou et al., 2007; Harayama et al., 2008). In a recent CRISPR-Cas9-based study investigating the role of ether lipids in the promotion of ferroptotic cell death, LPLAT3 (AGPAT3) emerged as a significant hit. This provided solid evidence that this isoform, already known to incorporate arachidonic and docosahexaenoic acid into ester lysophosphatidic acids (Yuki et al., 2009), is also crucial for generating *sn*-2-PUFA-containing ether phospholipids, which are essential for the susceptibility to ferroptosis (Zou et al., 2020). In previous work, where LPLAT3 (AGPAT3) had also popped up as potential hit in a CRISPR screen, LPLAT12 (LPCAT3) was shown to fuel ferroptosis (Dixon et al., 2015) and this effect was attributed to the enzyme's preference for arachidonic acid insertion into membrane phospholipids (Shindou and Shimizu, 2009).

3.2.2 Head group remodeling

Besides fast remodeling at the *sn*-2 position, plasmalogens also undergo polar head group remodeling. This exchange was shown to be 300 times faster than *de novo* plasmalogen synthesis - as measured by *sn*-1 alkyl chain incorporation - in studies using tritium-labeled choline or ethanolamine in contracting myocardium. Of note, this is in contrast to diacyl phospholipids, where *de novo* synthesis and remodeling happen at similar rates (Ford and Gross, 1994). Remodeling of PE[P] to PC[P] was proposed to occur through different mechanisms (Figure 1). Experimental evidence provided by Blank and coworkers in 1993 showed, that next to a multistep enzymatic cascade involving a PLA_2, followed by lysophospholipase D, acyltransferase, phosphohydrolase and cholinephosphotransferase steps [which resembles the *de novo* biosynthetic pathway presented in a comprehensive review (Nagan and Zoeller, 2001) and shown in Figure 1] also a more direct way exists. This involves either base exchange from ethanolamine to choline or a PLC-catalyzed removal of the phosphoethanolamine headgroup and introduction of phosphocholine through a choline phosphotransferase active in HL-60 cells (Blank et al., 1993). The existence of a PLC subtype which accepts plasmalogens as substrates was already proven 8 years earlier (Wolf and Gross, 1985).

Plasmalogens have been attributed a role in cardiolipin remodeling as they are substrates for the main enzyme responsible for producing mature cardiolipins, a transacylase named taffazin (Kimura et al., 2018). In tafazzin-deficient mouse heart, PC[P], arguably the most abundant phospholipid in this tissue, was strongly reduced, while PE[P]was unchanged and FAR1 protein expression was upregulated. This upregulation succeeded in maintaining PE[P] levels but was not able to counteract increased PC[P] degradation (Kimura et al., 2018). Follow-up studies from the same group then showed that other tissues including human brain and lymphoblasts obtained from Barth syndrome patients, characterized by taffazin deficiency, showed a marked reduction in PE[P] but at least in lymphoblasts no upregulation in FAR1 was found (Kimura et al., 2019). Supplementation of taffazin-deficient lymphoblasts with 1-*O*-hexadecyl-*sn*-glycerol, a precursor of plasmanyl and plasmenyl lipids, led to restoration of PE[P] and also cardiolipin levels (Bozelli et al., 2020). As tafazzin does not display a clear preference for certain acyl side chains and the molecular composition of cardiolipins differs from tissue to tissue, a systematic analysis of the impact of tissue phospholipid side chain composition on the cardiolipin side chain composition was performed. By applying machine learning, Oemer and others could show that the presence of high linoleic acid levels in the phospholipid pool was strongly linked to displacement of other fatty acids from the cardiolipin pool. Also oleic acid was a strong driver, however, oleic and linoleic acid inhibited each other's incorporation. In the brain, which is characterized by a unique fatty acyl side chain composition with many longer-chained essential fatty acids, the class of ether-linked phosphoethanolamine lipids displayed the highest profile similarities to cardiolipins (Oemer et al., 2020).

3.3 Regulation of degradation

3.3.1 Routes of degradation

This chapter only focuses on pathways and enzymatic reactions, which lead to degradation of the vinyl ether bond. Strictly speaking, on the level of individual plasmalogen subspecies, also the removal of fatty acyl chains or

plasmalogen head groups by PLs represents a way of degradation. However, for further details on species remodeling at the *sn*-2 and *sn*-3 positions, we kindly refer the reader to chapter 3.2 *Plasmalogen remodeling*.

3.3.1.1 Lysoplasmalogenase

Lysoplasmalogenase is an enzyme that acts, as its name suggests, on lysoplasmalogens, meaning that for its degradation of plasmalogens, the previous activity of a PLA_2 is required for removing the acyl side chain at the *sn*-2 position. The vinyl ether bond of lysoplasmalogens can then be hydrolyzed by lysoplasmalogenase (alternative name: alkenyl hydrolase) thus liberating a long chain fatty aldehyde and glycerophosphocholine/-ethanolamine. Already as early as 1961, a corresponding activity was detected in microsomes isolated from rat brain (Warner and Lands, 1961). Later, the enzyme was successfully purified and characterized in microsomes from rat liver (Jurkowitz-Alexander et al., 1989) and small intestine (Jurkowitz et al., 1999), two tissues, where its expression is reportedly high (Jurkowitz, 2015). However, it took until 2011 to assign a gene to this enzymatic function, when *TMEM86*B was identified as the gene coding for lysplasmalogenase in mammals (Wu et al., 2011). *TMEM86B* produces a transmembrane protein with six predicted transmembrane domains and was, accordingly, purified from membrane fractions. Interestingly, its activity is inhibited by LPA, which does not serve as a substrate (Wu et al., 2011). Unfortunately, LPA[P], the alkenyl analog of LPA, which has also been shown to be a bioactive compound (Dorninger et al., 2020), was not tested in that study. The enzyme encoded by *TMEM86B* accepts lysoplasmalogens with both headgroups, ethanolamine and choline (Wu et al., 2011), as substrates and, presumably, also acts on free alkenylglycerol (Gunawan and Debuch, 1985), a compound produced from lysoplasmalogen by the action of a PLC. Earlier studies, though, report the occurrence of a lysoplasmalogenase activity specific for individual head groups, i.e., for lysoplasmenylcholine (Warner and Lands, 1961; Arthur et al., 1986), thus feeding speculation that, apart from TMEM86B, additional, not yet identified lysoplasmalogenases exist in mammals (Watschinger and Werner, 2013). An obvious candidate is its paralog TMEM86A, a protein of long unknown function, which shares around 40% of its protein sequence with TMEM86B (Jurkowitz et al., 2015) and for which lysoplasmalogenase activity is predicted by the gene ontology (GO) project. No biologic function has been ascribed to the protein encoded by *TMEM86A* until recently. However, just during the production of the present review, a notable study was published demonstrating lysoplasmalogenase activity of TMEM86A in adipocytes and linking it to the development of obesity (Cho et al., 2022). Interestingly, the *TMEM86A* gene was also named in a recent study as a potential regulator of human epidermal keratinocyte differentiation (Zhang et al., 2021). Yet, the molecular mechanism underlying this finding remains unclear.

Interestingly, a protein with lysoplasmalogenase activity related to TMEM86B was discovered in bacteria of the *Legionella* genus. This is particularly remarkable considering that these bacteria do not possess plasmalogens themselves. However, it was speculated that the lysoplasmalogenase represents some kind of defense mechanism against host lysoplasmalogens, which could induce bacterial lysis (Jurkowitz et al., 2015). Just very recently, a similar mechanism was also revealed for another bacterial pathogen, *Mycobacterium tuberculosis* (Jurkowitz et al., 2022).

3.3.1.2 Plasmalogenase

The term plasmalogenase designates an enzyme with the ability to cleave the vinyl ether bond of plasmalogens. In contrast to the lysoplasmalogenase reaction (cf. chapter 3.3.1.1 *Lysoplasmalogenase*), the *sn*-2 position remains acylated prior to the action of plasmalogenase. A corresponding activity has been described in early studies on plasmalogens in mammalian brain and heart (Ansell and Spanner, 1968; Yavin and Gatt, 1972; D'Amato et al., 1975; Arthur et al., 1985) but proteins catalyzing the reaction could not be revealed for decades. Finally, in a hallmark study, cytochrome C, a mitochondrial enzyme most famous for its role in the respiratory chain and in apoptosis, was discovered as the first enzyme to exhibit plasmalogenase activity (Jenkins et al., 2018). The authors demonstrated that the peroxidase properties of cytochrome C lead to efficient hydrolytic cleavage of the vinyl ether bond under utilization of molecular oxygen. For activation of the plasmalogenase activity, though, the presence of either negatively charged lipids like cardiolipin and H_2O_2 or oxidized cardiolipin (or a similar lipid) are required. Even though some of the older reports indicated enzymatic activity only towards PE[P] (maybe due to their higher abundance) (Arthur et al., 1986), Jenkins et al. confirmed that both PE[P] and PC[P] are readily degraded by myocardial cytochrome C (Jenkins et al., 2018).

Yet, similarly as for lysoplasmalogenase, it remains a matter of debate if, apart from cytochrome C, also other enzymes possess plasmalogenase activity in mammals. One puzzling aspect is the fact that early reports described a considerable fraction of plasmalogenase activity to be located in the microsomal fraction after subcellular fractionation (Ansell and Spanner, 1968; Arthur et al., 1985), which is in apparent contradiction to the subcellular localization ascribed to cytochrome C. However, prominent activity was described in the mitochondrial fraction as well (Ansell and Spanner, 1968). Later, also cytosolic plasmalogenase activity was demonstrated in guinea pigs (McMaster et al., 1992), which would also fit to the idea of cytochrome C as responsible enzyme, as cytochrome C can be released into the cytosol under stress conditions (Garrido et al., 2006). Furthermore, the plasmalogenase activity of

cytochrome C requires highly specific conditions, i.e., the presence of O_2 and H_2O_2 or oxidized cardiolipin. Altogether, these facts may promote speculations that further enzymes capable of cleaving plasmalogens have to exist to explain the wide abundance of plasmalogenase activity as detailed in early studies.

3.3.1.3 Other enzymatic pathways

Myeloperoxidase is a lysosomal enzyme that is mainly expressed in neutrophils and monocytes and is an important regulator of inflammatory processes. Upon availability of H_2O_2, it converts chloride (Cl^-) and bromide (Br^-) ions to HOCl and HOBr, respectively. The vinyl ether bond of plasmalogens is susceptible to oxidation by both these compounds, resulting in the formation of lysolipids and the release of 2-halo fatty aldehydes (Albert et al., 2001), which themselves activate downstream signaling pathways and modulate immune reactions (Ebenezer et al., 2020). In the brain, upregulation of myeloperoxidase in response to microbiota attack has been implicated in neurodegeneration. The fact that HOCl-mediated oxidative attack of plasmalogens has been also proven *in vivo* in the mouse brain fueled speculation that plasmalogen degradation and subsequent defects in synaptic transmission are part of the underlying mechanism (Ullen et al., 2010).

Other than the hydrolases, which are important for the degradation of plasmalogens, plasmanyl lipids, which in contrast to plasmalogens do not harbor a vinyl ether bond next to the ether linkage, are degraded by the mixed function oxidase alkylglycerol monooxygenase (AGMO, E.C. 1.14.16.5) in the presence of the cofactor tetrahydrobiopterin (Watschinger et al., 2010). AGMO modulation in a knockdown macrophage cell line impacted the overall lipidome leading to increases in plasmanyl and plasmenyl lipids as well as strong reductions in glycosylated ceramides and cardiolipins (Watschinger et al., 2015). Recently, we established an AGMO knockout mouse, which presents with no obvious phenotype in unchallenged conditions (Sailer et al., 2021).

The fatty aldehydes resulting from the various degradation pathways, as outlined above, are toxic for cells due to their high reactivity in forming adducts with protein side chains and lipids and are therefore efficiently oxidized to the corresponding fatty acids by fatty aldehyde dehydrogenase (Weustenfeld et al., 2019). The fatty acids are then either catabolized for energy production or used in anabolic processes.

3.3.1.4 Non-enzymatic degradation of plasmalogens

Plasmalogens are susceptible to reactive oxygen species (ROS) that have been proposed to attack the vinyl ether double bond leading to enzyme-independent plasmalogen degradation and production of aldehydes. These aldehydes were either (n-1) carbons shorter than the original fatty alcohol or belonged to the class of α-hydroxyaldehydes. Both these product types are compatible with oxidative breakage of the vinyl ether double bond (Stadelmann-Ingrand et al., 2001). In contrast to diacyl phospholipids, plasmalogens have been discussed to be more prone to oxidation by such oxygen radicals (Khaselev and Murphy, 1999; Broniec et al., 2011). This feature has repeatedly evoked discussions about whether plasmalogens act as cellular antioxidants. For example, data from the Wanders group showed no changes in plasmalogen levels in cultured human skin fibroblasts incubated with or without intracellular ROS generator (Jansen and Wanders, 1997) and also Broniec et al. showed, 6 years after their first investigation (Broniec et al., 2011), that antioxidant properties in plasmalogens are not solely dependent on the vinyl ether (Broniec et al., 2017). In contrast, Zoeller et al. found that plasmalogen-deficient RAW264.7 cells were more susceptible to chemical hypoxia and supplementation with PE[P] reverted this hypersensitivity back to control levels (Zoeller et al., 1999) supporting the hypothesis of plasmalogens being antioxidants. In lupus erythematosus patients, which have elevated oxidative stress levels, it was found that plasmalogens were selectively decreased and *sn*-1 LPE (deacylated at the *sn*-1 position) and 4-hydroxy-2(E)-nonenal were increased (Hu et al., 2016).

3.3.2 Turnover of plasmalogens

A variety of studies have focused on different remodeling steps of plasmalogens (cf. chapter 3.2 *Plasmalogen remodeling*), but information on the turnover, i.e., the rate of degradation of the vinyl ether bond, is scarce. Although turnover rates most likely diverge strongly between organs and tissues, the few available data that have been gathered were derived almost exclusively from the brain. Early reports stated a relatively rapid turnover of brain plasmalogens, even of those in the myelin compartment (Horrocks and Fu, 1978), but indicated that half lives of PE[P] were longer than those of the corresponding diacyl phospholipids, even though exact numbers varied depending on the type of radioactively labeled precursor used (Miller et al., 1977). Later however, more detailed investigations involving intravenous infusion of radioactively labeled hexadecanol into anesthetized rats identified two different pools of brain PE[P] (Rosenberger et al., 2002) thus confirming earlier hypotheses (Freysz et al., 1969; Goracci et al., 1975): One is the metabolically less active myelin pool and the other a more dynamic pool of gray matter plasmalogens, which is turned over much more rapidly (Rosenberger et al., 2002) and may be a player in synaptic fusion and constriction processes like those in neurotransmission (Dorninger et al., 2019b). Strikingly, the half lives calculated in that study are in the magnitude of minutes, whereas another report estimated turnover times for myelin and microsomal PE[P] in the range of 4–58 days (Miller et al., 1977). The reason for this discrepancy may lie in the type or properties of the tracer used (Rosenberger et al., 2002) but illustrates that reliable absolute numbers for plasmalogen turnover are difficult to determine.

Notably, elaborate studies from the 1970s indicated that PC[P], which are comparatively rare in brain tissue, are metabolized more rapidly compared to their ethanolamine counterparts (Goracci et al., 1976). This is in accordance with the idea that the two subclasses fulfill fundamentally different roles in the brain. Whereas a large fraction of the much more abundant PE[P] likely are essential for membrane and myelin structure associated with a lower rate of turnover, PC[P] could serve other roles like acting as signaling mediators (Dorninger et al., 2020) and may thus be more short-lived.

3.3.3 Contributions of the different pathways and their regulation

The general view in literature appears to be that plasmalogen levels and composition are rather regulated via biosynthesis and remodeling than via cleavage of the vinyl ether bond. However, the reason for this may simply lie in the much higher number of studies on the former topics than on plasmalogen degradation. Actually, due to the fact that the genes and enzymes determining plasmalogen degradation have only been identified in recent years, knowledge on the interplay and regulation of these pathways is still in its infancy. Accordingly, the actual contributions of lysoplasmalogenases, plasmalogenases and other mechanisms to the turnover of plasmalogens can only be hypothesized, but is not yet supported by hard facts. A remarkable observation in this context is the seemingly reciprocal relationship between plasmalogen levels and lysoplasmalogenase activity (Gunawan and Debuch, 1981; Jurkowitz-Alexander et al., 1989; Wu et al., 2011). Most strikingly, lysoplasmalogenase expression and activity are high in the liver, an organ with particularly low amounts of plasmalogens, whereas heart and brain are characterized by both high plasmalogen levels and comparatively low lysoplasmalogenase activity. In addition, overexpression of *TMEM86B*, the gene coding for lysoplasmalogenase, in cultured cells resulted in lowered plasmalogen levels (Wu et al., 2011). This led several authors to speculate that lysoplasmalogenase is the major metabolic route for plasmalogen degradation or even for regulation of total plasmalogen levels (Braverman and Moser, 2012; Meikle and Summers, 2017).

In turn, a similar reciprocal association as for lysoplasmalogenase between expression and plasmalogen levels cannot be stated for cytochrome C, the only known plasmalogenase in mammals. *CYCS*, the gene encoding cytochrome C, is abundantly expressed in cardiac tissue, where its plasmalogenase activity was originally identified, but its expression is relatively low in the liver.

On the other hand, in the brain, plasmalogenase activity has been found to parallel the myelination process (Horrocks et al., 1978) and to increase in demyelinating lesions (Ansell and Spanner, 1968; Horrocks et al., 1978), possibly to get rid of phospholipids associated with myelin debris. However, it still needs to be established if cytochrome C acts as plasmalogenase in all tissues and/or if possibly other proteins capable of degrading plasmalogens exist.

What seems clear is that oxidative stress favors cleavage of the vinyl ether bond via different routes. Direct oxidative attack of the vinyl ether bond (see chapter 3.3.1.4 *Non-enzymatic degradation of plasmalogens*), increased activity of myeloperoxidase in certain cell types (see chapter 3.3.1.3 *Other enzymatic pathways*) and generation of oxidized phospholipids and H_2O_2 to support the plasmalogenase activity of cytochrome C (see chapter 3.3.1.2 *Plasmalogenase*) all take place under oxidative stress conditions. From this perspective, it is not surprising that a variety of human pathological conditions, which are associated with accumulation of reactive oxygen species, go along with a decrease of plasmalogen levels, like Alzheimer's disease (Han et al., 2001), spinal cord ischemia or hyperlipidemia (Brosche and Platt, 1998). For example, in the case of Alzheimer's disease, increased cytochrome C-mediated decay of plasmalogens as a consequence of oxidative stress has been hypothesized to be a driver of pathology (Jenkins et al., 2018). Similar mechanisms might be at work in other diseases, where H_2O_2 is excessively produced and serves as foundation for the plasmalogenase activity of cytochrome C. However, in mitochondria, where cytochrome C is normally localized, H_2O_2 is continuously produced by the respiratory chain (Sies, 2014) and, thus, probably present in every metabolically active cell. On the other hand, oxidized cardiolipin (another prerequisite for the plasmalogenase reaction mediated by cytochrome C) is apparently a marker of stress (Ji et al., 2012; Vähäheikkilä et al., 2018; Pizzuto and Pelegrin, 2020) and causes a domino effect eventually leading to neuronal death. Accordingly, future studies are needed to elucidate if cytochrome C acts as plasmalogenase to a relevant extent under physiological conditions or is only active upon excessive stress. Only then, its contribution to plasmalogen degradation in healthy cells and tissues can be assessed and put in the context of the other known routes of degradation, particularly the lysoplasmalogenase pathway.

4 Regulation of plasmalogen distribution across tissues in mammals

Even though humans (and most animals) have their own machinery to produce plasmalogens, these lipids can also be taken up from external sources. In this chapter, we discuss options for the supplementation with plasmalogens and current knowledge on how orally ingested plasmalogens are metabolized. Furthermore, we address the question, if and how plasmalogens are distributed to different tissues in mammals.

4.1 Dietary intake of plasmalogens

4.1.1 Plasmalogen content of conventional food

Plasmalogen ingestion via the diet happens already in early infancy, because several analytical studies have provided proof for the presence of plasmalogens and also lysoplasmalogens in breast milk from various mammalian species, including humans. Remarkably, the studies come to different conclusions as to the levels of the individual subclasses with one report stating that PC[P] account for the majority of human breast milk plasmalogens (Song et al., 2021), whereas other studies find PE[P] as the most abundant subclass (Garcia et al., 2012; Alexandre-Gouabau et al., 2018). Compared with other phospholipid classes (e.g., PE), PE[P] of breast milk has been described as particularly rich in PUFA (Moukarzel et al., 2016), which could be a major contributor to proper development of the newborn, given the importance of these fatty acids for brain formation and function (Bazinet and Layé, 2014). At later developmental stages, plasmalogen is mainly taken up by meat consumption. A comprehensive analysis of various meat subtypes revealed highest plasmalogen amounts in meat from livestock (especially beef, lamb and chicken) and considerably lower levels in different types of seafood, including fish and mussels (Wu et al., 2021). For meat bonvivants among the readers, it has been reported that meat derived from certain large deer species, i.e. moose and caribou, contains particularly high amounts of plasmalogens and lysoplasmalogens (Pham et al., 2021). Manipulation of foodstuff, like boiling, frying, or freeze-thawing, reportedly reduces plasmalogen content (Wu et al., 2020; Chen et al., 2022), which may in part be due to the propensity of these lipids for oxidation (cf. chapter 3.3.1.4 *Non-enzymatic degradation of plasmalogens*).

Not only plasmalogen content but also head group and side chain composition vary between meat from different species. Interestingly, analysis of the plasmalogens derived from the meat of certain marine invertebrates (shellfish) revealed high amounts of species with a serine headgroup, which is uncommon in mammalian tissue (Kraffe et al., 2004; Wang et al., 2021). Furthermore, a recent study investigating physiological effects of plasmalogen treatment detected considerably higher levels of docosahexaenoic acid and eicosapentaenoic acid in plasmalogens isolated from scallops compared with those of chicken, whereas oleic acid was enriched in chicken plasmalogens. Accordingly, scallop-derived plasmalogens showed more beneficial effects on memory tasks, when fed to mice (Hossain et al., 2022).

An essential question in the context of dietary plasmalogens is their metabolization and potential degradation in the course of the digestion process. In particular, the strongly acidic milieu in the stomach poses a considerable problem to the stability of plasmalogens, as the vinyl ether bond has been found to be sensitive to acid treatment already decades ago (Jones and Wood, 1964; Frosolono and Rapport, 1969). However, *in vitro* experiments exposing plasmalogens (embedded in sucrose-casein-based food pellets) for 1 h to conditions mimicking those in the mammalian stomach did not lead to plasmalogen degradation at a relevant rate. Likewise, the vinyl ether structure was largely preserved after incubation of emulsified plasmalogens with the intestinal contents of rats (Nishimukai et al., 2003). The exact extent of plasmalogen preservation in the stomach, though, may well depend on the exact pH of gastric juice. This can be deduced from other, yet unpublished data gathered by NMR spectroscopy, suggesting that plasmalogens can persist for 1 h at pH 2, but the rate of degradation increases considerably under lower pH and with increasing time (http://www.oilsfats.org.nz/wp-content/uploads/2016/02/Dawn-Scott-Nelson-talk-Nov-2016.pdf). Altogether, these data support the hypothesis that plasmalogens are not completely broken down in the alimentary tract after oral ingestion. Instead, at least a part of ingested plasmalogens, presumably after being packaged into chylomicron particles like other phospholipids (Iqbal and Hussain, 2009), is absorbed from the intestine into the lymph, as demonstrated by studies using duodenal infusion in rats (Hara et al., 2003). Remarkably, this process has been shown to be more effective for PC[P] than for PE[P] (Nishimukai et al., 2011). Furthermore, the *sn*-2 position appears to undergo remodeling with a clear preference for enrichment of arachidonic acid during absorption (Takahashi et al., 2020). Following the absorption process, chylomicrons likely serve as vehicles for plasmalogens to enter the circulation via the lymphatic system. In spite of these considerations, compared with endogenous biosynthesis, the contribution of the diet to tissue plasmalogen levels of mammals is supposed to be very low.

4.1.2 Plasmalogen supplementation as therapeutic strategy

Next to the ingestion via conventional dietary sources, the proactive supplementation with plasmalogens or their precursors represents an additional external source of plasmalogens, either as therapeutic strategy against pathological conditions or as a beneficial complement of the normal diet. Originally, the main intention for such an approach was the identification of treatment options for peroxisomal disorders with inborn ether lipid deficiency, as no cure for these dramatic diseases has been found yet. The most straightforward and also affordable strategy in this respect represents the supplementation with alkylglycerols like chimyl alcohol or batyl alcohol. These compounds contain a pre-formed ether bond and thus circumvent the peroxisomal steps of ether lipid biosynthesis, which are impaired in peroxisomal disorders associated with ether lipid deficiency. They are, therefore, readily converted to plasmalogens after oral ingestion and distributed to all peripheral organs, but not (at least not in substantial amounts) the brain, as shown by experiments in humans, mice and rats (Das and Hajra, 1988; Das et al., 1992; Brites et al., 2011; Paul et al., 2021). However, only limited and selective functional improvements have been

reported after alkylglycerol treatment in ether lipid-deficient mouse models (Brites et al., 2011; Todt et al., 2020) and no successful treatment with these compounds has yet been reported for human patients. Only recently, an unusual type of alkylglycerol with a C14 chain (tetradecylglycerol) has shown promising results particularly in the rescue of the myelination deficits in ether lipid-deficient animals and in *in vitro* assays (Malheiro et al., 2019). Interestingly, therapeutic application of alkylglycerols was also mentioned in other contexts apart from the treatment of ether lipid deficiency. Specifically, these substances are associated with antioxidative activity, immune system stimulation, anti-tumorigenic agents or facilitation of transport of other therapeutics (e.g., chemotherapeutics) across the blood-brain barrier (Erdlenbruch et al., 2003; Iannitti and Palmieri, 2010; Poleschuk et al., 2020).

In more recent years, with a continuously rising number of reports of pronounced plasmalogen deficits in human patients with common neurological disorders, particularly Alzheimer's disease, the interest in plasmalogens and their derivatives as a therapeutic option has markedly increased (Paul et al., 2019; Bozelli and Epand, 2021). Several preclinical studies have suggested that application of plasmalogens or their precursors has beneficial effects on cognitive or behavioral performance in mice and rats (Yamashita et al., 2017; Che et al., 2018; Fallatah et al., 2020; Hossain et al., 2022). A small-scale clinical study in Alzheimer's disease human patients even identified cognitive improvements in a subset of patients after oral administration of scallop-derived plasmalogens (Fujino et al., 2017). All these results are particularly astounding given the fact that none of the treatment strategies has succeeded in producing a measurable increase in brain plasmalogen levels, likely due to the fact that plasmalogens do not or only hardly cross the blood-brain barrier. Nevertheless, plasmalogens may unfold physiological actions relevant for the brain even without actually reaching it. One possibility that was suggested is a modulation of the gut microbiome (Hossain et al., 2022), which could also influence brain functions (Morais et al., 2021). Alternatively the supplemented plasmalogens could simply serve as vehicles for PUFA, which can be cleaved off the *sn*-2 position and reach the brain independently, where they may exert beneficial effects. Also, it is conceivable that minor amounts of plasmalogens or ether lipid species derived from them reach the brain without a measurable change in total levels, but still have biological effects, e.g., in signal transduction (Dorninger et al., 2020). Accordingly, plasmalogens are seen by some as a promising therapeutic target for the treatment of neurological diseases. In some markets, plasmalogens are even advertised as dietary supplements that should be taken prophylactically in order to avoid cognitive decline. However, an experimental proof for such an approach is not yet available.

With increasing commercial interest to exploit the therapeutic potential of plasmalogens, the strategies to increase their levels in humans have become manifold: Several different companies provide plasmalogens themselves, either as an oil formulation or encapsulated. Also, the individual formulations differ in their manufacturing; synthetically produced plasmalogens as well as plasmalogens extracted from natural sources, mostly from marine species like scallops, are available. Some commercially available plasmalogens show a specific chain distribution at *sn*-2 (e.g., DHA- or EPA-enriched), whereas others represent the whole spectrum of subspecies extracted from a certain source. In several marketed products, the actual plasmalogen amounts are surprisingly low and likely do not even exceed the levels present in meat products that are a normal part of the diet. Other providers pursue another strategy by offering precursors or derivatives that are transformed into plasmalogens after oral ingestion. One such option are alkylacylglycerols, which are closely related to the alkylglycerols described above but contain a pre-attached fatty acyl chain (in this case DHA) at sn-2. These compounds are metabolized to plasmalogens by introduction of a head group and the vinyl ether bond and *sn*-2 remodeling can occur in the tissues. Another company uses substances (PPI-1011, PPI-1025) with a pre-formed vinyl ether bond at *sn*-1, a fatty acyl chain (oleic acid or DHA) at *sn*-2 and a lipoyl group at *sn*-3 that increases stability and longevity. Also these precursors are converted into plasmalogens after oral intake and distributed across the body. Overall, the commercial enthusiasm about plasmalogens as nutritional or therapeutic supplements does not yet seem to match scientific evidence. Nevertheless, plasmalogen intake may have beneficial physiological effects under certain circumstances and involvement of these compounds or their derivatives in therapeutic strategies is a development to be monitored in the future.

4.2 Tissue-autonomous biosynthesis versus plasmalogen transport via the circulation

As outlined in chapter 2 *Steady state levels of plasmalogens in health and disease*, plasmalogen levels in the human body differ from tissue to tissue and are tightly regulated. How these tissue levels are reached, though, has not been shown. The liver has been proposed as the main location of plasmalogen synthesis with subsequent distribution via lipoproteins to the various tissues of the body (Snyder, 1972; Nagan and Zoeller, 2001; Braverman and Moser, 2012). Indeed, lipoproteins have high levels of plasmalogens and serum PE[P] levels reach 30% of total PE in rats and even 50% in humans. Different types of lipoproteins, including LDL, VLDL and HDL, all carry plasmalogens (Vance, 1990; Bräutigam et al., 1996) with highest levels reached in HDL (Ikuta et al., 2019). Regarding the role of plasmalogens in lipoproteins, there are reports showing them to be important for the protection from

oxidative stress (Vance, 1990; Engelmann et al., 1994; Hahnel et al., 1999) with LDL and VLDL plasmalogens being more efficiently oxidized than HDL plasmalogens (Felde and Spiteller, 1995). Another role for ether lipids was shown in cellular models of total ether lipid deficiency, where they were found to impact on reverse cholesterol transport via HDL but the underlying mechanism is not clear (Munn et al., 2003).

From these findings it clearly emerges that plasmalogens are abundantly present in lipoproteins and may fulfill important roles there. Whether their presence in lipoproteins is also causally linked to their arrival in all tissues is not clear so far. Restoration of plasmalogen content after alkylglycerol treatment in rodents and humans, however, supports the conclusion that lipoproteins or also serum albumin are capable of transporting ether lipids via the blood.

There are, however, also a couple of findings that are in sharp contrast to the hypothesis of tissue distribution of plasmalogens by lipoproteins from the liver to the periphery. First of all, plasmalogen levels in the liver are very low (Braverman and Moser, 2012) and this is presumably due to the fact that FAR1, the rate-limiting enzyme in plasmalogen biosynthesis, is hardly active in liver and liver cell lines (Lee et al., 1980). Also transport of relevant amounts of plasmalogens across the blood brain barrier has never been achieved in feeding or supplementation experiments using ether lipid-deficient or wild type rodents (Das and Hajra, 1988; Das et al., 1992; Brites et al., 2011) and there are already indications that brain plasmalogens are produced locally rather than imported from outside (Honsho and Fujiki, 2017). In a study using a mouse model with hepatocyte-specific deletion of Pex5 (Dirkx et al., 2005), the peroxisomal targeting signal 1 receptor, which is essential for assembly of functional peroxisomes (Dodt et al., 1995), we found that plasmalogen levels in seven tissues and plasma were not affected by the inability of hepatocytes to synthesize ether lipids (Werner et al., submitted).

5 Conclusion

The interest in plasmalogens has risen continuously since their discovery in the 1920s. In the last years, plasmalogens have not only drawn the attention of experts in the field of lipid research but also of a broader audience involving specialists from various disciplines. This is on the one hand due to rapid advancements in lipid analysis allowing the determination of plasmalogen subspecies in a wide variety of organisms, tissues and cell types and on the other hand, to recent discoveries linking plasmalogens to important cellular pathways like ferroptosis or indicating their involvement in common diseases, for example Alzheimer's disease or diabetes. However, to assess the role of plasmalogens in fundamental processes like ferroptosis or the etiology of complex diseases, it is imperative to understand in detail their physiological properties and regulation. Recent research has made big steps towards this goal, for example by the discovery of *TMEM189* as the gene coding for PEDS1 introducing the characteristic vinyl ether bond; or the revelation that strict homeostasis of plasmalogen levels is physiologically essential with both too high and too low levels causing similar and dramatic disease symptoms in humans. Nevertheless, several important aspects of plasmalogen biology remain in the dark. This is especially true for all facets of intra- and extracellular transport. Currently, it is still unclear, how ether lipid precursors are shuttled out of the peroxisome and, subsequently, to the ER for the last steps of plasmalogen biosynthesis. Similarly, little is known about plasmalogen transport between different tissues and here particularly, if and how plasmalogens can travel across the blood-brain barrier. Consequently, there is still a lot to learn about plasmalogens and their involvement in physiological and pathological processes and we are excited about what the future holds for research on these fascinating lipids.

Author contributions

FD conceived the review; FD, ERW, JB, and KW wrote the original draft of the manuscript; FD and KW revised the original draft; JB and KW acquired funding; FD, ERW, JB, and KW read and approved the final manuscript.

Funding

This work was supported by grants from the Austrian Science Fund (FWF; I2738-B26, P31082-B21, P30800-B26 and P34723-B) as well as RhizoKids International.

Conflict of interest

The authors declare that the research was conducted in the absence of any commercial or financial relationships that could be construed as a potential conflict of interest.

Publisher's note

References

Acar, N., Gregoire, S., Andre, A., Juaneda, P., Joffre, C., Bron, A. M., et al. (2007). Plasmalogens in the retina: *In situ* hybridization of dihydroxyacetone phosphate acyltransferase (DHAP-AT)--the first enzyme involved in their biosynthesis--and comparative study of retinal and retinal pigment epithelial lipid composition. *Exp. Eye Res.* 84, 143–151. doi:10.1016/j.exer.2006.09.009

Albert, C. J., Crowley, J. R., Hsu, F. F., Thukkani, A. K., and Ford, D. A. (2001). Reactive chlorinating species produced by myeloperoxidase target the vinyl ether bond of plasmalogens: Identification of 2-chlorohexadecanal. *J. Biol. Chem.* 276, 23733–23741. doi:10.1074/jbc.M101447200

Aldrovandi, M., and Conrad, M. (2020). Ferroptosis: The good, the bad and the ugly. *Cell Res.* 30, 1061–1062. doi:10.1038/s41422-020-00434-0

Alexandre-Gouabau, M.-C., Moyon, T., Cariou, V., Antignac, J.-P., Qannari, E. M., Croyal, M., et al. (2018). Breast milk lipidome is associated with early growth trajectory in preterm infants. *Nutrients* 10, E164. doi:10.3390/nu10020164

Alshenaifi, J., Ewida, N., Anazi, S., Shamseldin, H. E., Patel, N., Maddirevula, S., et al. (2019). The many faces of peroxisomal disorders: Lessons from a large Arab cohort. *Clin. Genet.* 95, 310–319. doi:10.1111/cge.13481

Altrock, K., and Debuch, H. (1968). Fettsäuren und Aldehyde von Gehirnphosphatiden während der fötalen und frühkindlichen Entwicklung des Menschen. *J. Neurochem.* 15, 1351–1359. doi:10.1111/j.1471-4159.1968.tb05914.x

Amunugama, K., Jellinek, M. J., Kilroy, M. P., Albert, C. J., Rasi, V., Hoft, D. F., et al. (2021). Identification of novel neutrophil very long chain plasmalogen molecular species and their myeloperoxidase mediated oxidation products in human sepsis. *Redox Biol.* 48, 102208. doi:10.1016/j.redox.2021.102208

Ansell, G. B., and Spanner, S. (1968). Plasmalogenase activity in normal and demyelinating tissue of the central nervous system. *Biochem. J.* 108, 207–209. doi:10.1042/bj1080207

Arthur, G., Covic, L., Wientzek, M., and Choy, P. C. (1985). Plasmalogenase in hamster heart. *Biochim. Biophys. Acta* 833, 189–195. doi:10.1016/0005-2760(85)90189-4

Arthur, G., Page, L., Mock, T., and Choy, P. C. (1986). The catabolism of plasmenylcholine in the Guinea pig heart. *Biochem. J.* 236, 475–480. doi:10.1042/bj2360475

Azad, A. K., Kobayashi, H., Md Sheikh, A., Osago, H., Sakai, H., Ahsanul Haque, M., et al. (2021). Rapid identification of plasmalogen molecular species using targeted multiplexed selected reaction monitoring mass spectrometry. *J. Mass Spectrom. Adv. Clin. Lab.* 22, 26–33. doi:10.1016/j.jmsacl.2021.09.004

Balakrishnan, S., Goodwin, H., and Cumings, J. N. (1961). The distribution of phosphorus-containing lipid compounds in the human brain. *J. Neurochem.* 8, 276–284. doi:10.1111/j.1471-4159.1961.tb13553.x

Bazinet, R. P., and Layé, S. (2014). Polyunsaturated fatty acids and their metabolites in brain function and disease. *Nat. Rev. Neurosci.* 15, 771–785. doi:10.1038/nrn3820

Bell, J. G., MacKinlay, E. E., Dick, J. R., MacDonald, D. J., Boyle, R. M., and Glen, A. C. A. (2004). Essential fatty acids and phospholipase A2 in autistic spectrum disorders. *Prostagl. Leukot. Essent. Fat. Acids* 71, 201–204. doi:10.1016/j.plefa.2004.03.008

Berger, J., Dorninger, F., Forss-Petter, S., and Kunze, M. (2016). Peroxisomes in brain development and function. *Biochim. Biophys. Acta* 1863, 934–955. doi:10.1016/j.bbamcr.2015.12.005

Blank, M. L., Fitzgerald, V., Lee, T. C., and Snyder, F. (1993). Evidence for biosynthesis of plasmenylcholine from plasmenylethanolamine in HL-60 cells. *Biochim. Biophys. Acta* 1166, 309–312. doi:10.1016/0005-2760(93)90112-m

Bozelli, J. C., Jr, and Epand, R. M. (2021). Plasmalogen replacement therapy. *Membranes* 11, 838. doi:10.3390/membranes11110838

Bozelli, J. C., Jr, Lu, D., Atilla-Gokcumen, G. E., and Epand, R. M. (2020). Promotion of plasmalogen biosynthesis reverse lipid changes in a Barth Syndrome cell model. *Biochim. Biophys. Acta. Mol. Cell Biol. Lipids* 1865, 158677. doi:10.1016/j.bbalip.2020.158677

Bräutigam, C., Engelmann, B., Reiss, D., Reinhardt, U., Thiery, J., Richter, W. O., et al. (1996). Plasmalogen phospholipids in plasma lipoproteins of normolipidemic donors and patients with hypercholesterolemia treated by LDL apheresis. *Atherosclerosis* 119, 77–88. doi:10.1016/0021-9150(95)05632-7

Braverman, N. E., and Moser, A. B. (2012). Functions of plasmalogen lipids in health and disease. *Biochim. Biophys. Acta* 1822, 1442–1452. doi:10.1016/j.bbadis.2012.05.008

Brites, P., Ferreira, A. S., da Silva, T. F., Sousa, V. F., Malheiro, A. R., Duran, M., et al. (2011). Alkyl-glycerol rescues plasmalogen levels and pathology of ether-phospholipid deficient mice. *PLoS One* 6, e28539. doi:10.1371/journal.pone.0028539

Broniec, A., Klosinski, R., Pawlak, A., Wrona-Krol, M., Thompson, D., and Sarna, T. (2011). Interactions of plasmalogens and their diacyl analogs with singlet oxygen in selected model systems. *Free Radic. Biol. Med.* 50, 892–898. doi:10.1016/j.freeradbiomed.2011.01.002

Broniec, A., Żądło, A., Pawlak, A., Fuchs, B., Kłosiński, R., Thompson, D., et al. (2017). Interaction of plasmenylcholine with free radicals in selected model systems. *Free Radic. Biol. Med.* 106, 368–378. doi:10.1016/j.freeradbiomed.2017.02.029

Brosche, T., and Platt, D. (1998). The biological significance of plasmalogens in defense against oxidative damage. *Exp. Gerontol.* 33, 363–369. doi:10.1016/s0531-5565(98)00014-x

Buchert, R., Tawamie, H., Smith, C., Uebe, S., Innes, A. M., Al Hallak, B., et al. (2014). A peroxisomal disorder of severe intellectual disability, epilepsy, and cataracts due to fatty acyl-CoA reductase 1 deficiency. *Am. J. Hum. Genet.* 95, 602–610. doi:10.1016/j.ajhg.2014.10.003

Bueno, A. A., Brand, A., Neville, M. M., Lehane, C., Brierley, N., and Crawford, M. A. (2015). Erythrocyte phospholipid molecular species and fatty acids of Down syndrome children compared with non-affected siblings. *Br. J. Nutr.* 113, 72–81. doi:10.1017/S0007114514003298

Che, H., Li, Q., Zhang, T., Ding, L., Zhang, L., Shi, H., et al. (2018). A comparative study of EPA-enriched ethanolamine plasmalogen and EPA-enriched phosphatidylethanolamine on Aβ42 induced cognitive deficiency in a rat model of Alzheimer's disease. *Food Funct.* 9, 3008–3017. doi:10.1039/c8fo00643a

Chen, Z., Jia, J., Wu, Y., Chiba, H., and Hui, S.-P. (2022). LC/MS analysis of storage-induced plasmalogen loss in ready-to-eat fish. *Food Chem.* 383, 132320. doi:10.1016/j.foodchem.2022.132320

Cheng, J. B., and Russell, D. W. (2004). Mammalian wax biosynthesis. I. Identification of two fatty acyl-Coenzyme A reductases with different substrate specificities and tissue distributions. *J. Biol. Chem.* 279, 37789–37797. doi:10.1074/jbc.M406225200

Cho, Y. K., Yoon, Y. C., Im, H., Son, Y., Kim, M., Saha, A., et al. (2022). Adipocyte lysoplasmalogenase TMEM86A regulates plasmalogen homeostasis and protein kinase A-dependent energy metabolism. *Nat. Commun.* 13, 4084. doi:10.1038/s41467-022-31805-3

Cui, W., Liu, D., Gu, W., and Chu, B. (2021). Peroxisome-driven ether-linked phospholipids biosynthesis is essential for ferroptosis. *Cell Death Differ.* 28, 2536–2551. doi:10.1038/s41418-021-00769-0

D'Amato, R. A., Horrocks, L. A., and Richardson, K. E. (1975). Kinetic properties of plasmalogenase from bovine brain. *J. Neurochem.* 24, 1251–1255. doi:10.1111/j.1471-4159.1975.tb03906.x

Das, A. K., and Hajra, A. K. (1988). High incorporation of dietary 1-O-heptadecyl glycerol into tissue plasmalogens of young rats. *FEBS Lett.* 227, 187–190. doi:10.1016/0014-5793(88)80895-0

Das, A. K., Holmes, R. D., Wilson, G. N., and Hajra, A. K. (1992). Dietary ether lipid incorporation into tissue plasmalogens of humans and rodents. *Lipids* 27, 401–405. doi:10.1007/BF02536379

de Vet, E. C., Zomer, A. W., Lahaut, G. J., and van den Bosch, H. (1997). Polymerase chain reaction-based cloning of alkyl-dihydroxyacetonephosphate synthase complementary DNA from Guinea pig liver. *J. Biol. Chem.* 272, 798–803. doi:10.1074/jbc.272.2.798

Dean, J. M., and Lodhi, I. J. (2018). Structural and functional roles of ether lipids. *Protein Cell* 9, 196–206. doi:10.1007/s13238-017-0423-5

Debuch, H., and Seng, P. (1972). The history of ether-linked lipids through 1960. *Ether Lipids Chem. Biol.*, 1–24. doi:10.1016/b978-0-12-654150-2.50008-7

Demopoulos, C. A., Pinckard, R. N., and Hanahan, D. J. (1979). Platelet-activating factor. Evidence for 1-O-alkyl-2-acetyl-sn-glyceryl-3-phosphorylcholine as the active component (a new class of lipid chemical mediators). *J. Biol. Chem.* 254, 9355–9358. doi:10.1016/s0021-9258(19)83523-8

Diez, E., Louis-Flamberg, P., Hall, R. H., and Mayer, R. J. (1992). Substrate specificities and properties of human phospholipases A2 in a mixed vesicle model. *J. Biol. Chem.* 267, 18342–18348. doi:10.1016/s0021-9258(19)36966-2

Dirkx, R., Vanhorebeek, I., Martens, K., Schad, A., Grabenbauer, M., Fahimi, D., et al. (2005). Absence of peroxisomes in mouse hepatocytes causes mitochondrial and ER abnormalities. *Hepatology* 41, 868–878. doi:10.1002/hep.20628

Dixon, S. J., Winter, G. E., Musavi, L. S., Lee, E. D., Snijder, B., Rebsamen, M., et al. (2015). Human haploid cell genetics reveals roles for lipid metabolism genes in nonapoptotic cell death. *ACS Chem. Biol.* 10, 1604–1609. doi:10.1021/acschembio.5b00245

Dodt, G., Braverman, N., Wong, C., Moser, A., Moser, H. W., Watkins, P., et al. (1995). Mutations in the PTS1 receptor gene, PXR1, define complementation group 2 of the peroxisome biogenesis disorders. *Nat. Genet.* 9, 115–125. doi:10.1038/ng0295-115

Dorninger, F., Brodde, A., Braverman, N. E., Moser, A. B., Just, W. W., Forss-Petter, S., et al. (2015). Homeostasis of phospholipids - the level of phosphatidylethanolamine tightly adapts to changes in ethanolamine plasmalogens. *Biochim. Biophys. Acta* 1851, 117–128. doi:10.1016/j.bbalip.2014.11.005

Dorninger, F., Forss-Petter, S., and Berger, J. (2017). From peroxisomal disorders to common neurodegenerative diseases - the role of ether phospholipids in the nervous system. *FEBS Lett.* 591, 2761–2788. doi:10.1002/1873-3468.12788

Dorninger, F., Forss-Petter, S., Wimmer, I., and Berger, J. (2020). Plasmalogens, platelet-activating factor and beyond - ether lipids in signaling and neurodegeneration. *Neurobiol. Dis.* 145, 105061. doi:10.1016/j.nbd.2020.105061

Dorninger, F., Gundacker, A., Zeitler, G., Pollak, D. D., and Berger, J. (2019a). Ether lipid deficiency in mice produces a complex behavioral phenotype mimicking aspects of human psychiatric disorders. *Int. J. Mol. Sci.* 20, E3929. doi:10.3390/ijms20163929

Dorninger, F., König, T., Scholze, P., Berger, M. L., Zeitler, G., Wiesinger, C., et al. (2019b). Disturbed neurotransmitter homeostasis in ether lipid deficiency. *Hum. Mol. Genet.* 28, 2046–2061. doi:10.1093/hmg/ddz040

Dorninger, F., Moser, A. B., Kou, J., Wiesinger, C., Forss-Petter, S., Gleiss, A., et al. (2018). Alterations in the plasma levels of specific choline phospholipids in Alzheimer's disease mimic accelerated aging. *J. Alzheimers Dis.* 62, 841–854. doi:10.3233/JAD-171036

Dragonas, C., Bertsch, T., Sieber, C. C., and Brosche, T. (2009). Plasmalogens as a marker of elevated systemic oxidative stress in Parkinson's disease. *Clin. Chem. Lab. Med.* 47, 894–897. doi:10.1515/CCLM.2009.205

Duker, A. L., Niiler, T., Kinderman, D., Schouten, M., Poll-The, B. T., Braverman, N., et al. (2020). Rhizomelic chondrodysplasia punctata morbidity and mortality, an update. *Am. J. Med. Genet. A* 182, 579–583. doi:10.1002/ajmg.a.61413

Ebenezer, D. L., Fu, P., Ramchandran, R., Ha, A. W., Putherickal, V., Sudhadevi, T., et al. (2020). S1P and plasmalogen derived fatty aldehydes in cellular signaling and functions. *Biochim. Biophys. Acta. Mol. Cell Biol. Lipids* 1865, 158681. doi:10.1016/j.bbalip.2020.158681

Engelmann, B., Bräutigam, C., and Thiery, J. (1994). Plasmalogen phospholipids as potential protectors against lipid peroxidation of low density lipoproteins. *Biochem. Biophys. Res. Commun.* 204, 1235–1242. doi:10.1006/bbrc.1994.2595

Erdlenbruch, B., Alipour, M., Fricker, G., Miller, D. S., Kugler, W., Eibl, H., et al. (2003). Alkylglycerol opening of the blood-brain barrier to small and large fluorescence markers in normal and C6 glioma-bearing rats and isolated rat brain capillaries. *Br. J. Pharmacol.* 140, 1201–1210. doi:10.1038/sj.bjp.0705554

Fabelo, N., Martín, V., Marín, R., Santpere, G., Aso, E., Ferrer, I., et al. (2012). Evidence for premature lipid raft aging in APP/PS1 double-transgenic mice, a model of familial Alzheimer disease. *J. Neuropathol. Exp. Neurol.* 71, 868–881. doi:10.1097/NEN.0b013e31826be03c

Fabelo, N., Martín, V., Santpere, G., Marín, R., Torrent, L., Ferrer, I., et al. (2011). Severe alterations in lipid composition of frontal cortex lipid rafts from Parkinson's disease and incidental Parkinson's disease. *Mol. Med.* 17, 1107–1118. doi:10.2119/molmed.2011.00119

Fallatah, W., Cui, W., Di Pietro, E., Carter, G. T., Pounder, B., Dorninger, F., et al. (2022). A Pex7 deficient mouse series correlates biochemical and neurobehavioral markers to genotype severity—implications for the disease spectrum of rhizomelic chondrodysplasia punctata type 1. *Front. Cell Dev. Biol.* 10, 886316. doi:10.3389/fcell.2022.886316

Fallatah, W., Schouten, M., Yergeau, C., Di Pietro, E., Engelen, M., Waterham, H. R., et al. (2021). Clinical, biochemical, and molecular characterization of mild (nonclassic) rhizomelic chondrodysplasia punctata. *J. Inherit. Metab. Dis.* 44, 1021–1038. doi:10.1002/jimd.12349

Fallatah, W., Smith, T., Cui, W., Jayasinghe, D., Di Pietro, E., Ritchie, S. A., et al. (2020). Oral administration of a synthetic vinyl-ether plasmalogen normalizes open field activity in a mouse model of rhizomelic chondrodysplasia punctata. *Dis. Model. Mech.* 13, dmm042499. doi:10.1242/dmm.042499

Farooqui, A. A., and Horrocks, L. A. (2001). Plasmalogens: Workhorse lipids of membranes in normal and injured neurons and glia. *Neuroscientist.* 7, 232–245. doi:10.1177/107385840100700308

Farooqui, A. A. (2010). Studies on plasmalogen-selective phospholipase A2 in brain. *Mol. Neurobiol.* 41, 267–273. doi:10.1007/s12035-009-8091-y

Felde, R., and Spiteller, G. (1995). Plasmalogen oxidation in human serum lipoproteins. *Chem. Phys. Lipids* 76, 259–267. doi:10.1016/0009-3084(94)02448-e

Fellmann, P., Hervé, P., and Devaux, P. F. (1993). Transmembrane distribution and translocation of spin-labeled plasmalogens in human red blood cells. *Chem. Phys. Lipids* 66, 225–230. doi:10.1016/0009-3084(93)90010-z

Ferdinandusse, S., McWalter, K., Te Brinke, H., IJlst, L., Mooijer, P. M., Ruiter, J. P. N., et al. (2021). Correction to: An autosomal dominant neurological disorder caused by de novo variants in FAR1 resulting in uncontrolled synthesis of ether lipids. *Genet. Med.* 23, 2467. doi:10.1038/s41436-021-01189-8

Fleming, P. J., and Hajra, A. K. (1977). 1-Alkyl-sn-glycero-3-phosphate: Acyl-CoA acyltransferase in rat brain microsomes. *J. Biol. Chem.* 252, 1663–1672. doi:10.1016/s0021-9258(17)40600-4

Ford, D. A., and Gross, R. W. (1994). The discordant rates of sn-1 aliphatic chain and polar head group incorporation into plasmalogen molecular species demonstrate the fundamental importance of polar head group remodeling in plasmalogen metabolism in rabbit myocardium. *Biochemistry* 33, 1216–1222. doi:10.1021/bi00171a022

Freysz, L., Bieth, R., and Mandel, P. (1969). Kinetics of the biosynthesis of phospholipids in neurons and glial cells isolated from rat brain cortex. *J. Neurochem.* 16, 1417–1424. doi:10.1111/j.1471-4159.1969.tb09893.x

Frosolono, M. F., and Rapport, M. M. (1969). Reactivity of plasmalogens: Kinetics of acid-catalyzed hydrolysis. *J. Lipid Res.* 10, 504–506. doi:10.1016/s0022-2275(20)43041-x

Fujino, T., Yamada, T., Asada, T., Tsuboi, Y., Wakana, C., Mawatari, S., et al. (2017). Efficacy and blood plasmalogen changes by oral administration of plasmalogen in patients with mild Alzheimer's disease and mild cognitive impairment: A multicenter, randomized, double-blind, placebo-controlled trial. *EBioMedicine* 17, 199–205. doi:10.1016/j.ebiom.2017.02.012

Gallego-García, A., Monera-Girona, A. J., Pajares-Martínez, E., Bastida-Martínez, E., Pérez-Castaño, R., Iniesta, A. A., et al. (2019). A bacterial light response reveals an orphan desaturase for human plasmalogen synthesis. *Science* 366, 128–132. doi:10.1126/science.aay1436

Garcia, C., Lutz, N. W., Confort-Gouny, S., Cozzone, P. J., Armand, M., and Bernard, M. (2012). Phospholipid fingerprints of milk from different mammalians determined by 31P NMR: Towards specific interest in human health. *Food Chem.* 135, 1777–1783. doi:10.1016/j.foodchem.2012.05.111

Garrido, C., Galluzzi, L., Brunet, M., Puig, P. E., Didelot, C., and Kroemer, G. (2006). Mechanisms of cytochrome c release from mitochondria. *Cell Death Differ.* 13, 1423–1433. doi:10.1038/sj.cdd.4401950

Glaser, P. E., and Gross, R. W. (1995). Rapid plasmenylethanolamine-selective fusion of membrane bilayers catalyzed by an isoform of glyceraldehyde-3-phosphate dehydrogenase: Discrimination between glycolytic and fusogenic roles of individual isoforms. *Biochemistry* 34, 12193–12203. doi:10.1021/bi00038a013

Goldfine, H. (2010). The appearance, disappearance and reappearance of plasmalogens in evolution. *Prog. Lipid Res.* 49, 493–498. doi:10.1016/j.plipres.2010.07.003

Goodenowe, D. B., Cook, L. L., Liu, J., Lu, Y., Jayasinghe, D. A., Ahiahonu, P. W. K., et al. (2007). Peripheral ethanolamine plasmalogen deficiency: A logical causative factor in Alzheimer's disease and dementia. *J. Lipid Res.* 48, 2485–2498. doi:10.1194/jlr.P700023-JLR200

Goracci, G., Francescangeli, E., Mozzi, R., Woelk, H., and Porcellati, G. (1976). The turnover of choline and ethanolamine plasmalogens in glial and neuronal cells of the rabbit *in vivo*. *Adv. Exp. Med. Biol.* 72, 123–129. doi:10.1007/978-1-4684-0955-0_11

Goracci, G., Francescangeli, E., Piccinin, G. L., Binaglia, L., Woelk, H., and Porcellati, G. (1975). The metabolism of labelled ethanolamine in neuronal and glial cells of the rabbit *in vivo*. *J. Neurochem.* 24, 1181–1186. doi:10.1111/j.1471-4159.1975.tb03895.x

Grimm, M. O. W., Grösgen, S., Riemenschneider, M., Tanila, H., Grimm, H. S., and Hartmann, T. (2011a). From brain to food: Analysis of phosphatidylcholins, lyso-phosphatidylcholins and phosphatidylcholin-plasmalogens derivates in Alzheimer's disease human post mortem brains and mice model via mass spectrometry. *J. Chromatogr. A* 1218, 7713–7722. doi:10.1016/j.chroma.2011.07.073

Grimm, M. O. W., Kuchenbecker, J., Rothhaar, T. L., Grösgen, S., Hundsdörfer, B., Burg, V. K., et al. (2011b). Plasmalogen synthesis is regulated via alkyl-dihydroxyacetonephosphate-synthase by amyloid precursor protein processing and is affected in Alzheimer's disease. *J. Neurochem.* 116, 916–925. doi:10.1111/j.1471-4159.2010.07070.x

Guan, Z., Wang, Y., Cairns, N. J., Lantos, P. L., Dallner, G., and Sindelar, P. J. (1999). Decrease and structural modifications of phosphatidylethanolamine plasmalogen in the brain with Alzheimer disease. *J. Neuropathol. Exp. Neurol.* 58, 740–747. doi:10.1097/00005072-199907000-00008

Gunawan, J., and Debuch, H. (1985). Alkenylhydrolase: A microsomal enzyme activity in rat brain. *J. Neurochem.* 44, 370–375. doi:10.1111/j.1471-4159.1985.tb05426.x

Gunawan, J., and Debuch, H. (1981). Liberation of free aldehyde from 1-(1-alkenyl)-sn-glycero-3-phosphoethanolamine (lysoplasmalogen) by rat liver microsomes. *Hoppe. Seylers. Z. Physiol. Chem.* 362, 445–452. doi:10.1515/bchm2.1981.362.1.445

Hahnel, D., Thiery, J., Brosche, T., and Engelmann, B. (1999). Role of plasmalogens in the enhanced resistance of LDL to copper-induced oxidation after LDL apheresis. *Arterioscler. Thromb. Vasc. Biol.* 19, 2431–2438. doi:10.1161/01.atv.19.10.2431

Hajra, A. K., Larkins, L. K., Das, A. K., Hemati, N., Erickson, R. L., and MacDougald, O. A. (2000). Induction of the peroxisomal glycerolipid-synthesizing enzymes during differentiation of 3T3-L1 adipocytes. Role in triacylglycerol synthesis. *J. Biol. Chem.* 275, 9441–9446. doi:10.1074/jbc.275.13.9441

Han, X., Holtzman, D. M., and McKeel, D. W., Jr (2001). Plasmalogen deficiency in early Alzheimer's disease subjects and in animal models: Molecular characterization using electrospray ionization mass spectrometry. *J. Neurochem.* 77, 1168–1180. doi:10.1046/j.1471-4159.2001.00332.x

Han, X. (2005). Lipid alterations in the earliest clinically recognizable stage of Alzheimer's disease: Implication of the role of lipids in the pathogenesis of alzheimer's disease. *Curr. Alzheimer Res.* 2, 65–77. doi:10.2174/1567205052772786

Hanel, A. M., Schüttel, S., and Gelb, M. H. (1993). Processive interfacial catalysis by mammalian 85-kilodalton phospholipase A2 enzymes on product-containing vesicles: Application to the determination of substrate preferences. *Biochemistry* 32, 5949–5958. doi:10.1021/bi00074a005

Hara, H., Wakisaka, T., and Aoyama, Y. (2003). Lymphatic absorption of plasmalogen in rats. *Br. J. Nutr.* 90, 29–32. doi:10.1079/bjn2003879

Harayama, T., Shindou, H., Ogasawara, R., Suwabe, A., and Shimizu, T. (2008). Identification of a novel noninflammatory biosynthetic pathway of platelet-activating factor. *J. Biol. Chem.* 283, 11097–11106. doi:10.1074/jbc.M708909200

Hayashi, D., Mouchlis, V. D., and Dennis, E. A. (2022). Each phospholipase A_2 type exhibits distinct selectivity toward sn-1 ester, alkyl ether, and vinyl ether phospholipids. *Biochim. Biophys. Acta. Mol. Cell Biol. Lipids* 1867, 159067. doi:10.1016/j.bbalip.2021.159067

Hazen, S. L., Stuppy, R. J., and Gross, R. W. (1990). Purification and characterization of canine myocardial cytosolic phospholipase A2. A calcium-independent phospholipase with absolute f1-2 regiospecificity for diradyl glycerophospholipids. *J. Biol. Chem.* 265, 10622–10630. doi:10.1016/s0021-9258(18)86992-7

Hermetter, A., Rainer, B., Ivessa, E., Kalb, E., Loidl, J., Roscher, A., et al. (1989). Influence of plasmalogen deficiency on membrane fluidity of human skin fibroblasts: A fluorescence anisotropy study. *Biochim. Biophys. Acta* 978, 151–157. doi:10.1016/0005-2736(89)90510-5

Hershkowitz, M., and Adunsky, A. (1996). Binding of platelet-activating factor to platelets of Alzheimer's disease and multiinfarct dementia patients. *Neurobiol. Aging* 17, 865–868. doi:10.1016/s0197-4580(96)00073-5

Heymans, H. S., Schutgens, R. B., Tan, R., van den Bosch, H., and Borst, P. (1983). Severe plasmalogen deficiency in tissues of infants without peroxisomes (Zellweger syndrome). *Nature* 306, 69–70. doi:10.1038/306069a0

Hirashima, Y., Farooqui, A. A., Mills, J. S., and Horrocks, L. A. (1992). Identification and purification of calcium-independent phospholipase A2 from bovine brain cytosol. *J. Neurochem.* 59, 708–714. doi:10.1111/j.1471-4159.1992.tb09426.x

Honsho, M., Abe, Y., and Fujiki, Y. (2017). Plasmalogen biosynthesis is spatiotemporally regulated by sensing plasmalogens in the inner leaflet of plasma membranes. *Sci. Rep.* 7, 43936. doi:10.1038/srep43936

Honsho, M., Asaoku, S., and Fujiki, Y. (2010). Posttranslational regulation of fatty acyl-CoA reductase 1, Far1, controls ether glycerophospholipid synthesis. *J. Biol. Chem.* 285, 8537–8542. doi:10.1074/jbc.M109.083311

Honsho, M., Dorninger, F., Abe, Y., Setoyama, D., Ohgi, R., Uchiumi, T., et al. (2019). Impaired plasmalogen synthesis dysregulates liver X receptor-dependent transcription in cerebellum. *J. Biochem.* 166, 353–361. doi:10.1093/jb/mvz043

Honsho, M., and Fujiki, Y. (2017). Plasmalogen homeostasis - regulation of plasmalogen biosynthesis and its physiological consequence in mammals. *FEBS Lett.* 591, 2720–2729. doi:10.1002/1873-3468.12743

Honsho, M., Tanaka, M., Zoeller, R. A., and Fujiki, Y. (2020). Distinct functions of acyl/alkyl dihydroxyacetonephosphate reductase in peroxisomes and endoplasmic reticulum. *Front. Cell Dev. Biol.* 8, 855. doi:10.3389/fcell.2020.00855

Horibata, Y., Ando, H., and Sugimoto, H. (2020). Locations and contributions of the phosphotransferases EPT1 and CEPT1 to the biosynthesis of ethanolamine phospholipids. *J. Lipid Res.* 61, 1221–1231. doi:10.1194/jlr.RA120000898

Horibata, Y., Elpeleg, O., Eran, A., Hirabayashi, Y., Savitzki, D., Tal, G., et al. (2018). EPT1 (selenoprotein I) is critical for the neural development and maintenance of plasmalogen in humans. *J. Lipid Res.* 59, 1015–1026. doi:10.1194/jlr.P081620

Horibata, Y., and Sugimoto, H. (2021). Differential contributions of choline phosphotransferases CPT1 and CEPT1 to the biosynthesis of choline phospholipids. *J. Lipid Res.* 62, 100100. doi:10.1016/j.jlr.2021.100100

Horrocks, L. A. (1972). Content, composition, and metabolism of mammalian and avian lipids that contain ether groups. *Ether Lipids Chem. Biol.*, 177–272. doi:10.1016/b978-0-12-654150-2.50016-6

Horrocks, L. A., and Fu, S. C. (1978). Pathway for hydrolysis of plasmalogens in brain. *Adv. Exp. Med. Biol.* 101, 397–406. doi:10.1007/978-1-4615-9071-2_37

Horrocks, L. A., and Sharma, M. (1982). Chapter 2 plasmalogens and O-alkyl glycerophospholipids. *New Compr. Biochem.*, 4, 51–93. doi:10.1016/s0167-7306(08)60006-x

Horrocks, L. A., Spanner, S., Mozzi, R., Fu, S. C., D'Amato, R. A., and Krakowka, S. (1978). Plasmalogenase is elevated in early demyelinating lesions. *Adv. Exp. Med. Biol.* 100, 423–438. doi:10.1007/978-1-4684-2514-7_30

Hossain, M. S., Mawatari, S., and Fujino, T. (2022). Plasmalogens, the vinyl ether-linked glycerophospholipids, enhance learning and memory by regulating brain-derived neurotrophic factor. *Front. Cell Dev. Biol.* 10, 828282. doi:10.3389/fcell.2022.828282

Hu, C., Zhou, J., Yang, S., Li, H., Wang, C., Fang, X., et al. (2016). Oxidative stress leads to reduction of plasmalogen serving as a novel biomarker for systemic lupus erythematosus. *Free Radic. Biol. Med.* 101, 475–481. doi:10.1016/j.freeradbiomed.2016.11.006

Huynh, K., Lim, W. L. F., Giles, C., Jayawardana, K. S., Salim, A., Mellett, N. A., et al. (2020). Concordant peripheral lipidome signatures in two large clinical studies of Alzheimer's disease. *Nat. Commun.* 11, 5698. doi:10.1038/s41467-020-19473-7

Iannitti, T., and Palmieri, B. (2010). An update on the therapeutic role of alkylglycerols. *Mar. Drugs* 8, 2267–2300. doi:10.3390/md8082267

Igarashi, M., Ma, K., Gao, F., Kim, H.-W., Rapoport, S. I., and Rao, J. S. (2011). Disturbed choline plasmalogen and phospholipid fatty acid concentrations in Alzheimer's disease prefrontal cortex. *J. Alzheimers Dis.* 24, 507–517. doi:10.3233/JAD-2011-101608

Ikuta, A., Sakurai, T., Nishimukai, M., Takahashi, Y., Nagasaka, A., Hui, S.-P., et al. (2019). Composition of plasmalogens in serum lipoproteins from patients with non-alcoholic steatohepatitis and their susceptibility to oxidation. *Clin. Chim. Acta.* 493, 1–7. doi:10.1016/j.cca.2019.02.020

Iqbal, J., and Hussain, M. M. (2009). Intestinal lipid absorption. *Am. J. Physiol. Endocrinol. Metab.* 296, E1183–E1194. doi:10.1152/ajpendo.90899.2008

Jackson, D. R., Cassilly, C. D., Plichta, D. R., Vlamakis, H., Liu, H., Melville, S. B., et al. (2021). Plasmalogen biosynthesis by anaerobic bacteria: Identification of a two-gene operon responsible for plasmalogen production in *Clostridium perfringens*. *ACS Chem. Biol.* 16, 6–13. doi:10.1021/acschembio.0c00673

James, P. F., Lake, A. C., Hajra, A. K., Larkins, L. K., Robinson, M., Buchanan, F. G., et al. (1997). An animal cell mutant with a deficiency in acyl/alkyl-dihydroxyacetone-phosphate reductase activity. Effects on the biosynthesis of ether-linked and diacyl glycerolipids. *J. Biol. Chem.* 272, 23540–23546. doi:10.1074/jbc.272.38.23540

Jansen, G. A., and Wanders, R. J. (1997). Plasmalogens and oxidative stress: Evidence against a major role of plasmalogens in protection against the superoxide anion radical. *J. Inherit. Metab. Dis.* 20, 85–94. doi:10.1023/a:1005321910248

Jean Beltran, P. M., Cook, K. C., Hashimoto, Y., Galitzine, C., Murray, L. A., Vitek, O., et al. (2018). Infection-Induced peroxisome biogenesis is a metabolic strategy for herpesvirus replication. *Cell Host Microbe* 24, 526–541.e7. doi:10.1016/j.chom.2018.09.002

Jenkins, C. M., Yang, K., Liu, G., Moon, S. H., Dilthey, B. G., and Gross, R. W. (2018). Cytochrome *c* is an oxidative stress-activated plasmalogenase that cleaves plasmenylcholine and plasmenylethanolamine at the *sn*-1 vinyl ether linkage. *J. Biol. Chem.* 293, 8693–8709. doi:10.1074/jbc.RA117.001629

Ji, J., Kline, A. E., Amoscato, A., Samhan-Arias, A. K., Sparvero, L. J., Tyurin, V. A., et al. (2012). Lipidomics identifies cardiolipin oxidation as a mitochondrial target for redox therapy of brain injury. *Nat. Neurosci.* 15, 1407–1413. doi:10.1038/nn.3195

Jones, D. M., and Wood, N. F. (1964). 1030. The mechanism of vinyl ether hydrolysis. *J. Chem. Soc.*, 5400. doi:10.1039/jr9640005400

Jurkowitz, M. (2015). Liver and small intestinal mucosa lysoplasmalogenase and nutrient metabolism/distribution. *FASEB J.* 29. doi:10.1096/fasebj.29.1_supplement.lb172

Jurkowitz, M. S., Azad, A. K., Monsma, P. C., Keiser, T. L., Kanyo, J., Lam, T. T., et al. (2022). *Mycobacterium tuberculosis* encodes a YhhN family membrane protein with lysoplasmalogenase activity that protects against toxic host lysolipids. *J. Biol. Chem.* 298, 101849. doi:10.1016/j.jbc.2022.101849

Jurkowitz, M. S., Horrocks, L. A., and Litsky, M. L. (1999). Identification and characterization of alkenyl hydrolase (lysoplasmalogenase) in microsomes and identification of a plasmalogen-active phospholipase A2 in cytosol of small intestinal epithelium. *Biochim. Biophys. Acta* 1437, 142–156. doi:10.1016/s1388-1981(99)00013-x

Jurkowitz, M. S., Patel, A., Wu, L.-C., Krautwater, A., Pfeiffer, D. R., and Bell, C. E. (2015). The YhhN protein of *Legionella pneumophila* is a Lysoplasmalogenase. *Biochim. Biophys. Acta* 1848, 742–751. doi:10.1016/j.bbamem.2014.11.011

Jurkowitz-Alexander, M., Ebata, H., Mills, J. S., Murphy, E. J., and Horrocks, L. A. (1989). Solubilization, purification and characterization of lysoplasmalogen alkenylhydrolase (lysoplasmalogenase) from rat liver microsomes. *Biochim. Biophys. Acta* 1002, 203–212. doi:10.1016/0005-2760(89)90288-9

Kaddurah-Daouk, R., McEvoy, J., Baillie, R., Zhu, H., K Yao, J., Nimgaonkar, V. L., et al. (2012). Impaired plasmalogens in patients with schizophrenia. *Psychiatry Res.* 198, 347–352. doi:10.1016/j.psychres.2012.02.019

Khaselev, N., and Murphy, R. C. (1999). Susceptibility of plasmenyl glycerophosphoethanolamine lipids containing arachidonate to oxidative degradation. *Free Radic. Biol. Med.* 26, 275–284. doi:10.1016/s0891-5849(98)00211-1

Kimura, T., Kimura, A. K., Ren, M., Berno, B., Xu, Y., Schlame, M., et al. (2018). Substantial decrease in plasmalogen in the heart associated with tafazzin deficiency. *Biochemistry* 57, 2162–2175. doi:10.1021/acs.biochem.8b00042

Kimura, T., Kimura, A. K., Ren, M., Monteiro, V., Xu, Y., Berno, B., et al. (2019). Plasmalogen loss caused by remodeling deficiency in mitochondria. *Life Sci. Alliance* 2, e201900348. doi:10.26508/lsa.201900348

Koch, J., Watschinger, K., Werner, E. R., and Keller, M. A. (2022). Tricky isomers—the evolution of analytical strategies to characterize plasmalogens and plasmanyl ether lipids. *Front. Cell Dev. Biol.* 10, 864716. doi:10.3389/fcell.2022.864716

Koivuniemi, A. (2017). The biophysical properties of plasmalogens originating from their unique molecular architecture. *FEBS Lett.* 591, 2700–2713. doi:10.1002/1873-3468.12754

Kou, J., Kovacs, G. G., Höftberger, R., Kulik, W., Brodde, A., Forss-Petter, S., et al. (2011). Peroxisomal alterations in Alzheimer's disease. *Acta Neuropathol.* 122, 271–283. doi:10.1007/s00401-011-0836-9

Kraffe, E., Soudant, P., and Marty, Y. (2004). Fatty acids of serine, ethanolamine, and choline plasmalogens in some marine bivalves. *Lipids* 39, 59–66. doi:10.1007/s11745-004-1202-x

Krakow, D., Williams, J., 3rd, Poehl, M., Rimoin, D. L., and Platt, L. D. (2003). Use of three-dimensional ultrasound imaging in the diagnosis of prenatal-onset skeletal dysplasias. *Ultrasound Obstet. Gynecol.* 21, 467–472. doi:10.1002/uog.111

Labadaridis, I., Moraitou, M., Theodoraki, M., Triantafyllidis, G., Sarafidou, J., and Michelakakis, H. (2009). Plasmalogen levels in full-term neonates. *Acta Paediatr.* 98, 640–642. doi:10.1111/j.1651-2227.2008.01205.x

Lee, T. C. (1998). Biosynthesis and possible biological functions of plasmalogens. *Biochim. Biophys. Acta* 1394, 129–145. doi:10.1016/s0005-2760(98)00107-6

Lee, T. C., Fitzgerald, V., Stephens, N., and Snyder, F. (1980). Activities of enzymes involved in the metabolism of ether-linked lipids in normal and neoplastic tissues of rat. *Biochim. Biophys. Acta* 619, 420–423. doi:10.1016/0005-2760(80)90091-0

Lee, T. C., Qian, C. G., and Snyder, F. (1991). Biosynthesis of choline plasmalogens in neonatal rat myocytes. *Arch. Biochem. Biophys.* 286, 498–503. doi:10.1016/0003-9861(91)90071-p

Lessig, J., and Fuchs, B. (2009). Plasmalogens in biological systems: Their role in oxidative processes in biological membranes, their contribution to pathological processes and aging and plasmalogen analysis. *Curr. Med. Chem.* 16, 2021–2041. doi:10.2174/092986709788682164

Levental, I., Levental, K. R., and Heberle, F. A. (2020). Lipid rafts: Controversies resolved, mysteries remain. *Trends Cell Biol.* 30, 341–353. doi:10.1016/j.tcb.2020.01.009

Liebisch, G., Fahy, E., Aoki, J., Dennis, E. A., Durand, T., Ejsing, C. S., et al. (2020). Update on LIPID MAPS classification, nomenclature, and shorthand notation for MS-derived lipid structures. *J. Lipid Res.* 61, 1539–1555. doi:10.1194/jlr.S120001025

Liu, D., Nagan, N., Just, W. W., Rodemer, C., Thai, T.-P., and Zoeller, R. A. (2005). Role of dihydroxyacetonephosphate acyltransferase in the biosynthesis of plasmalogens and nonether glycerolipids. *J. Lipid Res.* 46, 727–735. doi:10.1194/jlr.M400364-JLR200

Lodhi, I. J., Yin, L., Jensen-Urstad, A. P. L., Funai, K., Coleman, T., Baird, J. H., et al. (2012). Inhibiting adipose tissue lipogenesis reprograms thermogenesis and PPARγ activation to decrease diet-induced obesity. *Cell Metab.* 16, 189–201. doi:10.1016/j.cmet.2012.06.013

Lohner, K., Hermetter, A., and Paltauf, F. (1984). Phase behavior of ethanolamine plasmalogen. *Chem. Phys. Lipids* 34, 163–170. doi:10.1016/0009-3084(84)90041-0

Lohner, K. (1996). Is the high propensity of ethanolamine plasmalogens to form non-lamellar lipid structures manifested in the properties of biomembranes? *Chem. Phys. Lipids* 81, 167–184. doi:10.1016/0009-3084(96)02580-7

Maeba, R., Maeda, T., Kinoshita, M., Takao, K., Takenaka, H., Kusano, J., et al. (2007). Plasmalogens in human serum positively correlate with high- density lipoprotein and decrease with aging. *J. Atheroscler. Thromb.* 14, 12–18. doi:10.5551/jat.14.12

Malheiro, A. R., Correia, B., Ferreira da Silva, T., Bessa-Neto, D., Van Veldhoven, P. P., and Brites, P. (2019). Leukodystrophy caused by plasmalogen deficiency rescued by glyceryl 1-myristyl ether treatment. *Brain Pathol.* 29, 622–639. doi:10.1111/bpa.12710

Mapstone, M., Cheema, A. K., Fiandaca, M. S., Zhong, X., Mhyre, T. R., MacArthur, L. H., et al. (2014). Plasma phospholipids identify antecedent memory impairment in older adults. *Nat. Med.* 20, 415–418. doi:10.1038/nm.3466

Martínez, M., and Ballabriga, A. (1978). A chemical study on the development of the human forebrain and cerebellum during the brain "growth spurt" period. I. Gangliosides and plasmalogens. *Brain Res.* 159, 351–362. doi:10.1016/0006-8993(78)90540-1

McMaster, C. R., Lu, C. Q., and Choy, P. C. (1992). The existence of a soluble plasmalogenase in Guinea pig tissues. *Lipids* 27, 945–949. doi:10.1007/BF02535569

Meikle, P. J., and Summers, S. A. (2017). Sphingolipids and phospholipids in insulin resistance and related metabolic disorders. *Nat. Rev. Endocrinol.* 13, 79–91. doi:10.1038/nrendo.2016.169

Miller, S. L., Benjamins, J. A., and Morell, P. (1977). Metabolism of glycerophospholipids of myelin and microsomes in rat brain. Reutilization of precursors. *J. Biol. Chem.* 252, 4025–4037. doi:10.1016/s0021-9258(17)40228-6

Morais, L. H., Schreiber, H. L., 4thand Mazmanian, S. K. (2021). The gut microbiota-brain axis in behaviour and brain disorders. *Nat. Rev. Microbiol.* 19, 241–255. doi:10.1038/s41579-020-00460-0

Mouchlis, V. D., Hayashi, D., Vasquez, A. M., Cao, J., McCammon, J. A., and Dennis, E. A. (2022). Lipoprotein-associated phospholipase A_2: A paradigm for allosteric regulation by membranes. *Proc. Natl. Acad. Sci. U. S. A.* 119, e2102953118. doi:10.1073/pnas.2102953118

Moukarzel, S., Dyer, R. A., Keller, B. O., Elango, R., and Innis, S. M. (2016). Human milk plasmalogens are highly enriched in long-chain PUFAs. *J. Nutr.* 146, 2412–2417. doi:10.3945/jn.116.236802

Mozzi, R., Gramignani, D., Andriamampandr, C., Freysz, L., and Massarelli, R. (1989). Choline plasmalogen synthesis by the methylation pathway in chick neurons in culture. *Neurochem. Res.* 14, 579–583. doi:10.1007/BF00964921

Munn, N. J., Arnio, E., Liu, D., Zoeller, R. A., and Liscum, L. (2003). Deficiency in ethanolamine plasmalogen leads to altered cholesterol transport. *J. Lipid Res.* 44, 182–192. doi:10.1194/jlr.m200363-jlr200

Murphy, E. J., Schapiro, M. B., Rapoport, S. I., and Shetty, H. U. (2000). Phospholipid composition and levels are altered in Down syndrome brain. *Brain Res.* 867, 9–18. doi:10.1016/s0006-8993(00)02205-8

Nagan, N., Hajra, A. K., Das, A. K., Moser, H. W., Moser, A., Lazarow, P., et al. (1997). A fibroblast cell line defective in alkyl-dihydroxyacetone phosphate synthase: A novel defect in plasmalogen biosynthesis. *Proc. Natl. Acad. Sci. U. S. A.* 94, 4475–4480. doi:10.1073/pnas.94.9.4475

Nagan, N., and Zoeller, R. A. (2001). Plasmalogens: Biosynthesis and functions. *Prog. Lipid Res.* 40, 199–229. doi:10.1016/s0163-7827(01)00003-0

Nishimukai, M., Wakisaka, T., and Hara, H. (2003). Ingestion of plasmalogen markedly increased plasmalogen levels of blood plasma in rats. *Lipids* 38, 1227–1235. doi:10.1007/s11745-003-1183-9

Nishimukai, M., Yamashita, M., Watanabe, Y., Yamazaki, Y., Nezu, T., Maeba, R., et al. (2011). Lymphatic absorption of choline plasmalogen is much higher than that of ethanolamine plasmalogen in rats. *Eur. J. Nutr.* 50, 427–436. doi:10.1007/s00394-010-0149-0

Norton, W. T., Gottfried, E. L., and Rapport, M. M. (1962). The structure of plasmalogens: VI. Configuration of the double bond in the α, β-unsaturated ether linkage of phosphatidal choline. *J. Lipid Res.* 3, 456–459. doi:10.1016/s0022-2275(20)40391-8

Oemer, G., Koch, J., Wohlfarter, Y., Alam, M. T., Lackner, K., Sailer, S., et al. (2020). Phospholipid acyl chain diversity controls the tissue-specific assembly of mitochondrial cardiolipins. *Cell Rep.* 30, 4281–4291.e4. doi:10.1016/j.celrep.2020.02.115

Ofman, R., Hettema, E. H., Hogenhout, E. M., Caruso, U., Muijsers, A. O., and Wanders, R. J. (1998). Acyl-CoA:dihydroxyacetonephosphate acyltransferase: Cloning of the human cDNA and resolution of the molecular basis in rhizomelic chondrodysplasia punctata type 2. *Hum. Mol. Genet.* 7, 847–853. doi:10.1093/hmg/7.5.847

Panganamala, R. V., Horrocks, L. A., Geer, J. C., and Cornwell, D. G. (1971). Positions of double bonds in the monounsaturated alk-1-enyl groups from the plasmalogens of human heart and brain. *Chem. Phys. Lipids* 6, 97–102. doi:10.1016/0009-3084(71)90031-4

Paul, S., Lancaster, G. I., and Meikle, P. J. (2019). Plasmalogens: A potential therapeutic target for neurodegenerative and cardiometabolic disease. *Prog. Lipid Res.* 74, 186–195. doi:10.1016/j.plipres.2019.04.003

Paul, S., Rasmiena, A. A., Huynh, K., Smith, A. A. T., Mellett, N. A., Jandeleit-Dahm, K., et al. (2021). Oral supplementation of an alkylglycerol mix comprising different alkyl chains effectively modulates multiple endogenous plasmalogen species in mice. *Metabolites* 11, 299. doi:10.3390/metabo11050299

Peng, Z., Chang, Y., Fan, J., Ji, W., and Su, C. (2021). Phospholipase A2 superfamily in cancer. *Cancer Lett.* 497, 165–177. doi:10.1016/j.canlet.2020.10.021

Pham, T. H., Manful, C. F., Pumphrey, R. P., Hamilton, M. C., Adigun, O. A., Vidal, N. P., et al. (2021). Big game cervid meat as a potential good source of plasmalogens for functional foods. *J. Food Compos. Analysis* 96, 103724. doi:10.1016/j.jfca.2020.103724

Pike, L. J., Han, X., Chung, K.-N., and Gross, R. W. (2002). Lipid rafts are enriched in arachidonic acid and plasmenylethanolamine and their composition is independent of caveolin-1 expression: A quantitative electrospray ionization/mass spectrometric analysis. *Biochemistry* 41, 2075–2088. doi:10.1021/bi0156557

Pizzuto, M., and Pelegrin, P. (2020). Cardiolipin in immune signaling and cell death. *Trends Cell Biol.* 30, 892–903. doi:10.1016/j.tcb.2020.09.004

Poleschuk, T. S., Sultanov, R. M., Ermolenko, E. V., Shulgina, L. V., and Kasyanov, S. P. (2020). Protective action of alkylglycerols under stress. *Stress* 23, 213–220. doi:10.1080/10253890.2019.1660316

Rizzo, W. B., Craft, D. A., Judd, L. L., Moser, H. W., and Moser, A. B. (1993). Fatty alcohol accumulation in the autosomal recessive form of rhizomelic chondrodysplasia punctata. *Biochem. Med. Metab. Biol.* 50, 93–102. doi:10.1006/bmmb.1993.1050

Rog, T., and Koivuniemi, A. (2016). The biophysical properties of ethanolamine plasmalogens revealed by atomistic molecular dynamics simulations. *Biochim. Biophys. Acta* 1858, 97–103. doi:10.1016/j.bbamem.2015.10.023

Rosenberger, T. A., Oki, J., Purdon, A. D., Rapoport, S. I., and Murphy, E. J. (2002). Rapid synthesis and turnover of brain microsomal ether phospholipids in the adult rat. *J. Lipid Res.* 43, 59–68. doi:10.1016/s0022-2275(20)30187-5

Rouser, G., and Yamamoto, A. (1968). Curvilinear regression course of human brain lipid composition changes with age. *Lipids* 3, 284–287. doi:10.1007/BF02531202

Sailer, S., Coassin, S., Lackner, K., Fischer, C., McNeill, E., Streiter, G., et al. (2021). When the genome bluffs: A tandem duplication event during generation of a novel agmo knockout mouse model fools routine genotyping. *Cell Biosci.* 11, 54. doi:10.1186/s13578-021-00566-9

Shindou, H., Hishikawa, D., Harayama, T., Eto, M., and Shimizu, T. (2013). Generation of membrane diversity by lysophospholipid acyltransferases. *J. Biochem.* 154, 21–28. doi:10.1093/jb/mvt048

Shindou, H., Hishikawa, D., Nakanishi, H., Harayama, T., Ishii, S., Taguchi, R., et al. (2007). A single enzyme catalyzes both platelet-activating factor production and membrane biogenesis of inflammatory cells. Cloning and characterization of acetyl-CoA:LYSO-PAF acetyltransferase. *J. Biol. Chem.* 282, 6532–6539. doi:10.1074/jbc.M609641200

Shindou, H., and Shimizu, T. (2009). Acyl-CoA:lysophospholipid acyltransferases. *J. Biol. Chem.* 284, 1–5. doi:10.1074/jbc.R800046200

Sies, H. (2014). Role of metabolic H2O2 generation: Redox signaling and oxidative stress. *J. Biol. Chem.* 289, 8735–8741. doi:10.1074/jbc.R113.544635

Snyder, F. (1972). The enzymic pathways of ether-linked lipids and their precursors. *Ether Lipids Chem. Biol.*, 121–156. doi:10.1016/b978-0-12-654150-2.50014-2

Song, S., Liu, T.-T., Liang, X., Liu, Z.-Y., Yishake, D., Lu, X.-T., et al. (2021). Profiling of phospholipid molecular species in human breast milk of Chinese mothers and comprehensive analysis of phospholipidomic characteristics at different lactation stages. *Food Chem.* 348, 129091. doi:10.1016/j.foodchem.2021.129091

Stadelmann-Ingrand, S., Favreliere, S., Fauconneau, B., Mauco, G., and Tallineau, C. (2001). Plasmalogen degradation by oxidative stress: Production and disappearance of specific fatty aldehydes and fatty alpha-hydroxyaldehydes. *Free Radic. Biol. Med.* 31, 1263–1271. doi:10.1016/s0891-5849(01)00720-1

Steinberg, S. J., Dodt, G., Raymond, G. V., Braverman, N. E., Moser, A. B., and Moser, H. W. (2006). Peroxisome biogenesis disorders. *Biochim. Biophys. Acta* 1763, 1733–1748. doi:10.1016/j.bbamcr.2006.09.010

Stockwell, B. R., Friedmann Angeli, J. P., Bayir, H., Bush, A. I., Conrad, M., Dixon, S. J., et al. (2017). Ferroptosis: A regulated cell death nexus linking metabolism, redox biology, and disease. *Cell* 171, 273–285. doi:10.1016/j.cell.2017.09.021

Strum, J. C., and Daniel, L. W. (1993). Identification of a lysophospholipase C that may be responsible for the biosynthesis of choline plasmalogens by Madin-Darby canine kidney cells. *J. Biol. Chem.* 268, 25500–25508. doi:10.1016/s0021-9258(19)74420-2

Sugiura, T., Masuzawa, Y., Nakagawa, Y., and Waku, K. (1987). Transacylation of lyso platelet-activating factor and other lysophospholipids by macrophage microsomes. Distinct donor and acceptor selectivities. *J. Biol. Chem.* 262, 1199–1205. doi:10.1016/s0021-9258(19)75771-8

Tajima, Y., Ishikawa, M., Maekawa, K., Murayama, M., Senoo, Y., Nishimaki-Mogami, T., et al. (2013). Lipidomic analysis of brain tissues and plasma in a mouse model expressing mutated human amyloid precursor protein/tau for Alzheimer's disease. *Lipids Health Dis.* 12, 68. doi:10.1186/1476-511X-12-68

Takahashi, T., Kamiyoshihara, R., Otoki, Y., Ito, J., Kato, S., Suzuki, T., et al. (2020). Structural changes of ethanolamine plasmalogen during intestinal absorption. *Food Funct.* 11, 8068–8076. doi:10.1039/d0fo01666g

Thai, T. P., Heid, H., Rackwitz, H. R., Hunziker, A., Gorgas, K., and Just, W. W. (1997). Ether lipid biosynthesis: Isolation and molecular characterization of human dihydroxyacetonephosphate acyltransferase. *FEBS Lett.* 420, 205–211. doi:10.1016/s0014-5793(97)01495-6

Thai, T. P., Rodemer, C., Jauch, A., Hunziker, A., Moser, A., Gorgas, K., et al. (2001). Impaired membrane traffic in defective ether lipid biosynthesis. *Hum. Mol. Genet.* 10, 127–136. doi:10.1093/hmg/10.2.127

Tham, Y. K., Huynh, K., Mellett, N. A., Henstridge, D. C., Kiriazis, H., Ooi, J. Y. Y., et al. (2018). Distinct lipidomic profiles in models of physiological and pathological cardiac remodeling, and potential therapeutic strategies. *Biochim. Biophys. Acta. Mol. Cell Biol. Lipids* 1863, 219–234. doi:10.1016/j.bbalip.2017.12.003

Thomas, C., Jalil, A., Magnani, C., Ishibashi, M., Queré, R., Bourgeois, T., et al. (2018). LPCAT3 deficiency in hematopoietic cells alters cholesterol and phospholipid homeostasis and promotes atherosclerosis. *Atherosclerosis* 275, 409–418. doi:10.1016/j.atherosclerosis.2018.05.023

Thomas, R. H., Foley, K. A., Mepham, J. R., Tichenoff, L. J., Possmayer, F., and MacFabe, D. F. (2010). Altered brain phospholipid and acylcarnitine profiles in propionic acid infused rodents: Further development of a potential model of autism spectrum disorders. *J. Neurochem.* 113, 515–529. doi:10.1111/j.1471-4159.2010.06614.x

Tjoelker, L. W., Eberhardt, C., Unger, J., Trong, H. L., Zimmerman, G. A., McIntyre, T. M., et al. (1995). Plasma platelet-activating factor acetylhydrolase is a secreted phospholipase A2 with a catalytic triad. *J. Biol. Chem.* 270, 25481–25487. doi:10.1074/jbc.270.43.25481

Todt, H., Dorninger, F., Rothauer, P. J., Fischer, C. M., Schranz, M., Bruegger, B., et al. (2020). Oral batyl alcohol supplementation rescues decreased cardiac conduction in ether phospholipid-deficient mice. *J. Inherit. Metab. Dis.* 43, 1046–1055. doi:10.1002/jimd.12264

Ullen, A., Fauler, G., Köfeler, H., Waltl, S., Nusshold, C., Bernhart, E., et al. (2010). Mouse brain plasmalogens are targets for hypochlorous acid-mediated modification *in vitro* and *in vivo*. *Free Radic. Biol. Med.* 49, 1655–1665. doi:10.1016/j.freeradbiomed.2010.08.025

Vähäheikkilä, M., Peltomaa, T., Róg, T., Vazdar, M., Pöyry, S., and Vattulainen, I. (2018). How cardiolipin peroxidation alters the properties of the inner mitochondrial membrane? *Chem. Phys. Lipids* 214, 15–23. doi:10.1016/j.chemphyslip.2018.04.005

Valentine, W. J., Yanagida, K., Kawana, H., Kono, N., Noda, N. N., Aoki, J., et al. (2022). Update and nomenclature proposal for mammalian lysophospholipid acyltransferases, which create membrane phospholipid diversity. *J. Biol. Chem.* 298, 101470. doi:10.1016/j.jbc.2021.101470

Vance, D. E., Walkey, C. J., and Cui, Z. (1997). Phosphatidylethanolamine N-methyltransferase from liver. *Biochim. Biophys. Acta* 1348, 142–150. doi:10.1016/s0005-2760(97)00108-2

Vance, J. E. (1990). Lipoproteins secreted by cultured rat hepatocytes contain the antioxidant 1-alk-1-enyl-2-acylglycerophosphoethanolamine. *Biochim. Biophys. Acta* 1045, 128–134. doi:10.1016/0005-2760(90)90141-j

Wainberg, M., Kamber, R. A., Balsubramani, A., Meyers, R. M., Sinnott-Armstrong, N., Hornburg, D., et al. (2021). A genome-wide atlas of co-essential

modules assigns function to uncharacterized genes. *Nat. Genet.* 53, 638–649. doi:10.1038/s41588-021-00840-z

Wang, B., and Tontonoz, P. (2019). Phospholipid remodeling in physiology and disease. *Annu. Rev. Physiol.* 81, 165–188. doi:10.1146/annurev-physiol-020518-114444

Wang, J., Liao, J., Wang, H., Zhu, X., Li, L., Lu, W., et al. (2021). Quantitative and comparative study of plasmalogen molecular species in six edible shellfishes by hydrophilic interaction chromatography mass spectrometry. *Food Chem.* 334, 127558. doi:10.1016/j.foodchem.2020.127558

Warner, H. R., and Lands, W. E. M. (1963). The configuration of the double bond in naturally-occurring alkenyl ethers. *J. Am. Chem. Soc.* 85, 60–64. doi:10.1021/ja00884a012

Warner, H. R., and Lands, W. E. (1961). The metabolism of plasmalogen: Enzymatic hydrolysis of the vinyl ether. *J. Biol. Chem.* 236, 2404–2409. doi:10.1016/s0021-9258(18)64011-6

Watschinger, K., Keller, M. A., Golderer, G., Hermann, M., Maglione, M., Sarg, B., et al. (2010). Identification of the gene encoding alkylglycerol monooxygenase defines a third class of tetrahydrobiopterin-dependent enzymes. *Proc. Natl. Acad. Sci. U. S. A.* 107, 13672–13677. doi:10.1073/pnas.1002404107

Watschinger, K., Keller, M. A., McNeill, E., Alam, M. T., Lai, S., Sailer, S., et al. (2015). Tetrahydrobiopterin and alkylglycerol monooxygenase substantially alter the murine macrophage lipidome. *Proc. Natl. Acad. Sci. U. S. A.* 112, 2431–2436. doi:10.1073/pnas.1414887112

Watschinger, K., and Werner, E. R. (2013). Orphan enzymes in ether lipid metabolism. *Biochimie* 95, 59–65. doi:10.1016/j.biochi.2012.06.027

Weisser, M., Vieth, M., Stolte, M., Riederer, P., Pfeuffer, R., Leblhuber, F., et al. (1997). Dramatic increase of alpha-hydroxyaldehydes derived from plasmalogens in the aged human brain. *Chem. Phys. Lipids* 90, 135–142. doi:10.1016/s0009-3084(97)00089-3

Werner, E. R., Keller, M. A., Sailer, S., Lackner, K., Koch, J., Hermann, M., et al. (2020). The *TMEM189* gene encodes plasmanylethanolamine desaturase which introduces the characteristic vinyl ether double bond into plasmalogens. *Proc. Natl. Acad. Sci. U. S. A.* 117, 7792–7798. doi:10.1073/pnas.1917461117

Weustenfeld, M., Eidelpes, R., Schmuth, M., Rizzo, W. B., Zschocke, J., and Keller, M. A. (2019). Genotype and phenotype variability in Sjögren-Larsson syndrome. *Hum. Mutat.* 40, 177–186. doi:10.1002/humu.23679

Wiest, M. M., German, J. B., Harvey, D. J., Watkins, S. M., and Hertz-Picciotto, I. (2009). Plasma fatty acid profiles in autism: A case-control study. *Prostagl. Leukot. Essent. Fat. Acids* 80, 221–227. doi:10.1016/j.plefa.2009.01.007

Wolf, R. A., and Gross, R. W. (1985). Identification of neutral active phospholipase C which hydrolyzes choline glycerophospholipids and plasmalogen selective phospholipase A2 in canine myocardium. *J. Biol. Chem.* 260, 7295–7303. doi:10.1016/s0021-9258(17)39606-0

Wood, P. L., Barnette, B. L., Kaye, J. A., Quinn, J. F., and Woltjer, R. L. (2015). Non-targeted lipidomics of CSF and frontal cortex grey and white matter in control, mild cognitive impairment, and Alzheimer's disease subjects. *Acta Neuropsychiatr.* 27, 270–278. doi:10.1017/neu.2015.18

Wood, P. L., Filiou, M. D., Otte, D. M., Zimmer, A., and Turck, C. W. (2014). Lipidomics reveals dysfunctional glycosynapses in schizophrenia and the G72/G30 transgenic mouse. *Schizophr. Res.* 159, 365–369. doi:10.1016/j.schres.2014.08.029

Wu, L.-C., Pfeiffer, D. R., Calhoon, E. A., Madiai, F., Marcucci, G., Liu, S., et al. (2011). Purification, identification, and cloning of lysoplasmalogenase, the enzyme that catalyzes hydrolysis of the vinyl ether bond of lysoplasmalogen. *J. Biol. Chem.* 286, 24916–24930. doi:10.1074/jbc.M111.247163

Wu, Y., Chen, Z., Chiba, H., and Hui, S.-P. (2020). Plasmalogen fingerprint alteration and content reduction in beef during boiling, roasting, and frying. *Food Chem.* 322, 126764. doi:10.1016/j.foodchem.2020.126764

Wu, Y., Chen, Z., Jia, J., Chiba, H., and Hui, S.-P. (2021). Quantitative and comparative investigation of plasmalogen species in daily foodstuffs. *Foods* 10, 124. doi:10.3390/foods10010124

Yamashita, A., Hayashi, Y., Nemoto-Sasaki, Y., Ito, M., Oka, S., Tanikawa, T., et al. (2014). Acyltransferases and transacylases that determine the fatty acid composition of glycerolipids and the metabolism of bioactive lipid mediators in mammalian cells and model organisms. *Prog. Lipid Res.* 53, 18–81. doi:10.1016/j.plipres.2013.10.001

Yamashita, A., Sugiura, T., and Waku, K. (1997). Acyltransferases and transacylases involved in fatty acid remodeling of phospholipids and metabolism of bioactive lipids in mammalian cells. *J. Biochem.* 122, 1–16. doi:10.1093/oxfordjournals.jbchem.a021715

Yamashita, S., Hashimoto, M., Haque, A. M., Nakagawa, K., Kinoshita, M., Shido, O., et al. (2017). Oral administration of ethanolamine glycerophospholipid containing a high level of plasmalogen improves memory impairment in amyloid β-infused rats. *Lipids* 52, 575–585. doi:10.1007/s11745-017-4260-3

Yamashita, S., Kiko, T., Fujiwara, H., Hashimoto, M., Nakagawa, K., Kinoshita, M., et al. (2016). Alterations in the levels of amyloid-β, phospholipid hydroperoxide, and plasmalogen in the blood of patients with Alzheimer's disease: Possible interactions between amyloid-β and these lipids. *J. Alzheimers Dis.* 50, 527–537. doi:10.3233/JAD-150640

Yavin, E., and Gatt, S. (1972). Oxygen-dependent cleavage of the vinyl -ether linkage of plasmalogens. 2. Identification of the low-molecular-weight active component and the reaction mechanism. *Eur. J. Biochem.* 25, 437–446. doi:10.1111/j.1432-1033.1972.tb01713.x

Yu, T. W., Chahrour, M. H., Coulter, M. E., Jiralerspong, S., Okamura-Ikeda, K., Ataman, B., et al. (2013). Using whole-exome sequencing to identify inherited causes of autism. *Neuron* 77, 259–273. doi:10.1016/j.neuron.2012.11.002

Yuki, K., Shindou, H., Hishikawa, D., and Shimizu, T. (2009). Characterization of mouse lysophosphatidic acid acyltransferase 3: An enzyme with dual functions in the testis. *J. Lipid Res.* 50, 860–869. doi:10.1194/jlr.M800468-JLR200

Zhang, H., Weström, S., Kappelin, P., Virtanen, M., Vahlquist, A., and Törmä, H. (2021). Exploration of novel candidate genes involved in epidermal keratinocyte differentiation and skin barrier repair in man. *Differentiation.* 119, 19–27. doi:10.1016/j.diff.2021.04.001

Zhu, X. G., Nicholson Puthenveedu, S., Shen, Y., La, K., Ozlu, C., Wang, T., et al. (2019). CHP1 regulates compartmentalized glycerolipid synthesis by activating GPAT4. *Mol. Cell* 74, 45–58.e7. doi:10.1016/j.molcel.2019.01.037

Zoeller, R. A., Lake, A. C., Nagan, N., Gaposchkin, D. P., Legner, M. A., and Lieberthal, W. (1999). Plasmalogens as endogenous antioxidants: Somatic cell mutants reveal the importance of the vinyl ether. *Biochem. J.* 338 (Pt 3), 769–776. doi:10.1042/bj3380769

Zou, Y., Henry, W. S., Ricq, E. L., Graham, E. T., Phadnis, V. V., Maretich, P., et al. (2020). Plasticity of ether lipids promotes ferroptosis susceptibility and evasion. *Nature* 585, 603–608. doi:10.1038/s41586-020-2732-8

frontiers | Frontiers in Cell and Developmental Biology

TYPE Original Research
PUBLISHED 09 September 2022
DOI 10.3389/fcell.2022.921691

OPEN ACCESS

EDITED BY
Masanori Honsho,
Kyushu University, Japan

REVIEWED BY
Mikhail Y Golovko,
University of North Dakota,
United States
Thad A. Rosenberger,
University of North Dakota,
United States

*CORRESPONDENCE
Niyazi Acar,
niyazi.acar@inrae.fr

†These authors have contributed equally to this work

SPECIALTY SECTION
This article was submitted to Cellular Biochemistry, a section of the journal Frontiers in Cell and Developmental Biology

RECEIVED 16 April 2022
ACCEPTED 11 July 2022
PUBLISHED 09 September 2022

CITATION
Karadayi R, Pallot C, Cabaret S, Mazzocco J, Gabrielle P-H, Semama DS, Chantegret C, Ternoy N, Martin D, Donier A, Gregoire S, Creuzot-Garcher CP, Bron AM, Bretillon L, Berdeaux O and Acar N (2022), Modification of erythrocyte membrane phospholipid composition in preterm newborns with retinopathy of prematurity: The omegaROP study. *Front. Cell Dev. Biol.* 10:921691. doi: 10.3389/fcell.2022.921691

Modification of erythrocyte membrane phospholipid composition in preterm newborns with retinopathy of prematurity: The omegaROP study

Rémi Karadayi[1†], Charlotte Pallot[1,2†], Stéphanie Cabaret[3], Julie Mazzocco[1], Pierre-Henry Gabrielle[2], Denis S. Semama[4], Corinne Chantegret[4], Ninon Ternoy[4], Delphine Martin[4], Aurélie Donier[4], Stéphane Gregoire[1], Catherine P. Creuzot-Garcher[1,2], Alain M. Bron[1,2], Lionel Bretillon[1], Olivier Berdeaux[3] and Niyazi Acar[1*]

[1]Centre des Sciences du Goût et de l'Alimentation, Institut Agro, CNRS, INRAE, Université Bourgogne Franche-Comté, Eye and Nutrition Research Group, Dijon, France, [2]University Hospital, Department of Ophthalmology, Dijon, France, [3]Centre des Sciences du Goût et de l'Alimentation, Institut Agro, CNRS, INRAE, Université Bourgogne Franche-Comté, ChemoSens Platform, Dijon, France, [4]University Hospital, Neonatal Intensive Care Unit, Dijon, France

N-3 polyunsaturated fatty acids (PUFAs) may prevent retinal vascular abnormalities observed in oxygen-induced retinopathy, a model of retinopathy of prematurity (ROP). In the OmegaROP prospective cohort study, we showed that preterm infants who will develop ROP accumulate the n-6 PUFA arachidonic acid (ARA) at the expense of the n-3 PUFA docosahexaenoic acid (DHA) in erythrocytes with advancing gestational age (GA). As mice lacking plasmalogens —That are specific phospholipids considered as reservoirs of n-6 and n-3 PUFAs— Display a ROP-like phenotype, the aim of this study was to determine whether plasmalogens are responsible for the changes observed in subjects from the OmegaROP study. Accordingly, preterm infants aged less than 29 weeks GA were recruited at birth in the Neonatal Intensive Care Unit of University Hospital Dijon, France. Blood was sampled very early after birth to avoid any nutritional influence on its lipid composition. The lipid composition of erythrocytes and the structure of phospholipids including plasmalogens were determined by global lipidomics using liquid chromatography coupled to high-resolution mass spectrometry (LC-HRMS). LC-HRMS data confirmed our previous observations by showing a negative association between the erythrocyte content in phospholipid esterified to n-6 PUFAs and GA in infants without ROP (rho = −0.485, p = 0.013 and rho = −0.477, p = 0.015 for ethanolamine and choline total phospholipids, respectively). Phosphatidylcholine (PtdCho) and phosphatidylethanolamine (PtdEtn) species with ARA, namely PtdCho16:0/20:4 (rho = −0.511, $p < 0.01$) and PtdEtn18:1/20:4 (rho = −0.479, p = 0.015),

were the major contributors to the relationship observed. On the contrary, preterm infants developing ROP displayed negative association between PtdEtn species with n-3 PUFAs and GA (rho = −0.380, p = 0.034). They were also characterized by a positive association between GA and the ratio of ethanolamine plasmalogens (PlsEtn) with n-6 PUFA to PlsEtn with n-3 PUFAs (rho = 0.420, p = 0.029), as well as the ratio of PlsEtn with ARA to PlsEtn with DHA (rho = 0.843, p = 0.011). Altogether, these data confirm the potential accumulation of n-6 PUFAs with advancing GA in erythrocytes of infants developing ROP. These changes may be partly due to plasmalogens.

KEYWORDS

polyunsaturated (essential) fatty acids, plasmalogens, phospholipids, erythrocyte, retinopathy of prematurity

Introduction

Retinopathy of prematurity (ROP) is the leading cause of childhood blindness with an estimated incidence ranging from 6 to 34% in developed countries (Good & Hardy, 2001; Jordan, 2014). ROP is characterized by a first phase of vaso-obliteration in the central retina (phase 1), followed by the overexpression of pro-angiogenic growth factors such angiopoietins and VEGF (Sonmez, Drenser, Capone, & Trese, 2008; Sato, Shima, & Kusaka, 2011; Rivera et al., 2017) associated to neovascular events in the retina (phase 2) (Hellstrom, Smith, & Dammann, 2013). As a result, mature retinal vessels exhibit several major abnormalities, such as increased dilatation and tortuosity, as well as vascular leakage (Hellstrom et al., 2013).

Previous studies have reported that the polyunsaturated fatty acids (PUFAs) such as arachidonic acid (ARA, C20:4 n-6) and docosahexaenoic acid (DHA, C22:6 n-3) influence retinal vascularization processes in mouse models of oxygen-induced retinopathy, a mouse model of ROP (Connor et al., 2007; Sapieha et al., 2011). Moreover, human studies revealed alterations in blood levels of PUFAs in preterm newborns developing ROP (Martin et al., 2011; Lofqvist et al., 2018; Pallot et al., 2019). Particularly in the OmegaROP study, we have shown an accumulation of ARA at the expense of DHA in erythrocytes of preterm infants that will develop ROP. In cell membranes, PUFAs such as ARA and DHA are esterified on membrane phospholipids, from which they can be released by phospholipases for further intracellular metabolization and/or signaling. Within these phospholipids, plasmalogens represent a particular sub-class characterized by the presence of a vinyl-ether bond at *sn*-1 position of glycerol instead of an ester bond. Plasmalogens are considered as "reservoirs" for PUFAs such as ARA and DHA (Nagan & Zoeller, 2001) and are abundant in the human retina (Bretillon et al., 2008; Berdeaux et al., 2010; Acar et al., 2012). Interestingly, we have shown that plasmalogen-deficient mice exhibit retinal vascular abnormalities resembling to those observed in ROP (Saab-Aoude, Bron, Creuzot-Garcher, Bretillon, & Acar, 2013; Saab et al., 2014). Indeed, retinal vascular development in these mice was characterized by a delayed outgrowth followed by increased angiogenesis associated to the overexpression of pro-angiogenic factors such as angiopoietins (Saab et al., 2014).

In this work, we aimed to assess whether the differential accumulation of ARA and DHA in preterm infants of the OmegaROP study is associated to plasmalogens. By using high-resolution mass spectrometry (HRMS), we evaluated the concentrations of individual phospholipids species in erythrocytes of preterm infants that will or not develop ROP. In this study, blood was collected immediately after birth, in order to limit the interference with lipid nutritional intakes.

Materials and methods

Ethics statement

This study was conducted in accordance with the guidelines of the Declaration of Helsinki. The experimental procedures were approved by local ethics committee (CPP Est III, School of Medicine, Dijon, France) that waived the obtainment of a written consent as our study did not generate additional procedure to those of standard care. Instead of, an information note was given to parents and/or legal guardians. In accordance with "ethical considerations for clinical trials on medicinal products conducted with the pediatric population", the volume of blood collected in preterm infants was limited to 0.5 mL (European Union. 2008).

Selection of the patients

As described previously (Pallot et al., 2019), all preterm infants born before 29 weeks GA and hospitalized in the neonatal intensive care unit of the Dijon University Hospital, Dijon, France, between 31 July 2015 and 31 January 2018 were included in the study. A 0.5-mL blood sample was collected by venipuncture in a heparinized tube within the first 48 h of life. Red blood cells were immediately separated from plasma by

centrifugation at 1860 × g at 4°C. The red blood cell pellet was then washed three times with an isotonic saline solution. Samples were stored at −80°C until lipidomic analyses.

ROP screening was performed with the wide-field RETCAM II® camera (Clarity Medical Systems; Pleasanton, CA, United States) using a lid speculum after topical anesthesia by chlorhydrate oxybuprocaine, 1.6 mg/0.4 mL (Théa, Clermont-Ferrand, France). Pupillary dilation was previously performed using one drop of tropicamide, 2 mg/0.4 mL, Théa, Clermont-Ferrand, France). The procedure was completed by a trained nurse and all fundus photographs were analyzed by two trained pediatrics-specialized ophthalmologists. Screening began at 4–6 weeks of life but never before 31 weeks of postconceptional age (PCA). Fundus imaging was repeated every other week until 39 weeks PCA if no ROP was detected, and every week or up to twice a week in case of ROP. ROP staging was determined according to the International Classification of ROP (International Committee for the Classification of Retinopathy of, 2005). Subjects were classified in the group suffering from ROP (ROP group) or in the group of unaffected controls (no-ROP group). Within the ROP group, subjects were classified into type 1 ROP and type 2 ROP. The major risks of developing ROP, namely gestational age (GA), weight at birth, duration of mechanical ventilation, sepsis, use of erythropoietin, red blood cell transfusion and cerebral hemorrhage were documented.

Characterization and quantification of individual phospholipid species

Total lipids were extracted from red blood cells according to Moilanen and Nikkari by using chloroform/methanol (1:1, v:v) (Moilanen & Nikkari, 1981). The phosphorus content of the total lipid extracts was determined according to the method developed by Bartlett and Lewis (Bartlett & Lewis, 1970). The samples were then diluted at a concentration of 500 µg/mL in chloroform/methanol 1:1 (v/v). Quality control (QC) were prepared by pooling 10 µL of each resuspended lipid extract. The concentrations of individual phospholipids species of erythrocytes total lipids were determined by Hydrophilic Interaction Liquid Chromatography coupled to High Resolution Mass Spectrometry (HILIC-HR-MS).

Liquid chromatography analyses were performed using a Dionex UltiMate™ 3000 LC pump from Thermo Scientific (San Jose, CA, United States) equipped with an autosampler. The injection volume was 10 µL. Separation of lipid classes was achieved under HILIC conditions using an Accucore HILIC column (150 mm × 2.1 mm i. d., 2.6 µm, Thermo). The column was maintained at 40°C. The mobile phases consisted of (A) ACN/H_2O (99:1, v/v) containing 10 mM ammonium acetate and (B) ACN/H_2O (50:50, v/v) containing 10 mM ammonium acetate. The solvent-gradient system of the analytical pump was as follows: 0 min 100% A, 10 min 92% A, 40 min 50% A, 41–60 min 100% A. The flow rate was set to 500 µL.min−1. In order to guarantee analytical performance, Quality QC were used every eight test sample. HR-MS analyses of phospholipids were carried out using the Orbitrap FusionTM (Thermo Scientific, United States) Mass Spectrometer equipped with an EASY-MAX NGTM Ion Source (H-ESI). H-ESI source parameters were optimized and set as follows: Ion transfer tube temperature of 285°C, sheath gas flow rate of 35 au, auxiliary gas flow rate of 25 au, sweep gas of one au, and vaporizer temperature of 370°C. Positive and negative ions were monitored alternatively by switching polarity approach with a spray voltage set to 3500 V in positive and negative ion modes. The Orbitrap mass analyzer was employed to obtain all mass spectra in full scan mode with a mass range of 200–2000 Da, and a target resolution of 120,000 (FWHM at m/z 200). All MS data were recorded using a max injection time of 50 ms, automated gain control (AGC) at 4.105 and one microscan. An Intensity Threshold filter of 1.103 counts was applied. For MS/MS analyses, High-energy Collisional Dissociation (HCD) was employed for the fragmentation of PL species with optimized stepped collision energy of 30% (±5%). The linear ion trap (LIT) was used to acquire spectra for fragment ions in data-dependent mode. The AGC target was set to 2.104 with a max injection time of 50 ms. All MS and MS/MS data were acquired in the profile mode. The Orbitrap Fusion was controlled by XcaliburTM 4.1 software. The identification of PL species was performed, using the data of high accuracy and the information collected from fragmentation spectra (tolerance 5 ppm for MS1 and 20 ppm for MS2), with the help of the LipidSearchTM software and the LIPID MAPS® database (https://www.lipidmaps.org/).

Relative quantification of the abundances of choline glycerophospholipids (ChoGpl) [including phosphatidyl cholines (PtdCho) and plasmenyl cholines (choline plasmalogens or PlsCho)] and ethanolamine glycerophospholipids (EtnGpl) [including phosphatidylethanolamines (PtdEtn) and plasmenylethanolamines (ethanolamine plasmalogens or PlsEtn)] molecular species between samples was performed in the high resolution MS1 mode (positive for ChoGpl, negative for EtnGpl) by normalization of targeted phospholipid ion peak areas to the PtdCho14:0/14:0 or PtdEtn14:0/14:0 internal standards, respectively. Due to the lack of available lipid standards representing individual molecular species of EtnGpl and ChoGpl, the abundances of ChoGpl and EtnGpl molecular species was reported as the percentage of the total ChoGpl or EtnGpl ion abundance, respectively (after normalization on the PtdCho14:0/14:0 and PtdEtn14:0/14:0 internal standards).

Statistical analyses

Statistical analysis was performed using GraphPad Prism v6.05 (GraphPad Software, San Diego, CA, United States),

TABLE 1 Main characteristics of the OmegaROP population.

	ROP n = 27	No-ROP n = 25	p-value
Sampling time (h)	12 [12–21]	12 [12–30]	0.056
Male	14 (51.8)	12 (48.0)	0.781
Gestational age (weeks)	26.5 [25.5–27.1]	27.6 [27.1–28.4]	<0.001
Birth weight (g)	815 [735–967]	1020 [870–1160]	0.001
ROP	27 (100)	–	–
ROP treated	3 (11.1)	–	–
ROP detection (weeks)	8.2 [6.6–9.5]	–	–
Mechanical ventilation (days)	11.0 [5.5–16.5]	2.0 [1.0–7.0]	<0.001
Sepsis	16 (59.2)	7 (28.0)	0.023
Erythropoietin use	18 (66.6)	15 (60.0)	0.617
RBC transfusion	17 (62.9)	8 (32.0)	0.025
Cerebral haemorrhage	13 (48.1)	12 (48.0)	0.991

Continuous variables are expressed as median [IQR], categorical variables are expressed as No (%).
ROP: Retinopathy of prematurity; RBC: Red blood cells.
p-values in bold indicate a statistically significant difference ($p < 0.05$).

XLSTAT v2018.02.50494 (Addinsoft, Paris, France), and R Project v4.0.2 (Revolutions). Quantitative data were expressed as median and interquartile range [IQR]. The groups were compared using the nonparametric Mann-Whitney test for quantitative variables and the Chi-2 test or Fisher exact test for qualitative variables. The Benjamini-Hochberg false discovery adjusted p-value was applied to correct for multiple testing. Linear regression analyses were used to determine the R-squared (R^2) correlation coefficient values. Spearman correlations were carried out to compare the levels of individual or total levels of phospholipids and ratios as a function of GA. A p-value lower than 0.05 was considered as statistically significant and the tests were two-tailed.

Results

Characteristics of the population

The characteristics of the population are presented in Table 1. As described before (Pallot et al., 2019), fifty-eight preterm infants born before 29 weeks of GA were included in the study. Six infants died and the mortality rate was 11.5%. The final population included five sets of heterozygote twins. Blood samples were obtained from 52 infants at a median time of 12 h and a maximum time of 48 h after birth. No difference was observed between the ROP and the no-ROP groups for sampling time, gender, use of erythropoietin (EPO) and cerebral hemorrhage. ROP was associated with significantly higher sepsis and red blood cell transfusion ($p = 0.023$ and $p = 0.025$, respectively), lower GA and birth weight ($p < 0.001$ and $p = 0.001$, respectively) and higher duration of mechanical ventilation ($p < 0.001$). The mean follow-up for ROP screening was 11.3 ± 4.5 weeks of life.

The mean number of screening examinations was 3.6 ± 2.0 per infant. The incidence of ROP was 51.9%, including three cases of type 1 ROP (11.1%) and 24 cases of type 2 ROP (88.9%). Subjects with type 1 ROP underwent laser therapy on both eyes. No intravitreal injection of bevacizumab was performed. Twenty-six ROP cases were observed in zone 2 (96.3%) and one ROP case was observed in zone 3 (3.7%). We did not observe any ROP in zone 1. One case of ROP was stage 1 (3.7%), 19 cases were stage 2 (70.4%) and seven cases were stage 3 (25.9%). Four subjects were classified as a "plus" stage and three of them underwent laser treatment.

Individual phospholipid species distribution in erythrocytes

No significant difference was observed between groups in the proportions of individual EtnGpl and ChoGpl species as well as in total levels of PtdCho, PlsCho, PtdEtn, and PlsEtn (Figure 1 and Supplementary Table S1). The predominant species were PtdCho16:0/18:1, PtdCho16:0/16:0 and PtdCho16:0/20:4 + PtdCho16:1/20:3 for ChoGpl and PtdEtn16:0/18:1, PtdEtn16:0/20:4 + PtdEtn16:1/20:3, and PtdEtn18:0/20:4 + 16:0/22:4 for EtnGpl. The most represented plasmalogen species were PlsCho16:0/16:1, PlsCho18:0/16:0 and PlsCho18:1/18:2 for the choline subgroup and PlsEtn18:1/22:4 and PlsEtn18:0/22:4 the ethanolamine subgroup. The wide interquartile ranges confirmed the high interindividual variability previously observed for the fatty acid concentrations (Pallot et al., 2019).

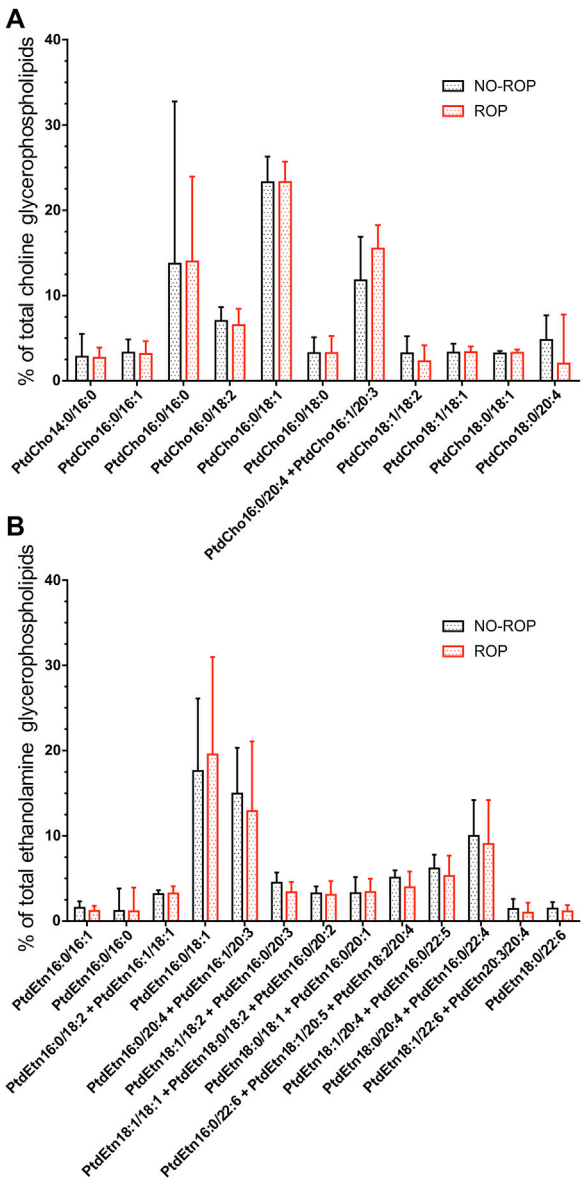

FIGURE 1
Concentrations of major individual ChoGpl species **(A)** and major EtnGpl species **(B)** of red blood cells of preterm infants without or with retinopathy of prematurity (% of total ChoGpl or % of total EtnGpl). No significant difference was observed between no-ROP and ROP groups for any specie. Abbreviations of individual phospholipid species are as follows: Position on the glycerol backbone as shown as sn-1/sn-2 of the fatty alcohol radicals (abbreviated as number of carbons: Number of double bonds). PtdCho: Phosphatidylcholine; PtdEtn: Phosphatidylethanolamine; ROP: Retinopathy of prematurity.

Associations between gestational age and erythrocyte phospholipid species

As in our previous work on the OmegaROP cohort and considering the results of the principal component analysis showing an interaction between GA and lipid data (Pallot et al., 2019), we checked for Spearman correlations between GA and individual phospholipid species (Table 2). In order to identify the phospholipid origin of the differential accumulation of ARA and/or DHA in subjects with or without ROP, we focused our attention on phospholipids carrying n-6 and n-3 PUFAs. Even if the correlations are weak, total ChoGpl and EtnGpl carrying n-6 PUFAs were negatively associated with GA in the no-ROP group (rho = −0.485, p = 0.013 and rho = −0.477, p = 0.015 for PtdCho + PlsCho and PtdEtn + PlsEtn, respectively). Within the choline subgroup, this negative association was weak but significant only for total PtdCho species esterified with n-6 PUFAs (rho = −0.509, p = 0.009), but not for PlsCho. PtdCho species carrying ARA are likely to contribute to this finding since total PtdCho species carrying ARA were also negatively associated with GA in the no-ROP group (rho = −0.495, p = 0.011, Panel B Figure 2), and particularly the individual PtdCho16:0/20:4, PtdCho18:1/20:4, and PtdCho18:0/20:4 species (Table 3). PC carrying ARA represented 28.8% of total PtdCho species (Panel A on Figure 2). Within EtnGpl, only PlsEtn carrying n-6 PUFAs were negatively associated with GA (rho = −0.587, p = 0.002). Although the correlation is not strong, PlsEtn18:1/20:4 may be a significant contributor to this observation (rho = −0.395, p = 0.049). No significant association with GA was observed for PtdEtn species.

In the no-ROP group, no significant association between GA and phospholipids carrying n-6 PUFAs was observed (Tables 2 and 3). Only a weak significant negative association was observed between GA and total EtnGpl esterified with n-3 PUFAs (rho = −0.380, p = 0.034). Probably as a consequence, the ratios of total PtdEtn with n-6 PUFAs to total PtdEtn with n-3 PUFAs, total PlsEtn with n-6 PUFAs to total PlsEtn with n-3 PUFAs, and total PtdEtn with ARA to total PtdEtn with DHA were impacted and positively associated with GA in the ROP group (rho = 0.420, 0.886, and 0.843, p = 0.029, 0.006, and 0.011, respectively; Table 2).

Discussion

This study characterizes the phospholipid composition of erythrocytes in preterm infants born before 29 weeks GA. The clinical characteristics of our population were comparable to those of several studies. Indeed, the incidence of ROP was high (51.9%) and in agreement with other very-low-GA populations (Austeng, Kallen, Ewald, Jakobsson, & Holmstrom, 2009).

Our data show a weak but negative association between ChoGpl and EtnGpl carrying n-6 PUFAs with GA in the no-ROP group, while no significant association was observed in the ROP group. These findings are in the line with our previous reports related to the OmegaROP study (Pallot et al., 2019). Considering that ChoGpl and EtnGpl species represent more than 90% of total phospholipids in erythrocytes (Acar et al., 2007;

TABLE 2 Spearman correlations between gestational age and erythrocyte ChoGpl and EtnGpl esterified with n-6 and/or n-3 PUFAs in preterm infants with or without retinopathy of prematurity.

	No-ROP $n = 25$					ROP $n = 27$				
	Median	[IQR][a]	rho	R^2	*p*-value	Median	[IQR]	rho	R^2	*p*-value
Total PtdCho and PlsCho with n-6 PUFAs	31.21	[9.27–43.84]	−0.485	0.202	0.013	36.86	[7.09–45.82]	0.079	0.001	0.693
Total PtdCho and PlsCho with n-3 PUFAs	1.81	[0.55–4.46]	−0.375	0.109	0.064	2.03	[0.58–4.50]	−0.160	0.010	0.422
Total PtdEtn and PlsEtn with n-6 PUFAs	64.70	[28.52–70.89]	−0.477	0.200	0.015	67.43	[25.10–69.83]	0.050	0.016	0.801
Total PtdEtn and PlsEtn with n-3 PUFAs	21.64	[15.28–24.81]	−0.117	0.004	0.575	19.62	[13.88–24.64]	−0.380	0.084	0.034
Total PtdCho with n-6 PUFAs	31.10	[9.27–42.67]	−0.509	0.208	0.009	36.56	[6.72–43.73]	0.122	0.002	0.544
Total PlsCho with n-6 PUFAs	0.80	[0.19–2.18]	−0.191	0.028	0.359	0.60	[0.05–2.07]	−0.198	0.029	0.319
Total PtdCho with n-3 PUFAs	1.55	[<0.01–4.04]	−0.391	0.126	0.052	2.03	[<0.01–3.89]	−0.011	0.000	0.953
Total PlsCho with n-3 PUFAs	0.16	[<0.01–0.42]	−0.093	0.000	0.657	0.28	[<0.01–0.83]	−0.352	0.105	0.071
Total PtdEtn with n-6 PUFAs	53.05	[28.52–63.07]	−0.311	0.123	0.129	45.36	[25.04–65.50]	0.211	0.050	0.288
Total PlsEtn with n-6 PUFAs	0.77	[0.33–12.68]	−0.587	0.075	0.002	0.58	[0.13–18.47]	0.027	0.019	0.892
Total PtdEtn with n-3 PUFAs	18.25	[13.88–21.64]	0.025	0.000	0.904	17.32	[12.68–19.94]	−0.260	0.063	0.189
Total PlsEtn with n-3 PUFAs	<0.01	[<0.01–3.26]	−0.326	0.062	0.111	<0.01	[<0.01–5.08]	−0.215	0.035	0.281
Total PtdCho with ARA	19.00	[3.06–30.88]	−0.495	0.204	0.011	26.57	[1.74–31.86]	0.062	0.000	0.756
Total PlsCho with ARA	<0.01	[<0.01–1.01]	−0.340	0.068	0.096	<0.01	[<0.01–1.04]	−0.104	0.003	0.603
Total PtdEtn with ARA	38.24	[17.95–46.04]	−0.319	0.130	0.119	32.92	[14.28–47.04]	0.243	0.039	0.221
Total PlsEtn with ARA	<0.01	[<0.01–9.33]	−0.286	0.066	0.164	<0.01	[<0.01–14.25]	−0.110	0.020	0.583
Total PtdCho with DHA	1.55	[<0.01–3.14]	−0.359	0.128	0.077	2.03	[<0.01–2.71]	−0.016	0.000	0.936
Total PlsCho with DHA	<0.01	[<0.01–0.16]	−0.308	0.053	0.133	<0.01	[<0.01–0.17]	−0.131	0.010	0.514
Total PtdEtn with DHA	8.93	[7.43–11.97]	0.189	0.069	0.364	8.77	[5.97–10.48]	−0.132	0.097	0.509
Total PlsEtn with DHA	<0.01	[<0.01–1.32]	−0.338	0.067	0.098	<0.01	[<0.01–2.04]	−0.206	0.028	0.300
Total PtdCho with n-6 PUFAs/total PtdCho with n-3 PUFAs	10.57	[<0.01–16.63]	−0.286	0.039	0.165	10.96	[<0.01–16.79]	0.312	0.090	0.112
Total PtdCho with ARA/total PtdCho with DHA	10.27	[<0.01–11.06]	−0.410	0.127	0.041	11.13	[<0.01–12.46]	0.242	0.052	0.222
Total PlsCho with n-6 PUFAs/total PlsCho with n-3 PUFAs	<0.01	[<0.01–2.27]	−0.355	0.062	0.081	<0.01	[<0.01–1.44]	−0.063	0.001	0.752
Total PlsCho with ARA/total PlsCho with DHA	<0.01	[<0.01–6.33]	−0.390	0.106	0.053	<0.01	[<0.01–6.27]	−0.088	0.001	0.661
Total PtdEtn with n-6 PUFAs/total PtdEtn with n-3 PUFAs	2.99	[2.57–4.11]	−0.072	0.027	0.731	3.19	[2.62–4.31]	0.420	0.032	0.029
Total PtdEtn with ARA/total PtdEtn with DHA	4.33	[3.88–5.15]	−0.239	0.033	0.249	4.58	[3.84–4.91]	0.366	0.057	0.060
Total PlsEtn with n-6 PUFAs/total PlsEtn with n-3 PUFAs	<0.01	[<0.01–2.71]	−0.308	0.059	0.133	<0.01	[<0.01–2.83]	0.886	0.269	0.006
Total PlsEtn with ARA/total PlsEtn with DHA	<0.01	[<0.01–5.70]	−0.296	0.056	0.150	<0.01	[<0.01–5.79]	0.843	0.214	0.011

[a]IQR: Interquartile range; median and IQR, values are given as % of total choline phospholipids or % of total ethanolamine phospholipids. ARA: Arachidonic acid; DHA, docosahexaenoic acid; PtdCho: Phosphatidylcholine; PlsCho: Plasmenylcholine; PtdEtn: Phosphatidylethanolamine; PlsEtn: Plasmenylethanolamine; ROP: Retinopathy of prematurity.

Acar et al., 2009; Acar et al., 2012), we assumed that the changes observed in their concentrations would be a reliable indicator of the whole phospholipid pool in erythrocytes. However, further analyses on phosphatidylserines and phosphatidylinositols could be of interest to draw a more complete picture of erythrocyte phospholipidome alterations in ROP.

In preterm infants who will not develop ROP, erythrocyte relative levels of phospholipids carrying ARA decrease as GA increases, while no change was observed in preterm infants who will develop ROP. This negative correlation mostly relies on PtdCho species and more specifically on individual PtdCho16:0/20:4, PtdCho18:1/20:4, and PtdCho18:0/20:4 species. This finding suggests an *in utero* accumulation of ARA in erythrocytes of preterm infants that will develop ROP relatively to those that will not develop ROP. This GA-related change is in line with the finding of Bernhard and collaborators that revealed a remodeling in plasma PtdCho species esterified with ARA in early preterm infants (Bernhard et al., 2016). They showed that the plasma PtdCho ARA to DHA ratio in preterm infants of less than 33 weeks GA largely exceeds that of term infants, thus likely contributing to the prematurity-related impaired overall health. The data we have obtained in 25- to 28-weeks GA newborns is then in agreement with this observation. However, it is important to keep in mind that

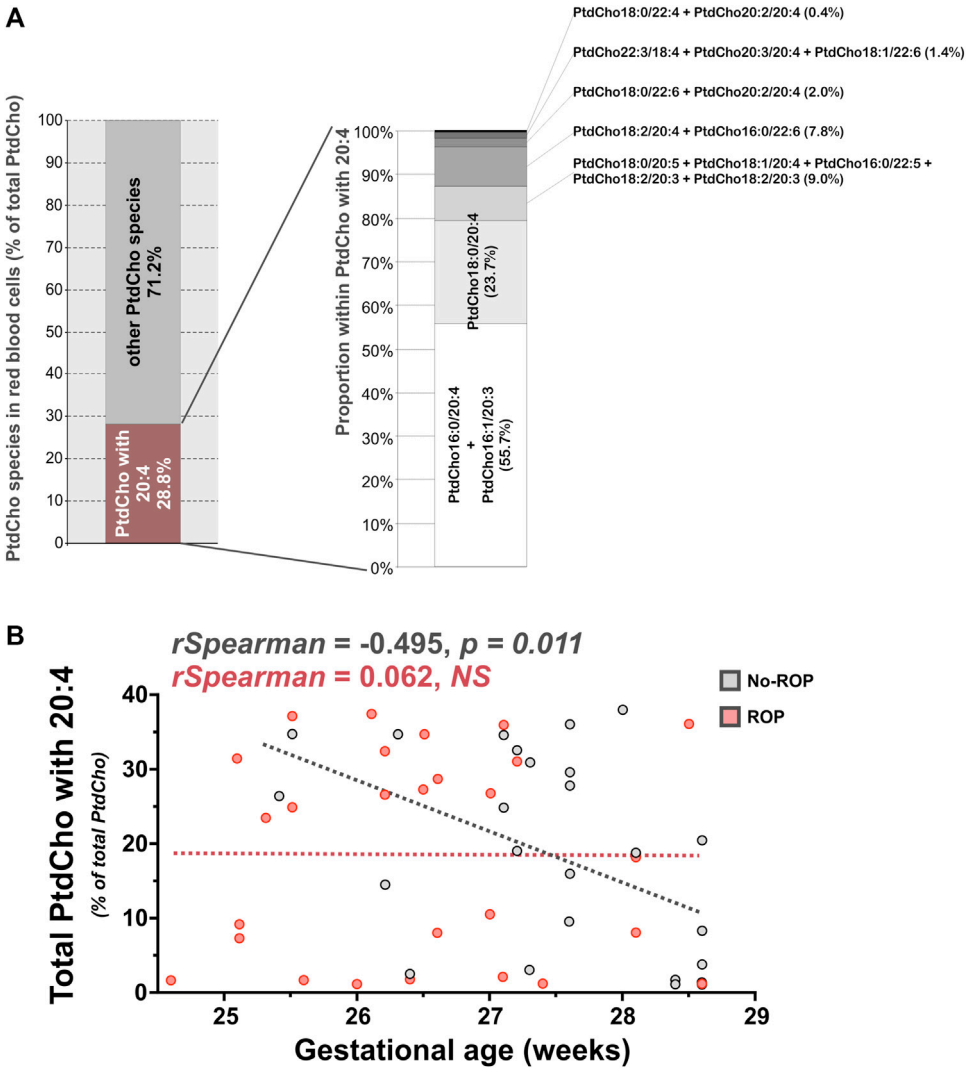

FIGURE 2
PtdCho with ARA are associated with GA in preterm infants without ROP. **(A)** PtdCho with ARA (20:4) accounted for 28.8% of total retinal PtdCho species. **(B)** The sum of PtdCho species carrying ARA was negatively associated to GA in erythrocytes of preterm infants of the no-ROP group (rho = −0.495, p = 0.011). Abbreviations of individual PtdCho species are as follows: Position on the glycerol backbone as shown as sn-1/sn-2 of the fatty alcohol radicals (abbreviated as number of carbons: Number of double bonds). PtdCho: Phosphatidylcholine; ROP: Retinopathy of prematurity.

the biological materials used in these two studies were different, making that further analyses on plasma PtdCho of our subjects would be of interest.

Whether the relative accumulation of ARA in erythrocytes is associated to the onset of ROP remains to be further investigated. Indeed, on one hand it is very clear that together with DHA, ARA is essential during gestation and early postnatal life for an optimal development of the infant (Tai, Wang, & Chen, 2013; Koletzko et al., 2020; Bernhard, Poets, & Franz, 2021). On the other hand, ARA is known to play a pivotal role in the promotion of inflammation, especially through its eicosanoid derivatives such as prostaglandin E2 (PGE2). PGE2 is known to be involved in abnormal angiogenesis and in the pathogenesis of proliferative retinopathies such as ROP (Yanni, Barnett, Clark, & Penn, 2009; Hartnett & Penn, 2012; Schoenberger et al., 2012; Xie et al., 2021). Accordingly, other studies have shown that inflammation is a significant risk factor for developing ROP (Holm et al., 2017; Rivera et al., 2017). Finally, it is recognized that ARA competes with DHA, the latter being known to inhibit retinal neovascularization in a mouse model of ROP (Connor et al., 2007). DHA and ARA are the most prevalent PUFAs in the human retina (Bretillon et al., 2008; Acar et al., 2012). As a subtle equilibrium in their needs may exist within this tissue, we cannot exclude that minor variations in the ARA to DHA ratio may impact retinal physiology.

TABLE 3 Spearman correlations between gestational age and erythrocyte individual phospholipids species esterified with n-6 and/or n-3 PUFAs in preterm infants with or without retinopathy of prematurity.

	[M + H]+ or [M-H]-[a]	No-ROP n = 25			ROP n = 27		
		rho	R^2	p-value	rho	R^2	p-value
Phosphatidylcholine species							
PtdCho16:0/20:4 + PtdCho16:1/20:3	782.5695	−0.511	0.225	0.009	0.013	0.001	0.945
PtdCho18:2/20:4 + PtdCho16:0/22:6	806.5695	−0.346	0.127	0.089	−0.016	0.000	0.936
PtdCho18:0/20:5 + PtdCho18:1/20:4 + PtdCho16:0/22:5 + PtdCho18:2/20:3 + PtdCho20:3/18:2	808.5851	−0.479	0.165	0.015	−0.023	0.033	0.906
PtdCho18:0/20:4	810.6008	−0.517	0.199	0.008	0.183	0.003	0.360
PtdCho20:5/22:6	828.5538	−0.338	0.073	0.097	−0.123	0.008	0.538
PtdCho22:3/18:4 + PtdCho20:3/20:4 + PtdCho18:1/22:6	832.5851	−0.304	0.069	0.138	−0.58	0.003	0.772
PtdCho18:0/22:6 + PtdCho20:2/20:4	834.6008	−0.331	0.068	0.105	−0.088	0.005	0.660
PtdCho18:0/22:4 + PtdCho20:0/20:4	838.6321	−0.350	0.087	0.086	−0.045	0.002	0.822
Plasmenylcholine species							
PlsCho18:1/20:4 + PlsCho16:1/22:4	792.5902	−0.352	0.057	0.083	−0.122	0.012	0.542
PlsCho18:0/20:4 + PlsCho16:0/22:4	794.6058	−0.336	0.070	0.100	−0.104	0.001	0.603
PlsCho18:0/22:6	818.6058	−0.308	0.053	0.133	−0.131	0.010	0.514
Phosphatidylethanolamine species							
PtdEtn16:0/20:4 + PtdEtn16:1/20:3	738.5079	−0.298	0.111	0.147	0.196	0.071	0.327
PtdEtn16:0/22:6 + PtdEtn18:1/20:5 + PtdEtn18:2/20:4	762.5079	−0.213	0.115	0.306	0.188	0.035	0.347
PtdEtn18:1/20:4 + PtdEtn16:0/22:5	764.5236	−0.432	0.215	0.030	0.082	0.010	0.683
PtdEtn18:0/20:4 + PtdEtn16:0/22:4	766.5392	−0.344	0.130	0.091	0.200	0.065	0.315
PtdEtn20:4/20:4 + PtdEtn18:2/22:6	786.5079	0.001	0.056	0.992	−0.185	0.128	0.354
PtdEtn18:1/22:6 + PtdEtn20:3/20:4	788.5236	−0.259	0.051	0.210	0.106	0.004	0.596
PtdEtn18:0/22:6	790.5392	−0.306	0.106	0.136	0.083	0.005	0.678
PtdEtn18:0/22:4 + PtdEtn20:0/20:4	794.5705	−0.282	0.148	0.171	0.314	0.062	0.110
PtdEtn20:4/22:6	810.5079	−0.047	0.002	0.821	−0.285	0.103	0.148
PtdEtn22:6/22:6	834.5079	0.439	0.168	0.027	−0.011	0.113	0.954
Plasmenylethanolamine species							
PlsEtn16:0/20:4	722.5130	−0.376	0.069	0.063	−0.179	0.018	0.369
PlsEtn16:0/22:6	746.5130	−0.343	0.070	0.092	−0.193	0.022	0.333
PlsEtn18:1/20:4	748.5287	−0.395	0.065	0.049	−0.214	0.019	0.283
PlsEtn18:0/20:4 + PlsEtn16:0/22:4	750.5443	−0.298	0.066	0.146	−0.117	0.021	0.560
PlsEtn18:1/22:6	772.5287	−0.326	0.064	0.111	−0.223	0.033	0.262
PlsEtn18:0/22:6 + PlsEtn18:1/22:5	774.5443	−0.326	0.059	0.111	−0.216	0.040	0.277

[a][M + H]+ for PtdCho and PlsCho, and [M + H]+ for PtdEtn and PlsEtn species. PtdCho: Phosphatidylcholine; PlsCho: Plasmenylcholine; PtdEtn: Phosphatidylethanolamine; PlsEtn: Plasmenylethanolamine; ROP: Retinopathy of prematurity. abrAbbreviationsof individual PtdCho, PlsCho, PtdEtn, and PlsEtn species are as follows: Position on the glycerol backbone as shown as sn-1/sn-2 of the fatty acid and fatty alcohol radicals (abbreviated as number of carbons: Number of double bonds).

In accordance with our previous observation on the same cohort (Pallot et al., 2019), our data display a high interindividual variability. This is especially true for ARA whose levels in total lipids were of 13.48 ± 7.29% and 13.86 ± 7.63% of total fatty acids in the no-ROP and ROP groups, respectively (Pallot et al., 2019). The present study shows that ARA levels were low especially in PtdCho, and independently from the development of ROP. Although extensive analyses, we were unable to connect these very low ARA levels to any other variable, including GA, blood sampling time after birth or any other parameter related to the

infants' health. Since we have used analytical QCs and as we have repeated our analyses several times, we believe that these changes are of physiologic origin and not the result of analytical bias. The probable physiological origin of these changes is reinforced by similar observations showing very-low levels of ARA (Glen et al., 1994; Khan et al., 2002) or even ARA levels close to zero (Li et al., 2022) in erythrocytes of human subjects with neurologic disorders or of infants with severe malnutrition (Smit et al., 1997). Such data may suggest a marked dysregulation of erythrocyte membrane fatty acids in some infants. It can be the result of either increased phospholipase A2 activity and/or enhanced lipid peroxidation. Free radical oxidation during technical steps of sample handling and lipid analysis can also be at the origin of the degradation of PUFAs such as AA, but also that of plasmalogens. To avoid such biases in our study, we took care to take a number of precautions starting from immediate processing of the blood sample after venipuncture, to the isolation and washing of red cells at a temperature of 4°C, their immediate storage at −80°C, and the use of the Moilanen & Nikkari procedure for lipid extraction. This last methodology doesn't use acidic conditions that are known to be deleterious for plasmalogens. Another hypothesis to explain the low levels of ARA would rely on a reduced bioavailability of ARA in maternal blood and/or its abnormal placental transfer. Further investigation is needed to better understand the origin of these modifications.

Circulating lipids are also subject to a postnatal remodeling. Indeed, several studies documented an increase in the plasma and erythrocyte levels of linoleic acid (the dietary precursor of ARA) and a decrease in the levels of ARA during the first weeks of life as a consequence of a LA-rich nutrition (Bernhard et al., 2014; Bockmann et al., 2021). Considering that the birth to blood sampling delay in our study exceeded 24 h in some cases, we cannot exclude the influence of the source of lipid (parenteral versus enteral nutrition) on the lipid data, especially in infants with lower GA for which the parenteral lipid supply is higher. Nevertheless, we did not find any association between erythrocyte lipids (and especially PtdCho16:0/20:4) and the sampling time in the subjects of our cohort (data not shown).

Interestingly, the n-6 to n-3 PUFA ratio in erythrocytes seems to display a similar pattern in the no-ROP group when considering PlsEtn species, as PlsEtn carrying n-6 PUFAs were negatively associated with GA (rho = −0.587, p = 0.002), with PlsEtn18:1/20:4 being the most significant contributor to this observation (rho = −0.395, p = 0.049). Considering that erythrocyte lipid composition could represent a reliable indicator of the lipid composition of the retina in newborns (Carlson, Carver, & House, 1986; Makrides, Neumann, Byard, Simmer, & Gibson, 1994; Sarkadi-Nagy et al., 2004), we may speculate that retinal lipids display similar modifications in ARA, DHA and plasmalogen levels of newborns developing ROP. On the contrary, infants that will develop ROP seem to accumulate n-6 PUFAs in their plasmalogens as the ratio of PlsEtn carrying n-6 PUFAs to PlsEtn carrying n-3 PUFAs is strongly positively associated to GA (rho = 0.886, p = 0.006), ARA and DHA being the major contributors to this observation (rho = 0.843, p = 0.011). These data are in line with the ROP-like phenotype observed in plasmalogen-deficient mice (Saab et al., 2014) and then reinforce the idea that plasmalogens may participate to the pathophysiology of this disease. It would be however interesting to check whether these mice display changes in the levels of PUFAs such as ARA and/or DHA in their erythrocytes in order to strengthen the conclusions of the present paper. While PUFAs status of the newborn correlates with maternal status (Bernhard et al., 2016), and as it can be influenced by dietary supplementation after birth (Schulzke, Patole, & Simmer, 2011), plasmalogen content of tissues only relies on fetal *de novo* synthesis as no materno-fetal transfer of ether-lipids has been demonstrated so far (Das, Holmes, Wilson, & Hajra, 1992). In our study, blood samples were collected within the first 48 h of life. Considering that the erythrocyte life-span ranges from 35 to 50 days in preterm infants (Pearson, 1967), the modifications observed in the present study might be assigned to differences *in situ* lipid metabolisms even if, again, a nutritional influence cannot be excluded for PUFAs.

Several limitations must be acknowledged in our study. First, the correlation coefficients found in this study are weak and deserve more investigations. Second, our population included a limited number of patients and subjects. Third, our population only included three preterm infants with severe ROP, while this population was specifically concerned by treatments targeting vascular events. Furthermore, while ChoGpl and EtnGpl species are the main contributors to erythrocytes phospholipidome, further lipidomic analyses including phosphatidylserine and phosphatidylinositol individual phospholipid species could provide useful complementary information.

Taken together, our results seem to confirm the alterations of erythrocyte PUFA profile in preterm infants developing ROP and suggest that plasmalogens may contribute to them. Considering the importance of plasmalogens in the cellular bioavailability of PUFAs and their involvement in the vascular development of the retina, our study suggests that investigating the relationships between plasmalogen metabolism and ROP could be of particular interest to decipher the pathophysiological mechanisms driving ROP.

Data availability statement

The datasets presented in this study can be found in online repositories. The names of the repository/repositories and accession number(s) can be found below: https://www.ebi.ac.uk/metabolights/MTBLS4219/descriptors

Ethics statement

The studies involving human participants were reviewed and approved by CPP Est III, School of Medicine, Dijon, France. Written informed consent from the participants' legal guardian/next of kin was not required to participate in this study in accordance with the national legislation and the institutional requirements.

Author contributions

CP, DS, CC-G, LB, NA designed the study. RK, CP, SC, JM, DS, CC, NT, DM, AD, SG, OB, NA acquired, analyzed and interpreted the data. RK, CP, JM, DS, AB, CC-G, LB, OB, NA drafted the manuscript. All authors reviewed the manuscript.

Funding

The authors thank National Research Institute for Agriculture, Food and Environment (INRAE); Regional Council of Burgundy (PARI Grant); European Regional Development Fund (FEDER); Agence Nationale de la Recherche (ANR-11-LABX-0021-01); VISIO Foundation; Fondation de France/Fondation de l'Oeil; Groupe Lipides et Nutrition (GLN) for their financial support.

Acknowledgments

The authors would like to thank all medical staff of the Neonatal Intensive Care Unit of Dijon University Hospital for their unique contribution to the study.

Conflict of interest

The authors declare that the research was conducted in the absence of any commercial or financial relationships that could be construed as a potential conflict of interest.

Publisher's note

All claims expressed in this article are solely those of the authors and do not necessarily represent those of their affiliated organizations, or those of the publisher, the editors and the reviewers. Any product that may be evaluated in this article, or claim that may be made by its manufacturer, is not guaranteed or endorsed by the publisher.

Supplementary material

The Supplementary Material for this article can be found online at: https://www.frontiersin.org/articles/10.3389/fcell.2022.921691/full#supplementary-material

References

Acar, N., Berdeaux, O., Gregoire, S., Cabaret, S., Martine, L., Gain, P., et al. (2012). Lipid composition of the human eye: Are red blood cells a good mirror of retinal and optic nerve fatty acids? *PLoS ONE* 7 (4), e35102. doi:10.1371/journal.pone.0035102

Acar, N., Berdeaux, O., Juaneda, P., Gregoire, S., Cabaret, S., Joffre, C., et al. (2009). Red blood cell plasmalogens and docosahexaenoic acid are independently reduced in primary open-angle glaucoma. *Exp. Eye Res.* 89 (6), 840–853. doi:10.1016/j.exer.2009.07.008

Acar, N., Gregoire, S., Andre, A., Juaneda, P., Joffre, C., Bron, A. M., et al. (2007). Plasmalogens in the retina: *In situ* hybridization of dihydroxyacetone phosphate acyltransferase (DHAP-AT) the first enzyme involved in their biosynthesis and comparative study of retinal and retinal pigment epithelial lipid composition. *Exp. Eye Res.* 84 (1), 143–151. doi:10.1016/j.exer.2006.09.009

Austeng, D., Kallen, K. B., Ewald, U. W., Jakobsson, P. G., and Holmstrom, G. E. (2009). Incidence of retinopathy of prematurity in infants born before 27 weeks' gestation in Sweden. *Arch. Ophthalmol.* 127 (10), 1315–1319. doi:10.1001/archophthalmol.2009.244

Bartlett, E. M., and Lewis, D. H. (1970). Spectrophotometric determination of phosphate esters in the presence and absence of orthophosphate. *Anal. Biochem.* 36 (1), 159–167. doi:10.1016/0003-2697(70)90343-x

Berdeaux, O., Juaneda, P., Martine, L., Cabaret, S., Bretillon, L., Acar, N., et al. (2010). Identification and quantification of phosphatidylcholines containing very-long-chain polyunsaturated fatty acid in bovine and human retina using liquid chromatography/tandem mass spectrometry. *J. Chromatogr. A* 1217 (49), 7738–7748. doi:10.1016/j.chroma.2010.10.039

Bernhard, W., Poets, C. F., and Franz, A. (2021). Parenteral nutrition for preterm infants: Correcting for arachidonic and docosahexaenoic acid may not suffice. *Arch. Dis. Child. Fetal Neonatal Ed.* 106 (6), 683. doi:10.1136/archdischild-2021-321871

Bernhard, W., Raith, M., Koch, V., Kunze, R., Maas, C., Abele, H., et al. (2014). Plasma phospholipids indicate impaired fatty acid homeostasis in preterm infants. *Eur. J. Nutr.* 53 (7), 1533–1547. doi:10.1007/s00394-014-0658-3

Bernhard, W., Raith, M., Koch, V., Maas, C., Abele, H., Poets, C. F., et al. (2016). Developmental changes in polyunsaturated fetal plasma phospholipids and feto-maternal plasma phospholipid ratios and their association with bronchopulmonary dysplasia. *Eur. J. Nutr.* 55 (7), 2265–2274. doi:10.1007/s00394-015-1036-5

Bockmann, K. A., von Stumpff, A., Bernhard, W., Shunova, A., Minarski, M., Frische, B., et al. (2021). Fatty acid composition of adipose tissue at term indicates deficiency of arachidonic and docosahexaenoic acid and excessive linoleic acid supply in preterm infants. *Eur. J. Nutr.* 60 (2), 861–872. doi:10.1007/s00394-020-02293-2

Bretillon, L., Thuret, G., Gregoire, S., Acar, N., Joffre, C., Bron, A. M., et al. (2008). Lipid and fatty acid profile of the retina, retinal pigment epithelium/choroid, and the lacrimal gland, and associations with adipose tissue fatty acids in human subjects. *Exp. Eye Res.* 87 (6), 521–528. doi:10.1016/j.exer.2008.08.010

Carlson, S. E., Carver, J. D., and House, S. G. (1986). High fat diets varying in ratios of polyunsaturated to saturated fatty acid and linoleic to linolenic acid: A comparison of rat neural and red cell membrane phospholipids. *J. Nutr.* 116 (5), 718–725. doi:10.1093/jn/116.5.718

Connor, K. M., SanGiovanni, J. P., Lofqvist, C., Aderman, C. M., Chen, J., Higuchi, A., et al. (2007). Increased dietary intake of omega-3-polyunsaturated fatty acids reduces pathological retinal angiogenesis. *Nat. Med.* 13 (7), 868–873. doi:10.1038/nm1591

Das, A. K., Holmes, R. D., Wilson, G. N., and Hajra, A. K. (1992). Dietary ether lipid incorporation into tissue plasmalogens of humans and rodents. *Lipids* 27 (6), 401–405. doi:10.1007/BF02536379

European Union (2008). Ethical considerations for clinical trials on medicinal products conducted with the paediatric population. *Eur. J. Health Law* 15 (2), 223–250.

Glen, A. I., Glen, E. M., Horrobin, D. F., Vaddadi, K. S., Spellman, M., Morse-Fisher, N., et al. (1994). A red cell membrane abnormality in a subgroup of schizophrenic patients: Evidence for two diseases. *Schizophr. Res.* 12 (1), 53–61. doi:10.1016/0920-9964(94)90084-1

Good, W. V., and Hardy, R. J. (2001). The multicenter study of early treatment for retinopathy of prematurity (ETROP). *Ophthalmology* 108 (6), 1013–1014. doi:10.1016/s0161-6420(01)00540-1

Hartnett, M. E., and Penn, J. S. (2012). Mechanisms and management of retinopathy of prematurity. *N. Engl. J. Med.* 367 (26), 2515–2526. doi:10.1056/NEJMra1208129

Hellstrom, A., Smith, L. E., and Dammann, O. (2013). Retinopathy of prematurity. *Lancet* 382 (9902), 1445–1457. doi:10.1016/S0140-6736(13)60178-6

Holm, M., Morken, T. S., Fichorova, R. N., VanderVeen, D. K., Allred, E. N., Dammann, O., et al. (2017). Systemic inflammation-associated proteins and retinopathy of prematurity in infants born before the 28th week of gestation. *Invest. Ophthalmol. Vis. Sci.* 58 (14), 6419–6428. doi:10.1167/iovs.17-21931

International Committee for the Classification of Retinopathy of, P (2005). The international classification of retinopathy of prematurity revisited. *Arch. Ophthalmol.* 123 (7), 991–999. doi:10.1001/archopht.123.7.991

Jordan, C. O. (2014). Retinopathy of prematurity. *Pediatr. Clin. North Am.* 61 (3), 567–577. doi:10.1016/j.pcl.2014.03.003

Khan, M. M., Evans, D. R., Gunna, V., Scheffer, R. E., Parikh, V. V., Mahadik, S. P., et al. (2002). Reduced erythrocyte membrane essential fatty acids and increased lipid peroxides in schizophrenia at the never-medicated first-episode of psychosis and after years of treatment with antipsychotics. *Schizophr. Res.* 58 (1), 1–10. doi:10.1016/s0920-9964(01)00334-6

Koletzko, B., Bergmann, K., Brenna, J. T., Calder, P. C., Campoy, C., Clandinin, M. T., et al. (2020). Should formula for infants provide arachidonic acid along with DHA? A position paper of the European academy of paediatrics and the child health foundation. *Am. J. Clin. Nutr.* 111 (1), 10–16. doi:10.1093/ajcn/nqz252

Li, N., Yang, P., Tang, M., Liu, Y., Guo, W., Lang, B., et al. (2022). Reduced erythrocyte membrane polyunsaturated fatty acid levels indicate diminished treatment response in patients with multi- versus first-episode schizophrenia. *NPJ Schizophr.* 8 (1), 7. doi:10.1038/s41537-022-00214-2

Lofqvist, C. A., Najm, S., Hellgren, G., Engstrom, E., Savman, K., Nilsson, A. K., et al. (2018). Association of retinopathy of prematurity with low levels of arachidonic acid: A secondary analysis of a randomized clinical trial. *JAMA Ophthalmol.* 136 (3), 271–277. doi:10.1001/jamaophthalmol.2017.6658

Makrides, M., Neumann, M. A., Byard, R. W., Simmer, K., and Gibson, R. A. (1994). Fatty acid composition of brain, retina, and erythrocytes in breast- and formula-fed infants. *Am. J. Clin. Nutr.* 60 (2), 189–194. doi:10.1093/ajcn/60.2.189

Martin, C. R., Dasilva, D. A., Cluette-Brown, J. E., Dimonda, C., Hamill, A., Bhutta, A. Q., et al. (2011). Decreased postnatal docosahexaenoic and arachidonic acid blood levels in premature infants are associated with neonatal morbidities. *J. Pediatr.* 159 (5), 743–742. doi:10.1016/j.jpeds.2011.04.039

Moilanen, T., and Nikkari, T. (1981). The effect of storage on the fatty acid composition of human serum. *Clin. Chim. Acta.* 114 (1), 111–116. doi:10.1016/0009-8981(81)90235-7

Nagan, N., and Zoeller, R. A. (2001). Plasmalogens: Biosynthesis and functions. *Prog. Lipid Res.* 40 (3), 199–229. doi:10.1016/s0163-7827(01)00003-0

Pallot, C., Mazzocco, J., Meillon, C., Semama, D. S., Chantegret, C., Ternoy, N., et al. (2019). Alteration of erythrocyte membrane polyunsaturated fatty acids in preterm newborns with retinopathy of prematurity. *Sci. Rep.* 9 (1), 7930. doi:10.1038/s41598-019-44476-w

Pearson, H. A. (1967). Life-span of the fetal red blood cell. *J. Pediatr.* 70 (2), 166–171. doi:10.1016/s0022-3476(67)80410-4

Rivera, J. C., Holm, M., Austeng, D., Morken, T. S., Zhou, T. E., Beaudry-Richard, A., et al. (2017). Retinopathy of prematurity: Inflammation, choroidal degeneration, and novel promising therapeutic strategies. *J. Neuroinflammation* 14 (1), 165. doi:10.1186/s12974-017-0943-1

Saab, S., Buteau, B., Leclere, L., Bron, A. M., Creuzot-Garcher, C. P., Bretillon, L., et al. (2014). Involvement of plasmalogens in post-natal retinal vascular development. *PLoS ONE* 9 (6), e101076. doi:10.1371/journal.pone.0101076

Saab-Aoude, S., Bron, A. M., Creuzot-Garcher, C. P., Bretillon, L., and Acar, N. (2013). A mouse model of *in vivo* chemical inhibition of retinal calcium-independent phospholipase A2 (iPLA2). *Biochimie* 95 (4), 903–911. doi:10.1016/j.biochi.2012.12.008

Sapieha, P., Stahl, A., Chen, J., Seaward, M. R., Willett, K. L., Krah, N. M., et al. (2011). 5-Lipoxygenase metabolite 4-HDHA is a mediator of the antiangiogenic effect of omega-3 polyunsaturated fatty acids. *Sci. Transl. Med.* 3 (69), 69ra12. doi:10.1126/scitranslmed.3001571

Sarkadi-Nagy, E., Wijendran, V., Diau, G. Y., Chao, A. C., Hsieh, A. T., Turpeinen, A., et al. (2004). Formula feeding potentiates docosahexaenoic and arachidonic acid biosynthesis in term and preterm baboon neonates. *J. Lipid Res.* 45 (1), 71–80. doi:10.1194/jlr.M300106-JLR200

Sato, T., Shima, C., and Kusaka, S. (2011). Vitreous levels of angiopoietin-1 and angiopoietin-2 in eyes with retinopathy of prematurity. *Am. J. Ophthalmol.* 151 (2), 353–357. doi:10.1016/j.ajo.2010.08.037

Schoenberger, S. D., Kim, S. J., Sheng, J., Rezaei, K. A., Lalezary, M., Cherney, E., et al. (2012). Increased prostaglandin E2 (PGE2) levels in proliferative diabetic retinopathy, and correlation with VEGF and inflammatory cytokines. *Invest. Ophthalmol. Vis. Sci.* 53 (9), 5906–5911. doi:10.1167/iovs.12-10410

Schulzke, S. M., Patole, S. K., and Simmer, K. (2011). Long-chain polyunsaturated fatty acid supplementation in preterm infants. *Cochrane Database Syst. Rev.* 2, CD000375. doi:10.1002/14651858.CD000375.pub4

Smit, E. N., Dijkstra, J. M., Schnater, T. A., Seerat, E., Muskiet, F. A., Boersma, E. R., et al. (1997). Effects of malnutrition on the erythrocyte fatty acid composition and plasma vitamin E levels of Pakistani children. *Acta Paediatr.* 86 (7), 690–695. doi:10.1111/j.1651-2227.1997.tb08569.x

Sonmez, K., Drenser, K. A., Capone, A., Jr., and Trese, M. T. (2008). Vitreous levels of stromal cell-derived factor 1 and vascular endothelial growth factor in patients with retinopathy of prematurity. *Ophthalmology* 115 (6), 1065–1070. doi:10.1016/j.ophtha.2007.08.050

Tai, E. K., Wang, X. B., and Chen, Z. Y. (2013). An update on adding docosahexaenoic acid (DHA) and arachidonic acid (AA) to baby formula. *Food Funct.* 4 (12), 1767–1775. doi:10.1039/c3fo60298b

Xie, T., Zhang, Z., Cui, Y., Shu, Y., Liu, Y., Zou, J., et al. (2021). Prostaglandin E2 promotes pathological retinal neovascularisation via EP4R-EGFR-Gab1-AKT signaling pathway. *Exp. Eye Res.* 205, 108507. doi:10.1016/j.exer.2021.108507

Yanni, S. E., Barnett, J. M., Clark, M. L., and Penn, J. S. (2009). The role of PGE2 receptor EP4 in pathologic ocular angiogenesis. *Invest. Ophthalmol. Vis. Sci.* 50 (11), 5479–5486. doi:10.1167/iovs.09-3652

frontiers | Frontiers in Molecular Biosciences

TYPE Review
PUBLISHED 14 November 2022
DOI 10.3389/fmolb.2022.962757

OPEN ACCESS

EDITED BY
Masanori Honsho,
Kyushu University, Japan

REVIEWED BY
Tomas Rezanka,
University of Chemistry and Technology, Prague/UCT, Czechia
Katrin Watschinger,
Medical University of Innsbruck, Austria

*CORRESPONDENCE
Howard Goldfine,
goldfinh@pennmedicine.upenn.edu

SPECIALTY SECTION
This article was submitted to Cellular Biochemistry,
a section of the journal
Frontiers in Molecular Biosciences

RECEIVED 06 June 2022
ACCEPTED 24 October 2022
PUBLISHED 14 November 2022

CITATION
Goldfine H (2022), Plasmalogens in bacteria, sixty years on.
Front. Mol. Biosci. 9:962757.
doi: 10.3389/fmolb.2022.962757

Plasmalogens in bacteria, sixty years on

Howard Goldfine*

Department of Microbiology, Perelman School of Medicine, University of Pennsylvania, Philadelphia, PA, United States

The presence of plasmalogens in bacteria has been known for 60 years. The recent discovery of two genes encoding reductases that convert diacyl lipids to 1-alk-1′-enyl 2-acyl lipids has confirmed the derivation of plasmalogens from the corresponding diacyl lipids in bacteria. These genes are widely distributed in anaerobic and in some facultatively anaerobic bacteria. Plasmalogens evolved very early in the history of life on earth. Their persistence during eons of evolution suggests that they play a fundamental role in living organism. The phase behavior of plasmalogens and their conformation in membranes is discussed.

KEYWORDS

bacteria, evolution, genetics, plasmalogen, biosynthesis

Introduction

An understanding of specific roles played by individual lipid types has expanded greatly in the past several decades. Specifically, the importance of a balance between lipids that assemble into bilayers readily, as opposed to those that easily transition to non-bilayer assemblages has become widely appreciated. In addition, specific roles played by unusual lipid species have been uncovered. Plasmalogens, with their alk-1′-enyl ether chain are different from the more common all acyl lipids chemically, in their phase behavior and in their three-dimensional structures in membranes. The recent discovery of the genes for plasmalogen synthesis in bacteria has confirmed their direct formation from the corresponding diacyl lipids. In this review, the presence of plasmalogens in many anaerobic and some facultatively anaerobic bacteria will be discussed. These lipids evolved very early in the history of life on earth. Their persistence suggests that they play a fundamental role in these living cells.

Abbreviations: CL, cardiolipin; DHAP, dihydroxyacetone phosphate; PE, phosphatidylethanolamine; PG, phosphatidylglycerol; PlsE, plasmenylethanolamine; PME, phosphatidyl-N-methylethanolamine; PlsG, plasmenylglycerol; PS, phosphatidylserine.

Distribution of plasmalogens in bacteria

The presence of plasmalogens in anaerobic bacteria was discovered in the early 1960s. The first report, by Allison *et al.* concerned the polar lipids of *Ruminococcus flavefaciens* (Allison et al., 1962). This anaerobic, Gram-positive species is related to *Clostridium*. The ratio of aldehydes released from plasmalogens to phosphorus was reported to be 0.56–0.80 suggesting that most of the polar lipid was plasmalogen. At the same time, Wegner and Foster (Wegner and Foster, 1963) were exploring the lipids of *Bacteroides succinogenes* and reported a similar high ratio of aldehyde to phosphorus. The major polar lipids are phosphatidylethanolamine and plasmenylethanolamine in this organism (Figures 1A,B).

The first reports on the presence of plasmalogens in *Clostridium* described the polar lipids of *Clostridium butyricum* ATCC 6015 (Goldfine, 1964; Baumann et al., 1965). The strain was subsequently reclassified as *Clostridium beijerinckii* because one of its major phospholipids, phosphatidyl-N-methylethanolamine (PME), is not present in *C. butyricum* (Goldfine, 1962; Johnston and Goldfine, 1983). The major lipids: phosphatidylethanolamine (PE), phosphatidyl-N-methylethanolamine (PME), phosphatidylglycerol (PG) and cardiolipin (CL), are all present as all acyl and 1-alk-1′-enyl, 2-acyl species. An additional ether lipid is present among the phospholipids and was later identified as a glycerol acetal of plasmenylethanolamine (Figure 1C) (Matsumoto et al., 1971). In *C. butyricum* all of the above lipid species except for PME are present (Johnston and Goldfine, 1983). As in *C. beijerinckii*, all the major lipids are present as all acyl and alk-1′-enyl, acyl species. Many Gram-positive bacteria have glycosyldiradylglycerols (Figure 1D) and a substantial portion of these is often 1-alk-1′-enyl 2-acyl lipids. There can be as many as four sugars, but in most cases, they have not been structurally identified (Guan and Goldfine, 2021).

In 1969 Kamio *et al.* published a survey of plasmalogens and saturated ether lipids in bacteria. The aldehyde/P ratio ranged from a low of 0.04 in *Clostridium perfringens* to a high of 1.04 in *Peptostreptococcus elsdenii,* now *Megasphaera elsdenii* (Kamio et al., 1969; Rogosa, 1984). Most species had very low levels of saturated ethers, which are characteristic of Archaea (Koga and Morii, 2005). Since then, there have been several reviews on plasmalogen distribution in bacteria (Goldfine and Johnston, 2005; Rezanka et al., 2012; Guan and Goldfine, 2021; Vitova et al., 2021).

Plasmalogen biosynthesis--the anaerobic pathway

The elucidation of the eukaryotic biosynthetic pathway for plasmalogen biosynthesis in the early 1970s revealed a requirement for molecular oxygen to affect the desaturation of a saturated ether precursor (Snyder, 1972; Snyder, 1999). It became apparent that nature has evolved two mechanisms for formation of lipids containing an alk-1′-enyl ether bond (Goldfine, 2010). Since early life evolved in an anaerobic environment, the anaerobic pathway is presumably the more

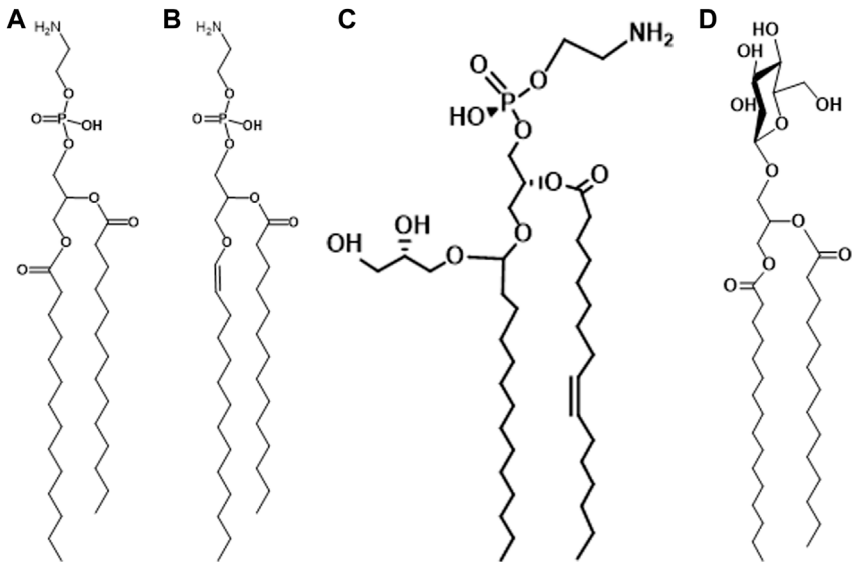

FIGURE 1
(A) phosphatidylethanolamine; **(B)** plasmenylethanolamine; **(C)** glycerolacetal of plasmenylethanolamine; **(D)** glycosyldiacylglycerol.

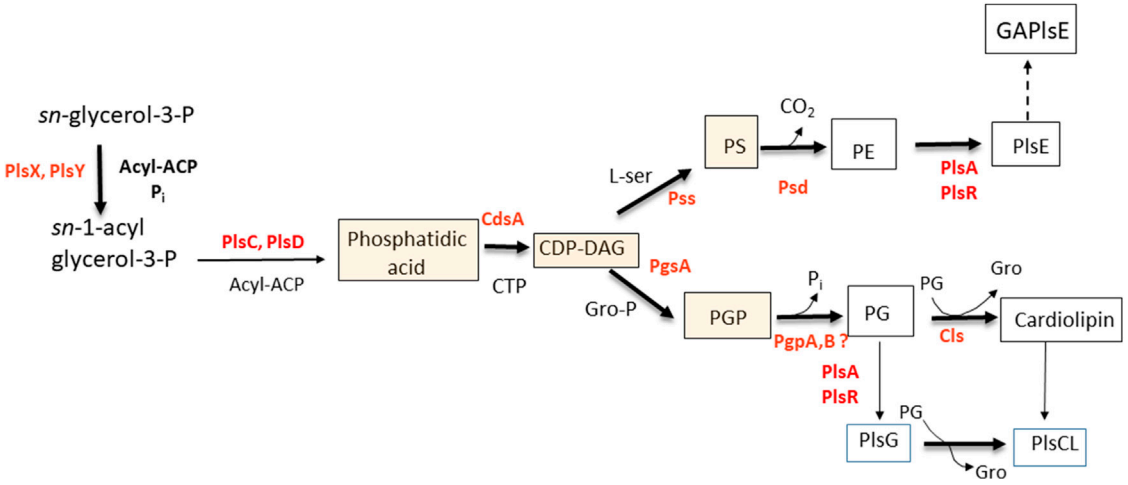

FIGURE 2
Pathway for the biosynthesis of plasmalogens in *Clostridium butyricum*. The shaded boxed intermediates have essentially no plasmalogen species in *C. novyi* and *C. tetani*. Abbreviations: ACP, acyl carrier protein; CL, cardiolipin; DAG, diacylglycerol; GAPlsE, glycerolacetal of plasmenylethanolamine; PE, phosphatidylethanolamine; PG, phosphatidylglycerol; PlsE, plasmenylethanolamine; PlsG, plasmenylglycerol, PS, phosphatidylserine.

ancient. At that time in Earth's history, respiration had not yet evolved. When respiration appeared as the concentration of O_2 in the earth's atmosphere increased, reactive oxygen species (ROS) were produced as a by-product of respiration. Plasmalogens are highly sensitive to ROS and thus became undesirable membrane constituents. Aerobic and facultative organisms were able to survive and reproduce with lipids containing only acyl ester lipids (Goldfine, 2010).

As described in other articles in this series, the eukaryotic pathway to plasmalogens begins with the synthesis of a saturated ether lipid formed first by the acylation of dihydroxyacetone phosphate (DHAP) catalyzed by glycerone phosphate acyl transferase (GNPAT). A long-chain alcohol then displaces the *sn*-1 acyl chain to form 1-*O*-alkyl-2-hydroxy-glycerol-3-P catalyzed by alkylglycerone phosphate synthase (AGPS) on the luminal side of the peroxisomal membrane (da Silva et al., 2012). After acylation of the sn-2 hydroxyl group to form 1-O-alkyl-2-acyl glycerol-2-P and the subsequent formation of 1-O-alkyl-2-acyl-glycerol-P-ethanolamine, there is an oxygen-dependent desaturation of the 1-O-alkyl chain to produce plasmenylethanolamine (PlsE) (Figure 1B) (Gallego-García et al., 2019; Werner et al., 2020).

It has been clear for several decades that the formation of plasmalogens in anaerobes succeeds the formation of the cognate diacylglycerol-phospholipids. The earliest studies indicated a precursor-product relationship between PE and PlsE (Baumann et al., 1965). DHAP was eliminated as a precursor of plasmalogens in *Clostridium beijerinckii* (Hill and Lands, 1970), *Veillonella parvulla*, and *Megasphaera elsdenii* (Prins and Van Golde, 1976). DHAP is also not a precursor to plasmalogens in two anaerobic protozoa, indicating that the dividing line is anaerobic vs. aerobic, rather than prokaryotic vs. eukaryotic (Prins and Van Golde, 1976). Long-chain alcohols were not utilized for plasmalogen biosynthesis in bacteria, but long-chain aldehydes were (Goldfine and Hagen, 1972). The formation of plasmalogens in bacteria from diacylphospholipids received further support in later experiments with whole cells in which the decarboxylation of phosphatidylserine (PS) was inhibited. The mostly diacyl PS that accumulated was rapidly converted to PE followed by PlsE when *the* block was removed (Koga and Goldfine, 1984). Mass spectrometric analysis showed that precursors of phospholipids in bacteria including: phosphatidic acid, CDP-diacylglycerol, and PS were essentially devoid of alk-1′-enyl ether species (Johnston et al., 2010; Guan et al., 2011). In more recent experiments, PS containing odd-chain fatty acids (C_{17}), not present in *C. beijerinckii*, was taken up by growing cells, it was then decarboxylated to form PE, which was transformed to PlsE containing the identical odd-chains (Figure 2) (Goldfine, 2017).

The long-sought bacterial genes for the formation of plasmalogens by direct reduction of the *sn*-1 acyl chain were identified in *Clostridium perfringens* (Jackson et al., 2021). The genes *plsA* and *plsR* encode reductases that sequentially convert the acyl ester to an alk-1′-enyl ether. As expected, these genes are present in many Firmicutes, which includes Costridiales, Veillonellales, Tissierallales, Selenomonadeles, Erysipelotrichales and Acidaminococcales. Among Actinobacteria, these genes are also present in Propionibacteriales, Eggerthellales, Coriobacteriales, Bifidobacteriales and Actinomycetales. Some groups of Proteobacteria have orthologs of these genes (Jackson et al., 2021).

Unexpectedly, these studies have revealed the presence of *plsA* and *plsR* orthologs in facultatively anaerobic bacteria such as *Listeria*, which appear to be active when the cells are grown under anaerobic conditions, confirming earlier reports of the presence of plasmalogens in *L. monocytogenes* and *Enterococcus* faecalis (Farizano et al., 2019). A TetR/AcrR-like transcriptional regulator (EF1326) is present directly upstream of the *pls* gene in *E. faecalis* (EF1327) and other facultative anaerobes. This potentially O_2-sensing transcriptional regulator is not present in strict anaerobes. These findings open the question of the need for plasmalogens under anaerobic, but not aerobic conditions, which is discussed below.

The conformation of plasmalogens and their biophysical properties

With respect to gel to liquid phase transition temperatures, the presence of the *sn*-1-vinyl ether bond has a modest, but measurable effect, lowering the transition temperature 4–6°C (Goldfine et al., 1981; Lohner et al., 1984). A more dramatic effect is seen in the transition from a lamellar to non-lamellar phase. The lamellar to hexagonal II (L → H) for a semi-synthetic PlsE was 30°C compared to 68°C for the diacyl form (Lohner et al., 1984). In biological membranes rich in PlsE, the ability to prevent this transition, which is incompatible with normal membrane function, is necessary. This is usually accomplished by the presence of negatively charged lipids such as PG, CL or PS, and in the case of solvent-producing bacteria, by the presence of a glycerolacetal of PlsE (Figure 1C) (Johnston and Goldfine, 1985; Goldfine et al., 1987).

Diacyl PE molecules in model membranes display a bend at C-2 in the *sn*-2 acyl chain so that the first and second carbon atoms lie essentially parallel to the bilayer plane (Hitchcock et al., 1974). In contrast, this chain in plasmalogens appears to be perpendicular to the bilayer surface (Malthaner et al., 1987a; Malthaner et al., 1987b; Han and Gross, 1990). A molecular dynamics simulation study supports the closer packing of the proximal regions, which results in thicker lipid bilayers. These simulation studies have shown that in plasmalogens the vinyl-ether linkage increases the ordering of the sn-1 chain and the sn-2 acyl chains in PlsCs and PlsEs (Rog and Koivuniemi, 2016; Koivuniemi, 2017). Taken together, these studies indicate tighter packing of plasmalogens in biomembranes, consistent with studies showing that artificial membranes with plasmalogens are less permeable to small molecules (Chen and Gross, 1994; Zeng et al., 1998).

Functions of plasmalogens

Animals including humans require plasmalogens for normal development and function. As discussed in other articles in this series, humans lacking plasmalogens suffer from Rhizomelic chondrodysplasia punctata (RCDP), a condition that impairs normal development of the bones in the upper arms and thighs (rhizomelia). Other consequences of the absence of plasmalogens include intellectual disability, cataracts and heart defects (Braverman and Moser, 2012).

The recent discovery of an operon in bacteria that encodes two reductases needed for plasmalogen biosynthesis in bacteria has opened the field to discovery of the effects of plasmalogen deficiency in bacteria. As of now, there have been no reports on the effects of these mutations on bacterial structures and physiology. In the past, plasmalogen-deficient strains of *Megasphaera elsdenii* were isolated after serial subculture. Strains of this species were isolated in which the normal ratio of plasmalogen to lipid phosphorus was reduced from 0.8 to less than 0.05. Only small changes in morphology and end-products of fermentation were reported. A notable change was a large decrease in saturated fatty acids in the major lipids (Kaufman et al., 1988; Kaufman et al., 1990). Physical studies that compared the membranes and lipids of the wild type and the plasmalogen-deficient strain revealed somewhat lower ordering of the phospholipids compared to the wild type. Both ^{31}P NMR and X-ray diffraction revealed that lipids from the wild-type strain underwent transition from the bilayer arrangement to a hexagonal phase, beginning at 30°C. Phospholipids from plasmalogen-deficient strains appeared to form a relatively stable lamellar phase. Thus, the presence of plasmalogens promoted the formation of non-lamellar phases as found in studies with model membranes (Lohner et al., 1984).

Examination of the polar lipids of *Clostridium tetani* ATCC 10779, the parent strain of strain E88, which was the first *C. tetani* strain to have its genome sequenced, revealed that it did not have plasmalogens. Analysis of several other *C. tetani* strains showed that they all had mixtures of all acyl and plasmalogen polar lipids including PE, PG, CL and N-acetylglucosaminyl diradylglycerol (Johnston et al., 2010). Strain ATCC 10779 was used for production of tetanus toxoid, and it is possible that the ability to form plasmalogens was lost during serial passage. No physical studies were done on the polar lipids of the wild-types and the plasmalogen-deficient strain ATCC 10779.

In general, the results with natural membrane lipids from *M. elsdenii*, support previous work with semisynthetic plasmalogens and those isolated from fatty acid auxotrophic bacteria. The presence of plasmalogens results in closer packing and destabilization of the lamellar organization. As Koivuniemi has pointed out, it seems probable that plasmalogens play an important role in exosome fission, but this is an unlikely general role in bacteria. More likely is the tighter packing they provide resulting from the absences of a bend at the C-2/C-3 carbons of the *sn*-2 acyl chains. The retention of the ability to synthesize plasmalogens in anaerobic and facultatively anaerobic species over eons of evolution speaks to a generalized function. One characteristic of fermentative organisms is the production of acids and expulsion of protons into the

extracellular space. This is true for saccharolytic and proteolytic species of *Clostridium* (Holdeman et al., 1977). As the surrounding medium acidifies, the concentration of protons increases and it is imperative that protons do not return to the cytoplasm. Hence, membranes containing plasmalogens that are less permeable than those containing diacyl phospholipids alone would be favored. As the concentration of oxygen in the atmosphere increased, the development of respiration disfavored fermentation and the concomitant production of acids. As noted above, respiration produces reactive oxygen species, which are destructive of plasmalogens. As organisms that are more complex evolved, plasmalogens again appeared, but in animal cells, they were formed by an oxygen-dependent mechanism. It is instructive to note that in higher organisms, plasmalogens are concentrated in conductive tissues such as the heart and central nervous system, where their enhanced barrier function plays an important role.

Author contributions

Manuscript was written by HG.

Acknowledgments

The author appreciates the lipid structures provided by Ziqiang Guan.

Conflict of interest

The author declares that the research was conducted in the absence of any commercial or financial relationships that could be construed as a potential conflict of interest.

Publisher's note

References

Allison, M. J., Bryant, M. P., Keeney, M., and Katz, I. (1962). Metabolic function of branched-chain volatile fatty acids, growth factors for ruminococci. II. Biosynthesis of higher branched-chain fatty acids and aldehydes. *J. Bacteriol.* 83, 1084–1093. doi:10.1128/JB.83.5.1084-1093.1962

Baumann, N. A., Hagen, P.-O., and Goldfine, H. (1965). Phospholipids of *Clostridium butyricum*: Studies on plasmalogen composition and biosynthesis. *J. Biol. Chem.* 240, 1559–1567. doi:10.1016/s0021-9258(18)97471-5

Braverman, N. E., and Moser, A. B. (2012). Functions of plasmalogen lipids in health and disease. *Biochim. Biophys. Acta* 1822, 1442–1452. doi:10.1016/j.bbadis.2012.05.008

Chen, X., and Gross, R. W. (1994). Phospholipid subclass-specific alterations in the kinetics of ion-transport across biologic membranes. *Biochemistry* 33, 13769–13774. doi:10.1021/bi00250a030

Da Silva, T. F., Sousa, V. F., Malheiro, A. R., and Brites, P. (2012). The importance of ether-phospholipids: A view from the perspective of mouse models. *Biochim. Biophys. Acta* 1822, 1501–1508. doi:10.1016/j.bbadis.2012.05.014

Farizano, J. V., Masias, E., Hsu, F., Salomon, R. A., Freitag, N. E., Hebert, E. M., et al. (2019). PrfA activation in *Listeria monocytogenes* increases the sensitivity to class IIa bacteriocins despite impaired expression of the bacteriocin recepto. *Biochim. Biophys. Acta. Gen. Subj.* 1863, 1283–1291. doi:10.1016/j.bbagen.2019.04.021

Gallego-García, A., Monera-Girona, A. J., Pajares-Martínez, E., Bastida-Martínez, E., Pérez-Castaño, R., Iniesta, A. A., et al. (2019). A bacterial light response reveals an orphan desaturase for human plasmalogen synthesis. *Science* 366, 128–132. doi:10.1126/science.aay1436

Goldfine, H. (1964). Composition of the aldehydes of *Clostridium butyricum* plasmalogens: Cyclopropane aldehydes. *J. Biol. Chem.* 239, 2130–2134. doi:10.1016/s0021-9258(20)82210-8

Goldfine, H., and Hagen, P.-O. (1972). "Bacterial plasmalogens," in *Ether lipids: Chemistry and biology*. Editor F. Snyder (New York: Academic Press).

Goldfine, H., Johnston, N. C., Mattai, J., and Shipley, G. G. (1987). The regulation of bilayer stability in *Clostridium butyricum*: Studies on the polymorphic phase behavior of the ether lipids. *Biochemistry* 26, 2814–2822. doi:10.1021/bi00384a024

Goldfine, H., and Johnston, N. C. (2005). "Membrane lipids of clostridia," in *Handbook on clostridia*. Editor P. Dürre (Boca Raton, FL: Taylor & Francis).

Goldfine, H., Johnston, N. C., and Phillips, M. C. (1981). Phase behavior of ether lipids from *Clostridium butyricum*. *Biochemistry* 20, 2908–2916. doi:10.1021/bi00513a030

Goldfine, H. (2017). The anaerobic biosynthesis of plasmalogens. *FEBS Lett.* 591, 2714–2719. doi:10.1002/1873-3468.12714

Goldfine, H. (2010). The appearance, disappearance and reappearance of plasmalogens in evolution. *Prog. Lipid Res.* 49, 493–498. doi:10.1016/j.plipres.2010.07.003

Goldfine, H. (1962). The characterization and biosynthesis of an N-methylethanolamine phospholipid from *Clostridium butyricum*. *Biochim. Biophys. Acta* 59, 504–506. doi:10.1016/0006-3002(62)90212-3

Guan, Z., and Goldfine, H. (2021). Lipid diversity in clostridia. *Biochim. Biophys. Acta. Mol. Cell Biol. Lipids* 1866 (9), 158966. doi:10.1016/j.bbalip.2021.158966

Guan, Z., Johnston, N. C., Aygun-Sunar, S., Daldal, F., Raetz, C. R., and Goldfine, H. (2011). Structural characterization of the polar lipids of *Clostridium novyi* NT. Further evidence for a novel anaerobic biosynthetic pathway to plasmalogens. *Biochim. Biophys. Acta* 1811, 186–193. doi:10.1016/j.bbalip.2010.12.010

Han, X., and Gross, R. W. (1990). Plasmenylcholine and phosphatidylcholine membrane bilayers possess distinct conformational motifs. *Biochemistry* 29, 4992–4996. doi:10.1021/bi00472a032

Hill, E. E., and Lands, W. E. M. (1970). Formation of acyl and alkenyl glycerol derivatives in *Clostridium butyricum*. *Biochim. Biophys. Acta* 202, 209–211. doi:10.1016/0005-2760(70)90239-0

Hitchcock, P. B., Mason, R., Thomas, K. M., and Shipley, G. G. (1974). Structural chemistry of 1, 2- Dilauroyl-DL-phosphatidylethanolamine:Molecular conformation and intermolecular packing of phospholipids. *Proc. Natl. Acad. Sci. U. S. A.* 71, 3036–3040. doi:10.1073/pnas.71.8.3036

Holdeman, L. V., Cato, E. P., and Moore, W. E. C. (1977). *Anaerobe laboratory manual*. Blacksburg, VA: Virginia Polytechnic Institute and State University.

Jackson, D. R., Cassilly, C. D., Plichta, D. R., Vlamakis, H., Liu, H., Melville, S. B., et al. (2021). Plasmalogen biosynthesis by anaerobic bacteria: Identification of a two-gene operon Responsible for plasmalogen Production in *Clostridium perfringens*. *ACS Chem. Biol.* 16, 6–13. doi:10.1021/acschembio.0c00673

Johnston, N. C., Aygun-Sunar, S., Guan, Z., Ribeiro, A. A., Daldal, F., Raetz, C. R., et al. (2010). A phosphoethanolamine-modified glycosyl diradylglycerol in the polar lipids of *Clostridium tetani*. *J. Lipid Res.* 51, 1953–1961. doi:10.1194/jlr.M004788

Johnston, N. C., and Goldfine, H. (1983). Lipid composition in the classification of the butyric acid-producing clostridia. *J. Gen. Microbiol.* 129, 1075–1081. doi:10.1099/00221287-129-4-1075

Johnston, N. C., and Goldfine, H. (1985). Phospholipid aliphatic chain composition modulates lipid class composition, but not lipid asymmetry in *Clostridium butyricum*. *Biochim. Biophys. Acta* 813, 10–18. doi:10.1016/0005-2736(85)90339-6

Kamio, Y., Kanegasaki, S., and Takahashi, H. (1969). Occurrence of plasmalogens in anaerobic bacteria. *J. Gen. Appl. Microbiol.* 15, 439–451. doi:10.2323/jgam.15.439

Kaufman, A. E., Goldfine, H., Narayan, O., and Gruner, S. M. (1990). Physical studies on the membranes and lipids of plasmalogen-deficient *Megasphaera elsdenii*. *Chem. Phys. Lipids* 55, 41–48. doi:10.1016/0009-3084(90)90147-j

Kaufman, A. E., Verma, J. N., and Goldfine, H. (1988). Disappearance of plasmalogen-containing phospholipids in *Megasphaera elsdenii*. *J. Bacteriol.* 170, 2770–2774. doi:10.1128/jb.170.6.2770-2774.1988

Koga, Y., and Goldfine, H. (1984). Biosynthesis of phospholipids in *Clostridium butyricum*: The kinetics of synthesis of plasmalogens and the glycerol acetal of ethanolamine plasmalogen. *J. Bacteriol.* 159, 597–604. doi:10.1128/JB.159.2.597-604.1984

Koga, Y., and Morii, H. (2005). Recent advances in structural research on ether lipids from archaea including comparative and physiological aspects. *Biosci. Biotechnol. Biochem.* 69, 2019–2034. doi:10.1271/bbb.69.2019

Koivuniemi, A. (2017). The biophysical properties of plasmalogens originating from their unique molecular architecture. *FEBS Lett.* 591, 2700–2713. doi:10.1002/1873-3468.12754

Lohner, K., Hermetter, A., and Paltauf, F. (1984). Phase behavior of ethanolamine plasmalogen. *Chem. Phys. Lipids* 34, 163–170. doi:10.1016/0009-3084(84)90041-0

Malthaner, M., Hermetter, A., Paltauf, F., and Seelig, J. (1987a). Structure and dynamics of plasmalogen model membranes containing cholesterol; a deuterium NMR study. *Biochim. Biophys. Acta* 900, 191–197. doi:10.1016/0005-2736(87)90333-6

Malthaner, M., Seelig, J., Johnston, N. C., and Goldfine, H. (1987b). Deuterium NMR studies on the plasmalogens and the glycerol acetals of plasmalogens of *Clostridium butyricum* and *Clostridium beijerinckii*. *Biochemistry* 26, 5826–5833. doi:10.1021/bi00392a037

Matsumoto, M., Tamiya, K., and Koizumi, K. (1971). Studies on neutral lipids and a new type of aldehydogenic ethanolamine phospholipid in *Clostridium butyricum*. *J. Biochem. (Tokyo)* 69, 617–620.

Prins, R. A., and Van Golde, L. M. G. (1976). Entrance of glycerol into plasmalogens of some strictly anaerobic bacteria and protozoa. *FEBS Lett.* 63, 107–111. doi:10.1016/0014-5793(76)80204-9

Rezanka, T., Kresinova, Z., Kolouchova, I., and Sigler, K. (2012). Lipidomic analysis of bacterial plasmalogens. *Folia Microbiol.* 57, 463–472. doi:10.1007/s12223-012-0178-6

Rog, T., and Koivuniemi, A. (2016). The biophysical properties of ethanolamine plasmalogens revealed by atomistic molecular dynamics simulations. *Biochim. Biophys. Acta* 1858, 97–103. doi:10.1016/j.bbamem.2015.10.023

Rogosa, M. (1984). "Anaerobic gram-negative cocci," in *Bergey's manual of systematic bacteriology V. 1*. Editors N. R. Krieg and J. G. Holt (Baltimore, MD: Williams & Wilkins).

Snyder, F. (1972). "The enzymic pathways of ether-linked lipids and their precursors," in *Ether lipids. Chemistry and biology*. Editor F. Snyder (New York: Academic Press).

Snyder, F. (1999). The ether lipid trail: A historical perspective. *Biochim. Biophys. Acta* 1436, 265–278. doi:10.1016/s0005-2760(98)00172-6

Vitova, M., Palyzova, A., and Rezanka, T. (2021). Plasmalogens - ubiquitous molecules occurring widely, from anaerobic bacteria to humans. *Prog. Lipid Res.* 83, 101111. doi:10.1016/j.plipres.2021.101111

Wegner, G. H., and Foster, E. M. (1963). Incorporation of isobutyrate and valerate into cellular plasmalogen by Bacteroides succinogenes. *J. Bacteriol.* 85, 53–61. doi:10.1128/JB.85.1.53-61.1963

Werner, E. R., Keller, M. A., Sailer, S., Lackner, K., Koch, J., Hermann, M., et al. (2020). The TMEM189 gene encodes plasmanylethanolamine desaturase which introduces the characteristic vinyl ether double bond into plasmalogens. *Proc. Natl. Acad. Sci. U. S. A.* 117, 7792–7798. doi:10.1073/pnas.1917461117

Zeng, Y. C., Han, X. L., and Gross, R. W. (1998). Phospholipid subclass specific alterations in the passive ion permeability of membrane bilayers: Separation of enthalpic and entropic contributions to transbilayer ion flux. *Biochemistry* 37, 2346–2355. doi:10.1021/bi9725172

Frontiers in
Cell and Developmental Biology

Explores the fundamental biological processes of life, covering intracellular and extracellular dynamics.

The world's most cited developmental biology journal, advancing our understanding of the fundamental processes of life. It explores a wide spectrum of cell and developmental biology, covering intracellular and extracellular dynamics.

Discover the latest Research Topics

See more →

Frontiers

Avenue du Tribunal-Fédéral 34
1005 Lausanne, Switzerland
frontiersin.org

Contact us

+41 (0)21 510 17 00
frontiersin.org/about/contact